Revision of basal sauropods from the Middle Jurassic of Patagonia and the early evolution of eusauropods

Dissertation zur Erlangung des Doktorgrades
an der Fakultät für Geowissenschaften
der Ludwig- Maximilians-Universität München

Vorgelegt von Femke Marleen Holwerda

München, 23. Januar 2019

Erstgutachter: PD Dr. Oliver Walter Mischa Rauhut

Zweitgutachter: Dr. Diego Pol

Tag der mündlichen Prüfung: 05.06.2019

Statutory declaration and statement

I hereby confirm that my thesis entitled "**Revision of basal sauropods from the Middle Jurassic of Patagonia and the early evolution of eusauropods**", is the result of my own original work. Furthermore, I certify that this work contains no material which has been accepted for the award of any other degree or diploma in my name, in any university and, to the best of my knowledge and belief, contains no material previously published or written by another person, except where due reference has been made in the text. In addition, I certify that no part of this work will, in the future, be used in a submission in my name, for any other degree or diploma in any university or other tertiary institution without the prior approval of the Ludwig-Maximilians-University Munich.

Munich, 23.01.2019 Femke Holwerda

Contents

Chapter 3: Revising associated material of *Patagosaurus fariasi* BONAPARTE 1979, with notes on the species diversity of the Cerro Condor bonebeds

Chapter 4: The phylogeny of *Patagosaurus fariasi* and implications for evolutionary relationships of Early-Middle Jurassic sauropods and their biogeography

Chapter 5: Geometric morphometrics on *Patagosaurus fariasi* and Jurassic sauropods: implications for diversity and ontogeny

Acknowledgements

I would never have made it this far but for the support of Diego Pol, who took me on as a MSc student and then kept supporting me throughout. And we still work together! Thanks to Oliver Rauhut for providing the DFG grant so that I could work on this great group, the sauropods! #sauropodsrule #gosauropodsgo

Thanks also to the members of the workgroup Mesozoic Vertebrates.

And thanks to:

Munich: Gertrud, Nicola, Martin&Camila, Mike, Warren, Bill, and the awesome student gang Tom, Lukardis, Sara

Nederland: Sofie, Eva, De Bioloogjes; Petra, Madelon, Tryntsje, Linda, Tammo, Anne Schulp, Jelle Reumer, Wilma Wessels, en mijn familie.

Argentina:
Trelew: Diego, Jose, Nacho, Juli&Juli, Marcos, Andrea, Marcelo, Pablo, Dudu, Leandro&Lorena
Buenos Aires: Alejandro Kramarz, Stella Alvarez, Juli Desojo, Chorno, Agus,
Tucuman: Jaime Powell, Rodrigo, Graci
…..and a huge thanks to The Randomers Becky and Santi!!

Portugal: João, João, Nury (just counting you there fofinha) Alex, Christophe, Emanuel, Alexandra

UK: Paul&Paul (the sauropauls), Mark Evans, Hillary Ketchum, Sandra Chapman, Mike Taylor, Matt Wedel, Steve Brusatte, Stig Walsh, Elsa Panciroli, David Button, Phil Mannion

Germany: Daniela Schwarz, Nils Knötschke, Martin Sander, Heinrich Mallison, Ulrich Joger

Paris: Ronan Allain, Claire PdF, Emilie Läng

My Sauroporacles: a word of my own invention (sauropod + oracle) which stands for amazing people who've helped me with *every stupid question imaginable* concerning sauropods, and that on a regular (sometimes daily) basis. Without (at least audibly) getting annoyed with me. Without complaining. A magnificent thank you goes to Emanuel Tschopp, Jose Luis Carballido, Phil Mannion and Veronica Díez Díaz.

Moral support (very important); listening to me when I needed someone to listen, giving sound advice and swearing along with my cursing: Madelon, Liz, Nicola, Franzi, Roland, the EAVP gossip group, and Jon and Daenerys for a right proper swooning.

And last, but certainly not least: My husband Jeff. I'm looking forward to a long life together and becoming Fat like Pat ☺

Lastly, a big thank you to Fat Pat and the Patsies (#FatPat, #gosauropodsgo, #sauropodsrule). I may go on to date Cetio and Rut and Moos, but you will always be My Pat.

And finally, this thesis is dedicated to the memory of Jaime Powell.

Abstract

The Early and Middle Jurassic are widely regarded as the critical time for sauropod radiation and worldwide dispersal. The accepted theory is that the common ancestor of Early Jurassic sauropods had its provenance in South Africa, South Gondwana at the time. The major sauropod diversification and dispersal out of South Africa happened between the Early and Middle Jurassic (±180-160 Ma), with major clades being firmly established by the Late Jurassic (±150 Ma). The Early and Middle Jurassic, however, have a generally poor sauropod body fossil record with the exception of a few taxa from Gondwana (e.g. *Patagosaurus, Volkheimeria, Amygdalodon, Vulcanodon, Tazoudasaurus, Spinophorosaurus, Barapasaurus, Bothriospondylus, Lapparentosaurus*) and even fewer from Laurasia (e.g. *Cetiosaurus, Cetiosauriscus, Shunosaurus, Klamelisaurus, Mamenchisaurus, Omeisaurus*).

The Gondwanan sauropod with the most material preserved is *Patagosaurus fariasi,* from the Cañadón Asfálto Formation of west-central Chubut province, Patagonia, Argentina. It has a holotype consisting of axial and appendicular elements, and associated material consisting of cranial, axial, appendicular and dermal bones. The completeness of the material makes it valuable for Middle Jurassic sauropod research. Moreover, recent dating of the sediments belonging to the Cañadón Asfálto Formation resulted in a much older age range for the latter, redating it and all vertebrates found there from a Callovian to a much older Aalenian-Bajocian age, and thus placing *Patagosaurus* in a critical time for sauropod evolution; the latest Early to the early Middle Jurassic. *Patagosaurus* has been found in two bonebeds, not far apart; the holotype and several other associated specimens from Cerro Condor Norte, north of the village of Cerro Cóndor by the Chubut river, and more associated material, as

well as another sauropod taxon, *Volkheimeria chubutensis*, from Cerro Condor Sur, a site close to the Chubut river. Both beds are lacustrine deposits. However, the original 1986 description of *Patagosaurus* consisted of a blend of the holotype and associated material, without clearly distinguishing the former from the latter. Moreover, some material from Cerro Condor Sur, specimen MACN-CH 934, has since been considered to be a taxon other than *Patagosaurus* or *Volkheimeria*. Thus, a revision of all material has been done. The holotype has been revised and the alpha taxonomy of *Patagosaurus fariasi* has been established, confirming or discarding old diagnostic characters as appropriate, and generating new diagnostic characters for the new assignment of associated material to *Patagosaurus fariasi, Volkheimeria*, sauropod indet., or a new taxon.

After the revision of all material, the Cerro Condor Norte bonebed was found to be monospecific, and includes an ontogenetic series of a small juvenile *Patagosaurus*, an intermediate juvenile, a subadult, the holotype (being a subadult to adult specimen) and another adult specimen. Cerro Condor Sur proved to be more problematic; yielding *Patagosaurus* material of an adult and a fully grown large adult, material that can only be assigned to an indeterminate sauropod, due to the fragmentary nature, and finally, two potential new taxa, one of which is more likely a valid new taxon than the other: MACN-CH 934 and MACN-CH 230.

A phylogenetic analysis using all confirmed material of *Patagosaurus*, and the MACN-CH 934 as OTU, as well as a recoding of *Volkheimeria, Spinophorosaurus, Tazoudasaurus, Cetiosaurus oxoniensis* and the Rutland *Cetiosaurus, Lapparentosaurus, Bothriospondylus*, confirms *Patagosaurus* to be a derived non-neosauropodan eusauropod, sister taxon to the Rutland *Cetiosaurus,* and nested within *Cetiosaurus*, both from the UK, thus confirming the existence of Cetiosauridae. *Barapasaurus*, an Indian taxon, which is traditionally closely associated with

Patagosaurus, was retrieved as being more basal than the Cetiosauridae, and is thus considered a more basal non-neosauropodan eusauropod, and not closely related to *Patagosaurus*. Interestingly, the new, unnamed taxon MACN-CH 934 is retrieved as a derived non-neosauropodan eusauropod or even a basal neosauropod, and sister-taxon to *Lapparentosaurus*, a taxon from Madagascar. *Volkheimeria* comes out as sister-taxon to the North African *Spinophorosaurus*. The addition of MACN-CH 230 as a potential new OTU, however, destabilizes the tree, and forces MACN-CH 230, and *Bothriospondylus* and *Lapparentosaurus* from Madagascar together, while MACN-CH 934 remains a basal neosauropod. This means there is probably not enough information on *Lapparentosaurus*, *Bothriospondylus*, or MACN-CH 230, to provide valid results, and future research should establish their phylogenetic relationships better. Moreover, geometric morphometric analysis on limb bones important for stance and gait, the femora and tibiae, provide different patterns compared to those shown by the phylogenetic results. Early and Middle Jurassic sauropods show more morphological variability in the tibiae, which may reflect on differences in mobility between basal sauropods and more derived non-neosauropod eusauropods. The femora show a low amount of morphological variability throughout the Jurassic, with an increase in size towards the Late Jurassic, which reflects on the trend of sauropods becoming larger towards the Late Jurassic, when neosauropods were firmly established.

The grouping together of taxa from across the Gondwanan continent, and even together with Laurasian taxa, shows a greater mobility for sauropods in the Middle Jurassic than previously assumed. The evolution of Gondwanan sauropods was thought to be bracketed by their diversification wave after the Toarcian mass extinction, and by a physical barrier in the form of the Central Gondwanan Desert, preventing taxa from dispersing, and thus creating

endemic radiation patterns in South Africa and Argentina. However, this study shows that sauropods would be able to migrate through the physical barrier, and questions the existence of a real barrier, or whether the desert was periodically (in)accessible. Future research on the more unstable taxa of the tree, and more revisions of poorly known basal eusauropods, will hopefully clarify this.

Chapter 1 introduces the thesis, Chapters 2 and 3 revise the holotype and associated material respectively, and Chapter 4 shows the phylogenetic study. Chapter 5 shows geometric morphometric analysis on adult and juvenile *Patagosaurus* elements compared to other Jurassic sauropods. Thus, the revision of *Patagosaurus* aids in sauropod taxonomic, evolutionary, ontogenetic, and phylogenetic research.

1 Introduction

1.1 Sauropods

Sauropods were a group of large, quadrupedal, herbivorous dinosaurs (see Figure 1), and possibly the 'quintessential' dinosaur for the general public (McIntosh, 1990; Upchurch et al., 2004; Barrett and Upchurch, 2005; Tschopp et al., 2015). Sauropod body fossils have been found in all continents, even Antarctica, and their presence in the fossil record stretches over almost the entire Mesozoic period, from the Late Triassic (±227 Ma) to the Late Cretaceous (±66 Ma), see for instance (Bonaparte, 1986a; McIntosh, 1990; Barrett, 1999; Upchurch et al., 2004; Barrett and Upchurch, 2005; Allain and Aquesbi, 2008; Lloyd et al., 2008; Läng and Mahammed, 2010; Mannion, 2010a; Mannion and Upchurch, 2011; Cerda et al., 2012; Benson et al., 2013; McPhee et al., 2016; Lallensack et al., 2017).

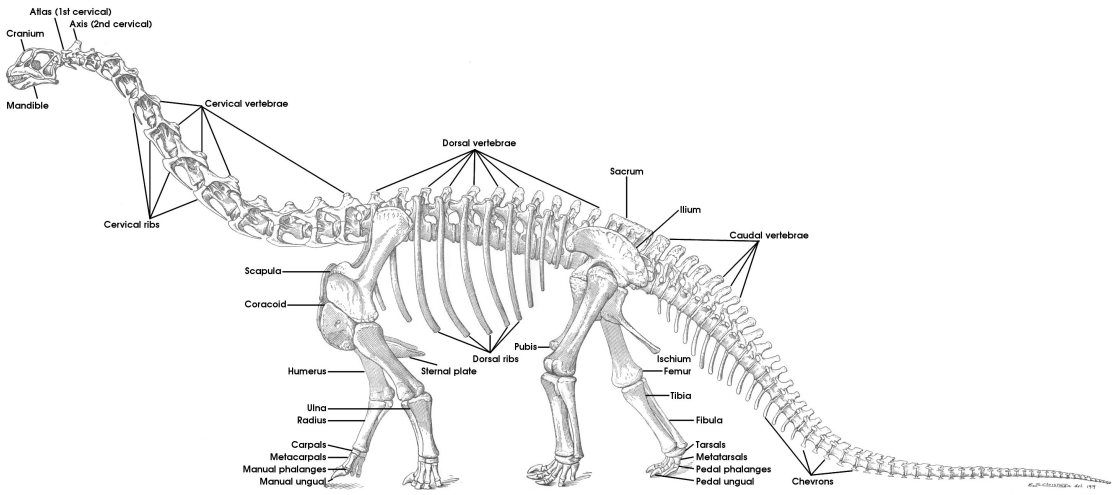

Figure 1: Basic sauropod skeletal anatomy, based on Camarasaurus (after Osborn and Mook, (1921), courtesy of Mike Taylor at SVPOW.com).

They were thus a successful clade, and their evolutionary strategies have been extensively studied, and traced to a number of factors. The first is their bauplan; consisting of a diminutive cranium, an (in some cases extremely) elongated neck, a large round torso, columnar limbs, and a long tail (McIntosh, 1990; Sander et al., 2004, 2011; Upchurch et al., 2004; Wilson, 2005a; Sander and Clauss, 2008; Rauhut et al., 2011; Stoinski et al., 2011;

Sander, 2013; de Souza and Santucci, 2014). The elongation of the neck in particular is a sauropod trait, and has been linked to feeding, thermoregulation, sexual selection and mobility (Frey and Martin, 1997; Martin et al., 1998; Stevens and Parrish, 2005a; Parrish, 2006; Christian and Dzemski, 2007, 2011; Seymour, 2009; Taylor et al., 2009, 2011; Christian, 2010; Preuschoft and Klein, 2013; Taylor and Wedel, 2013; Hughes et al., 2016). The long tail function is thought to be used for balance and mobility, but possibly also as a defense mechanism against predators (Holland, 1915; Zhang, 1988; Dong et al., 1989, 1989; Christiansen, 1996; Myhrvold and Currie, 1997; Remes et al., 2009; Butler et al., 2013; Vidal and Díaz, 2017). The large body contained an efficient digestive system, and this combined with the long neck, small head, and the existence of a high tooth replacement rate, provided an efficient feeding strategy (Christiansen, 2000; Upchurch and Barrett, 2000; Sereno and Wilson, 2005; Stevens and Parrish, 2005; Barrett and Upchurch, 2007; Yates et al., 2010; Hummel and Clauss, 2011; Whitlock, 2011; Young et al., 2012; D'Emic et al., 2013; Button et al., 2014; Holwerda et al., 2015; Schwarz et al., 2015; Wiersma and Sander, 2016).

Next to their bauplan, their reproductive strategy of having many young, as well as their fast growth from vulnerable, precocious juveniles to (sub)adults, added to their success (Carpenter and McIntosh, 1994; Chiappe et al., 1998, 2001, 2005; Curry, 1999; Klein and Sander, 2008; García and Cerda, 2010; Werner and Griebeler, 2011; Sander, 2013; Waskow and Sander, 2014; García et al., 2015). An evolutionary cascade model for their success is shown in Figure 2 (adapted after Sander et al., 2013).

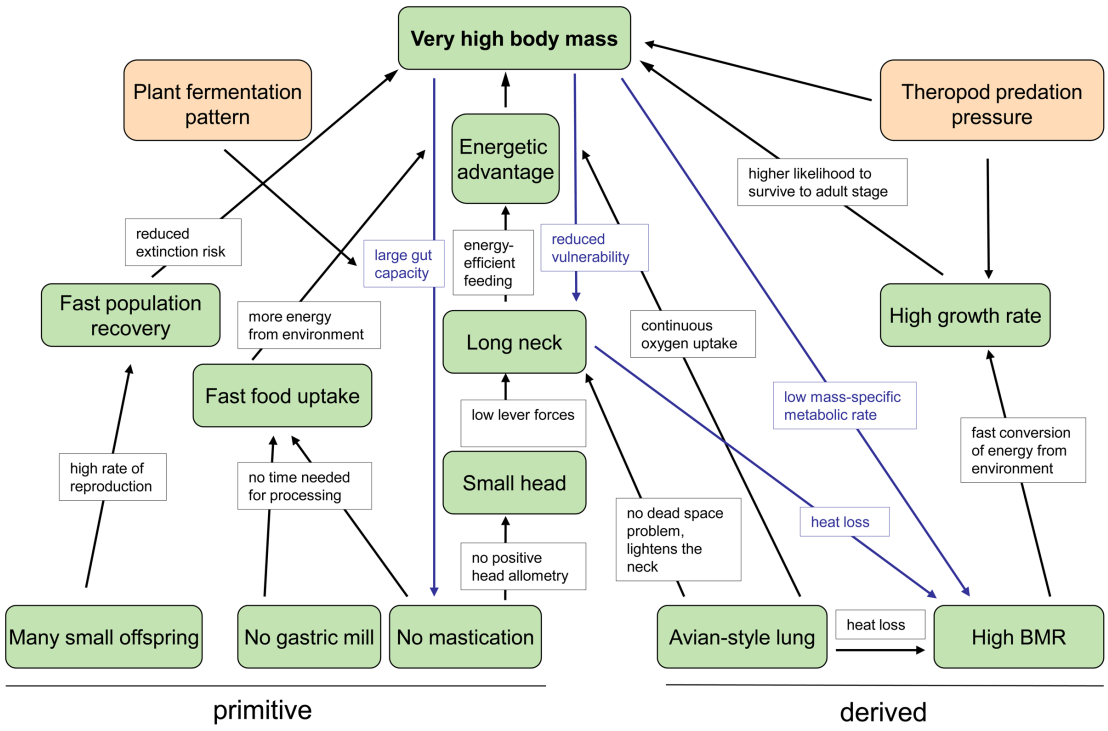

Figure 2: Evolutionary cascade model of sauropod gigantism, from Sander et al., (2013).

1.2 Evolution of early sauropods

Though eventually growing to gigantic proportions, the early evolution of sauropods started in the early Late Triassic (Carnian, ±237 Ma) with a split from saurischia; small, bipedal, omnivorous to carnivorous dinosaurs, to sauropodomorphs, medium to large-sized, (facultatively) bipedal to quadrupedal dinosaurs (Galton, 1990; Galton and Upchurch, 2004; Barrett and Upchurch, 2005, 2007; Martinez and Alcober, 2009; Ezcurra, 2010; McPhee et al., 2015a). They had a worldwide distribution at the time of the Late Triassic (Norian-Rhaetian, ±227-208 Ma) when the first basal sauropods appear in the fossil record, which were subsequently established as a clade in the Early Jurassic (±200 Ma; Raath, 1972; Jain et al., 1975; Cooper, 1984; Yates and Kitching, 2003; Kutty et al., 2007; Yates et al., 2010; Pol et al., 2011a; McPhee 2014; McPhee et al., 2015b; McPhee and Choiniere, 2016; Lallensack et al., 2017; Rauhut et al., in prep). Originally, sauropods were thought to originate in South Africa, from where they dispersed over the rest of Gondwana, and Laurasia (Raath, 1972; Cooper, 1984; Bonaparte, 1986a; Galton, 1998; Yadagiri, 2001; Wilson, 2005a; Kutty et al., 2007;

McPhee et al., 2015b), however, the potential presence of sauropods in the Late Triassic of Europe, as well as Thailand, might change this (Buffetaut *et al*., 2000, 2002; Racey & Goodall, 2009; Lallensack et al., 2017).

After their initial appearance, the radiation and evolution of sauropods most likely took place between the Early Jurassic and the Middle Jurassic (±170 Ma, Upchurch et al., 2004; Barrett and Upchurch, 2005; Wilson, 2005b; Mannion, 2010a; Mannion and Upchurch, 2010a, 2010b; Mannion et al., 2011). By the late Middle to Late Jurassic (± 150 Ma), all major clades were established (McIntosh, 1990; Upchurch et al., 2004; Barrett and Upchurch, 2005; Wilson, 2005b), see Figure 3 and 4). Figure 4 shows the major sauropod groups and their phylogenetic relationships; however, these continuously change with new phylogenetic research (see Chapter 4 for a more extensive overview of sauropod phylogeny). Eusauropoda (Figure 4) is defined as the group including *Shunosaurus, Saltasaurus*, their most recent common ancestor, and all descendants (Yates and Kitching, 2003; Wilson, 2005b; Yates et al., 2010; McPhee et al., 2014). The term was coined by Upchurch in 1995 as the group including all sauropods except vulcanodontids (Upchurch, 1995). More recent analyses added Gravisauria as the most basal sauropod clade, including *Vulcanodon, Tazoudasaurus*, and *Saltasaurus* and all descendants (Allain and Aquesbi, 2008). However, not all phylogenetic studies agree on including Gravisauria. Neosauropoda is defined as *Diplodocus*, *Saltasaurus*, their common ancestor, and all its descendants (Bonaparte 1986, Wilson and Sereno 1998). Neosauropoda (Figure 4) is split further into Diplodocoidea, (which includes Rebbachisauridae, Dicraeosauridae and Diplodocidae), Macronaria, Titanosauriformes and Titanosauria (Wilson, 2002, 2005b; Allain and Aquesbi, 2008; Remes et al., 2009; Sander et al., 2011). This thesis will focus mostly on the early evolution of non-neosauropodan eusauropods.

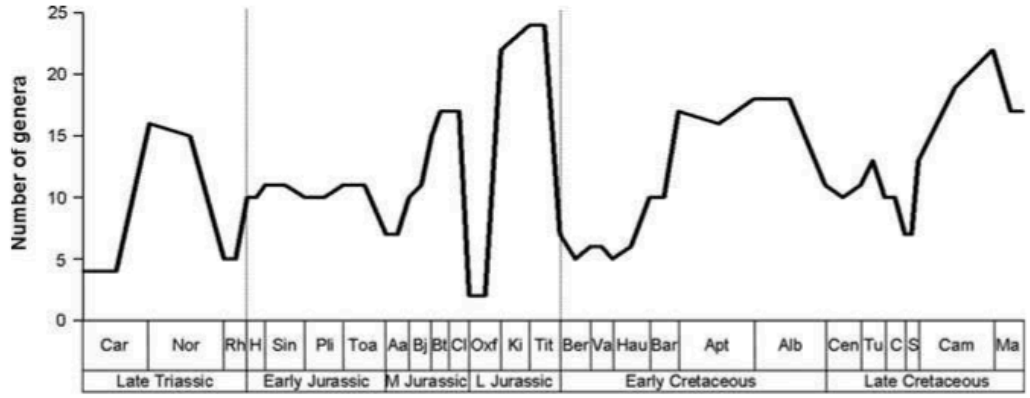

Figure 3: Sauropodomorph diversity through time after (Mannion et al., 2011).

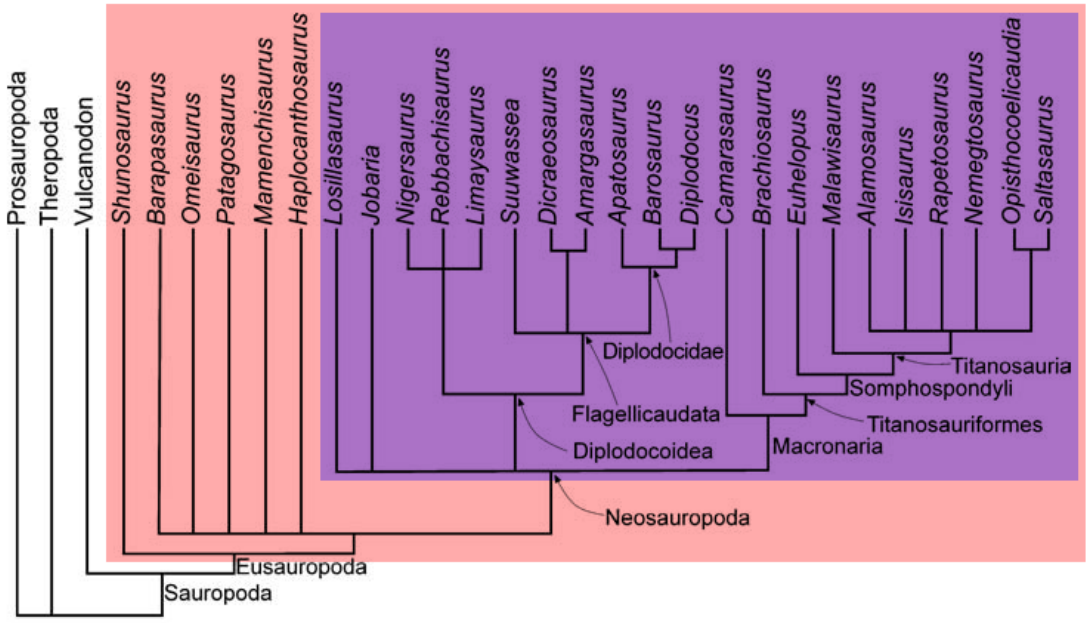

Figure 4: Simplified sauropod phylogeny with all major clades. Note Sauropoda, Eusauropoda and Neosauropoda (after Harris 2006; courtesy of Mike Taylor at SVPOW.com).

1.3 The world during the Jurassic: a sauropod perspective

The early radiation of sauropods in the Jurassic was mainly controlled by environmental factors. The Pliensbachian-Toarcian exctinction (±190-182 Ma) was a mass-extinction event most likely triggered by a global cooling , induced by extensive and prolonged volcanism at the Karoo Basin. This cooling subsequently caused a global drop in sea level, after which plant life colonized the newly exposed continental shelves (Morard et al., 2003; Wignall et al.,

2005; Wignall and Bond, 2008; Gómez and Goy, 2011). A period of warming followed, which caused this organic mass to accumulate on the sea floor, which triggered massive ocean anoxia, the Toarcian Ocean Anoxic Event (OAE; Morard et al., 2003; Wignall et al., 2005; Wignall and Bond, 2008; Gómez and Goy, 2011). The mass extinction and associated climate change would be responsible for the clearing of an ecological niche for large herbivores (Jenkyns, 1988; Bailey et al., 2003; van de Schootbrugge et al., 2005; Hesselbo et al., 2007; Allain and Aquesbi, 2008; Läng, 2008; Al-Suwaidi et al., 2010; Läng and Mahammed, 2010; Mannion, 2010a; Hesselbo and Pieńkowski, 2011; McPhee et al., 2015b; Stumpf et al., 2015). The second controlling factor on sauropod radiation was and the presence of physical barriers such as deserts, and new seaways by the splitting up of Pangaea into Gondwana and Laurasia in the Early Jurassic (Dietz and Holden, 1970; Hallam, 1980, 1983; Rauhut and Lopez-Arbarello, 2008; Rauhut and López-Arbarello, 2009; Remes et al., 2009; Pol et al., 2011b; Pol and Rauhut, 2012). The Jurassic in general had a more humid climate than the Triassic, and gymnosperms were more common, as well as podocarps, conifers, Araucariaceae and gingkos (Hallam, 1985; Escapa et al., 2008, 2013; Gee, 2010, 2011; Bodnar et al., 2013; Elgorriaga et al., 2015).

1.4 Systematic overview of important Jurassic taxa for this study

The most relevant Early and Middle Jurassic basal non-neosauropod sauropod taxa used in this thesis are briefly described below. All of these taxa are used in the phylogeny of Chapter 4, and are also considered in the biogeographical analysis of Chapter 4. Several taxa that are known from the Jurassic but are too fragmentary/poorly known are not discussed here, such as *Ferganasaurus, Cetiosaurus mogrebiensis,* and *Datousaurus*. See Upchurch et al. (2004), Wilson (2005) as well as Läng (2010) for systematics on the outgroups (basal sauropodomorphs and neosauropods). A fuller review of the Cetiosaurs is planned in the future (P.Upchurch and P. Mannion, pers.comm).

Amygdalodon patagonicus is an Early Jurassic sauropod from Patagonia, Argentina. It was found in the Cerro Carnerero Formation at Pampa Agnia, Patagonia, Argentina, which was thought to be Bajocian, but may now be as old as Pliensbachian-Toarcian (see Rauhut, 2003; Cúneo et al., 2013). It was first described in 1947 (Cabrera, 1947), redescribed in 1963, and redescribed once more in 2003 (Casamiquela, 1963; Rauhut, 2003a). The material consists of dentition, several appendicular elements and some fragmentary axial elements. It usually is retrieved as a basal sauropod, more closely related to *Tazoudasaurus* and *Vulcanodon*, than to more derived (eu)sauropods. The dentition, in particular the enamel wrinkling pattern, thus far has been found to be unique amongst other basal sauropods (Carballido and Pol, 2010).

Vulcanodon karibaensis is an Early Jurassic (Toarcian, ±180 Ma) sauropod from Zimbabwe, South Africa. It is in need of redescription, since its last descriptions were in 1972 and 1984 (Raath, 1972; Cooper, 1984). A redescription is planned, however (P.Barrett, pers.comm.). It is usually used as the oldest sauropod in the definition of sauropoda by Salgado et al. (1997), as it was the oldest sauropod known until recently (Upchurch et al., 2004). Cooper (1984) erected the clade Vulcanodontidae, which is still supported by Allain et al. (2008), although encompassed within Gravisauria (Allain et al., 2008).

Tazoudasaurus naimi was found in the High Atlas Mountains in Morocco, North Africa, from the Azilal/Wazzant Formation, which is thought to be Toarcian to Aalenian in age, with *Tazoudasaurus* coming most probably from the Toarcian layers (Allain et al., 2004; Allain and Aquesbi, 2008). It is known from several individuals, both juveniles and adults, which sheds light on early sauropod ontogenetic variation. The material consists of dentition, cranial, axial, and appendicular material. A reconstruction of *Tazoudasaurus* has been recently

attempted as well (Peyer and Allain, 2010). The discovery and osteological description led to the erection of the new sauropod clade Gravisauria, which encompasses *Vulcanodon*+*Tazoudasaurus*, and all other sauropods (Allain et al., 2008).

Barapasaurus tagorei is an Indian taxon from the Early Jurassic Kota Formation of Deccan Province, India. It was first described in the 1970's (Jain et al., 1975, Jain, 1980) and redescribed recently (Bandyopadhyay et al., 2010). Next to the basal sauropodiform *Kotasaurus* (Yadagiri, 2001; Kutty et al., 2007) it is the only Indian Middle Jurassic taxon known to date, and therefore important for the study of Gondwanan sauropod evolution. It is known from several specimens, and includes dentition, as well as axial and appendicular elements including pelvic and pectoral elements, however, the taxon is slightly problematic due to the holotype possibly being a composite specimen, and due to uncertainties regarding the provenance of the specimens.

Shunosaurus lii was found in 1977 and named in 1983 and further described in 1988 (Dong et al., 1983; Zhang, 1988). It was found in the Lower Xiashaximiao Formation near Dashanpu, Zigong, China, which is Bathonian to Oxfordian in age (±168-157 Ma), however, recent redating of the depositional sediments yields a maximum age of 159 ±2 Ma, giving it an Oxfordian age (Wang *et al*., 2018). It is the most common sauropod from the Xiashaximiao Formation. It was thought to be a euhelopodid sauropod, until Wilson (2002) retrieved it as a basal eusauropod. A redescription of cranial material was done more recently, which found a unique curvature in both the maxillae as well as the dentaries (Zheng, 1996; Chatterjee and Zheng, 2002). A more recent description of the postcranial material, however, has not been performed recently. More redescriptions of Chinese sauropods from the Middle Jurassic will tell more on the phylogenetic position of *Shunosaurus*. Currently, it is usually found at the base of the eusauropods in phylogenetic analyses, and, as noted

before, defines the Eusauropoda as the group including *Shunosaurus, Saltasaurus*, their most recent common ancestor, and all descendants (Yates and Kitching, 2003; Yates et al., 2010; McPhee et al., 2014). Finally, It is peculiar amongst Jurassic sauropods due to the presence of a tailclub.

Spinophorosaurus nigerensis is a relatively new basal eusauropod from the Middle Jurassic of Niger, Africa (Remes et al., 2009). It is known from several specimens, most of which is still under preparation. A full osteology is currently in the making (F. Knoll, pers.comm.). The holotype consists of several axial elements, cranial elements, teeth, and several pectoral, pelvic and appendicular elements. A braincase was described in 2012, which found a combination of primitive and derived characters (Knoll et al., 2012), which is not unusual for basal eusauropods, as is found in Chapter 2 and 3 of this thesis. Lastly, it is peculiar for Jurassic sauropods in that it probably possessed tail spines (Remes et al., 2009).

Volkheimeria chubutensis is a sauropod from the locality of Cerro Condor Sur, Cañadón Asfálto Fm., west-central Chubut, Patagonia, Argentina. It is known from several dorsal elements, and several appendicular elements, as well as pelvic elements. It was found together with *Patagosaurus*, and described in 1979 and 1986. The material is in need of a redescription however, and is currently being prepared for that purpose (D.Pol pers.comm.). In the phylogenetic analysis in Chapter 4, it comes out as more basal than *Patagosaurus*, and it remains a valid taxon.

Cetiosaurus oxoniensis is historically speaking the oldest sauropod to be described, though explicitly left out of the first paper naming Dinosauria, and not described as a real sauropod until 1871 (see Owen, 1842, 1841; Phillips, 1871; Taylor, 2010; Upchurch and Martin, 2003), it's first description dating from 1841 (as sauropod skeletal remains, since *Cardiodon* was

described the same year but based only on an isolated tooth (Owen, 1841; Taylor, 2010). The genus has unfortunately become a wastebasket for many nomina dubia and nomina nudem over the years. The type species was strictly based under ICZN regulations on *Cetiosaurus medius*, which is a very incomplete series, however since 2009 the *Cetiosaurus* specimen known as the Bletchingdon specimen, from near Oxford, which is a large individual with many more skeletal elements than *C. medius*, is the type species (Upchurch and Martin, 2003; Upchurch et al., 2009; Taylor, 2010). It is from the Forest Marble of Oxfordshire, UK, which is Bathonian in age (±168 Ma). The specimen includes a caudal series, one partial cervical, a partial dorsal, and many appendicular elements, and also pectoral and pelvic elements. This material is extensively used for the phylogenetic analysis in Chapter 4.

The Rutland *Cetiosaurus* is sauropod that was found in Rutland, Leicestershire, UK, in 1968 in a brick pit, which is dated to be Upper Bajocian (±175 Ma). The specimen is the most complete sauropod from the UK to date, consisting of a well-preserved cervical and dorsal series, several caudals, and several appendicular (though more fragmentary) elements. It was originally ascribed to *Cetiosaurus* (*oxoniensis*), however, recently several differences have been found between the Rutland *Cetiosaurus* and *Cetiosaurus oxoniensis*, noteably in the axial width of the acetabulum, which is wider in C. xxoniensis than in the Rutland *Cetiosaurus*. Also the femur of *C. oxoniensis* is more stout and anteroposteriorly compressed, whilst the Rutland *Cetiosaurus* has a more slender femur. Finally, the chevrons of the Rutland *Cetiosaurus* have a dorsally open haemal canal, which is a derived feature that *C. oxoniensis* does not share.

Patagosaurus fariasi is the main subject of this thesis. Found in the late '70's and early '80's, it was coined in 1979 and more fully described in 1986 (Bonaparte, 1979, 1986b). Several specimens were found from two localities, Cerro Condor Norte (which yielded the holotype

specimen) and Cerro Condor Sur, both in the Cañadón Asfálto Fm., west-central Chubut, Patagonia, Argentina. The age lies roughly between the Aalenian-Bajocian, but could be as old as the Toarcian, which is significantly older than the original Callovian age given (Bonaparte 1986; Cúneo et al., 2013). The holotype is described in Chapter 2, the other material in Chapter 3. It is now believed that the material of *Patagosaurus* yields another taxon, and possibly, two other taxa. This is discussed in Chapter 3 and Chapter 4.

Lapparentosaurus madagascariensis (Bonaparte, 1986a198, 1986b) is a Middle Jurassic sauropod from Madagascar. The holotype is based on juvenile material, and consists of teeth, axial and appendicular material (Bonaparte, 1986a). However, adult material also exists, which has not had much study yet (Läng, 2008). It is retrieved as a basal eusauropod, in a polytomy with *Cetiosaurus mogrebiensis, Cetiosaurus oxoniensis, Chebsaurus* and *Ferganasaurus* (Läng, 2008; Läng and Mahammed, 2010) and more recently as a derived eusauropod, more derived than most other eusauropods, and basal to *Jobaria* (Mannion et al., 2013).

Bothriospondylus ?suffosus is another Middle Jurassic sauropod from Madagascar. The name *Bothriospondylus*, however, has become a wastebasket taxon, with French, English, Malagasi and other material ascribed to it (Owen, 1875; Lydekker, 1895; Nopcsa, 1902). The material in the collections of the NHM has been redescribed by Mannion, (2010b), and found to be a nomen dubium. The Malagasi material comes from several localities from the Bathonian (± 168 Ma) of the Isalo III Formation in Madagascar, and is briefly described by Läng (2010), and found to be valid, however, there is still uncertainty over which material comes from which locality, and which material is *Bothriospondylus*, since several elements seem to be titanosauriform rather than basal eusauropod. Until more clarity is produced, only the material from Mannion (2010) is used. The French material is found to be a basal

titanosauriform (Mannion et al., 2017).

Mamenchisaurus is a colloquical name for many different species, the most important for this study being *Mamenchisaurus youngi and Mamenchisaurus hochuanensis* (Young and Zhao, 1972; Russell and Zheng, 1993; Pi et al., 1996; Ouyang and Ye, 2002). It is a group of Middle Jurassic of Laurasian sauropods with extreme neck elongation, and their remains have been found in China, Thailand, and Mongolia (Suteethorn et al., 2012; Xing et al., 2015). Their interrelationships are a work of ongoing progress, as in many eusauropod phylogenies they emerge as more derived than most eusauropods (e.g. Wilson, 2002; Upchurch et al., 2004; Allain and Aquesbi, 2008; Remes et al., 2009), and within a mamenchisaurid-based phylogeny they are retrieved as more basal than most eusauropods (Xing et al., 2015).

Klamelisaurus gobiensis is a relatively new mamenchisaurid which is currently under revision. It is found to be different from Mamenchisaurids, and comes out more basal to Mamenchisaurus. The material consists of a nearly complete skeleton (Zhao, 1993; Zhao and Downs, 1993; Moore et al., 2017). It is currently being redescribed, and its osteology and phylogenetic analysis will be published in the future by Moore et al. (in prep; see Moore et al., 2017).

Omeisaurus is a group of sauropods that includes *Omeisaurus maoianus, Omeisaurus junghsiensis*, and many others. It was found in the Shaximiao Formation of Sichuan Province, China, which dates to the Bathonian-Callovian (±178-168 Ma). It was first described in 1939, and more specimens were added to the genus in the 1970's and 1980's. The most recent descriptions are from the early 2000's, however (Young, 1939; Dong et al., 1983; He et al., 1984, 1988; Tang et al., 2001; Wings et al., 2011). The most complete specimen has been used for this analysis in Chapter 2, 3 and 4 (Tang et al., 2001).

1.5 The importance of *Patagosaurus fariasi* for this thesis

Sauropods were one of the major components of terrestrial Mesozoic faunas, however, their early evolution in the Late Triassic to Early Middle Jurassic is poorly understood. This has much to do with an incomplete fossil record, with few taxa coming from Laurasia (*Cetiosaurus, Shunosaurus*) and with most taxa from this time coming from Gondwana. Within Gondwana however, sauropod-containing localities are still scarce, with most material coming from North Africa (*Tazoudasaurus, Spinophorosaurus*), India (*Barapasaurus*) and Argentina. The fossil record of Argentina is particularly good, with especially abundant sauropod material from the early Middle Jurassic Cañadón Asfálto Formation in west-central Chubut, Patagonia, Argentina. Thus far, *Patagosaurus fariasi* and *Vokheimeria chubutensis* are known from these beds, but more taxa are likely present. *Patagosaurus* is by far the more common sauropod, with over eight specimens found in two localities, Cerro Condor Norte and Cerro Condor Sur, near the village of Cerro Condor by the Chubut river. Both sauropods were found and collected during excavations in the 1970's and 1980's by Bonaparte and his crew. *Patagosaurus* and *Volkheimeria* were described in 1979 and 1986 (Bonaparte, 1979; 1986), however, the emphasis was laid on *Patagosaurus*. Since then, several studies showed that material ascribed to *Patagosaurus* may in fact belong to a different taxon, and moreover, yet another taxon has since than been uncovered from the Cañadon Asfalto Formation, providing a total of at least four sauropod taxa from this formation (Rauhut, 2003b; Pol et al., 2009; Holwerda et al., 2015a). Since the Cañadón Asfálto Formation was recently redated from an assumed Callovian age to a much older Aalenian-Bajocian age, the significance of *Patagosaurus* and the other sauropods from the Cañadón Asfálto Formation shifts towards the crucial time of early sauropod evolution and dispersal. Moreover, since the earliest sauropods are thought to come from South Africa, and thereafter dispersed towards other Gondwanan and finally Laurasian lands, the provenance of the Cañadon Asfalto

Formation in south-west Gondwana makes it an important checkpoint for sauropod dispersal. Indeed, the diversity of sauropods in this locality (*Patagosaurus, Vokheimeria* and the other unnamed sauropod taxa) show that sauropod evolution and dispersal was already likely at a peak development. Therefore, the redescription of *Patagosaurus i*s relevant not only for sauropod evolution, but also for dispersal patterns in the early Middle Jurassic.

1.6 Overview of Chapters 2-5 of this thesis

After this initial introduction, Chapter 2 reviews in detail the osteology of the holotype of *Patagosaurus fariasi,* PVL 4170, which is housed in the Instituto Miguel Lillo in Tucuman, Argentina. It consists of most of the axial skeleton, as well as the ilium, right pubis, and both distal fused parts of the ischia. It also has a right femur. The original diagnosis is discussed and a new diagnosis is given, together with old and new autapomorphies. Finally, it is compaired to other Early and Middle Jurassic sauropods, and the evolution of vertebral laminae in sauropods is discussed, based on the results from the osteological redescription of the vertebrae of *Patagosaurus*.

Chapter 3 reviews in detail the associated material of *Patagosaurus*, housed both in the Instituto Miguel Lillo in Tucuman, as well as the Museo Argentino de Ciencias Naturalus Bernardo Rivadavia in Buenos Aires, Argentina (PVL and MACN collection references). Several specimens can be ascribed to *Patagosaurus*; PVL 4076 and PVL 4176, as well as MACN-CH 932, 933, 935, 936, 1299, 231. Two specimens, MACN-CH 934 and MACN-CH 230, probably show sufficient significant differences to the *Patagosaurus* holotype and associated material to merit the erection of new taxa. The rest of the material, unfortunately, will remain Sauropoda indet., due to lack of information on taxonomy and provenance. Since there is material that can safely be attributed to *Patagosaurus*, showing ontogenetic variation, tentative ontogenetic patterns in the osteology of basal eusauropods are discussed.

The phylogenetic analysis is discussed in Chapter 4, where several resulting cladograms are

discussed. The different cladograms arise from adding different taxa to the matrix. Problematic taxa are discussed, and the phylogenetic position in relation to other Early and Middle Jurassic sauropods is discussed. Furthermore, a tentative biogeographic dispersal scenario is suggested for Gondwanan sauropods in the Early and Middle Jurassic, and their relations to Laurasian taxa are discussed.

Finally, Chapter 5 builds on the osteological revision as well as the phylogenetic results by performing a geometric morphometric analysis on matching longbones of *Patagosaurus* and several other Jurassic sauropods. The results show significant differences between both the juvenile and the adult *Patagosaurus* material, but also between these latter elements and other sauropods. Moreover, *Patagosaurus* significantly differs morphologically from other Jurassic sauropods.

References

Allain R., Aquesbi N., Dejax J., Meyer C., Monbaron M., Montenat C., Richir P., Rochdy M., Russell D., Taquet P. 2004. A basal sauropod dinosaur from the Early Jurassic of Morocco. *Comptes Rendus Palevol* 3:199–208.

Allain R., Aquesbi N. 2008. Anatomy and phylogenetic relationships of *Tazoudasaurus naimi* (Dinosauria, Sauropoda) from the late Early Jurassic of Morocco. *Geodiversitas* 30:345–424.

Al-Suwaidi AH., Angelozzi GN., Baudin F., Damborenea SE., Hesselbo SP., Jenkyns HC., Manceñido MO., Riccardi AC. 2010. First record of the Early Toarcian oceanic anoxic event from the Southern Hemisphere, Neuquén Basin, Argentina. *Journal of the Geological Society* 167:633–636.

Bailey TR., Rosenthal Y., McArthur JM., van de Schootbrugge B., Thirlwall MF. 2003. Paleoceanographic changes of the Late Pliensbachian–Early Toarcian interval: a possible link to the genesis of an Oceanic Anoxic Event. *Earth and Planetary Science Letters* 212:307–320.

Bandyopadhyay S., Gillette DD., Ray S., Sengupta DP. 2010. Osteology of *Barapasaurus tagorei* (Dinosauria: Sauropoda) from the Early Jurassic of India. *Palaeontology* 53:533–569.

Barrett PM. 1999. A sauropod dinosaur from the Lower Lufeng Formation (Lower Jurassic) of Yunnan Province, People's Republic of China. *Journal of Vertebrate Paleontology* 19:785–787.

Barrett PM., Upchurch P. 2005. Sauropodomorph diversity through time. In: Curry Rogers, K., Wilson J eds. *The Sauropods: evolution and paleobiology*. Berkeley, CA: University of California Press, 125–156.

Barrett PM., Upchurch P. 2007. The evolution of herbivory in sauropodomorph dinosaurs. *Special Papers in Palaeontology* 77:91-112.

Benson RBJ., Mannion PD., Butler RJ., Upchurch P., Goswami A., Evans SE. 2013. Cretaceous tetrapod fossil record sampling and faunal turnover: Implications for biogeography and the rise of modern clades. *Palaeogeography, Palaeoclimatology, Palaeoecology* 372:88–107.

Bodnar J., Escapa I., Cúneo NR., Gnaedinger S. 2013. First record of conifer wood from the Cañadón Asfalto Formation (Early-Middle Jurassic), Chubut Province, Argentina. *Ameghiniana* 50:227–239.

Bonaparte JF. 1979. Dinosaurs: A Jurassic Assemblage from Patagonia. *Science* 205:1377–1379.

Bonaparte JF. 1986a. The early radiation and phylogenetic relationships of the Jurassic sauropod dinosaurs, based on vertebral anatomy. In: Padian K ed. *The Beginning of the Age of Dinosaurs*. Cambridge: Cambridge University Press, 247–258.

Bonaparte JF. 1986b. Les dinosaures (Carnosaures, Allosauridés, Sauropodes, Cétosauridés) du Jurassique Moyen de Cerro Cóndor (Chubut, Argentina). *Annales de Paléontologie (Vert.-Invert.)* 72:247–289.

Buffetaut, E., Suteethorn, V., Cuny, G., Tong, H. 2000. The earliest known sauropod dinosaur. *Nature* 407:72.

Buffetaut, E., Suteethorn, V., Le Loeuff, J., Cuny, G., Tong, H., Khansubha, S. 2002. The first giant dinosaurs: a large sauropod from the Late Triassic of Thailand. *Comptes Rendus Palevol*, 1:103–109.

Butler RJ., Yates AM., Rauhut OWM., Foth C. 2013. A pathological tail in a basal sauropodomorph dinosaur from South Africa: evidence of traumatic amputation? *Journal of Vertebrate Paleontology* 33:224–228.

Button DJ., Rayfield EJ., Barrett PM. 2014. Cranial biomechanics underpins high sauropod diversity in resource-poor environments. *Proceedings of the Royal Society B* 281:20142114.

Cabrera A. 1947. Un saurópodo nuevo del Jurásico de Patagonia. *Notas del Museo de La Plata, Paleontologia* 95:1–17.

Carballido JL., Pol D. 2010. The dentition of *Amygdalodon patagonicus* (Dinosauria: Sauropoda) and the dental evolution in basal sauropods. *Comptes Rendus Palevol* 9:83–93.

Carpenter, K., and J. McIntosh. 1994. Upper Jurassic sauropod babies from the Morrison Formation. In: K. Carpenter, K. F. Hirsch, and J. R. Horner (eds.), *Dinosaur eggs and babies.* Cambridge University Press, Cambridge, UK, 265–278.

Casamiquela RM. 1963. Consideraciones acerca de *Amygdalodon* Cabrera (Sauropoda, Cetiosauridae) del Jurasico Medio de la Patagonia. *Ameghiniana* 3:79–95.

Cerda IA., Carabajal AP., Salgado L., Coria RA., Reguero MA., Tambussi CP., Moly JJ. 2012. The first record of a sauropod dinosaur from Antarctica. *Naturwissenschaften* 99:83–87.

Chatterjee S., Zheng Z. 2002. Cranial anatomy of *Shunosaurus*, a basal sauropod dinosaur from the Middle Jurassic of China. *Zoological Journal of the Linnean Society* 136:145–169.

Chiappe LM., Coria RA., Dingus L., Jackson F., Chinsamy A., Fox M. 1998. Sauropod dinosaur embryos from the Late Cretaceous of Patagonia. *Nature* 396:258–261.

Chiappe LM., Jackson F., Coria RA., Dingus L. 2005. Nesting titanosaurs from Auca Mahuevo and adjacent sites. In: Curry Rogers K, Wilson eds. *The Sauropods: Evolution and Paleobiology*. Berkeley, CA: University of California Press, 285–302.

Chiappe LM., Salgado L., Coria RA. 2001. Embryonic skulls of titanosaur sauropod dinosaurs. *Science* 293:2444.

Christian A. 2010. Some sauropods raised their necks—evidence for high browsing in *Euhelopus zdanskyi*. *Biology letters* 6:823.

Christian A., Dzemski G. 2007. Reconstruction of the cervical skeleton posture of *Brachiosaurus brancai* Janensch 1914 by an analysis of the intervertebral stress along the neck and a comparison with the results of different approaches. *Fossil Record* 10:38–49.

Christian A., Dzemski G. 2011. Neck posture in sauropods. In: Klein, N, Remes, K, Gee, C, Martin P eds. *Biology of the sauropod dinosaurs: Understanding the life of giants*. Bloomington: Indiana University Press, 251-261.

Christiansen P. 1996. The "whiplash" tail of diplodocid sauropods: was it really a weapon? In: Morales M ed. *The Continental Jurassic.* The Museum of Northern Arizona Bulletin 60:51–58.

Christiansen P. 2000. Feeding mechanisms of the sauropod dinosaurs *Brachiosaurus*, *Camarasaurus*, *Diplodocus* and *Dicraeosaurus*. *Historical Biology* 14:137–152.

Cooper MR. 1984. A reassessment of *Vulcanodon karibaensis* Raath (Dinosauria: Saurischia) and the origin of the Sauropoda. *Palaeontologia africana* 25:203–231.

Cúneo R., Ramezani J., Scasso R., Pol D., Escapa I., Zavattieri AM., Bowring SA. 2013b. High-precision U–Pb geochronology and a new chronostratigraphy for the Cañadón Asfalto Basin, Chubut, central Patagonia: Implications for terrestrial faunal and floral evolution in Jurassic. *Gondwana Research* 24:1267–1275.

Curry KA. 1999. Ontogenetic histology of *Apatosaurus* (Dinosauria: Sauropoda): new insights on growth rates and longevity. *Journal of Vertebrate Paleontology* 19:654–665.

D'Emic MD., Whitlock JA., Smith KM., Fisher DC., Wilson JA. 2013. Evolution of high tooth replacement rates in sauropod dinosaurs. *PLoS ONE* 8:e69235.

Dietz RS., Holden JC. 1970. Reconstruction of Pangaea: breakup and dispersion of continents, Permian to present. *Journal of Geophysical Research* 75:4939–4956.

Dong Z., Peng G., Huang D. 1989. The discovery of the bony tail club of sauropods. *Vertebrata PalAsiatica* 27:218–224.

Dong Z., Zhou SW., Zhang Y. 1983. Dinosaurs from the Jurassic of Sichuan. *Palaeontologica Sinica, New Series C* 162:1–136.

Elgorriaga A., Escapa IH., Bomfleur B., Cúneo R., Ottone EG. 2015. Reconstruction and phylogenetic significance of a new Equisetum Linnaeus species from the Lower Jurassic of Cerro Bayo (Chubut Province, Argentina). *Ameghiniana* 52:135–152.

Escapa IH., Sterli J., Pol D., Nicoli L. 2008. Jurassic tetrapods and flora of Cañadón Asfalto Formation in Cerro Cóndor area, Chubut province. *Revista de la Asociación Geológica Argentina* 63:613–624.

Escapa IH., Cúneo NR., Rothwell G., Stockey RA. 2013. *Pararaucaria delfueyo*i sp. nov. from the Late Jurassic Cañadón Calcáreo Formation, Chubut, Argentina: insights into the evolution of the Cheirolepidiaceae. *International Journal of Plant Sciences* 174:458–470.

Ezcurra MD. 2010. A new early dinosaur (Saurischia: Sauropodomorpha) from the Late Triassic of Argentina: a reassessment of dinosaur origin and phylogeny. *Journal of Systematic Palaeontology* 8:371–425.

Frey E., Martin J. 1997. Long necks of sauropods. In: Currie PJ, Padian K eds. *Encyclopedia of Dinosaurs.* Academic Press, San Diego, 406–409.

Galton PM. 1990. Basal Sauropodomorpha - Prosauropoda. In: Weishampel DB, Dodson P, Osmolska H eds. *The Dinosauria*. Berkeley: University of California Press, 320–344.

Galton PM. 1998. Saurischian dinosaurs from the Upper Triassic of England: *Camelotia* (Prosauropoda, Melanorosaridae) and *Avalonianus* (Theropoda,? Carnosauria). *Palaeontographica Abteilung A*:155–172.

Galton PM., Upchurch P. 2004. Stegosauria. In: Weishampel DB, Dodson P, Osmolska H eds. *The Dinosauria, 2nd Edition*. Berkeley: University of California Press, 343–362.

García RA., Cerda IA. 2010. Dentition and histology in titanosaurian dinosaur embryos from Upper Cretaceous of Patagonia, Argentina. *Palaeontology* 53:335–346.

García RA., Salgado L., Fernández MS., Cerda IA., Paulina Carabajal A., Otero A., Coria RA., Fiorelli LE. 2015. Paleobiology of titanosaurs: reproduction, development, histology, pneumaticity, locomotion and neuroanatomy from the South American fossil record. *Ameghiniana* 52:29–68.

Gee CT. 2010. *Plants in Mesozoic time: morphological innovations, phylogeny, ecosystems*. Bloomington: Indiana University Press, 424 pp.

Gee CT. 2011. Dietary options for the sauropod dinosaurs from an integrated botanical and paleobotanical perspective. In: Klein N, Remes K, Sander PM, Gee CT eds. *Biology of the Sauropod Dinosaurs: Understanding the life of giants*. Life of the Past. Bloomington: Indiana University Press, 34–56.

Gómez JJ., Goy A. 2011. Warming-driven mass extinction in the Early Toarcian (Early Jurassic) of northern and central Spain. Correlation with other time-equivalent European sections. *Palaeogeography, Palaeoclimatology, Palaeoecology* 306:176–195.

Hallam A. 1980. A reassessment of the fit of Pangaea components and the time of their initial breakup. *The Continental Crust and its Mineral Deposits*: 375–87.

Hallam A. 1983. Supposed Permo-Triassic megashear between Laurasia and Gondwana. *Nature* 301:499–502.

Hallam A. 1985. A review of Mesozoic climates. *Journal of the Geological Society* 142:433–445.

Harris, J.D., 2006. The significance of *Suuwassea emilieae* (Dinosauria: Sauropoda) for flagellicaudatan intrarelationships and evolution. *Journal of Systematic Paleontology* 4:185–198.

He X., Li K., Cai K. 1988. *The Middle Jurassic dinosaur fauna from Dashanpu, Zigong, Sichuan. Vol. IV. Sauropod Dinosaurs (2) Omeisaurus tianfuensis.* Chengdu, China: Sichuan Publishing House of Science and Technology. 143 pp.

He X., Li K., Cai K., Gao Y. 1984. *Omeisaurus tianfuensis*—a new species of *Omeisaurus* from Dashanpu, Zigong, Sichuan. *Journal of Chengdu College Geology, Supplement* 2:13–32.

Hesselbo SP., Jenkyns HC., Duarte LV., Oliveira LC. 2007. Carbon-isotope record of the Early Jurassic (Toarcian) Oceanic Anoxic Event from fossil wood and marine carbonate (Lusitanian Basin, Portugal). *Earth and Planetary Science Letters* 253:455–470.

Hesselbo SP., Pieńkowski G. 2011. Stepwise atmospheric carbon-isotope excursion during the Toarcian oceanic anoxic event (Early Jurassic, Polish Basin). *Earth and Planetary Science Letters* 301:365–372.

Holland WJ. 1915. Heads and tails: a few notes relating to the structure of the sauropod dinosaurs. *Annals of the Carnegie Museum* 9:272–278.

Holwerda FM., Pol D., Rauhut OWM. 2015. Using dental enamel wrinkling to define sauropod tooth morphotypes from the Cañadón Asfalto Formation, Patagonia, Argentina. *PLOS ONE* 10:e0118100.

Holwerda F., Schmitt A D., Tschopp E. 2015. Ontogenetic differences in tooth replacement rates in adult and juvenile diplodocids. *Journal of Vertebrate Paleontology, Program and Abstracts 36 (Supplement 2),* 145A.

Hughes S., Barry J., Russell J., Bell R., Gurung S. 2016. Neck length and mean arterial pressure in the sauropod dinosaurs. *Journal of Experimental Biology* 219:1154–1161.

Hummel J., Clauss M. 2011. Sauropod feeding and digestive physiology. In: Klein N, Remes K, Gee CT, Sander PM eds. *Biology of the sauropod dinosaurs: Understanding the life of giants*. Bloomington: Indiana University Press, 11–33.

Jain SL. 1980. The continental lower Jurassic fauna from the Kota formation, India. *Aspects of Vertebrate History: Museum of Northern Arizona Press, Flagstaff* 99–123.

Jain SL., Kutty TS., Roy-Chowdhury T., Chatterjee S. 1975. The sauropod dinosaur from the Lower Jurassic Kota formation of India. *Proceedings of the Royal Society of London B: Biological Sciences* 188:221–228.

Jenkyns H. 1988. The early Toarcian (Jurassic) anoxic event-stratigraphic, sedimentary, and geochemical evidence. *American Journal of Science* 288:101–151.

Klein N., Sander PM. 2008. Ontogenetic stages in the long bone histology of sauropod dinosaurs. *Paleobiology* 34:247–263.

Knoll F., Witmer LM., Ortega F., Ridgely RC., Schwarz-Wings D. 2012. The braincase of the basal sauropod dinosaur *Spinophorosaurus* and 3D reconstructions of the cranial endocast and inner ear. *PLoS ONE* 7:e30060.

Kutty TS., Chatterjee S., Galton PM., Upchurch P. 2007. Basal sauropodomorphs (Dinosauria: Saurischia) from the Lower Jurassic of India: their anatomy and relationships. *Journal of Paleontology* 81:1218-1240.

Lallensack JN., Klein H., Milàn J., Wings O., Mateus O., Clemmensen LB. 2017. Sauropodomorph dinosaur trackways from the Fleming Fjord Formation of East Greenland: Evidence for Late Triassic sauropods. *Acta Palaeontologica Polonica,* 62, 833-843.

Läng É. 2008. Les cétiosaures (Dinosauria, Sauropoda) et les sauropodes du Jurassique moyen: révision systématique, nouvelles découvertes et implications phylogénétiques. Ph. D. dissertation Thesis. Paris, France: Centre de recherche sur la paléobiodiversité et les paléoenvironnements. 639 pp.

Läng E., Mahammed F. 2010. New anatomical data and phylogenetic relationships of *Chebsaurus algeriensis* (Dinosauria, Sauropoda) from the Middle Jurassic of Algeria. *Historical Biology* 22:142–164.

Lloyd GT., Davis KE., Pisani D., Tarver JE., Ruta M., Sakamoto M., Hone DWE., Jennings R., Benton MJ. 2008. Dinosaurs and the Cretaceous terrestrial revolution. *Proceedings of the Royal Society of London B: Biological Sciences* 275:2483–2490.

Lydekker R. 1895. On bones of a sauropodous dinosaur from Madagascar. *Quarterly Journal of the Geological Society* 51:329–336.

Mannion PD. 2010a. A revision of the sauropod dinosaur genus '*Bothriospondylus*' with a redescription of the type material of the Middle Jurassic form '*B. madagascariensis*.' *Palaeontology* 53:277–296.

Mannion PD. 2010b. Environmental and geological controls on the diversity and distribution of the sauropodomorpha. Ph.D. Dissertation Thesis. London: University College London.

Mannion PD., Upchurch P. 2010a. A quantitative analysis of environmental associations in sauropod dinosaurs. *Paleobiology* 36:253–282.

Mannion PD., Upchurch P. 2010b. Completeness metrics and the quality of the sauropodomorph fossil record through geological and historical time. *Paleobiology* 36:283–302.

Mannion PD., Upchurch P. 2011. A re-evaluation of the 'mid-Cretaceous sauropod hiatus' and the impact of uneven sampling of the fossil record on patterns of regional dinosaur extinction. *Palaeogeography, Palaeoclimatology, Palaeoecology* 299:529–540.

Mannion PD., Upchurch P., Carrano MT., Barrett PM. 2011. Testing the effect of the rock record on diversity: a multidisciplinary approach to elucidating the generic richness of sauropodomorph dinosaurs through time. *Biological Reviews* 86:157–181.

Mannion PD., Upchurch P., Barnes RN., Mateus O. 2013. Osteology of the Late Jurassic Portuguese sauropod dinosaur *Lusotitan atalaiensis* (Macronaria) and the

evolutionary history of basal titanosauriforms. *Zoological Journal of the Linnean Society* 168:98–206.

Mannion PD., Allain R., Moine O. 2017. The earliest known titanosauriform sauropod dinosaur and the evolution of Brachiosauridae. *PeerJ* 5:e3217.

Martin J., Martin-Rolland V., Frey E. 1998. Not cranes or masts, but beams: the biomechanics of sauropod necks. *Oryctos* 1:113–120.

Martinez RN., Alcober OA. 2009. A Basal Sauropodomorph (Dinosauria: Saurischia) from the Ischigualasto Formation (Triassic, Carnian) and the Early Evolution of Sauropodomorpha. *PLoS ONE* 4:e4397.

McIntosh JS. 1990. Sauropoda. In: Weishampel DB, Dodson P, Osmólska H eds. *The Dinosauria*. Berkeley, CA: University of California Press, 345–401.

McPhee BW., Yates AM., Choiniere JN., Abdala F. 2014. The complete anatomy and phylogenetic relationships of *Antetonitrus ingenipes* (Sauropodiformes, Dinosauria): implications for the origins of Sauropoda. *Zoological Journal of the Linnean Society* 171:151–205.

McPhee BW., Bonnan MF., Yates AM., Neveling J., Choiniere JN. 2015a. A new basal sauropod from the pre-Toarcian Jurassic of South Africa: evidence of niche-partitioning at the sauropodomorph–sauropod boundary? *Scientific reports* 5:13224.

McPhee BW., Choiniere JN., Yates AM., Viglietti PA. 2015b. A second species of *Eucnemesaurus* Van Hoepen, 1920 (Dinosauria, Sauropodomorpha): new information on the diversity and evolution of the sauropodomorph fauna of South Africa's lower Elliot Formation (latest Triassic). *Journal of Vertebrate Paleontology* 35:e980504.

McPhee BW., Choiniere JN. 2016. A hyper-robust sauropodomorph dinosaur ilium from the Upper Triassic–Lower Jurassic Elliot Formation of South Africa: Implications for the

functional diversity of basal Sauropodomorpha. *Journal of African Earth Sciences* 123:177–184.

McPhee BW., Mannion PD., de Klerk WJ., Choiniere JN. 2016. High diversity in the sauropod dinosaur fauna of the Lower Cretaceous Kirkwood Formation of South Africa: Implications for the Jurassic–Cretaceous transition. *Cretaceous Research* 59:228–248.

Moore A., Xu X., Clark J. 2017. Anatomy and systematics of *Klamelisaurus gobiensis*, a mamenchisaurid sauropod from the Middle-Late Jurassic Shishugou Formation of China. *Journal of Vertebrate Paleontology, Program and Abstracts*, *37 (Supplement 2),* 165A.

Morard A., Guex J., Bartolini A., Morettini E., de Wever P. 2003. A new scenario for the Domerian-Toarcian transition. *Bulletin de la Société géologique de France* 174:351–356.

Myhrvold NP., Currie PJ. 1997. Supersonic sauropods? Tail dynamics in the diplodocids. *Paleobiology* 23:393–409.

Nopcsa FB. 1902. Notizen über die Cretacischen Dinosaurier. Pt. 3. Wirbel eines südamerikanischen Sauropoden. *Sitzungsberichte der Berliner Akademie der Wissenschaften* 3:108–114.

Osborn HF., Mook CC. 1921. *Camarasaurus*, *Amphicoelias*, and other sauropods of Cope. *Memoirs of the American Museum of Natural History, New Series* 3:249–387.

Ouyang H., Ye Y. 2002. *The first mamenchisaurian skeleton with complete skull,* Mamenchisaurus youngi. Chengdu, China: Sichuan Publishing House of Science and Technology, 138pp.

Owen R. 1841. Report on British fossil reptiles. *Reports of the British Association for the Advancement of Science* 11:60-204.

Owen R. 1842. A description of a portion of the skeleton of *Cetiosaurus*, a gigantic extinct saurian occurring in the Oolitic Formation of different parts of England. *Proceedings of the Geological Society of London*. 457–462.

Owen R. 1875. Monographs on the British fossil Reptilia of the Mesozoic Formations, Part II (Genera *Bothriospondylus, Cetiosaurus, Omosaurus*). *Palaeontographical Society (Monograph)* 1–93.

Parrish JM. 2006. 7 The Origins of High Browsing and the Effects of Phylogeny and Scaling on Neck Length in Sauropodomorphs. In: Carrano MT, Gaudin TJ, Blob RW, Wible JR (ed), *Amniote paleobiology: perspectives on the evolution of mammals, birds, and reptiles: a volume honoring James Allen Hopson*, 201-224.

Peyer K., Allain R. 2010. A reconstruction of *Tazoudasaurus naimi* (Dinosauria, Sauropoda) from the late Early Jurassic of Morocco. *Historical Biology* 22:134–141.

Phillips J. 1871. *Geology of Oxford and the Valley of the Thames*. Clarendon Press, Oxford, UK, 532 pp.

Pi L., Ou Y., Ye Y. 1996. A new species of sauropod from Zigong, Sichuan, *Mamenchisaurus youngi*. In: *Papers on geosciences contributed to the 30th International Geological Congress*. 87–91.

Pol, D., Rauhut, O.W.M., Carballido, J.L., 2009. Skull anatomy of a new basal eusauropod from the Cañadon Asfalto Formation (Middle Jurassic) of Central Patagonia. *Journal of Vertebrate Paleontology, Program and Abstracts 29 (Supplement 3)*, 100A.

Pol D., Garrido A., Cerda IA. 2011a. A new sauropodomorph dinosaur from the Early Jurassic of Patagonia and the origin and evolution of the sauropod-type sacrum. *PloS one* 6:e14572.

Pol D., Rauhut OW., Becerra M. 2011b. A Middle Jurassic heterodontosaurid dinosaur from Patagonia and the evolution of heterodontosaurids. *Naturwissenschaften* 98:369–379.

Pol D., Rauhut OWM. 2012. A Middle Jurassic abelisaurid from Patagonia and the early diversification of theropod dinosaurs. *Proceedings of the Royal Society B: Biological Sciences* 279:3170–3175.

Preuschoft H., Klein N. 2013. Torsion and bending in the neck and tail of sauropod dinosaurs and the function of cervical ribs: insights from functional morphology and biomechanics. *PLoS ONE* 8:e78574.

Raath MA. 1972. Fossil vertebrate studies in Rhodesia: a new dinosaur (Reptilia: Saurischia) from near the Trias-Jurassic boundary. *Arnoldia (Rhodesia)* 7:1–7.

Racey, A. & Goodall, J.G. 2009. Palynology and stratigraphy of the Mesozoic Khorat Group red bed sequences from Thailand. *Geological Society London Special Publications* 315:69–83.

Rauhut OWM. 2003a. Revision of *Amygdalodon patagonicus* Cabrera, 1947 (Dinosauria, Sauropoda). *Fossil Record* 6:173–181.

Rauhut OWM. 2003b. A dentary of *Patagosaurus* (Sauropoda) from the Middle Jurassic of Patagonia. *Ameghiniana* 40:425–432.

Rauhut OWM., Lopez-Arbarello A. 2008. Archosaur evolution during the Jurassic: a southern perspective. *Revista de la Asociación Geológica Argentina* 63:557–585.

Rauhut OWM., López-Arbarello A. 2009. Considerations on the age of the Tiouaren Formation (Iullemmeden Basin, Niger, Africa): implications for Gondwanan Mesozoic terrestrial vertebrate faunas. *Palaeogeography, Palaeoclimatology, Palaeoecology* 271:259–267.

Rauhut OWM., Fechner R., Remes K., Reis K. 2011. How to get big in the Mesozoic: the evolution of the sauropodomorph body plan. In: Klein N, Remes K, Gee CT, Sander PM eds. *Biology of the Sauropod Dinosaurs: Understanding the life of giants*. Bloomington: Indiana University Press, 119–149.

Remes K., Ortega F., Fierro I., Joger U., Kosma R., Ferrer JMM., Ide OA., Maga A. 2009. A new basal sauropod dinosaur from the Middle Jurassic of Niger and the early evolution of Sauropoda. *PLoS One* 4:e6924.

Russell DA., Zheng Z. 1993. A large mamenchisaurid from the Junggar Basin, Xinjiang, People's Republic of China. *Canadian Journal of Earth Sciences* 30:2082–2095.

Salgado L., Coria RA., Calvo JO. 1997. Evolution of titanosaurid sauropods: Phylogenetic analysis based on the postcranial evidence. *Ameghiniana* 34:3–32.

Sander PM., Klein N., Buffetaut E., Cuny G., Suteethorn V., Le Loeuff J. 2004. Adaptive radiation in sauropod dinosaurs: bone histology indicates rapid evolution of giant body size through acceleration. *Organisms Diversity & Evolution* 4:165–173.

Sander PM., Clauss M. 2008. Sauropod gigantism. *Science* 322:200–201.

Sander PM., Christian A., Clauss M., Fechner R., Gee CT., Griebeler E-M., Gunga H-C., Hummel J., Mallison H., Perry SF., Preuschoft H., Rauhut OWM., Remes K., Tutken T., Wings O., Witzel U. 2011. Biology of the sauropod dinosaurs: the evolution of gigantism. *Biological Reviews of the Cambridge Philosophical Society* 86:117–155.

Sander PM. 2013. An evolutionary cascade model for sauropod dinosaur gigantism - overview, update and tests. *PLoS ONE* 8:e78573.

van de Schootbrugge B., McArthur JM., Bailey TR., Rosenthal Y., Wright JD., Miller KG. 2005. Toarcian oceanic anoxic event: An assessment of global causes using belemnite C isotope records. *Paleoceanography* 20:1-10.

Schwarz D., Kosch JCD., Fritsch G., Hildebrandt T. 2015. Dentition and tooth replacement of *Dicraeosaurus hansemanni* (Dinosauria, Sauropoda, Diplodocoidea) from the Tendaguru Formation of Tanzania. *Journal of Vertebrate Paleontology* 35:e1008134.

Sereno PC., Wilson JA. 2005. Structure and evolution of a sauropod tooth battery. In: Curry Rogers K, Wilson JA eds. *The Sauropods: Evolution and Paleobiology*. Berkeley, CA: University of California Press, 157–177.

Seymour RS. 2009. Raising the sauropod neck: it costs more to get less. *Biology Letters* 5:317–319.

de Souza LM., Santucci RM. 2014. Body size evolution in Titanosauriformes (Sauropoda, Macronaria). *Journal of Evolutionary Biology*:n/a-n/a.

Stevens KA., Parrish JM. 2005a. Neck posture, dentition, and feeding strategies in Jurassic sauropod dinosaurs. In: Carpenter K, Tidwell V eds. *Thunder Lizards: The Sauropodomorph Dinosaurs*. Bloomington: Indiana University Press, 212–232.

Stevens KA., Parrish JM. 2005b. Digital reconstructions of sauropod dinosaurs and implications for feeding. In: Curry Rogers K, Wilson J (ed) *The Sauropods: Evolution and Paleobiology*, 178–200.

Stoinski S., Suthau T., Gunga H-C. 2011. Reconstructing body volume and surface area of dinosaurs using laser scanning and photogrammetry. In: Klein N, Remes K, Gee C, Sander PM eds. *Biology of the Sauropod Dinosaurs: Understanding the life of giants*. Life of the Past. Bloomington: Indiana University Press, 94-104.

Stumpf S., Ansorge J., Krempien W. 2015. Gravisaurian sauropod remains from the marine late Early Jurassic (Lower Toarcian) of North-Eastern Germany. *Geobios* 48:271–279.

Suteethorn S., Loeuff JL., Buffetaut E., Suteethorn V., Wongko K. 2012. First evidence of a mamenchisaurid dinosaur from the Upper Jurassic-Lower Cretaceous Phu Kradung Formation of Thailand. *Acta Palaeontologica Polonica* 58:459–469.

Tang F., Jing X., Kang X., Zhang G. 2001. *Omeisaurus maoianus:* a complete sauropod from Jingyuan, Sichuan. Beijing, China: China Ocean Press, 112pp.

Taylor MP. 2010. Sauropod dinosaur research: a historical review. *Geological Society, London, Special Publications* 343:361–386.

Taylor MP., Hone DW., Wedel MJ., Naish D. 2011. The long necks of sauropods did not evolve primarily through sexual selection. *Journal of Zoology* 824:1-12.

Taylor MP., Wedel MJ. 2013. Why sauropods had long necks; and why giraffes have short necks. *PeerJ* 1:e36.

Taylor MP., Wedel MJ., Naish D. 2009. Head and neck posture in sauropod dinosaurs inferred from extant animals. *Acta Palaeontologica Polonica* 54:213–220.

Tschopp E., Mateus O., Benson RBJ. 2015. A specimen-level phylogenetic analysis and taxonomic revision of Diplodocidae (Dinosauria, Sauropoda). *PeerJ* 3:e857.

Upchurch, P. 1995. The evolutionary history of sauropod dinosaurs. *Philosophical Transactions of the Royal Society of London. Series B: Biological Sciences* 349:365–390.

Upchurch P., Barrett PM. 2000. The evolution of sauropod feeding mechanisms. In: Sues H-D ed. *Evolution of herbivory in terrestrial vertebrates: perspectives from the fossil record.* Cambridge: Cambridge University Press, 79–122.

Upchurch P., Barrett PM., Dodson P. 2004. Sauropoda. In: Weishampel DB, Dodson P, Osmólska H eds. *The Dinosauria. Second edition*. Berkeley, CA: University of California Press, 259–322.

Upchurch P., Martin J. 2003. The anatomy and taxonomy of *Cetiosaurus* (Saurischia, Sauropoda) from the Middle Jurassic of England. *Journal of Vertebrate Paleontology* 23:208–231.

Upchurch P., Martin J., Taylor MP. 2009. Case 3472: *Cetiosaurus* Owen, 1841 (Dinosauria, Sauropoda): proposed conservation of usage by designation of *Cetiosaurus oxoniensis* Phillips, 1871 as the type species. *Bulletin of Zoological Nomenclature* 66:51–55.

Vidal D., Díaz VD. 2017. Reconstructing hypothetical sauropod tails by means of 3D digitization: *Lirainosaurus astibiae* as case study. *Journal of Iberian Geology* 43:293–305.

Wang, J., Ye, Y., Pei, R., Tian, Y., Feng, C., Zheng, D. & Chang, S.-C. 2018. Age of Jurassic basal sauropods in Sichuan, China: A reappraisal of basal sauropod evolution. *Geological Society of America Bulletin*, 130, 1493–1500.

Waskow K., Sander PM. 2014. Growth record and histological variation in the dorsal ribs of *Camarasaurus* sp. (Sauropoda). *Journal of Vertebrate Paleontology* 34:852–869.

Werner J., Griebeler EM. 2011. Reproductive Biology and Its Impact on Body Size: Comparative Analysis of Mammalian, Avian and Dinosaurian Reproduction. *PLoS ONE* 6:e28442.

Whitlock JA. 2011. Inferences of diplodocoid (Sauropoda: Dinosauria) feeding behavior from snout shape and microwear analyses. *PLoS ONE* 6:e18304.

Wiersma K., Sander PM. 2017. The dentition of a well-preserved specimen of *Camarasaurus* sp.: implications for function, tooth replacement, soft part reconstruction, and food intake. *Paläontologische Zeitschrift* 91:1–17.

Wignall PB., Bond DP. 2008. The end-Triassic and Early Jurassic mass extinction records in the British Isles. *Proceedings of the Geologists' Association* 119:73–84.

Wignall PB., Newton RJ., Little CT. 2005. The timing of paleoenvironmental change and cause-and-effect relationships during the Early Jurassic mass extinction in Europe. *American Journal of Science* 305:1014–1032.

Wilson JA. 2002. Sauropod dinosaur phylogeny: critique and cladistic analysis. *Zoological Journal of the Linnean Society* 136:215–275.

Wilson JA. 2005a. Integrating ichnofossil and body fossil records to estimate locomotor posture and spatiotemporal distribution of early sauropod dinosaurs: a stratocladistic approach. *Paleobiology* 31:400–423.

Wilson JA. 2005b. Overview of sauropod phylogeny and evolution. In: Curry Rogers K, Wilson J (ed) *The sauropods: evolution and paleobiology*, 15–49.

Wilson, J.A., Sereno, P.C., 1998. Early evolution and higher-level phylogeny of sauropod dinosaurs. *Journal of Vertebrate Paleontology* 18:1–79.

Wings O., Schwarz-Wings D., Fowler DW. 2011. New sauropod material from the Late Jurassic part of the Shishugou Formation (Junggar Basin, Xinjiang, NW China). *Neues Jahrbuch für Geologie und Paläontologie - Abhandlungen* 262:129–150.

Xing L., Miyashita T., Zhang J., Li D., Ye Y., Sekiya T., Wang F., Currie PJ. 2015. A new sauropod dinosaur from the Late Jurassic of China and the diversity, distribution, and relationships of mamenchisaurids. *Journal of Vertebrate Paleontology* 35:e889701.

Yadagiri P. 2001. The osteology of *Kotasaurus yamanpalliensis*, a sauropod dinosaur from the Early Jurassic Kota Formation of India. *Journal of Vertebrate Paleontology* 21:242–252.

Yates AM., Bonnan MF., Neveling J., Chinsamy A., Blackbeard MG. 2010. A new transitional sauropodomorph dinosaur from the Early Jurassic of South Africa and the evolution of sauropod feeding and quadrupedalism. *Proceedings of the Royal Society of London B: Biological Sciences* 277:787–794.

Yates AM., Kitching JW. 2003. The earliest known sauropod dinosaur and the first steps towards sauropod locomotion. *Proceedings of the Royal Society of London. Series B: Biological Sciences* 270:1753–1758.

Young C-C. 1939. On a new Sauropoda, with notes on other fragmentary reptiles from Szechuan. *Bulletin of the Geological Society of China* 19:279–315.

Young C-C., Zhao X. 1972. Description of the type material of *Mamenchisaurus hochuanensis*. *Institute of Vertebrate Paleontology and Paleoanthropology Monograph Series I* 8:1–30.

Young MT., Rayfield EJ., Holliday CM., Witmer LM., Button DJ., Upchurch P., Barrett PM. 2012. Cranial biomechanics of *Diplodocus* (Dinosauria, Sauropoda): testing

hypotheses of feeding behaviour in an extinct megaherbivore. *Naturwissenschaften,* 99:1–7.

Zhang Y. 1988. *The Middle Jurassic dinosaur fauna from Dashanpu, Zigong, Sichuan, vol. 1: sauropod dinosaur (I): Shunosaurus*. Chengdu, China: Sichuan Publishing House of Science and Technology, 114pp.

Zhao, X. J. 1993. A new mid-Jurassic sauropod (*Klamelisaurus gobiensis* Gen. et sp. Nov.) from Xinjiang, China. Vertebrata PalAsiatica 2:132-138.

Zhao XJ., Downs TBW. 1993. A new Middle Jurassic sauropod subfamily (Klamelisaurinae subfam. nov.) from Xinjiang Autonomous Region, China. *Vertebra PalAsiatica* 31:132–138.

Zheng Z. 1996. Cranial anatomy of *Shunosaurus* and *Camarasaurus* (Dinosauria: Sauropoda) and the phylogeny of the Sauropoda. Ph. D. dissertation Thesis. Lubbock, TX, USA: Texas Tech University, 188 pp.

2 Osteological revision of the holotype of *Patagosaurus fariasi* BONAPARTE 1979

Femke M Holwerda[123], Oliver W M Rauhut[13], Diego Pol[45]

1 Staatliche Naturwissenschaftliche Sammlungen Bayerns (SNSB), Bayerische Staatssamlung für Paläontologie und Geologie, Richard-Wagner-Strasse 10, 80333 München, Germany

2 GeoBioTec, Departamento de Ciências da Terra, Faculdade de Ciências e Tecnologia (FCT), Universidade Nova de Lisboa, 2829-526 Caparica, Portugal

3 Department of Earth and Environmental Sciences and GeoBioCenter, Ludwig Maximilians Universität, 80333 München, Germany

4 Consejo Nacional de Investigaciones Científicas y Técnicas (CONICET), Argentina

5 Museo Paleontológico Egidio Feruglio, Avenida Fontana 140, Trelew, Argentina

Author contributions: Designed study: FH, OWM, DP. Conducted study: FH. Wrote the manuscript and prepared the figures: FH.

2.1 Abstract

While neosauropod diversity and evolution in the Late Jurassic and Cretaceous is becoming more studied and more and more taxa are revised, the Middle Jurassic sauropod taxa are less well known. This is partly due to stratigraphic bias towards only a few localities yielding Middle Jurassic sauropods. One of these localities is the Cañadón Asfálto Formation in central-north Patagonia, dated to latest Early-Middle Jurassic age. Four sauropod taxa are known so far from this Formation; of which only two have been formally described. Here, we revise the holotype of *Patagosaurus fariasi* Bonaparte 1986, a basal eusauropod from the Cañadon Asfálto Formation, Cerro Condor, Patagonia, Argentina. The holotype material consists of large parts of the axial skeleton, the pelvic girdle, and the right femur. *Patagosaurus* is mainly characterised by a combination of diagnostic features, rather than a range of autapomorphies, although at least one possible autapomorphy is discussed here. Diagnostic features are mainly identified on the axial skeleton; stout cervicals with low EI,

high projection of the postzygodiapophyseal lamina (podl) in an angle of ~45 degrees to the horizontal in cervicals, deep anterior pleurocoels that are sometimes compartmentalized in cervicals, high elongation of the neural arch in cervico-dorsals and in dorsals, high projection of the neural spine in cervico-dorsals, dorsals, and anterior(most) caudals, deep pneumatic foramina in posterior dorsals which connect into an internal pneumatic chamber, anterior caudals with elongated and 'saddle'shaped neural spines. Some other diagnostic features are distinguished on the appendicular skeleton, however, only the right femur, right ilium and pubis and the fused distal ischia are preserved. Diagnostic features on the appendicular skeleton include a transversely wide and axially short femur, a medial placement of the fourth trochanter on the femur, and an axially elongated ilium with a rounded dorsal rim, and with hook-shaped anterior lobe. Diagnostic features are illustrated and discussed. New characters potentially useful for phylogenetic analysis are discussed, and the osteology of *Patagosaurus* is compared to that of Early Jurassic and Middle Jurassic (eu)sauropods from both Laurasia and Gondwana (e.g. *Cetiosaurus, Barapasaurus, Amygdalodon, Spinophorosaurus, Tazoudasaurus, Vulcanodon, Shunosaurus, Omeisaurus, Mamenchisaurus*, and neosauropods).

2.2 Introduction

The late Early to Middle Jurassic is an important time window for sauropod evolution; phylogenetic studies indicate this was the time when all major lineages diversified and spread worldwide; even though the Late Jurassic shows a diversity peak, the earlier stages of the Jurassic (or perhaps even the latest Triassic) seem to have been the time of the start of this rise in sauropods (Yates, 2003; Barrett and Upchurch, 2005; Irmis et al., 2007; Allain and Aquesbi, 2008; Mannion and Upchurch, 2010; Yates et al., 2010; McPhee et al., 2014, 2015, 2016). Not many terrestrial deposits remain from the specific time window that is the Early-early Middle Jurassic, and fewer still contain diagnostic basal sauropod or basal non-

neosauropod eusauropod material. Notable examples are *Cetiosaurus oxoniensis*, the Rutland *Cetiosaurus*, and cetiosaurid and gravisaurian material from England, Scotland and Germany in Europe (von Huene, 1927; Upchurch and Martin, 2002, 2003; Liston, 2004; Galton, 2005; Barrett, 2006; Buffetaut et al., 2011; Brusatte et al., 2015; Stumpf et al., 2015; Clark and Gavin, 2016); the Asian *Shunosaurus, Mamenchisaurus, Omeisaurus, Datousaurus, Bellusaurus, Klamelisaurus, Barapasaurus, Kotasaurus* from China and India and possibly early sauropod material from Thailand (Young and Zhao, 1972; Dong and Tang, 1984; He et al., 1984, 1988; Zhang, 1988; Russell and Zheng, 1993; Pi et al., 1996; Tang et al., 2001; Yadagiri, 2001; Buffetaut et al., 2002; Chatterjee and Zheng, 2002; Peng et al., 2005; Bandyopadhyay et al., 2010; Mo, 2013); *Vulcanodon*, *Spinophorosaurus*, *Tazoudasaurus, Chebsaurus, Bothriospondylus* and *Lapparentosaurus* from Madagascar, Morocco, and South Africa (Raath, 1972; Cooper, 1984; Bonaparte, 1986a; Bonaparte, 1986c; Yates and Kitching, 2003; Allain et al., 2004; Allain and Aquesbi, 2008; Buffetaut, 2005; Mahammed et al., 2005; Remes et al., 2009; Mannion, 2010; Yates et al., 2010; McPhee et al., 2015); *Rhoetosaurus* from Australia (Nair and Salisbury, 2012), and *Patagosaurus fariasi*, *Volkheimeria chubutensis* and *Amygdalodon patagonicus* (Cabrera, 1947; Bonaparte, 1979; Bonaparte, 1986a; Rauhut, 2003) from Argentina.

In Patagonia, Argentina, the Cañadón Asfálto Formation (Stipanicic et al., 1968; Tasch and Volkheimer, 1970), is one of the few geological units worldwide to contain a multitude of latest Early to early Middle Jurassic eusauropod fossils. It crops out in west-central Patagonia, Argentina, and has recently been dated as ranging from the Toarcian to the Aalenien/Bajocian (Cúneo et al., 2013). The sauropod diversity of this unit includes *Patagosaurus fariasi*, *Volkheimeria chubutensis* (Bonaparte, 1979), and at least two undescribed taxa (Rauhut 2002, 2003; Pol et al., 2009).

Patagonia first came under the attention of vertebrate palaeontologists by the discovery of the basal sauropod *Amygdalodon patagonicus* by Cabrera (1947), and later by Casamiquela (1963) from the Pampa de Agnia locality, Cerro Carnerero Formation (Rauhut, 2003). These beds were revisited in 1976, but no further discovery was made, until another excursion in Patagonia, about 50 Km further away, in 1977, was successful. José Bonaparte led numerous more expeditions to the region between 1977 and 1986, during which *Patagosaurus fariasi*, *Volkheimeria chubutensis* and the theropod *Piatnitzkysaurus floresi* were found and described (Bonaparte 1979, 1986b, 1996; Rauhut, 2004). Since then, numerous other dinosaurs and other vertebrates have been discovered in the Cañadón Asfálto Formation; see Escapa et al. (2008), Cuneo et al (2013) and Olivera et al. (2015). The MPEF in Trelew has more recently started excavations of Cerro Condor South to uncover more material, of which only one element has been described (Rauhut, 2003).

Thus far*, Patagosaurus* is the only well-known sauropod taxon from this area, and one of the few sauropods from the Middle Jurassic outside of China with abundant material. It was coined by Bonaparte in 1979; *Patagosaurus* for Patagonia, and *fariasi* to honour the owners of the Farias farmland, on which it was discovered. It has been included in numerous phylogenetic studies (e.g. Upchurch, 1998; Wilson, 2002; Upchurch et al., 2004; Harris, 2006; Allain and Aquesbi, 2008; Wilson and Upchurch, 2009; Carballido et al., 2011, 2012). However, the only description of this taxon published so far (Bonaparte, 1986a) is not only based on the holotype, but also draws information from a selection of associated material, representing several individuals. These individuals come partially from the same bonebed as the holotype, but also from a bonebed nearby (Bonaparte, 1979; Bonaparte, 1986a). Since this description, new sauropod finds from the Cañadón Asfálto Formation show a higher sauropod diversity for this unit than previously assumed (Pol et al., 2009). Furthermore, recent study of *Patagosaurus* material revealed the probable presence of another taxon in

the associated material (Rauhut, 2002; Rauhut, 2003). In light of this, a revision of *Patagosaurus* is needed. This paper is the first in a series on the osteology, taxonomy and phylogeny of *Patagosaurus*, starting with a redescription of the holotype.

2.3 Material and methods

2.3.1 Anatomical Abbreviations

Laminae

acdl: anterior centrodiapophyseal lamina**; acpl**: anterior centroparapophyseal lamina**; cpol**: centropostzygapophyseal lamina**; cprl**: centroprezygapophyeseal lamina**; tprl**: intraprezygapophyseal lamina**; stprl**: single-intraprezygapophyseal lamina**l; tpol**: intrapostzygapophyseal lamina**; stpol**: single intrapostzygapophyseal lamina**; podl**: postzygadiapophyseal lamina**; ppdl**: parapodiapophyseal lamina**; pcdl**: posterior centrodiapophyseal lamina**; prdl:** prezygodiapophyseal lamina; **sprl**: spinoprezygapophyseal lamina**; spol**:; spinopostzygapophyseal lamina**; spdl**: spinodiapophyseal lamina**; prsl**: prespinal lamina**; posl**: postspinal lamina

Fossae

cdf, centrodiapophyseal fossa (fenestrae for some posterior dorsals); **cpof**, centropostzygapophyseal fossa; **cprf**, centroprezygapophyseal fossa; **pocdf**, postzygapophyseal centrodiapophyseal fossa; **posdf**, postzygapophyseal spinodiapophyseal fossa; **prcdf**, prezygapophyseal centrodiapophyseal fossa; **prsdf**, prezygospinodiapophyseal fossa; **sdf**, spinodiapophyseal fossa; **spof**, spinopostzygapophseal fossa; **sprf**, spinoprezygapophseal fossa

2.3.2 Terminology

Wilson (1999) is followed for the terminology of vertebral laminae, with some modifications based on Carballido and Sander (2014). The terminology of vertebral fossae follows Wilson *et al.* (2011).

As was already pointed out by Carballido and Sander, (2014), the term pleurocoel has not been rigourously defined. The term, however, was used in that paper for a lateral excavation on the vertebral centrum with clearly defined anterior, ventral and dorsal margins, and a usually less clearly defined but still visible posterior margin (Carballido and Sander, 2014). As this description is applicable for the lateral pneumatopores found in *Patagosaurus*, it will be used in this sense.

The use of 'anterior' and 'posterior' is preferred instead of 'cranial' and 'caudal'. This is to avoid confusion when describing, for instance, the caudal vertebrae.

2.3.3 Institutional abbreviations:

LEICT: New Walk Museum and Art Gallery, Leicester Arts and Museum Service, Leicester, UK.

MACN: Museo Argentino de Ciencias Naturales 'Bernardino Rivadavia', Buenos Aires, Argentina.

MNHN-MAA: Musee National d'Histoire Naturelle, Paris, France.

OUMNH: Oxford University Museum of Natural History, Oxford, UK.

PVL: paleovertebrados, Instituto Miguel Lillo, Tucuman, Argentina.

2.3.4 Systematic paleontology

SAURISCHIA SEELEY 1887

SAUROPODA MARSH 1878

EUSAUROPODA UPCHURCH 1995

CETIOSAURIDAE LYDEKKER 1888

PATAGOSAURUS BONAPARTE 1979

PATAGOSAURUS FARIASI BONAPARTE 1979

2.3.5 Holotype

PVL 4170, consisting of several anterior, middle and posterior cervical vertebrae, PVL 4170 1-9, anterior, mid- and posterior dorsals, PVL 4170 10-17, anterior caudals 19-25 and middle to posterior caudals 26-32, the sacrum, PVL 4170 18, fused ischia, PVL 4170 36, the right ilium, PVL 4170 34, right pubis, PVL 4170 35, and the right femur, PVL 4170 37. See Table 1 and 2 for vertebral measurements, and Table 3 for appendicular measurements. The holotype was said to also contain a scapula and coracoid (Bonaparte, 1986a), but these could unfortunately not be located in the collections. In the collections of the MACN we found two elements labelled as MACN-CH 1986 scapula 'A' and coracoid 'B', which might be these holotypic elements; however at present the association of these bones with the holotype is uncertain, and the association with another *Patagosaurus* specimen, MACN-CH 935, is also likely, due to close association of these elements with MACN-CH 935 on the excavation map. A large humerus is also indicated in the original quarry map for the holotype, however, the only large humerus retrieved from the collections of the Instituto Miguel Lillo is from another locality, Cerro Condor South. Originally, associated teeth with typical eusauropod wrinkled enamel were mentioned (Bonaparte 1986a). However, no

directly associated teeth or tooth-bearing bones are known for the holotype specimen, so that these teeth are not regarded as part of the holotype here and were not used in the diagnosis, even though some are ascribed to *Patagosaurus* (Holwerda et al., 2015). Ribs and chevrons appear on the quarry map of the holotype, but are mixed in with ribs and chevrons of other *Patagosaurus* specimens, and will therefore be omitted from the holotype description.

2.3.6 Original Diagnosis (Bonaparte 1986a): Cetiosaurid of large size, with tall dorsal vertebrae; posterior dorsals with elevated neural arches and well-developed neural spines, formed from 4 divergent laminae and with a massive dorsal region; dorsoventrally-oriented neural spine cavities, more expanded than in *Barapasaurus*. Anterior and lateral regions of the neural arch similar to that of *Cetiosaurus* and *Barapasaurus*. Sacrum with 5 vertebrae, elevated neural spines, and a large dilation of the neural canal forming a neural cavity. Pelvis with pubis showing distal and proximolateral expansions, more developed than in *Barapasaurus*, and a less expanded pubic symphysis than in *Amygdalodon*. Ischium slightly transversely compressed, with a ventromedial ridge of sublaminar type, and with a clear distal expansion. Ratio of tibia-femur lengths from 1:1.5 in juveniles, reaching 1:1.7 in adults. Mandible with weak medial torsion. Spatulate teeth with occlusal traces.

2.3.7 Emended diagnosis: *Patagosaurus fariasi* is a non-neosauropodan eusauropod dinosaur that can be diagnosed on the basis of the following morphological features, and the following combination of characters (features with * are tentatively considered autapomorphies): cervicals and anterior dorsals with marked pleurocoel, which is deep in cervicals but more shallow in dorsals. In cervicals, the pleurocoel is deeper anteriorly with well defined margins, but becomes shallow posteriorly and has only well defined dorsal and

ventral margins. In several cervicals, a faint oblique accessory lamina is present, dividing the pleurocoel into an anterior deeper part and a posterior more shallow part. The cervicals have a relatively high neural spine, accompanied by high dorsal placement of postzygapophyses, which results in a high angle between the postzygodiapophyseal and posterior centrodiapophyseal laminae of about 55°. Posterior dorsal neural arches with a centrodiapopohyseal fossa that extends internally as a pneumatic structure, which is separated by the mirroring structure by a thin septum, and both of which connect into a ventral, oval shaped internal pneumatic chamber, which is dorsal to and well separated from the neural canal*. Posterior dorsals with small round excavations on the posterior side of the distal extremity of the diapophyses*. Posteriormost dorsals have rudimentary aliform processes. All dorsals display an absence of the spinodiapophyseal lamina in all dorsals, with a contact between the lateral spol and podl in posterior-most dorsals instead, Sacrals with dorsoventrally high neural spine. Ilium with round dorsal rim, hooks-shaped anterior lobe and dorsoventrally elongated pubic peduncle. Fused distal ischia with the paired distal shafts creating an angle of 110°, pubis with torsion and kidney-shaped pubic foramen. Femur with posteromedially placed fourth trochanter, and laterally convex surface of femoral shaft.

2.3.8 Horizon, locality and age

Patagosaurus fariasi was found in what are now considered latest Early to early Middle Jurassic beds of the Cañadón Asfálto Formation in west-central Chubut, Patagonia, South Argentina (Cúneo et al., 2013). The Cañadón Asfálto Formation is a continental unit, consisting of mainly lacustrine deposits. *Patagosaurus* was found in the Cerro Condor area. The type locality of the holotype of *Patagosaurus fariasi* is Cerro Condor North, which lies around 4-5 km North of the first discovery site of *Patagosaurus* remains: Cerro Condor South, close to the village of Cerro Condor, near the Chubut river, not far from the town of Paso de Indios (Figure 1).

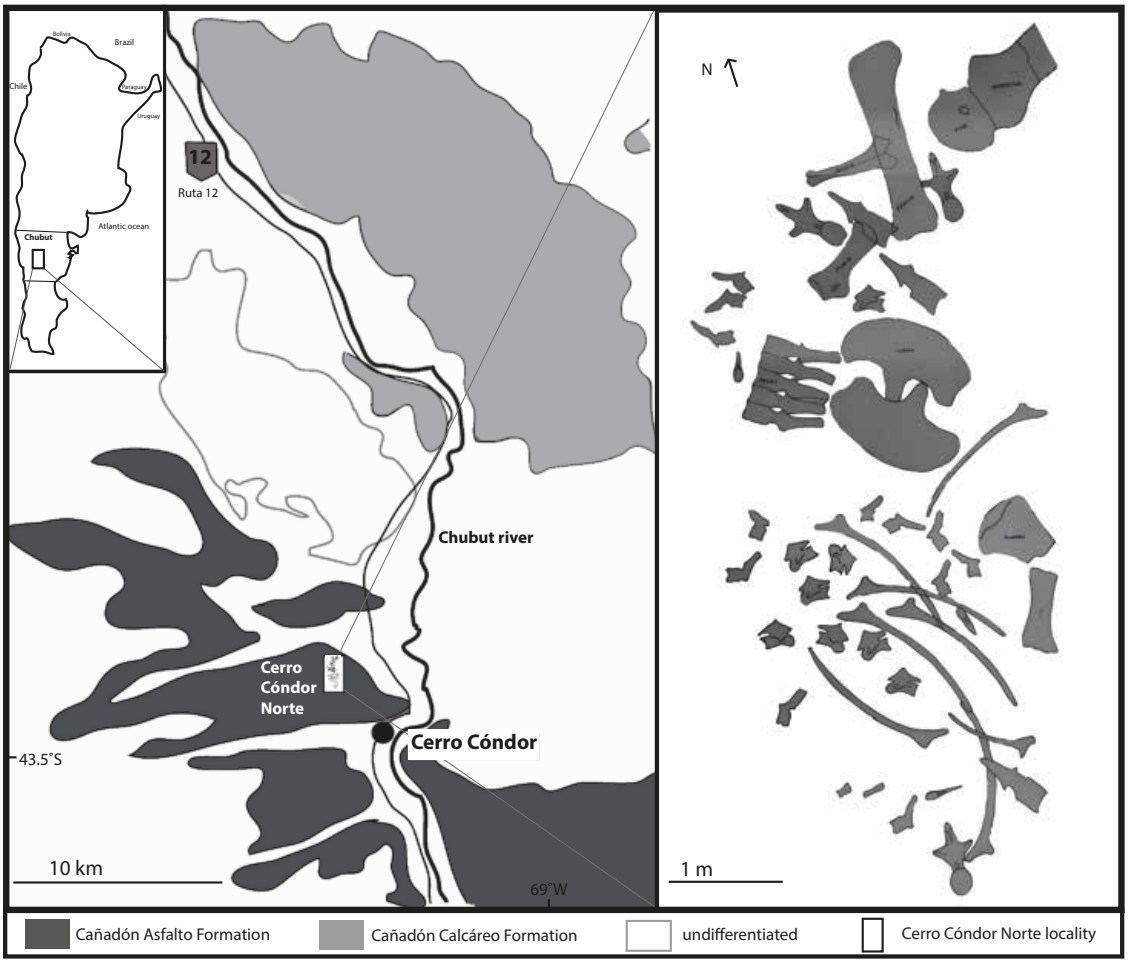

Figure 1: Geological setting of Cerro Condor Norte, and bonebed with holotype highlighted

2.3.9 Geological Setting

The Cañadon Asfálto Formation (west-central Chubut province, Patagonia, Argentina, see Figure 1) was first studied by Piatnitzky, (1936), after which it was formally described and named by Stipanicic et al., (1968) and further described by Nullo, (1983). It is part of the eponymous Cañadon Asfálto Basin, which consists of different subunits of Lower Jurassic to Upper Cretaceous sediments. The Cañadon Asfálto Formation is the uppermost unit of the lower megasequence of the Cañadon Asfálto basin, which has sedimentary infill of the Lower Jurassic (Figari et al., 2015). This unit lies between the Chubut province towns of Paso del Sapo and Paso de Indios (Olivera et al., 2015). The early Middle Jurassic (Toarcian-Bajocian, possibly earliest Bathonian) Cañadon Asfálto Formation conformably overlies the

Early Jurassic (Pliensbachian-early Toarcian; Cúneo et al., 2013; Figari et al., 2015; Volkheimer et al., 2015) Lonco Trapial Formation. It has been the subject of numerous geological studies in recent years to determine its sedimentology and age, since the age of the Cañadón Asfálto Formation has long been considered to be Callovian-Oxfordian (and thus the South American equivalent of several other Jurassic beds worldwide, such as the Oxford Clay; Bonaparte, 1979; Bonaparte, 1986; Frenguelli, 1949; Rauhut, 2003). However, a recent detailed chronostratigraphic study showed otherwise, using zircon grains from several tuff samples from the Cañadón Asfálto Formation (Cuneo et al., 2013). These were pre-treated by the chemical abrasion, or CA-TIMS technique, in order to constrain radiation-induced Pb loss. This method (using U/PB isotopes) is considered to be one of the most precise dating methods (Mattinson, 2005). The U/Pb isotope ratios show a latest Early (early-mid Toarcian), to early Middle Jurassic age range (Aalenian or Bajocian, Cúneo et al., 2013), although the youngest radiometric age for this Formation has been given as Bajocian-Bathonian (Cabaleri et al., 2010a). This much older age of the Formation is also consistent with palynological and other radiometric studies (e.g. Volkheimer et al., 2008, Cabaleri et al., 2010; Zavattieri et al., 2010; Hauser et al., 2017). Moreover, this new age also puts the vertebrate fossils found in the Cañadón Asfálto Formation in a new light.

Since its discovery, over 20 species of different taxonomic groups (including sauropod, theropod, and ornithischian dinosaurs, pterosaurs, sphenodonts, mammals, fishes, frogs, turtles and crocodiles have been discovered (Sterli et al. 2010; Olivera et al., 2015). This makes it an important unit for the study of Middle Jurassic tetrapods, and the diversification of Middle Jurassic dinosaurs in particular.

The outcrops of the Cañadón Asfálto Formation are dominated by microbial limestones, often tuffaceous mudstones and shales with conchostracans, and conglomeratic

intercalations (Silva Nieto et al., 2002; Tasch and Volkheimer, 1970). They provide mainly disarticulated dinosaur remains, as well as a few articulated skeletons, as shown in the quarry map of the sauropod bonebed of Cerro Condor North (Figure 1). The Cañadón Asfálto Formation shows evidence of both folding and faulting, which makes correlation of the different localities impossible, until further study is performed.

The region was dominated by a warm and relatively humid climate in the Middle Jurassic, evidenced by palynology (Volkheimer et al., 2001) and by macrofloral remains (e.g. Cheirolepidiaceae and Araucariaceae; Volkheimer et al., 2008, Volkheimer et al. 2015). Lacustrine sedimentation cycles found in paleolakes in the Cañadón Asfálto Formation provide evidence of climatic fluctuations and cyclicity (Cabaleri and Armella, 2005; Cabaleri et al., 2005).

José Bonaparte started excavations in the Cañadón Asfálto Formation with a team of scientists and preparators, and with funding from the National Geographic Society, in 1977. They found bones, on the Farias farm estate close to the river Chubut. After this, in 1978, they found a sauropod skeleton 4-5 km north of Cerro Condor. This site was then dubbed Cerro Condor Norte (North), and the original site Cerro Condor Sur (South). The Cerro Condor North site was excavated until 1982; in 1980, however, most material was uncovered and visible, as demonstrated in the quarry map of Figure 1. From this site, the holotype PVL 4170 originates, as well as at least seven other individuals, most likely of *Patagosaurus*.

The sediments of Cerro Condor North are dark grey, and hard. The bones from this quarry are similarly dark grey or dark brown in colour. The sediments of Cerro Condor North were interpreted by Bonaparte as fluvial deposits, however, they have more recently been interpreted as mainly lacustrine deposits.

Cerro Condor South was thought to be fluvial, but from observations by O.R. is now thought to be originating from an alluvial fan within a shallow lacustrine environment. Sediments from Cerro Condor South are fine-grained to paraconglomeratic, light-coloured and contain small freshwater shell fragments of invertebrates. Bonaparte also hinted that this locality consists of multiple layers of sediment with fossils.

2.4 Description

2.4.1 Axial skeleton

Cervicals

PVL 4170 has seven cervical vertebrae preserved, ranging from anterior to posterior cervicals. The atlas and axis are missing. The most anterior cervical preserved (PVL 4170 1) is probably the third or fourth cervical, based on comparisons with the Rutland *Cetiosaurus* (LEICT 468.1968.40; Upchurch and Martin, 2002).

Given the incomplete preservation of the neck in *Patagosaurus*, the exact cervical count in this taxon cannot be established. At the very least, the atlas, axis and first one or two cervicals are missing, given the high projection of the neural spine in the first cervical preserved, and compared to the Rutland *Cetiosaurus,* where neural arches and spines are low in the first 2-3 cervicals after the axis. Only very few non-neosauropodan sauropods with complete cervical series are known, making a comparison of the preserved elements difficult. Of the basal eusauropods with complete cervical series, *Shunosaurus* and *Jobaria* have 12 cervicals (Zhang, 1988; Sereno et al., 1999), whereas *Spinophorosaurus* has 13 (Remes et al. 2009). The Rutland *Cetiosaurus* was said to have 14 cervicals by Upchurch and Martin (2002), but several of these vertebrae, including the possibly last two cervicals, have only parts of the neural arch preserved, so that it cannot be established with certainty if these two last vertebrae are cervicals or might already be anterior dorsals (Upchurch & Martin 2002). The derived non-neosauropodan mamenchisaurids have apomorphically increased the cervical vertebral count to as much as 18 cervicals (Ouyang & Ye, 2002). The primitive number of cervicals in eusauropods thus seems to be either 12 or 13, and this is the condition we assume for *Patagosaurus*. As the exact position of the different cervicals preserved can thus not be established, the numbering used here starts with the first bone

preserved, therefore cervical no. 3 or 4 is numbered cervical 1. For convenience we will adhere to this numbering.

The cervical centra are longer than high and opisthocoelous, as in most sauropods. In comparison with other sauropods, cervicals are rather stout, with an average elongation index (aEI; Chure *et al.*, 2010) ranging from 1.9-2 in anterior to 1.2-1.4 in posterior cervicals and the 'traditional' elongation index (EI, Upchurch, 1998) ranging from 2.1 in anterior to 1.2 in posterior cervicals, compared to ~3.5 on average in *Spinophorosaurus* (Remes et al., 2009b), ~3.1 in the only cervical known from *Amygdalodon* (Rauhut, 2003, MLP 46-VIII-21-1/8), and 2,1 in anterior to 5,3 in mid cervicals in an undescribed sauropod from the Bagual site in the Cañadón Asfálto Formation (MPEF-PV 'Bagual' C2-4; Pol et al., 2009). This index is thus on average lower if compared to other eusauropods (see Table 1). The condyle has an anterior protrusion slightly dorsal to its center, and the condyle is 'cupped' by a ca. 1-2 cm thick rugose layer, similar to that in the Rutland *Cetiosaurus* (see Upchurch and Martin, 2003, LEICT 468.1968 cervical series). The cotyles are concave; with the deepest concavity slightly dorsal to the midpoint. As in most saurischians, the parapophyses are placed on the anteroventral end of the centra. In lateral view, the centra are ventrally concave posterior to the parapophysis. The posteriormost 1/3rd of the ventral side of the centra is convex, and the dorsoventral height increases posteriorly. Pleurocoels are developed as large, but only partially well-defined lateral depressions on the centra. In anterior cervicals, the pleurocoel is deeper than in posterior cervicals, and has a well-defined anterior, dorsal and ventral margin. In mid- and posterior cervicals the posterior margin of the pleurocoel is less clearly defined and the depression gradually fades into the lateral surface of the centrum. In some mid- to posterior cervicals, the left and right pleurocoels are only separated by thin septa (which are damaged or broken in some elements), but they do not invade the centrum and ramify within the bone, as is the case in neosauropods, (Wedel et al., 2005). Some cervicals show a faint compartmentalization of anterior and posterior pleurocoels, but they generally

lack the oblique lateral lamina that subdivides the cervical pleurocoels in neosauropods and some derived basal eusauropods.

In ventral view, the centra are constricted directly posterior to the condyle, as in most sauropods. A prominent ventral keel is present, which extends to about 2/3rd of the length of the ventral axial midline of the cervicals, after which it fades and disappears into the ventral surface of the centrum. It is present in all cervicals preserved (and possibly in the first dorsal as well as a marginally developed keel). The keel is developed as a thin, ventrally protruding ridge, with a very small hypapophysis anteriorly. The latter is developed as a transversely thin, rounded, sail-like ventral protrusion present immediately behind the ventral rim of the condylar 'cup'. This structure is accompanied by elliptical lateral fossae, as in *Amygdalodon* (Rauhut, 2003), *Tazoudasaurus* (MNHM To1-64; 81; 112; 354) *Lapparentosaurus* (MNHM MAA 13; 172; 5) and *Spinophorosaurus* (NMB-1699-R), but in contrast to *Cetiosaurus* (Leict 468.1968.40; 42; 7) and *Mamenchisaurus hochuanensis* (Young and Zhao, 1972) and derived sauropods.

Table 1: EI and aEI for several sauropod cervicals

Taxon	**cervical**	**aEI**
Patagosaurus	ant	1,4
	mid	1,7
	post	1
Cetiosaurus	ant	2,4
	mid	2,7
	post	2,3
Amygdalodon	ant	2,8
Spinophorosaurus	ant	2,0
	mid	2,7
Lapparentosaurus	ant	2,0
	mid	1,7
	post	1,3
Tazoudasaurus	ant	1,6
Bagual sauropod	ant	3,8
	mid	4,3
	mid-post	5,3

Neurocentral sutures are visible on the lateral side of the centrum in some cervical vertebrae, a possible sign of morphological immaturity in archosaurs (Brochu 1996, Irmis 2007). The neural arches of the cervicals are axially elongated, transversely narrow and higher posteriorly than the vertebral centrum, as in most sauropods. The diapophyses are placed on ventrolaterally directed transverse processes, which are attached to the neural arch by bony laminae, which are described in detail below for the individual vertebrae. The prezygapophyses are more prominent than the postzygapophyses, being placed on stout, elongated, beam-like stalks projecting anteriorly from the neural arch. The postzygapophyses are less prominent as they do not project much posteriorly from the neural arch. With the increasing height of the neural arch in more posterior cervicals, the postzygodiapophyseal lamina becomes more steeply inclined. In mid cervicals, this inclination of the postzygodiapophyseal lamina is ± 45-50°, measured from the axial plane, which is larger than in most basal sauropods, but comparable to the situation in diplodocids (see also McPhee et al 2015).

At the anterior end of the cervical neural arches the intraprezygapophyseal laminae are separated medially, as in *Tazoudasaurus* (Allain and Aquesbi, 2008) and the Rutland *Cetiosaurus* (LEICT 468.1968). The intrapostzygapophyseal laminae do meet at the midline. However, there are no centropostzygapophyseal laminae, as in *Tazoudasaurus* (Allain and Aquesbi, 2008), but unlike the Rutland *Cetiosaurus* (Leict 468.1968). Cervical PVL 4170 (7) is the only cervical with a single centropostzygapophyseal lamina. This lamina is found more commonly in middle and posterior cervicals of neosauropods, *Haplocanthosaurus* and *Cetiosaurus* (Upchurch et al., 2004). As this is the last cervical before the cervico-dorsal transition (which happens at cervical PVL 4170 (8), this could be feature enabling ligament attachement for stability and strength at the base of the neck, however, this has not been investigated.

The cervical neural spines project higher than in most basal sauropods, especially in the middle and posterior cervicals. The spines are connected to the zygapophyses by well-developed spinopre- and spinopostzygapophyseal laminae. Whereas the summit of the spine is more or less flush with the spol in the anteriormost vertebra, it protrudes dorsally beyond that lamina in more posterior elements. The spol are robust in all cervicals, but the sprl is only extensive in anterior elements and becomes short and thin in more posterior cervicals. From cervical 4 onwards the neural spine forms a rounded protrusion which is transversely wider than long anteroposteriorly. The neural spine is slightly anteriorly inclined in anterior cervicals (to at least the fifth preserved element), but becomes more erect towards the end of the cervical series, with a straight anterior margin; this is also seen in *Shunosaurus* (Zhang, 1988, T5402).

vertebra #	greatest length	greatest height	centrum length	centrum minimum width	length diapophyses	length postzygapophyses	length prezygapophyses	width across diapophyses	width across prezygapophyses	width across postzygapophyses	pleurocoel length	pleurocoel height	width posterior cotyle	height posterior cotyle	width anterior condyle	height anterior condyle	height neural spine	length neural spine	height neural arch posterior (dorsals)	height neural arch anterior (dorsals)	centrum length without condyle	nc anterior (height)	nc posterior (height)	width between parapophyses	length parapophyses
1	19	19	19	4	6,5	4	9	14	13	10	11	5	7	9	7	6	10	8	n.a.	n.a.	15		2	9	3
2	29	?	29	8	4	5	11	18	16	16	17	8	13	11	11	8	?	?	n.a.	n.a.	23	4	4	13	6
3	29	33	29	?	7,5	10	15	22	18	13	22	8	14	12	?	14	16	9	n.a.	n.a.	26	?	4	14	5
4	30	33	30	8	8	9	15	30	20	14	22	8	14	14	12	12	18	9	n.a.	n.a.	25	6	3	15	3
5	30	36	30	8	6	7	14	25	18	14	23	8	17	15	13	13	18	5	n.a.	n.a.	26	6	3	17	7
6	33	27	33	8	9	8	12	27	23	24	22	9	19	16	15	13	20	4	n.a.	n.a.	27	7	4	15	8
7	30	48	30	7	10	7	10	30	24	18	18	8	19	17	17	14	24	4	n.a.	n.a.	22	7	4	18	5
8	26	49	26	7	12	11	12	37	26	19	15	9	22	17	18	15	26	4	n.a.	n.a.	20	7	4	18	5
9	23	53	23	11	11	7	13	45	32	22	11	10	21	19	?	16	36	4	n.a.	n.a.	16	?	4	?	4
10	15	55	15	9	11	10	13	46	27	23	6	10	26	19	22	16	35	4	n.a.	n.a.	10	8	6	20	4
11	16	56	16	?	14	11	10	64	30	23	8	8	15	12	18	16	42	4	5	7	12	8	4	?	?
12	16	12	55	40	12	?	10	40	26	?	9	9	19	16	20	15	43	3	9	12	12	9	5	15	5
13	18	68	18	12	13	10	8	44	18	18	11	6	17	18	19	16	56	7	12	15	16	5	10	20	7
14	14	67	14	10	14	8	8	36	16	15	10	8	21	22	24	22	52	7	11	15	13	5	12	24	7
15	18	?	?	12	?	?	?	?	?	?	10	8	25	23	23	23	?	?	11	20	15	?	?	?	?
16	15	70	15	11	?	?	?	?	13	20	10	8	24	25	24	21	50	9	11	16	14	12	6	17	7
17	15	74	15	11	?	?	?	?	20	15	9	10	24	24	20	18	55	10	8	18	13	9	4	21	8
18,1	23	80	23	?	15	?	10	24	16	?	?	?	?	20	?	20	34	10	?	?	n.a.	14	?	38	7
18,2	?	?	?	?	?	?	?	?	?	?	?	?	?	?	?	?	34	9	?	?	n.a.	?	?	?	?
18,3	?	?	?	?	?	?	?	?	?	?	?	?	?	?	?	?	33	11	?	?	n.a.	?	?	?	?
18,4	28	?	?	?	33	?	?	?	?	9	?	?	?	?	?	?	30	8	?	?	n.a.	?	?	?	?
18,5	17	?	?	?	13	?	?	?	?	9	?	?	27	25	?	?	30	8	?	?	n.a.	9	?	?	?
19	10	47	10	12	8	4	6	29	9	6	n.a.	n.a.	16	18	18	20	29	7	n.a.	n.a.	n.a.	4	5	n.a.	n.a.
20	11	47	11	13	8	4	6	27	9	6	n.a.	n.a.	15	17	19	20	30	7	n.a.	n.a.	n.a.	4	4	n.a.	n.a.
21	13	45	13	7,2	5	4	5	?	10	11	n.a.	n.a.	16	17	18	17	27	7	n.a.	n.a.	n.a.	3	3	n.a.	n.a.
22	13,5	32	13,5	11,4	3,5	4	3	15	6	4	n.a.	n.a.	16	11	18	15	?	5	n.a.	n.a.	n.a.	4	4	n.a.	n.a.
23	12	39	12	7,6	5	3	4	19	5	4	n.a.	n.a.	13	14	12	14	26	6	n.a.	n.a.	n.a.	3	3	n.a.	n.a.
24	14	33	14	10	n.a.	?	4	n.a.	7	2	n.a.	n.a.	11	14	12	15	23	5	n.a.	n.a.	n.a.	3	3	n.a.	n.a.
25	12	33	12	8,4	n.a.	4	6	n.a.	7	2	n.a.	n.a.	10	13	12	14	23	5	n.a.	n.a.	n.a.	3	3	n.a.	n.a.
26	13	23,1	16,8	4	n.a.	2,43	4,7	n.a.	5	3,5	n.a.	n.a.	13	12	10	13	12	6	n.a.	n.a.	n.a.	2	2	n.a.	n.a.
27	14	21	16,6	6,6	n.a.	?	?	n.a.	4	?	n.a.	n.a.	10	12	11	12	11	5	n.a.	n.a.	n.a.	2	2	n.a.	n.a.
28	14	18	18,2	n.a.	n.a.	?	?	n.a.	?	?	n.a.	n.a.	11	11	11	9	?	?	n.a.	n.a.	n.a.	2	2	n.a.	n.a.
29	10	9	10	n.a.	n.a.	?	?	n.a.	?	?	n.a.	n.a.	9	9	8	9	?	?	n.a.	n.a.	n.a.	?	?	n.a.	n.a.
30	8,5	8	8,5	n.a.	n.a.	?	?	n.a.	?	?	n.a.	n.a.	8	7	8	9	?	?	n.a.	n.a.	n.a.	?	?	n.a.	n.a.
31	10,5	7,5	10,5	n.a.	n.a.	?	?	n.a.	?	?	n.a.	n.a.	8	6	7,5	6	?	?	n.a.	n.a.	n.a.	?	?	n.a.	n.a.

Previous page: Table 2: measurements of all presacral (1-17, blue), sacral (18, red), and caudal (19-30, green) vertebrae.

Cervical vertebra PVL 4170 (1)

This is the smallest and anteriormost of the cervical vertebrae preserved. The element is generally complete and well-preserved, but the right prezygapophysis is broken off at the base (see Figure 2). A lump of sediment is still attached to the anterior part of the neural arch, above the condyle.

The centrum is relatively shorter than in the mid-cervicals, with an EI of 1,55 and an aEI of 1,43. The articular ends are notably offset from each other, with the anterior end facing anteroventrally in respect to the posterior cotyle (Figure 2E,F). The cotyle is not as concave as in the other cervicals of the series. The ventral keel is strongly developed in the anterior 1/3rd of the centrum, after which it gradually fades into ventral surface. In ventral view, the parapophyses are visible as lateral oval bulges, the articular surfaces of which are confluent with the condyle rim (Figure 2E).

The centrum shows a distinct pleurocoel, present laterally on the vertebral body (Figure 2A,B). It is deeper anteriorly than posteriorly and developed as a rounded concavity that follows the rim of the condyle on the lateral anterior side of the centrum. Posteriorly it extends almost to the posterior end of the centrum; however, it fades gently into the lateral surface from about 2/3rd of the centrum axial length. Within the pleurocoel there appears to be a slight bulge at about the height of the diapophysis, which is similar to the oblique accessory lamina in neosauropods (Upchurch 1998), dividing the pleurocoel in two subdepressions. This subdivision is also seen to some extent in mamenchisaurids (e.g. Ouyang and Ye, 2002; Tang et al., 2001; Young, 1939; Young and Zhao, 1972; Zhang et al., 1998), and also in the Rutland *Cetiosaurus* (Upchurch and Martin, 2003). This incipient subdivision is also present in some other cervicals of *Patagosaurus*, but it is best developed in this element. The parapophysis is positioned anteroventrally on the lateral side of the centrum, and is connected to the rugose rim of the condyle. The dorsal side is excavated,

with the recess being confluent with the deep anterior part of the pleurocoel. A stout lamina extends horizontally posteriorly from the parapophysis and forms the ventral border of the pleurocoel and the border between the lateral and the ventral side of the centrum. This lamina becomes less prominent posteriorly (Figure 2A,B).

The posterior region of the neural arch is approximately as high as the posterior end of the centrum. It extends over most of the length of the centrum, but is slightly offset anteriorly from the posterior end of the latter. The neural canal is rather small and round in outline, but only its posterior opening is visible, as the anterior end is still covered in matrix. Despite the anterior position of the vertebrae, lateral neural arch lamination is well-developed, with prominent prdl, podl and pcdl. The diapophysis is developed as a small, lateroventrally projecting process on the anterior third of the neural arch (Figure 2A,C,D). It is connected to the prezygapophysis by a slightly anterodorsally directed prdl. The latter is in line with the pcdl, which meets the diapophysis from posteroventral. The podl is steeply anteroventrally inclined and meets the prdl just anterior to the diapophysis. A short and stout acdl is present, but hidden in lateral view by the diapophysis.

The prezygapophysis is placed on a stout, anteriorly and slightly dorsally directed process that slightly overhangs the anterior condyle of the centrum (Figure 2A,C). The base of this process is connected to the centrum by a short and almost vertical cprl, which here meets the prdl in an acute angle; from this point onwards only a single, very robust lateroventral lamina continues anteriorly onto the stall and braces the prezygapophysis from lateroventral. The prezygapophyseal articular suface is flat, triangular to elliptic in shape and measures about 3 by 3 cm. It is inclined dorsomedially at an angle of approximately 30-40° from the horizontal. The intraprezygapophyseal lamina is very short and widely separated from its counterpart in the middle of the anterior surface of the neural arch.

A slightly asymmetrical centroprezygapophyseal fossa is present below the intraprezygapophyseal and centroprezygapophyseal laminae on either side of the neural arch, with the right fossa being hidden by sediment (Figure 2C). Anteroventral to the diapophysis an axially elongated prcdf is visible, contra Upchurch and Martin (2003), who reported this to be absent in *Patagosaurus*. A slightly larger cdf is present posteroventral to the diapophysis, and a very large, triangular pocdf is present between the pcdl and podl.

The postzygapophysis is placed on the posterodorsal edge of the neural arch, above the posterior end of the centrum, which it does not overhang it posteriorly. It is developed as a large, lateroventrally facing facet which is dorsally bordered by the slightly curved podl and dorsally braced by the stout spol. The stout and almost vertical cpol connects the centrum to the medial margin of the postzagypophysis. The tpol is directed ventromedially and connects the medial side of the postzygapophysis to the dorsal margin of the neural canal, where it is separated from its counterpart.

The neural spine is relatively low, barely extending dorsally beyond the postzygapophysis, but it is anteroposteriorly elongate and robust, becoming wider transversely posteriorly (Figure 2A, B, C, D). It is placed more over the anterior side of the centrum and is almost 2/3 of the length of the latter. Its anterior margin is inclined anterodorsally. The spine is connected to the medial side of the prezygapophyseal process by a short sprl, which meets its counterpart at about one third of the height of the neural spine, thus defining a small sprf. The spol is robust, but also short and connects the posterior end of the spine with the dorsal surface of the postzygapophysis. A large, diamond-shaped spof is bordered by the spols and tpols, with the latter being longer than the former. The entire dorsal surface of the neural spine is rugose.

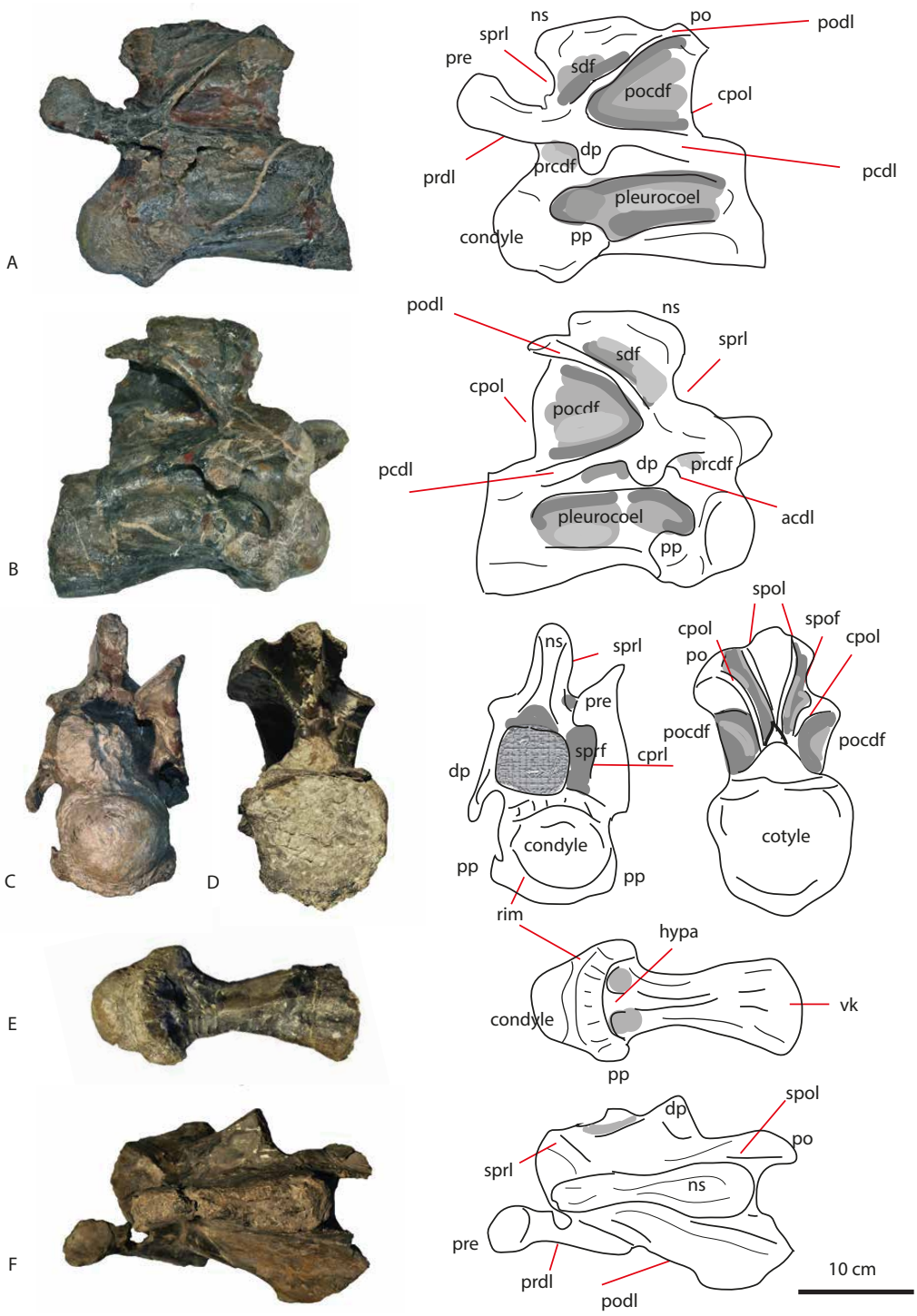

Figure 2: Cervical PVL 4170 (1) in lateral (A,B), anterior (C), posterior (D), ventral (E) and dorsal (F) views. Abbreviations: acdl = anterior centrodiapophyseal lamina, cprl = centroprezygapophyseal lamina, cpol = centropostzygapophyseal lamina, dp = diapophysis, hypa = hypapophysis, nc = neural canal, ns = neural spine, pcdl = posterior centrodiapophyseal lamina, pp = parapophysis, po = postzygapophysis, prcdf = prezygapophyseal centrodiapophyseal fossa, pocdf = postzygapophyseal centrodiapophyseal fossa, prdl = prezygapophyseal diapophyseal lamina, pre = prezygapophysis, spof = spinopostzygapophyseal fossa, spol = spinopostzygapophyseal lamina, sprf = spinoprezygapophyseal fossa, sprl = spinoprezygapophyseal lamina, vk = ventral keel.

Cervical vertebra PVL 4170 (2)

This anterior cervical vertebra is the second element preserved after the anteriormost cervical, and appears to be directly sequential based on the size similarity in cotylar and condylar size between PVL 4170 (1) and (3). It is incomplete, missing the neural arch and neural spine, which are broken off, see Figure 3. The centrum, prezygapophyses and the right postzygapophysis, however, are complete. The left postzygapophysis is also broken. The vertebra is slightly flattened/displaced towards the right lateral side, most likely due to compression.

The centrum is stout and robust, although slightly more elongated than that of the previous cervical PVL 4170 (1). Its EI is 1,64 and its aEI is 1,97. The overall shape is not as curved as in PVL 4170 (1), but rather straight along the axial plane, with a slight concave curvature of the ventral side of the centrum. The condyle is convex, although slightly more dorsoventrally flattened than in the previous cervical. In lateral view it shows a slightly pointy 'nose', i.e. a pointed protrusion, on its dorsal side (Figure 3A,B). The cotyle is slightly flattened dorsoventrally as well, and it is wider transversely than dorsoventrally. Because the condyle and cotyle show a high amount of osteological detail, this flattening might be natural, and not caused by compression. On the ventral side of the cotyle, a lateral flange extends on the left side but not on the right (Figure 3E) . This flange extends further posteriorly than the dorsal rim of the cotyle, extending posteriorly and laterally. The dorsal side of the rim of the cotyle shows a U-shaped indentation in dorsal and posterior view, posterior to the neural canal. As in the first preserved cervical, the parapophyses are placed at the anteroventral end of the centrum and extend from the thick condylar rim to the lateral and posterior sides of the condyle. They are generally conical in shape and elongated towards the rest of the centrum. The parapophyseal articular surfaces are more elongated axially than in the previous cervical (PVL 4170 1). In ventral view, the ventral keel on the centrum is clearly

present anteriorly on the vertebral body, but fades after about 2/3rd of the vertebral length towards the posterior side where it is not clearly visible (Figure 3E).

On the lateral sides of the centrum, pleurocoels are clearly visible as deep round anterior depressions, directly behind the rim of the anterior condyle (Figure 3A,C). These depressions fade into the lateral side of the centrum posteriorly. In this cervical, as in the first preserved cervical, the right pleurocoel slightly ramifies anteriorly near the right parapophysis; however, this is not visible on the left side of the centrum. As in the previous cervical, the ventrolateral side of the centrum and ventral border of the pleurocoel is formed by a stout lamina that extends from the posterior edge of the parapophyses to the posterior end of the cotyle.

The neural arch is only partially preserved (Figure 3A.B). Its height is similar to the height of the cotyle. The neural arch in this element is limited to the middle/posterior end of the vertebra; however, this is probably due to the fact that the neural spine is missing. The neural canal, however, is clearly visible in this vertebra, being round to oval in anterior view and more rounded triangular in posterior view. As in the previous vertebra, the lateral neural arch lamination is well-developed, with the stoutest laminae being the prdl, the pcdl, and the right podl. The acdl is also visible; however, it is smaller and shorter than the pcdl. Both diapophyses are present on the neural arch, and are positioned dorsal and slightly posterior to the parapophyses. The diapophyses are developed as small, lateroventrally projecting protrusions of bone, being oval in shape in lateral view and conical in anterior view. The left diapophysis is flexed more towards the centrum than the right, this is probably due to deformation. The right prdl runs straight in a slight anterodorsal slope from the diapophysis towards the prezygapophysis, where it meets with the cprl. Similarly, the right sprl runs more or less parallel to the prdl. The left prdl, however, forms a much steeper

angle from the left diapophysis to the left prezygapophysis, due to the taphonomical deformation. Towards the posterior end of the neural arch, the pcdl is in alignment with the prdl. However, the former is directed slightly posteroventrally. The right podl is visible but is damaged. It is a stout lamina and it forms a steep angle of 50° from the horizontal axis in its course from the right diapophysis towards the right postzygapophysis.

The prezygapophyses are much more elongated than in the previous cervical PVL 4170 (1), (Figure 3B,C). They project further anteriorly from the vertebral condyle than PVL 4170 (1) by about 9 cm. Moreover, unlike in PVL 4170 (1), they project mostly anteriorly and only slightly dorsally from the neural arch. Once more the taphonomical deformation of this cervical is apparent, as the left prezygapophysis is displaced and bent towards the vertebral body, while the right projects more lateral and away from the vertebral body. The prezygapophyses are supported by very stout stalks, which are formed by the prdl on the dorsolateral side, the cprl on the lateral, and, partially, the sprl on their dorsal side. The prdl meets the cprl in an acute angle, which is obscured from view by the prezygapophyseal articular surfaces. A small, short, pair of intraprezygapophyseal laminae is present, which meet in a wide acute angle, dorsal to the neural canal (Figure 3C). Lateral to these laminae, small, paired, rounded to oval prcdfs are visible underneath the prezygapophyses. They are also transversely convex.

The only preserved, right postzygapophysis is flexed slightly medially in dorsal view, and has its articular surface directed dorsally and tipped slightly anteriorly and laterally (Figure 3B,D). It is supported by the stout podl and an acutely angled, thin cpol, which together with the pcdl creates a triangular, wing-like structure, which is offset from the neural arch dorsally and posteriorly. The thin sheet of bone between the podl and the pcdl is pierced. The distal end of the postzygapophysis is rounded to triangular in shape. A relatively deep right pocdf is visible between the cpol and the podl. No tpol is visible here.

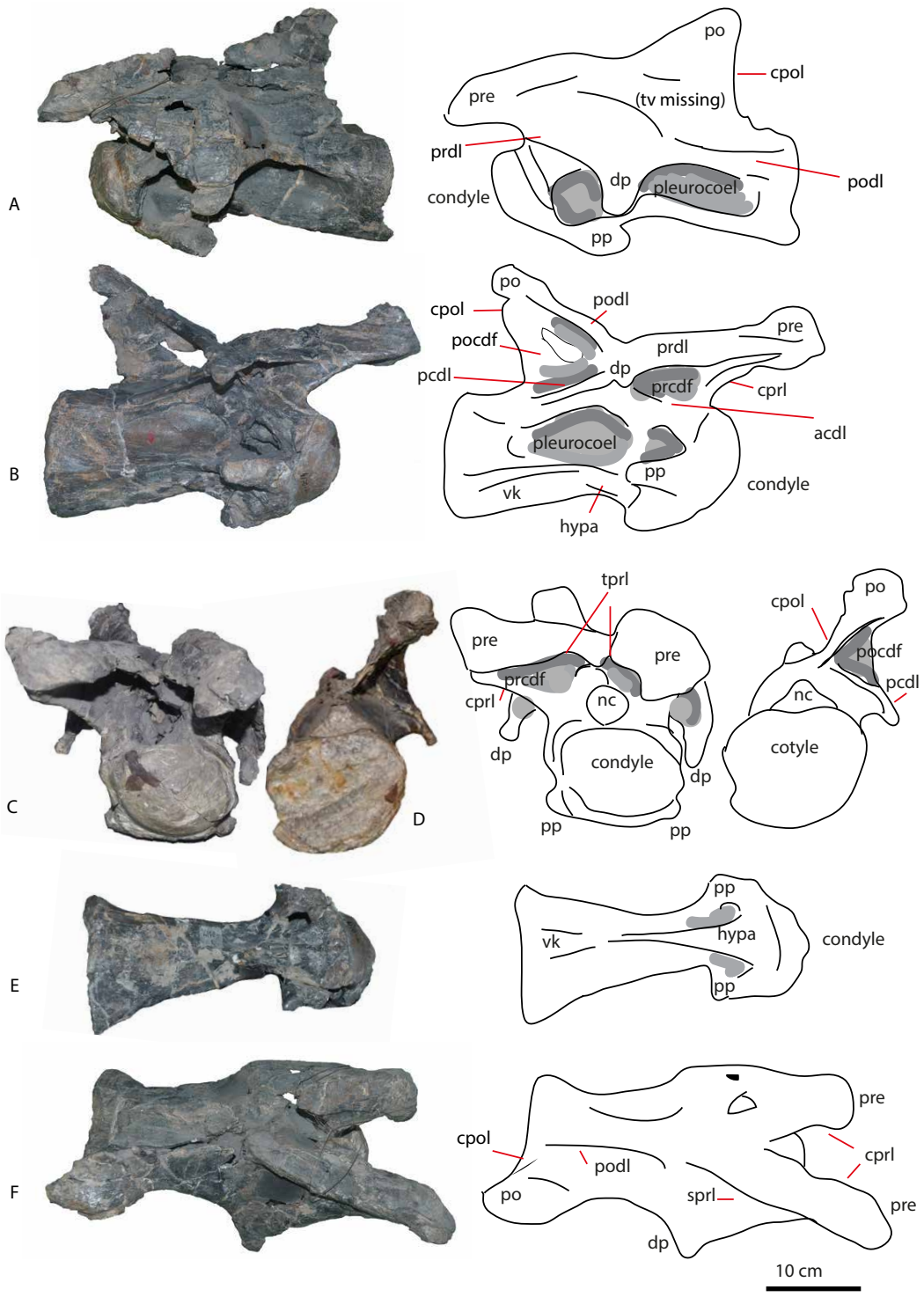

Figure 3: Cervical PVL 4170 (2) in lateral (A,B), anterior (C), posterior (D),, ventral (E) and dorsal (F) views. Abbreviations: acdl = anterior centrodiapophyseal lamina, cprl = centroprezygapophyseal lamina, cpol = centropostzygapophyseal lamina, dp = diapophysis, hypa = hypapophysis, nc = neural canal, ns = neural spine, pcdl = posterior centrodiapophyseal lamina, pp = parapophysis, po = postzygapophysis, prcdf = prezygapophyseal centrodiapophyseal fossa, pocdf = postzygapophyseal centrodiapophyseal fossa, prdl = prezygapophyseal diapophyseal lamina, pre = prezygapophysis, spof = spinopostzygapophyseal fossa, spol = spinopostzygapophyseal lamina, sprf = spinoprezygapophyseal fossa, sprl = spinoprezygapophyseal lamina, tprl = intraprezygapophyseal lamina, vk = ventral keel.

Cervical vertebra PVL 4170 (3)

This is the third cervical preserved in the series; it probably corresponds to the 5-6th cervical (compared to the Rutland *Cetiosaurus* Leict LEICT 468.1968). It is well-preserved, but lacks both diapophyses, see Figure 4. The cervical is stout, and is similar to PVL 4170 (2) in that the centrum is generally straight, and the anterior and posterior ends are not as offset from each other as in the first preserved cervical. Nevertheless, the cotyle is slightly offset to the ventral side, and the condyle bends slightly ventrally from the relatively straight vertebral body (Figure 4A,B). The prezygapophyses are slightly displaced, the right projects further laterally than the left; this might be caused by deformation.

Both the condyle and cotyle are larger in this cervical than in the previous two (Figure 4A,B). The condyle is oval in shape, and is transversely wider than dorsoventrally. It has a small rounded protrusion, visible slightly dorsal to the midpoint of the condyle (Figure 4E). A thick rugose rim surrounds the condyle, from which the parapophyses protrude at the lateroventral sides. The cotyle is more or less equally wide transversely as high dorsoventrally. It has its deepest depression slightly dorsal to the midpoint. The cotyle does not have a rugose rim; however, its ventral rim projects further posterior and slightly lateral than its dorsal rim. In ventral view, (as well as in lateral view) the parapophyses are clearly visible as rugose, oval structures that protrude from behind the condylar rim to the posterior and lateral sides. Also emerging from this condylar rim is the ventral keel, which is prominently visible for about 2/3rds of the length of the centrum, after which it fades into the ventral body of the centrum. At the onset of the keel, a small round hypapophysis protrudes ventrally from the centrum. Two oval depressions are visible on the lateral sides of the hypapophysis.

In lateral view, the centrum shows neurocentral sutures between the lower part of the centrum and the upper part of the vertebral body (Figure 4A,B). The suture is better

preserved on the right side than on the left side of the centrum. On both lateral sides of the centrum, a prominent pleurocoel is visible as a deep oval depression, which becomes more shallow posteriorly but spans almost the entire length of the vertebral body. Unlike in the previous two cervicals, no compartmentalization of the pleurocoel is visible in this element. The dorsal and ventral rim of the pleurocoels are marked by two stout laminae that define the ventral and dorsal sides of the centrum.

The neural arch becomes more dorsoventrally elevated in this cervical, with the neural arch being slightly higher than the dorsoventral height of the cotyle (Figure 4A,B). The neural canal is triangular to slightly teardrop-shaped in anterior view, in contrast to the previous two cervicals. In posterior view, the neural canal is oval, with a flat ventral surface. Because the diapophyses are damaged, the lamination underneath the diapophyses is clearly visible in lateral view. The acdl is developed as a short lamina, running anteroventrally in an oblique slope towards the anterodorsal end of the pleurocoel. The pcdl is a very stout, elongated lamina in this cervical. It runs from directly underneath the diapophysis to the posterior end of the vertebral body, but fades into the centrum shortly before the rim of the cotyle. The anterior and posterior centrodiapophyseal laminae delimit a small triangular centrodiapophyseal fossa, while a much wider postzygodiapophyseal fossa is bordered by the slightly convex, stout postzygodiapophyseal lamina (Figure 4A,B,C). This lamina runs at an oblique angle of about 40 degrees to the horizontal from the diapophysis to the postzygapophysis. Shortly before reaching the postzygapophysis, the curvature of the lamina changes from straight to slightly concave (ventrally), giving the podl a slight sinusoidal appearance. The prdl runs from the diapophyses to the prezygapophyses in an oblique angle similar to the podl. The four major laminae on this cervical, prdl, acdl, pcdl, and podl, together create an X shape (in near symmetrical oblique angles) on the midpoint of this cervical.

The prezygapophyses project anteriorly, dorsally, and slightly laterally, with the angle between each prezygapophyseal summit being about 110-120° (Figure 4D). They project assymetrically; this is probably due to taphonomical deformation. The stout stalks supporting the prezygapophyses are concave ventrally, and convex dorsally, and project 9 cm anterior from the vertebral body (Figure 4A,B,D). The articular surfaces are triangular in shape. The prezygapophyses are supported by the prdl from the dorsolateral side, and by the cprls ventrally. The cprls extend in a near vertical axis from the ventral side of the neural arch, but at about the height of the neural canal project laterally towards the prezygapophyseal articular surface in an angle of about 30 degrees. In anterior view, the stout, sinusoidal intraprezygapophyseal laminae join together from the medial articular surface of the prezygapophyses to the ventral side of the prezygapophyses, just dorsal to the neural canal. Here a very short, stout, single intraprezygapophyseal lamina is present. The paired prcdfs, seen as triangular depressions, bordered by the tprls and the cprls, are larger than in previous cervicals PVL 4170 (1) and (2).

The postzygapophyses are triangular in shape in posterior view, and their articular surfaces in posterior/ventral view are rounded to triangular in shape (Figure 4C). There is a slight V-shaped indentation on the medial side of each postzygapophysis between the posterior termination of the podl and the cpol at the postzygapophyses. The cpols run in a curved, oblique angle of ±55 degrees to the horizontal, from the postzygapophyseal articular surfaces to the dorsal rim of the posterior neural canal. No stpol is visible here. On each lateral side of the paired cpols, large triangular paired pocdf are visible, bordered by the vertically aligned podls.

The neural spine is already prominent in this cervical, more so than in PVL 4170 (1) and (2) (Figure 4A,B, F). In dorsal view, the neural spine appears solid, and is rounded in shape, and the anterior, posterior and lateral rims are clearly visible and protrude slightly dorsally (Figure 4F). The dorsalmost part shows rugosities, probably for ligament attachment. In anterior view, the neural spine is kite-shaped, and shows rugosities on the anterior surface. Relatively thin, paired sprls curve down from the anterior lateral sides of the neural spine, where they extend in an inverted V-shape to the lateral sides of the prezygapophyses. Medial to these laminae, an oval sprf is visible, ventrally bordered by the tprls. Similarly, in posterior view, the spols form an inverted V towards the postzygapophyses, dorsally bordering the spof, which is clearly visible as a deep and large fossa, which in turn is bordered laterally by the paired cpols. The neural spine in lateral view as well as in posterior view is seen to incline anteriorly, making the neural spine summit less prominent in posterior view (Figure 4A,B,C).

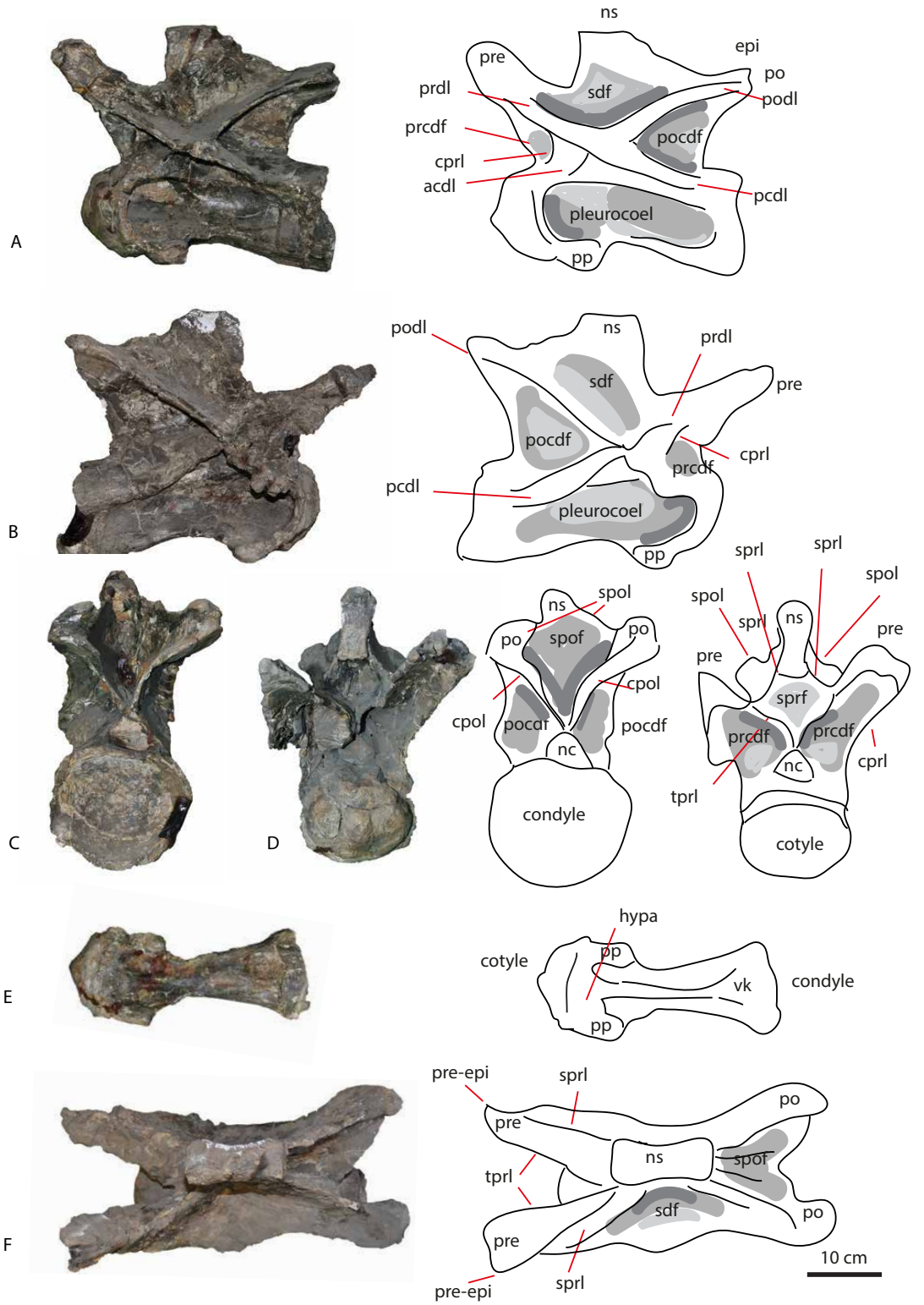

Figure 4: Cervical PVL 4170 (3) in lateral (A,B), posterior (C) anterior, (D), ventral (E) and dorsal (F) views. Abbreviations: acdl = anterior centrodiapophyseal lamina, cprl = centroprezygapophyseal lamina, cpol = centropostzygapophyseal lamina, dp = diapophysis, hypa = hypapophysis, nc = neural canal, ns = neural spine, pcdl = posterior centrodiapophyseal lamina, pp = parapophysis, po = postzygapophysis, prcdf = prezygapophyseal centrodiapophyseal fossa, pocdf = postzygapophyseal centrodiapophyseal fossa, prdl = prezygapophyseal diapophyseal lamina, pre = prezygapophysis, sdf = spinodiapophysal fossa, spof = spinopostzygapophyseal fossa, spol = spinopostzygapophyseal lamina, sprf = spinoprezygapophyseal fossa, sprl = spinoprezygapophyseal lamina, tprl = intraprezygapophyseal lamina, vk = ventral keel.

Cervical vertebrae PVL 4170 (4)

The fourth preserved cervical is generally well-preserved. However, the left diapophysis and part of the neural arch are missing, and the right neural arch, between the neural spine and the diapophysis, is partially reconstructed, see Plate IV. The left prezygapophysis, and the articular surface of the postzygapophysis are also partially missing. This cervical could have been more robust than the next one, and the neural spine could have projected further dorsally, making this cervical in fact cervical (5), however, as it is reconstructed, this cannot be ascertained for certain.

The centrum is more elongated then that of the previous cervical (Figure 5A,B). The centrum only shows a mild curvature, and the cotyle and condyle are not offset from one another; the condyle bends slightly ventrally and the cotyle also mildly curves ventrally. The lateroventral rims of the cotyle flare out slightly laterally and posteriorly, and are more enlongated ventrally than dorsally. In anterior view, the condyle is oval and slightly dorsoventrally flattened (Figure 5D). It has a thick, prominent rim surrounding it, from which the parapophyses are offset in anterior view. In posterior view, the cotyle is larger than the condyle, and more or less equally wide transversely as dorsoventrally. In ventral view, the thick rim that cups the condyle is clearly visible (Figure 5E). From this rim, the hypapophysis protrudes ventrally as a small rounded bulge. The ventral keel is prominently visible, and runs along the ventral surface of the centrum until it fades into the posterior 1/3rd of the centrum, where it widens transversely towards its posterior end. This is also seen to some extent in *Lapparentosaurus* (MNHM MAA 13; 172; 5), although this fanning includes a dichotomous branching of the posterior end of the ventral keel in the latter taxon. In lateral view, the ventral keel protrudes slightly more ventrally than the stout lamina that defines the ventral lateral end of the centrum. In lateral view, the pleurocoels are visible as deep depressions on the lateral side of the centrum, being deepest behind the rim of the condyle, and fading into the posterior 1/3rd of the lateral centrum. Interestingly, this cervical shows

pleurocoels with well-defined posterior margins (as well as anterior, dorsal and ventral), which differs from the pleurocoels in the previous cervicals (Figure 5A,B). Moreover, the pleurocoels in this element are slightly compartmentalized (a deeper depression of the pleurocoel is visible anteriorly and posteriorly, while the mid section is less deep in the lateral body of the centrum), as in the first two cervicals.

The neural arch is slightly more elongated than the condyle; in that it overhangs the condyle (Figure 5A,B), but not by much, which makes this cervical similar to PVL 4170 (3). As in the previous three cervicals, the neural arch extends over most of the length of the centrum, but ends a short way anterior to the posterior end of the centrum. The neural canal is rounded to teardrop-shaped in anterior view, and oval to triangular in posterior view, with an abrupt transverse ventral rim, as in PVL 4170 (3). The configuration of the four prominent laminae on the lateral neural arch is similar to that of PVL 4170 (3) in that pcdl, prdl, podl and acdl form an X-shaped structure. However, the right diapophysis (the left is missing) of this element is larger than in the previous cervicals. The right diapophyis is developed as a ventrolaterally projecting process, which is supported posteriorly by the very stout pcdl, and anteriorly by a smaller, shorter acdl. The diapophysis is oval in shape and is axially shorter than dorsoventrally.

The right prezygapophysis is supported laterally and dorsally by the stout prdl, which extends from the anterodorsal side of the diapophysis to approximately 2/3rds of the length of the stalk of the prezygapophysis (Figure 5B,D). Ventrally, the prezygapophysis is supported by the cprl, which is nearly vertically positioned on the neural arch. The prezygapophysis has a triangular articular surface. As in the previous cervicals, the cprl and tprl meet at the distal end of the prezygapophysis in an acute angle of approximately 30

degrees. The paired tprls slope steeply down and meet on the dorsal rim of the anterior neural canal. The cprl and tprls enclose paired, rhomboid prcdfs.

In posterior view, the left postzygapophysis is only partially preserved, as the articular surface is missing, but the right structure is present, showing a flattened articular surface (Figure 5C). The intrapostzygapophyseal laminae form a V shape with an angle of about 55 degrees from the sagittal plane of the centrum, which is similar to PVL 4170 (3). They meet only on the dorsal rim of the posterior neural canal. The paired, triangular pocdfs, which are demarcated by the cpols and the podls, are also similar to the third preserved cervical.

The neural spine is robust in anterior view (Figure 5D). It is narrower at the base (at the onset of the spinoprezygapophyseal lamina) and expands transversely towards the summit, which in anterior view is shaped like a rounded hexagon. The right spinoprezygapophyseal lamina is a near-vertically positioned, prominent structure that extends from about 1/3rd under the neural spine summit to the ventral pairing of the tprls. In lateral view, the neural spine is anteroposteriorly shorter, with respect to the length of the centrum, than in previous cervicals. Its anterior margin is slightly inclined anteriorly. In posterior view, the neural spine summit has a more rounded, rectangular shape, and is clearly inclined towards the anterior side of the cervical. The (only preserved) right spinopostzygapophyseal lamina curves concavely towards the postzygapophysis (Figure 5A,B,C). The spinopostzygapophyseal fossa is deep and triangular in shape.

In dorsal view, the neural spine summit is roughly quadrangular in outline, although it is slightly wider transversely than long anteroposteriorly (Figure 5F). On the anterior rim of the summit, the spine slightly bulges out convexly, with an indent on the midline, rendering the anterior rim slightly heart-shaped. The posterior side of the neural spine summit is slightly concave in dorsal view, with the spinopostzygapophyseal laminae sharply protruding from each lateral side.

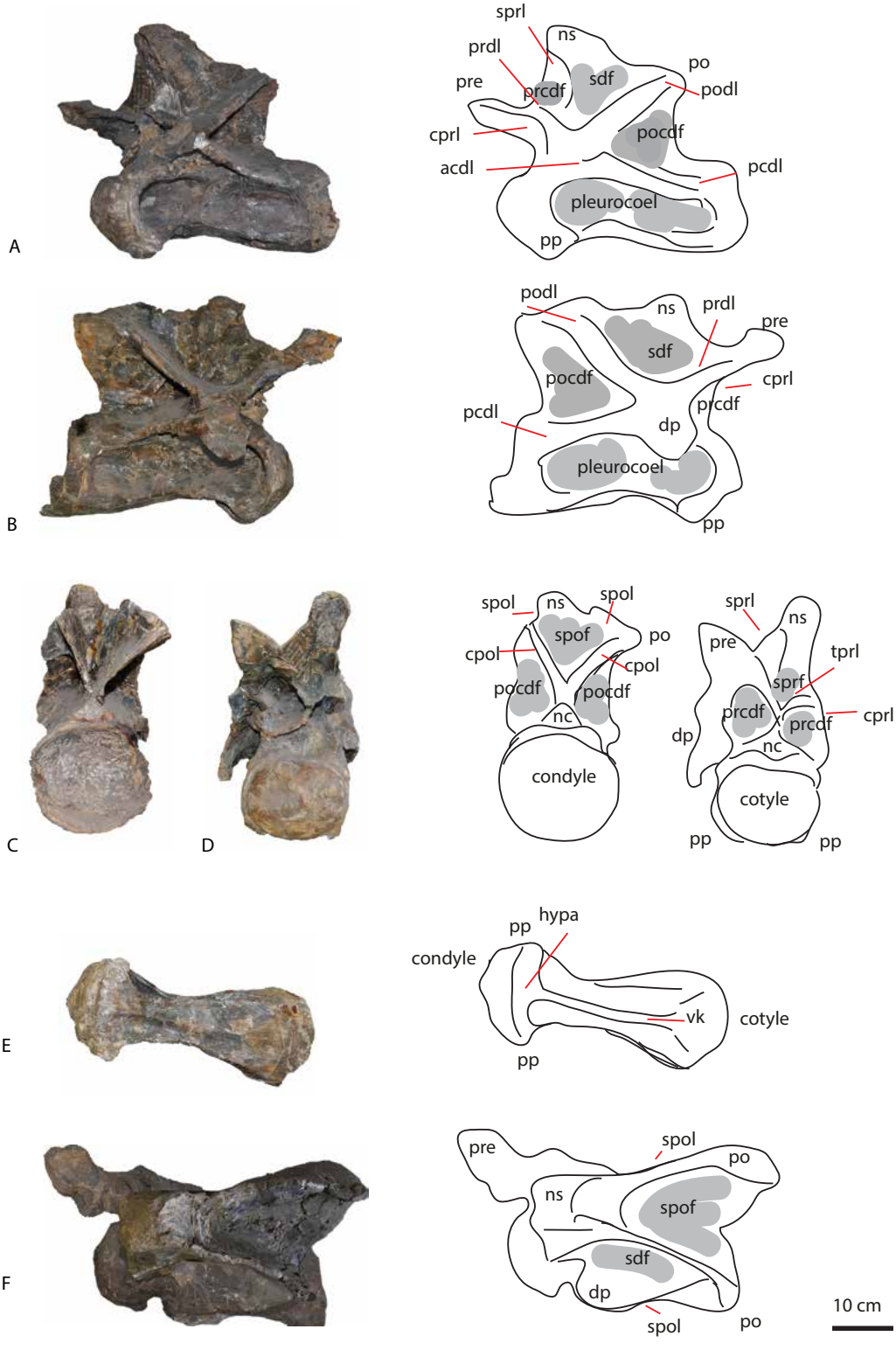

Figure 5: Cervical PVL 4170 (4) in lateral (A,B), posterior (C), anterior (D), ventral (E) and dorsal (F) views. Abbreviations: acdl = anterior centrodiapophyseal lamina, cprl = centroprezygapophyseal lamina, cpol = centropostzygapophyseal lamina, dp = diapophysis, hypa = hypapophysis, nc = neural canal, ns = neural spine, pcdl = posterior centrodiapophyseal lamina, pp = parapophysis, po = postzygapophysis, prcdf = prezygapophyseal centrodiapophyseal fossa, pocdf = postzygapophyseal centrodiapophyseal fossa, prdl = prezygapophyseal diapophyseal lamina, pre = prezygapophysis, sdf = spinodiapophysal fossa, spof = spinopostzygapophyseal fossa, spol = spinopostzygapophyseal lamina, sprf = spinoprezygapophyseal fossa, sprl = spinoprezygapophyseal lamina, tprl = intraprezygapophyseal lamina, vk = ventral keel.

Cervical vertebra PVL 4170 (5)

This is a mid-posterior cervical, which is well-preserved, with all zygapophyses and diapophyses intact, although the neural spine is slightly taphonomically deformed, and the diapophyses are slightly asymmetrical, also probably due to deformation. The left parapophysis is also missing, see Figure 6A.

The centrum is different from the previous cervicals in that it is more robust, less axially elongated and the condyle, cotyle and neural spine are dorsoventrally larger (Figure 6A,B). The anterior condyle is rounded, robust and slightly dorsoventrally flattened. The anterior end of the condyle has a rounded protrusion on the midpart. The rim of the condyle is clearly visible and protrudes slightly dorsally (Figure 6C). Posteriorly, the cotyle is deeply concave and is larger transversely and dorsoventrally than the condyle. The posterior end of the centrum, ventral to the cotyle, flares out laterally, however, it shows a U-shaped indent in the midpart, seen in posterior view (Figure 6D). In lateral view, the centrum is concavely constricted anteriorly, directly posterior to the rim of the condyle. As in the other cervicals, the dorsal end of the posterior cotyle extends a little further posteriorly from the neural canal in lateral and ventral view. The right parapophysis is visible in lateral view at the ventrolateral end of the condylar rim (Figure 6B). It is oval in shape and protrudes ventrally and posteriorly. The pleurocoel on the lateral side of the centrum is deeper anteriorly than posteriorly, and spans almost the entire lateral side of the condyle anteriorly (Figure 6A,B). Posteriorly it fades into the centrum. In ventral view, the ventral keel is clearly visible, and stretches over the entire length of the centrum, but flattens in the posteriormost part (Figure 6E). The hypapophysis protrudes less in this cervical than in the previous ones. The parapophysis is more elongated axially than transversely in ventral view, and less rounded

than in the previous cervicals; rather than having a rounded rectangular shape in ventral view, it is more elliptical in shape, and is slightly more offset to the lateral sides of the centrum (Figure 6E). Both posterior centroparapophyseal laminae are clearly visible in this element as short but strong laminae that are confluent with the ventrolateral edges of the vertebral body.

The neural arch is higher dorsoventrally in this element than in the previous ones. In lateral view, the neural arch spans almost the entire axial length of the centrum, however, as in the previous cervicals, it is slightly offset from the anterior dorsal end of the centrum (Figure 6A,B). In anterior view, the neural canal is slightly teardrop-shaped, and dorsoventrally is more elongated than transversely. In posterior view, the neural canal is also teardrop-shaped, however here it is more dorsoventrally flattened and transversely widened at the base. The diapophyses, in lateral view, appear as rounded appendices, which are offset from the vertebral body as ventral and lateral projection. They are transversely thin and flattened. In anterior view they are more complex in shape, created by a conjoining of the acdl, pcdl and prdl in a triangular shape, which shows a ventral hook-shaped distal protrusion. In posterior view the diapophyses are enclosed in sheets of bone. The prezygapophyses on this cervical rest on more dorsoventrally elongate stalks than in previous cervicals (Figure 6A,B,C). These stalks have a pedestal-like appearance, and show lateral rounded bulges at their base, dorsal and lateral to the thick condylar rim. The prezygapophyses project anteriorly and slightly medially and dorsally, and are anteriorly triangular in shape. There are deep rhomboid prcdfs visible as dorsoventrally narrow, slit-like fossae, ventral to the prezygapophyses. The centroprezygapophyseal laminae form an oblique angle towards the centrum. The prezygodiapophyseal laminae run ventrally from the prezygapophyses in a sharp angle. These laminae meet dorsally in an acute angle. The intraprezygapophyseal laminae meet dorsal to the neural canal in a wider angle than in the previous cervicals,

showing a widening of the space between the prezygapophyses towards more posterior cervicals in *Patagosaurus*.

The postzygapophyses and prezygapophyses are both more aligned with the axial column than in previous cervicals (Figure 6F). In lateral view, the articular surface of the postzygapophyses is aligned with the horizontal axis, and in dorsal and posterior view the articular surfaces are triangular in shape (Figure 6A,B). In lateral view, the postzygodiapophyseal laminae form a wide angle with the axial column, owing to the further elongation of the centropostzygapophyseal laminae (producing more elevated postzygapophyses). The cpols show an acute angle from the postzygapophyses to the anterior and ventral side, and are slightly ragged in appearance. They meet the centrum anteriorly to the dorsal rim of the cotyle. In posterior view, the centropostzygapophyseal laminae run at an acute angle, and in a slightly concave way, to the ventral side of the postzygapophysis (Figure 6D). This angle is smaller than in previous cervicals, being about 35 degrees, due to the elongation of the neural arch and higher dorsal position of the postzygapophyses. Between the cpol and podl, large, triangular postzygocentrodiaopophyseal fossae are visible.

The neural spine in anterior view is slightly sinusoidal, probably due to taphonomic deformation (Figure 6C). In lateral view, the neural spine is further reduced in its axial length compared to the previous cervicals (Figure 6A,B). The spine summit is prominent; it is seen to protrude dorsally and anteriorly, clearly separated from the vertebral body as a rounded rectangular bony mass. In dorsal view, the neural spine summit is wider than the neural spine body, and is of a teardrop-shaped protuberant shape (Figure 6F). It is also expanded transversely. Anteriorly on the neural spine, a prominent protuberance is visible anteriorly, possibly an attachment site for ligaments. The sprls are seen, in dorsal view, to protrude

from the anterior side of the neural spine summit (Figure 6C). They run nearly vertically towards the dorsal base of the prezygapophyseal stalks. At the base of the neural spine they are slightly transversely constricted. The spinopostzygapophyseal laminae are positioned as near-horizontally aligned with the axial plane of the cervical. They are thin, prominent laminae.

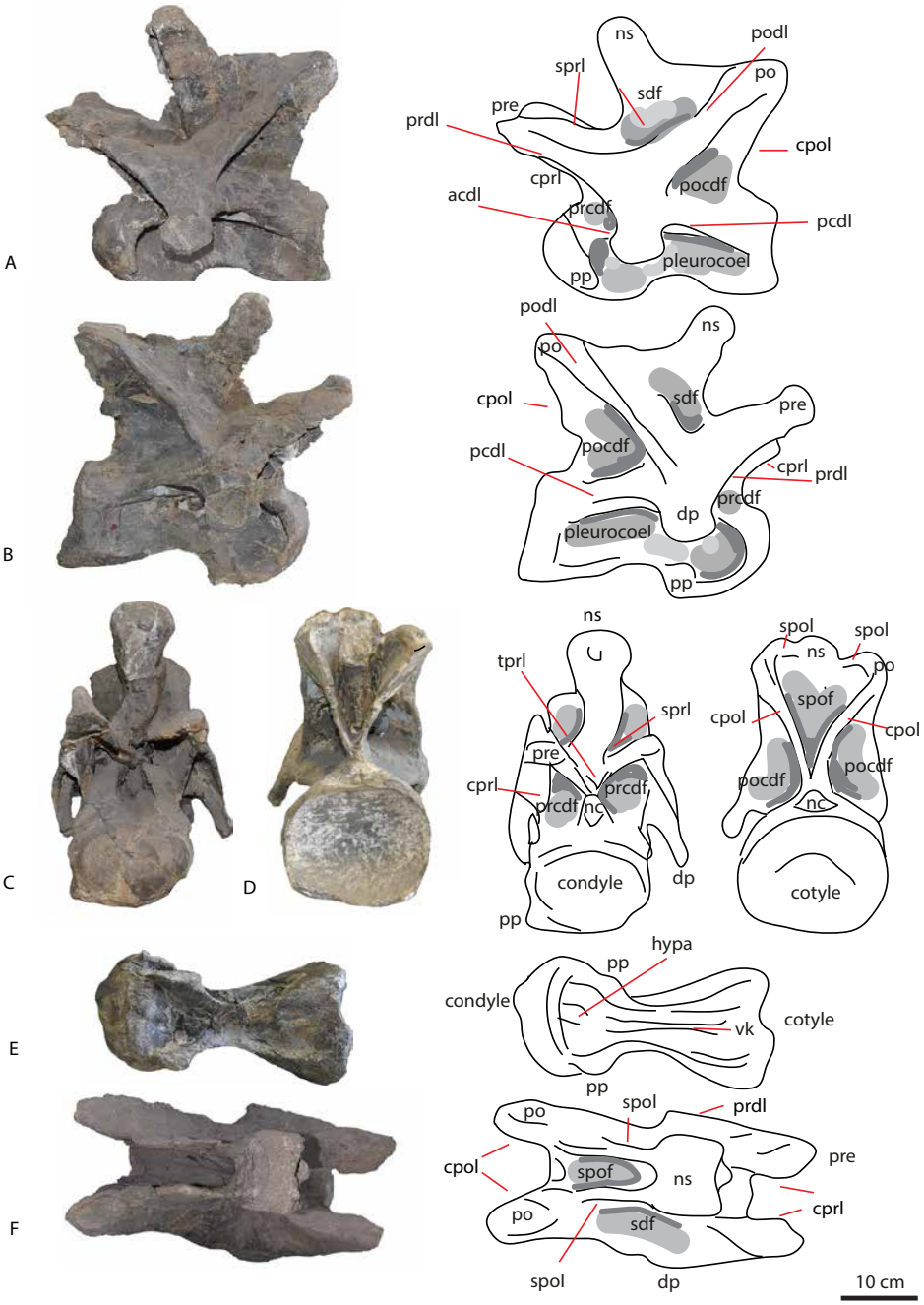

Figure 6 (previous page): Cervical PVL 4170 in lateral (A,B), anterior (C), posterior (D), ventral (E) and dorsal (F) views. Abbreviations: acdl = anterior centrodiapophyseal lamina, cprl = centroprezygapophyseal lamina, cpol = centropostzygapophyseal lamina, dp = diapophysis, hypa = hypapophysis, nc = neural canal, ns = neural spine, pcdl = posterior centrodiapophyseal lamina, pp = parapophysis, po = postzygapophysis, prcdf = prezygapophyseal centrodiapophyseal fossa, pocdf = postzygapophyseal centrodiapophyseal fossa, prdl = prezygapophyseal diapophyseal lamina, pre = prezygapophysis, sdf = spinodiapophysal fossa, spof = spinopostzygapophyseal fossa, spol = spinopostzygapophyseal lamina, sprf = spinoprezygapophyseal fossa, sprl = spinoprezygapophyseal lamina, tprl = intraprezygapophyseal lamina, vk = ventral keel.

Cervical vertebrae PVL 4170 (6)

This is a well-preserved posterior cervical with some damaged/broken thin septa. The centrum is robust, as in PVL 4170 (5), but unlike the more elongated anterior cervicals. The cervical is further distinguished by having an axially more elongated neural arch than in the previous cervical, see Figure 7.

The centrum is shorter than in previous cervicals, and more stout, with a transversely flattened condyle with a small rounded protrusion slightly higher than the midpoint (Figure 7A,B). The cotyle is slightly larger and higher dorsoventrally than the condyle, as in the other cervicals.

In ventral view, the ventral keel is developed as a protruding ridge between two concavities, which are flanked by the ventrolateral ridges of the centrum (Figure 7E). This keel flattens towards the caudal end into a bulge and is no longer visible at the posterior end of the ventral side of the centrum. Instead there is a slight depression on the distal end of the keel. The centrum is constricted directly posterior to the parapophyses, which shows a deep concavity of the centrum in lateral view, after which the centrum curves more gently towards a convex posterior end of the centrum (Figure 7A,B). The pleurocoel is anteriorly deep, and the thin septum that separated it from its mirroring pleurocoel is broken, creating

an anterior fenestra. On the left side of the centrum the neurocentral suture is visible. In anterior view, the neural canal is oval, being higher dorsoventrally than wide transversely, and in posterior view, the neural canal is subcircular with a pointed dorsal side.

In anterior view, the prezygapophyses are a triangular shape, due to the tapering of both cprl and prdl towards the dorsal tip of the prezygapophyses, where they meet in an inverted V-shape, as in PVL 4170 (5), see Figure 7C. The centroprezygapophyseal fossae are not as deep as in the previous cervicals. The dorsal end of the prezygapophyses is not as convex as in the previous cervicals. In ventral and posterior view, the postzygapophyseal articular surfaces are triangular (Figure 7D, E). In lateral view, the spinoprezygapophyseal lamina is positioned less vertical than in PVL 4170 5, and instead slopes in a gentle curve towards the prezygapophyses (Figure 7A,B). In posterior view, the thick cpols and the spols support the laterally canted, 'wing-tip'-shaped sheet of bones that are supported by the podl and pcdl on the lateral side (Figure 7D). The cpols do not meet, while there is no tpol. In dorsal view, the postzygapophyses and spinopostzygapophyseal laminae expand further beyond the centrum than the prezygapophyses overhang the centrum anteriorly, which is the reversed condition compared to the more anterior cervicals in PVL 4170. The spinopostzygapophyseal lamina is also less oblique than in previous cervicals, and curves gently concavely towards the postzygapophyses (Figure 7D).

The neural spine is craniocaudally flattened but transversely broader than PVL 4170 (5). The base of the neural spine is only supported by a rather thin bony sheet, both anteriorly and posteriorly, as can be seen due to a break. The dorsal end and summit of the neural spine, however, are formed by solid bone. In anterior view, the spine is not as teardrop-shaped as in PVL 4170 (5), but is more rectangular, and widens towards its summit. The neural spine does not tilt notably forward as in PVL 4170 (5), but cants only slightly anteriorly. The neural

spine summit extends dorsally beyond the spinopostzygapophyseal laminae as an oval to rhomboid protuberance. The neural spine and the postzygapophyses, together with the postzygodiapophyseal lamina are more axially elongated and dorsally elevated in this cervical than in the previous ones. In dorsal view, the neural spine summit is a stout, transverse strut. It is slightly transversely expanded, and thicker at the lateral ends.

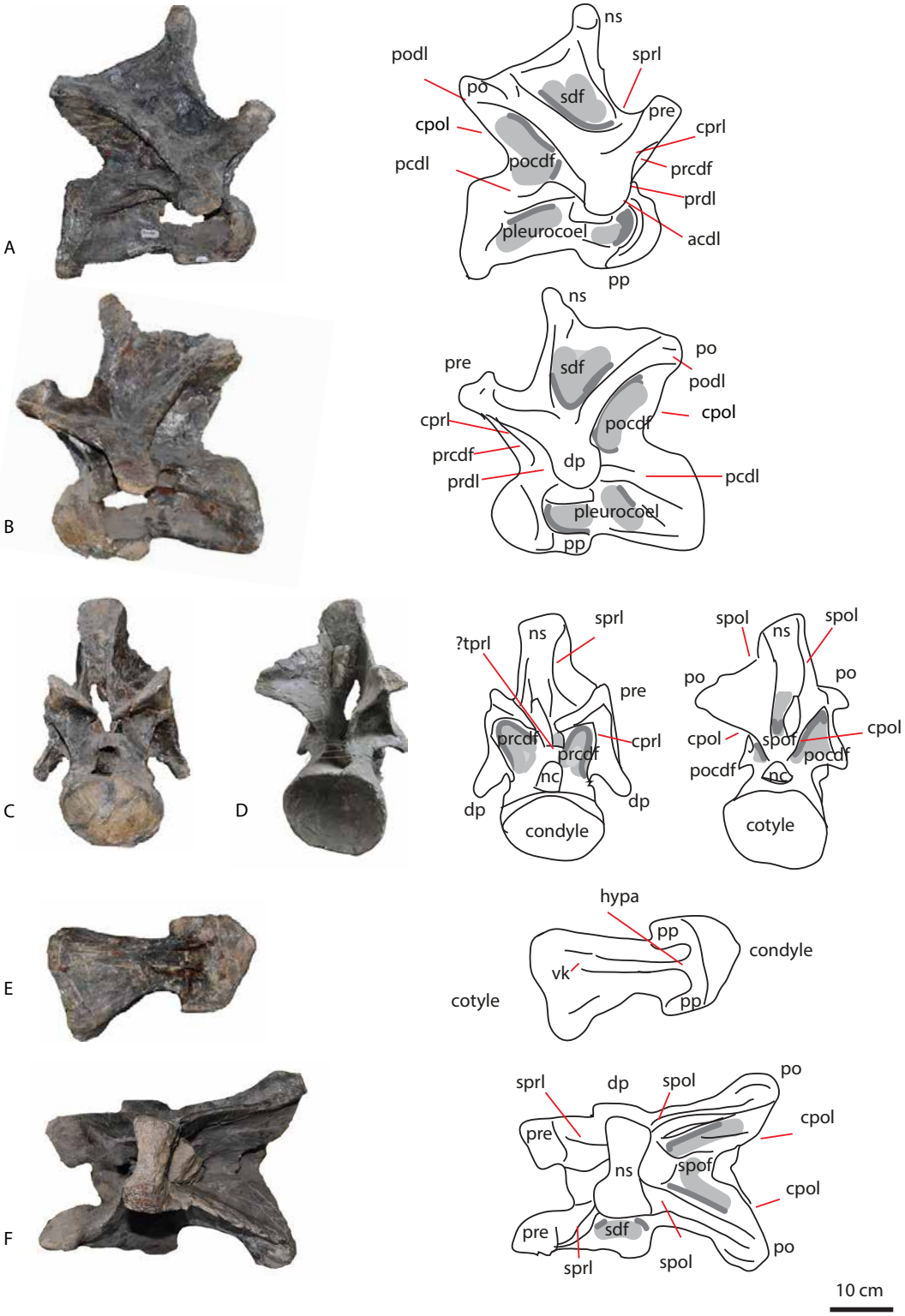

Plate 7: Cervical PVL 4170 (6) in lateral (A,B), anterior (C), posterior (D), ventral (E) and dorsal (F) view. Abbreviations: acdl = anterior centrodiapophyseal lamina, cprl = centroprezygapophyseal lamina, cpol = centropostzygapophyseal lamina, dp = diapophysis, hypa = hypapophysis, nc = neural canal, ns = neural spine, pcdl = posterior centrodiapophyseal lamina, pp = parapophysis, po = postzygapophysis, prcdf = prezygapophyseal centrodiapophyseal fossa, pocdf = postzygapophyseal centrodiapophyseal fossa, prdl = prezygapophyseal diapophyseal lamina, pre = prezygapophysis, sdf = spinodiapophysal fossa, spof = spinopostzygapophyseal fossa, spol = spinopostzygapophyseal lamina, sprf = spinoprezygapophyseal fossa, sprl = spinoprezygapophyseal lamina, tprl = intraprezygapophyseal lamina, vk = ventral keel.

Cervical vertebra PVL 4170 (7).

This is a partially reconstructed posterior cervical, with the left diapophysis missing, see Figure 8. The vertebra is shorter axially and higher dorsoventrally than previous cervicals (Figure 8A,B). The centrum is stout. In anterior view, the condyle is dorsoventrally compressed and transversely widened (Figure 8 F). The 'cup' is very distinct. The cotyle is larger than the condyle, more rounded, and shows an indentation dorsally for the neural canal, making the cotyle slightly heart-shaped (Figure 8E). In ventral view, this centrum is less elongated and transversely wider than previous cervicals. The keel is still well developed, as are the lateral concavities coinciding with the hypapophysis, which is present as a sharp ridge (Figure 8C). The posterior ventral side of the centrum is ventrally offset from the anterior ventral side, due to the larger size of the cotyle in this specimen, and due to the ventral bulge of the distal half of the centrum.The parapophyses are more aligned with the centrum, in that they do not project ventrolaterally, but more posteriorly, in contrast to previous cervicals (Figure 8C). The parapophyses are oval in ventral view and more triangular in lateral view. The neural canal is dorsoventrally flattened and teardrop-shaped (Figure 8E,F).

The prezygapophyses differ from previous cervicals in that they form a more accute angle with the vertebral body and have a flat, dorsally directed articular surface in lateral view (Figure 8A,B). The beams supporting the prezygapophyseal articular surface are stout, as in the previous cervicals. The prezygapophyses are inverted V-shaped in anterior view (Figure 8F). However, this structure is wider transversely than in previous cervicals. The intraprezygapophyseal laminae tilt ventromedially, whereas the distal tips of the prezygadiapophyseal laminae tilt ventrolaterally, creating an inverted V-shape in anterior view of each prezygapophysis, as in the previous cervical. The single intraprezygapophyseal

lamina is not present. In dorsal view, the articular surface of the prezygapophysis is more rounded than in previous cervicals. The postzygapophyses are supported from the lateral and ventral sides by the prominent postzygodiapophyseal laminae, which project in a wide angle of about 70 degrees from the posterior side of the diapophysis to the postzygapophyses; this lamina curves gently convexly (Figure 8A,B,E). In lateral view, the postzygapophyses are present as triangular structures at the distal end of the thick postzygodiapophyseal laminae. Dorsal to the postzygapophyses, triangular epipophyses are visible (Figure 8A,B,E). Also in lateral view, the tpols run ventral to the postzygadiapophyses in a vertical line towards a U-shaped recess, formed by the single intrapostzygapophyseal lamina. In posterior view, the intrapostzygapophyseal laminae form a V-shape. The tpols are much shorter than in PVL 4170 (6), which also limits the size of the spinopostzygapophyseal fossa. A short stpol is present as a thin lamina that recedes towards the neural arch (Figure 8E). This is the only cervical that has an stpol that is longer than 1 cm. It separates paired rhomboid centropostzygapophyseal fossae. These are flanked by the thick postzygodiapophyseal laminae, which are more elongated in this vertebra than in cervical PLV 4170 (6). The right diapophysis expands from the lateral side of the neural arch, and shows a strong ventral bend towards its distal end. This strong bend could be the product of deformation. The left diapophysis also bends ventrally and laterally, but not as strongly as the right one (Figure 8A,B,E,F). The diapophyses are clearly visible both in anterior and posterior view. Ventrally and anteriorly they are concave, with elongated but axially short prcdfs. They are dorsally supported by the convergence of the prdl and the podl, which form a thick rugose, rounded plate of bone on the dorsal tips of the diapophyses.

The neural spine is transversely broad and axially short, and rectangular in shape (Figure 8F). In dorsal view, it fans out transversely at the apex, but, together with the spinoprezygapophyseal laminae, becomes constricted ventrally (Figure 8D). This cervical is

further distinguished from the previous cervicals by the dorsoventral elongation of the neural spine, and the accompanying elongation of the intrapostzygapophyseal laminae in lateral view (Figure 8A,B).

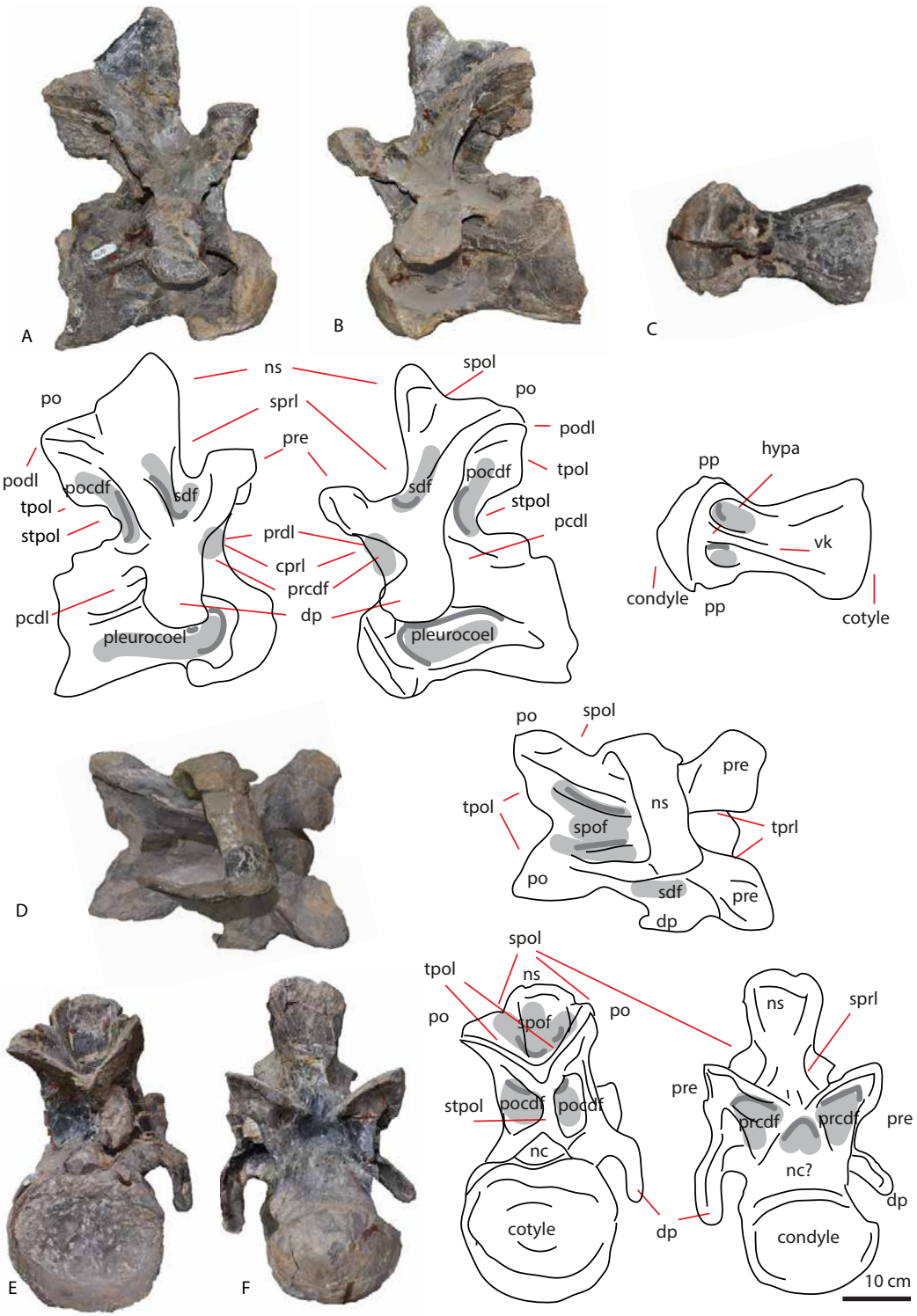

Figure 8 (previous page): Cervical PVL 4170 (7) in lateral (A,B), ventral (C), dorsal (D), anterior (E)and posterior (F) views. Abbreviations: acdl = anterior centrodiapophyseal lamina, cprl = centroprezygapophyseal lamina, cpol = centropostzygapophyseal lamina, dp = diapophysis, hypa = hypapophysis, nc = neural canal, ns = neural spine, pp = parapophysis, po = postzygapophysis, prcdf = prezygapophyseal centrodiapophyseal fossa, pocdf = postzygapophyseal centrodiapophyseal fossa, prdl = prezygapophyseal diapophyseal lamina, pre = prezygapophysis, sdf = spinodiapophysal fossa, spof = spinopostzygapophyseal fossa, spol = spinopostzygapophyseal lamina, sprf = spinoprezygapophyseal fossa, sprl = spinoprezygapophyseal lamina, tprl = intraprezygapophyseal lamina, tpol = intrapostzygapophyseal lamina, stpol = single intrapostzygapophyseal lamina, vk = ventral keel.

Cervicodorsal PVL 4170 (8)

The neural arch is dorsoventrally elongated in this transitional vertebra between cervicals and dorsals; a trend that persists throughout the anterior and posterior dorsals. The posterior articular surface (cotyle) is dorsoventrally higher than the anterior condyle, (see Figure 9).

The condyle is of similar shape to that in PVL 4170 (7) (Figure 9A,B,C). The cotyle of this vertebra is well-preserved and has an oval, slightly dorsoventrally flattened shape, with a small concave recess at the base of the neural canal (Figure 9D).

On the ventral side of the centrum, the ventral keel and adjacent fossae are still clearly visible (Figure 9F). In lateral view, the ventral margin of the centrum is strongly concave in the first half of its length (slightly damaged but still visible) and in the posterior part becomes more convex and robust (Figure 9F). The ventral keel extends over the first 1/3 of the length, as in the other vertebrae, and then becomes a bulge, adding to the convexity of the posterior ventral end of the centrum. In lateral view, the pleurocoels of either side show a cut through the centrum, creating a foramen (Figure 9A,B). This supports the observation that the pleurocoels are very deep in the cervicals of *Patagosaurus*, and that they are normally only separated from the adjacent pleurocoel by a very thin midline septum (Carballido and Sander, 2014), which in this vertebra did not preserve. The parapophyses are present as rounded to triangular extensions on the lateral sides of the condylar rim (Figure

9F). They are not clearly visible in anterior or lateral view, but are visible in ventral view. At the base of the prezygapophyseal stalks, however, similar triangular protrusions exist (Figure 9C).

The centroprezygapophyseal laminae project slightly laterally from the centrum (Figure 9A,B). The prezygodiapophyseal fossae are larger than in previous vertebrae, due to the wider lateral projection of the diapophyses. These fossae are triangular in shape (Figure 9C). The prezygapophyses are roughly square with rounded edges in dorsal view. The spinoprezygapophyseal fossa is very deep. The prezygodiapophyseal laminae are prominently developed as sinusoidal thick laminae, supporting the prezygodiapophyseal laminae from below and from the lateral side, and supporting the diapophyses anteriorly. The prezygapophyseal articular surfaces are flat and axially longer than in previous vertebrae (Figure 9E). The angle of lateral expansion of the spinoprezygapophyseal laminae however, is greater than in previous vertebrae.

In posterior view, the postzygapophyses project to the lateral side (Fgure 9D). The tpols do not meet, but run down parallel in the dorsoventral plane to the neural canal. A faint right cpol seems to be present in this vertebra, however, it could also be an anomaly of the pocdf. This elongates the spinopostzygapophyseal fossa. The postzygodiapophyseal laminae project dorsally and posteriorly in a high angle. Towards about 2/3rd of the total vertebral height these project in a straight line, after which they bend in a convex curve to the posterior side. The posterior centrodiapophyseal laminae make a similar bending curve towards the centrum, due to the elongation of the posterior neural arch. Prominent postzygocentrodiapophyseal fossae are present as shallow triangular fossae.

In dorsal view, as in PVL 4170 (7), the neural spine is transversely wide and axially short (Figure 9E). It is constricted towards the postzygapophyses so that it 'folds' posteriorly. In anterior view, the neural spine is ventrally more constricted than in the previous vertebra

(Figure 9C). It is more elongated dorsoventrally, and the neural spine is transversely overall less wide than the previous vertebra.

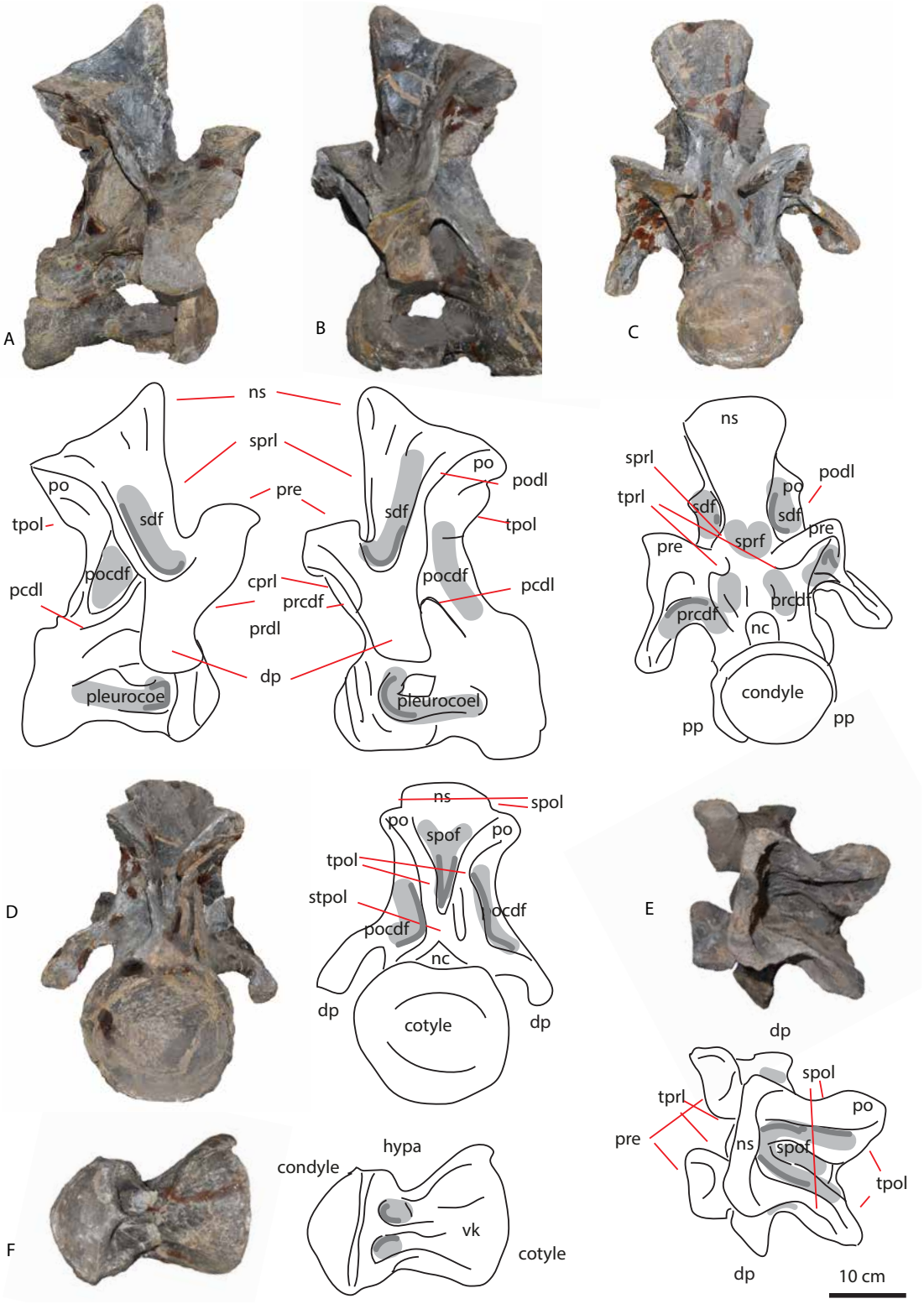

Figure 9 (previous page): Cervicodorsal PVL 4170 (8) in lateral (A,B), anterior (C), posterior (D), dorsal (E) and ventral(F) views. Abbreviations: acdl = anterior centrodiapophyseal lamina, cprl = centroprezygapophyseal lamina, cpol = centropostzygapophyseal lamina, dp = diapophysis, hypa = hypapophysis, nc = neural canal, ns = neural spine, pp = parapophysis, po = postzygapophysis, prcdf = prezygapophyseal centrodiapophyseal fossa, pocdf = postzygapophyseal centrodiapophyseal fossa, prdl = prezygapophyseal diapophyseal lamina, pre = prezygapophysis, sdf = spinodiapophysal fossa, spof = spinopostzygapophyseal fossa, spol = spinopostzygapophyseal lamina, sprf = spinoprezygapophyseal fossa, sprl = spinoprezygapophyseal lamina, tprl = intraprezygapophyseal lamina, tpol = intrapostzygapophyseal lamina, stpol = single intrapostzygapophyseal lamina, vk = ventral keel.

Dorsals

The holotype specimen has nine dorsals preserved, including a transitional cervicodorsal vertebra. Most neural arches and spines are conserved; except dorsal PVL 4170 (15) has only the centrum preserved. The centra become axially longer and dorsoventrally higher towards the posterior dorsals, and the centra also change from being opisthocoelus to amphicoelus. The pleurocoel, however, remains visible on the lateral side of the centrum throughout the dorsal series, but becomes more of an oval depression. Towards the posterior end of the dorsal column, the neural arches increase in height to twice that of the posterior cervicals. The neural spines become axially shorter and transversely broader, however, the posteriormost dorsals have protuberant neural spines that are nearly as high as the combined length of the neural arch and centrum. The neural canal becomes elongated dorsoventrally in the elongated neural arches, and is oval.

Anteriormost dorsals (PVL 4170 9-10) are already more elongated dorsoventrally than the cervicals, however, they are still opisthocoelous, and are morphologically distinct from the posterior dorsals, in that they have transversely wide neural spines, which are flattened axially. The neural canal is transversely wide and oval. The diapophyses are bent ventrally as in the cervicals, and the prezygapophyses are placed higher dorsally than the diapophyses.

Prezygapophyses are also directed obliquely dorsally. The hyposphene appears here, as a small, rhomboid structure, accompanied by very faint centropostzygapophyseal laminae which are embedded in the posterior neural arch. The hyposphene is a few cm more dorsal to the neural canal (about 5 cm). The spinopostzygapophyseal laminae flare out ventrally, giving the neural spine a broad exterior. As in the cervicals, the angle made between the postzygodiapophyseal laminae and the posterior centrodiapophyseal laminae is high.

Middle dorsals (PVL 4170 11-12) become more transversely slender in the neural arch, and the prezygapophyses have a more horizontally positioned articular surface. The transverse processes are also more elongated than the anterior dorsals. The pedicels become more elevated, and the neural spine more elongated dorsoventrally. The spinopostzygapophyseal laminae still flare out, but less posteriorly than in anterior dorsals, creating a more 'compact' neural spine complex.

At the transition from middle to posterior dorsals, anteriorly, the centroprezygapophyseal laminae lengthen as the neural arch and the pedicels elongate. Posteriorly, first the intrapostzygapophyseal laminae meet, then the centropostzygapophyseal laminae disappear, and instead a single intracentropostzygapophyseal lamina appears (see Table 2).

The posterior dorsals (PVL 4170 13-17) possess the most discriminating combination of features for *Patagosaurus*. The holotype posterior dorsals show an extensive elongation of the neural arch, both at the pedicels as well as at the neural spine. Elongation of the neural spine towards posterior dorsals is common for sauropods (e.g. *Cetiosaurus*, *Barapasaurus*, *Haplocanthosaurus, Omeisaurus,* (Hatcher, 1903; He et al., 1984; Upchurch and Martin, 2003; Bandyopadhyay et al., 2010), however this in combination with the elevation of the pedicels is not seen to this degree, save for *Cetiosaurus*, and then the elongation is still

higher in *Patagosaurus*. The elongation of the neural arch and pedicels is only seen in *Mamenchisaurus youngi* (Pi et al., 1996). The lateral elongation of the transverse processes is reduced. Next to being elongated, the pedicels also show a lateral, ragged sheet of bone that stretches from the base of the prezygapophyses to the ventral end of the centroprezygapophyseal laminae. This is seen in a more rudimentary form in *Cetiosaurus* (Upchurch and Martin, 2003, OUMNH J13644/2). The relatively horizontal lateral projection of the transverse processes also distinguishes *Patagosaurus* from many (more or less) contemporary basal eusauropods, as these tend to project more dorsally in *Cetiosaurus*, *Mamenchisaurus*, *Omeisaurus*, and *Haplocanthosaurus* (Hatcher, 1903; Young and Zhao, 1972; Pi et al., 1996; Tang et al., 2001; Upchurch and Martin, 2002, 2003). In anterior view, the neural arch is characterized by two dorsoventrally elongated oval excavations; the centroprezygapophyseal fossae, which are separated by a single intraprezygapophyseal lamina. The single intraprezygapophyseal lamina runs down to the dorsal rim of the neural canal. This is also seen in *Cetiosaurus oxoniensis* OUMNH J13644/2, and to some extent in *Tazoudasaurus* (Allain and Aquesbi, 2008), and Spinophorosaurus (Remes et al., 2009), howecer, in these taxa, this lamina is shorter, as the neural arch is less dorsoventrally elongated. In *Patagosaurus* dorsals, the neural canal itself is also dorsoventrally elongated and oval, this is also seen in *Cetiosaurus oxoniensis* OUMNH J13644/2, although not to the extent of *Patagosaurus*. It is not slit-like however, as seen in *Amygdalodon* (Rauhut, 2003; Carballido et al., 2011) and *Barapasaurus* ISIR 700 (Bandyopadhyay et al., 2010). In posterior view, the spinopostzygapophyseal laminae remain close to the body of the neural spine, i.e. they do not flare out laterally as in the anterior and mid-dorsals. The hyposphene is prominently visible below the postzygapophyses, which now are aligned at 90° with the neural spine, and have a horizontal articular surface. Posteriorly, during the transition from mid- to posterior dorsals, the intrapostzygapophyseal lamina becomes shorter, and eventually dissapears as the postzygapophyses approach each other medially. Instead, the

spinopostzygapophyseal laminae split into the medial and lateral spinopostzygapophyseal laminae (see Table 2). The postzygodiapophyseal laminae include the lateral spinopostzygapophyseal laminae. The single intrapostzygapophyseal lamina continues to run down to the hyposphene. Posterior dorsals have a very rudimentary aliform process, sensu Carballido and Sander, (2014).

The most noted autapomorphy of *Patagosaurus* is the presence of paired centrodiapophyseal fossae, or fenestrae, which appear from dorsals PVL 4170 13 onwards. It was long thought that these were connected to the neural canal, however, recent CT data reveals that a a thin septum separates the adjacent fenestrae from each other, and from the neural canal, ventrally these fenestrae form a central chamber, still well above the neural canal (see PVL 4170 13).

Dorsal PVL 4170 (9)

Anterior-mid dorsal with the centrum drastically reduced in anteroposterior length, making it stouter than the cervicals, but still clearly opisthocoelous., see Figure 10. The left diapophysis, neural arch and part of the neural spine are partially reconstructed.

The condyle has a slightly pointed protrusion on the midpoint, as in the cervicals (See Figure 10A,B, F). Ventrally, the centrum constricts strongly immediately posterior to the anterior condyle (Figure 10F). The ventral keel marginally visible, and exists more as a scar running down the midline from the small hypapophysis. The ventral side of the posterior cotyle is slightly deformed, with the left lateral end projecting further than the right. As in the other ventral posterior surfaces of the vertebrae, the lateral ends flare out slightly further posteriorly than the axial midpart (Figure 10 A,B,F).

The neural canal in anterior view is subtriangular in shape, and transversely wider than dorsoventrally high (Figure 10C). Directly above it, there is a small protrusion present of the hypapophysis. In posterior view, the shape of the neural canal is similar, however, the posterior opening is less triangular and more rounded (Figure 10D).

The neural arch of this vertebra is still transversely wide, as in the cervicals, however, it is also becoming dorsoventrally higher (See Figure 10A,B,C,D). Because of this, the centroprezygapophyseal fossae, which are placed medially to the prezygapophyseal stalks, are not as deep as in the cervicals (Figure 10C). In lateral view, the prezygapophyseal pedestals are directed nearly vertically in the dorsoventral plane (Figure 10A,B).

The prezygapophyses are leaning slightly medially and ventrally towards the single intraprezygapophyseal lamina that runs along the midline of the vertebral neural arch on the anterior side (Figure 10C). In dorsal view, the prezygapophyses are subtriangular in shape and are widely spaced apart, with about 1/3rd of the spinal summit width between them (Figure 10E).

The postzygapophyses are raised even higher dorsally in this anterior dorsal than in the cervicals, at about 2/3rd of the height of the neural spine (Figure 10A,B,D). Consequently, the postzygadiapophyseal laminae are more elongated and makes a high angle, of about 130°, with respect to the axial plane and to the posterior centrodiapophyseal lamina. Both podl's are slightly arched towards the postzygapophyses (Figure 10A,B). Because of the extension of the postzygadiapophyseal lamina, the posdf takes in a large portion of the posterior lateral surface of the vertebra (Figure 10A,B). The tpols in posterior view are prominent, convexely curving laminae, which meet right above the posterior neural canal. In lateral view, the tpols show a triangular recess below the postzygapophyses, after which the tpols expand posteriorly before meeting the hypopshene dorsal to the neural canal (Figure 10D).

In this vertebra, the cpol's are no longer clearly visible, and indeed, only the left cpol is seen as a thin lamina on the neural arch, lateral and ventral to the left tpol (Figure 10D). Here, a rudimentary hyposphene is present as a small teardrop-shape ventral to the ventral fusion of the tpols. The fusion of the tpols and the hyposphene are also visible as a triangular protruding complex in dorsal view.

The right diapophysis is prominent in anterior, posterior and lateral view as a stout, lateroventrally positioned element (Figure 10A,B,C,D). It is transversely broader than in the cervicals. In anterior view, the prdl and acdl/pcdl are all positioned in an inverted V-shape

with oblique angles of about 45° to the horizontal. In anterior view, the cprl divides the cprf neatly from the prcdf, which is similarly inverted V-shaped as the outline of the diapophyseal laminae (Figure 10C). In posterior view, the pocdf is confluent with the posterior flat surface of the diapophysis (Figure 10D). The posterior centrodiapophyseal lamina in posterior view, curves convexly towards the ventral side of the vertebra.

The articular surface of the diapophysis is flat to concave, and rounded to rectangular in shape. Posteriorly, they show small, elliptic depressions, on the distal end of the diapophyses (Figure 10D).

Note that the spinoprezygapophyseal laminae are reconstructed, and will not be discussed here. The spinopostzygapophyseal laminae are clearly seen in anterior view; they flare out transversely in a steep sloping line (Figure 10C). The spinopostzygapophyseal laminae are rugose, and the intrapostzygapophyseal laminae as well, these appear ragged in lateral view. In this anterior dorsal, the spinopostzygapophyseal fossae are more rectangular than in the cervicals, and also more deep (Figure 10D).

The neural spine is constricted transversely around the dorsoventral midlength, and fans out transversely towards the summit. The spine summit consists of a thick transverse ridge, which folds posteriorly on each lateral side, before smoothly transitioning to the spols (Figure 10E). The neural spine summit is positioned higher dorsally in this anterior dorsal than in the cervicals (so that the spinopostzygapophyseal laminae are consequently more elongated).

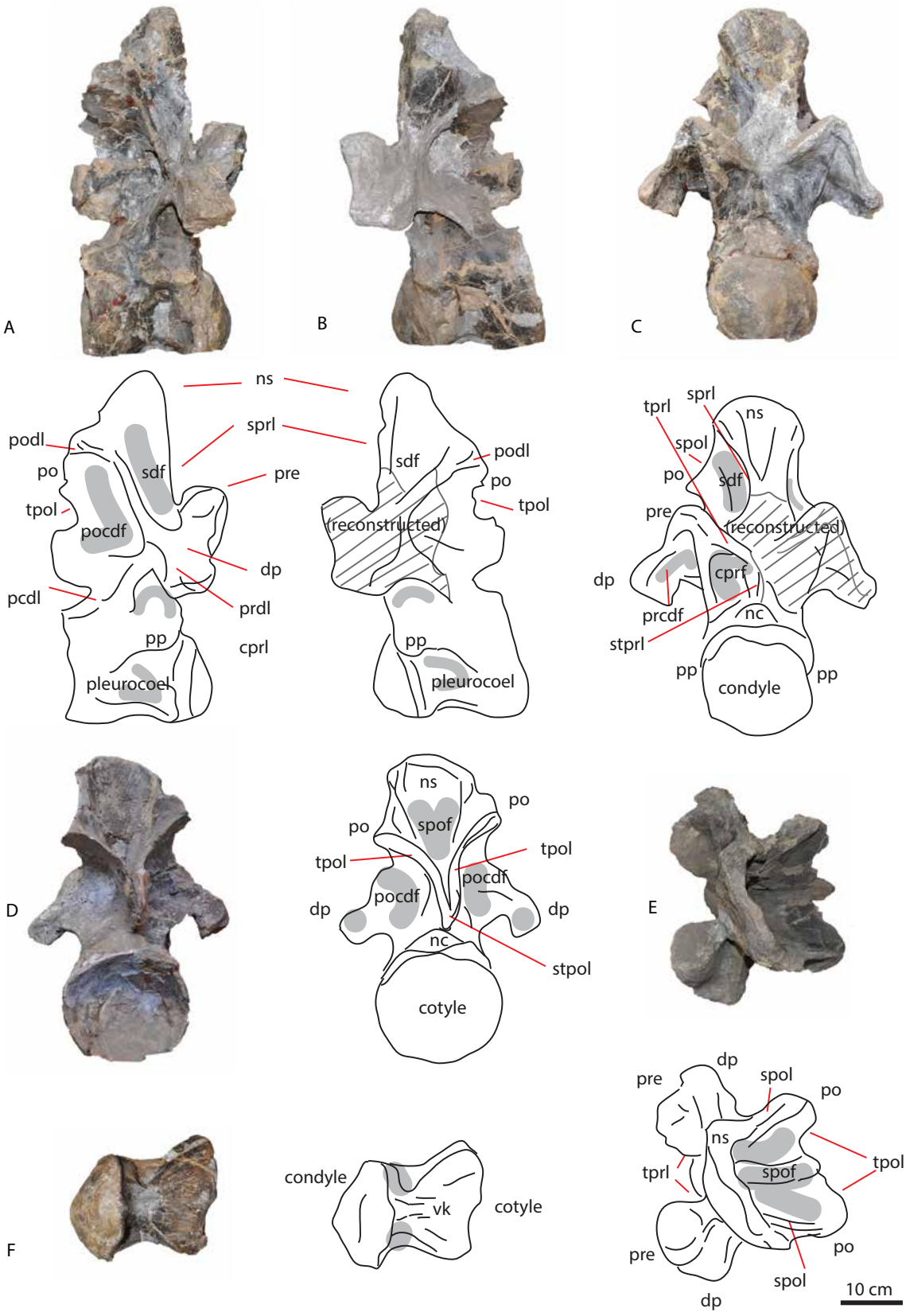
A
B
C
ns
sprl
podl
po
sdf
pre
tpol
pocdf
dp
pcdl
prdl
pp
cprl
pleurocoel
sdf
podl
po
tpol
(reconstructed)
pp
pleurocoel
tprl
sprl
ns
spol
po
sdf
pre
(reconstructed)
dp
cprf
prcdf
nc
stprl
pp
condyle
pp
D
E
ns
po
po
spof
tpol
tpol
pocdf
pocdf
dp
dp
nc
stpol
cotyle
F
condyle
vk
cotyle
dp
pre
spol
po
ns
tpol
tprl
spof
pre
po
spol
dp
10 cm

Figure 10 (previous page): Dorsal PVL 4170 (9) in lateral (A,B), anterior (C), posterior (D), dorsal (E) and ventral (F) views. Note part of this vertebra is reconstructed. Abbreviations: acdl = anterior centrodiapophyseal lamina, cprl = centroprezygapophyseal lamina, cpol = centropostzygapophyseal lamina, dp = diapophysis, hypa = hypapophysis, nc = neural canal, ns = neural spine, pcdl = posterior centrodiapophysesal lamina, pp = parapophysis, po = postzygapophysis, prcdf = prezygapophyseal centrodiapophyseal fossa, pocdf = postzygapophyseal centrodiapophyseal fossa, prdl = prezygapophyseal diapophyseal lamina, pre = prezygapophysis, sdf = spinodiapophysal fossa, spof = spinopostzygapophyseal fossa, spol = spinopostzygapophyseal lamina, sprf = spinoprezygapophyseal fossa, sprl = spinoprezygapophyseal lamina, tprl = intraprezygapophyseal lamina, tpol = intrapostzygapophyseal lamina, stpol = single intrapostzygapophyseal lamina, stprl = single intrapostzygapophyseal lamina, vk = ventral keel.

Dorsal PVL 4170 (10)

This partially reconstructed anterior-middle dorsal (Figure 11) is slightly taphonomically distorted, in that the right transverse process is bent slightly more ventrally, and the neural spine is slightly tilted to the left side (see Figure 11). Parts of the centrum, the middle anterior part of the neural arch, and ventral parts of the diapophyses are partially reconstructed.

The centrum is still slightly opisthocoelous in lateral view, as in PVL 4170 (9), and as in the cervicals,, with the characteristic stout rim cupping the anterior condyle (Figure 11A,B). It is noteworthy however, that the centrum and neural arch do not entirely match, possibly due to this vertebra being partially reconstructed. The centrum in ventral view is transversely constricted posterior to the rim that cups the condyle (Figure 11F). The rim stands out transversely from the centrum body. The parapophyses are located dorsal to this this expansion, as triangular protrusions. The cotyle in posterior view is concave, and is slightly transversely wider than dorsoventrally high.

The neural arch transversely narrows slightly, dorsal to the parapophyses (both at its anterior and posterior side) (Figure 11C). The anterior neural canal is embedded in this narrowing, and is rounded to rectangular in shape. It is less wide transversely as in the posterior cervicals (Figure 11C). The posterior neural canal is equally rectangular to rounded in shape. About 5 cm dorsal to it, the hyposphene is present as a rhomboid, small structure (Figure 11D).

The diapophyses in this dorsal are creating a wider angle with respect to the horizontal than in the last dorsal PVL 4170 (9), see Figure 11C,D. The prdl, the acdl, and posteriorly, the pcdl, all arch into a less oblique angle, creating an inverted V-shape of about 50°. (note that the right diapophysis is slightly distorted due to taphonomical damage). The diapophyseal articular surface is triangular, with the tip pointing ventrally, and the flat surface pointing dorsally, in lateral view (Figure 11A,B). Ventral to the diapophyses, in lateral view, the anterior and posterior centrodiapophyseal laminae are more or less equally distributed in length and spacing on the lateral surface of the neural arch. A roughly triangular but deep centrodiapophyseal fossa can be seen between these laminae.

The prezygapophyses in dorsal view make a wide wing-like structure together with the diapophyses and the prezygodiapophyseal laminae (Figure 11E). There is a U-shaped, wide recess between the prezygapophyses. In anterior view, the prezygapophyses stand widely apart from one another, and are supported by stout centroprezygapophyseal laminae, creating stout pedicels that expand laterally above the centrum, dorsal to a slight recess right above the centrum (Figur 11C). The articular surface of the prezygapophyses is rounded to rectangular in shape, and in anterior view is tilted ventrally towards the midline of the vertebra (Figure 11C,E). The prezygapophyseal spinodiapophyseal fossae are present between the prezygapophyseal pedicels, on the neural arch. They are rounded to

rectangular ins hape, dorsoventrally elongated, and shallow, the deepest point being near the onset of the spinoprezygapophyseal laminae (Figure 11C).

The postzygapophyseal articular surfaces are obliquely offset from the hyposphene. The articular surfaces are roughly triangular in shape (Figure 11D). In posterior view, the intrapostzygapophyseal laminae are distinctly flaring out from the dorsal end of the hyposphene to the postzygapophyses. The cpols are present only as very faint, low ridges embedding the hyposphene on the lateral side (Figure 11D). The postzygodiapophyseal lamina is short and stout, therefore dramatically reduced in length and angle compared to dorsal PVL 4170 9 (Figure 11A,B), leading to believe at least one dorsal between PVL 4170 (9) and (10) should have existed. The spinopostzygapophyseal fossa is deeply excavated, occupying about 1/3rd of the transverse length of the neural spine (Figure 11D,E). The postzygapophyseal centrodiapophyseal fossae are shallow, and only a bit more excavated near the ventral rim of the postzygapophyseal pedicels.

The spinoprezygapophyseal laminae run from the top of the spine to the prezygapophyses in an oblique angle of about 40°. They flank the entire length of the neural spine, creating roughly a V-shape (Figure 11C,E). The spinopostzygapophyseal laminae are clearly visible in anterior view in this vertebra, as they flare out laterally from the neural spine, giving the neural arch and spine a triangular appearance.

In anterior view, the neural spine is roughtly V-shaped, with a transversely broad dorsalmost rim (Figure 11C). In posterior view, the neural spine combined with spinopostzygapophyseal laminae and postzygapophyses are slightly bell-shaped. The neural spine tapers dorsally to a point, exposing a stout rim. In dorsal view, the neural spine summit is clearly seen as an anteroposteriorly thin rim, transversely wide, reaching to the level of the onset of the postzygapophyses (Figure 11E).

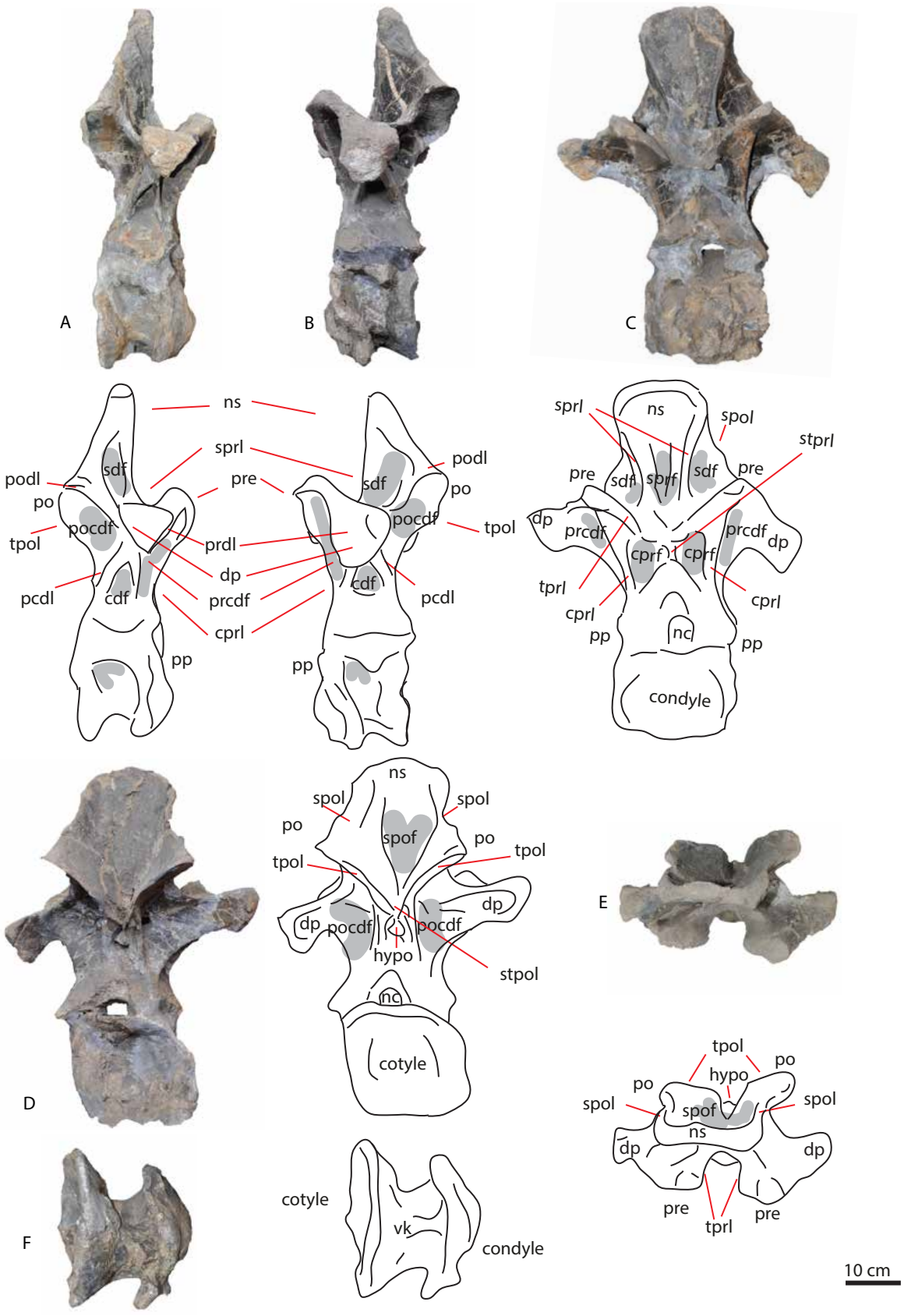
A
B
C
ns
sprl
podl
sdf
pre
po
pocdf
tpol
prdl
dp
pcdl
cdf
prcdf
cprl
pp
sprl
ns
spol
stprl
pre
sdf
sprf
sdf
pre
dp
prcdf
prcdf
dp
cprf
cprf
tprl
cprl
cprl
pp
nc
pp
condyle
D
ns
spol
spol
po
spof
po
tpol
tpol
dp
dp
pocdf
pocdf
hypo
stpol
nc
cotyle
E
tpol
po
hypo
po
spol
spof
spol
ns
dp
dp
pre
pre
tprl
F
cotyle
vk
condyle
10 cm

Figure 11 (previous page): MACN-CH 4170 (10) dorsal vertebra in lateral (A,B) anterior (C), posterior (D), dorsal (E) and ventral (F) views. Abbreviations: acdl = anterior centrodiapophyseal lamina, cdf = centrodiapophyseal fossa, cprl = centroprezygapophyseal lamina, dp = diapophysis, hypa = hypapophysis, nc = neural canal, ns = neural spine, pcdl = posterior centrodiapophyseal fossa, pp = parapophysis, po = postzygapophysis, prcdf = prezygapophyseal centrodiapophyseal fossa, pocdf = postzygapophyseal centrodiapophyseal fossa, prdl = prezygapophyseal diapophyseal lamina, pre = prezygapophysis, sdf = spinodiapophysal fossa, spof = spinopostzygapophyseal fossa, spol = spinopostzygapophyseal lamina, sprf = spinoprezygapophyseal fossa, sprl = spinoprezygapophyseal lamina, tprl = intraprezygapophyseal lamina, tpol = intrapostzygapophyseal lamina, stpol = single intrapostzygapophyseal lamina, stprl = single intrapostzygapophyseal lamina, vk = ventral keel.

Dorsal PVL 4170 (11)

Partially reconstructed dorsal; the centrum is a replica, which will not be described. The neural arch and spine and transverse processes, however, are original, see Figure 12. The diapophyses of this vertebrae are elongated laterally compared to the other dorsals, and the transition between this and the previous and next vertebrae, leads to believe a transitional dorsal could have existed originally.

The neural arch is mainly shaped by the acdl in anterior view, and the pcdl in posterior view. It is about as long and wide, as PVL 4170 (10), see Figure 12A,B. The neural canal in anterior view is rounded to rectangular in shape, with a dorsoventral elongation (Figure 12C). The posterior neural canal is more flattened, and triangular to round in shape. The hyposphene is seen as a small rhomboid structure, about 5 cm dorsal to the posterior neural canal (Figure 12D).

In this dorsal, the diapophyses are more prominent and extend wider transversely than in previous dorsals (Fig2C,D). Their shape in anterior and posterior view is near rectangular. They are directed laterally and slightly ventrally in anterior view (Figue 12C). The articular

surface of the diapophyses is more rounded than triangular (Figure 12A,B). The diapophyses in posterior view are slightly expanded towards their extremities (Figure 12D). The posterior centrodiapophyseal laminae are slightly damaged and have a frayed appearance, but arch convexly towards the transverse processes.

The prezygapophyses are more or less perpendicularly placed towards the neural spine, and slightly canted medially in anterior view (Figure 12C). Their articular surface lies in the dorsal plane. The articular surface of the prezygapophyses is roughly square in shape (Figure 12E). In dorsal view, a U-shaped recess is seen between the prezygapophyseal articular surfaces. The prezygodiapophyseal laminae are stout and run in a convex arch transversely to the diapophyses. In this vertebra, the single intraprezygapophyseal lamina (stprl) is visible, as the interprezygapophyseal laminae (tprl) run down in a curved V-shape towards the neural canal (Figure 12C). The paired centroprezygapophyseal fossae, positioned laterally to the stprl, are more excavated than in previous dorsals, and also have a more defined rim.

The postzygapophyses are more pronounced in this vertebra than in previous dorsals, and also protrude posteriorly more than in previous dorsals (Figure 12D). Their articular surface is triangular in shape. There is a similar U-shaped recess between the postzygapophyses, though not as wide, as with the prezygapophyses (Figure 12C,D). The tpols are shorter in this vertebra, as they do not reach as far down ventrally to reach the hyposphene. Below the tpols, two cpols are seen to strut the hyposphene on lateral sides. The triangular and shallow pocdf's are positioned on each lateral side of the cpols, and ventral to the tpols (Figure 12D).

The neural spine is transversely wide and anteroposteriorly short, but protrudes out posteriorly at both lateral sides and on the midline (Figure 12D). This midline could be a rudimentary scar of a postspinal lamina, but that is not clearly visible. In anterior view, the

neural spine resembles that of PVL 4170 10, however the neural spine is more dorsoventrally elongated, and the spinopostzygapophyseal laminae are more dented than straight as they run down to the postzygapophyses. The morphology of the neural spine posteriorly, towards the postzygapophyses is similar to PVL 4170 10 in that the composition looks bell-shaped in posterior view, and the posterior half contains a deep V-shaped spof. The neural spine is more dorsally elevated however, and the summit is less transversely broad than in the previous dorsal (Figure 12E).

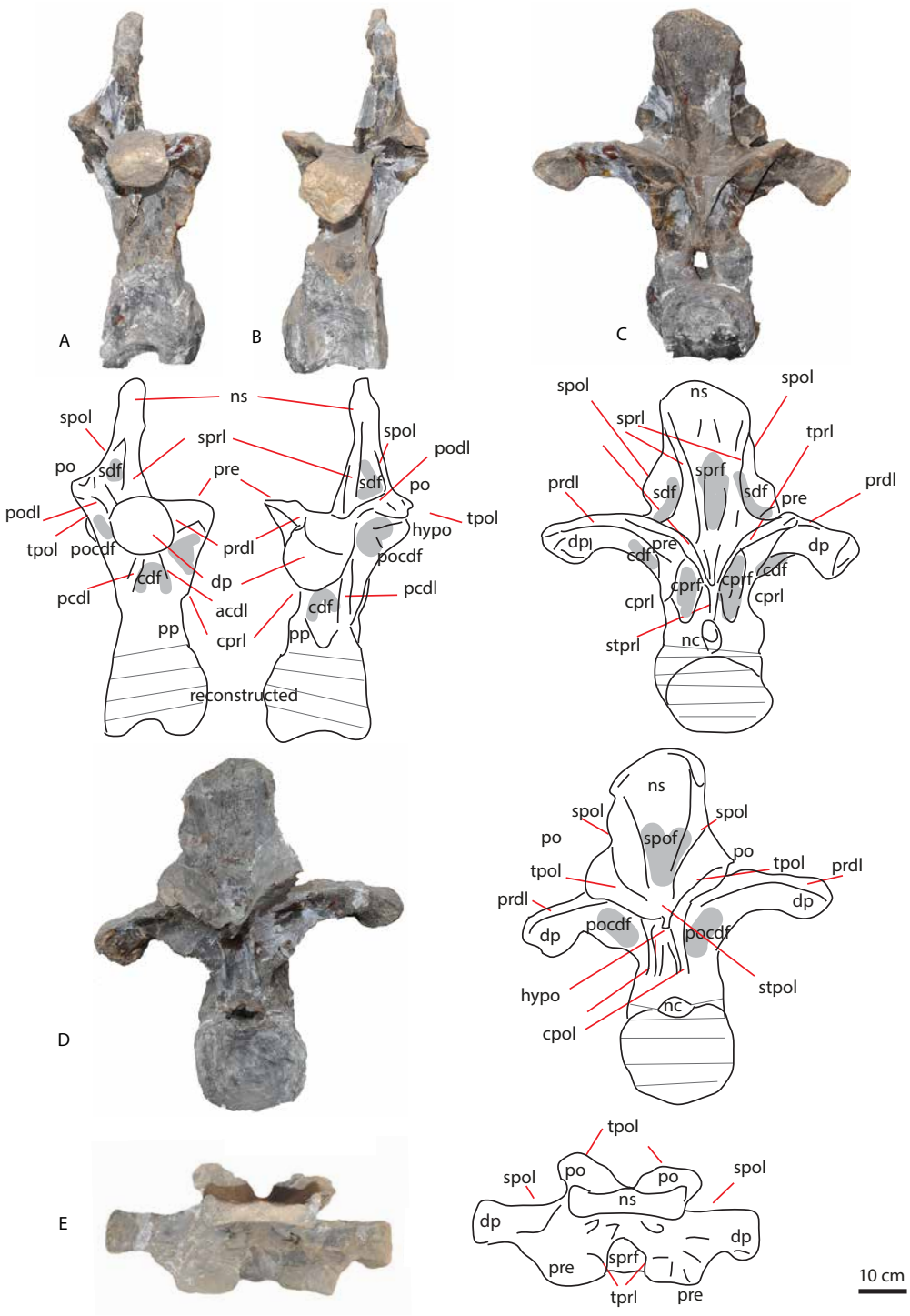

Figure 12: Dorsal MACN-CH 4170 (11) in lateral (A,B) anterior (C), posterior (D), and dorsal (E) views. Note that the centrum is reconstructed, and a ventral view is therefore not given. Abbreviations: acdl = anterior centrodiapophyseal lamina, cdf = centodiapophyseal fossa, cpol = centropostzygapophyseal lamina, cprl = centroprezygapophyseal lamina, dp = diapophysis, hypa = hypapophysis, nc = neural canal, ns = neural spine, pcdl = posterior centrodiapophyseal lamina, pp = parapophysis, po = postzygapophysis, prcdf = prezygapophyseal centrodiapophyseal fossa, pocdf = postzygapophyseal centrodiapophyseal fossa, prdl = prezygapophyseal diapophyseal lamina, pre = prezygapophysis, sdf = spinodiapophysal fossa, spof = spinopostzygapophyseal fossa, spol = spinopostzygapophyseal lamina, sprf = spinoprezygapophyseal fossa, sprl = spinoprezygapophyseal lamina, tprl = intraprezygapophyseal lamina, tpol = intrapostzygapophyseal lamina, stpol = single intrapostzygapophyseal lamina, stprl = single intrapostzygapophyseal lamina, vk = ventral keel.

Dorsal PVL 4170 (12)

Mid-posterior dorsal with partially reconstructed neural spine (which will therefore be omitted from description). The transition from middle to posterior dorsals is perhaps the most drastic morphological transition in *Patagosaurus* (see Figure 13).

The centrum is clearly opisthocoelous, though the condyle is not as convex as in previous anterior dorsals (Figure 13A,B). The centrum is posteriorly still wider transversely than anteriorly. The condyle still has a rugose rim, as in the cervicals. The parapophyses are positioned on the dorsolateral side of this rim, and are visible as rounded rugose protrusions. The pleurocoel is still clearly visible, and has a deep, rounded dorsal rim, and a clear rectangular posterior rim. The ventral side of the cotyle extends further posteriorly than the dorsal side (Figure 13E). The cotyle is heart-shaped in posterior view, with a rounded 'trench' below the neural canal (Figure 13D). In ventral view, the centrum is not as constricted as in previous vertebrae; even though there is still a slight constriction posterior to the rim of the condyle. The ventral keel is no longer present.

The neural canal in anterior view is elongated to an oval to teardrop shape, which is dorsoventrally longer than transversely wide (Figure 13C). The neural canal in posterior view is oval to rectangular in shape, and is also dorsoventrally elongated.

The neural arch in this dorsal is rather rectangular and straight in anterior and posterior view, widens axially in lateral view, towards the prezygapophyses (Figure 13 A,B,C,D). A fenestra is formed instead of the centrodiapophyseal fossa. The centrodiapophyseal laminae run smoothly in a convex curve towards the centrum.

The pedicels of the prezygapophyses are stout, and expand laterally towards the ventral side of the prezygapophyses (Figure 13C). The intraprezygapophyseal laminae meet ventrally and at the midpoint between the prezygapophyses, where a rudimentary hypantrum is formed, below which a single intraprezygapophyseal lamina runs down to the dorsal roof of the neural canal. This lamina separates two parallel, rhomboid, deep centroprezygapophyseal fossae.

In posterior view, the postzygapophyses form a wide V-shape, and the tpols meet dorsal to a small diamond-shaped hyposphene, below which a stpol runs down to the neural canal, which is oval and dorsoventrally elongated (Figure 13D). The podl is a sharply curved, short lamina, not to be confused with the spdl, which is not present in this vertebra (Figure 13A,B). Two parallel cpols might be present, but this is not entirely clear as the posterior part of this vertebra is partially reconstructed (Figure 13D).

In anterior view, the diapophyses are no longer ventrally and laterally positioned, but dorsally and laterally, in an oblique angle dorsally (Figure 13C). In lateral view, posterior centrodiapophyseal lamina runs in a sinusoidal shape down from the diapophysis to the neural arch, while the prdl is convex (Figure 13A,B). The diapophyses extend a bit further ventrally in a subtriangular protrusion. The diapophyses are slightly excavated between the podl and the pcdl. In dorsal view, the diapophyses are seen to extend to nearly the entire width of the centrum (Figure 13F). They are slightly pointed posteriorly as well.

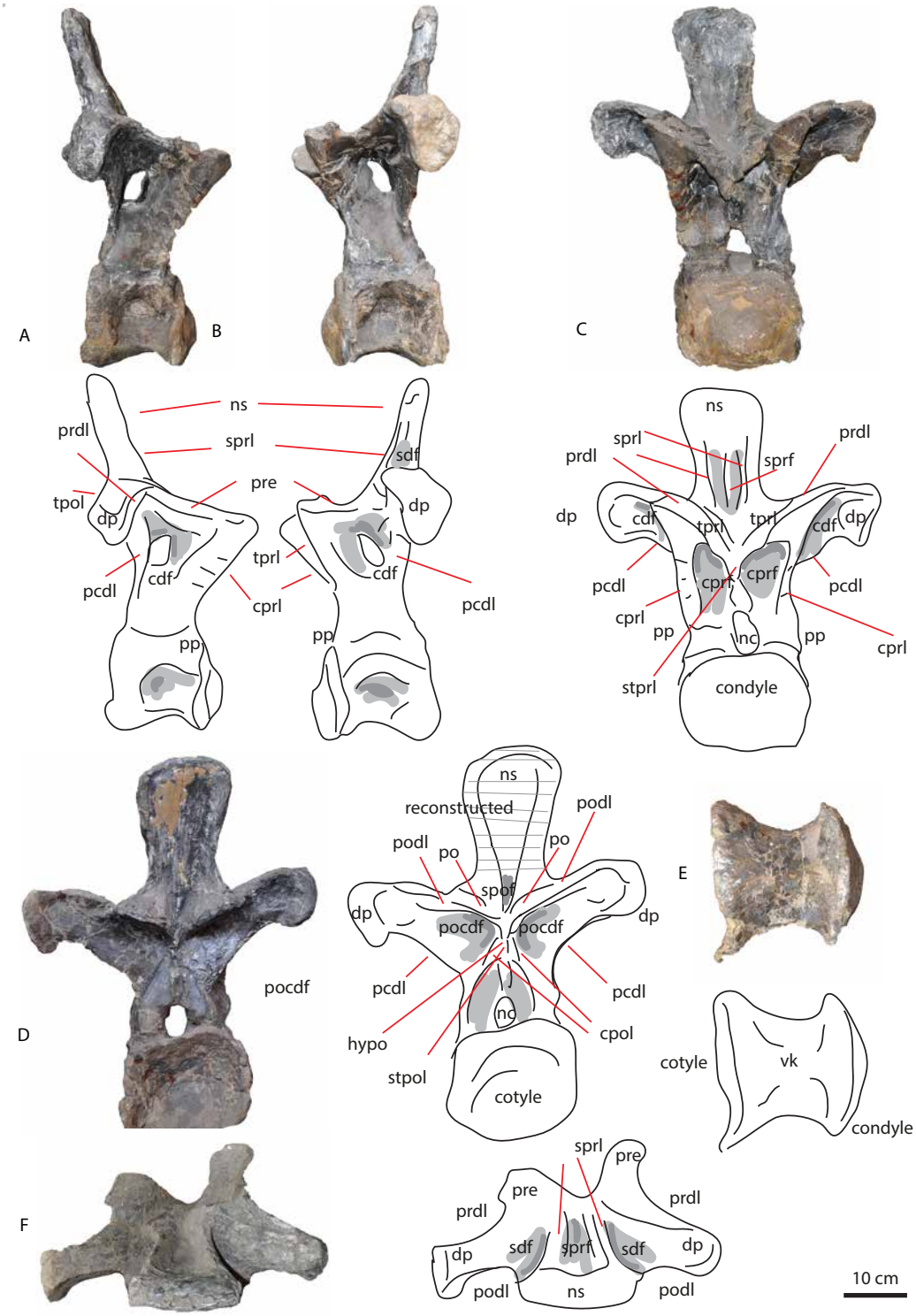

Figure 13: Dorsal MACN-CH 4170 (12) in lateral (A,B) anterior (C), posterior (D), ventral (E) and dorsal (F) views. Note that a large part of the posterior neural arch and spine is reconstructed. Abbreviations: acdl = anterior centrodiapophyseal lamina, cprl = centroprezygapophyseal lamina, dp = diapophysis, hypa = hypapophysis, nc = neural canal, ns = neural spine, pcdl = posterior centrodiapophyseal lamina, pp = parapophysis, po = postzygapophysis, prcdf = prezygapophyseal centrodiapophyseal fossa, pocdf = postzygapophyseal centrodiapophyseal fossa, prdl = prezygapophyseal diapophyseal lamina, pre = prezygapophysis, sdf = spinodiapophysal fossa, spof = spinopostzygapophyseal fossa, spol = spinopostzygapophyseal lamina, sprf = spinoprezygapophyseal fossa, sprl = spinoprezygapophyseal lamina, tprl = intraprezygapophyseal lamina, tpol = intrapostzygapophyseal lamina, stpol = single intrapostzygapophyseal lamina, stprl = single intrapostzygapophyseal lamina, vk = ventral keel.

Dorsal PVL 4170 (13)

This is the most complete posterior dorsal of the holotype.

The anterior articular surface of the centrum is oval in anterior view, with a slight constriction at about two-thirds of the dorsoventral height. Consequently, the ventral side is transversely wider than the dorsal side. In posterior view, the posterior articular surface of the centrum is heart-shaped at its dorsal side, and flattened on its ventral side. The articular surface itself is slightly oval, and is constricted towards the upper 1/3rd as in the anterior side. In ventral view, the centrum is more or less equally flaring out at each articular surface, and slightly constricted in the midpoint. No keel is visible, but on the anterior ventral side of the centrum, a small triangular 'lip' is seen. In lateral view, the centrum is ventrally concave, with the posterior ventral side expanding further ventrally than the anterior side. There is a slight depression on the lateral side of each centrum.

The dorsal anterior side of the centrum is expanding a bit further anteriorly beyond the pedicels of the neural arch, but the dorsal posterior side of the centrum expands considerably further posteriorly from the neural arch.

The parapophyses are not clearly visible in anterior view, however, they are visible in lateral and ventral view as rugose oval protrusions on the rugose lateral sides of the cprls.

In anterior view, the neural canal is clearly visible in this specimen. It is oval and dorsoventrally much more elongated than in the previous vertebrae. It is transversely narrow, and slightly above the midpoint is constricted, so that the neural canal looks like a figure 8-shape. The neural canal is not clearly visible in posterior view, however, the neural arch is excavated in a triangular shape around the neural canal. It is surrounded by stout centropostzygapophyseal laminae. Dorsal to this depression, the stpol supports the rhomboid hyposphene from below (see description of postzygapophyses).

The neural arch itself is ventrally restricted transversely. The pedicels of the neural arch are equally dorsoventrally elongated and transversely narrow. The anterior side of the neural arch is characterised by a dorsoventrally oriented, long single intraprezygapophyseal lamina, dividing two mirror image, shallow, oval to bean-shaped centroprezygapophyseal fossae. The lateral sides of the neural arch tilt towards the midline in posterior view, giving the neural arch a constricted look towards its dorsal end. On the lateral side of the neural arch, the centrodiapophyseal foramen is visible as a dorsoventrally elongated oval, opening slightly posterior to the midpoint of the neural arch.

The diapophyses project laterally in a near perpendicular angle from the neural arch. They are ventrally excavated, with the prezygodiapophyseal laminae running concavely from the lateral side of the prezygapophyses to the diapophyses. In dorsal view, the diapophyses are seen to bend slightly posteriorly as well as laterally. The tips point sharply to the posterior side. The diapophyseal articular surfaces are triangular, with a rounded posterior rim, in lateral view. The dorsal distal ends of the diapophyses have a small triangular protrusion, projecting dorsally, in anterior view. The diapophyses show round excavations on the posterior side of their distal ends. The ventral side of the diapophyses is also concavely curved with a concave paradiapophyseal lamina running parallel to the prdl. The posterior centrodiapophyseal laminae curve concavely from the diapophyses down to the ventralmost side of the neural arch. These sustain a thin sheet of bone that holds the diapophyses on each lateral side in posterior view.

.

The prezygapophyses are transversely shorter than in previous dorsals, and are stout; almost as thick dorsoventrally as transversely. They tilt at an oblique angle anteriorly and dorsally from this narrow arch. The prezygapophyseal articular surfaces are horizontally aligned in the axial plane, and are near perpendicular to the neural spine. In dorsal view,

prezygapophyses are directed mostly anteriorly, and there is a deep U-shaped recess between them. On the lateral side of the prezygapophyses, running from the lateral ends of the centrodiapophyseal fossae, the centroprezygapophyseal laminae are characterized by laterally flaring, rugose, rugged bony flanges, that spread anteriorly as well as laterally. In anterior and lateral view, prdl and the ppdl run parallel in a convex arch at the ventral end of the neural spine. They are equally thin and dorsoventrally flattened.

The postzygapophyses are triangular in shape, and are positioned slightly more dorsally on the neural arch than the prezygapophyses. The postzygapophyses are flat to slightly convex on articular surface, seen from lateral and ventral view. The single intrapostzygapophyseal lamina tapers dorsally and posteriorly in an oblique angle from the rhomboid hyposphene to the neural arch. The postzygapophyses are not visible in lateral view as they are obscured by the diapophyses. The postzygapophyses connect with the diapophyses through a strongly bending postzygodiapophyseal lamina, which is often mistaken for a spinodiapophyseal lamina (Wilson, 2011a, Carballido and Sander, 2014).

In this dorsal, the prdl and the podl are seen to support wide, but thin plates of bone between the prezyga- dia- and postzygapophyses.

The neural spine is roughly cone-shaped, and is constricted toward the summit both anteriorly and posteriorly. In anterior view, the spinoprezygapophyseal laminae flare out towards the ventral contact of the prezygapophyses. The sprls are seen as sharply protruding thin laminae. The sprdfs, bordered by the sprls, are visible as deep triangular depressions in dorsal view. The neural spine shows a triangular excavated prezygospinodiapophyseal fossa on each lateral side, which have clear posterior rims.

Similar to the sprls, in posterior view, the spinopostzygapophyseal laminae are seen to flare out towards the ventral side of the neural spine. In this dorsal, the spol has divided into a lateral spol and medial spol, visible as running from the ventral one-third of the neural spine to the postzygapophyses. On the midline between these laminae, a deep but transversely narrow rudimentary spof is present. The lateral spols flare out on the lateral sides, giving the spine a 'rocket-shape' in posterior view. A slight transverse thickening of this stout lateral spinopostzygodiapophyseal lamina is visible at about two-thirds of the spinal dorsoventral length.

On the dorsoventral midline of the spine, in posterior view, a rough scar is visible, which could be a very rudimentary postspinal lamina.

The spine itself tilts very slightly posteriorly, especially the most distal one-third part. This distal end is solid, and cone-shaped, with a rounded summit. The spine summit has a slight bulge on each lateral side, which might be a rudimentary aliform process (see Carballido and Sander, 2014), and the summit is more rounded than flattened. The summit of the neural spine in dorsal view is rounded, but has a constricted anterior end, where it points towards the sprls. The posterior end projects more posteriorly and is round, though with a slightly pointed end at the posterior midline.

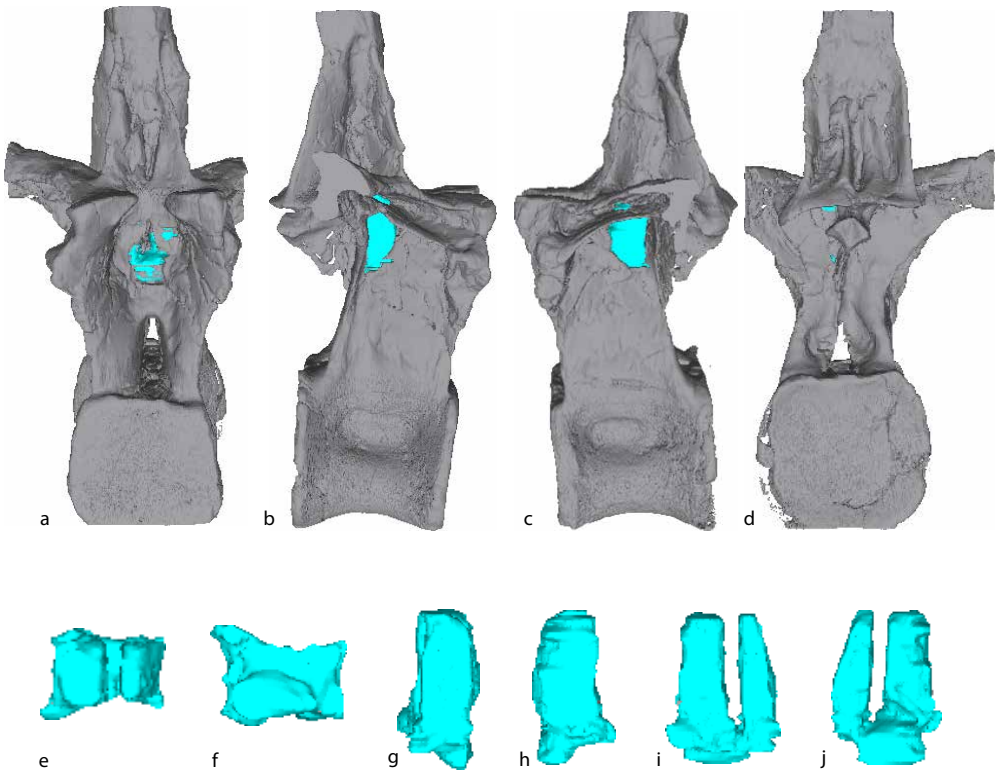

Figure 14: CT scan of PVL 4170 (13) in anterior (A), lateral (B,C) and posterior (D) views, with the shape of the internal pneumatic feature highlighted in light blue, in dorsal (E), ventral (F) lateral (G,H), anterior (I) and posterior (J) views.

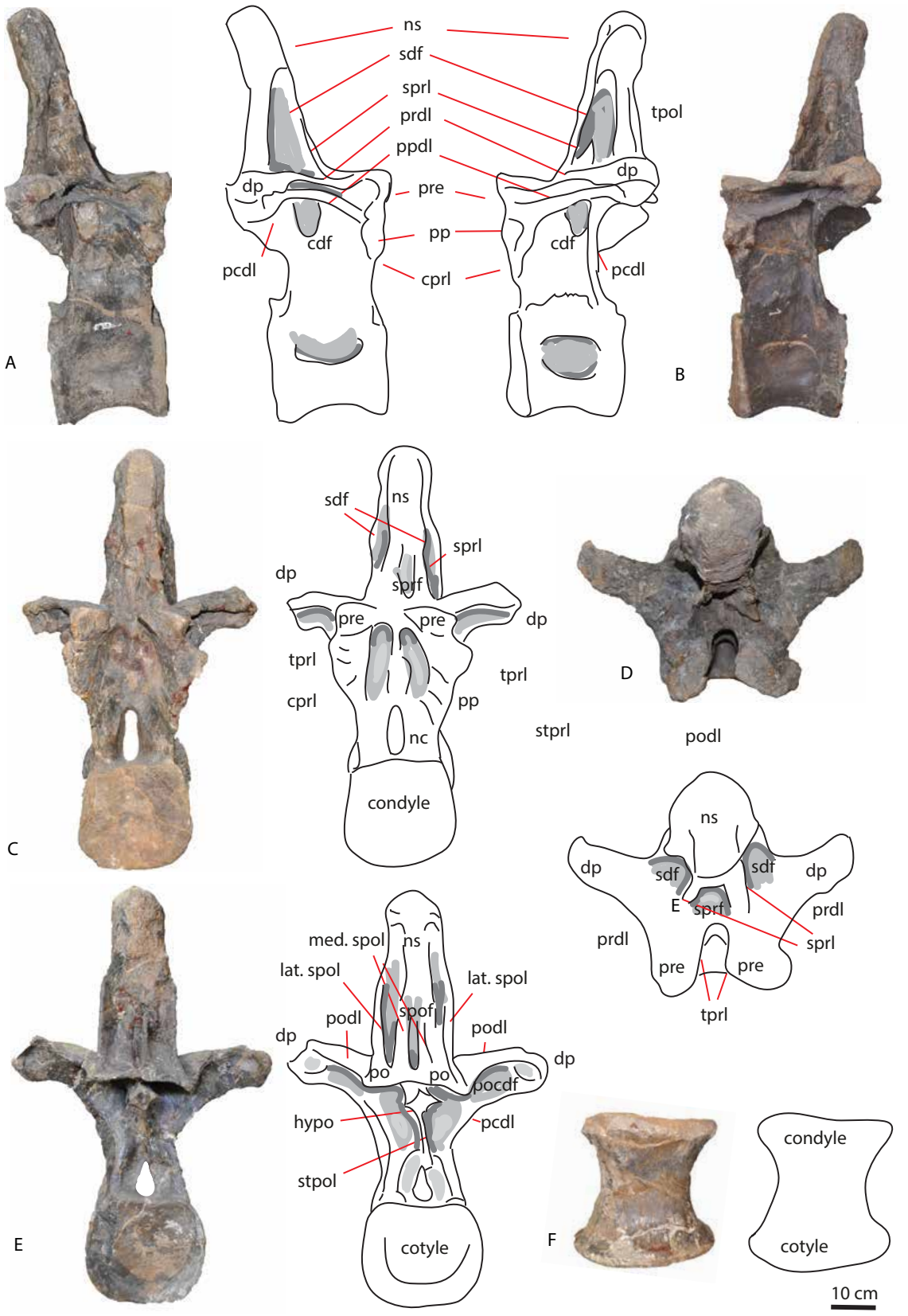
A
ns
sdf
sprl
prdl
ppdl
dp
pre
pp
cdf
pcdl
cprl
tpol
dp
cdf
pcdl
B
C
sdf
ns
sprl
dp
sprf
pre
pre
dp
tprl
tprl
cprl
pp
nc
condyle
stprl
podl
D
ns
dp
sdf
sdf
dp
E
sprf
prdl
sprl
prdl
pre
pre
tprl
E
med. spol
ns
lat. spol
lat. spol
spof
podl
podl
dp
dp
po
po
pocdf
hypo
pcdl
stpol
cotyle
F
condyle
cotyle
10 cm

Figure 15 (previous page): Dorsal MACN-CH 4170 (13) in lateral (A,B), anterior (C), dorsal (D), posterior (E) and ventral (F) views. Abbreviations: acdl = anterior centrodiapophyseal lamina, cprl = centroprezygapophyseal lamina, dp = diapophysis, hypa = hypapophysis, nc = neural canal, ns = neural spine, pcdl = posterior centrodiapophyseal lamina, pp = parapophysis, po = postzygapophysis, prcdf = prezygapophyseal centrodiapophyseal fossa, pocdf = postzygapophyseal centrodiapophyseal fossa, prdl = prezygapophyseal diapophyseal lamina, pre = prezygapophysis, sdf = spinodiapophysal fossa, spof = spinopostzygapophyseal fossa, spol = spinopostzygapophyseal lamina, sprf = spinoprezygapophyseal fossa, lat.spol/med.spol = lateral/medial spinopostzygapophyseal lamina, sprl = spinoprezygapophyseal lamina, tprl = intraprezygapophyseal lamina, tpol = intrapostzygapophyseal lamina, stpol = single intrapostzygapophyseal lamina, stprl = single intrapostzygapophyseal lamina, vk = ventral keel.

Dorsal PVL 4170 (14)

Posterior dorsal with preserved neural arch, spine and centrum. Because of its fragile state, a ventral image could not be obtained. Parts of the diapophyses and neural arch are damaged.

In anterior view, the anterior articular surface of the centrum is oval, and dorsoventrally flattened, so that the transverse width is greater than the dorsoventral height. The dorsal end is slightly heart-shaped. The anterior articular surface of the centrum is dorsoventrally longer than the posterior side. The posterior dorsal rim of the articular surface of the centrum extends further posteriorly than the ventral side. The extension is rounded and is visible on both lateral sides of this dorsal vertebra. The width of the centrum extends beyond the width of the pedicels of the neural arch. In posterior view, the centrum is dorsoventrally flattened and expands a little transversely on the midline. The dorsal end of the posterior articular surface is slightly excavated dorsally, as are posterior surfaces of the pedicels surrounding the neural canal, embedding the neural canal. In lateral view, the centrum is ventrally concave. It is slightly reconstructed however, so there might not be

more original curvature preserved. There are shallow, elliptical depressions visible on each lateral side of the centrum.

The anterior side of the neural canal is oval and dorsoventrally elongated, and narrows in the upper one-third towards its dorsal end. The posterior side is more triangular in shape, but overall roughly similar to the anterior one.The medial sides of the pedicels of the neural arch are excavated, forming an oval excavation around the neural canal.

The anterior central part of the neural arch is damaged, thereby revealing the pneumatic centrodiapophyseal fenestra, which connects to each lateral side of the neural arch below the diapophyses. These openings perforate the neural arch to the posterior side, indicating there must have been only a thin sheet of bone covering them. The neural arch tapers towards the midpoint on both the anterior and posterior sides in lateral view, however, the anterior end expands towards the posterior side again together with the parapophysis and the base of the prezygapophysis. The neural arch constricts around the central part of the vertebra in posterior view. On the right lateral neural arch a neurocentral suture is present. Posteriorly, the hyposphene is visible as a clear triangular protrusion below the postzygapophyses. The hyposphene is smaller than in the previous dorsals.

The left lateral side of this dorsal is missing the diapophyses, however, this does give a good view of the proximal bases of the diapophyseal laminae; the prezygodiapophyseal lamina is a relatively delicate and short lamina that runs obliquely to the ventral anterior base of the prezygapophysis; the postzygodiapophyseal lamina lies on the same oblique sagittal plane and projects dorsally and posteriorly towards the postzygapophysis. The right lateral side in lateral view shows the partial right diapophysis, of which the distal end is broken, revealing two laminae, the distal side of the prdl and the distal side of the posterior centrodiapophyseal lamina. Also, a thin short lamina runs from the posterior end of the

diapophysis to the postzygapophyses; this lamina connects also to the lateral spinopostzygapophyseal lamina, therefore is the podl+lspol complex. On both lateral sides, ventral to the diapophyseal base, the centrodiapophyseal fenestra is clearly visible and perforates the neural arch completely; however, there would probably have been a thin septum separating them.

The right diapophysis is partially preserved; it is shorter than in the previous dorsals, and stout. It projects laterally, slightly dorsally and posteriorly, unlike the diapophyses of the previous dorsals. he diapophysis is wing-shaped in posterior view; the pcdl encircles a wide sheet of bone on its posterior side. The prezygodiapophyseal lamina is visible in anterior view, as it curves convexly to the lateral distal end of the diapophysis. The ventral lateral side of the transverse process is marked by the prcdf.

The only prezygapophysis present is reconstructed. On the right lateral side, a rugose parapophysis is supported by an anterior centroparapophyseal lamina, which runs along a ragged lateral rim of bone from the prezygapophyses to the ventral end of the pedicel of the neural arch, which is similar to those in PVL 4170 (13). The actual prezygapophyses are missing or reconstructed, therefore there is no information known about these in this particular dorsal.

Because most zygapophyseal structures are either broken or reconstructed, not much can be said about the shape of these in dorsal view, however, the wide sheet of bone between the prdl and the pcdl is clearly visible in dorsal view. The left pedicel of the neural arch is partially visible. It is positioned slightly posterior to the anterior rim.

The postzygapophyses are ventrally convex, and dorsally stand out from the neural spine, making the spols protrude from the spine in an equal fashion. The podl + lspol complex is seen curving sharply convexely from the lateral end of the right postzygapophysis to the distal end of the diapophysis.

The neural spine in anterior view is straight and square in the upper one-third of its dorsoventral height, however, the anterior side tapers to a V-shaped point towards its ventral end. The 'V' is rugose. On each lateral side, slightly dorsal to this point, the spinoprezygapophyseal laminae widen the lowermost one-third of the neural spine. The summit of the neural spine is rugose and shows a small oval protrusion on its anterior midline. The lower half of the neural spine shows a clear division between the lateral and medial spols, between which are evenly sized, slit-like fossae. The spof completely perforates the area between the postzygapophyses in a elliptical shape. The top of the neural spine is cone-shaped and rugose. There is no trace of a postspinal scar, as in more anterior dorsals. The neural spine in lateral view is excavated by the prsdf, which is triangular and relatively deep. The lspol is thick in the ventral half of the neural spine, however, at the lateral sides of the dorsal half of the neural spine it is only a thin edge that protrudes posteriorly from the spine. The lateral spols form a bell-shaped sheet around the lower half of the neural spine in posterior view, whereas the upper half has the base of the lateral spol only visible as a thin lateral ridge. As in the previous dorsals, the distal end of the neural spine is massive, and cone-shaped. In this posterior dorsal however, the lower half of the spine is bending anteriorly, the upper half of the spine is bending posteriorly. At the base of the upper half, a ridge is seen curving from the anterior lateral side to the posterior lateral side. In dorsal view, the summit of the neural spine is transversely wider posteriorly than anteriorly, giving it a trapezoidal shape. The surface is rugose.

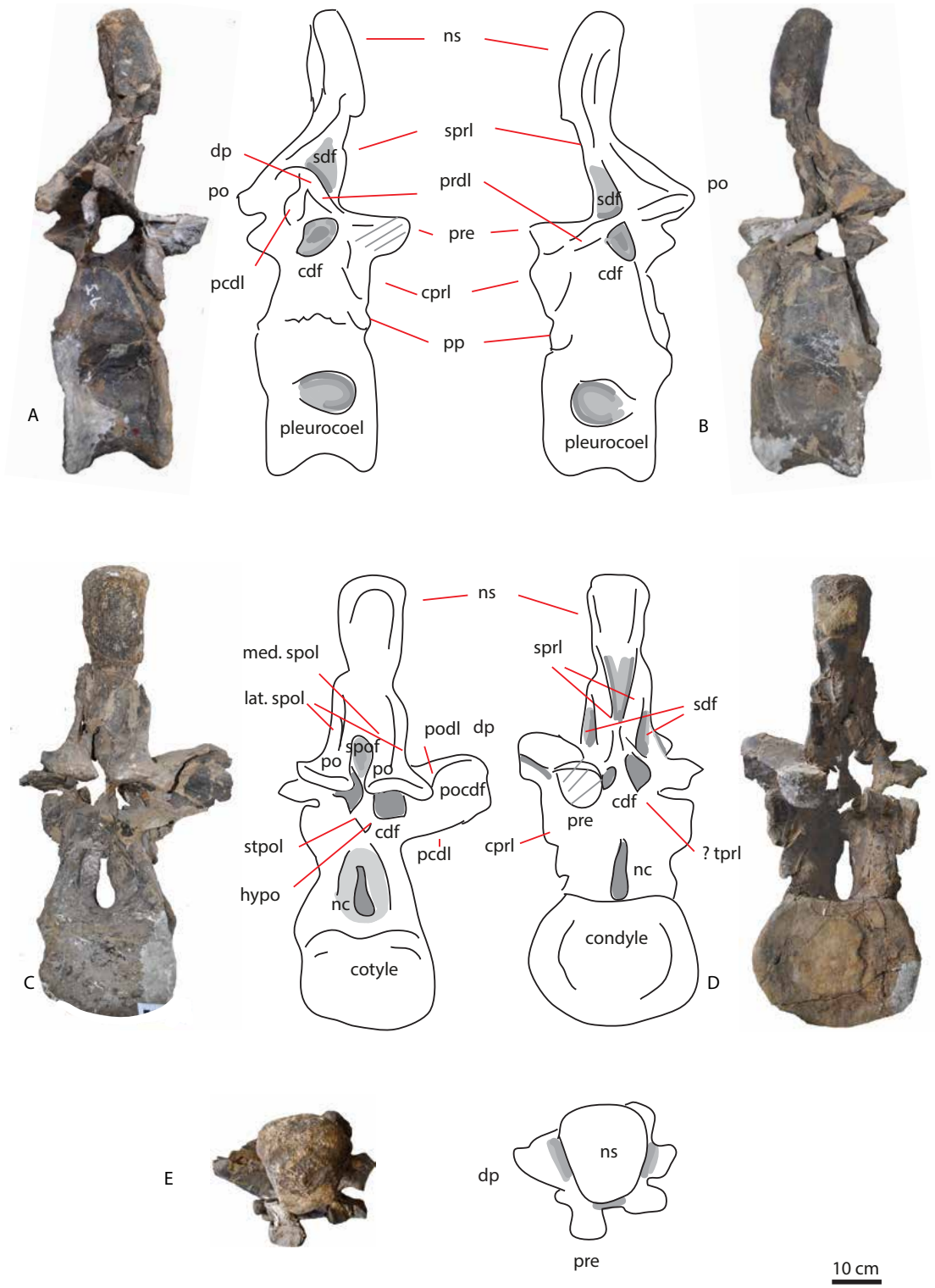

Figure 16: Dorsal MACN-CH 4170 (14) in lateral (A,B), posterior (C) , anterior (D), and dorsal (E) views.Abbreviations: acdl = anterior centrodiapophyseal lamina, cprl = centroprezygapophyseal lamina, dp = diapophysis, hypa = hypapophysis, nc = neural canal, ns = neural spine, pp = parapophysis, po = postzygapophysis, prcdf = prezygapophyseal centrodiapophyseal fossa, pocdf = postzygapophyseal centrodiapophyseal fossa, prdl = prezygapophyseal diapophyseal lamina, pre = prezygapophysis, sdf = spinodiapophysal fossa, spof = spinopostzygapophyseal fossa, spol = spinopostzygapophyseal lamina, sprf = spinoprezygapophyseal fossa, sprl = spinoprezygapophyseal lamina, tprl = intraprezygapophyseal lamina, tpol = intrapostzygapophyseal lamina, lat.spol/med.spol = lateral/medial spinopostzygapophyseal lamina, stpol = single intrapostzygapophyseal lamina, stprl = single intrapostzygapophyseal lamina, vk = ventral keel.

Dorsal PVL 4170 (15)

This dorsal vertebra only has its centrum preserved (Figure 17, part 15). In anterior view, the anterior articular surface of the centrum is almost trapezoidal in shape, with lateral protrusions on the midline. The anterior articular surface is equally as high as it is wide. The posterior articular surface in lateral view is broken and not clearly visible. In lateral view, the centrum shows a concave ventral side, and a slightly more convex than flat anterior articular surface. Towards the dorsal middle part of the centrum, in lateral view, a shallow elliptical fossa is visible. The ventral floor of the neural canal is visible, and the lowermost lateral walls, indicating an elongated elliptical shape of the neural canal, as in the other posterior dorsals. In dorsal view, the neural canal is seen to cut deeply into the centrum, and shows a widening transversely towards the posterior opening. In dorsal view, the neurocentral sutures are either broken or unfused; the former is the more likely option, as the sutures are fused in the other dorsals of PVL 4170.

Dorsal PVL 4170 (16)

This dorsal, though well-preserved, and only partially reconstructed, is unfortunately stuck behind a low bar on the ceiling of the Instituto Miguel Lillo, in the hallway where the holotype is mounted. As a result, only the right lateral side and some oblique views of the anterior side could be obtained (Figure 17, part 16).

The centrum is partially reconstructed, however, the dorsal end is original and is heart-shaped. In right lateral view, the centrum is almost quadrangular in shape. The dorsoventral height is slightly greater than the anteroposterior length. The posterior dorsal side of the centrum flares slightly laterally and posteriorly, and the neural canal creates a little 'gutter'

on the dorsal surface of the centrum. On the lateral side of the centrum, dorsal to the axial midpoint, is an oval fossa, which is axially longer than dorsoventrally high. This fossa is dorsoventrally higher than in the previous dorsals, making it appear more round than elliptical.

The neural arch is supported by lateral pedicels, which rest more on the anterior side of the centrum than on the posterior. The pedicels of the neural arch in anterior view are of irregular shape, and show an almost anastomosing structure. The posterior part of the pedicels rests a few centimeters medial to the dorsal posterior rim of the posterior articular surface. From there, the posterior part of the pedicel inclines towards the medial side in lateral view. The dorsal end of the pedicels is axially constricted. The right lateral pedicel is broken off laterally. The anterior medial area, between the prezygapophyses, is excavated; this is probably due to a thin sheet of bone having been broken away, revealing the internal pneumatic structure.

The diapophysis is not very clearly visible in anterior view.The diapophyses are located slightly posterior to the midline of the neural arch. In lateral view, the articular surface is a thin, semi-lunate dorsoventrally elongated ridge.

The prezygapophyses are supported below by stout colums that project obliquely anteriorly and dorsally; these are also convex anteriorly.

The prezygapophyses have a flat axial articular surface, and are supported from below by stout convex columns.

The postzygapophyses are situated at around the same elevation as the prezygapophyses. The articular surface of the postzygapophyses is slightly inclined ventrally. The hyposphene

extends further posteriorly than the postzygapophyses, and has a ragged outline in lateral view; this could however be caused by damage to the bone.

The neural spine is slightly inclined towards the posterior side in its lower half, the upper half is more or less erect in the dorsoventral plane. It is slightly wider at its base, however the upper 2/3rd is of an equal axial width. The summit is rod-shaped. The accessory lamina seen in the previous two dorsals is seen around halfway to the summit, running in a semicircular line from anterior dorsal to posterior ventral.

Dorsal PVL 4170 (17)

The posteriormost dorsal is only partially preserved, and therefore is partially reconstructed (Figure 17, part 17). It is also not possible to unmount this dorsal, therefore the view is limited to the anterior side and the (partial) lateral side. The centrum shows deep lateral depressions, and is more oval than round, as in the previous dorsals. The neural arch is similar in morphology to the previous posterior dorsals, with stout prpls and a deep depression between each lateral side of the neural arch. The prezygapophyses are inclined medially, rather than being horizontally aligned with the sagittal plane. The neural spine has very sharp outstanding sprls and spols between which the spine has deep depressions on anterior and lateral sides, which are oriented dorsoventrally. The spine summit is a massive block of bone, and has a square shape. Two rudimentary but clearly visible aliform processes are positioned slightly ventral to the dorsal spine summit on each lateral side.

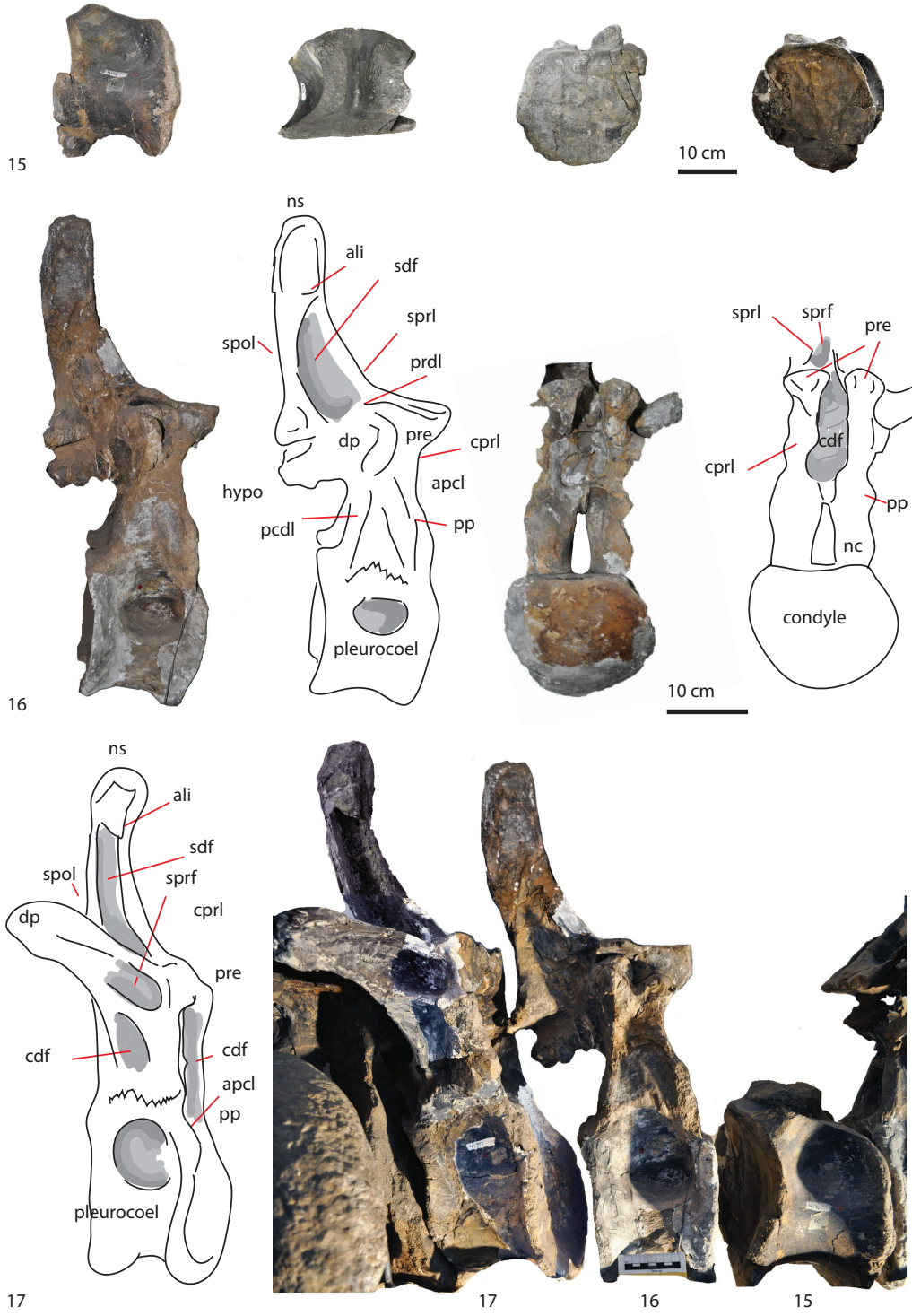

Figure 17: Dorsals PVL 4170 (15,16,17). PVL 4170 (15) in lateral, dorsal, anterior, posterior (oblique) view. PVL 4170 (16) in lateral and anterior view. PVL 4170 (17) in lateral view. Abbreviations: acdl = anterior centrodiapophyseal lamina, ali = aliform process, cprl = centroprezygapophyseal lamina, cpol = centropostzygapophyseal lamina, dp = diapophysis, hypa = hypapophysis, nc = neural canal, ns = neural spine, pp = parapophysis, po = postzygapophysis, prcdf = prezygapophyseal centrodiapophyseal fossa, pocdf = postzygapophyseal centrodiapophyseal fossa, prdl = prezygapophyseal diapophyseal lamina, pre = prezygapophysis, sdf = spinodiapophysal fossa, spof = spinopostzygapophyseal fossa, spol = spinopostzygapophyseal lamina, sprf = spinoprezygapophyseal fossa, sprl = spinoprezygapophyseal lamina, tprl = intraprezygapophyseal lamina, tpol = intrapostzygapophyseal lamina, stpol = single intrapostzygapophyseal lamina, stprl = single intrapostzygapophyseal lamina, vk = ventral keel.

To summarize, there are eight cervicals preserved, and nine dorsals (including one cervico-dorsal) for the holotype of *Patagosaurus* PVL 4170. At least the anteriormost cervical and the atlas-axis are missing, and most likely several dorsals are missing as well. In general, the order of numbering of the specimens is correct, save for a possible switch between PVL 4170 4-5. See Figure 18 for all presacral and vertebrae in lateral view.

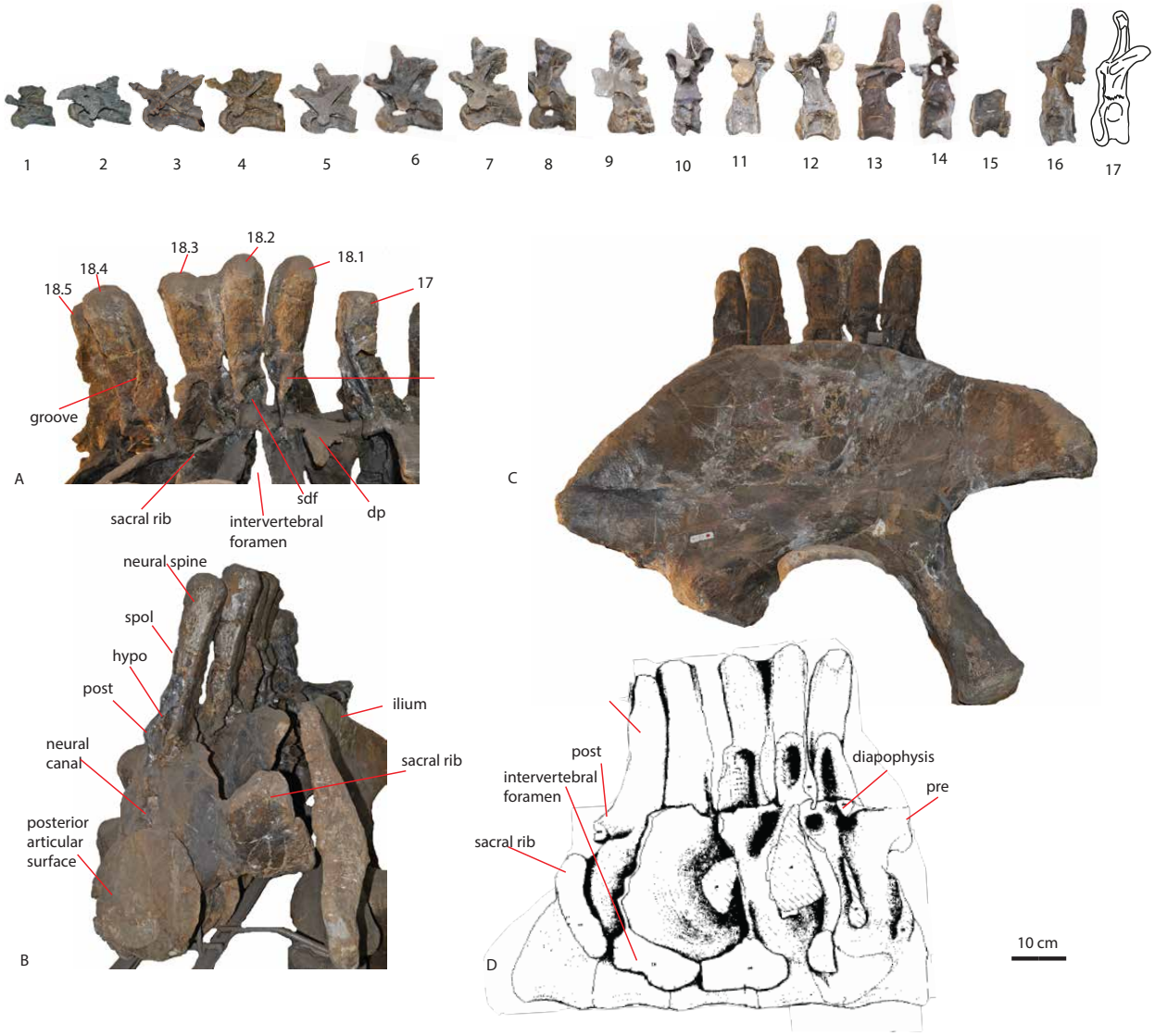

Figure 18: Upper row: All presacral vertebrae of MACN-CH 4170 (1-17) in left lateral view (not to scale). Lower row: all sacral vertebrae of PVL 4170 (18) sacrum. A: PVL 4170 (18.1-5) sacral neural arches and spines in right lateral view. with dorsal PVL 4170 (17) on the right. B: PVL 4170 (18) in posterior view. C: PVL 4170 (18) associated with ilium PVL 4170 (34). D: Original drawing of PVL 4170 (Bonaparte, 1986b). Abbreviations: hypo = hyposphene, pre = prezygapophysis, post = postzygapophysis, spol = spinopostzygapophyseal lamina.

Sacrals PVL 4170 (18)

The complete sacrum is well-preserved (see Bonaparte 1986a, Figures 43 and 44, and Figure 18, lower row, A-D). Unfortunately, because the specimen is mounted, it is difficult to access. Most recent pictures can only show the neural arches and the spines, as the rest of the view is blocked by the ilium laterally (Figure 18C), by the dorsals anteriorly, and by the caudals posteriorly, although the caudals can be unmounted. Bonaparte's 1986 paper shows a detailed illustration however; see Bonaparte, (1986a), and Figure 18D. The sacrum consists of five sacral vertebrae, of which all centra are fused. The second, and third of the neural spines are fused together by their anterior and posterior sides. This is different from neosauropods; e.g. diplodocids fuse the sacral neural spines 2-4, whereas *Camarasaurus* and *Haplocanthosaurus* fuse sacral neural spines 1-3 (Upchurch 2004). All neural spines are rugosely striated (Figure 18B). They all possess spinoprezygapophyseal and spinopostzygapophyseal laminae, which are roughly similar to the morphology of the posteriormost dorsal vertebrae. The dorsal rim of the ilium terminates at about the diapophysis height of the sacrum (Figure 18C). The neural spines extend dorsally beyond the upper rim of the ilium for about 30 cm. In *Mamenchisaurus youngi* and other mamenchisaurids, as well as in *Camarasaurus* and basal titanosauriforms, the neural spines of the sacrum are much shorter (not as dorsoventrally high as the neural arch and centrum combined), and more robust (Ouyang and Ye, 2002; Taylor, 2009). In neosauropods such as *Apatosaurus*, *Diplodocus* and *Haplocanthosaurus*, however, the neural spines do extend further beyond the ilium, and are as dorsoventrally high as the neural arch and centrum together, like in *Patagosaurus* (Gilmore, 1936; Hatcher, 1901, 1903).

The first sacral PVL 4170 18.1 is, as in most sauropods, relatively similar to the posteriormost dorsal (Upchurch 2004). The centrum is oval, and dorsoventrally elongated (Figure 18D). The neural canal is oval and also dorsoventrally elongated, as in the posterior dorsals. The

sacral rib is unattached to the diapophysis in this sacral vertebra. It is a lateral dorsoventrally elongated extension, as in most sauropods, a C-shaped plate that extends laterally towards the medial side of the ilium (Upchurch et al., 2004). The prezygapophyses are anteriorly elongated, and flat dorsally, and have a deep U-shaped recess between them, as in the posterior dorsals (Figure 18A). They connect to the neural spine via the spinoprezygapophyeal laminae, which project as sharp ridges off the lateral sides of the anterior side of the neural spine. Lateral and anterior to the postzygapophysis, the postzygodiapophyseal lamina runs to the transverse process of the first sacral. As in the posterior dorsals, dorsal to the postzygapophyses, a rudimentary aliform process is present. From here, the lateral spinopostzygapophyseal lamina flares out laterally and dorsally before it joins the postzygapophysis. The sprl encases a deep triangular depression, which is visible on the lateral side of the neural spine, which could be the sacral equivalent of the spinodiapophyseal fossa in *Patagosaurus* (see Wilson et al., 2011).

The neural spine inclines slightly anteriorly, as in the posteriormost dorsals. The anterior surface of the neural spine shows rugosities for ligament attachments. On the lateral side of the neural spine, a triangular depression runs over about 2/3rds of the dorsoventral length (Figure 18A,D), with a sharp dorsal semicircular rim. Dorsal to this rim, the spine becomes solid. The spine summit is rounded laterally and has a crest-like shape in anterior view.

The second and third sacral neural spines PVL 4170 18.2 and 18.3 are fused (Figure 18A,C,D). Both the second and third sacral vertebrae have large C-shaped sacral ribs that connect to the medial side of the ilium. These sacral ribs project laterally and slightly posteriorly from the neural arch above the centra. Between these sacral ribs, dorsoventrally elongated and axially short slitlike apertures are visible, which seem to be fenestrae that connect to large internal pneumatic chambers inside the sacrum.

The second sacral neural spine is projecting mainly dorsally, and only slightly anteriorly (Figure 18A,C,D). At the base of the spine, the spinopre- and spinopostzygapophyseal laminae and the dorsal side of the sacral transverse process border a triangular fossa, as in the first sacral. This fossa is more oval-to-triangular, which is different from the first sacral. This fossa is also present on the third sacral and is more pronounced there; being axially wider and more triangular. Between both neural spines, a thin plate of bone was probably present, as there is a small slit, which does not appear natural. The neural spines are dorsally connected by rugose bone tissue. In lateral view, this connection has a U-shaped concavity between both neural spine summits.

The fourth sacral vertebra PVL 4170 18.4 inclines slightly more posteriorly than the previous sacrals (Figure 18A,C,D). The sacral rib of this sacral is a C-to-butterfly-wing shaped laterally projecting bony plate. Between this sacral rib and the sacral rib of the third sacral, a large dorsoventrally elongated slitlike opening is seen to connect to the internal pneumatic chamber of the sacrum.

The prezygapophyses are not visible; the postzygapophyses are diamond-shaped, laterally projecting protrusions. The hyposphene is equally diamond-shaped.

In anterior view, the neural spine is transversely shorter than the previous sacrals, however, axially it is equally wide, giving the spine summit a rhomboidal shape. At the anterior side of the base of the spine, a triangular protrusion is visible, which appears broken, therefore this sacral might have been connected to the third sacral by a bony protrusion at the bases of the neural spines. On the lateral side of the spine, a deep groove is seen to run concavely from the dorsal anterior lateral side to the ventral posterior lateral side, as in some caudals (see caudals later). The dorsal lateral side of the neural spine shows a weakly developed aliform process. In posterior view, the lateral spinopostzygapophyseal laminae are seen to protrude dorsally from the neural spine, which is very rugosely dorsoventrally striated.

The fifth sacral PVL 4170 18.5 is slightly different in morphology from the previous four, in that it is slightly posteriorly offset from the others (Figure 18A,B). The posterior articular surface of the centrum is clearly visible in this last sacrum, and is flat to slightly amphicoelous. It is oval in shape, and slightly dorsoventrally elongated, and slightly transversely flattened. The neural canal is a dorsoventrally elongated oval shape. Directly dorsal to the neural canal, a small triangular and posteriorly projected protrusion is visible, which resembles the small anteriorly projected protrusions above the neural canal of some of the dorsal vertebrae. The lamina that projects laterally towards the sacral rib has a dorsolaterally directed bulge, so that the rib projects laterally in two stages (Figure 18B). The main body of the sacral ribs of this last sacral are directed laterally, but also bend anteriorly towards the other sacrals. The postzygapophyses are diamond-shaped, as is the hyposphene. The spinopostzygapophyseal laminae in posterior view are slightly offset from the spine, and at about half of the dorsoventral height of the spine, protrude in a rounded triangular shape. This might have been a ligament attachment site. The spine itself is rugosely striated and resembles the fourth sacral in morphology.

Caudals

The holotype PVL 4170 has a few anterior, mid, and mid-posterior caudals preserved. The caudal numbering is rather discontinuous, indicating that the caudal series was already incomplete when it was found. Two caudals are unnumbered but will be described here and positioned in the caudal series relative to their size and morphology. Two caudals are probably repeated, as one is a cast of the other.

Anterior- to anterior-mid caudals (PVL 4170 19-20-21) have dorsoventrally high, and axially short centra (Figure 19). They display rounded triangular-to-heart-shaped anterior vertebral articular surfaces, and slightly more heart-shaped posterior vertebral articular surfaces, the most acute tip being the ventral side. The centrum in lateral view is concavely curved on the ventral side, with the slope on the anterior half less acute than on the posterior half. A faint raised ridge of bone is seen in some caudals on the lateral centrum, ventral to the diapophyses. This is also seen in *Cetiosaurus*, and could be a rudimentary lateral ridge as seen in neosauropods (Tschopp et al., 2015). The posterior dorsal rim of the centrum shows an inlet for the neural canal, as in the cervicals and dorsals, and stretches slightly beyond the posterior end of the base of the neural spine.

In ventral view, two parallel axially positioned struts are visible, between which is a 'gully'; an axially running depression. This feature is seen in other eusauropods (*Cetiosaurus oxoniensis* and the Rutland *Cetiosaurus* (Upchurch and Martin, 2002, 2003) as well as an unnamed specimen from Skye, UK (Liston, 2004), though is not as prominently developed in *Patagosaurus* as in the latter taxa. This feature is named the ‘ventral hollow’ in neosauropods, and is also found in derived non-neosauropodan eusauropods (Mocho et al., 2016). Chevron facets are present, as in most eusauropods (e.g. *Cetiosaurus oxoniensis, Lapparentosaurus, ‘Bothriospondylus madagascariensis’* and in caudals from unnamed taxa

from the Late Jurassic of Portugal (Upchurch and Martin, 2003; Mannion, 2010; Mocho et al., 2016)) but not as prominent as in *Vulcanodon* (Raath, 1972; Cooper, 1984) or *Cetiosaurus*.

The transverse processes are short and blunt, and project slightly posteriorly as well as laterally. Below them, rounded shallow depressions are visible, which are a vestigial caudal remnant of the pleurocoels. These depressions are both in anterior and middle caudals bordered by slight rugosities protruding laterally from the centrum, which could be very rudimentary lateral and ventrolateral ridges, but this is unsure, and not recorded in non-neosauropodan eusauropods (Mocho et al., 2016). The neural arch is both dorsoventrally as well as axially shortened compared to the dorsals and sacrals. Lamination is rudimentarily present; in particular the sprl, spol, stpol and tprl are visible anteriorly and posteriorly. Small, blunt pre- and postzygapophyses are also present. The prezygapophyses rest on short, stout stalks that project anteriorly and dorsally. The postzygapophyses are considerably smaller than the prezygapophyses, and project only posteriorly as small triangular protrusions. These are, however, still prominent in anterior caudals; more so than in *Spinophorosaurus* (Remes et al., 2009). Prezygapophyses and postzygapophyses are strongly diminished in the anterior caudals and continue to do so towards the posterior caudals. Prezygapophyses are expressed as small oval protrusions, in anterior caudals still projecting from stalks, in middle and posterior simply projecting from the neural arch. The postzygapophyses are even further diminished, are only seen as small triangular protrusions from the base of the neural spine, and disappear completely in posterior caudals. The hypophsene remains visible, however, as a straight rectangular structure projecting at 90 degrees with the horizontal. The neural spine is dorsoventrally high, and projects dorsally and posteriorly.

The most distinctive features of this set of vertebrae, however, are the elongated neural spines. These taper posteriorly, and dorsally, in a gradual gentle curve, which becomes more straightened towards the dorsal end. Towards the tip of the neural spine, the lateral surface

expands axially. The spine summit displays the same characteristic saddle shape as in the posterior dorsals, in that in lateral view both anterior and posterior dorsal ends bulge slightly, with a slight depression on the midline between these bulges. In lateral view, as well as posterior view, the posterior side of the spine shows long coarse rugose dorsoventrally running striations, probably for ligament attachments. In particular, one or two grooves of ± 1 cm wide are seen aligned in the dorsoventral plane, a few centimeters from the posterior rim in lateral view. These run from the midline of the spine, a few centimeters below the spine summit, to the posterior rim of the spine, just above the hyposphene.

Figure 19: Anterior Caudals PVL 4170 (19-20-21) in lateral view.

Middle caudals (PVL 4170 22-25) are more elongated axially, with the axial length slightly higher than the height or width of the centrum (Figure 20). However, the centrum height and width are still similar to the anterior-mid caudals. The centrum in lateral view shows a concave surface between two slightly raised ridges, as seen in *Cetiosaurus*. The ventral side

of the centra is concavely and symmetrically curved, as opposed to the more anterior caudals. The base of the spine is axially wider than in the anterior caudals, and together with the base of the prezygapophyses, forming the simplified neural arch, rest more on the anterior half of the centrum, a feature commonly seen in eusauropods and neosauropods (Tschopp et al., 2015). The posterior dorsal side of the centrum inclines slightly dorsally. The diapophyses are reduced to small rounded stumps that protrude laterally and slightly dorsally. They are positioned on the ventral and posterior side of the neural spine bases. Below the transverse processes a very shallow depression can be seen, unlike in *Tazoudasaurus* where well-defined round fossae are still present on the middle caudals (To1-288, Allain and Aquesbi, 2008). Most prezygapophyses are broken; their bases are visible as broad stout bulges. The base of the neural spine bulges out laterally, and is extended axially to the base of the prezygapophyses, creating a broad stout pillar in lateral view. The spine is inclined posteriorly, and shows a gentle sinusoidal curvature on the posterior rim. The neural arch and spine shift towards the anterior side of the centrum in middle and posterior caudals.

Figure 20: Middle Caudals PVL 4170 (22-23-24) in lateral view.

Posterior-mid caudals (PVL 4170 26-27-28-29-30) increase in axial centrum length and decrease in centrum height, giving the centrum a dorsoventrally flattened oval shape. The posterior articular surfaces of the centra have a small inlet on their dorsal rim, rendering them heart-shaped. From PVL 4170 (26) the transverse processes diminish into slight bulges underneath which a small shallow elliptical depression is visible. The postzygapophyses are present as stunted, slightly square ventral protrusions on the neural spine; the prezygapophyses are more developed and protrude as short stout struts anteriorly and dorsally from just above the base of the neural spine. The neural spine inclines heavily posteriorly, and becomes rectangular; losing the sinusoidal curvature.

The last preserved, posteriormost caudals of the holotype (note that these are not the posterior-most caudals of the skeleton) (PVL 4170 31-34) display an elongated centrum, further decreased centrum height and a symmetrically curved concave ventral side. Most neural spines are broken off or damaged; only PVL 4170 (32) has a neural spine that curves posteriorly and aligns with the axial plane. The diapophyses are further reduced as small rugose stumps, and the elliptical depression below these is barely discernible. The prezygapophyses are short stunted protrusions on the anterior end of the spine, nearly equal in height with the spine. The articular surfaces are round rather than heart-shaped.

PVL 4170 (19)

The first caudal that is preserved is an anterior- to mid- caudal. The centrum is dorsoventrally higher than transversely wide, and is axially short, as in the posterior dorsals and sacrals (Figure 21 A,B).

In anterior view, the anterior articular surface of the centrum is oval, and dorsoventrally higher than transversely wide (Figure 21D). However, the upper 1/3rd of the anterior articular surface is transversely broader than the transverse width of the midpoint, and towards the lower 1/3rd this width decreases further. The ventral side of the articular surface is slightly V-shaped (Fgiure 21E). The dorsal section of the articular surface shows a protruding sharp 'lip-like' rim. 'Lips' on the dorsal rim of the articular surface of the caudals are an autapomorphy in *Cetiosaurus* (Upchurch and Martin, 2003). However, *Patagosaurus* has less distinctive 'lips' than *Cetiosaurus,* potentially hinting at a shared feature for Cetiosaurids. The articular surface is concave, with the deepest point slightly dorsal to the midpoint. In posterior view, the articular surface of the centrum is heart-shaped, due to two parallel elevations of the dorsal rim between which a gully for the neural canal exists (Figure 21C). The articular surface is less concave than its anterior counterpart, and also less extensive; the outer rim stretches towards the centre of the articular surface, which is flattened, and only the area slightly dorsal to the midpoint is slightly concave. In lateral view, the centrum is ventrally mildly concave, and the rims of both posterior and anterior articular surfaces show thick circular striations, seen in weight-bearing bones of sauropods, e.g. *Cetiosaurus, Giraffatitan, Tornieria* (H.Mallison pers. comm.; see Figure 21A,B). The centrum is much dorsoventrally higher than it is axially long, however, this length has decreased with respect to the sacrals and the posterior dorsals. The neural canal is triangular to rounded in shape, both in anterior and posterior views.

The diapophyses project laterally and dorsally in anterior view, and in dorsal view, they are also seen to project slightly posteriorly (Figure 21D,F). Their shape is triangular with a stunted distal tip; the dorsal angle made with the centrum is less acute than the ventral one. Between the diapophyses and the neural arch, a raised ridge of bone is present, similar to

that of anterior caudals of *Cetiosaurus* (Upchurch and Martin, 2003). Whether this is a rudimentary lateral ridge, seen in neosauropods (Tschopp et al., 2015) is unsure.

The neural arch is formed of a square elevated platform upon which the prezygapophysis and the neural spine rest (Figure 21A,B,F). The prezygapophysis projects anteriorly and dorsally from the neural arch, at an angle of ±100° with the horizontal. The base of the prezygapophyses is stout, after which it tapers towards the distal end. The medial articular surface of the prezygapophysis is round with an internal rounded depression. In posterior and lateral view, the hyposphene is visible as a squared protrusion at the posterior base of the neural spine. It makes an angle of 90° with respect to the axial and dorsoventral planes. The postzygapophyses are only visible as raised oval facades, dorsal to the hyposphene. The postzygapophyses are formed as triangular lateral protrusions, which project from the base of the neural spine, between which is an oval depression, likely a rudimentary caudal spof.

The neural spine is diverted to the left lateral side in anterior view; this is probably a taphonomic alteration (Figure 21D). It has roughly the same morphology as in the dorsals; a constricted base and a widened summit, with gently curving lateral sides. The spine is heavily striated on the surface of the upper 2/3rds of the dorsoventral height. The neural spine in lateral view gently curves convexly posteriorly and concavely anteriorly. The summit has a distinct saddle shape in lateral view. The spine summit is elevated in the centre and has two anterior and posterior rims, which are at a lower elevation than the middle part, as is seen in the neural spine summits of the dorsal vertebrae. The neural spine is rugosely striated in the dorsoventral plane in posterior view, and is offset to the right (Figure 21C). Two spols are clearly visible.

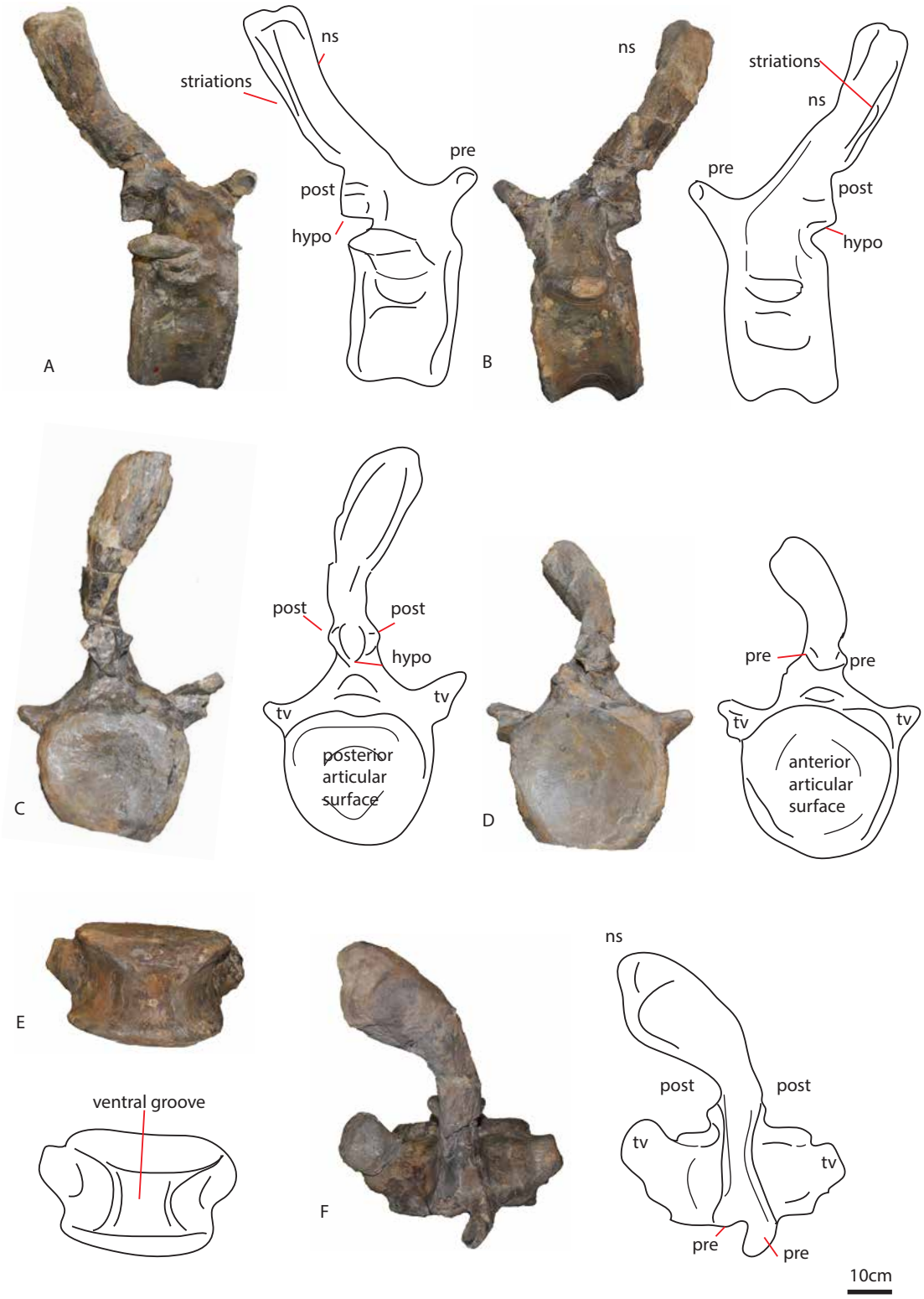

Figure 21: Caudal PVL 4170 (19) in lateral (A,B), posterior (C), anterior (D) and ventral (E) and dorsal (F) views. Abbreviations: hypo = hyposphene, ns = neural spine, post = postzygapophysis, pre = prezygapophysis, tv = transverse process.

PVL 4170 (20)

This anterior caudal resembles PVL 4170 (19). In anterior view, the anterior articular surface is asymmetrically oval, with a slightly flattened dorsal rim, and a slightly triangular ventral one (Figure 22D). It is also transversely broadest slightly dorsal to the midline. The dorsal edge shows lateral elevations, between which a slight rounded indentation exists on the midline. In posterior view, the articular surface of the centrum is more heart-shaped than oval (Figure 22C). It has a thick rim, showing circular striation marks, which is not as concave as the inner part of the articular surface. This concave surface, however, is less concave than the anterior articular surface. The posterior dorsal rim of the centrum does not extend posteriorly, but it faces ventrally in an oblique angle towards the axial plane, as in PVL 4170 (19), however, the posterior dorsal rim of the centrum extends further ventrally in PVL 4170 (20). In lateral view, the centrum is axially short and dorsoventrally elongated as in the posterior dorsals and the sacrals. The ventral side of the centrum, however, is symmetrically concavely curved, with posterior and anterior rims bulging out concavely towards the ventral side.

The neural canal is visible as a semi-circular indentation in the neural arch. It is much broader ventrally than in PVL 4170 (19), see Figure 22C,D.

In ventral view, the anterior chevron facets are broken off Figure 22F). The centrum is concave on both lateral sides, and shows a slight depression beneath the diapophysis. Right at the base of the diapophysis however, it shows a slight convexity.

The centrum is anteriorly slightly convex, and posteriorly slightly convex, in dorsal view.

The left diapophysis is preserved, and this projects laterally in anterior view, with an angle of 90° with respect to the dorsoventral plane (Fgiure 22C,D). The diapophysis in dorsal view projects posteriorly and slightly dorsally. The diapophysis is flat and rectangular in dorsal view, with the anterior edge being convex and the posterior one concave.

The prezygapophyses are visible above the neural canal as short rounded triangular stubs, which project dorsally and slightly laterally (Figure 22A,B,D). In dorsal view, the prezygapophyses are rounded-triangular protrusions that fork from the base of the neural arch, and which bend slightly medially, towards each other. The postzygapophyses are broken off, although the bases are present, showing a dorsoventrally elongated, dorsally triangular and ventrally oval shape (Figure 22C).

The neural spine is stout and cone-shaped in anterior view, and displays paired spinoprezygapophyseal laminae (Figure 22D). The base of the neural spine is axially constricted; the neural spine broadens axially towards its dorsal end. The spine shows rugose longitudinal striations on its lateral sides (Figure 22A,B). Though possibly broken and damaged, it shows a similar curve as in PVL 4170 (19), in that the posterior side curves convexly and the anterior concavely, allowing the neural spine to curve gently in a sort of L-shape. The tip of the neural spine is not as saddle-shaped as in PVL 4170 (19), however, there is still a slight curvature of the neural spine summit visible on its posterior side (Figure 22A,B). The spine summit is similar in shape to those of the posterior dorsals of PVL 4170 (19), in that the sides of the summit are tapering slightly ventrally from a 'platform' that is the dorsalmost part. The summit is a rhomboid-shaped knob, which is transversely broader anteriorly than posteriorly (Figure 22E).

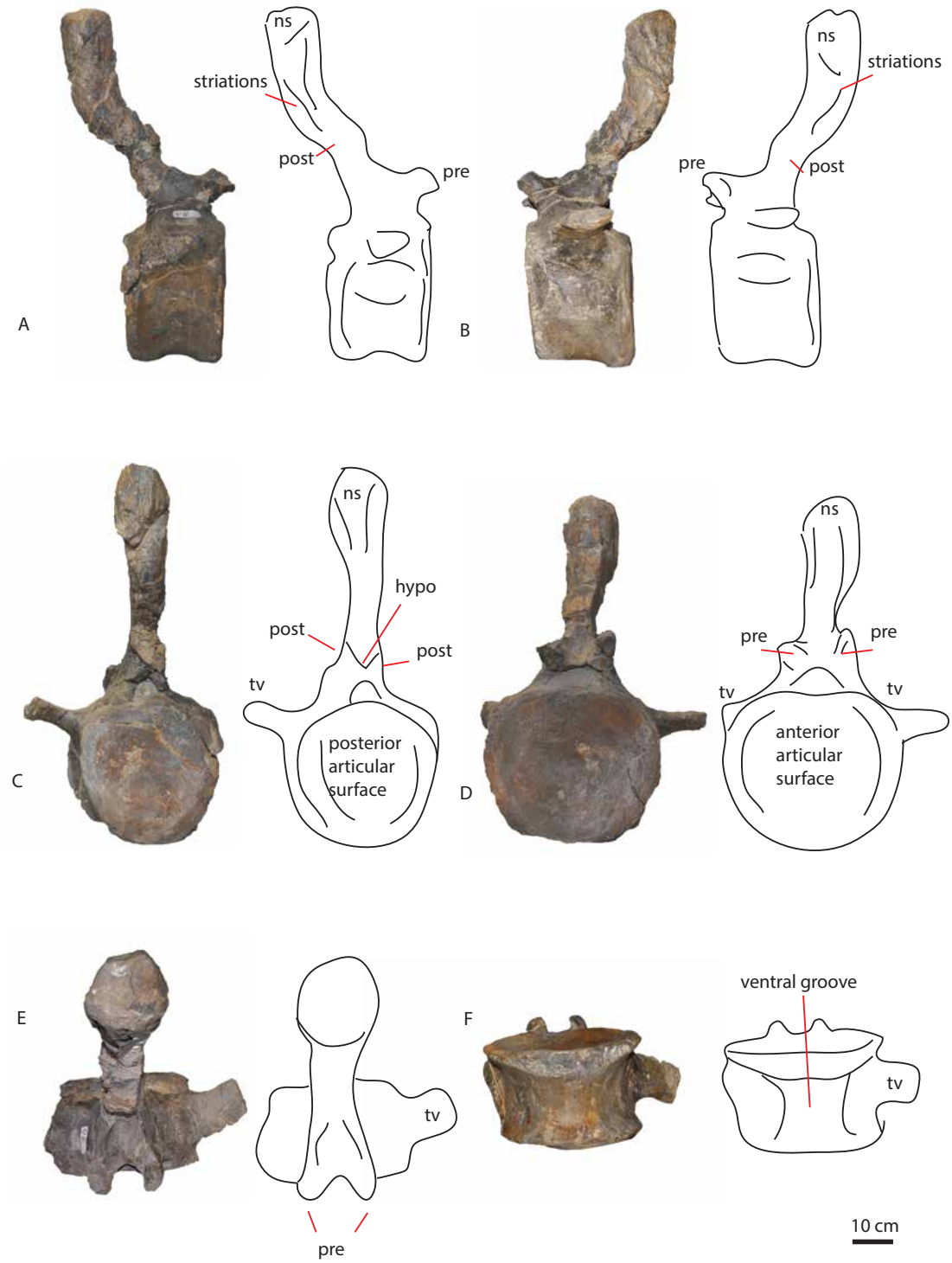

Figure 22:: Caudal PVL 4170 (20) in lateral (A,B), posterior (C), anterior (D), dorsal (E) and ventral (F) views. Abbreviations: hypo = hyposphene, ns = neural spine, post = postzygapophysis, pre = prezygapophysis, tv = transverse process.

PVL 4170 (21)

This anterior - mid caudal has a much more heart-shaped anterior articular surface than PVL 4170 (19-20), however, the lower half of the articular surface is reconstructed, therefore it is not certain that the original form persists (Figure 23D). The deepest concavity is not at the midpoint but slightly above it, about 1/3rd of the dorsoventral length of the articular surface down from its dorsal rim. The dorsal rim has a slight 'lip'; an anteriorly protruding part of the rim that cups the articular surface. The midpart of this lip is bent ventrally with two lateral bulges, giving it a heart-shape, as in PVL 4170 (19-20), see Figure 23C. In posterior view, the articular surface of the centrum is rounded-to-triangular in shape. The posterior articular surface is less concave than the anterior articular surface. In lateral view the centrum is more elongated than in PVL 4170 (19-20). In ventral view, the posterior edge of the centrum shows slightly developed chevron facets (Figure 23E). The lateral sides of the centrum are strongly concave, the axial centrum length is increased in this caudal vertebra, compared to PVL 4170 (19-20).

The neural canal is near semi-circular with the horizontal axis on the ventral side. In dorsal view, the posterior dorsal rim of the centrum retreats towards the neural arch in a U-shaped recess, posterior to the neural canal opening (Figure 23C).

The left diapophysis is preserved; the right is broken off (Figure 23C,D). The left diapophysis is a stout straight element in anterior view, and is slightly tilted towards the anterior and dorsal side. The extremity is roughly triangular in outline (Figure 23B). In dorsal view, the diapophysis is seen to bend posteriorly as in PVL 4170 (19-20). The prezygapophyses are flattened in dorsal view, and slightly spatulate. The diapophysis is seen to deflect slightly posteriorly Figur 23F).

The prezygapophyses are stout dorsoventrally broad struts (Figure 23A,B,D). They are triangular in shape, with dorsoventrally elongated struts, and are directed dorsally. The neural arch is tilted, probably due to taphonomical alteration. The postzygapophyses are small rounded triangular bosses posterior to a large bulge on the neural spine (Figure 23A,B,C). This bulge is set right ventral to an axial constriction of the neural spine, after which it constricts slightly again.

The spine summit is similar to PVL 4170 (19-20). . It constricts transversely at about 1/3rd of the dorsoventral length towards the summit, after which it slightly transversely widens towards the summit; the spinoprezygapophyseal laminae follow a similar pattern (Figure 23A,B,F). Dorsal to the postzygapophyses, the spine also bends more posteriorly after this bulge, similar to PVL 4170 (20). The top 1/3rd of the spine shows ligament attachment sites in lateral view. The neural spine expands slightly towards the summit in a rhomboid shape, with dorsoventrally deep striations for ligament attachments. The summit is' saddle shaped', as in the other anterior caudals PVL 4170 (19-20), see Figure 23F.

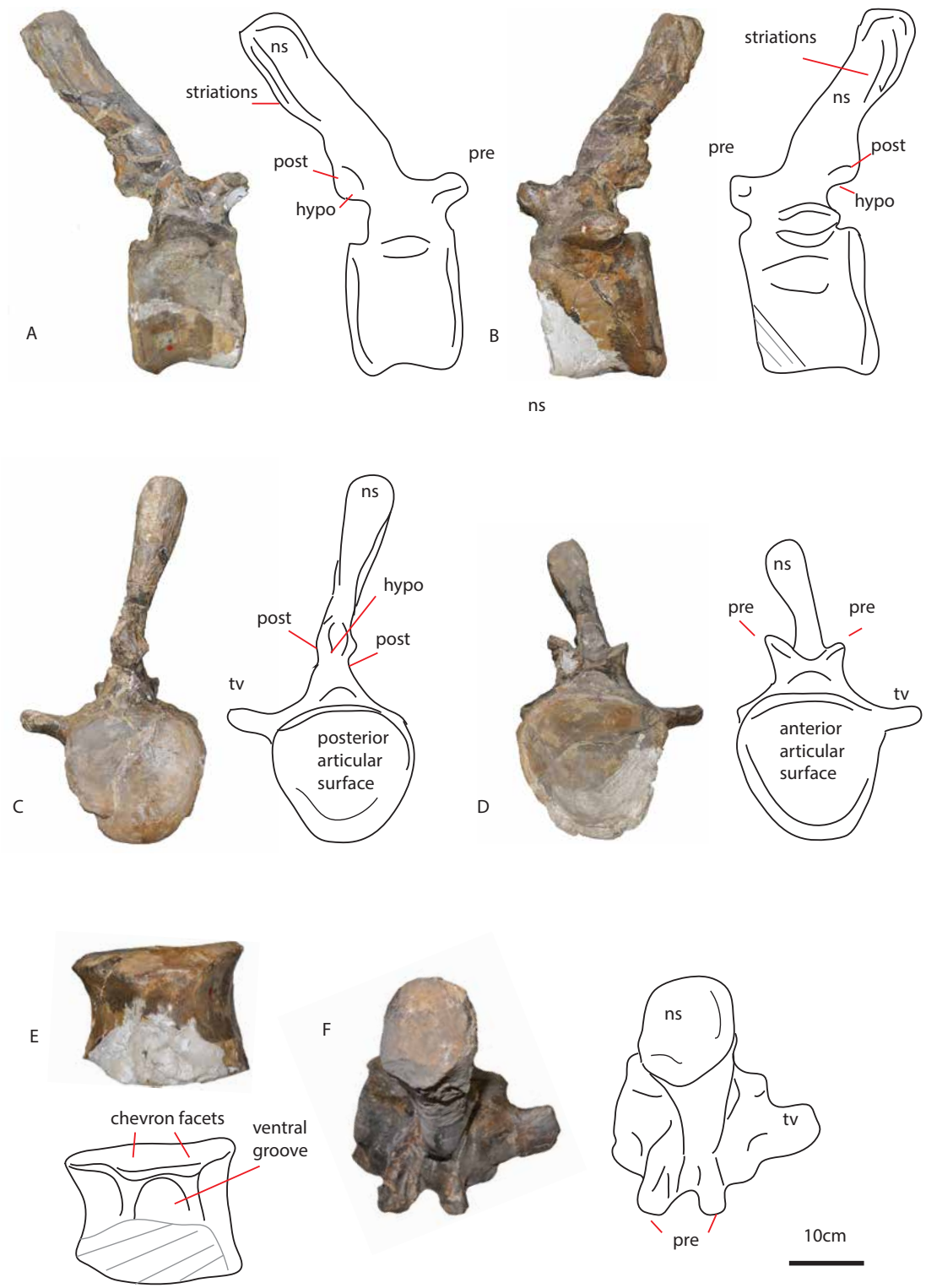

Figure 23: Caudal PVL 4170 (21) in lateral (A,B), posterior (C), anterior (D), ventral (E) and dorsal (F) views. Abbreviations: hypo = hyposphene, ns = neural spine, post = postzygapophysis, pre = prezygapophysis, tv = transverse process.

PVL 4170 (22)

This anterior middle caudal has a partially broken neural spine and partially broken right prezygapophysis IFigure 24A,B). In anterior view, the articular surface of the centrum is oval, with the dorsal edge similar to PVL 4170 (19-21), see Figure 24D. In posterior view, the articular surface is oval to round, with the long axis on the dorsoventral plane (Figure 24C). The rim that cups the articular surface is thinner than in PVL 4170 (19-21). In lateral view, the ventral side of the centrum is concave, and in ventral view the anterior rim showing chevron facets (Figure 24A,E). Because the ventral side of the centrum slopes down, the posterior end lies lower than the anterior end (Figue 24A). In ventral view, the centrum is symmetrically concave transversely. The axial midline is smooth, with no keel or struts, however, anteriorly two large, rugose semi-circular chevron facets are visible, and posteriorly two smaller semi-circular ones (Figure 24E).

The neural canal is triangular to semi-circular. In posterior view,the neural canal is semi-oval (Figure 24C,D).

The prezygapophyses are less triangular than in PVL 4170 (21), rather they are blunted triangular to rounded (Figure 24A,D). The prezygapophyses are stout struts that protrude anteriorly and dorsally from the neural arch. They have a rounded tip at their extremities. In dorsal view, the prezygapophyses show stout beams and stout spinoprezygapophyseal laminae. Posteriorly, the same U-shaped recess is visible as in PVL 4170 (19-20-21), ventral to the hyposphene and postzygapophyses, which together have the same morphology as the previous caudals PVL 4170 (19-20-21) and the posterior dorsals PVL 4170 (16-17, see Figure 24A,C).

The diapophyses bend towards the posterior side (Fgiure 24B). The centrum is broadened transversely around the diapophyses.

The neural spine is inclined posteriorly, directly dorsally from an axial thickening of the neural spine (Figure 24A). This part however, is broken off.

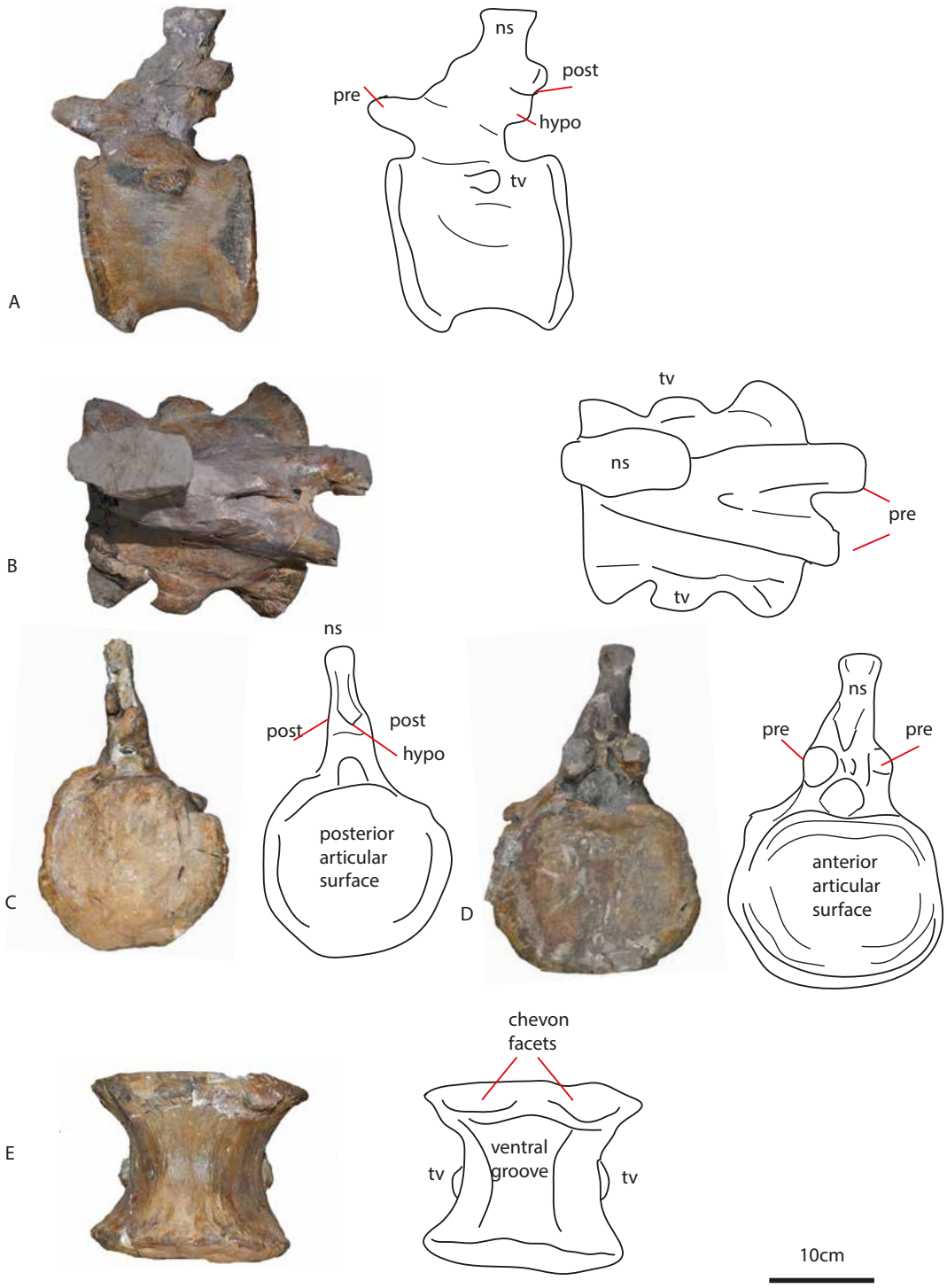

Figure 24: Caudal PVL 4170 (22) in lateral (A), dorsal (B), posterior (C), anterior (D) and ventral (E) views. Abbreviations: hypo = hyposphene, ns = neural spine, post = postzygapophysis, pre = prezygapophysis, tv = transverse process.

PVL 4170 (23)

In anterior view, this middle caudal has a round articular surface (Figure 25C). The articular surface is concave, with the deepest point in the center. The same thick rim is present as in PVL 4170 (19-22), however it is less rugose in this caudal. In posterior view, the articular surface is round (Figure 25D). The rim surrounding the articular surface shows rounded striations as in the previous caudals. In ventral view, the centrum is of a similar morphology to in PVL 4170 (22), see Figure 25E. It has two well-developed chevron facets on the anterior ventral rim of the anterior articular surface. These chevron facets are connected medially by a rugose elevated ridge of bone. On the posterior rim two small semi-circular chevron facets are discernible.

The neural canal is rounded to triangular in shape, with the horizontal plane on the ventral side (Fgiure 25C,D).

The prezygapophyses are directed more dorsally than anteriorly (Figure 25A,C). In dorsal view, the prezygapophyses are bent towards their medial side, as in PVL 4170 (22), see Figure 25B. In lateral view, the neural arch is of similar morphology as in PVL 4170 (22), however, the prezygapophyses are directed more dorsally than ventrally and the diapophyses are shorter in length (Figure 25A).

The diapophyses are thickened axially compared to previous caudals, and remain more close to the central body, where the centrum is thickened transversely (Figure 25B). Both the diapophyses and postzygapophyses are reduced in size compared to previous caudals. The postzygapophyses are present as small triangular bosses (Figure 25A,D).

The neural spine is of equal transverse width, unlike the previous caudals (Figure 25A). The neural spine is still elongated as in previous caudals, however it is more straight and does not bend dorsally more than 1/3rd of its dorsoventral length onwards. The axial thickening however, is still visible as in the previous caudals. The spine summit is slightly saddle shaped as in the previous anterior caudals (Figure 25B). The neural spine summit does still show the elevated rhomboid morphology as in the previous anterior caudals and in the posterior dorsals of PVL 4170.

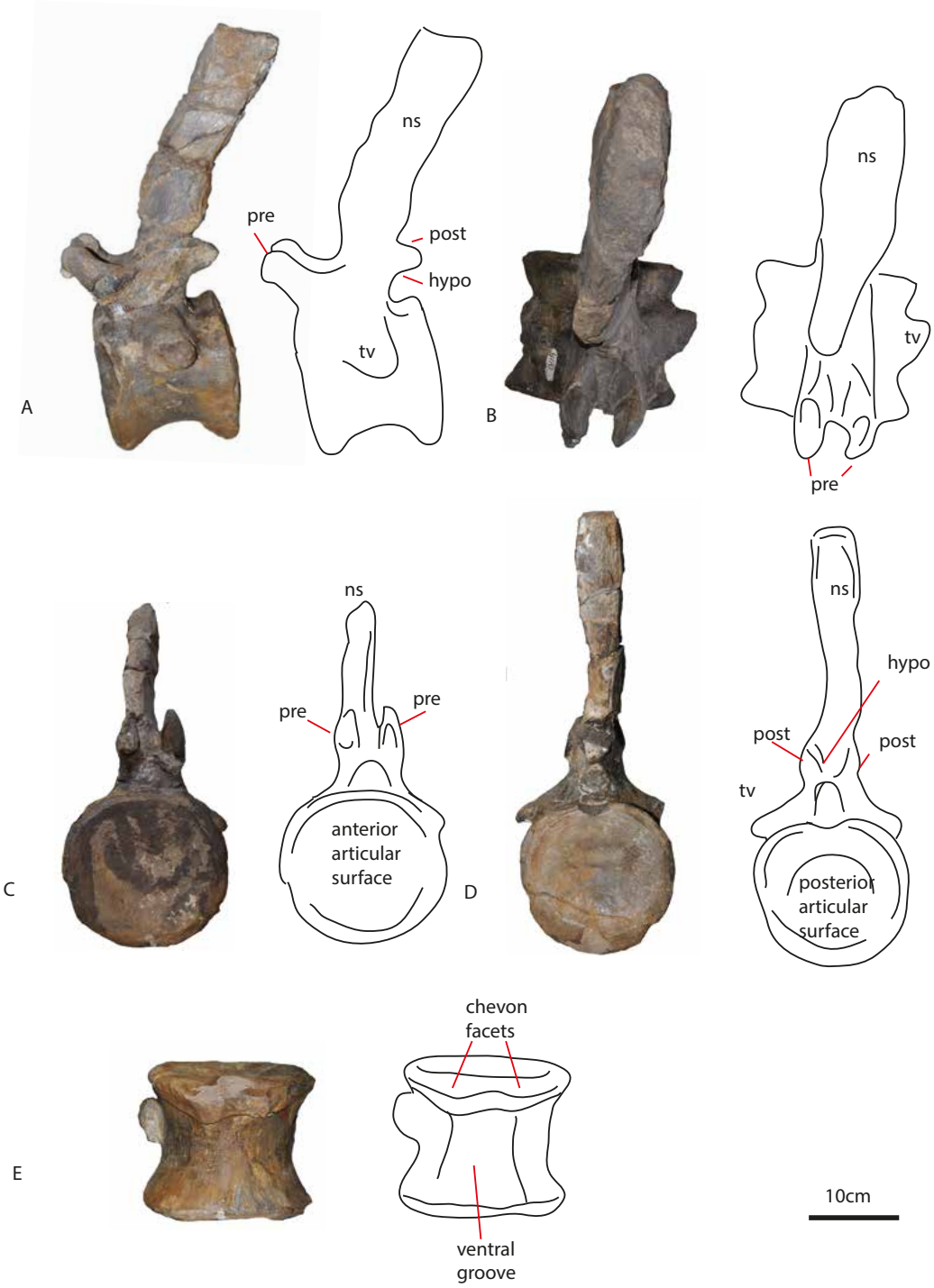

Figure 25: Caudal PVL 4170 (23) in lateral (A), dorsal (B), anterior (C), posterior (D) and ventral (E) views. Abbreviations: hypo = hyposphene, ns = neural spine, post = postzygapophysis, pre = prezygapophysis, tv = transverse process.

PVL 4170 (24)

In anterior view, this caudal has a more oval than round articular surface, with the long axis in the dorsoventral plane (Figure 26D). This is different to the other caudals, however, it and its surrounding thick rim are also partially damaged on the anterior surface. In posterior view, the articular surface of the centrum is oval, with the long axis in the transverse axis, giving the articular surface a more flattened appearance (Figure 26C). In lateral view, the centrum shows an elliptical fossa ventral to the diapophyses (Figure 26A,B). In ventral view, the centrum is smooth, without a keel or rugosities, with only a faint ventral groove, and is transversely concave (Figure 26F). The anterior chevron facets are similar to those in PVL 4170 (23), however they are less developed (Figure 26F).

The neural canal is more semi-circular than triangular (Figure 26C,D). The neural arch supporting the posterior neural canal opening is triangular in shape, and the neural canal itself is oval with an elongation on the dorsoventral plane (Figure 26C).

The right prezygapophysis is slightly damaged; the left is complete (Figure 26A,B,E). Its articular surface bends towards the lateral side, unlike in the previous caudals. The prezygapophyses are more elongated, and the postzygapophyses (Figure 26C) are more pronounced in this caudal, unlike PVL 4170 (23), which might mean that this caudal should be switched with the former caudal, in terms of vertebral order.

The neural spine is straight and rectangular in shape in anterior, posterior and lateral view, showing a more simple morphology than the previous caudals (Figure 26A,B,E). The spine summit has a faint saddle shape, however not as pronounced as in previous anterior caudals; the summit shows a more flat surface, with only a slight posterior elevation (Figure A,B,E).

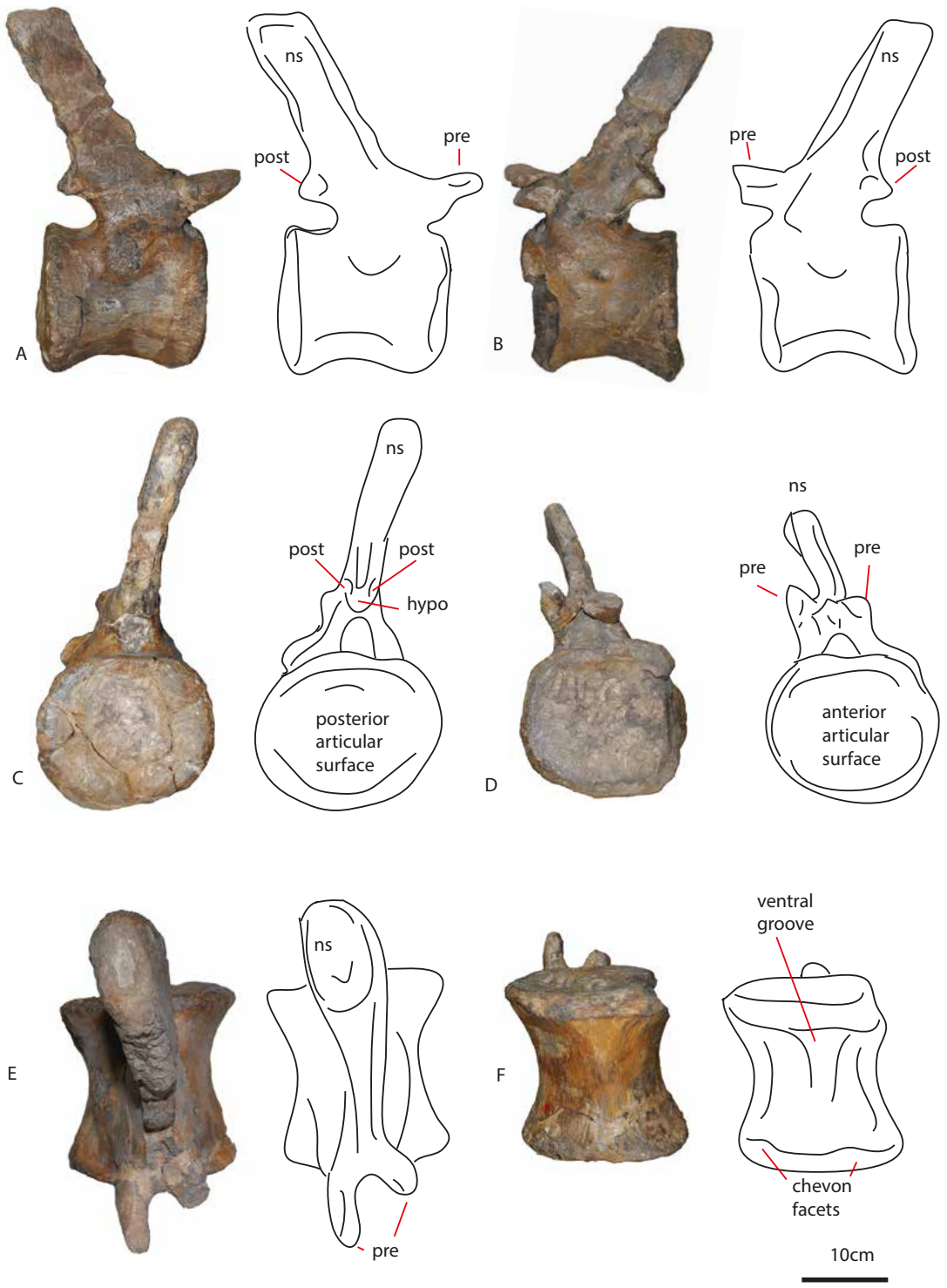

Figure 26: Caudal PVL 4170 (24) in lateral (A,B), posterior(C), anterior (D), dorsal (E) and ventral (F) views. Abbreviations: hypo = hyposphene, ns = neural spine, post = postzygapophysis, pre = prezygapophysis, tv = transverse process.

PVL 4170 25

In anterior view, the dorsal rim of the anterior articular surface is well developed, and shows a slight indentation below the neural canal, giving it a small heartshape as in the more anterior caudals (Figure 27D). In posterior view, the articular surface of the centrum is round, and shows pronounced round striations on the rim (Figure 27E). In lateral view, the centrum displays a larger anterior articular surface than posteriorly (Figure 27A,B), as in other middle caudals of eusauropods (Upchurch 2004). The anterior rim is also more rugose than the posterior one. In ventral view, the centrum shows two large chevron facets on the anterior side, and two smaller ones on the posterior side (Figure 27C). The neural canal is similar in morphology to that of PVL 4170 (23-24), see Figure 27D,E.

The prezygapophyses are connected medially by a ridge of bone, which is different from the previous caudal vertebrae, where a deep U-shaped gap between the prezygapophyses exists (Fgiure 27A,B,D,F). The prezygapophyses themselves are damaged. In dorsal view, the prezygapophyses and spinoprezygapophyseal laminae are clearly visible as stout beams, as in PVL 4170 (22). The posterior dorsal rim of the centrum shows a sharp U-shaped recess towards the postzygapophyses, which are positioned in an angle at almost 90 degrees, Figure 27A,B,E). The postzygapophyses are visible as lateral triangular protrusions ventral to the neural spine.

The diapophyses in this caudal are reduced to small protrusions on the more dorsal side of the centrum, indicating the transition from the middle caudals to a more posterior caudal morphology (Figure 27E,F). They are shaped as round bosses on the lateral sides of the centrum, in dorsal view.

The neural spine is straight, and increases in axial width towards the summit (Figure 27A,B,F). It is more inclined posteriorly than dorsally, confirming its middle-posterior caudal position. On the lateral side, rugose dorsoventrally positioned striations are visible. The spine summit is not straight, but shows a faint saddle shape (Figure 27A,B).

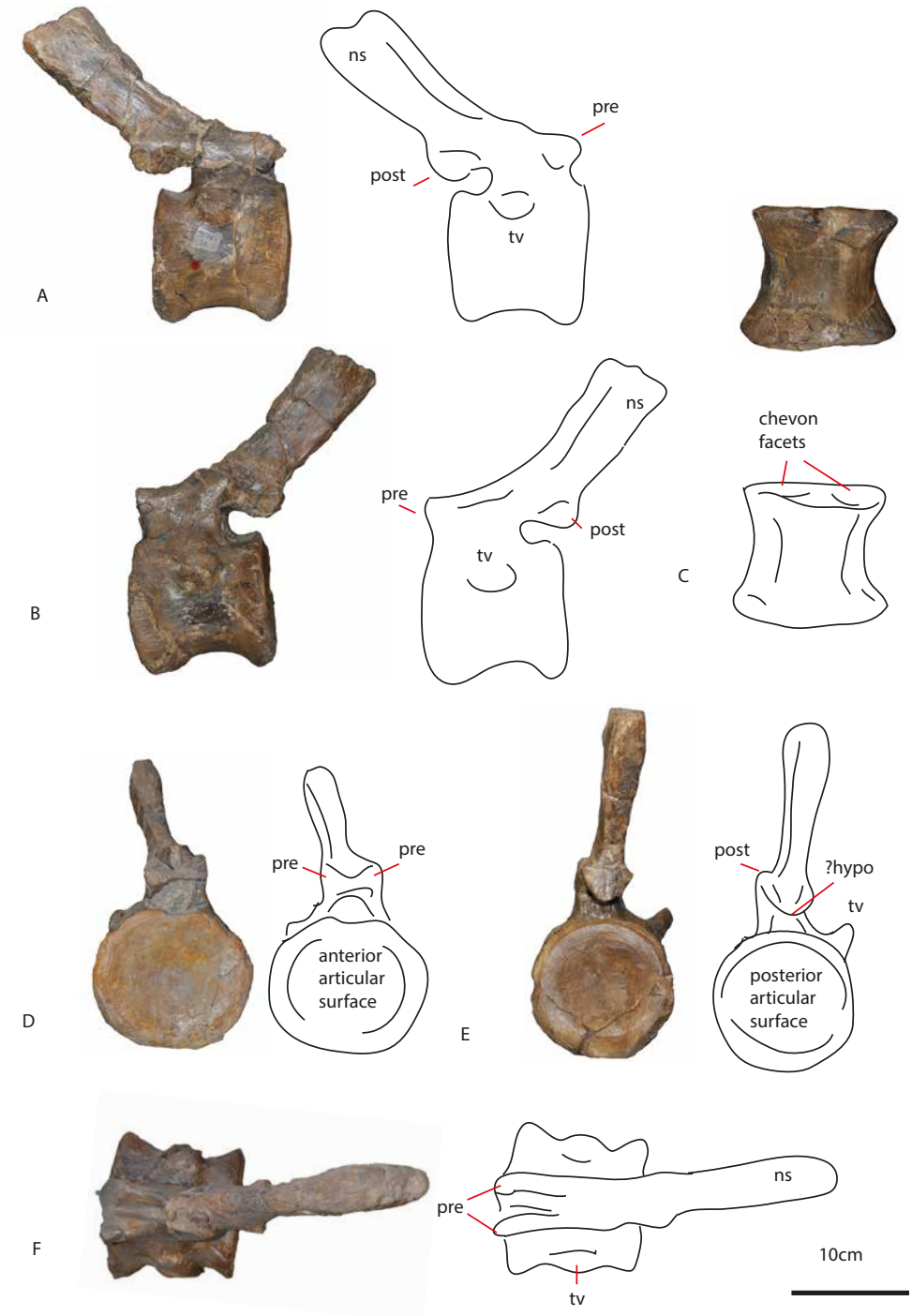

Figure 27: Caudal PVL 4170 (25) in lateral (A,B), ventral (C), anterior (D), posterior (E), and dorsal (F) views. Abbreviations: hypo = hyposphene, ns = neural spine, post = postzygapophysis, pre = prezygapophysis, tv = transverse process.

PVL 4170 (26)

In anterior view, the articular surface of the centrum is oval and dorsoventrally flattened as in PVL 4170 (25), see Figure 28B. In posterior view, the articular surface is oval and elongated in the dorsoventral axis (Figure 28A). It has rough circular striations as in the other caudals. In lateral view, the centrum is axially elongated, suggesting a possibly more posterior position than the numbering might indicate (Figure 28C,D). In dorsal view, the axial elongation of the centrum is apparent, again indicating this caudal might be more posterior than middle (Figure 28F). This could also imply that some caudals that originally existed between PVL 4170 (25) and (26) are missing here. The outline of the centrum is symmetrical in dorsal view; the flaring of the extremities and the constriction of the centrum in the middle (Figure 28F). In ventral view, the centrum is smooth and concave, and the chevron facets are not pronounced (Figure 28E).

The same indentation as in most caudals, ventral to the neural canal, is visible, however, this part is also partially broken. The anterior neural canal is large and triangular to oval in shape (Figure 28B). It occupies most of the anterior surface of the neural arch. The posterior neural canal is oval and also dorsoventrally elongated (Figure 28A).

The prezygapophyses are still protruding anteriorly, however as in PVL 4170 (25), the recess between them is not pronounced (Figure 28B,C,D). The prezygapophyses are inclined dorsally and medially, and make an angle of about 45 degrees with respect to the centrum, with the triangular articular surface on the medial side. The postzygapophyses are reduced to triangular bosses ventral to the neural spine (Figure 28A,C,D).

The diapophyses are reduced to bulges on the lateral side of the centrum, beneath which a slight depression still remains (Figure 28C,D,F).

The neural spine is partially broken off at the base. Dorsal to the postzygapophyses, the neural spine displays rough dorsoventrally elongated striations (Figure 28C,D). The neural spine is projecting dorsally and posteriorly, being parallel to the centrum. In dorsal view, all extremities are symmetrical, giving the caudal the outline of a cross in dorsal view (Figure 28F).

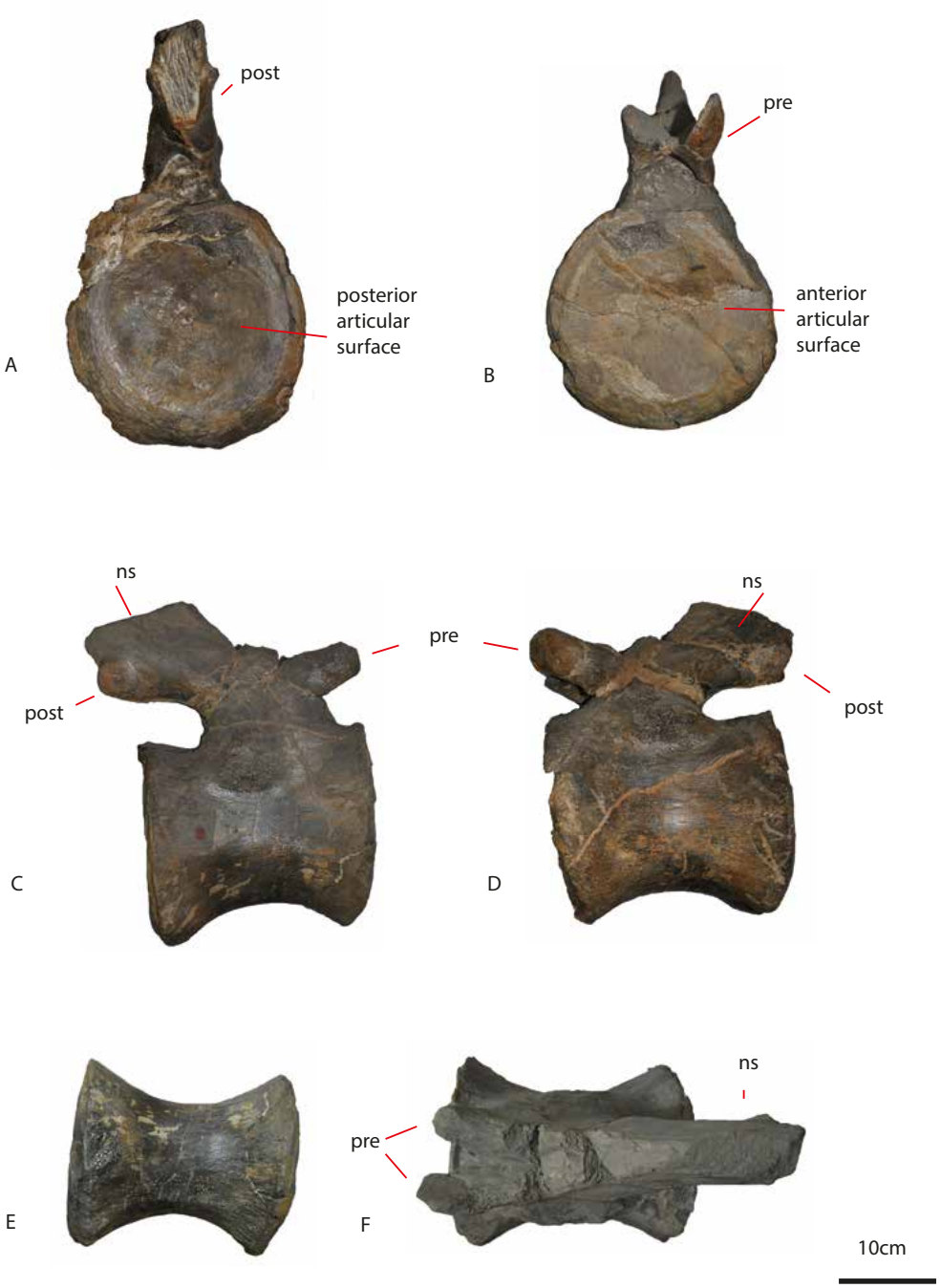

Figure 28: Caudal PVL 4170 (26) in posterior (A), anterior (B), lateral (C,D), ventral (E), and dorsal (F) views. Abbreviations: ns = neural spine, post = postzygapophysis, pre = prezygapophysis, tv = transverse process.

PVL 4170 (27)

The centrum of this middle-posterior caudal is symmetrically amphicoelously shaped. In anterior view, the articular surface is oval and dorsoventrally flattened as in PVL 4170 (25-26, see Figure 29F). Similarly, the dorsal rim of the articular surface is heart-shaped. In lateral view, the anterior articular surface is slightly longer dorsoventrally than the posterior one (Figure 29C,D). The anterior also shows the chevron facets clearly as ventral rugose protrusions. The centrum on the ventral side is concave, and on the lateral axial surface the centrum seems to be slightly transversely flattened (Figure 28B). In posterior view, the articular surface is oval, with the elongation in the dorsoventral plane (Figure 28E). It is also flattened transversely. In ventral view, no chevron facets are visible, however, the centrum shows a flattening in the axial midline, which is slightly concave (Figure 29B).

On the lateral sides of the centrum, the diapophyses are visible as rudimentary, rugose rounded bulges (Figure 29C,D). The prezygapophyses are damaged, however, this renders the neural canal clearly visible as a semi-circular/triangular structure (Figure 29E,F).

The neural spine is broken, however, it is straight and directed posteriorly and dorsally, it being more flattened towards the centrum than in previous caudals, indicating again a more posterior caudal morphology (Figure 29C,D). In dorsal view, the spine is clearly flattened towards the centrum (Figure 29A).

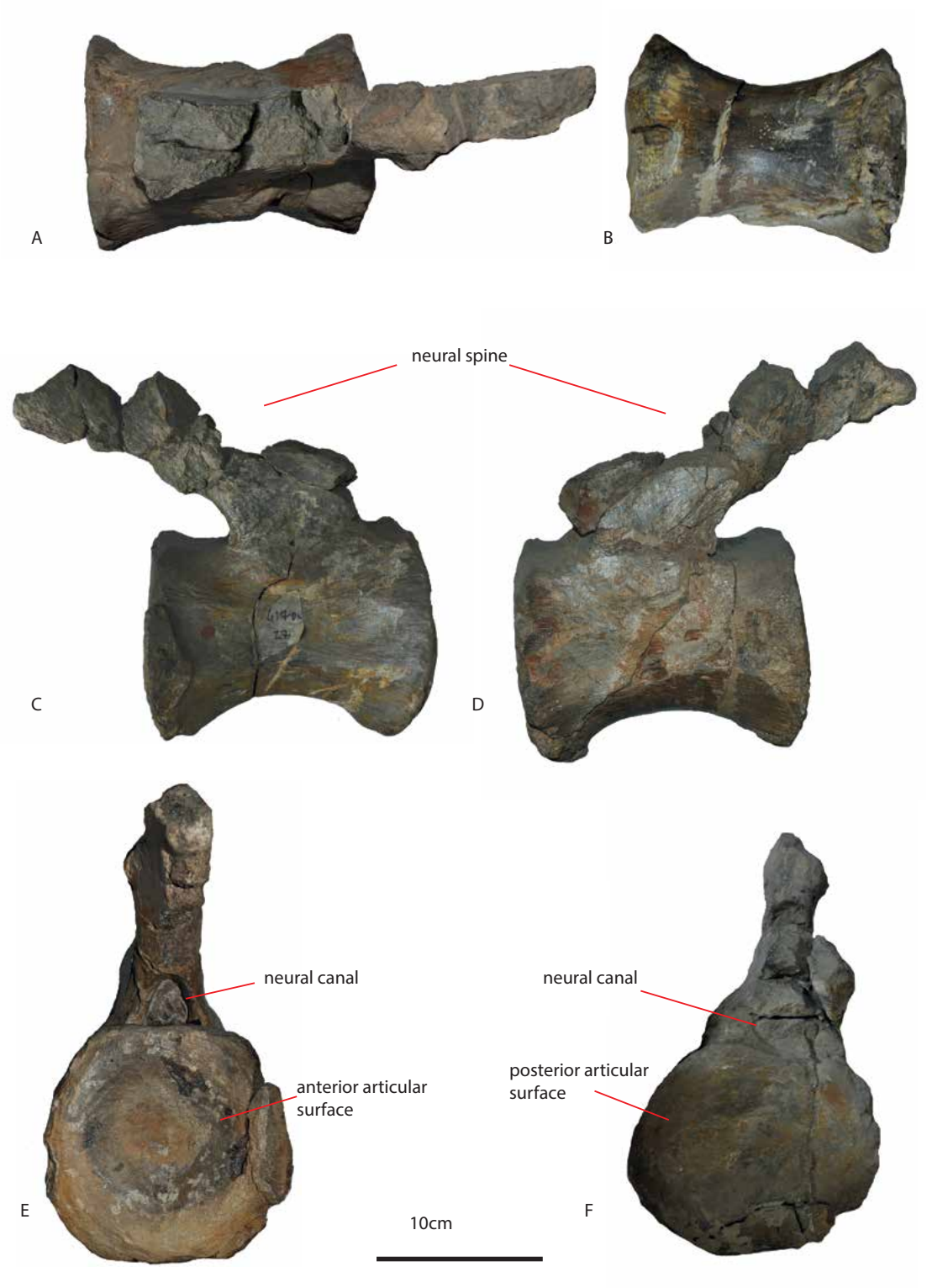

Figure 29: Caudal PVL 4170 (27) in dorsal (A), ventral (B), lateral (C,D), posterior (E), anterior (F) views. Abbreviations:.

PVL 4170 (30 / 31 /32)

The last preserved caudals are middle/posterior caudals. They are dorsoventrally and transversely smaller than previous caudals, and show an even more simplified morphology than middle caudals. The anterior articular surface is oval with the elongation axis on the dorsoventral plane, see Figure 30A. The posterior articular surface is smaller in size and more rounded than oval (Figure 30B). These caudals do not have the prezygapophyses, postzygapophyses or neural spines preserved (Figure 30), except for PVL 4170 (32). In lateral view, PVL 4170 (32 has) prezygapophyses present as small rounded protrusions that project anteriorly. The postzygapophyses are no longer visible. PVL 4170 (32) has a short, robust spine. It is inclined posteriorly and ventrally, back towards the centrum, indicating a posterior caudal position.

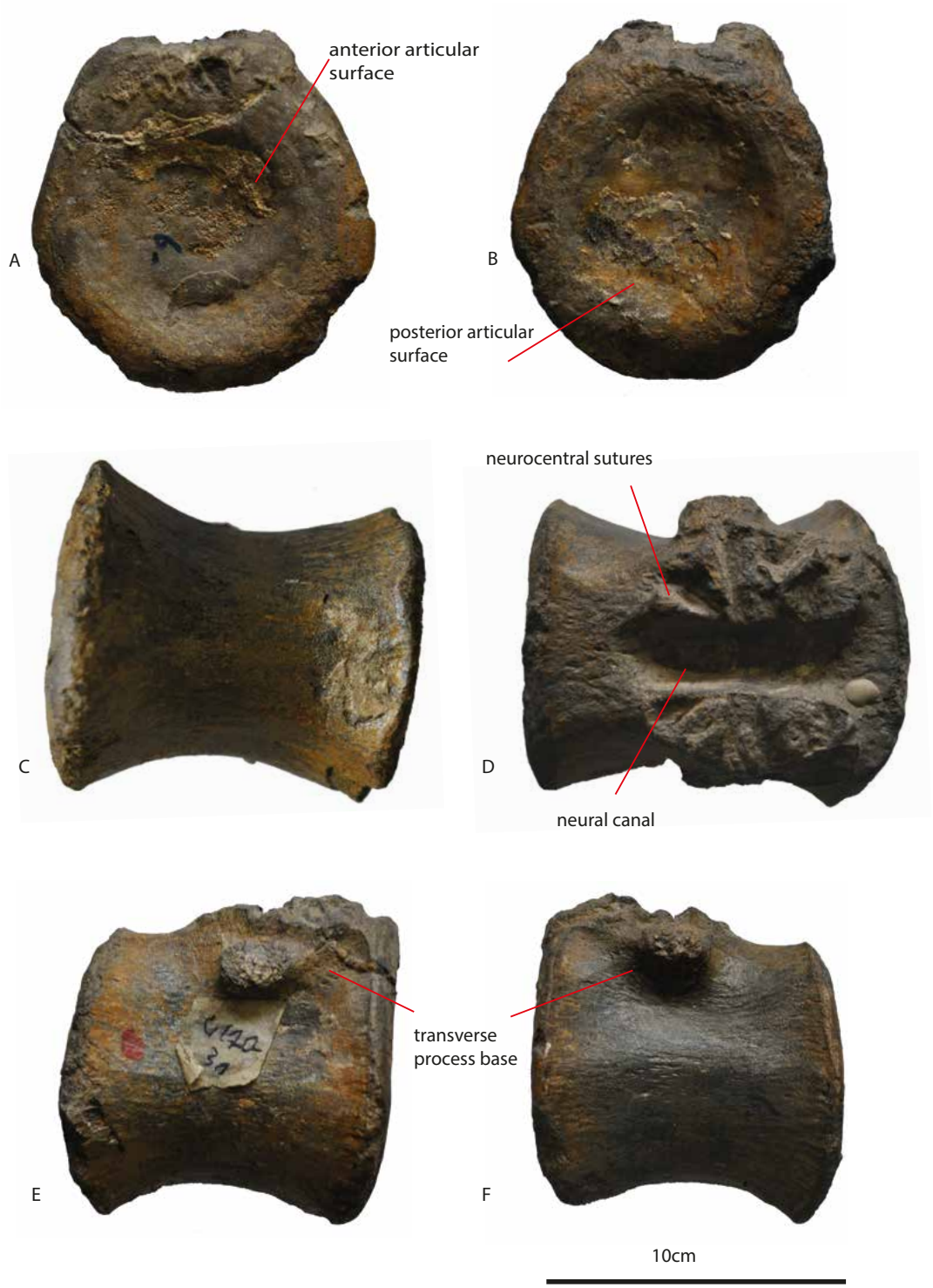

Figure 30 Caudal PVL 4170 (30) in anterior (A), posterior (B), ventral (C), dorsal (D), lateral E,F) views.

2.4.2 Appendicular skeleton

Pelvic girdle

Table 3: Measurements on appendicular elements of PVL 4170.

Element	Measurement	cm
Femur	proximodistal length	117,5
	mediolateral width proximal end with condyle	40
	mediolateral width proximal end without condyle	28
	distance from proximal end to distal tip of fourth trochanter	25
	midshaft mediolateral width	24
	midshaft anteroposterior maximum length	9
	midshaft minimum circumference	53
	distal end maximum anteroposterior length	40
	mediolateral width tibial condyle	10
	mediolateral width fibular condyle	7
	proximodistal length 4th trochanter	18
	anteroposterior length 4th trochanter	5
Ilium	anteroposterior maximum length	97
	dorsoventral maximum height	54
	acetabular anteroposterior length	33
	acetabular mediolateral depth (width)	18
	preacetabular (anterior lobe) anteroposterior length	30
	anterior lobe mediolateral width	12
	postacetabular maximum anteroposterior length	37
	postacetabular minumum mediolateral width	3
	postacetabular maximum mediolateral width	9
	pubic peduncle proximodistal length	31
	pubic peduncle mediodistal width	18
	ischial peduncle anteroposterior length	19
	ischial peduncle mediodistal width	10
Pubis	proximodistal length	55
	midshaft mediodistal width	9
	pubic apron maximum length (proximodistal)	35
	pubic apron maximum width (anteroposterior)	17
	iliac peduncle mediodistal width	9
	iliac peduncle anteroposterior length	13
	ischial peduncle mediodistal width	6
	ischial peduncle proximodistal length	18
	pubic foramen length	4
	pubic foramen width	3
Ischia	mediodistal width of the distal end	27
	proximodistal length	35

Ilium PVL 4170 (34)

According to the Cerro Condor Norte quarry map (Fig 1), two ilia were recovered in the original excavations. However, the whereabouts of the second ilium are unknown. Even though the MACN in Buenos Aires hosts several ilia, which can be attributed to *Patagosaurus* (See Chapter 3), none of these are large enough to match the one ilium in the collections of the Instituto Miguel Lillo in Tucuman.

The right ilium is axially longer than dorsoventrally high (Figure 31C). The dorsal rim is convex as in most sauropods, however, the curvature resembles the high dorsal rim of basal neosauropods/derived eusauropods (e.g. *Apatosaurus, Haplocanthosaurus, Diplodocus, Cetiosaurus*) more than those of more basal forms, which tend to be less convex, as seen in *Plateosaurus* and *Tazoudasaurus* (Allain et al., 2004, Allain and Acquiesbi 2008). The iliac body is not entirely straight; it is offset from the axial plane to the lateral side at the anterior lobe, whereas the midsection is axially aligned, and the posterior end is slightly offset to the medial side. The ilium of the eusauropod *Lapparentosaurus* also follows this curvature. *Cetiosaurus oxoniensis* shows a more or less straight anterior half of the iliac body, though the posterior half is also slightly offset medially.

The preacetabular process in lateral view is hook-shaped (Figure 31C); a common feature among sauropods, and found in the eusauropods *Cetiosaurus*, *Barapasaurus*, *Omeisaurus junghsiensis*, and *Shunosaurus lii* (Tang et al., 2001; Upchurch and Martin, 2003; Bandyopadhyay et al., 2010), although not in *Tazoudasaurus* (Allain and Aquesbi, 2008). The anteriormost part of the process has a thickened rugose dorsal side, which is much thicker than the dorsal edge of the more posterior part of the ilium, and is slightly constricted dorsoventrally. However, the posteriormost dorsal rim of the iliac blade shows another

thickened ridge. Ventrally the preacetabular process slopes down gently, not in a sharp curve, towards the pubic peduncle of the ilium.

The preacetabular process in anterior view (Figure 31A) is dorsally rugose and pitted for muscle and cartilage attachment. It is slightly bent towards the lateral side, thus not entirely aligned in the axial plane. The pubic peduncle in anterior view is a stout element, which flares out distally and is less wide at its proximal base. The articular surface of the distal end of the pubic peduncle is not symmetrical, but slightly triangular in shape. The dorsal part of the preacetabular lobe is similar to *Haplocanthosaurus* in that it has a similar thickening rugosity of the anteriormost hook-shaped process, but differs from *Haplocanthosaurus* in that it constricts slightly behind this process, whereas in *Haplocanthosaurus* the dorsal rugosity behind the anterior process continues smoothly (Hatcher, 1903; Upchurch et al., 2004). The constriction does seem to be natural and not due to damage.

The pubic peduncle is a slender rod-shaped element, which widens towards the distal end, both anteriorly and posteriorly, in lateral view (Figure 31C). The anterior distal side of this peduncle bulges slightly convexly. The posterior side of the pubic peduncle (or the anterior edge of the acetabulum) is concave. The extremity of the peduncle is convex anteriorly and flat posteriorly, and the surface is rugose.

The acetabulum is relatively wide as in *Barapasaurus*, *Haplocanthosaurus*, and diplodocids (Hatcher, 1903; Upchurch et al., 2004; Bandyopadhyay 2010), but differs from *Cetiosaurus*, *Tazoudasaurus* and titanosauriforms (Upchurch and Martin, 2003; Allain and Aquesbi, 2008; Díez Díaz et al., 2013; Poropat et al., 2014), see Figure 31C. Its dorsal rim is transversely acute towards the medial side. The rim itself is concave.

The ischial lobe is clearly visible as the ventral half of the butterfly-wing like posterior end of the illiac blade (Figure 31B,C). In lateral view it is a semi-round structure. The surface of the ischial peduncle bulges out laterally, giving it a slight offset from the iliac blade to the lateral and ventral side. It is also offset ventrally and posteriorly from the acetabulum (Figure 31B). The articular surface for the ischium is oval in shape and rugosely pitted and striated. The ischial peduncle of the ilium in lateral view is a semi-round, non-prominent lobe.

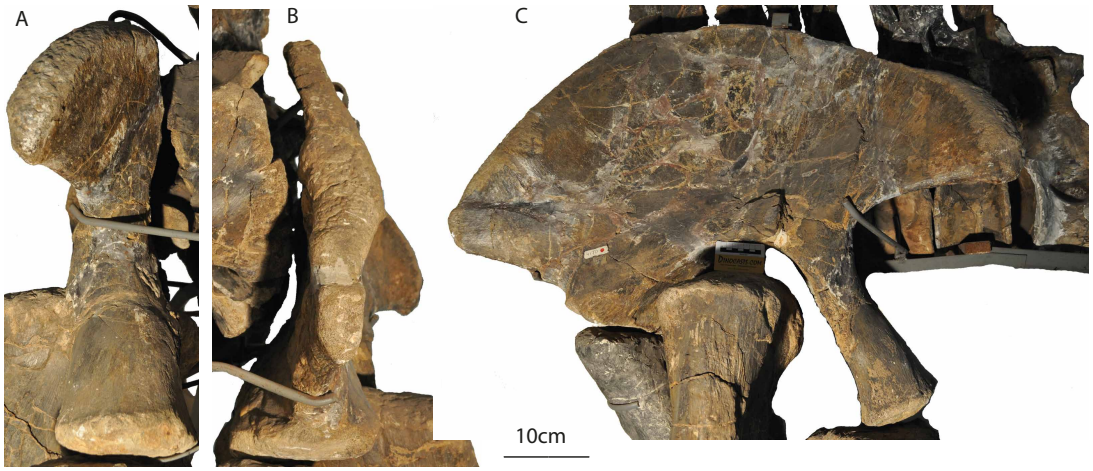

Figure 31: PVL 4170 (34) ilium in anterior (A) posterior (B) and lateral (C) view.

Pubis PVL 4170 (35)

The right pubis is almost complete. In lateral view, the pubic shaft shows a slightly convex dorsal side and a slightly concave ventral side of the shaft, providing the shaft with a slight curvature in lateral view (Figure 32A). The shaft is gracile, taking up approximately 2/3rds of the entire pubic length. The shaft is more compressed lateromedially than that of *Cetiosaurus oxoniensis* (Upchurch and Martin, 2003) *Mamenchisaurus youngi* (Pi et al., 1996), or *Bothriospondylus madagascariensis* (Mannion, 2010). Moreover, the length of the pubis is more or less similar to that of the ischium. In this way it more resembles that of *Haplocanthosaurus* than other sauropods (Hatcher, 1903). The shaft and proximal part are aligned (Figure 32A); in that there is no torsion of the pubis as in more derived sauropods (Upchurch and Martin 2003; Upchurch et al., 2004). Interestingly, the African basal eusauropods *Spinophorosaurus* and *Bothriospondylus* have a much more 'robust' pubis than *Patagosaurus* (Remes et al., 2009; Läng, 2010). The pubis of *Tazoudasaurus* appears to be of the more robust type as well, however this is not entirely clear, as it belongs to a juvenile (Allain et al., 2008). The elongated and slender shaft is also seen in *Vulcanodon* (Cooper, 1984), however in this taxon the pubic apron is smaller. Also, in *Vulcanodon*, the pubis is much shorter than the ischium, as in most sauropods (Cooper, 1984; Upchurch et al., 2004).

The distal expansion of the pubis in lateral view flares more dorsally than ventrally, and tapers acutely to a point (Figure 32B,D). This distal shape is similar to that of *Barapasaurus* (Bandhyopadhyay, 2010) is more flared than *Haplocanthosaurus* (Hatcher, 1903). The distal end of the pubis in distal view is suboval in shape (Figure 32B,D).

The pubic apron is slightly convex ventrally in lateral view, with the ischial peduncle tapering obliquely (Figure 32A). The pubic peduncle of the pubis projects medially and slightly ventrally. Even though the mirroring pubis is not present, the pubic basin can be estimated to be wider than that of *Barapasaurus,* in which taxon the pubic basin is narrow.

The pubic foramen is 'pear-shaped' in lateral view; a dorsoventrally elongated oval that is constricted slightly dorsal to the middle (Figure 32A).

The pubic rim of the acetabulum is a steeply sloping surface from the iliac peduncle to the ischial peduncle in lateral view. This rim tapers ventrally and posteriorly towards the acetabulum.

The ischial peduncle has a roughly triradiate, transversely narrow and dorsoventrally elongated articulation surface, with the narrowest point on the ventral side. The length of the ischial peduncle of the pubis is less than 33% of the length of the entire pubis; further reinforcing the elongation of this pubis. In *Haplocanthosaurus* the length of the ischial peduncle is also less than 33%, in *Cetiosaurus* as well (Hatcher, 1903; Upchurch and Martin 2003). The iliac peduncle is dorsally elevated from the pubic apron and the shaft, as in *Cetiosaurus*. The iliac articulation surface is rugose, and curves slightly medially and posteriorly. There is no 'hook'-shaped ambiens process present as in *Lapparentosaurus*, *Bothriospondylus* or derived sauropods (Mannion, 2010). The pubic symphysis projects medially and ventrally, as in most sauropods (Upchurch et al., 2004)

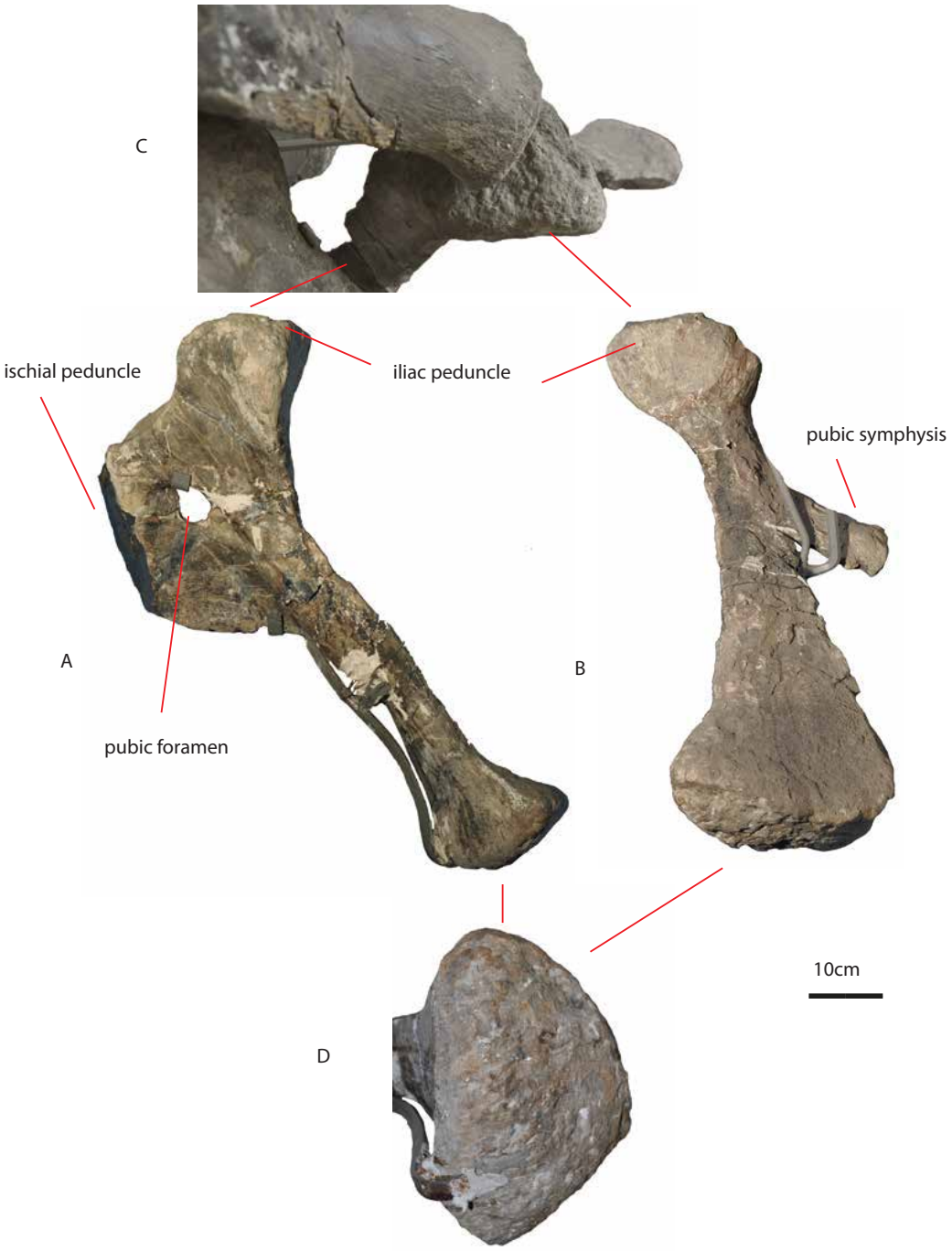

Figure 32: PVL 4170 (35) Pubis in lateral (A), distal (B), dorsal (C) and distal-most (D) view. Note that D is not to scale.

Ischia PVL 4170 (36)

The fused distal parts of both ischia are preserved, with fusion occurring at around 2/3 of the shaft length (Figure 33). The proximal parts are recreated in plaster, therefore these will not be described; however, part of the shaft of the right ischium is preserved (Figure 33C). In lateral view, the ventral side is concave, and the shaft expands both dorsally and ventrally towards the limit of the distal end (as far as it is preserved).

There is a peculiar oval depression on the lateral side of the right ischium, approximately at the height of the fusion with the left ischium (Figure 33A). This could be a pathology, however, seeing as the femur originally was overlaying the ischium in situ during excavations (see Figure 1), this depression is most probably taphonomic. The extremities of the fused ischia flare out distally towards the sagittal plane. In posterior view, the distal ends are directed laterodorsally and medioventrally (Figure 33B). The fusion forms a wide V-shape with an angle of ±110°, an intermediate stage between the coplanar *Camarasaurus* ischial fusion state and that of *Cetiosaurus, 'Bothriospondylus madagascariensis'* and *Vulcanodon* (Janensch, 1961; Cooper, 1984; Upchurch and Martin, 2003; Mannion, 2010). In dorsal view, the shaft of the right ischium bends and bulges slightly towards the lateral side at 2/3rd of shaft length, but this is probably due to the taphonomic/pathological damage, as the left ischial shaft is concave laterally in dorsal view. The surfaces of the ischial extremities are convex and rugose (Figure 33B).

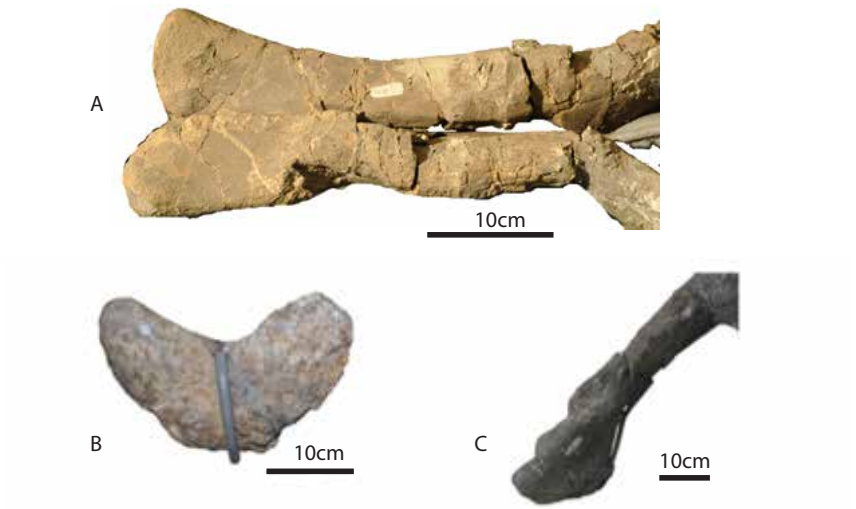

Figure 33: PVL 4170 (36) ischia in dorsal (A) view, distal (B) view, and lateral (C) view.

Femur PVL 4170 (37)

The right femur is well-preserved (Figure 34). It is a stout element, transversely nearly three times wider than axially long. This makes it anteroposteriorly shorter than transversely, as in most sauropods other than Titanosauriformes. The stoutness already distinguishes it from *Lapparentosaurus* (MAA 67), which has a more slender femur, albeit a juvenile one. The shaft has an elliptical cross-section. There is no lateral bulge present as in Titanosauriformes (Upchurch et al., 2004). The fourth trochanter is positioned slightly medial to the dorsoventral midpoint of the shaft, therefore it is not entirely medially positioned. This is also seen in *Tazoudasaurus, Cetiosaurus, Volkheimeria*, and neosauropods like *Tornieria* (Bonaparte 1986a; Upchurch and Martin, 2003; Allain and Aquesbi, 2008; Remes, 2009).

In anterior view, on the proximal side of the femur, a distinct groove is present, which runs along the midline from the proximal end to about 3/5th of the femoral length (Figure 34). This groove ends in a square-shaped depression, which has a rugose surface on its lateral side. The lateral side of the femur is slightly convex, and the medial side slightly concave,

giving the femur a curved appearance. It is not entirely certain whether this is due to taphonomy, or if it is the actual natural curvature. In the latter case, this could have implications for the stance and gait of *Patagosaurus*, (Wilson and Carrano, 1999), as the pubic basin could be wide compared to other sauropods. This can not be proven, however, without the other pubis present, which was never recovered from the Cerro Condor Norte locality.

The distal end of the anterior side of the femur shows a slight sub-quadrangular depression between the lateral and medial condyles, which forms a triangular shape more dorsally, as is common in basal sauropods. The lateral condyle is slightly offset, but this could be due to the taphonomic deformation slightly dorsal to it.

In posterior view, the curvature of the femur is still visible (Figure 34). A deep longitudinal muscle attachment scar is visible at around the midpart of the shaft. The greater trochanter is clearly visible in posterior view, as a small rounded protrusion, projecting dorsally from the proximolateral end of the femur. Directly medial to this, the proximal end of the femur shows a slight depression, before the medial onset of the femoral head. Distally, in posterior view, the tibial condyle is slightly damaged. It expands strongly medially, and medioposteriorly; this is also seen in *Cetiosaurus* (Upchurch and Martin, 2003). Between the tibial and fibular condyles the distal end of the posterior part of the femur shows a deep depression, also seen in *Cetiosaurus*, and possibly *Lapparentosaurus* (MAA 64). The fibular condyle is offset to the lateral side, and clearly protrudes posteriorly as a teardrop-shaped solid structure. The distal lateral condyle flares to the lateral side.

In dorsal view, the proximal end of the femur is strongly rugose and pitted, for cartilage and muscle attachments. Medial to the greater trochanter, the proximal end is axially constricted, after which the femoral head widens again. Unfortunately, the femoral head is not very clearly visible due to the mounting of the specimen, however, it is rounded,

standing out medially at about 20 cm. The medial end of the femoral head is not completely rounded, but a little pointed, though not as abruptly as in *Cetiosaurus*.

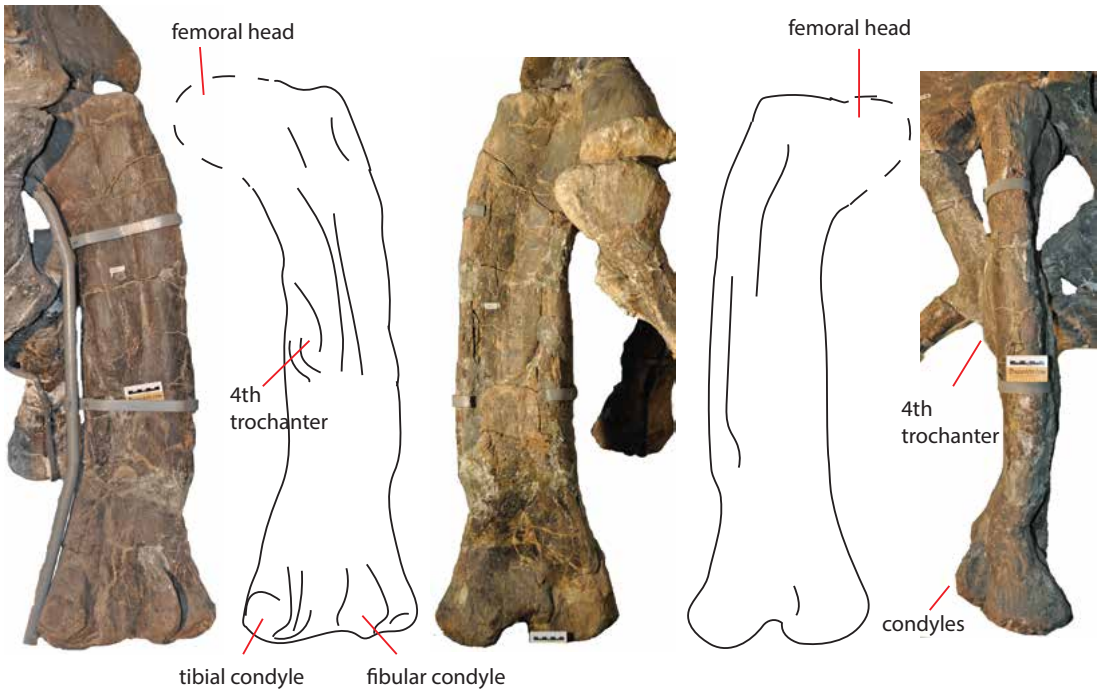

Figure 34: PVL 4170 (37) Femur in posterior, anterior, and lateral view. Scalebar equals 7 cm.

2.5 Discussion and conclusions

2.5.1 Diagnostic combination of characters of *Patagosaurus fariasi*

Cervicals

Diagnostic characters on the cervicals are anteriorly deep pleurocoels with a gradual shallowing towards the posterior side, and with clearly defined anterior, dorsal and ventral rims, but no clearly defined posterior rim. The anteriorly deep part of the pleurocoel is visible as a circular concavity. Damage in some cervicals show that only a thin plate of bone divided mirroring pleurocoels (e.g PVL 4170 6). Bonaparte (1979, 1986a, 1999) already noted the presence pleurocoel. Note that the pleurocoel is existing, but is more shallow in the dorsals, as is also noted by Bonaparte (1986a). The pleurocoel is defined for sauropods either as a pneumatopore or as a pneumatic structure (Wilson, 2002; Wedel, 2003, 2005, 2013; Upchurch et al., 2004), however, Carballido and Sander (2014) defined the structure using *Patagosaurus* as an example, as a lateral excavation on the centrum, with clear anterior, dorsal and ventral margins, and a posterior margin that could be either well-defined or more merging with the lateral body of the centrum (Carballido and Sander, 2014). As already remarked on by Bonaparte (1986a, 1999) and Carballido and Sander (2014), *Patagosaurus* does not show the internal pneumatic structure that neosauropods display. This type of pleurocoel outline, is seen in other Jurassic non-neosauropodan eusauropods, such as the Rutland *Cetiosaurus, Barapasaurus*, *Tazoudasaurus, Spinophorosaurus, Lapparentosaurus* (Bonaparte 1986c; Upchurch and Martin, 2003; Allain and Aquesbi 2008; Remes et al, 2009). The lack of a clear posterior margin of the pleurocoel is also common, except in the Rutland *Cetiosaurus* (Upchurch and Martin, 2003). The anterior depth of the pleurocoel in *Patagosaurus*, however, is probably unique to this taxon. In S*pinophorosaurus*

(Remes et al., 2009), as well as *Lapparentosaurus* (MAA 13), the pleurocoel is shallow at its anterior margin, and even shows a shallowing at its anterior ventral margin. in *Barapasaurus* (Bandyopadhyay, 2010), the entire pleurocoel is shallow. In *Shunosaurus*, the pleurocoel is anteriorly deep, but the concavity is more elongated and elliptic in shape, while in *Patagosaurus* this is circular and restricted to the anterior-most part of the pleurocoel. In *Klamelisaurus* (Zhao, 1993) the pleurocoel is entirely shallow, and in mamenchisaurs *Mamenchisaurus youngi* (Ouyang and Ye, 2002), *Zigongosaurus* (Hou et al., 1976), *Tonganosaurus* (Liu et al., 2010), and *Qijianglong* (Xing et al., 2015) the pleurocoel is compartmentalized by one or more accessory laminae into small deep pockets over the length of the centrum. Only in the Rutland *Cetiosaurus* (Upchurch and Martin, 2003), the pleurocoel is anteriorly deep as well. In some cervicals, an oblique accessory lamina is faintly present, which divides the pleurocoel into a deeper anterior section and a more shallow posterior section. This feature is also seen in the Rutland *Cetiosaurus*, in mamenchisaurs, and in neosauropods like *Apatosaurus* (Upchurch and Martin, 2003; Xing et al., 2015; Taylor and Wedel 2017). The faintness of this oblique accessory lamina, however, and the irregularity of its presence are probably not enough to make it a character. Note that in the contemporaneous Rutland *Cetiosaurus* (Upchurch and Martin, 2003) this lamina is more consistently present.

Another diagnostic feature of *Patagosaurus* is the wide angle between the postzygodiapophyseal laminae and the posterior centrodiapophyseal lamina. This angle is as wide as 55° to the horizontal (contra McPhee et al., (2016) who measured 41°) and is not found in any basal non-neosauropodan eusauropod (all have an angle between the podl and pcdl of between 30 and 40°) except *Shunosaurus* and *Kotasaurus* (Tang et al., 2001,; Yadagiri 2001), who have a high projection of the podl, but not a lower projection of the pcdl, therefore still not equating the high angle of *Patagosaurus.* In neosauropods, higher angles are reached with higher projections of the podl (Upchurch et al, 2004).

Finally, the cervicals of *Patagosaurus* are different from most other Early and Middle Jurassic non-neosauropodan eusauropods in that they are rather stout and short but dorsoventrally high. The aEI is on average lower than most other eusauropods (e.. *Cetiosaurus*, *Spinophorosaurus*, *Lapparentosaurus*, *Amygdalodon, see Table 1*). However, as the cervical series is not complete, some cervicals that are missing could have a higher aEI, the absence of which lowers the aEI. The aEI is possibly similar to that of *Tazoudasaurus*, however, the morphology of the cervicals between these two taxa is different, and also *Tazoudasaurus* does not have a complete cervical series.

Dorsals

The CDF, the pneumatic structure on dorsal neural arches, appearing first in the middle dorsal neural arches and expanding in the posterior dorsal neural arches, is the key feature that Bonaparte mentioned for *Patagosaurus*, also using it to distinguish it from *Volkheimeria*, the other sauropod described from Cerro Condor (Bonaparte, 1979, 1986a, 1999). This feature is still the main autapomorphy for *Patagosaurus,* and marks new pneumatic features for basal eusauropods that were previously unknown. Pneumaticity in sauropods is well-known for neosauropods (Wedel, 2003; Wedel et al., 2005; Schwarz and Fritsch, 2006; Schwarz et al., 2007; Fanti et al., 2013; Taylor and Wedel, 2013). However, it is not well understood for basal eusauropods, and *Patagosaurus* is the first to give conclusive evidence for this structure. However, more basal eusauropods may have this structure (e.g. *Cetiosaurus, Barapasaurus, Tazoudasaurus, Spinophorosaurus*), therefore future research will show if the presence/absence of a pneumatic structure is a diagnostic feature alone, or if it is the combination with the ventral pneumatic air chamber that is well-separated from the neural canal. A detailed pneumatic study is beyond the scope of this paper. The CDF is present in both *Cetiosaurus oxoniensis* and the Rutland *Cetiosaurus*. In *C. oxoniensis*, the

dorsal shows triangular openings underneath the diapophyses (and maybe bordered by the acdl and pcdl).

The centrodiapophyseal fenestrae, which extend ventrally in a pneumatic chamber separated from the neual canal, is a feature possibly shared with *Cetiosaurus* and *Barapasaurus* (Bandyopadhyay et al., 2010); (this feature often pairing these taxa with *Patagosaurus* as sister-taxa in phylogenetic analyses, e.g. Remes et al., (2009a); however, it is not clearly shown whether these latter taxa possess the same ventral pneumatic chamber as in *Patagosaurus*. This feature has however been shown in the basal neosauropod *Haplocanthosaurus* (Foster and Wedel, 2014, M. Wedel pers. Comm.).

The inconspicuous small round depressions on the posterior side of some of the more well preserved posterior dorsals is a feature thus far not seen in any other sauropod, and could be an autapomorphy, however, as it is a small feature, it might have been missed in osteological descriptions of contemporaneous sauropods to *Patagosaurus*. Most (eu)sauropods do have a rectangular fossa or depression at the posterior side of the transverse process of (posterior) dorsals, bordered by the pcdl, and the podl, which is named the pocdf, or postzygocentrodiapophyseal fossa (Wilson, 2011). Whether this has compartmentalized in *Patagosaurus* is not clear, as the pocdf is rather prominently present, however, in *Patagosaurus* this fossa is more expressed towards the neural arch than towards the distal end of the diapophysis, as is the case in *Spinophorosaurus* and *Cetiosaurus* (Rutland *Cetiosaurus* and *C. oxoniensis;* Upchurch and Martin, 2002, 2003; Remes et al., 2009). One observation is that these latter taxa have more dorsally projecting diapophyses, in an angle of about 45 degrees to the horizontal, compared to a more horizontal and lateral projection in *Patagosaurus*. However, whether or not the extra fossa in Patagosaurus is correlated to the projection of the diapophyses (e.g. as extra ligament attachement site for additional support) remains an unanswered question. In *Barapasaurus*,

no such fossa is seen, whilst the diapophyses of that taxon also project laterally as in *Patagosaurus*.

The rudimentary aliform process is seen in better stages of development in Europasaurus, where it projects as a triangular protrusion dorsal to the spinal onset of the sprl in anterior view, and dorsal to the lateral spdl + spol complex in posterior view (Carballido and Sander, 2014). However, in *Patagosaurus*, this feature is more seen dorsal to the lspol+podl complex. This feature could be a convergence of a laterally projecting triangular process for ligament attachement, found in basal eusauropods in the configuration as in *Patagosaurus*, and in neosauropods in the configuration of Europasaurus. Note also that this feature develops more in mature specimens of Europasaurus and that the holotype of *Patagosaurus* PVL 4170 is a (sub)adult and still growing, and in *Patagosaurus* is only seen in posteriormost dorsals as a very rudimentary form.

The absence of a spinodiapophyseal lamina on dorsal vertebrae, finally, is the last diagnostic dorsal feature in *Patagosaurus*. This lamina is seen in dorsals of basal sauropods such as *Tazoudasaurus* and *Barapasaurus*, then disappears in *Patagosaurus*, *C. oxoniensis* and Rutland *Cetiosaurus*, then reappears in neosauropods such as *Apatosaurus, Diplodocus, Haplocanthosaurus, Camarasaurus, Dicraeosaurus* and *Amargasaurus* (Wilson, 1999). In *Patagosaurus*, the diapophyses of dorsal are supported solely by the acdl, pcdl from the ventral and lateral sides, and prdl and podl from the lateral and dorsal sides. In posterior dorsals, the diapophysis is additionally supported by the lspol+podl complex, which is sometimes mistaken for spdl (Allain et al., 2008). This podl+lspol complex is also seen in the Rutland *Cetiosaurus*. This complex could possibly be the 'replacement' of the spdl found in basal sauropods and neosauropods. More intensive research on the cetiosaurs and their interrelationships is needed to clarify this. In any case, the absence of the spdl in *Patagosaurus* and *Cetiosaurus* cannot be connected with either neural spine elongation, as

neosauropods (and especially diplodocids) display similar spine elongation. Neither can the spdl be correlated with neural spine bifurfaction, as the spdl is found in basal non-neosauropodan sauropods.

Caudals

The elongated neural spines, which are not straight but curve convexly posteriorly at 2/3rd of the height of the spine, that are seen in the anterior caudals of *Patagosaurus,* are another diagnostic feature that is not seen in other sauropods, even though anterior neural spine elongation is seen in *Cetiosauriscus*, and diplodocids (Charig, 1980; Upchurch et al., 2004; Noè et al., 2010).

Other elements

The round dorsal rim and hook-shaped anterior lobe of the ilium, together with the elongated pubic peduncle are diagnostic features for the ilium of *Patagosaurus.* Whereas *Cetiosaurus oxoniensis* displays a more flattened dorsal rim (Upchurch and Martin, 2002), *Barapasaurus* does share a round one (Bandyopadyay, 2010), however, not as highly dorsally projecting as in *Patagosaurus*. This morphology is more shared with *Haplocanthosaurus,* and with diplodocids (Hatcher 1903, Tschopp et al., 2015). Similarly, a hook-shaped anterior lobe is shared with many neosauropods, especially diplodocids (Hatcher 1903, Tschopp et al., 2015), however, also with *Cetiosaurus oxoniensis*. Together with the sacrum which is similar to (basal) neosauropods (*Haplocanthosaurus, Diplodocus* and *Apatosaurus*), it is safe to say the sacricostal complex of *Patagosaurus* is more of a neosauropod build, supporting a position as derived eusauropod (see Chapter 4). Similarly, the 110° angle of the fused distal ischia, shows an intermediate stage between neosauroods and basal eusauropods. Finally, the intermediate morphology of the pubis, showing a torsion more seen in neosauropods like *Tornieria* (Remes, 2009), but showing a kidney-shaped pubic

foramen as *in Cetiosaurus oxoniensis*, adds to *Patagosaurus* being a derived non-neosauropodan eusauropod (or basal neosauropod, but see Chapter 4).

The slightly convex femur towards the lateral side shows a possible gait modification that is diagnostic for *Patagosaurus* and that has not been found in other Jurassic sauropods (e.g. *Barapasaurus, Tazoudasaurus, Lapparentosaurus, Haplocanthosaurus*, diplodocids). In *Cetiosaurus*, the femoral morphology is similar to that of *Patagosaurus*, however, the femur is more straight. A wide-gait is more common in titanosaurs (Henderson, 2006), however, a footprint site from the early Middle Jurassic from the UK shows the presence of both a narrow-, as well as wide-gait sauropod track (Day et al., 2004). The trackmaker from this site unfortunately cannot be identified. One theory, however, is that wide-gait is an adaptation for a more forested environment, whereas narrow-gait is commonly seen in animals that inhabit coastal environment (P.Upchurch, pers. comm.). Seeing as *Cetiosaurus* lived in lagunal settings, and *Patagosaurus* is found in more lacustrine deposits, this could be a theory that could be tested in the future, with a larger sample size.

2.5.2 Other characteristics and comparison with other eusauropods

Cervicals

The anterior condyle of the cervicals is most comparable to those of *Cetiosaurus*, especially as there is a rugose rim that cups the condyle, and as there is a protrusion on the condyle. The condylar rim of *Cetiosaurus,* however, is more rugose than in *Patagosaurus* (Upchurch and Martin, 2002; 2003). The cervicals of *Cetiosaurus* used in this study belong to the Rutland *Cetiosaurus*, which itself might be slightly more derived than the holotype of

Cetiosaurus oxoniensis (Läng 2008, P.Upchurch, M. Evans pers.comm.). The next outstanding feature of *Patagosaurus* cervicals is the high angle between the postzygodiapophyseal laminae and the posterior centroprezygapophyseal lamina. This feature is seen more in (basal) neosauropods than in eusauropods, like *Haplocanthosaurus* and *Diplodocus* (Hatcher, 1901; 1903), however, it is also seen in *Shunosaurus* (Zhang, 1988). However, the other cervical features, such as a pronounced ventral keel and posteriorly extending ventral end of the posterior cotyle, are more typical eusauropod features shared with *Lapparentosaurus, Amygdalodon, Tazoudasaurus*, and *Spinophorosaurus*. However, *Cetiosaurus oxoniensis* (Upchurch and Martin, 2003; 2002) does not seem to have a ventral keel on its anterior cervicals. *Lapparentosaurus* shows a posterior V-shaped forking of the keel, which is not seen in *Patagosaurus.* Moreover, more derived sauropods possess ventral keels, such as the Titanosauria *Opisthocoelicaudia* and *Diamantinasaurus*, which have ventral keels (Poropat et al., 2015).

The lamination of the cervicals stands out with the high projection (as stated in diagnostic characters) of the postzygodiapophyseal lamina. In basal sauropods and sauropodomorphs, this angle is much lower, and even in many eusauropods this extremity of angle is not reached (McPhee et al 2015). Thus, this elevation seems to mark the transgression from sauropodomorphs to sauropods. The next interesting feature is the non-juncture of the intrapostzygapophyseal laminae and the absence of centropostzygapophyseal laminae. This is a feature that distinguishes *Patagosaurus* from *Cetiosaurus*, and unites it with *Tazoudasaurus*, therefore a connection between this non-juncture and the elevation of the neural spine can be ruled out. Whether or not this is a feature shared between Gondwanan sauropods is uncertain. The single intraprezygapophyseal lamina is a feature shared with *Cetiosaurus* and *Tazoudasaurus*. The centrodiapophyseal fossa, as seen in *Patagosaurus*, is not shared with *Tazoudasaurus*, rather, it is shared with *Mamenchisaurus*. The

centroprezygapophyseal fossa is however shared with *Tazoudasaurus* (To1-354, contra Wilson, 2011).

Dorsals

The anterior dorsals and middle dorsals of *Patagosaurus* resemble other non-neosauropodan eusauropods, particularly *Cetiosaurus*, *Tazoudasaurus* and *Lapparentosaurus*. The posterior dorsals display non-neosauropodan eusauropod features such as unbifurcated neural spines, simple hyposphene/hypantrum complexes (hyposphene rhomboid and small, hypanthrum a rugose scar) and unexcavated parapophyses, however, the neural spine summits resemble more those of the non-neosauropodan eusauropod *Lapparentosaurus* and also of the basal neosauropod *Haplocanthosaurus*. The phylogenetic position of *Lapparentosaurus* is not completely resolved, as the type specimen is a juvenile, and has been retrieved as either a brachiosaurid by Bonaparte (1986c) or as a eusauropod by Läng (2008), therefore it is not possible to draw any conclusions from this.

The lamination of the anterior dorsals is largely similar to that of *Cetiosaurus* and *Tazoudasaurus*, in that the spinopostzygapophyseal laminae flare out laterally and ventrally, broadening the neural spine. However, the transition from anterior to middle to posterior brings some changes in lamination. The centroprezygapophyseal laminae extend dorsoventrally as the neural arch, pedicels and neural canal extend in dorsoventral height. This is seen in several other sauropods, however, not in the same degree as in *Patagosaurus*. The configuration of the intrapostzygapophyseal laminae shifts from a non-juncture to a juncture, and then these laminae disappear. Instead, a single intrapostzygapophyseal lamina appears. This seems to be unique for a select group of eusauropods (see Allain and Aquesbi, 2008; Carballido and Sander, 2014). The posterior dorsals then also display a split in the spinopostzygapophyseal laminae, namely a medial and a lateral running lamina. This is

described in *Europasaurus* (Carballido, 2012), a basal macronarian. However, this pattern is also observed in the Rutland *Cetiosaurus*, which might be a slightly more derived eusauropod than the holotype of *Cetiosaurus*. The centropostzgyapophyseal fossa is present in *Patagosaurus*, however it is only weakly developed. It is more developed in *Cetiosaurus*.

Throughout the dorsal vertebral column, the cpol becomes a rather secondary lamina to the tpols and stpol. In *Europasaurus*, this feature coincides with a division of the cpol into a lateral and medial one, however, in *Patagosaurus*, only one cpol exists, which matches the description of the medial cpol of *Europasaurus*.

Furthermore, the posterior dorsals show the dorsoventrally elongated neural spine seen in *Cetiosaurus*, and also in *Haplocanthosaurus* and diplodocids (Hatcher, 1901; 1903). The posterior inclination of the neural spines of posterior dorsals is also seen in *Klamelisaurus, Mamenchisaurus* and *Omeisaurus* (Xijing, 1993; Tang et al., 2001; Ouyang and Ye, 2002; Moore et al., 2017). The deep excavations of the fossae on the posterior dorsal neural spines, especially on the lateral sides, noted by Bonaparte (1986a), is also seen in *Cetiosaurus*, mamenchisaurids and neosauropods, suggesting a widespread character (Upchurch and Martin, 2002, 2003; Upchurch et al., 2004).

Posterior dorsal neural arches with rudimentary aliform processes are now known for *Patagosaurus*, and are also seen in more distinct form in *Europasaurus, Bellusaurus* and *Haplocanthosaurus* (Hatcher, 1903; Mo, 2013; Carballido and Sander, 2014; Foster and Wedel, 2014).

The presence of a single intraprezygapophyseal and single intrapostzygapophyseal lamina is a relatively new feature for sauropods, as this was named a median strut or single lamina below the hypapophysis/hyposphene (Upchurch et al., 2004; Wilson, 1999) before Carballido and Sander (2014) named it the stprl. These laminae are noted only for *Camarasaurus* and the titanosauriform *Tehuelchesaurus* (Carballido et al., 2011; Carballido and Sander, 2014), however, they now appear to also be present in *Patagosaurus*.

The presence of a small stprl accompanied by a large oval cprf on either lateral side, is however shared with many other eusauropods, therefore this combination is not a definitive diagnostic character.

The posterior dorsals also display the separation of the spinopostzygapophyseal laminae in a lateral and medial spol configuration, as in the basal macronarian *Europasaurus* (Carballido and Sander, 2014). This spinopostzygapophyseal laminar configuration, however, is also seen to some extent in *Cetiosaurus*. It is therefore possibly a more widespread configuration than for solely (basal) macronarians, and also existed in eusauropods.

Sacrum

One possible source of bias in the comparison of the sacrum of *Patagosaurus* with other (eu/neo)sauropods is that not many sacra of basal eusauropods are preserved. Sacral elements are known from *Lapparentosaurus* and *Tazoudasaurus*, and mostly from juvenile individuals. Therefore the sacrum of *Patagosaurus* is more easily compared to that of *Haplocanthosaurus* and diplodocids. The morphology of the neural spines and the elongation of the neural spines resembles that of *Haplocanthosaurus* in particular (Hatcher, 1903). This latter taxon is currently under redescription, therefore in a later phylogenetic analysis more might be discussed about the phylogenetic relationship of these two taxa.

Caudals

The anterior caudal vertebrae of *Patagosaurus* show a potential autapomorphic morphology of the neural spine, however, the neural spine tips strongly resemble those of *Spinophorosaurus* and *Cetiosauriscus* (P. Upchurch pers. comm*.,* (Charig, 1993; Heathcote and Upchurch, 2003; Noè et al., 2010). *Cetiosauriscu*s is currently under revision, however, it

is possibly not a eusauropod. The middle and posterior caudals of *Patagosaurus* are more typically eusauropod however, resembling those of the holotype of *Cetiosaurus* and those of other Argentine eusauropods (Gallina and Otero, 2009).

Appendicular elements

The femur of the holotype of *Patagosaurus* is a stout element, which does not resemble neosauropod elongated femora, but rather that of *Cetiosaurus, Tazoudasaurus* and *Barapasaurus*.

The *Patagosaurus* ilium, however, is another element that matches the morphology of several eu- and (non)neosauropods, save for the elongation of the pubic peduncle and the wide acetabulum. The typically sauropod tapering anterior lobe is seen in *Cetiosaurus*, *Bothriospondylus* (Mannion, 2010) and *Lapparentosaurus*, but also is common in neosauropods. The dorsoventrally high dorsal rim, however, is more seen in *Haplocanthosaurus* and *Apatosaurus* (Wedel and Taylor, 2013).

To summarize, *Patagosaurus fariasi* shows a set of morphological features that are typically eusauropod and are shared with other eusauropods. However, some elements seem to slightly more derived, and are found in derived eusauropods and/or (non)-neosauropods. A thorough phylogenetic analysis will clarify the position of *Patagosaurus* with respect to other sauropods and consequently will aid in resolving the early evolution of eusauropods.

2.6 Acknowledgements

The author would like to thank Jaime Powell (PVL, Tucuman), Sandra Chapman (NHM London), Mark Evans (NWM Leicester), Hillary Ketchum (OUMNH Oxford), Ronan Allain (MNHM Paris), Daniela Schwarz (Naturkundemuseum, Berlin), Ulrigh Joger (NHM Braunschweig), Stig Walsh (NMS Edinburgh). Many thanks also to José Carballido, Emanuel Tschopp, Phill Mannion and Veronica Diez for their unwavering support and help concerning sauropod morphology.

The author would like to dedicate this manuscript to the memory of Jaime Powell.

2.7 References

Allain, R., Aquesbi, N., Dejax, J., Meyer, C., Monbaron, M., Montenat, C., Richir, P., Rochdy, M., Russell, D., Taquet, P., 2004. A basal sauropod dinosaur from the Early Jurassic of Morocco. *Comptes Rendus Palevol* 3:199–208.

Allain, R., Aquesbi, N., 2008. Anatomy and phylogenetic relationships of *Tazoudasaurus naimi* (Dinosauria, Sauropoda) from the late Early Jurassic of Morocco. *Geodiversitas* 30:345–424.

Bandyopadhyay, S., Gillette, D.D., Ray, S., Sengupta, D.P., 2010. Osteology of *Barapasaurus tagorei* (Dinosauria: Sauropoda) from the Early Jurassic of India. *Palaeontology* 53:533–569.

Barrett, P.M., 2006. A sauropod dinosaur tooth from the Middle Jurassic of Skye, Scotland. *Transactions of the Royal Society of Edinburgh, Earth and Environmental Sciences* 97:25–29.

Barrett PM., Upchurch P. 2007. The evolution of herbivory in sauropodomorph dinosaurs. *Special Papers in Palaeontology* 77:91-112.

Barrett PM., Upchurch P. 2005. Sauropodomorph diversity through time. In: Curry Rogers, K., Wilson J eds. *The Sauropods: evolution and paleobiology*. Berkeley, CA: University of California Press, 125–156.

Bonaparte, J.F., 1979. Dinosaurs: A Jurassic Assemblage from Patagonia. *Science* 205:1377–1379.

Bonaparte JF. 1986a. The dinosaurs (Carnosaurs, Allosaurids, Sauropods, Cetiosaurids) of the Middle Jurassic of Cerro Cóndor (Chubut, Argentina). *Annales de Paléontologie (Vert.-Invert.)*. 72:325–386.

Bonaparte JF. 1986b. Les dinosaures (Carnosaures, Allosauridés, Sauropodes, Cétosauridés) du Jurassique Moyen de Cerro Cóndor (Chubut, Argentina). *Annales de Paléontologie (Vert.-Invert.)* 72:247–289.

Bonaparte, J.F., 1986c. The early radiation and phylogenetic relationships of the Jurassic sauropod dinosaurs, based on vertebral anatomy, in: Padian, K. (Ed.), The Beginning of the Age of Dinosaurs. Cambridge University Press, Cambridge, 247–258.

Bonaparte JF. 1996. *Dinosaurios de America del Sur*. Museo Argentino de Ciencias Naturales. 174 pp.

Bonaparte, J. F. 1999. Evolución de las vértebras presacras en Sauropodomorpha. *Ameghiniana* 36:115–187.

Brusatte, S. L., T. J. Challands, D. A. Ross, and M. Wilkinson. 2015. Sauropod dinosaur trackways in a Middle Jurassic lagoon on the Isle of Skye, Scotland. *Scottish Journal of Geology,* 5:1-9

Buffetaut E. 2005. A new sauropod dinosaur with prosauropod-like teeth from the Middle Jurassic of Madagascar. *Bulletin de la Société Géologique de France* 176:467-473.

Buffetaut, E., Suteethorn, V., Le Loeuff, J., Cuny, G., Tong, H., Khansubha, S., 2002. The first giant dinosaurs: a large sauropod from the Late Triassic of Thailand. *Comptes Rendus Palevol* 1: 103–109.

Cabaleri, N., Volkheimer, W., Silva Nieto, D., Armella, C., Cagnoni, M., Hauser, N., Matteini, M., Pimentel, M.M., 2010. U-Pb ages in zircons from las Chacritas and Puesto Almada members of the Jurassic Cañadón Asfálto Formation, Chubut province, Argentina, in: VII South American Symposium on Isotope Geology, 190–193.

Cabaleri, N.G., Armella, C., 2005. Influence of a biohermal belt on the lacustrine sedimentation of the Cañadón Asfálto Formation (Upper Jurassic, Chubut province, Southern Argentina). *Geologica Acta* 3:205-214.

Cabaleri, N.G., Armella, C., Nieto, D.G.S., 2005. Saline paleolake of the Cañadón Asfálto

Formation (Middle-Upper Jurassic), Cerro Cóndor, Chubut province (Patagonia), Argentina. *Facies* 51: 350–364.

Cabrera A. 1947. Un saurópodo nuevo del Jurásico de Patagonia. *Notas del Museo de La Plata, Paleontologia* 95:1–17.

Carballido, J.L., Rauhut, O.W.M., Pol, D., Salgado, L., 2011. Osteology and phylogenetic relationships of *Tehuelchesaurus benitezii* (Dinosauria, Sauropoda) from the Upper Jurassic of Patagonia. *Zoological Journal of the Linnean Society.* 163:605–662.

Carballido, J.L., Salgado, L., Pol, D., Canudo, J.I., Garrido, A., 2012. A new basal rebbachisaurid (Sauropoda, Diplodocoidea) from the Early Cretaceous of the Neuquén Basin; evolution and biogeography of the group. *Historical Biology* 24:631–654.

Carballido, J.L., Sander, P.M., 2014. Postcranial axial skeleton of *Europasaurus holgeri* (Dinosauria, Sauropoda) from the Upper Jurassic of Germany: implications for sauropod ontogeny and phylogenetic relationships of basal Macronaria. *Journal of Systematic Palaeontology* 12: 335–387.

Casamiquela RM. 1963. Consideraciones acerca de *Amygdalodon* Cabrera (Sauropoda, Cetiosauridae) del Jurasico Medio de la Patagonia. *Ameghiniana* 3:79–95.

Charig, A. J. 1993. Case 1876. *Cetiosauriscus* von Huene, 1927 (Reptilia, Sauropodomorpha): proposed designation of *C. stewarti* Charig, 1980 as the type species. *Bulletin of Zoological Nomenclature* 50:282–283.

Charig, A.J., 1980. A diplodocid sauropod from the Lower Cretaceous of England, in: Jacobs, L.L. (Ed.), Aspects of Vertebrate History. Essays in Honor of Edwin Harris Colbert. Museum of Northern Arizona Press, Flagstaff, 231–244.

Chatterjee, S., Zheng, Z., 2002. Cranial anatomy of *Shunosaurus*, a basal sauropod dinosaur from the Middle Jurassic of China. *Zoological Journal of the Linnean Society* 136:145–169.

Chure, D., Britt, B., Whitlock, J., Wilson, J., 2010. First complete sauropod dinosaur skull from the Cretaceous of the Americas and the evolution of sauropod dentition. *Naturwissenschaften* 97:379–391.

Clark, N.D., Gavin, P., 2016. New Bathonian (Middle Jurassic) sauropod remains from the Valtos Formation, Isle of Skye, Scotland. *Scottish Journal of Geology* 52:71-75.

Cooper MR. 1984. A reassessment of *Vulcanodon karibaensis* Raath (Dinosauria: Saurischia) and the origin of the Sauropoda. *Palaeontologia africana* 25:203–231.

Cúneo, R., Ramezani, J., Scasso, R., Pol, D., Escapa, I., Zavattieri, A.M., Bowring, S.A., 2013. High-precision U–Pb geochronology and a new chronostratigraphy for the Cañadón Asfálto Basin, Chubut, central Patagonia: Implications for terrestrial faunal and floral evolution in Jurassic. *Gondwana Research* 24:1267–1275.

Díez Díaz V., Tortosa T., Le Loeuff J. 2013. Sauropod diversity in the Late Cretaceous of southwestern Europe: The lessons of odontology. *Annales de Paléontologie* 99:119–129.

Dong, Z., Tang, Z., 1984. Note on a new mid-Jurassic sauropod (*Datousaurus bashanensis* gen. et sp. nov.) from Sichuan Basin, China. *Vertebrata Palasiatica*. 2: 69–75.

Foster, J.R., Wedel, M.J., 2014. Haplocanthosaurus (Saurischia: Sauropoda) from the lower Morrison Formation (Upper Jurassic) near Snowmass, Colorado. *Volumina Jurassica* 12:197–210.

Figari, E. G., R. A. Scasso, R. N. Cúneo, and I. Escapa. 2015. Estratigrafía y evolución geológica de la Cuenca de Cañadón Asfalto, provincia del Chubut, Argentina. *Latin American Journal of Sedimentology and Basin Analysis* 22:135–169.

Frenguelli, J. 1949. Los estratos con “Estheria” en el Chubut (Patagonia). *Revista de La Asociación Geológica Argentina* 1:1-4.

Galton, P. M. 2005. Bones of large dinosaurs (Prosauropoda and Stegosauria) from the Thaetic Bone Bed (Upper Triassic of Aust Cliff, southwest England. *Revue de Paléobiologie* 24:1-51.

Harris, J.D., 2006. The axial skeleton of the dinosaur *Suuwassea emilieae* (Sauropoda: Flagellicaudata) from the Upper Jurassic Morrison Formation of Montana, USA. *Palaeontology* 49: 1091–1121.

Hatcher, J.B., 1901. *Diplodocus* (Marsh): its osteology, taxonomy, and probable habits, with a restoration of the skeleton. *Memoirs of the Carnegie Museum* 1:1–63.

Hatcher, J.B., 1903. Osteology of *Haplocanthosaurus*, with description of a new species and remarks on the probable habits of the Sauropoda and the age and origin of the *Atlantosaurus* beds: Additional remarks on *Diplodocus*. *Memoirs of the Carnegie Museum*. 2:1–72.

He X., Li K., Cai K. 1988. *The Middle Jurassic dinosaur fauna from Dashanpu, Zigong, Sichuan. Vol. IV. Sauropod Dinosaurs (2) Omeisaurus tianfuensis*. Chengdu, China: Sichuan Publishing House of Science and Technology. 143 pp.

He, X., Li, K., Cai, K., Gao, Y., 1984. *Omeisaurus tianfuensis*—a new species of *Omeisaurus* from Dashanpu, Zigong, Sichuan. *Journal of Chengdu College Geology, (Supplemen)t* 2:13–32.

Heathcote, J., Upchurch, P., 2003. The relationships of *Cetiosauriscus stewarti* (Dinosauria; Sauropoda): implications for sauropod phylogeny. *Journal of Vertebrate Paleontology Program and Abstracts 23, (Supplement)* 60A.

Henderson, D.M., 2006. Burly gaits: centers of mass, stability, and the trackways of sauropod dinosaurs. *Journal of Vertebrate Paleontology* 26:907–921.

Hou, L., Zhou, S., Cao, Y., 1976. New discovery of sauropod dinosaurs from Sichuan. *Vertebrata PalAsiatica* 14:160–165.

von Huene, F., 1927. Sichtung der Grundlagen der jetzigen Kenntnis der Sauropoden.

Eclogae Geologica Helvetiae 20:444–470.

Irmis, R.B., 2010. Evaluating hypotheses for the early diversification of dinosaurs. *Transactions of the Royal Society of Edinburgh, Earth and Environmental Sciences* 101: 397–426.

Janensch, W., 1961. Die Gliedmassen und Gliedmassengürtel der Sauropoden der Tendaguru-Schichten. *Palaeontographica*-Supplementbände 4:177–235.

Läng, É., 2008. Les cétiosaures (Dinosauria, Sauropoda) et les sauropodes du Jurassique moyen: révision systématique, nouvelles découvertes et implications phylogénétiques (Ph. D. dissertation). Centre de recherche sur la paléobiodiversité et les paléoenvironnements, Paris, France, 639 pp.

Läng, E., and F. Mahammed. 2010. New anatomical data and phylogenetic relationships of Chebsaurus algeriensis (Dinosauria, Sauropoda) from the Middle Jurassic of Algeria. *Historical Biology* 22:142–164.

Liston, J.J., 2004. A re-examination of a Middle Jurassic sauropod limb bone from the Bathonian of the Isle of Skye. *Scottisch Journal of Geology* 40:119–122.

Liu, L.K.Y.C.-Y., Zheng-Xin, J.W., 2010. A New Sauropod From The Lower Jurassic Of Huili, Sichuan, China. *Vertebrata Palasiatica* 3:185-202.

Mahammed, F., Läng, É., Mami, L., Mekahli, L., Benhamou, M., Bouterfa, B., Kacemi, A., Chérief, S.-A., Chaouati, H., Taquet, P., 2005. The “Giant of Ksour”, a Middle Jurassic sauropod dinosaur from Algeria. *Comptes Rendus Palevol* 4:707–714.

Mattinson, J. M. 2005. Zircon U–Pb chemical abrasion (“CA-TIMS”) method: combined annealing and multi-step partial dissolution analysis for improved precision and accuracy of zircon ages. *Chemical Geology* 220:47–66.

Mannion, P.D., 2010. A revision of the sauropod dinosaur genus “*Bothriospondylus*” with a redescription of the type material of the Middle Jurassic form “*B. madagascariensis*.” *Palaeontology* 5:277–296.

Mannion, P.D., Upchurch, P., 2010. Completeness metrics and the quality of the sauropodomorph fossil record through geological and historical time. *Paleobiology* 36:283–302.

McPhee, B.W., Yates, A.M., Choiniere, J.N., Abdala, F., 2014. The complete anatomy and phylogenetic relationships of *Antetonitrus ingenipes* (Sauropodiformes, Dinosauria): implications for the origins of Sauropoda. *Zoological Journal of the Linnean Society* 171: 151–205.

McPhee, B.W., Bonnan, M.F., Yates, A.M., Neveling, J., Choiniere, J.N., 2015. A new basal sauropod from the pre-Toarcian Jurassic of South Africa: evidence of niche-partitioning at the sauropodomorph–sauropod boundary? *Scientific Reports* 5:13224.

McPhee, B.W., Upchurch, P., Mannion, P.D., Sullivan, C., Butler, R.J., Barrett, P.M., 2016. A revision of Sanpasaurus yaoi Young, 1944 from the Early Jurassic of China, and its relevance to the early evolution of Sauropoda (Dinosauria). *PeerJ* 4:e2578.

Mo, J. 2013. Topics in Chinese Dinosaur Paleontology-*Bellusaurus sui* . Henan Science and Technology Press, Zhengzhou, China, 231 pp.

Moore A., Xu X., Clark J. 2017. Anatomy and systematics of *Klamelisaurus gobiensis*, a mamenchisaurid sauropod from the Middle-Late Jurassic Shishugou Formation of China. *Journal of Vertebrate Paleontology, Program and Abstracts*, *37 (Supplement 2),* 165A.

Nair, J.P., Salisbury, S.W., 2012. New anatomical information on *Rhoetosaurus brownei* Longman, 1926, a gravisaurian sauropodomorph dinosaur from the Middle Jurassic of Queensland, Australia. *Journal of Vertebrate Paleontology* 32:369–394.

Noè, L.F., Liston, J.J., Chapman, S.D., 2010. 'Old bones, dry subject': the dinosaurs and pterosaur collected by Alfred Nicholson Leeds of Peterborough, England. Geological Society, London, Special Publications 343:49–77.

Nullo, F.E., 1983. Descripción geológica de la Hoja 45 c, Pampa de Agnia, provincia del Chubut: carta geológico-económica de la República Argentina, escala 1: 200.000. *Servicio Geológico Nacional* 199:1-94.

Olivera, D.E., Zavattieri, A.M., Quattrocchio, M.E., 2015. The palynology of the Cañadón Asfálto Formation (Jurassic), Cerro Cóndor depocentre, Cañadón Asfálto Basin, Patagonia, Argentina: palaeoecology and palaeoclimate based on ecogroup analysis. *Palynology* 39:362–386.

Ouyang, H., Ye, Y., 2002. *The first mamenchisaurian skeleton with complete skull, Mamenchisaurus youngi*. Sichuan Publishing House of Science and Technology, Chengdu, China, 138 pp.

Peng, Z., Ye, Y., Gao, Y., Shu, C.K., Jiang, S., 2005. Jurassic Dinosaur Faunas in Zigong. Sichuan Peoples Publishing House, Chengdu, China, 98 pp.

Pi, L., Ou, Y., Ye, Y., 1996. A new species of sauropod from Zigong, Sichuan, *Mamenchisaurus youngi*, in: Papers on Geosciences Contributed to the 30th International Geological Congress, 87–91.

Piatnitzky, C. 1936. Informe preliminar sobre el estudio geológico de la región situada al norte de los lagos Colhué Huapi y Musters. *Boletín Informaciones Petroleras, Yacimientos Petrolíferos Fiscales* 137:2–15.

Pol, D., Rauhut, O.W.M., Carballido, J.L., 2009. Skull anatomy of a new basal eusauropod from the Cañadon Asfalto Formation (Middle Jurassic) of Central Patagonia. *Journal of Vertebrate Paleontology, Program and Abstracts 29 (Supplement 3)*, 100A.

Poropat, S.F., Upchurch, P., Mannion, P.D., Hocknull, S.A., Kear, B.P., Sloan, T., Sinapius, G.H.K., Elliott, D.A., 2015. Revision of the sauropod dinosaur *Diamantinasaurus matildae* Hocknull et al. 2009 from the mid-Cretaceous of Australia: Implications for Gondwanan titanosauriform dispersal. *Gondwana Research* 27:995–1033.

Raath, M.A., 1972. Fossil vertebrate studies in Rhodesia: a new dinosaur (Reptilia:

Saurischia) from near the Trias-Jurassic boundary. *Arnoldia Rhodesia* 7:1–7.

Rauhut, O.W., 2004. Braincase structure of the Middle Jurassic theropod dinosaur *Piatnitzkysaurus*. *Canadian Journal of Earth Sciences*. 41:1109–1122.

Rauhut, O.W.M., 2002. Dinosaur evolution in the Jurassic: a South American perspective. *Journal of Vertebrate Paleontology, Program and Abstracts 22 (Supplement)* 89A.

Rauhut, O.W., 2003a. A dentary of *Patagosaurus* (Sauropoda) from the Middle Jurassic of Patagonia. *Ameghiniana* 40:425–432.

Rauhut, O.W.M., 2003b. Revision of *Amygdalodon patagonicus* Cabrera, 1947 (Dinosauria, Sauropoda). *Fossil Record* 6:173–181.

Remes, K., Ortega, F., Fierro, I., Joger, U., Kosma, R., Ferrer, J.M.M., Ide, O.A., Maga, A., 2009a. A new basal sauropod dinosaur from the Middle Jurassic of Niger and the early evolution of Sauropoda. *PLoS One* 4:e6924.

Remes, K., 2009b. Taxonomy of Late Jurassic diplodocid sauropods from Tendaguru (Tanzania). *Fossil Record* 12:23–46.

Russell, D.A., Zheng, Z., 1993. A large mamenchisaurid from the Junggar Basin, Xinjiang, People's Republic of China. *Canadian Journal of Earth Sciences* 30:2082–2095.

Silva Nieto, D.G., Cabaleri, N.G., Salani, F.M., Coluccia, A., 2002. Cañadón Asfálto, una cuenca tipo "pull apart" en el área de Cerro Cóndor, provincia del Chubut, in: XV Congreso Geológico Argentino, El Calafate, Acta, I, 238–244.

Stipanicic, P. N., F. Rodrigo, O. L. Baulies, and C. G. Martínez. 1968. Las formaciones presenonianas en el denominado Macizo Nordpatagónico y regiones adyacentes. *Revista de La Asociación Geológica Argentina* 23: 67–98.

Stumpf, S., Ansorge, J., Krempien, W., 2015. Gravisaurian sauropod remains from the marine late Early Jurassic (Lower Toarcian) of North-Eastern Germany. *Geobios* 48:271–279.

Tang, F., Jing, X., Kang, X., Zhang, G., 2001. *Omeisaurus maoianus*: a complete sauropod from Jingyuan, Sichuan. China Ocean Press, Beijing, China, 112 pp.

Tasch, P., Volkheimer, W., 1970. Jurassic conchostracans from Patagonia. *The University of Kansas Paleontological Contributions* 50:1-23.

Taylor, M.P., 2009. A re-evaluation of *Brachiosaurus altithorax* Riggs 1903 (Dinosauria, Sauropoda) and its generic separation from *Giraffatitan brancai* (Janensch 1914). *Journal of Vertebrate Paleontology* 29, 787–806.

Tschopp, E., Mateus, O., Benson, R.B.J., 2015. A specimen-level phylogenetic analysis and taxonomic revision of Diplodocidae (Dinosauria, Sauropoda). *PeerJ* 3:e857.

Upchurch, P., 1998. The phylogenetic relationships of sauropod dinosaurs. *Zoological Journal of the Linnean Society* 124:43–103.

Upchurch, P., Barrett, P.M., Dodson, P., 2004. Sauropoda, in: Weishampel, D.B., Dodson, P., Osmólska, H. (Eds.), The Dinosauria. Second Edition. University of California Press, Berkeley, CA, 259–322.

Upchurch, P., Martin, J., 2003. The anatomy and taxonomy of *Cetiosaurus* (Saurischia, Sauropoda) from the Middle Jurassic of England. *Journal of Vertebrate Paleontology* 23:208–231.

Upchurch, P., Martin, J., 2002. The Rutland *Cetiosaurus*: the anatomy and relationships of a Middle Jurassic British sauropod dinosaur. *Palaeontology* 45:1049–1074.

Volkheimer, W., Quattrocchio, M.E., Cabaleri, N.G., García, V. 2008. Palynology and paleoenvironment of the Jurassic lacustrine Cañadón Asfalto Formation at Cañadón Lahuincó locality, Chubut Province, Central Patagonia, Argentina. *Revista Española de Microplaeontología* 40:77-96.

Volkheimer, W., Quattrocchio, M.E., Cabaleri, N.G., Narvaez, P.L., Rosenfeld, U., 2015. Environmental and climatic proxies for the Cañadón Asfálto and Neuquén basins (Patagonia, Argentina): review of Middle to Upper Jurassic continental and near coastal sequences. *Revista Brasileira de Paleontologia* 18:71–82.

Volkheimer, W., Rauhut, O.W., Quattrocchio, M.E., Martinez, M.A., 2008. Jurassic

paleoclimates in Argentina, a review. *Revista de la Asociación Geológica Argentina* 63:549–556.

Wedel, M.J., Taylor, M.P., 2013. Caudal pneumaticity and pneumatic hiatuses in the sauropod dinosaurs *Giraffatitan* and *Apatosaurus*. PLoS ONE 8: e78213.

Wedel, M.J., Wilson, J.A., Rogers, K.C., 2005. Postcranial skeletal pneumaticity in sauropods and its implications for mass estimates. In: Curry Rogers, K, Wilson, J, (Eds). The sauropods: evolution and paleobiology, 201–228.

Wedel, M.J., 2003. Vertebral pneumaticity, air sacs, and the physiology of sauropod dinosaurs. *Paleobiology* 29:243-255.

Wilson, J.A., 1999. A nomenclature for vertebral laminae in sauropods and other saurischian dinosaurs. *Journal of Vertebrate Paleontology* 19:639–653.

Wilson JA., Carrano MT. 1999. Titanosaurs and the origin of ”wide-gauge” trackways: a biomechanical and systematic perspective on sauropod locomotion. *Paleobiology* 25:252–267.

Wilson, J.A., 2002. Sauropod dinosaur phylogeny: critique and cladistic analysis. *Zoological Journal of the Linnean Society* 136:215–275.

Wilson, J.A., Upchurch, P., 2009. Redescription and reassessment of the phylogenetic affinities of *Euhelopus zdanskyi* (Dinosauria: Sauropoda) from the Early Cretaceous of China. *Journal of Systematic Palaeontology* 7: 199–239.

Wilson, J.A., 2011. Anatomical terminology for the sacrum of sauropod dinosaurs. *Contributions from the museum of Paleontology, University of Michigan 32:59-69.*

Wilson, J.A., D’Emic, M.D., Ikejiri, T., Moacdieh, E.M., Whitlock, J.A., 2011. A nomenclature for vertebral fossae in sauropods and other saurischian dinosaurs. PLoS ONE 6:e17114.

Woodward, A.S., 1905. On parts of the skeleton of *Cetiosaurus leedsi*, a sauropodous dinosaur from the Oxford Clay of Peterborough. *Proceedings of the Zoological*

Society London 1:232–243.

Xing, L., Miyashita, T., Zhang, J., Li, D., Ye, Y., Sekiya, T., Wang, F., Currie, P.J., 2015. A new sauropod dinosaur from the Late Jurassic of China and the diversity, distribution, and relationships of mamenchisaurids. Journal of Vertebrate Paleontology 35:e889701.

Yadagiri, P., 2001. The osteology of Kotasaurus yamanpalliensis, a sauropod dinosaur from the Early Jurassic Kota Formation of India. J. Vertebr. Paleontol. 21:242–252.

Yates, A.M., Bonnan, M.F., Neveling, J., Chinsamy, A., Blackbeard, M.G., 2010. A new transitional sauropodomorph dinosaur from the Early Jurassic of South Africa and the evolution of sauropod feeding and quadrupedalism. *Proceedings of the Royal Society London B: Biological Sciences* 277:787–794.

Yates, A.M., Kitching, J.W., 2003. The earliest known sauropod dinosaur and the first steps towards sauropod locomotion. *Proceedings of the Royal Society London B: Biological Sciences* 270:1753–1758.

Young, C.-C., 1939. On a new sauropoda, with notes on other fragmentary reptiles from Szechuan. *Bulletin of the Geological Society China* 19:279–315.

Young, C.-C., Zhao, X., 1972. Description of the type material of *Mamenchisaurus hochuanensis*. *Institute of Vertebrate Paleontology and. Paleoanthropology. (Monograph Series)* 8:1–30.

Zavattieri, A.M., Escapa, I.H., Scasso, R.A., Olivera, D., 2010. Contribución al conocimiento palinoestratigráfico de la Formación Cañadón Calcáreo en su localidad tipo, provincia del Chubut, Argentina. *X Congreso Argentino de Paleontología Y Bioestratigrafía-VII Congreso Latinoamericano de Paleontología,* 51 pp.

Zhang Y. 1988. *The Middle Jurassic dinosaur fauna from Dashanpu, Zigong, Sichuan, vol. 1: sauropod dinosaur (I): Shunosaurus*. Chengdu, China: Sichuan Publishing House of Science and Technology, 114 pp.

Zhang, Y., Li, K., Zeng, Q., Downs, T.B.W., 1998. A new species of sauropod from the Late Jurassic of the Sichuan Basin (*Mamenchisaurus jingyanensis* sp. nov.). *Journal of the Chengdu University of Technology* 25:61-68.

Zhao, Z. 1993. A New Mid-Jurassic Sauropod (*Klamelisaurus gobiensis* Gen. Et Sp. Nov.) From Xinjiang, China. *Vertebrata Palasiatica* 2: 243-265.

Zhao, X.J., Downs, T.B.W., 1993. A new Middle Jurassic sauropod subfamily (Klamelisaurinae subfam. nov.) from Xinjiang Autonomous Region, China. Vertebra PalAsiatica 31, 132–138.

3 Revision of associated material of *Patagosaurus fariasi* BONAPARTE 1979, with notes on the species diversity of the Cerro Condor bonebeds

Femke M Holwerda[123], Oliver W M Rauhut[13], Diego Pol[45]

1 Staatliche Naturwissenschaftliche Sammlungen Bayerns (SNSB), Bayerische Staatssamlung für Paläontologie und Geologie, Richard-Wagner-Strasse 10, 80333 München, Germany

2 GeoBioTec, Departamento de Ciências da Terra, Faculdade de Ciências e Tecnologia (FCT), Universidade Nova de Lisboa, 2829-526 Caparica, Portugal

3 Department of Earth and Environmental Sciences and GeoBioCenter, Ludwig Maximilians Universität, 80333 München, Germany

4 Consejo Nacional de Investigaciones Científicas y Técnicas (CONICET), Argentina

5 Museo Paleontológico Egidio Feruglio, Avenida Fontana 140, Trelew, Argentina

Author contributions: Designed study: FH, OWM, DP. Conducted study: FH. Wrote the manuscript and prepared the figures: FH.

3.1 Abstract

The early Middle Jurassic eusauropod *Patagosaurus fariasi* has been described on the basis of abundant remains two localities of the Cañadón Asfálto Formation in west-central Chubut, Patagonia, Argentina. It has been featured in numerous phylogenetic analyses of sauropods, as it comes from a pivotal time in sauropod evolutionary history; the Early-Middle Jurassic. However, the original description of this sauropod in 1979 and 1986 do not address the complicated associations of the paratypes, all found in two bonebeds during the original excavations, which also led to the discovery and description of the holotype. Now that the holotype is redescribed, it is clear that not all elements that are originally assigned to the holotype and the hypodigm in fact belong to *Patagosaurus*. Moreover, uncertainty has arisen whether the two bonebeds in which *Patagosaurus* was found are monospecific, or whether multiple taxa are actually present. This paper describes in detail the remaining non-holotypic material originally referred to *Patagosaurus*, and gives an overview of the

most likely associations of specimens. Apart from six more specimens that can be safely assigned to *Patagosaurus fariasi*, two potentially new taxa are found, all of which differ from *Volkheimeria*, the only other sauropod taxon formally described from these localities, indicating a higher species diversity in the Cerro Condor area in the Middle Jurassic. Moreover, the different ontogenetic stages of the specimens may help to shed light on sauropod ontogenetic development.

3.2 Introduction

Patagosaurus fariasi, a Middle Jurassic eusauropod, was named in 1979 and described in 1979 and 1986 (Bonaparte, 1979; Bonaparte, 1986a). During extensive excavations in the 1970's and 1980's a wealth of material was collected, including several large and some smaller sauropod individuals, as well as theropod material (Bonaparte 1979, 1986a, and fieldnotes from 1976-1979). Over several field campaigns the remains were extracted and stored in the collections of the Museo Argentino de Sciencias Naturales Bernardo Rivadavia in Buenos Aires (MACN), and the Instituto Miguel Lillo in Tucuman (PVL). Several, but by far not all, elements were featured in the main monograph by Bonaparte in 1986. The original papers on *Patagosaurus* (Bonaparte 1979, 1986a) describe mainly the holotype and several of the better preserved referred materials of the collection to complete the anatomical description of the taxon. Therefore, the collection in its entirety has not yet received a full review. Now that the holotype has been osteologically revised, (Holwerda et al., in prep, see Chapter 2), the associated material can fill in any missing information on axial or appendicular elements for the taxon *Patagosaurus*. Since this sauropod comes from the Middle Jurassic, a critical time in sauropod evolution, and has featured in numerous phylogenetic analyses of sauropod dinosaurs (Upchurch and Martin, 2002; Wilson, 2002; Harris, 2006; Allain and Aquesbi, 2008; Remes et al., 2009; Wilson and Upchurch, 2009;

Carballido et al., 2011; Carballido and Sander, 2014; Mocho et al., 2014), more information on all material would therefore aid sauropod research in general, and especially eusauropod research. Next to the evolutionary importance of (re)examining *Patagosaurus*, there is also the question of local species diversity within the Cañadón Asfalto Formation. The material was found in two localities; Cerro Condor Norte and Cerro Condor Sur, therefore it is likely that not all material is *Patagosaurus* (moreover, two other taxa, the sauropod *Volkheimeria* and the theropod *Piatnitzkysaurus* were found in Cerro Condor Sur). In fact, most recent studies find high sauropod diversity rates in almost all geological units that contain sauropod dinosaurs, and the Cañadón Asfálto Fm localities prove no exception (see for instance Rauhut, 2003; Pol et al., 2009; Holwerda et al., 2015). Since the Cañadón Asfálto Formation yields more sauropod taxa than *Patagosaurus*, the associated material needs to be carefully cross-checked, not only with the holotype PVL 4170 (housed in Tucuman), but also with *Volkheimeria chubutensis* (Bonaparte 1979), which was discovered together with *Patagosaurus*. In this study, all the *Patagosaurus* material besides the holotype (that could be retrieved) is (re)described. We adhere to all originally composed specimens by Bonaparte (1979, 1986a) as much as possible; since Bonaparte was at the original excavations, and for some specimens no other information is preserved other than it being a likely association of material. Unfortunately, only one quarry map of one locality, Cerro Condor Norte, has been retrieved, no quarry map has been found of the other locality, Cerro Condor Sur. Therefore not all material could definitely be ascribed to *Patagosaurus*, *Volkheimeria* or an unnamed taxon, and several elements remain 'Sauropoda indet'.

3.3 Horizon, locality and material:

Cerro Condor Norte and Cerro Condor Sur, Cañadón Asfálto Formation, Chubut province, Patagonia, Argentina. These two localities are named and briefly described by Bonaparte,

(Bonaparte, 1986a,b). They are more extensively described in Holwerda et al., (2015). For a more extensive description of the geological setting however, see Geological Setting and Chapter 2.

Cerro Condor Norte (see Figure 1) yielded a bonebed of several *Patagosaurus* individuals, including the holotype PVL 4170. The locality of Cerro Condor Sur yielded numerous elements, as well as skeletons of individual sauropods (see material).

3.3.1 Material

Bonaparte and his team numbered elements and individual skeletons, and we adhere to this numbering (see Table 1). For Cerro Condor Norte, at least, a quarry map exists, which shows the associations to be more or less logically done, according to direct association, and size (related to the Morphological Ontogenetic Stage, MOS). For Cerro Condor Sur, however, the associations have to be based on both the assignment of specimens by Bonaparte, as well as the size associations; since there is no quarry map available. Moreover, The Cerro Condor Sur locality may consist of several bonebeds and/or layers. One final informative element is the colour of the fossils; since direct associations tend to have similar coloration. This is, however, not the most reliable method. Several specimens show unclear associations, as wil be discussed in the paper. The abbreviations stand for:

PVL – Instituto Miguel Lillo, Tucuman, Argentina

MACN-CH – Museo Argentino de Ciencias Naturales Bernardo Rivadavia, Buenos Aires, Argentina

MPEF-PV – Museo Paleontologico Egidio Feruglio, Trelew, Argentina

Some elements that are listed in collection databases could not be retrieved; which is unfortunate but not uncommon for decade-old collections (see for instance Sander, 2000; Upchurch and Martin, 2003; Liston, 2004a; Liston and Noè, 2004; Noè et al., 2010). Some elements are currently housed in museum deposits for a European traveling exhibition, and could not be studied first-hand for this study. (Note: the holotype, PVL 4170, is also from Cerro Condor Norte, and is housed in the PVL Tucuman).

Table 1: List of elements and provenance of *Patagosaurus* material

NUMBER	Material	LOCALITY		STORAGE	
		Cerro Condor Norte	Cerro Condor Sur	MACN Buenos Aires	PVL Tucuman
MACN-CH 932	Several appendicular and axial elements	x		x	
MACN-CH 933	Several appendicular, axial and cranial elements	x		x	
MACN-CH 934	Axial and cranial elements		x	x	
MACN-CH 935	Several appendicular and axial elements	x		x	
MACN-CH 936	Cervical series		x	x	
MACN-CH 1299	Femur, tibia, caudals		x	x	
PVL 4075	Humerus and tibia		x		x
PVL 4076	Axial and premaxilla		x		x
PVL 4617	Ungual phalanx		x		x
MACN-CH 219	Right ischium (=934)		x	x	
MACN-CH 223	Cervical w/o neural arch, caudals, sacral		x	x	
MACN-CH 225	Scapula and coracoid (=935)		x	x	
MACN-CH 229	Dorsal centrum and proximal shaft of dorsal rib		x	x	
MACN-CH 230	Several dorsals		x	x	
MACN-CH 231	Caudal vertebrae		x	x	
MACN-CH 232	Fragments of vertebrae and pelvis		x	x	
MACN-CH	Right ischium (=933)		x	x	

233					
MACN-CH 244	**Dorsal rib (=935)**		**x**	**x**	
MACN-CH 245	**Dorsal rib (=935)**		**x**	**x**	
MACN-CH 1986	**Femur and tibia**	**x?**		**x**	

Material from Buenos Aires, MACN (both from Cerro Condor Norte and Sur):

MACN-CH 932
This material belonged to a small individual, and consists of a right radius, right ulna, right humerus, ?right sternal plate, right ilium, right pubis, ?left tibia, two dorsal neural spines, two dorsal centra, a cervical centrum and a sacral neural arch, as well as a left pes. According to Bonaparte (1986a), and the quarry map (Fig 1 and Fig 2) this specimen also should possess a scapula and coracoid, however these could not be retrieved from the collections of the MACN. Instead, a right sternal plate was found in the collections.

MACN-CH 933
The material belonged to the smallest individual of the Cerro Condor Norte bonebed, and consists of a right femur, left pubis, left ilium, as well as several centra of cervicals and anterior dorsals, and a neural arch of a cervicodorsal. Finally, it contains a right dentary. There is a right ischium attributed to this specimen; however, the numbering of this specimen has next to 'MACN-CH 933' also an extra numbering of '233'; which is actually a specimen from Cerro Condor South.

MACN-CH 934
This material belongs to a small individual, and also some larger elements are attributed to this number. It consists of several axial neural arches and spines, as well as an ilium, a pubis, ?two or ?three ischia, and two maxillae. The sizes of the several specimens do not match, however, therefore it is more likely that this specimen consists of two different specimens of differing body size.

MACN-CH 935
This material consists of a large individual, with four dorsal neural arches and spines, several anterior caudal vertebrae, four sacral vertebrae, several dorsal ribs, a scapulacoracoid and an ilium. A scapula attributed to this specimen could not be seen first-hand, because it is currently part of a traveling exhibition. NB: Several rib fragments were under the specimen number MACN-CH 244-245.

MACN-CH 936
This material consists of a series of large cervical vertebrae, from the axis to ~cervical 9, and anterior to middle dorsals. More than half of this material, however, could not be seen first-hand, because it is currently part of a traveling exhibition.

MACN-CH 230
This material consists of several dorsal vertebrae.

MACN-CH 231

This material consists of several caudal vertebrae.

MACN-CH 232
This material belongs to a small individual or several small individuals. It consists of several fragments of neural arches, centra, and ribs, as well as an enigmatic fragment of a dermal or a pelvic bone.

MACN-CH 1299
This material consists of a series of anterior caudals, a right femur (inaccessible, measurements only) and a right tibia.

MACN-CH 219
An ilium and several disarticulated axial elements.

MACN-CH 223 (-221)
This is one isolated sacral vertebra, as well as two ischia. One ischium is potentially part of MACN-CH 934, however, has the number 221.

MACN-CH 1986
A right femur and a tibia. The tibia could not be found in the MACN collections.

Material from Tucuman, PVL (both from Cerro Condor Norte and Cerro Condor Sur):

PVL 4170
Holotype (see osteological revision of holotype, Holwerda et al in prep/Chapter 2).

PVL 4075
Humerus and tibia of a large individual (or individuals). A femur was also ascribed to this specimen by Bonaparte (1986a), however, this could not be found in the collections of the Instituto Lillo in Tucuman.

PVL 4076
Several partially preserved cervical and caudal elements, and a premaxilla with dentition. According to Bonaparte (1986a) originally a left femur and left tibia were ascribed to this specimen, however, these elements were not found with this specimen in the PVL storage.

PVL 4617
Several partially preserved cervicals, ungual phalanx.

3.3.2 Anatomical abbreviations

Laminae and fossae terminology follows that of (Wilson, 1999, 2012; Wilson et al., 2011; Carballido & Sander, 2014):

Laminae:

acdl: anterior centrodiapophyseal lamina

acpl: anterior centroparapophyseal lamina

cpol: centropostzygapophyseal lamina

cprl: centroprezygapophyeseal lamina

tprl: intraprezygapophyseal lamina

stprl: single intraprezygapophyseal lamina

tpol: intrapostzygapophyseal lamina

stpol: single intrapostzygapophyseal lamina

podl: postzyga-iapophyseal lamina

ppdl: parapodiapophyseal lamina

pcdl: posterior centro-diapophyseal lamina

sprl: spinoprezygapophyseal lamina

spol: spinopostzygapophyseal lamina (mspol: medial; lspol: lateral spol)

spdl: spinodiapophyseal lamina

prsl: prespinal lamina

posl: postspinal lamina

Fossae

cdf, centrodiapophyseal fossa; **cpof**, centropostzygapophyseal fossa; **cprf**, centroprezygapophyseal fossa; **pocdf**, postzygapophyseal centrodiapophyseal fossa; **posdf**, postzygapophyseal spinodiapophyseal fossa; **prcdf**, prezygapophyseal centrodiapophyseal

fossa; **prsdf**, prezygospinodiapophyseal fossa; **sdf**, spinodiapophyseal fossa; **spof**, spinopostzygapophseal fossa; **sprf**, spinoprezygapophseal fossa

3.3.3 Geological setting (Cerro Condor Norte and Cerro Condor Sur)

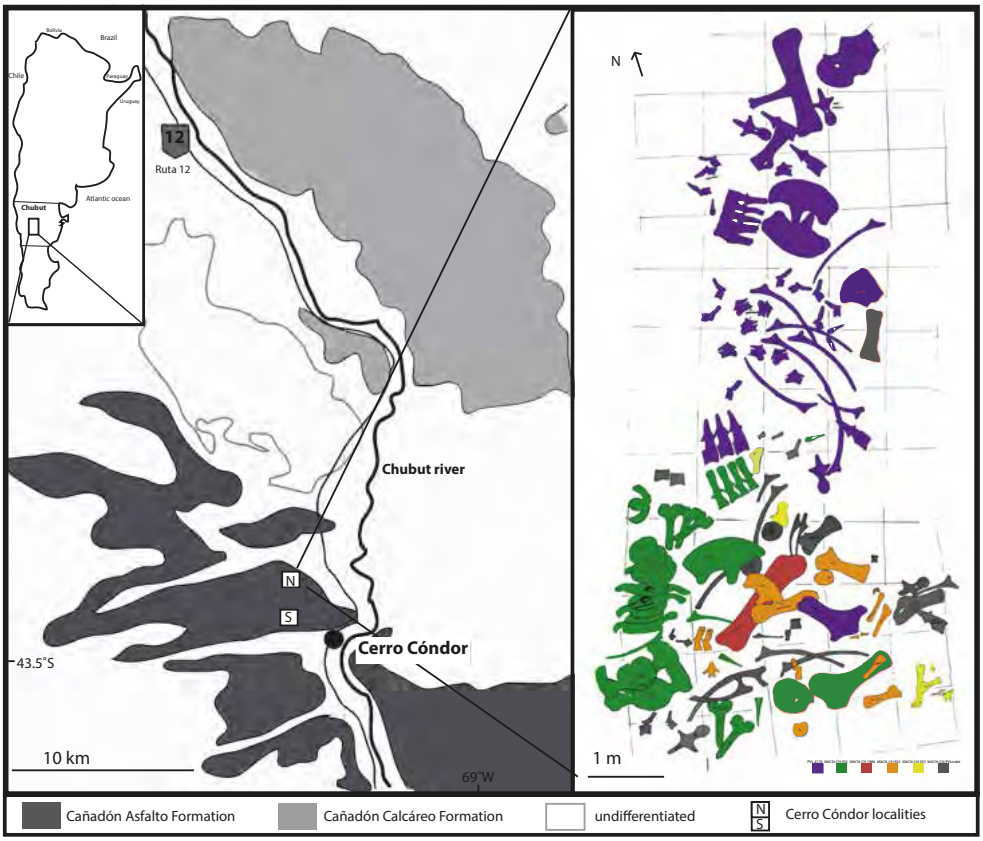

Figure 1: Geological setting of Cerro Condor localities, and the Cerro Condor bonebed.

All material of *Patagosaurus* and the associated remains come from the, west-central Chubut, Patagonia, Argentina (*Patagosaurus* = lizard from Patagonia). The Cañadón Asfálto Formation was long considered to be Callovian in age, however, recent re-dating of various localities (though excluding the Cerro Condor localities) by U/Pb isotope analysis, an Aalenian-Bajocian age has been found, putting the Cañadón Asfálto Formation sauropods in a much older time-window in their evolutionary history (Cúneo et al., 2013). This much older age is also consistent with palynological and other radiometric studies (Volkheimer et al.,

2008; Cabaleri et al., 2010; Zavattieri et al., 2010; Volkheimer et al., 2015; Hauser et al., 2017). The two localities, Cerro Condor Norte and Cerro Condor Sur, both near the village of Cerro Condor, close to Paso de Indios, and near the river Chubut (see Figure 1).

Excavations in the region of Cerro Condor (Cañadón Asfálto Formation) were begun in 1977, by Jose Bonaparte and a team of palaeontologists and geologists. The following year, bones were found on the Farias farm estate, approximately 5 Km North of the village of Cerro Condor. This locality was then named Cerro Condor Norte, and excavated in the next years up to 1982 (Bonaparte, 1986a, 1996, Bonaparte fieldnotes 1977-1980) The bonebed is documented in Figure 1&2. Cerro Condor Sur, the second locality, lies not far from Cerro Condor Norte (a few Km to the south and close to the river Chubut).

Cerro Condor Norte shows dark-coloured sediments, interpreted by Coria and Bonaparte to be calcareous tuffs including carbonaceous plant remains, intercalated with thin sandstones (Bonaparte, 1979; Bonaparte, 1986a; Coria, 1994). Five to seven skeletons of sauropods were found here disarticulated, and fossils are dark grey to dark brown in colour. The quarry map of this locality is found in Figure 2. Coria (1994) and Bonaparte (1986a) argue that Cerro Condor North's sauropod bonebed is evidence of gregariousness, however, this can be disputed, (see Discussion below). Lacustrine bonebeds are not uncommon, but are not the most common bonebed type; making up only 6% of total bonebed depositional environments (Rogers et al., 2010).

The bonebed depicted in the quarry map of Cerro Condor Norte shows several elements which could not be retrieved from the collections, or which are unknown to any collections since the original excavations. These are shown in grey on the map. The other elements are colour coded according to association with specimens MACN-CH 933, 932, 935, and PVL 4170 (the holotype), 4076 and 4176.

Cerro Condor Sur shows fine to coarse grained, yellow to beige sediments with small fragments of shells of bivalves. It is interpreted by DP and OR as a conglomeratic

intercalation in lacustrine deposits, which is evidenced by the presence of freshwater shells. The fossils from this locality have lighter colours and are thus easily identified as coming from Cerro Condor South. This bonebed probably consists of several depositional layers, accumulated over time, and was excavated over several years. Because of this accumulation, it is unclear if all elements represent the same depositional environment, or indeed the same depositional time/event (see Discussion). Several elements and specimens originate from this locality. Unfortunately, no quarry map has ever been known from this site, and it is thus likely the Cerro Condor Sur map was never produced.


Purple = holotype PVL 4170
red = unknown/possibly holotype
green = MACN CH 935
orange = MACN CH 932
yellow = MACN CH 933

Figure 2 (previous page): Cerro Condor Norte quarry map (enlarged excerpt from Figure 1). Purple = PVL 4170, red = MACN-CH 1986, green = MACN-CH 935, orange = MACN-CH 932, yellow = MACN-CH 933, grey = indet.

3.4 **Description**

Material from Cerro Condor Norte

The material from Cerro Condor Norte was originally ascribed all to *Patagosaurus*, and even gregarious behaviour was inferred. There are two elements, however, that cannot be safely ascribed to *Patagosaurus*; these will be discussed last.

The holotype PVL 4170 also comes from Cerro Condor Norte. A brief diagnosis with characteristic features that define *Patagosaurus fariasi* (arisen from the redescription of the holotype) is repeated here, as all associated specimens are subsequently compared to the holotype.

PVL 4170 can be diagnosed on the basis of the following combination of morphological features (features with * are tentatively considered autapomorphies): opisthocoelous cervicals and anterior dorsals with marked pleurocoel, which is deep in cervicals but more shallow in dorsals, and which is deeper anteriorly with well defined rims, but becomes shallow posteriorly and has only well defined dorsal and ventral rims; a small protrusion slightly dorsal to the midpoint on the anterior condyle of cervical vertebrae; relatively high neural spine on cervicals, accompanied by high dorsal placement of postzygapophyses (resulting in a high angle between the axial plane and the podl); cervicals with pronounced ventral keels, accompanied by an anterior protrusion at the onset of the keel and lateral excavations, with the keel running over 2/3 of the ventral surface in cervicals and 1/3 in anterior dorsals; lateral small flanges of bone on the ventral side of the posterior cotyle of cervical vertebrae; mid-posterior dorsals with high neural arches; mid-posterior dorsals with anterior neural arches separated by dorsoventrally elongated stprl accompanied by large oval cprf; dorsal neural arches with a CDF that extends internally as a cone-shaped pneumatic structure, which is separated by the mirroring structure by a thin septum, and both of which connect in a ventral, oval shaped internal pneumatic chamber, which is dorsal

to and well separated from the neural canal*; dorsals with small round excavations on the posterior side of the distal extremity of the diapophyses; posterior dorsal neural arches inclined posteriorly; high dorsal neural spines with lateral excavations; dorsal neural spines with rudimentary aliform processes; anterior caudals with saddle shaped spine summits and elongated neural spines which are not straight but curve convexly posteriorly at 2/3rd of spine height*; ilium with axially wide acetabulum, hook-shaped preacetabular lobe, and anteriorly projecting pubic peduncle; distal ends of ischia fused with ~100 degree angle between left and right ischium; pubis with 'kidney' shaped pubic foramen; femur with absent dorsolateral bulge but laterally concave along the shaft in anterior and posterior view*.

Table 2 (next page): Vertebral measurements of all associated MACN-CH and PVL material; first half = cervical and dorsal vertebrae, second half = caudal vertebrae. *EI (Elongation index, centrum length without condyle/height posterior cotyle) **aEI (average Elongation Index, (centrum length/height posterior cotyle).

vertebra MACN-CH/PVL	greatest length	greatest height	centrum length	centrum minimum width	width across diapophyses	width across prezygapophyses	width across postzygapophyses	pleurocoel length	pleurocoel height	width posterior cotyle	height posterior cotyle	width anterior condyle	height anterior condyle	height neural spine	length neural spine	height neural arch	centrum length without condyle	nc anterior	nc posterior	width between parapophyses	EI*	aEI**
936 1	18	?		?	?	?	?	12	4	?	7	?	?	9	9	?	?	?	?	?	?	?
936 2	17	16	16	?	?	?	?	14	4	?	7	?	5	8	11	?	15	?	?	?	2,1	?
936 3	17	15	15	?	?	?	?	10	3	?	5	?	3	7	13	?	15	?	?	?	3	?
936 4	17	12	12	?	?	?	?	12	3	?	6	?	5	?	13	?	12	?	?	?	2	?
936 5	22	?		?	?	?	?	9	4	?	10	?	7	14		?	15	?	?	?	1,5	?
936 6	22	23	23	?	?	?	?	18	3	?	10	?	7	14	15	?	20	?	?	?	2	?
936 7	21	25	25	?	?	?	?	10	5	?	10	?	9	16	17	?	15	?	?	?	1,5	?
936 8	20	27	27	?	?	?	?	12	5	?	9	?	8	17	15	?	14	?	?	?	1,6	?
936 9	34	44	30	10	38	22	28	17	7	13	15	14	15	26	20	6	24	4	3	?	1,6	1,723
936 10	44	39	40	10	?	24	20	22	11	20	17	21	17	23	26	6	27	4	3	?	1,6	1,469
dorsal 1	32	34	32	12	42	28	25	16	8	?	?	21	16	19	4	10	24	?	?	?	?	?
dorsal 2	20	64	20	12	48	30	29	6	8	23	20	20	20	24	2	14	10	?	?	?	0,5	0,467
dorsal 3	20	77	16	10	66	24	22	10	10			23	20	36	10	20	14	?	?	?	?	?
dorsal 4	32	84	15	13	?	20	27	8	8	26	22	24	19	33	12	28	12	7		?	0,5	0,503
936 axis	15	15	15	?	?	?	?	10	4	?	6	?	3	9	10	?	13	?	?	?	2,2	?
932 250	15	45	?	?	?	10	15	?	?	?	?	?	?	22	8	15	?	?	?	15	?	?
932 253	21	29	?	?	17	19,5	14	?	?	?	?	?	?	18	7	13	?	?	?	?	?	?
932 278	25	?	25	3,5	?	?	?	16	6	9	10	8	10	?	?	?	20		?	9	2	2,111
932 251	15	45	?	?	25	9	8	?	?	?	?	?	?	20	5	10		8?	?	14	?	?
933 309	15,8	6,25	15,8	?	?	?	?	10,6	?	5,3	6	4	4	?	?	?	11	?	?	6	1,8	1,954
933 279	13	?	13	3	?	?	?	8	3	6,5	7	6	6	?	?	?	9	?	?	7	1,3	1,335
933 295	10	?	10	4	16	?	?	5	4	6	7	7	8	?	?	?	7	?	?	8	1	0,583
230 1	12	49	12	7	24	?	?	5,5	3	11	15	11	12	20	6	10	8	6	5	14	0,5	0,364
230 2	12	30	12	5	?	6	?	5	3	6	8	6	8	15	4	8	6	5	3	?	0,8	0,5
934 1	7	22,5	?	?	?	6,6	5,5	?	?	?	?	?	?	15,5	4,3	10,5	?	?	?	11,5	?	?
934 2	11	23	?	?	?	7,5	6,4	?	?	?	?	?	?	13	3,5	8,7	?	?	?	9,5	?	?
934 3	6	22	?	?	?	6,2	7,5	?	?	?	?	?	?	11,5	3	9,5	?	?	?	12	?	?
934 4	5	19	?	?	24	6,5	8,5	?	?	?	?	?	?	12	2,5	10	?	?	?	8	?	?
934 5	8,5	26	?	?	?	9	7,5	?	?	?	?	?	?	17	3,5	11	?	?	?	14	?	?
934 6a	7	23,5	?	?	?	7	6	?	?	?	?	?	?	15,5	6,5	12	?	?	?	12	?	?
934 6b	8	25	?	?	?	7,5	6,5	?	?	?	?	?	?	15	5,5	11	?	?	?	12	?	?
934 7	6	29	?	?	21,5	7	6	?	?	?	?	?	?	17	5	12,5	?	?	?	12,5	?	?
934 8	8,5	27	?	?	?	9,5	8,5	?	?	?	?	?	?	18	6	10	?	?	?	11	?	?
934 9	8,5	25,5	?	?	?	8	7	?	?	?	?	?	?	15,5	5,5	10	?	?	?	10	?	?
935 1	19	16	?	?	46	16	21	?	?	?	?	?	?	33	10		?	7	6	?	?	?
935 2	17	16	?	?	40	20	20	?	?	?	?	?	?	34	10		?	?	?	?	?	?
935 3	12	20	?	?	36	19	18	?	?	?	?	?	?	37	8		?			?	?	?
935 4	20	17	?	?	40	19	20	?	?	?	?	?	?	37	11		?	?	?	?	?	?
4076 1	33	30	25	3,5	?	13,5	11,5	16,5	3,5	8,5	11	7	7	13	12	5,5	17	3	3	8	1,5	1
4076 2	22	17	19,5	2,7	14	14	16,5	13,8	2,5	8,5	8,5	11	8,5	?	?	5,5	14	2	2,5	11	1,6	0,824
4076 3	15	44	?	?	36	16,6	13,8	?	?	?	?	?	?	22	5,5	12	?	?	?	?	?	?

vertebra MACN-CH/PVL	greatest length	greatest height	centrum length	centrum minimum width	width across diapophyses	width across prezygapophyses	width across postzygapophyses	pleurocoel length	pleurocoel height	width posterior cotyle	height posterior cotyle	width anterior condyle	height anterior condyle	height neural spine	length neural spine	height neural arch	centrum length without condyle	nc anterior	nc posterior	width between parapophyses	EI*
935 1	12	55	12	?	38	8	6	n.a.	n.a.	15	16	15	16	20	6	10	n.a.	3	3	n.a.	0,8
935 2	15	55	15	13	35	8	5	n.a.	n.a.	15	18	15	18	25	5	10	n.a.	4	4	n.a.	0,8
935 3	13	52	13	12	35	7	6	n.a.	n.a.	17	15	18	15	28	7	10	n.a.	3	3	n.a.	0,9
935 4	12	52	12	10	35	8	7	n.a.	n.a.	17	15	17	19	22	6	10	n.a.	5	3	n.a.	0,8
935 5	15	50	15	12	35	10	7	n.a.	n.a.	18	15	17	17	25	6	10	n.a.	5	4	n.a.	1
935.1	18,5	12,5	14	7	?	?	?	n.a.	n.a.	9	7,5	7	6	10	7	?	n.a.	2	2	n.a.	1,9
935.2	16,5	12	13,5	8	?	?	?	n.a.	n.a.	6,5	7,6	8,8	9	9	5	?	n.a.	1,5	1,5	n.a.	1,8
934	13	?	13	?	15	?	?	n.a.	n.a.	16	15	16	15	?	?	?	n.a.	1,8	2	n.a.	0,9
1299 1	13	35	13	10	16,5	8,5	?	n.a.	n.a.	12	12	17	15	17	5	3	n.a.	2	2	n.a.	1,1
1299 2	?	41,6	?	10	20	6,7	4	n.a.	n.a.	?	20	13	22	18	4	3	n.a.	2	2	n.a.	?
1299 3	13	45	12	10	?	7	?	n.a.	n.a.	10	18	15	20	22	5	5	n.a.	2	2	n.a.	0,6
1299 4	14,5	30	14,5	13	20	7	?	n.a.	n.a.	15	14	15	16	8	4	?	n.a.	2	2	n.a.	1
1299 5	12	46	12	10	?	?	?	n.a.	n.a.	13	20	15	23	23	6	6	n.a.	2	2	n.a.	?
1299 6	10	40	10	9	?	6,5	4	n.a.	n.a.	14	17	14	20	16	5	3	n.a.	2	2	n.a.	0,6
1299 7	15	50	15	12	?	?	4,5	n.a.	n.a.	16	16	14	16,5	26	6	9	n.a.	2,5	2	n.a.	?
4076	14	25	8,5	11	?	7,7	?	n.a.	n.a.	13,8	14	14	14,2	12	3	?	n.a.	1,1	1,6	n.a.	0,6
933 345	?	?	?	?	20	10	13	n.a.	n.a.	?	?	?	?	14	5	?	n.a.	?	?	n.a.	?

Table 3: measurements of non-vertebral elements in cm. *pubic peduncle length is only for ilia. **GI (Gracility Index) is total proximodistal length/minimum mediolateral width.

MACN-CH	max length	pubic peduncle length*	min width	distal end length	distal end width	prox end length	prox end width	4th trochanter (lxw)	GI**
933 femur	56	-	12	10	16	8	18	5,5x2,5	4,6
933 pubis	39	-	6	6	10	10	20	-	6,5
933 ischium	35	-	6	5	-		20	-	5,8
933 ilium	29	14	-	-	-	-	-	-	-
932 sternal plate	25	-	-	-	-	-	-	-	-
932 humerus	61	-	10	6	18	6	22	-	6,1
932 radius	40	-	5	5	9	5	9	-	8
932 ulna	44	-	7	8	6	12	14	-	6,3
932 tibia	35	-	6	5	9	6	12	-	5,8
932 pubis	49	-	8	6	15	8	18	-	6,1
932 ilium	35	8	-	-	-	-	-	-	-
934 ischium	34	-	4	4	7	7	14	-	8,5
934 pubis	35	-	6	5	12	7	18	-	5,8
934 ilium	57	17	-	-	-	-	-	-	-
935 coracoid	23,5	-	-	-	-	-	-	-	-
935 scapula	70,5	-	-	-	-	-	-	-	-
935 ilium	43,5	16	-	-	-	-	-	-	-
1986 femur	120	-	26	18	26	20	40	11,5x5	4,6
1299 femur	119	-	25	20	28	17	35	-	4,76
1299 tibia	66	-	20		10	25	17	-	3,3

Associated material

MACN-CH 932

Several small to medium sized elements have been gathered from Cerro Condor Norte (see Fig 1). The material consists of a pubis, radius, ulna, humerus, sternal plate, ilium, tibia, two dorsal neural spines, a cervicodorsal neural arch, a cervical centrum and a sacral neural arch. It is not entirely certain whether all material belongs to one specimen or several; especially the two dorsal neural spines, which have a morphology that slightly deviates from the holotype of *Patagosaurus.* Most elements have a collection or field number besides the generic MACN-CH 932 group number, and, where present, we will adhere to these numbers to avoid confusion.

Axial elements

Cervical centrum MACN-CH 932 '278'

This small centrum is moderately well preserved (See Plate I, 278). The left parapophysis is missing, as are the neural arch and spine. The centrum shows unfused neurocentral sutures (see Plate I, 278 A), indicating that it represents a young individual (Morphological Ontogenetic Stage, MOS, 1 or 2; early immature animal, sensu Carballido and Sander, 2014; Marpmann et al., 2015). It is a stout but moderately elongated element, with an EI of 2,22 and an aEI of 2,11 (sensu Upchurch, 1998; Chure et al., 2010, See Table 2). This EI is relatively high compared to PVL 4170, but could correspond to the most elongated cervical PVL 4170 (6). In lateral view, the centrum curves gently, so that the cotyle is offset to a lower position than the condyle (Plate I, 278 B). The condyle is round, and displays the condylar rim characteristic of *Patagosaurus* PVL 4170 and *Cetiosaurus oxoniensis* (Plate I,

278 E). It also has a 'nose', a small protrusion slightly dorsal to the midpoint, as in anterior to mid-cervicals of PVL 4170. The cotyle is deep and slightly higher dorsoventrally than wide transversely (Plate I, 278 D). Ventrally, it has two lateral flanges that fan out, as in *Patagosaurus* PVL 4170. In ventral view, a ventral keel is present, which is visible as a prominent ridge on the ventral surface of the centrum, and fades into the centrum at about 2/3rds of the length of the centrum, as in PVL 4170 (Plate I, 278 C). The round, small parapophysis is confluent with this rim, and is not offset from the centrum. There is a depression present on the lateral side of the centrum (Plate I, 278 B), which is probably an early stage of the pleurocoel, further confirming an early ontogenetic stage (Schwarz et al., 2007; Carballido et al., 2012;).

Cervicodorsal neural arch MACN-CH 932 '253'

This element is a small neural arch with a high dorsal spine, and unfused neurocentral sutures, indicating an immature, small individual (MOS 1, MOS 2 ; Carballido et al., 2012; Carballido and Sander, 2014; Marpmann et al., 2015; Schwarz et al., 2007). It is, however, quite badly damaged, not completely prepared out of its matrix, and glued together; the glue obscures certain laminae (Plate I, 253). Also, the left postzygapophysis, as well as both diapophyses, are missing. It is a cervicodorsal element, due to the anterior and dorsally, elongated prezygapophyses, and the ventrally projecting diapophyseal laminae. In comparison with PVL 4170, it is likely the equivalent of PVL 4170 (7) or (8), see Chapter 2.

The neural arch and spine are dorsoventrally high, as is characteristic for *Patagosaurus, (*see Holwerda et al. in prep/Chapter 2).

The visible laminae on the lateral side of the neural arch are the acdl, the pcdl, and the podl (Plate I, 253 B, D). The acdl is visible as an oblique, anteroventrally projecting thick lamina that runs from the 'scar' of the (missing) diapophysis to the anteroventral side of the neural

arch. The pcdl projects posteriorly and ventrally, and is seen to follow the lateral ventral rim of the neural arch. Below this, a small fossa is partially visible on the lateral side of the neural arch, indicating that even in an early stage of development, some possible pneumaticity was already present (see Discussion for more ontogenetic features in *Patagosaurus*). Similarly, anterior on the neural arch, a faint, triangular prcdf is present, and posteriorly a possible pocdf (Plate I, 253 C). No aperture in the cdf is visible, however; implying a possible delay in the development of this particular pneumatic feature, which is present in the holotype PVL 4170 (see Discussion).

The prezygapophyses project anteriorly and dorsally from the neural arch (Plate I, 253 B, D); in lateral view they are supported by the strongly curving cprl ventrally and the mildly oblique sprl dorsally (which follows the same angle of the prezygapophyses of about 50 degrees to the horizontal). The prezygapophyses have a flat but slightly posteriorly canted articular surface, which is rounded to triangular in shape. In anterior view, there is a wide U-shaped recess between the tprls. Ventral to where the tprls meet, the dorsal rim of the anterior neural canal is visible, which, if this is the case, would have most likely been elliptical in shape.

The postzygapophysis is a small triangular protrusion, with a possible epipophysis visible (this is unfortunately not entirely clear). The postzygapophysis projects high from the neural arch, supported by the high projecting podl (around 60-70 degrees to the horizontal); another feature that is shared with *Patagosaurus* (Plate I, 253 A). The spol is poorly visible because it is obscured by a thick layer of glue. In posterior view, the scar of the missing spol is partially visible, as well as a deep, prominent and triangular spof. No cpols are visible, however, a possible stpol runs down to what might be the dorsal rim of the posterior neural canal, which is slightly triangular in shape.

The neural spine is a straight and rectangular in shape, and projects at nearly 90 degrees to the horizontal. The anterior side is rugosely striated, and the summit is square in dorsal view.

Dorsal neural spine MACN-CH 932 '250'

This element is a well-preserved neural arch and spine, with only the right diapophysis missing, see Plate I, 251. It has unfused neurocentral sutures on the neural arch, indicating skeletal immaturity (MOS 1, MOS 2; Carballido et al., 2012; Carballido and Sander, 2014; Marpmann et al., 2015; Schwarz et al., 2007). It is still partially embedded in sediment, however, which obscures views of the anterior and left lateral side. This lump of sediment contains some elements of bone directly anterior and dorsal to the prezygapophyses, indicating this element was once probably connected to another neural arch and might have been found in association with another vertebra. The perpendicularity of the prezygapophyses and the neural spine, together with the lateral projection of the diapophyses, indicates this dorsal to have been one of the posteriormost dorsals, as compared to the holotype PVL 4170.

In left lateral view, the element is well exposed; it shows the unfused neurocentral sutures ventral to the neural arch, the parapophysis, the left prezygapophysis, diapophysis, lamination, fossae and the neural spine (Plate I, 250 B). The lamination on the neural arch shows prominent cprl, pcdl, and prdl/prpl. The cprl supports the prezygapophysis on the lateral side, in a slightly oblique angle (of about 70 degrees to the horizontal). Ventral to the prezygapophysis it meets the prpl, which shows a gentle curvature before it reaches the small, rounded parapophysis. The pcdl supports the diapophysis from the ventral side and is nearly vertically projected. There is a possible remnant visible of the acdl, therefore, the orientation of these laminae indicate this element is posterior dorsal. A prominent, squared, deep cdf is visible between these three laminae, as is seen in posterior dorsals of

Patagosaurus PVL (4170). It is seen to connect to an internal pneumatic chamber, however, any septa that might have been present to separate it from its adjacent chamber are missing. It connects to the fossa around the hyposphene, however, as is seen in the posteriormost dorsal of the holotype PVL (4170). The diapophysis shows a rounded articular surface, and it projects perpendicular to the vertically aligned neural spine.

In posterior view, both postzygapophyses are well-preserved, as small, triangular protrusions (Plate I, 250 A). They are supported by the lateral spol (l.spol) and the podl on the dorsal and lateral side, and from the dorsal side by the medial spol. The l.spol runs down from around 2/3rds of the dorsoventral height of the neural spine, down to the dorsal end of the postzygapophyses, where it constricts slightly with the spine before it flares out to the postzygapophyses and to the diapophysis where it meets with the podl in the l.spol+podl configuration, after (Carballido et al., 2012). The m.spol runs along the medial side of the neural spine where it meets with its counterpart in a shallow gully, dorsal and medial to the postzygapophyses. It is interesting to note that at this ontogenetic stage, both the l.spol and the m.spol are present in this element. The hyposphene is partially damaged, but shows a squared to rhomboid appearance, and the stpol is not visible in this element. Ventral to the missing hyposphene, however, an oval posterior opening, possibly the neural canal, is visible. Both pocdfs are visible as shallow oval fossae.

The neural spine in lateral view is a straight, stout element, anteriorly supported by the sprl and posteriorly by the spols (Plate I, 250 B). In left lateral view, the prsdf is visible. In posterior view, the spine is rugosely striated and shows a small but relatively deep spof.

MACN-CH 932 '251'

This element is a well-preserved posterior dorsal with neural arch and spine, with all zygapophyses and diapophyses intact, though slightly taphonomically distorted. It is possible that this element originally was associated with MACN 932 '250', since these elements

match in size and general morphology, making this element also a posterior(most) dorsal. This is also apparent from the Cerro Condor quarry map (see Fig 1 and 2, orange coloured elements). The element shows unfused neural sutures as in MACN-CH 932 '250'. These are particularly clearly visible in ventral view. This indicates the dorsal was at the same ontogenetic stage as MACN-CH 932 '251'. The neural arch on the shows the cprl, prpl, prdl/acdl and pcdl present on the lateral side (Plate I, 251 C). They encompass a triangular, prominent cdf, infilled with sediment. The diapophysis projects laterally, with a mild dorsal convex curvature, and its articular surface is rounded to triangular in shape and bulges slightly. The prezygapophysis in lateral view shows a flat horizontal articular surface, which protrudes anteriorly (Plate I, 251 B). The cprl cants slightly to the anterior side, making the neural arch slightly wider laterally towards the prezygapophyses. The posterior side of the neural arch shows the postzygapophyses as small triangular protrusions, and it shows the hyposphene ventral to the postzygapophyses as a dorsoventrally elongated triangular protrusion.

In anterior view, the element shows some taphonomic deformsyion, with the right diapophysis being bent to the dorsal side and the neural spine slightly bent to the left lateral side (Plate I, 251 B). The anterior neural canal is clearly visible as an elongated ellipse, as in posterior dorsals of the holotype PVL (4170). The prezygapophyses are supported by stout short stalks, which bulge slightly on the lateral sides together with the cprls. There is no sign of a stprl, and only two short tprls are seen to run from the medial sides of the articular surfaces to the neural arch. The prdl is clearly visible as it runs in a convex dorsal curve from the prezygapophyses to both diapophyses. No cprf are present, but two prcdfs are visible underneath the diapophyses.

In posterior view, the postzygapophyses are clearly visible as two triangular protrusions (Plate I, 251 A). They are supported by the lateral spol and medial spol from the dorsal side (and lateral and medial dorsal side, respectively), and by the podl on the lateral side. The

l.spol is slightly damaged, however, it can be seen to have flared out to the lateral side from the neural spine towards the postzygapophyses. The m.spol shows the same morphology as in MACN-CH 932 '250'. No stpol is visible here, however, a prominent, elongated and squareshaped hyposphene is present ventral to where the tpols meet. This element is particularly large in comparison to the posterior dorsals of the adult holotype specimen PVL (4170). Paired pocdf are visible between the diapophyses and the postzygapophyses.

The neural spine is more elongated dorsoventrally in this element than in the previous adjacent element MACN-CH 932 '251'. It shows a more irregular shape however, due to taphonomic deformation. Its anterior and posterior surfaces are strongly rugosely striated (Plate I, 251 A,B). The lateral sides show a clear prsdf before the dorsalmost 1/3rd of the spine becomes slightly more convex and rugose. This change occurs together with a rugose striation that runs from the dorsal anterior side of the lateral spine to the more ventral posterior side. This is also seen in the holotype PVL (4170). The summit of the spine also shows a slight 'saddle shape' in lateral view, as in the holotype PVL (4170). In posterior view, a prominent but shallow spof is visible. The spine summit in dorsal view is rectangular in shape.

Sacral neural arch (932?) unnumbered

This sacral element is partially preserved; the neural arch, left transverse process, prezygapophysis, sacral rib, and the neural spine are preserved, see Plate I, bottom right (sacral unnumbered). In anterior view, the neural arch is unfused, indicating a juvenile stage (Plate I, bottom right, A). Only the rim of the neural canal is preserved, however, it seems that the anterior neural canal in anterior view is oval and extremely dorsoventrally elongated, as in the holotype of *Patagosaurus* PVL (4170). The left prezygapophysis is supported from the ventral side by a prominent tprl and cprl on both lateral side of the stout prezygapophyseal pedicel. The articular surface of the prezygapophysis is horizontally flat

and triangular in shape. The prdl runs from the lateral side of the prezygapohysis to the short and stout diapophysis in a convex dorsal curve. Ventral to this lamina, a wide and prominent prcdf is present, which stretches down to the ventral side of the neural arch. The sacral rib is rounded to C-shaped and stretches to about the height of the articular surface of the diapophysis, as in *Patagosaurus* PVL (4170).There is a gap between the diapophysis and the sacral rib, which might indicate a division between the latter two, indicating this element to be one of the first sacrals of the sacrum (Plate I, bottom right, A, B). The neural spine is dorsoventrally high as in *Patagosaurus* PVL (4170) and is rugosely striated. Two sprl are visible as sharply-protruding ridges. In lateral view, the spine summit is saddle-shaped, as in the holotype. In lateral view, the diapophyseal articular surface is triangular and rugose (Plate I, bottom right, C). Ventral to the diapophyseal articular surface, a second, semilunar and rugose attachment site is present for the attachment of the sacricostal yoke. The neural spine shows a shallow prsdf on the lateral side. In posterior view, the sacral element shows the left postzygapophysis to be well-preserved, while the right is slightly damaged. The left is a small triangular lateral protrusion at around 2/3rd of the height of the neural spine. The pcdl is seen running to the dorsal end of the sacral rib, where it terminates just below the hyposphene. The hyposphene is small and triangular, and is clearly separated from the postzygapophysis. The spine in dorsal view shows the rhomboid shape of the posteriormost dorsals, sacrals and anterior caudals of *Patagosaurus* PVL (4170), see Plate I, bottom right, D.

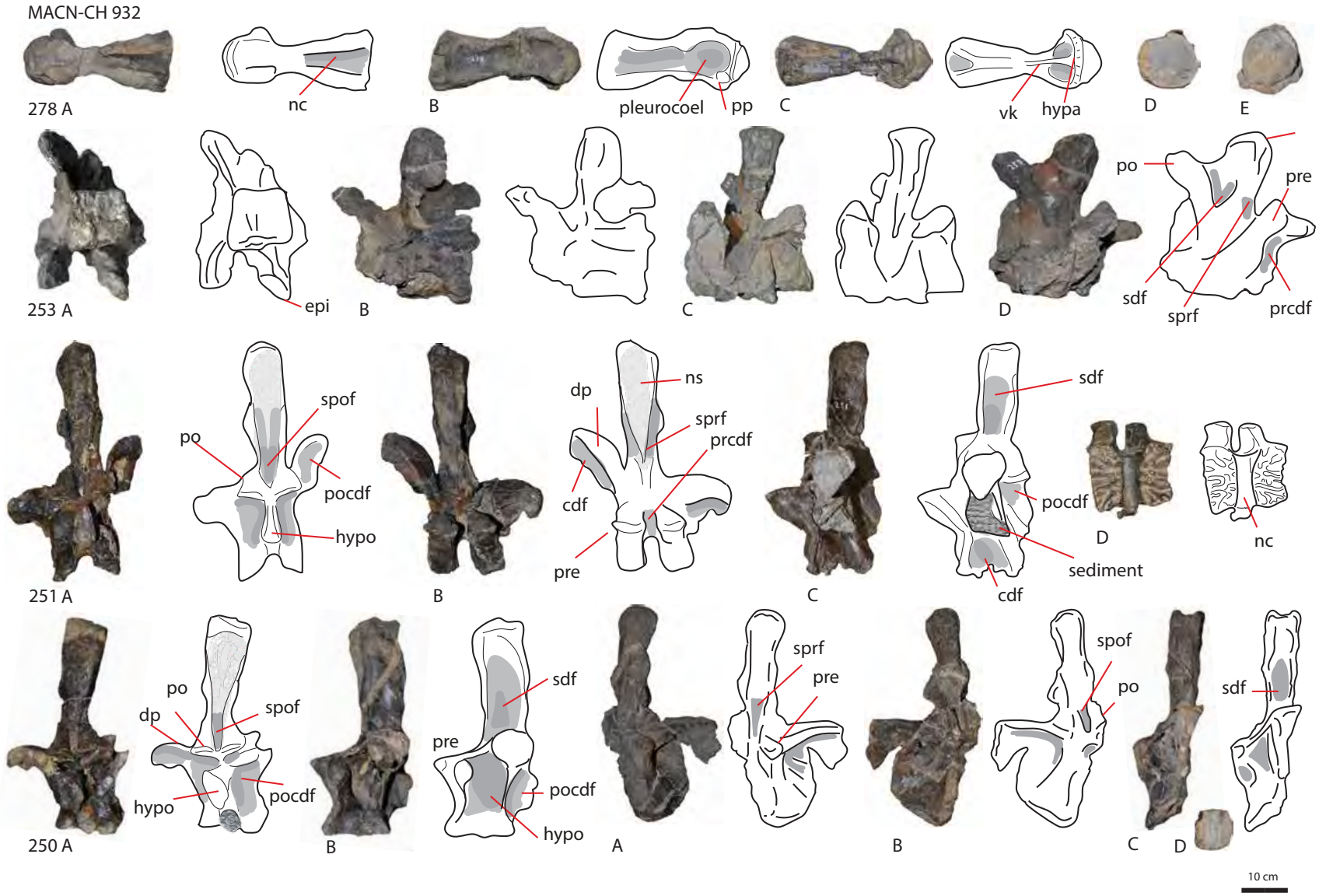
MACN-CH 932
278 A
nc
B
pleurocoel
pp
C
vk
hypa
D
E
253 A
epi
B
C
D
po
pre
sdf
sprf
prcdf
251 A
spof
po
pocdf
hypo
B
dp
ns
sprf
prcdf
cdf
pre
C
sdf
pocdf
D
sediment
cdf
nc
250 A
po
dp
spof
hypo
pocdf
B
sdf
pre
pocdf
hypo
A
sprf
pre
B
spof
po
C
D
sdf
10 cm

Plate I (previous page): MACN-CH 932 axial material. Top row: cervical centrum MACN-CH 932 278 in dorsal (A), lateral (B), ventral (C), posterior (D) and anterior (E) view. Second row: cervicodorsal neural arch MACN-CH 932 253 in dorsal (A), left lateral (B), anterior (C) and right lateral (D) views. Third row: dorsal neural arch MACN-CH 932 251 in posterior (A), anterior (B), lateral (C) and ventral (D) views. Bottom row: dorsal neural arch MACN-CH 932 250 in posterior (A), lateral (B), views. MACN-CH 932 sacral neural arch (unnumbered) in anterior (A), posterior (B) and lateral (C) views. Abbreviations: cdf = centrodiapophyseal fossa, dp = diapophysis, epi = epipophysis, hypa = hypapophysis, hypo = hyposphene, nc = neural canal, ns = neural spine, pp = parapophysis, pre = prezygapphysis, po = postzygapophysis, pocdf = postzygapophyseal centrodiapophyseal fossa, sdf = spinodiapophyseal fossa, spof = spinopostzygapophyseal fossa, sprf = spinoprezygapophyseal fossa, vk = ventral keel.

Sternal plate MACN-CH 932 (unnumbered)

Thus far, this is the only sternal plate found in the entire hypodigm (of the MACN) ascribed to *Patagosaurus*. It is a stout but transversely narrow element, perhaps in appearance somewhat similar to a coracoid, but lacking the coracoid foramen (or even the juvenile unclosed state of it). It is most likely a left sternal plate. It is roughly bean-shaped and convex in ventral (=anterior) view, (Plate II, sternal plate A), in that it is axially elongated, with tapering proximal and distal ends, but with a broader transverse part in the midsection, which makes it most similar to *Shunosaurus* (Tschopp and Mateus, 2013a) and slightly different from *Cetiosaurus* (Upchurch and Martin, 2002). On the distal half, a ridge is visible, which splits into a forked ridge at the distalmost part of the plate, possibly representing a ligament attachment site. On the left lateral side, a small rugose articular surface exists (Plate II, sternal plate B). This articular surface is dorsoventrally relatively broad and transversely narrow. On the medial side, a rugose articular surface exists for the attachment to the parallel sternal plate (Plate II, sternal plate C). In dorsal view (=posterior view, Plate II, sternal plate B), it is concave, and slightly more pear-shaped, in that the proximal end is rounded and narrower than the distal end, which is also rounded, but broader. Another small articular surface exists on the right lateral side, possibly for the attachment of a ligament or even a gastralium.

Ilium MACN-CH 932

This is a fragment of a small right ilium, with the pubic peduncle, the acetabulum and part of the posterior lobe preserved (Plate II, ilium, A). The anterior lobe and the dorsal rim are missing. The acetabulum is wide, as in the holotype PVL 4170, with an angle between the pubic peduncle and the posterior lobe of around 100-120 degrees. The acetabular rim is concave in lateral view, as is seen in the holotype PVL 4170. The pubic peduncle is a slender rod-shaped element, which does not widen towards its extremity as much as in the holotype PVL 4170 (Plate II, ilium, B), however, this could be an ontogenetic difference. The lobe of the ischial peduncle is rounded, and the same 'butterflywing'-shape is seen in the first half of the posterior lobe as in the holotype, however, the other half of this lobe is unfortunately missing. The ischial peduncle is roughly rounded triangular in shape (Plate II, ilium, C).

Pubis MACN-CH 932

This small to medium-sized left pubis is well-preserved, with almost no damage or taphonomic alteration visible, however the shaft has been broken off near the pubic apron and glued back together (Plate II, pubis, A,B). It is generally robust, as in the holotype PVL 4170. There is no torsion between the pubic apron and the shaft, which is similar to the holotype PVL 4170 (Plate II, pubis, A,B). In lateral view, the pubic apron shows a rectangular iliac peduncle, which is offset and dorsally elevated from the apron, as in PVL 4170 and *Cetiosaurus oxoniensis*. In this specimen, however, the iliac peduncle is slightly more confluent with the pubic apron than in the latter two adult specimens, which again can reflect ontogeny. In lateral view, the articular surface appears flat. The articular surface of the iliac peduncle in anterior view is roughly triangular, with the posterior rim more squared and the anterior rim more triangular (Plate II, pubis, C). The pubic symphysis shows only a small, rugose, rounded to rectangular articulation surface (Plate II, pubis, D). The pubic

foramen is kidney-shaped as in *Patagosaurus* PVL 4170, and is closed, contrary to the state of neosauropod juvenile pubes, such as Tornieria (Remes 2009). The shaft is not as sinusoidal in ventral/dorsal view as the holotype PVL 4170, and is rather straight. The shaft flares out towards its distal end, however, the ventral end runs a little further distally than the dorsal end, as is seen in PVL 4170 (Plate II, pubis, E).

Appendicular elements

Humerus MACN-CH 932 '268'

This right humerus is a small and slender element (Plate II, 268 A,B,C). As in most sauropods, the midpoint of the shaft is considerably smaller transversely than either of the extremities, and is elliptical in cross-section. The expansion of proximal and distal ends are not as wide as in more derived sauropods (neosauropods, titanosauriforms), see Plate II, 268 A,C, (Upchurch, Barrett & Dodson, 2004). The gracility index (total proximodistal length/minimum mediolateral width) is 6,0 (See Table 3). This is lower than in *Cetiosaurus oxoniensis* (6,7) and in the juvenile *Lapparentosaurus* (7,8). The proximal end is transversely wider than the distal end. In posterior view, the proximal end of the shaft is convex, and the distal end is flat to concave (Plate II, 268 C). Compared to *Cetiosaurus*, the proximal end of the humerus is flat in anterior and posterior view (Upchurch and Martin 2003), and resembles more the state of the mamenchisaurid *Tonganosaurus*, but is unlike the state in *Omeisaurus* and *Mamenchisaurus youngi* (He, Li and Cai, 1988; Ouyang and Ye, 2002; Liu and Zheng-Xin, 2010).

The proximal articular surface in dorsal view is roughly triradiate and shows a rugose bulge of the humeral head on the posterior rim, approximately midway on the surface (Plate II, 268 D). This is not as prominent as in more derived neosauropods from the Late Jurassic or Early Cretaceous such as *Giraffatitan* or *Haestasaurus* (Taylor, 2009; Upchurch et al., 2015). The proximal articular surface (in dorsal view) is more symmetrical in outline than in

mamenchisaurids or *Omeisaurus* (Tang et al., 2001; Ouyang and Ye, 2002) and thus is closer to the condition of *Cetiosaurus oxoniensis* and an unnamed sauropod from the Early-Middle Jurassic of Skye, UK (Liston, 2004b) and neosauropods (Upchurch et al. , 2004).

The distal articular surface shows two small round condyles for the radius and ulna, wich are more or less similar in size (Plate II, 268 E), and less pronounced than those in the Skye sauropod (Liston, 2004b). The posterior side of the distal articular surface shows a relatively prominent anconeal fossa, as in Cetiosaurus oxoniensis (Upchurch and Martin, 2003) between the condyles, where rugose ridges border the concavity.

The deltopectoral crest is a small low ridge, although the end of the crest is broken off, so it could be that this element was slightly more pronounced (Plate II, 268 B). In its current state, it is far less prominent than in *Cetiosaurus oxoniensis* or *Lapparentosaurus*. It runs to about 1/3rd of the length of the humeral shaft.

Radius MACN-CH 932 '272'

This radius is well preserved, and only slightly taphonomically distorted (Plate II, 272 A,B). It is a slender element, of typical sauropod morphology (sensu Upchurch, 2004). It belongs to a small-medium sized individual, and therefore it likely can be associated with the ulna of the MACN-CH 932 specimen. The proximal end of the shaft shows the medial and lateral processes to be not as pronounced as in neosauropods (Upchurch, Barrett & Dodson, 2004; Upchurch, Mannion & Taylor, 2015). The proximal end is rather rounded to squared with no prominent protrusions (Plate II, 272 C). The proximal end of this radius also differs from the Rutland *Cetiosaurus* J13611 in that it lacks the prominent triangular medial process on the distal shaft; instead it is more rounded in this element. The lateral side of the distal end shows a concavely curved surface, rendering the distal end mildly kidney-shaped (Plate II, 272 D). This shape is seen also in *Camarasaurus*, *Haestasaurus* and *Ferganasaurus*

(Upchurch et al., 2015). A rugose ridge runs from the distal end to about 1/4th of the length of the shaft; this is probably the ligament attachment site for the ulna (Plate II 272 A).

Ulna MACN-CH 932 '271'

The ulna is well-preserved and not taphonomically altered; only the distal shaft is slightly damaged; giving it a blunt appearance. (Plate II, 271 A,B,C). In terms of size, it fits well with the radius MACN-CH 932 '272', and the two were likely associated. The proximal shaft (Plate II, 271 D) shows the typical sauropod triradiate ulna surface (sensu Upchurch, 2004). The shaft widens considerably towards its proximal end, as in most sauropods (Upchurch, 2004). The anteromedial extremity, in dorsal view, is more pronounced and is triangular in shape, and almost going towards a hook-shaped morphology (Plate II, 271 D). This latter hook-shape is also seen on the medial process of the ulna of *Lapparentosaurus* MAA 154.

The anterolateral extremity, in dorsal view, is less pronounced and resembles a rounded hook-shape (Plate II, 271 D). The medial and lateral processes are also not as pronounced as in *Omeisaurus*; in *Omeisaurus* these protrude further from the proximal center, and show a deep radial articulation. The proximal end of the ulna of *Mamenchisaurus*, however, is less pronounced than in this juvenile *Patagosaurus*; in *Mamenchisaurus* the extension of the medial and lateral processes are more or less symmetrical, whereas in MACN-CH 932 these are asymmetrical. The anteromedial process also does not show the extensive lobe as in *Haestasaurus* (Barrett et al., 2010; Upchurch, Mannion & Taylor, 2015). The proximal end of MACN-932 does not show the dorsally protruding ridges as in the Rutland *Cetiosaurus*, but rather shows low ridges/rugosities and a convex dorsal proximal rim, whereas this surface in the Rutland *Cetiosaurus* is more concave. The convex proximal side of MACN-CH 932 is not likely an olecranon process however, as it is not as pronounced as in derived sauropods (Upchurch et al., 2004).

The distal shaft shows a medially triangular side and a lateral rounded side (Plate II, 271 E). The shaft flares out to both lateral sides at its distal extremity. The distal half of the shaft shows rugose ridges on both lateral and medial sides.

Tibia MACN-CH 932 '273'

This element is a small tibia, belonging to a juvenile specimen (Plate II, 273, A,B). In anterior view, the proximal end of the shaft is straight, however, towards the distal end, the lateral rim of the tibia tapers towards the medial side (Plate II, 273 A). In lateral view, the shaft shows a slight sinusoidal shape from the posterior proximomedial end to the anterior lateral distal end. The medial distal end of the shaft projects slightly further distally than the lateral, allowing for the medial malleolus. The typical 'step', however, seen in sauropod tibiae (Upchurch et al., 2004), is very low, and not prominent in this element (Plate II, 273 A,B). This is in contrast to most other sauropods, including other Middle Jurassic sauropods such as *Cetiosaurus* and *Lapparentosaurus* (Upchurch and Martin, 2003), but could be an ontogenetic feature. In posterior view, the medial ridge of the cnemial crest is seen to run along the shaft, crossing the posterior side of the shaft to the medial distal end, which creates a triangular shape. The proximal articular surface is transversely wider than the distal articular surface (Plate II, 273 C).

Pes MACN-CH 932

Several metatarsals of a small pes are associated with this specimen, as well as a small ungual phalanx. Metatarsals I, II, and IV, and the pedal ungual are preserved, as well as phalanges I-1, II-1, III-1, IV-1, and two small phalanges that could not be definitely determined, however, these are likely IV-1 and V-1.

Metatarsal I (unnumbered) is a roughly rectangular element (Plate III Metatarsal I A, B, C, D), with distinctly tapering lateral ends, both dorsally and ventrally (Plate III Metatarsal I D, E), in

dorsal and plantar view (Plate III Metatarsal I A,B). This is similar to the state in the metatarsal I of the Late Jurassic *Vouivria* (Mannion et al., 2017), and in the Middle Jurassic *Lapparentosaurus* MAA 149, however, in MACN-CH 932, the distal tapering is slightly more pronounced, which is similar to the state of *Cetiosauriscus stewarti* NHMUK R3078, from the Callovian of the UK. Metatarsal II '283' is a more elongated element, with on its proximal end a beveled medial slope and protruding lateral side (Plate III Metatarsal II A, B, C, D). The beveled surface is more prominent than in *Lapparentosaurus* MAA 96, however, the lateral protrusion is more prominent in *Lapparentosaurus*. The proximal end (Plate III Metatarsal II E) furthermore resembles the state of basal titanosauriforms from the Late Jurassic, *Giraffatitan* (Janensch, 1961) and an unknown brachiosaurid from the USA (Maltese et al., 2018).

Metatarsal IV is a slender, rod-like element, with a triangular, wider proximal end and a distal end tapering to a point (Plate III Metatarsal IV A, B, C). On its distal end, it displays a flattened surface for ligament attachement. In this regard it resembles metatarsal IV of *Cetiosauriscus stewarti*, but does not resemble any neosauropod state (Maltese et al., 2018). None of the metatarsals show similarities with those of diplodocids (Maltese et al., 2018).

The phalanges (Plate III) are small and squared elements, wider than long, and with slightly wider proximal ends, which is typical for eusauropods (Upchurch et al., 2004).

The ungual (Plate III Ungual phalanx A,B) is small and delicate, and tapers to an acute point. It is uncertain whether or not it is the first or second ungual, since several ichnofossils indicate that basal sauropods had two unguals (Wilson, 2005; Marty et al., 2016; Lallensack et al., 2017). However, the small size and moderate curvature do suggest it is not the first ungual. The shape of the metatarsals suggests a plantigrade spreading, as is usual for basal eusauropods, and in contrast to neosauropods (Upchurch, 2004).


MACN-CH 932
D
deltopectoral crest
humeral head
anconeal fossa
268
A
B
C
E
A
B
C
Sternal plate
anterolateral process
anteromedial process
D
C
ridge
A
B
272
D
A
B
C
271
E
C
cnemial crest
A
B
273
D
Ilium
A
pubic peduncle
ischial peduncle
B
C
C
iliac peduncle
ischial peduncle
D
pubic foramen
A
E
B
Pubis
10 cm

Plate II (previous page): MACN-CH 932 axial and appendicular elements. MACN-CH 932 ‘268’ humerus, in anterior (A), lateral (B), posterior (C), proximal (D) and distal (E) views. MACN-CH 932 sternal plate (unnumbered) in ventral/anterior view (A), dorsal/posterior view (B), lateral view (C). MACN-CH ‘273’ tibia, in anterior (A), posterior (B), proximal (C), and distal view (D). MACN-CH ‘272’ radius in anterolateral (A) and posterolateral (B), proximal (C) and distal (D) views. MACN-CH 932 ‘271’ in lateral (A), anterior (B), posterior (C), proximal (D), and distal (E) views. MACN-CH 932 Ilium (unnumbered) in lateral (A) view, pubic peduncle (B) and ischial peduncle (C). MACN-CH 932 pubis (unnumbered) in lateral (A), medial (B), proximal iliac peduncle (C), ischial peduncle (D) and distal view (E).

MACN-CH 932

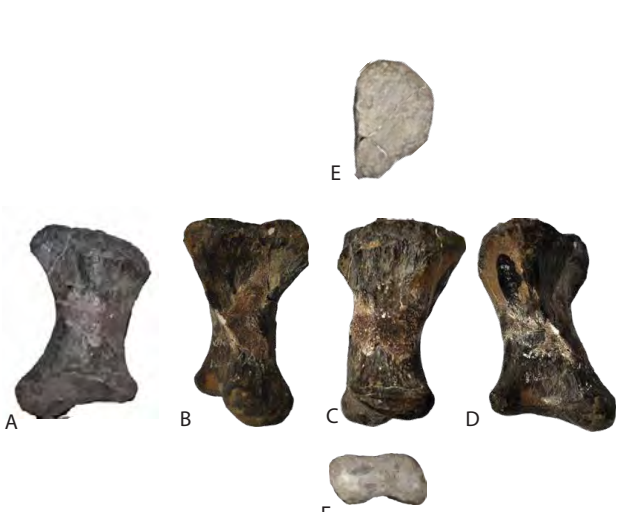

Metatarsal I

Metatarsal II

Metatarsal IV

Phalanx I-1

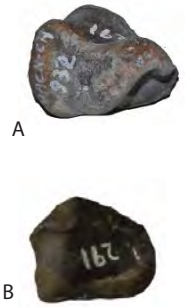

Phalanx II-1

Phalanx III-1

Phalanx ? IV-1

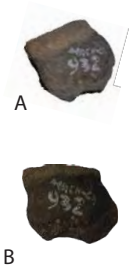

Phalanx ? V-1

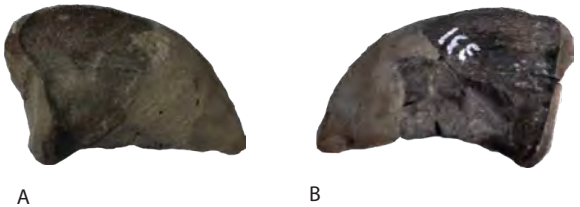

Ungual Phalanx

5cm

Plate III (previous page): MACN-CH 932 pes. Metatarsal I in plantar (A), dorsal (B), lateral (C), medial (D), proximal (E) and distal (F) views. Metatarsal II in planter (A), dorsal (B), lateral (C) and medial (D), proximal (E) and distal (F) views. Metatarsal IV in plantar (A), lateral (B) and dorsal (C) views. Phalanges I-1, II-1, III-1, IV-1 and ?V-1 in plantar (A) and dorsal (B) views. Ungual phalanx in lateral (A) and medial (B) views.

Comparison with *Patagosaurus* PVL 4170

Based on the following combination of characters shared by (and based on comparisons with) the holotype specimen PVL (4170), it is fairly certain that this specimen is a *Patagosaurus*. For the cervical and cervicodorsal elements (MACN-CH 932 250, 251 and 278) these are: the morphology of the centrum, with ventral keel, parapophyses and deep pleurocoel, the morphology of the prezygapophyses and U-shaped recess between the prezygapophyses, and the asymmetry (in dorsal view) between the projection of the prezygapophyses and the postzygapophyses (in the cervicals), as well as the configuration of the tprl, prdl, and the high projection of the podl (in the dorsal). These characters of MACN-CH 932 match those of the mid and posterior cervicals of *Patagosaurus* PVL 4170. These are: the lateral lamination of the neural arch with square to triangular configuration of the prdl, pcdl and cprl/prpl, the open cdf that connects to an internal pneumatic chamber in the neural arch, the oval and dorsoventrally elongated neural canal, the morphology of the neural spine and the morphology of the hyposphene. These characters of MACN-CH 932 match the posterior cervicals of PVL 4170 (7) and PVL 4170 (8) and the posteriormost dorsals of PVL 4170 (14) and (16) and (17).

Interestingly, one main feature that differs in MACN-CH 932 from PVL 4170 is the absence of an stprl and sprf. This could be an ontogenetic feature, as the neural arch is not elongated as in PVL 4170, and the neurocentral sutures are still unfused in MACN-CH 932.

The ilium of MACN-CH 932 shows a similar posterior lobe as in the holotype. The pubis shows a few slight differences compared to the holotype; especially in the proximal end, which could still reflect ontogeny.

New information from MACN-CH 932

New elements in this specimen, which are not present in the holotype are: the humerus, radius, ulna, tibia and sternal plate, as well as pedal elements. Originally, the holotype PVL

4170 was associated with a humerus (see quarry map of Cerro Condor Norte, Figure 1 and 2); however, the only humerus that is kept with the holotype in the PVL collections, is from Cerro Condor South, whereas the holotype is from Cerro Condor North. The MACN-CH 932 humerus unfortunately lacks a femur for the purpose of elongation and gracility index comparisons.

The ulna does not show an overly prominent anterolateral and mediolatesal process, which implies it is not derived as in neosauropods. However, it is also dissimilar from that of *Cetiosaurus*, thus giving it a unique set of characters; the assymmetry between medial and lateral process, without extreme extension as in neosauropods, combined with a convex proximal surface (but without olecranon process) for subsequent phylogeny. It resembles more closely the state of that of the Middle Jurassic Malagasi *Lapparentosaurus*.

The radius does not show many important phylogenetic characters, however potentially in conjunction with the ulna (as it is a possibility that the two were paired) indicates something about the stance and gait of *Patagosaurus*, particularly in combination with the humerus. This seems to be a rather stout forelimb altogether, with low gracility index and moderate slenderness of the humerus.

The sternal plate is the final new item to add to *Patagosaurus*. The morphology is similar to the large sternal plate of *Cetiosaurus oxoniensis* and to those of *Shunosaurus* and *Camarasaurus* (Upchurch and Martin, 2002; Upchurch et al., 2004), indicating an intermediate stage of phylogenetic development between basal non-neosauropod eusauropods and neosauropods.

The pes, finally, sheds light on the stance of *Patagosaurus*, which was plantigrade, which, combined with the slightly laterally convex femur of the holotype, suggests a more basal sauropod stance and gait, as opposed to the style in neosauropods. The metatarsals of *Patagosaurus* show an intermediate stage between non-neosauropod eusauropods

(*Lapparentosaurus, Cetiosauriscus*) and neosauropods (*Vouivria, Giraffatitan*), but do not share any similarities with diplodocids.

Comparison with *Volkheimeria chubutensis* (PVL 4077)

The only elements that can be compared to *Volkheimeria* are the dorsal neural arches, the ilium and the tibia.

The dorsal neural arches of MACN-CH 932 do not show the accessory lamina on the anterior side of the neural spine or the prespinal lamina that defines *Volkheimeria* PVL 4077 (Bonaparte, 1979; Bonaparte, 1986a), nor do they possess the axially elongated dorsal neural spine. They are rather more axially compressed and dorsoventrally elongated, which brings them much closer to *Patagosaurus* than to *Volkheimeria*. Finally, *Volkheimeria* shows another accessory lamina on both sides of the neural arch, which runs from the parapophyses to the ventral posterior side of the centrodiapophyseal fossae at an angle of about 40 degrees to the horizontal; this accessory lamina is not found in MACN-CH 932. The neural arch shows a large open fossa ventral to the diapophysis, which in adults shows the cdf, which is one of the most notable autapomorphies of *Patagosaurus*.

The ilium does not show the same shortening of the pubic peduncle as in *Volkheimeria*. However, the dimensions of the acetabulum are rather similar between PVL 4077 and MACN-CH 932. This could be due to both being in early ontogenetic stages of development, since the ischial peduncle of both are dissimilar in shape; the one in MACN-CH 932 is slightly more rectangular in shape than PVL 4077.

The tibia of this specimen is very small and of an early ontogenetic stage, therefore lacking in much anatomical information. Compared to the *Volkheimeria* PVL 4077, however, the

proximal end of MACN-CH 932 flares out less transversely. The medial malleolus in MACN-CH 932 is prominent, while PVL 4077 has a less pronounced medial malleolus.

Ontogenetic features of MACN-CH 932

The unfused neurocentral sutures, absence of neural arch elongation, absence of an stprl, overall smaller size than the holotype, but presence of laminae and fossae show it was a juvenile to subadult *Patagosaurus*, probably in MOS 2.

MACN-CH 933

The material of this juvenile specimen consists of a right femur, left pubis, right ischium, partial left ilium, several centra of cervical, dorsal and caudal vertebrae, and a dorsal neural arch.

Cranial element MACN-CH 933

A small left dentary is associated with this specimen, bearing teeth. The dentition as well as the dentary have been extensively described elsewhere (Rauhut, 2003; Holwerda et al., 2015). The dentition is morphologically dissimilar to the other isolated teeth associated with *Patagosaurus* (Bonaparte, 1986a), however, the enamel wrinkling pattern is comparable (Holwerda et al., 2015).

The dentary is partially embedded in sediment, obscuring the surangular and splenial. The distal tip of the surangular is visible in dorsal view (Plate IV C). Anteriorly (Plate IV A,B), the dentary lacks the deep 'chin' seen in diplodocids (Upchurch 2004, Tschopp et al., 2015). The ventral side of the dentary is rather straight and does not show the shallow concavity seen in *Shunosaurus, Camarasaurus, Giraffatitan or Europasaurus* (Janensch, 1935; Madsen, et al., 1995; Chatterjee and Zheng, 2002; Marpmann et al., 2015). The straight ventral side is also seen in another dentary ascribed to Patagosaurus from the Cañadón Asfalto Fm., MPEF-PV 1670. Both elements lack a prominent chin-like process on the anterior side, which is also shared with *Archaeodontosaurus* (though this element is incomplete) from the Middle Jurassic of Madagascar (Buffetaut, 2005). The symphysis shows a slight concave medial curvature, which is also shared with MPEF-PV 1670. Estimated from the curvature of the dentary in dorsal view (Plate IV C) he small juvenile dentary MACN-CH 933 would create a less clear U-shaped mandible than MPEF-PV 1670 (Rauhut 2003), however, this could be

ontogenetic, as this is also seen as a difference in ontogenetic stages of dentaries of *Europasaurus* (Marpmann et al., 2015).

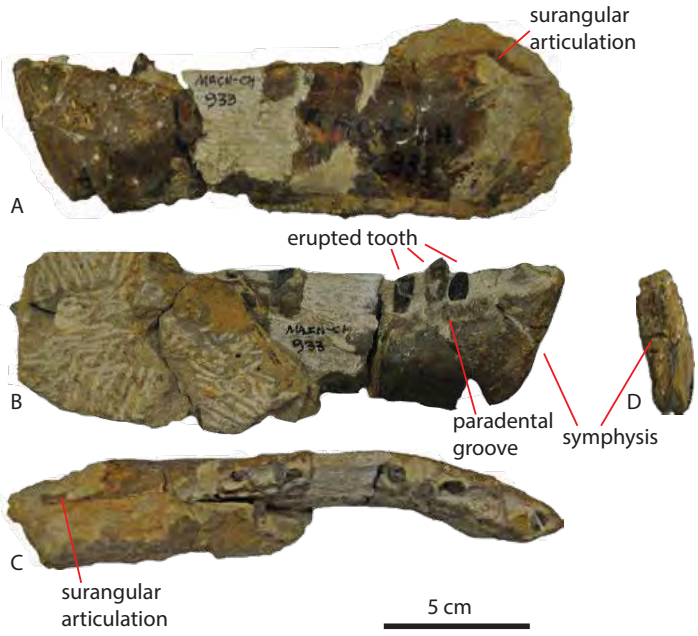

Plate IV: MACN-CH 933 Dentary in lateral (A), medial (B) and dosal (C) and proximal view (D).

Axial elements (See Plate V)

Cervical centrum MACN-CH 933 '309'

This unfused cervical centrum is partially embedded in matrix (Plate IV 309 A). Only the ventral side, and anterior and posterior are partially visible. The anterior condyle is rounded, and shows a slight protrusion dorsal to the midpoint (Plate V 309 C). It is cupped by a small rim, as in the holotype PVL 4170. The cotyle is filled-in with sediment (Plate V 309 B). On its ventral side, a lateral flange is seen, as in the cervicals of the holotype PVL 4170. The body of the centrum, only visible in ventral side, is anteroposteriorly elongated, and transversely narrow, with an EI of 2,0. It is constricted posterior to the condyle, where a small hypapophysis protrudes ventrally, and where laterally small rounded parapophyses protrude posteriorly and laterally. The ventral keel is visible, and runs to about 3/4ths of the axial length of the centrum, where it fades at the posterior 1/4th into a triangular elevated surface. It is unclear if a fork-like structure as in *Lapparentosaurus* is visible (Plate V 309 A).

Cervical centrum MACN-CH 933 '279'

This unfused cervical centrum is generally well-preserved, with only the left parapophysis partially preserved (Plate V 279 A, B, C). It also has a lump of matrix still attached to the right lateral side. The anterior end is not much offset from the posterior end, and the ventral side in lateral view is only mildly concave.

The condyle is round and smooth (Plate V 279 D). It has a small anterior protrusion slightly dorsal to the midpoint, which is seen in the holotype PVL 4170, and in many other basal eusauropods. The condyle is supported by a thick rugose rim. Confluent with this rim, and on the ventral lateral side, the parapophyses protrude ventrally and laterally as small elliptical rugose protrusions (Plate V 279 B). The rim of the condyle, in lateral view, struts the pleurocoel, which invades the lateral anterior side of the condyle, and runs along almost the

entire lateral surface of the centrum, where it fades into the centrum a few centimeters away from the lateral rim of the cotyle (Plate V 279 A, C). It is deepest at the anterior side however, as in the holotype PVL 4170. The cotyle is slightly larger than the condyle, is round and filled with matrix. As in the holotype PVL 4170, it is slightly wider on each lateral ventral side. The ventral side of the centrum shows a constriction of the centrum directly posterior to the condyle and the postzygapophyses (Plate V 279 B). Here, there is also a prominent ventral keel, which runs along 2/3rds of the ventral surface before it fades into the centrum (Plate V 279 B). Here, however, a triangular depression is seen as in MACN-CH 932 '278' and in *Lapparentosaurus*. The anterior side of the keel is supported by a small but rugose hypapophysis, which shows oval shallow fossae on each lateral side, as in the holotype PVL 4170 (Plate V 279 B). In dorsal view, the neural canal gully is visible on the posterior half of the centrum. The unfused neurocentral sutures, however, are not visible.

Cervicodorsal centrum MACN-CH 933 '295'

This element is a small but stout unfused centrum. On one side of the neural arch, the neurocentral sutures are preserved. It is strongly opisthocoelous, making it one of the last cervicals, or the first dorsal (Plate V 295 A, B, C, D). The condyle is dorsoventrally elongated, making it more likely to be a dorsal (Plate V 295 F). It is surrounded by a rugose rim, as in the holotype PVL 4170. The parapophyses are elevated towards around midway up the dorsoventral height of the condyle, and appear as small rugose protrusions (Plate V 295 A, D). The cotyle is filled with sediment, but shows an elongation posteriorly of its ventral rim compared to its dorsal side (Plate V 295 E). In posterior view, it is slightly triangular in shape due to a V-shaped ventral side, while the dorsal side of the cotylar rim is rounded. The ventral side has a clear ventral keel and a pronounced hypapophysis, which is more pronounced in this small vertebra than in adult vertebrae (Plate V 295 B). The centrum is

slightly constricted behind the hypapophysis, as in most cervicals and the anteriormost dorsal of PVL 4170. In lateral view, the centrum has a shallow, oval pleurocoel, which is not as pronounced as in the adult specimens (Plate V 295 A, D). In dorsal view, the neurocentral sutures and the neural canal groove are visible, though damaged (Plate V 295 C). The right suture is better preserved than the left, and shows rugosities on its dorsal surface.

Dorsal centrum MACN-CH 933 '276'

This partially preserved middle dorsal centrum shows a slightly convex anterior articular surface in lateral view, as in most non-neosauropod eusauropods (Plate V 276 E). It is also slightly asymmetrical, with a larger and deeper anterior face. It has an oval to rectangular shaped anterior articular surface (Plate V 276 A) and a more rectangular shaped posterior articular surface (Plate V 276 B). The ventral surface of the posterior articular face is slightly triangular, as in MACN-CH 933 '295'. The centrum is smooth in ventral view, with no keel visible (Plate V 276 D). On the lateral side, no depressions are visible (Plate V 276 E). In dorsal view (Plate V 276 C), the neurocentral sutures show rugosities, as in '295'.

Caudal centrum MACN-CH 933 '345'

This posterior caudal centrum and neural spine is relatively well-preserved compared to the other elements, and has a part of the postzygapophyses and neural spine still intact (Plate V 345 A, B). The centrum is symmetrical and smooth both ventrally and laterally (Plate V 345 A, B, D); only anteriorly on the ventral rim of the articular surface, very faint chevron facets are visible (Plate V 345 D). The anterior and posterior articular surfaces are flat to concave, and both are oval in shape. The neural arch is low, and shows slight oval depressions on both lateral sides (Plate V 345 A,B). The prezygapophyses do not project further anteriorly than the centrum, and are small, blunt triangular elements (Plate V A,B, C, E). The neural spine is

directed strongly posteriorly and only slightly dorsally, and projects further than the posterior end of the centrum. It tapers to a point towards its distal end.

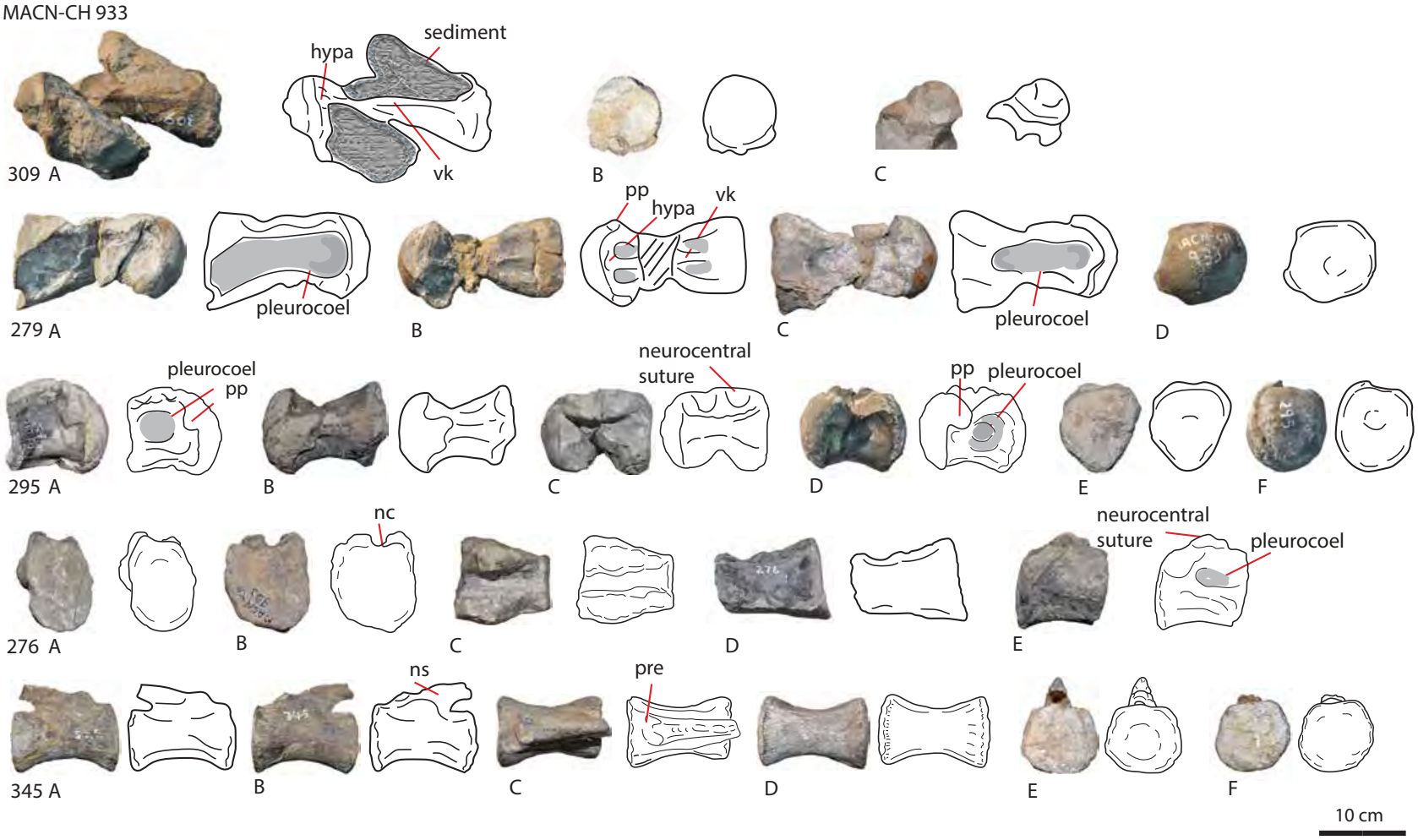
MACN-CH 933
sediment
hypa
vk
309 A
B
C
pp
hypa
vk
pleurocoel
279 A
B
C
pleurocoel
D
pleurocoel
pp
neurocentral
suture
295 A
B
C
D
pp
pleurocoel
E
F
nc
276 A
B
C
D
neurocentral
suture
pleurocoel
E
ns
pre
345 A
B
C
D
E
F
10 cm

Plate V (previous page): MACN-CH 933 axial vertebral elements. MACN-CH 933 ‘309’ in ventral (A), posterior (B), and anterior (C) views. MACN-CH 933 ‘279’ in right lateral (A) ventral (B), left lateral (C), and anterior (D) views. MACN-CH 933 ‘295’ in right lateral (A), ventral (B), dorsal (C), left lateral (D), posterior (E), and anterior (F) views. MACN-CH 933 ‘276’ in anterior (A), posterior (B), dorsal (C), ventral (D) and lateral views (E). MACN-CH 933 ‘345’ in right lateral (A), left lateral (B), dorsal (C), ventral (D), posterior (E) and anterior (F) views. Abbreviations: hypa = hypapophysis, ns = neural spine, pp = parapophysis, pre = prezygapophysis, vk = ventral keel.

Pubis MACN-CH 933

This small left pubis is relatively well-preserved. The shaft is slender in the mid-section, and flares out equally towards each distal end (Plate VI K, L, N). The proximal end of the pubis is less pronounced than in MACN-CH 932, and shows a small, kidney-shaped pubic foramen (Plate VI L, N). It stretches between about ½ and 2/3rds of the length of the shaft. In lateral view, the pubic apron is strongly sinuous, but the pubic shaft only curves slightly (Plate VI N). The distal end is rounded, and shows prominent rugosities on its surface and rim (Plate VI O). The distal surface is strongly rugose and is oval in shape, with a slight tapering on its medial side, as in the holotype PVL 4170. The peduncle for the ilium is slightly offset from the shaft, and is pedestal-like, as in the holotype PVL 4170 (Plate VI L, M, N). The articular surface is less rugose than on the distal surface, and is more rectangular in shape. The ischial peduncle on the distal side of the pubic apron is roughly triangular in shape, elongated, tapering, and rugose (Plate VI L). As in PVL 4170, the pubic symphysis is also sinusoid in shape (Plate VI K,L).

Ischium MACN-CH 933

This small ischium has a slightly different colouration from the other elements ascribed to specimen MACN-CH 933. It is slightly more yellow/beige than the average dark grey colours of the Cerro Condor Norte material. Therefore, it is not entirely certain whether this element is from Cerro Condor Norte or Cerro Condor Sur.

It is a small and slender element, and well preserved (Plate VI H, I). The shaft, however, is more stout than in the holotype PVL 4170. The lateral side of the shaft shows a slightly sinusoidal shape, whereas the shaft in medial view shows a rod-like shape (Plate VI H, I). The peduncle for the ilium is elongated in the sagittal plane. The articular surface is triangular and rugosely striated and pitted. The pubic peduncle is smaller than the iliac one, and is more rounded in shape and less rugosely striated (Plate VI F). The space between both

peduncles is semi-circular and shallow (Plate VI E, H, I). On the dorsal side of the shaft, a small, ragged, semicircular process is visible, which is offset to the dorsal side. This is most likely a ligament attachment site. The angle between the shaft and distal ends when combined with its mirroring ischial element would probably have been more V-shaped than coplanar, as in the holotype PVL 4170, *Vulcanodon*, and unlike in neosauropods (Cooper, 1984; Upchurch, 2004).

Ilium MACN-CH 933

A fragment of a small ilium is preserved, with the anterior lobe, preacetabulum, part of the pubic peduncle, and part of the acetabulum preserved (Plate VI P,Q). The acetabulum is low, measuring about 10 cm from the pubic peduncle to the highest point of the dorsal rim of the acetabulum, and it is wide, as in the holotype PVL 4170 (Plate VI Q). The anterior lobe is hook-shaped, with a strongly tapered point, as in the holotype PVL 4170 (Plate VI P). The dorsal rim of the ilium is broken away, however, the projection of the dorsal rim of the anterior lobe suggests a rather high dorsal rim of the ilium (Plate VI P), as in the holotype PVL 4170, *Cetiosaurus*, *Barapasaurus*, and *Haplocanthosaurus* (Hatcher, 1903; Upchurch and Martin, 2002, 2003; Bandyopadhyay et al., 2010).

Appendicular elements

Femur MACN-CH 933

A small and stout femur is well preserved in this specimen. The element has a Gracility Index (GI) of 4,6, which slightly lower than in the holotype (GI of 4,9), but this could be ontogenetic (See Table 3). The shaft is slightly convex laterally and slightly concave medially, as in the holotype PVL 4170, indicating a similar stance and gait in this specimen (Plate VI A,B). The

femoral head is prominently present, and projects further medially than the tibial condyle (Plate VI B). In dorsal view, the femoral head is anteroposteriorly wider than the greater trochanter, as in PVL 4170, but unlike *Vulcanodon* and PVL 4077, and neosauropods (Bonaparte, 1986; Cooper, 1984; Upchurch et al., 2004). The fourth trochanter is not pronounced, which might also be an ontogenetic feature (Plate VI B). It is placed posteromedially, as in the holotype PVL 4170 and *Cetiosaurus* (Upchurch and Martin, 2003). It is a sharp protruding ridge that occurs at about the level of the midpoint of the shaft. The greater trochanter is visible as a bulge on the lateral proximal side of the femur, at the same height as the ventral tip of the femoral head. The distal condyles are both prominent, and asymmetrical, as in the holotype PVL 4170 (Plate VI B). The tibial condyle is rounded and blunt, and projects posteriorly as well as medially. The fibular condyle is more triangular, but it is also damaged, only projecting posteriorly. There is a deep depression between both condyles, as in the holotype PVL 4170. In ventral view, the distal end shows a sharp hook-shaped protrusion of the tibial condyle towards the posterior side (Plate VI D). This is seen in other basal sauropods and in some basal sauropodomorphs (Yates, 2003; Upchurch 2005; McPhee et al., 2015), but also in neosauropods (Upchurch et al., 2004).


MACN-CH 933
A
B
femoral head
C
fourth
trochanter
D
tibial condyle
fibular condyle
E
F
pubic
peduncle
G
iliac
peduncle
H
I
J
M
K
L
N
ischial
peduncle
iliac
peduncle
pubic
foramen
pubic
symphysis
O
P
anterior lobe
Q
acetabulum
pubic
peduncle
10 cm

Plate VI (previous page): MACN-CH 933 appendicular material. MACN-CH 933 Femur in anterior (A), posterior (B), dorsal (C) and ventral views (D), MACN-CH 933 ischium proximal articular surface (E), pubic peduncle (F), iliac peduncle (G), lateral (H), medial (I), and distal (J) views. MACN-CH 933 pubis in ventral (K), medial (L), proximal (M), lateral (N), and distal (O) views. MACN-CH 933 ilium in lateral (P) and ventrolateral (Q) views.

Comparison with *Patagosaurus* PVL 4170

MACN-CH 933 shows similarities with *Patagosaurus* PVL 4170 in the shape and morphology of the cervical centra. The condyle and the condylar rim, together with the parapophyses and the ventral keel and hypapophyses and accompanying oval depressions are similar to those in PVL 4170. The dorsal centra are slightly more nondescript and more common for sauropods in general than when the first description of *Patagosaurus* was written in 1986. The stoutness of '279' is similar to that of PVL 4170, however, '309' is slightly more slender and elongated than in *Patagosaurus* PVL 4170 dorsals.

The proximal end of the pubis shows a difference between MACN-CH 933 and PVL 4170, but this could be due to ontogeny. The peduncle for the ilium is semi-circular wheareas this is more square in *Patagosaurus* PVL 4170. The femur is more slender and not so anteroposteriorly compressed and transversely wide as in *Patagosaurus* PVL 4170 or as in *Cetiosaurus oxoniensis* (Upchurch & Martin, 2003). It does however show the posteromedial placement of the fourth trochanter, as well as the slight lateral convexity of the shaft, as in PVL 4170 and unlike in *Cetiosaurus oxoniensis* (Upchurch and Martin, 2003).

Comparison with *Volkheimeria chubutensis* (PVL 4077)

As *Volkheimeria* PVL 4077 is also a juvenile, the femora and pubes can be compared for ontogenetic and anatomical features. The femora look relatively similar, in that they both have slender shafts and large condyles. In anterior and posterior view, the femoral heads look similar, however, in dorsal view the MACN-CH 933 condyle is more asymmetrical and shows a wider condyle transversely than the greater trochanter, whereas this is all a similar width (and thus more symmetrical) in *Volkheimeria* PVL 4077. The distal condyles of MACN-CH 933 are very asymmetrical, however, whereas *Volkheimeria* shows more symmetrical distal condyles in ventral view. The medial condyle of MACN-CH 933 in ventral view shows a sharp hook-shape, whereas this condyle in *Volkheimeria* only projects anteriorly. The fourth

trochanter unfortunately cannot be compared fully as this is damaged in MACN-CH 933, however, this element is smaller in *Volkheimeria*, despite not being damaged.

Ontogenetic features

The small size and unfused state of the neurocentral sutures, show that this specimen is most probably in MOS 1 (Schwarz et al., 2007; Carballido et al., 2012; Carballido and Sander, 2014). As isometric growth is assumed for sauropods (Taylor, 2009; Carballido et al., 2012), this smaller and more slender femur fits with an early ontogenetic stage of development. This might also explain why the pubis shows a smaller ossified apron than in PVL 4170 and MACN-CH 932, since a large part of this element would likely have been cartilaginous and not completely ossified yet; a similar feature is seen in the pubis of the juvenile *Lapparentosaurus* MAA 117, which shows an incompletely closed pubic foramen and a pubic apron of the same shape as in MACN-CH 933.

MACN-CH 935

The material ascribed to this specimen consists of four posterior dorsal neural arches, four sacral centra and sacral ribs, with one sacral neural arch, five complete caudals, one cervical rib, and several dorsal rib fragments, several chevrons, and one left ilium.

Axial elements

MACN-CH 935 Dorsal neural arch 1

This unfused neural arch and spine is slightly reconstructed with lab putty, metal rods and wires (Plate VII A-D). It is probably the first of the series of four, as the neural spine is slightly inclined anteriorly, as in the holotype PVL 4170 is the case with the anterior to mid-dorsals (Plate VII 1C,D). The zygapophyses, hyposphene and neural arch, however, are relatively well preserved. The parapophyses are not clearly visible in this specimen. The neural canal is visible anteriorly as an elliptical canal (Plate VII 1A), as in PVL 4170, and posteriorly as a slightly transversely wider elliptical canal (Plate VII 1B). The spine is damaged, and the diapophyses are missing.

The major laminae that are preserved are the sprl, cprl, spol, podl. The prezygapophyses are supported from below by the cprl and from the lateral sides by the (not well visible) prdl (Plate VII 1A). As in the holotype PVL 4170, a prominent single stprl is visible, running between the two prezygapophyseal pedestals, down towards the neural canal (Plate VII 1A). On either side of the stprl, oval cprfs are visible. The prezygapophyses project anteriorly and slightly dorsally, and are both slightly canted to the medial side (Plate VII 1A, C, D). They are rounded to triangular in shape. The postzygapophyses are supported by the prominent spols from above and by a prominent tpol (Plate VII 1B). They are triangular in shape, and the articulation surfaces are slightly elliptical in shape. A prominent, rhomboid-shaped hyposphene is visible below the postzygapophyses, and this structure is supported by the

cpols (Plate VII 1B). The hyposphene is slightly offset to the lateral side, probably a preservational artefact. Two shallow but large oval cpofs are visible on either side of the hyposphene.

The neural arch is square-shaped and shows large triangular CDFs as in *Patagosaurus* PVL 4170 and MACN-CH 932. They are both filled with sediment (Plate VII 1C, D).

The neural spine is robust and elongated, as in PVL 4170, and MACN-CH 932 and 933. It is slightly constricted on its anterior side by the narrowing of the sprls, but it shows a wider posterior side, with ventrally flaring spols (Plate VII 1A,B). The lateral spol is broken, however, but the medial spol is clearly present, which also suggests the existence of the lspol+spdl complex in this element (Plate VII 1D), however, the diapophysis is broken and the lamination here is not clearly visible due to sediment infill and taphonomic damage. Two prominent aliform processes are visible on the lateral side of the dorsal end of the spine (Plate VII 1 A, B).

MACN-CH 935 Dorsal neural arch 2 (Plate VII 2)

This unfused neural arch is better preserved than the previous element, and has in addition to the pre- and postzygapophyses, the parapophysis and neural spine also completely preserved (Plate VII 2A-E). The diapophyses are broken off, however, the base of the left is preserved.

The anterior neural canal is elliptical in shape, and the posterior is more teardrop-shaped, as in PVL 4170 mid-posterior dorsal vertebrae (Plate VII 2A). The major laminae are shared with the previous element. The prezygapophyses project more anteriorly than dorsally, however, although they are also canted medially. They are supported by a prominent cprl from the ventral side, and from the ventrolateral side by the prominent prpl, which connects the laterally projecting, rounded and rugose parapophyses to the prezygapophyses (Plate VII 2A). The space between both pedestals is larger in this specimen than in the previous, and

the prcdfs are larger and deeper in this specimen. The morphology of the postzygapophyses is similar to that of the previous element (Plate VII 2B). The hyposphene is better preserved, and is a symmetrical rhomboidal shape, supported by two cpols from below. This specimen shows both cpofs as well as two extra, circular fossae that accompany the neural canal on both lateral sides (Plate VII 2B).

The neural arch is rectangular in shape, and shows the CDF, which is open and connects to the other lateral CDF, as well as to a ventral pneumatic chamber, as in PVL 4170 (Plate VI 2D,E). The neural spine shows four distinct laminae, which create a near pyramid-shaped spine. The posterior side is wider transversely however, due to the ventral flaring of the lateral spols (Plate VII 2A,B). Anteriorly, a deep V-shaped sprf is visible, and posteriorly an equally deep and V-shaped spof is visible. On each lateral side a deep triangular to rectangular sdf is visible, which covers most of the surface area of the lateral side of the spine (Plate VII 2E,D). The tip of the spine is robust and rectangular in shape, and shows lateral aliform processes. In dorsal view, the spine is rounded to rectangular in shape, and shows rugosities (Plate VII 2E).

MACN-CH 935 dorsal neural arch 3 (Plate VII, 3)

This unfused neural arch has the neural spine, zygapophyses, parapophyses and the left diapophysis preserved (Plate VII 3A-E). The morphology of the prezygapophyses, prcdf, neural canal and parapophyses is largely the same as in the previous element, only the prezygapophyses are slightly canted slightly more medially (Plate VII 3A). The postzygapophyses also have a similar morphology to the previous element, only the ventral and articular surfaces are slightly sinusoidal in this element, and the tpols are equally sinusoidal (Plate VII 3B). The neural arch is rectangular, but is smaller in width than in the previous elements (Plate VII A,B). Posteriorly, the hyposphene is present as a prominent

rhomboid structure. The CDFs are visible as triangular fossae, however, they are infilled with sediment (Plate VII 3C,D).

The left diapophysis is a stout, laterally, and posteriorly and slightly dorsally projecting element (Plate VII D). It is supported by a prominent prdl on its dorsal side, and by a stout pcdl on its posterior and ventral side, as well as the ppdl from the ventral side (Plate VII 3A,B,D,E). The diapophysis shows a prominent fossa ventrally on the neural arch, as well as a small rounded fossa on its posterior distal side. A rounded process protrudes from the dorsal side on the midpoint (Plate VII B). The neural spine morphology is largely the same as in the previous element, including the constricted sprl, flaring spol, and prominent lateral and medial spol (Plate VII A,B). In this element, however, the lspol+spdl is clearly visible, showing an incipient spdl, as in the posterior(most) dorsals of the holotype PVL 4170.

MACN-CH 935 dorsal neural arch 4 (plate VII, 4)

This stout unfused neural arch shows a similar morphology to the previous element, except that the CDF penetrates the anterior side of the neural arch, leaving a large open space with a ventral pneumatic chamber that is situated well above the neural canal (Plate VII 4 B, C, D). This is also seen in the posteriormost dorsals of *Patagosaurus* PVL 4170. The prezygapophyses are more stout in this element than in previous elements, and more rugose (Plate VII 4A, C, D, E). The parapophyses are similar to previous elements, however, they are more dorsoventrally elongated and cover more of the surface of the lateral neural arch (Plate VII 4A). The element has the left diapophysis preserved at the base, however, the right diapophysis, postzygapophysis and part of the neural arch are missing and/or damaged (Plate VII 4A, D).

The neural arch in lateral view shows the CDF, which is divided here by an oblique ppdl. The diapophysis base shows a similar morphology to that in the previous element (Plate VII 4C,D).

The posterior neural arch shows the CDF as well, which means the entire neural arch is pneumatized (Plate VII 4C). The postzygapophysis is canted ventrally and medially, unlike in previous elements. There is no V-shaped spof visible (Plate VII 4C).

The neural spine is solid, and of a similar morphology to those of the previous elements. It has deep fossae on anterior and lateral sides, and prominent aliform processes underneath the spine summit, which is rugosely striated (Plate VII 4E).

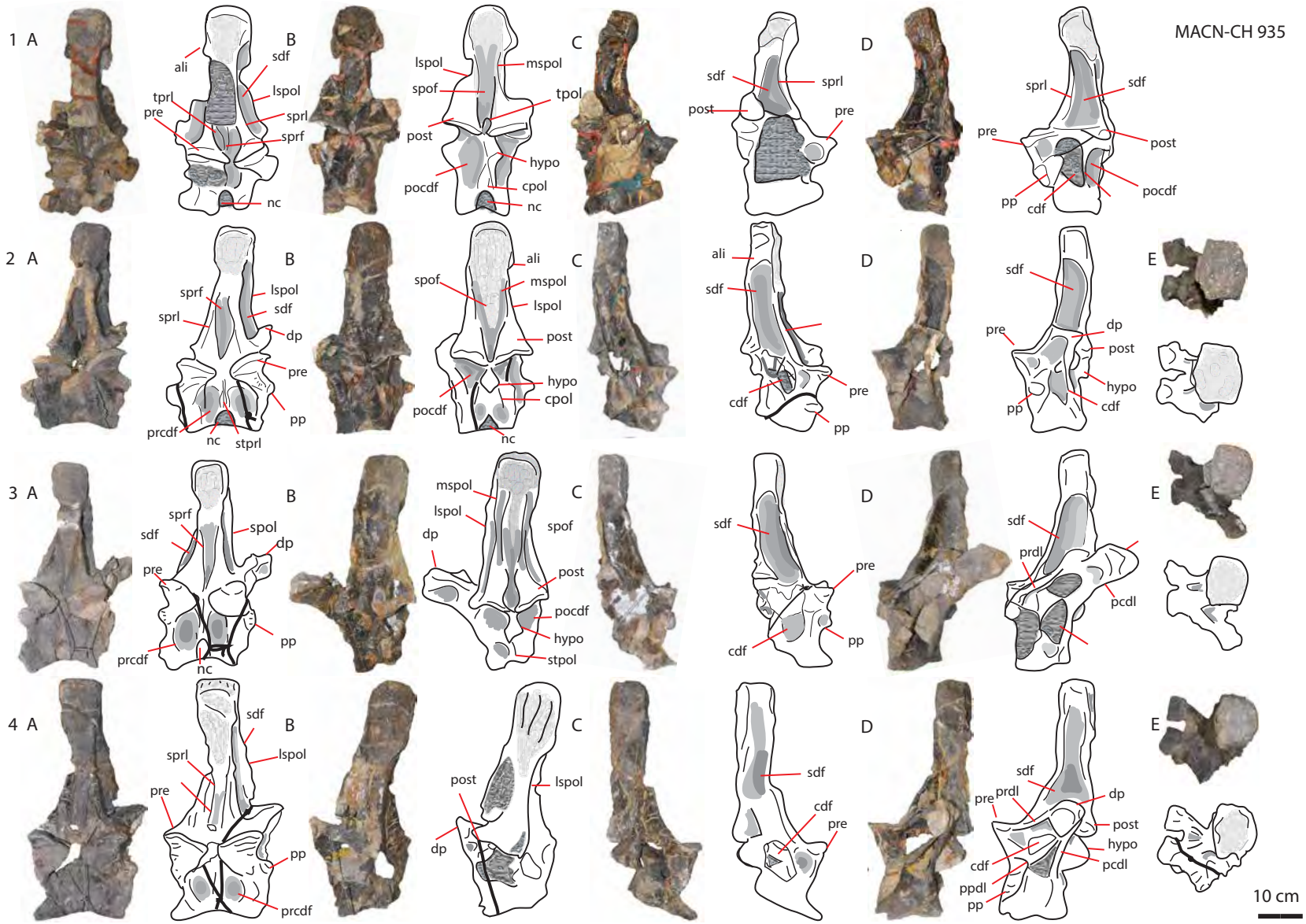
MACN-CH 935
1 A
B
ali
sdf
tprl
pre
lspol
sprl
sprf
nc
C
lspol
mspol
spof
tpol
post
hypo
pocdf
cpol
nc
D
sdf
sprl
post
pre
sprl
sdf
pre
post
pocdf
pp
cdf
2 A
B
sprf
lspol
sprl
sdf
dp
pre
pp
prcdf
nc
stprl
C
ali
spof
mspol
lspol
post
hypo
cpol
pocdf
nc
D
ali
sdf
cdf
pre
pp
sdf
pre
dp
post
hypo
pp
cdf
E
3 A
B
sprf
sdf
spol
dp
pre
pp
prcdf
nc
C
mspol
lspol
dp
spof
post
pocdf
hypo
stpol
D
sdf
pre
cdf
pp
sdf
prdl
pcdl
E
4 A
B
sdf
sprl
lspol
pre
pp
prcdf
C
post
lspol
dp
D
sdf
cdf
pre
sdf
pre
prdl
dp
post
hypo
pcdl
cdf
ppdl
pp
E
10 cm

Plate VII: MACN-CH 935 dorsal neural arches 1-4. Dorsal neural arch 1 in anterior (A), posterior (B), right and left lateral C, D views. Dorsal neural arch 2 in anterior (A), posterior (B), right lateral (C), left lateral (D), and dorsal (E) views. Dorsal neural arch 3 in anterior (A), posterior (B), right lateral (C), left lateral (D), and dorsal (E) views. Dorsal neural arch 3 in anterior (A), posterior (B), right lateral (C), left lateral (D), and dorsal (E) views. Dorsal neural arch 4 in anterior (A), posterior (B), right lateral (C), left lateral (D), and dorsal views (E).

Abbreviations: cdf = centrodiapophyseal fossa, cpol = centropostzygapophyseal lamina, dp = diapophysis, hypo = hyposphene, nc = neural canal, ns = neural spine, pp = parapophysis, pre = prezygapphysis, po = postzygapophysis, pocdf = postzygapophyseal centrodiapophyseal fossa, podl = postzygadiapophyseal lamina, ppdl= paradiapophyseal lamina, prcdf = prezygapophyseal centrodiapophyseal fossa, sdf = spinodiapophyseal fossa, spof = spinopostzygapophyseal fossa, l.spol, m. spol = lateral/medial spinopostzygapophyseal lamina, sprf = spinoprezygapophyseal fossa, sprl = spinoprezygapophyseal lamina, tpol = intrapostzygapophyseal lamina, tprl = intraprezygapophyseal lamina, stpol = single intrapostzygapophyseal lamina, stprl = single intraprezygapophyseal lamina.

MACN-CH 935 sacrals (Plate VIII)

Three sacral vertebral centra and attached sacral ribs are preserved, and one sacral neural arch (Plate VIII). The sacrals show unfused neurocentral sutures as in the dorsals.

As a direct comparison with *Patagosaurus* PVL 4170 is not possible due to the sacrum being mounted, the correct order of attachment of the sacrals not being entirely certain.

The first element, however, resembles the articular surface of the posterior dorsal centra (Plate VIII 2A,B). The articular surface is oval and dorsoventrally elongated, as in PVL 4170. In dorsal view, the centrum is constricted transversely at the midsection. The sacral ribs are directed laterally and anteriorly, and are constricted at about ½ of their distal length (Plate VIII 2A,B). They flare out towards their distal ends though, and have rounded, blunt, rugose articular surfaces for the sacricostal yoke. In dorsal view, the sacral ribs are C-shaped and consist of large sheets of bone (Plate VIII 2B).

The second element has a round articular surface on its anterior and posterior side. (Plate VIII 3A,B). The anterior side is slightly more convex than flat, and the posterior side is flat. In ventral view, the centrum is transversely constricted at the midpoint, and flares out towards both articular surfaces (Plate VIII 3C). The transverse sacral ribs are constricted dorsoventrally at their base, after which they fan out towards their distal rugose tips, which creates a C-shaped sacral rib as in the first element (Plate VIII 3A,B). The distal ends are rugosely striated for ligament attachments and the sacricostal yoke.

The third element has flattened, round to rectangular articular surfaces of the centrum, although the anterior surface is dorsoventrally elongated, and the posterior one is transversely wider (Plate VIII 4A,B). The centrum is equally constricted transversely as in the other elements. The sacral ribs in ventral view are similar to the previous element, however, in anterior, posterior and dorsal views they are more complex in shape (Plate VIII

A, B, D). They fan out towards both the ventral and dorsal sides, and on each lateral end show elongated notches, creating a butterfly-wing morphology. Both ventral and dorsal distal ends are thick and rugose. In dorsal view (Plate VIII 4D), the ventral distal tip of the sacral ribs is seen to project anteriorly. The shape of the neurocentral suture matches that of the only sacral neural arch preserved for this specimen, but it is not entirely certain whether they are associated.

The sacral neural arch (Plate VIII 1 A, B) is elongated, as in PVL 4170, with particular elongation of the neural spines, which is also seen in PVL 4170. The transverse processes are preserved on both lateral sides, as ventrally and laterally fanning shapes with rugose distal rims. (Plate VIII 1A, B) The prezygapophyes are prominent, rounded anterior protrusions, although the right is slightly offset to the dorsal side due to taphonomy. The prezygapophyses are well separated from one another, and are supported from the ventral side by stout pedestals (Plate VIII 1A). The neural arch shows a large oval depression between the prezygapophyses. The postzygapophyses are also large compared to the previous dorsal neural arches, and prominent. They are supported by thick tpols, which join directly dorsal to the hyposphene (Plate VIII 1B). The neural arch shows prominent, rugose, dorsoventrally elongated and transversely slim hyposphene and hypantrum processes. The neural spine shows the sprl and spols, as thick supporting laminae for the lateral sides. Also the sprf and the spof are clearly visible as V-shaped deep depressions at the base of the spine. The spine is constricted at around ½ of the dorsoventral length, after which it flares slightly outwards towards the summit. The spine has rugose striations over the entire surface.

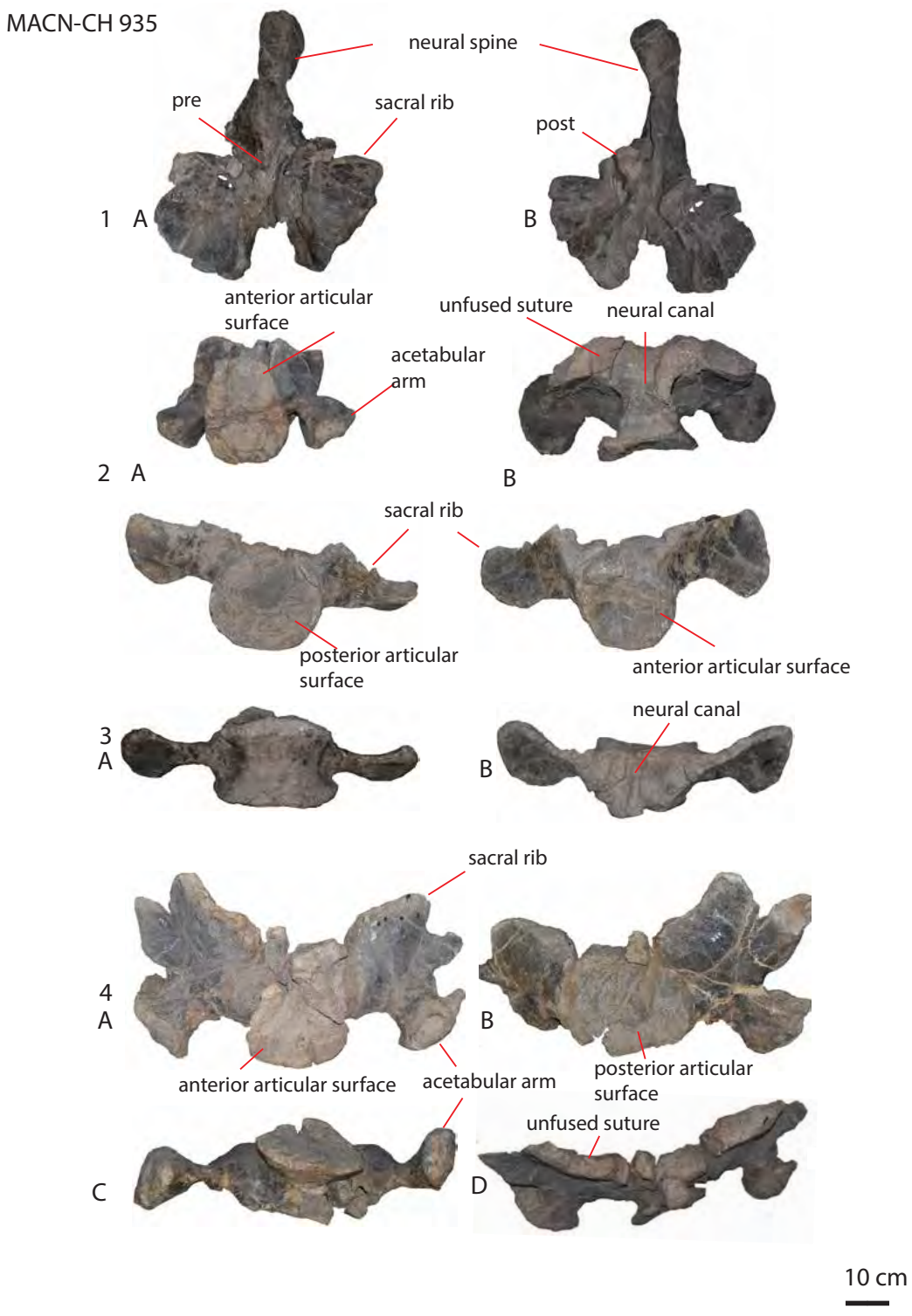

Plate VIII: MACN-CH sacral centra and sacral neural arches. MACN-CH 935 sacral neural arch 1 in anterior (A), and posterior (B) views. MACN-CH 935 sacral centrum 2 in anterior (A) and dorsal (B) views. MACN-CH 935 sacral centrum 3 in posterior (A), anterior (B), ventral (C), and dorsal (D), views. MACN-CH 935 sacral centrum 4 in anterior (A), posterior (B), ventral (C) and dorsal (D) views. Abbreviations: pre = prezygapophysis, post = postzygapophysis.

MACN-CH 935 caudals. (Plate IX 1-5)

This set of five associated caudals is the most complete anterior caudal vertebral series that the Cerro Condor Norte material has (Plate IX 1-5). Two small posterior caudals are also associated with this specimen (Plate IX 1,2). The anterior caudals are characterized by round to oval articular surfaces on both anterior and posterior sides (Plate IX 1-5 C,D). The anterior surface, however, has a slightly more tapering ventral side, which makes the anterior surface appear slightly heart-shaped Plate IX 1-5 C). The centra are amphicoelous, as in most basal eusauropods. The posterior surface, however, shows a slight convexity in lateral view (Plate IX 1-5 A,B). This is not as extensive as in titanosaurs (e.g. *Saltasaurus,* Powell, 1992) and is closer to, but less pronounced than, the condition of that in *Mamenchisaurus*, *Klamelisaurus* and *Omeisaurus* (but not *Shunosaurus*; Ouyang and Ye, 2002; Powell, 1992; Russell and Zheng, 1993; Xijing, 1993; Zhang, 1988; Zhao and Downs, 1993; Tang et al., 2001). It is possibly also present in *Losillasaurus* (Casanovas, Santafé & Sanz, 2001), as well as in *Ferganasaurus* (Alifanov & Averianov, 2003). In ventral view, the anterior ventral rim shows two rugose chevron facets, similar to those in *Cetiosaurus* and *Vulcanodon* (Cooper, 1984; Upchurch & Martin, 2003). The midline groove that these latter taxa have is not visible.

All elements have both zygapophyses preserved (Plate IX 1-5 A,B), as well as the diapophyses (Plate IX 1-5 C,D) and the neural spine, although some elements have been partially reconstructed. The neural arch is rectangular in shape as in the dorsal neural arches of MACN-CH 935, and as in PVL 4170. The anterior and posterior neural canals are oval with the elongation in the dorsoventral plane, as in *Patagosaurus* PVL 4170 (Plate IX 1-5 C,D). The diapophyses project laterally, and slightly posteriorly. Some diapophyses are slightly taphonomically pushed towards the dorsal side. Ventral to the diapophyses, small elliptical depressions are visible.

The prezygapophyses are directed anteriorly and dorsally, and taper acutely at their distal ends (Plate IX 1-5 A,B, C). The articular surfaces are canted sharply medially, in an oblique

angle, which is nearly vertical. The articular surfaces are triangular in shape (Plate IX 1E, 2F, 3E, 4E, 5E). The postzygapophyses are small and are situated at the base of the neural spine, and make an angle of almost 90 degrees with the horizontal. They are rectangular in lateral view (Plate IX 1-5 A,B), and triangular in posterior view (Plate IX 1E, 2F, 3E, 4E, 5E), and project posteriorly and laterally. Some caudals have a rectangular hyposphene preserved, which project posteriorly as a small triangular protrusion.

The neural spine is constricted at its base on anterior, posterior and lateral sides. It widens towards the summit, where it becomes rounded to rhomboid in shape (Plate IX 1-5 A,B,C,D). The dorsalmost 1/3rd is rugosely striated. The sprf and spof are present as deep teardrop-shaped fossae at the base of both anterior and posterior spinal surfaces. In lateral view, the spine curves slightly sinusoidally at the lower half, which is characteristic for *Patagosaurus* PVL 4170 caudal spines as well (Plate IX 1-5 A,B). The spine summit in lateral view shows a saddle-shaped summit (Plate IX 3-4A,B), which PVL 4170 displays, as well as *Spinophorosaurus* and *Cetiosauriscus* (Charig, 1993; Remes et al., 2009).

MACN-CH 935

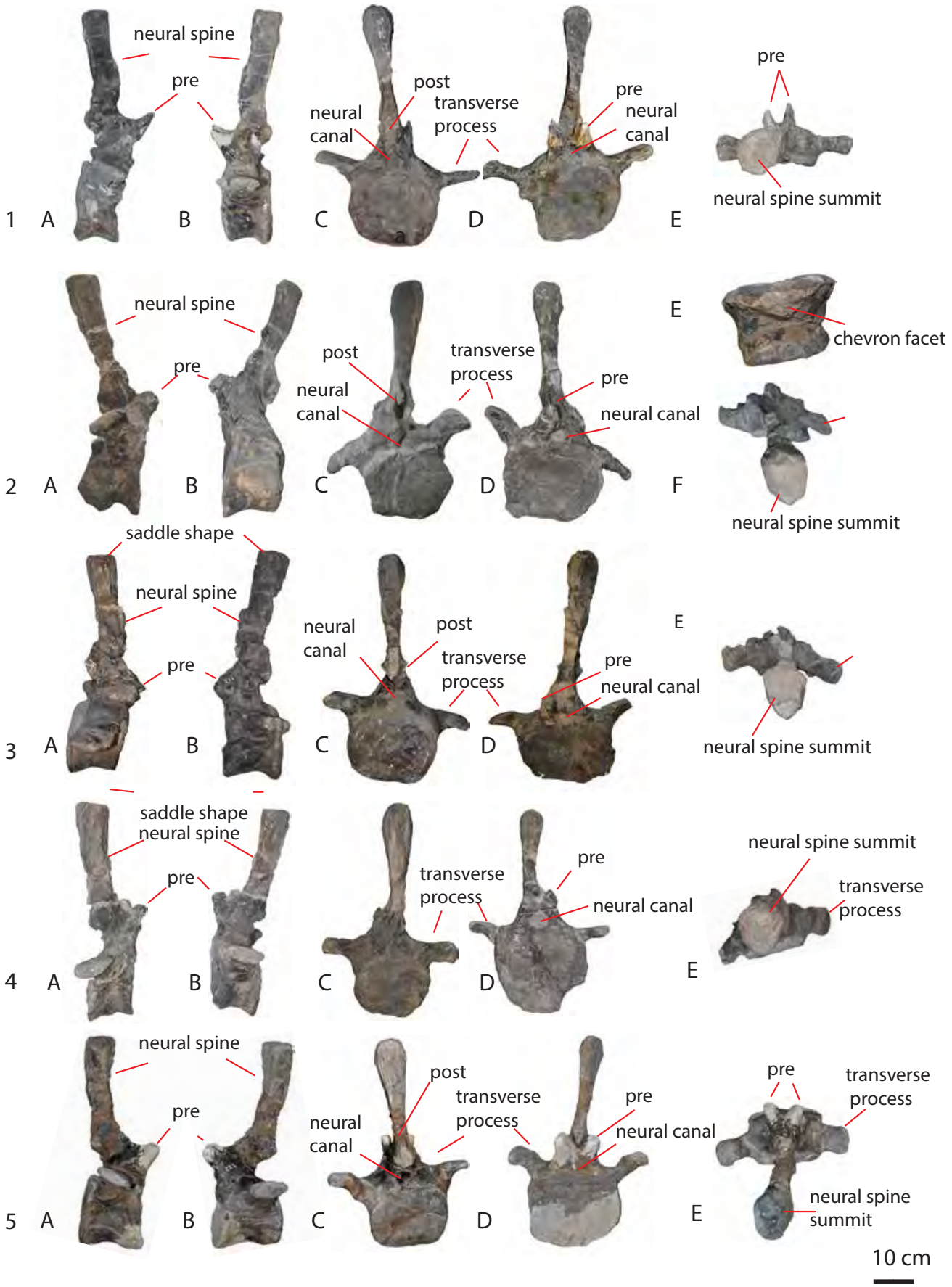
1
A
neural spine
pre
B
C
post
neural canal
transverse process
D
pre
neural canal
E
pre
neural spine summit
2
A
neural spine
pre
B
C
post
neural canal
transverse process
D
pre
neural canal
E
chevron facet
F
neural spine summit
3
A
saddle shape
neural spine
pre
B
C
neural canal
post
transverse process
D
pre
neural canal
E
neural spine summit
4
A
saddle shape
neural spine
pre
B
C
transverse process
D
pre
neural canal
E
neural spine summit
transverse process
5
A
neural spine
pre
B
C
post
neural canal
transverse process
D
pre
neural canal
E
pre
transverse process
neural spine summit
10 cm

Plate IX: MACN-CH 935 caudal vertebrae. MACN-CH caudal 1 in right lateral (A), left lateral (B), anterior (C) posterior (D), and dorsal (E) views. MACN-CH 935 caudal 2 in right lateral (A), left lateral (B), anterior (C) posterior (D), and, ventral (E) and dorsal (F) views. MACN-CH 935 caudal 3 in right lateral (A), left lateral (B), anterior (C) posterior (D), dorsal (E) views. MACN-CH 935 caudal 4 in right lateral (A), left lateral (B), anterior (C) posterior (D), and dorsal (E) views. MACN-CH 935 caudal 5 in right lateral (A), left lateral (B), anterior (C) posterior (D), and dorsal (E) views. Abbreviations: pre = prezygapophysis, post = postzygapophysis.

The posterior caudals (Plate X) are small and axially elongated elements. They are symmetrical in shape, being constricted at their midsection and flaring out towards anterior and posterior articular surfaces (Plate X 1A-C, 2A,B)). They are amphicoelous, with both articular surfaces being flat with a small rounded depression on the midpoint (Plate X 1D,E, 2C,F). Ventrally, on both ventral rims, small rounded rugose chevron facets are present. No midline groove is seen. The neural canal is both anteriorly and posteriorly semicircular, and transversely wide, as in PVL 4170. As in MACN-CH 933, the prezygapophyses are small and taper to a point, and project anteriorly and slightly dorsally in an oblique angle (Plate IX 1A). The postzygapophyses are barely visible as small bulges on the ventral posterior surface of the spine, dorsal to the neural canal (Plate X 1E, 2C)l. The neural spine tapers to a rounded tip and projects posteriorly and dorsally (Plate X 1A, 2A,B). In lateral view, it has a mild curvature on the dorsal side which makes the spine slightly convexly curved.

MACN-CH 935

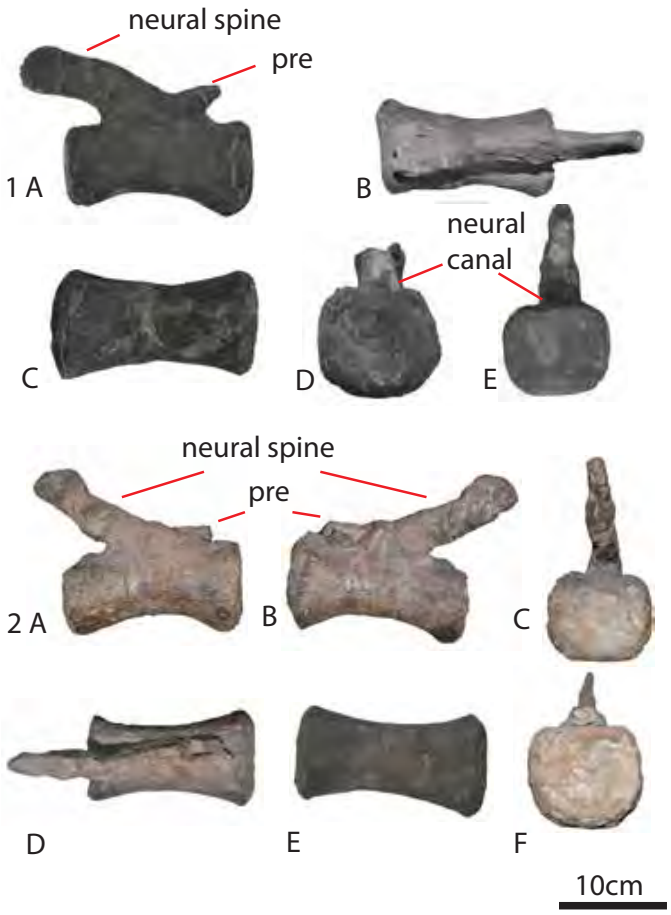

Plate X: MACN-CH 935 posterior caudals. MACN-CH 935 posterior caudal 1 in lateral (A), dorsal (B), ventral (C), anterior (D) and posterior (E) views. MACN-CH 935 posterior caudal 2 in right lateral (A), left lateral (B), posterior (C), dorsal (D) ventral (E) and anterior (F) views. Abbreviations: pre = prezygapophysis.

MACN-CH 935 cervical rib (Plate XI 1)

One isolated incomplete cervical rib is recovered for this specimen, of about 22 cm long. It is a slender, elongated element, with two symmetrical proximal heads. The angle between the heads is about 90 degrees. The articular surfaces are flat and rounded. There are no cervicals to compare this rib to in MACN-CH 935, however, when compared to the holotype PVL 4170

cervicals, the small size of the proximal end of the rib could indicate this to be an anterior cervical rib.

MACN-CH 935 dorsal ribs (Plate XI 2-3)

Several dorsal rib fragments are recovered for this specimen, all of which are the proximal ends. These are rugose elements, with a widening of the axial shaft towards the proximal heads, and a flattening of the transverse shaft. The tuberculum and capitulum are asymmetrical, with one longer tuberculum for the diapophyseal articulation, which is the more stout of the two, and one shorter capitulum for the parapophyseal articulation.

MACN-CH 935 chevrons (Plate XI 4-7)

Several chevrons are associated with this specimen, which are all dorsoventrally elongated, rod-like shapes. The haemal canals are oval and transversely and dorsoventrally wide, and the chevron proximal heads are closed, creating a closed-in haemal canal, unlike in the Rutland *Cetiosaurus* (Upchurch and Martin, 2002). The shafts are flattened transversely towards the distal end, and expand towards the distal end in sail-like structures (Plate XI 4C,D), which is not seen in the Rutland *Cetiosaurus*. These structures are usually seen in anterior chevrons of neosauropods (e.g. *Dicraeosaurus*, *Apatosaurus*, Tschopp et al., 2015; though non-neosauropod eusauropod chevrons are not common and could have had similar structures), and might have been used as ligament attachment for large tail muscles (H. Mallison pers. comm.). Based on these structures, the chevrons are likely the anteriormost chevrons, and could have been associated with the anterior caudals of MACN-CH 935.

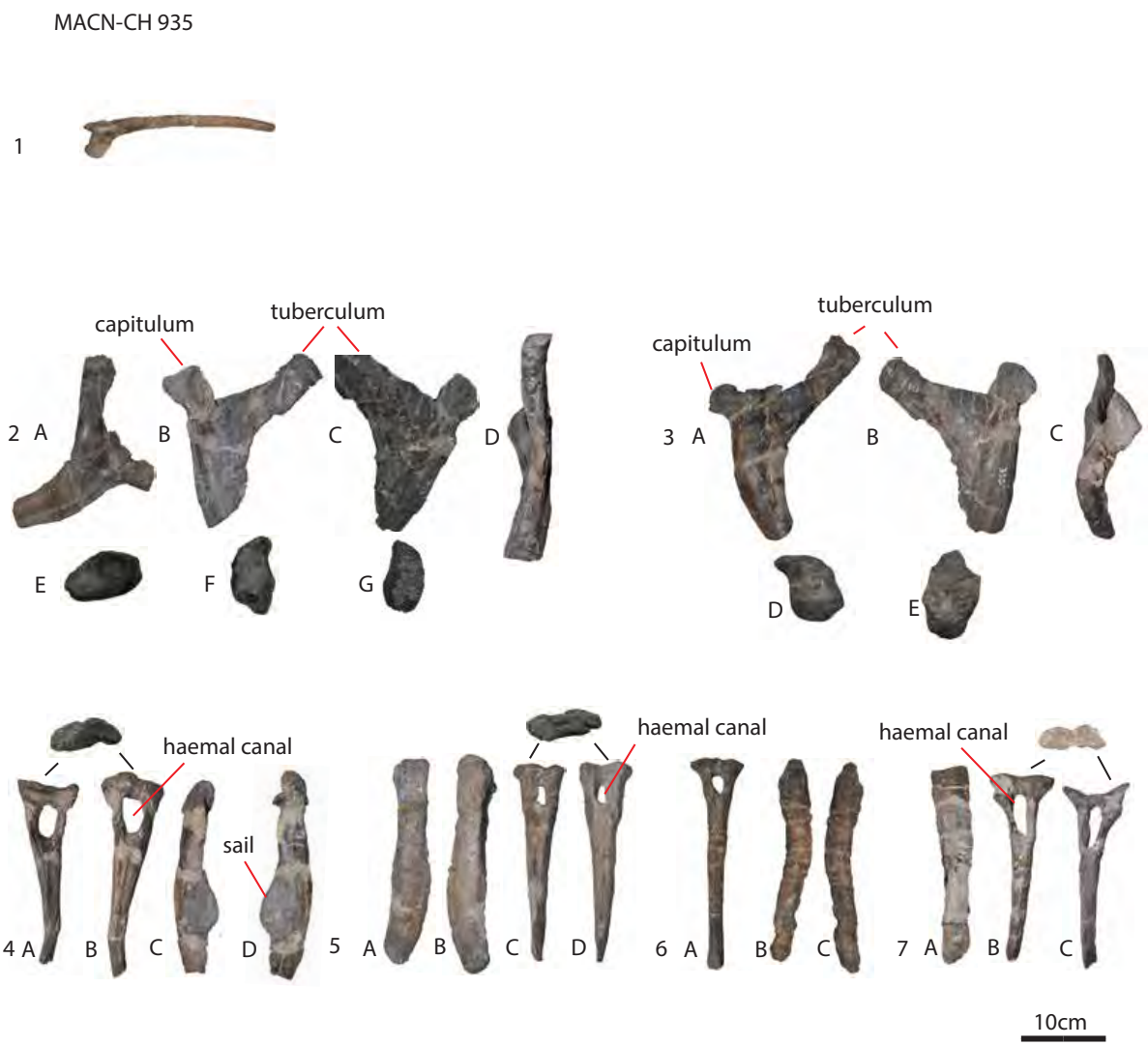

Plate XI: MACN-CH 935 cervical rib (1) in lateral view. MACN-CH 935 dorsal rib (2) in antelateral (A), lateral (B), medial (C) and posterior (D) view, with cross-section of shaft (E), capitulum (F) and tuberculum (G). MACN-CH 935 dorsal rib (3) in lateral (A), medial (B), and posterior (C) view, with capitulum cross-section (D) and tuberculum cross-section (E). MACN-CH 935 chevrons (4-7) in anterior, posterior and lateral views.

MACN-CH 935 Scapula

This right scapula is well-preserved, however, because it is mounted on a metal rod, it can only be viewed in anterior/lateral view. It is a large element, matching the rest of the MACN-CH 935 material in size, however, it also matches the holotype in size. In the quarry map (Figure 1, Figure 2), two scapulae are indicated, of which only one has been retrieved from the collections so far (Plate XII 3). The holotype should have a partial scapula and a coracoid closely associated. However, MACN-CH 935 should also have a scapula and coracoid closely associated, and that scapula was more or less intact, therefore, this rather complete scapula, marked 'A' together with an associated coracoid marked 'B', is most likely MACN-CH 935. The scapula has a more prominent proximal expansion than in more basal sauropods, however, it is not as prominent as in neosauropods (Upchurch et al., 2004). It shows a rather small and flat acromion process (Plate XII 3), as in *Cetiosaurus oxoniensis* and *Lapparentosaurus* MAA 44, and unlike *Mamenchisaurus* (Ouyang and Ye, 2002; Upchurch and Martin, 2003), however, the scapula is also slightly damaged here. The acromial area of the scapula is rounded in shape, as in *Cetiosaurus oxoniensis* (Upchurch and Martin, 2003) The proximal midsection of the scapula is damaged, but shows a V-shaped indentation. The glenoid region is a prominently fanning out, rounded lobe (Plate XII 3), as in most eusauropods and neosauropods (Upchurch, et al., 2004). The shaft of the scapula is obliquely directed towards the posterior side, and slightly to the ventrolateral side, unlike in *Mamenchisaurus*, *Lapparentosaurus*, and *Cetiosaurus*. It curves gently convexly on the dorsal side.

MACN-CH 935 Coracoid

The coracoid is a stout, thick element with the coracoid foramen infilled with sediment (Plate XII 2A-C). It is rounded in shape, as in most sauropods besides titanosauriforms

(Upchurch, Barrett & Dodson, 2004). It is partially broken, however, the thick glenoid margin is clearly visible, and is rugosely pitted (Plate XII 2C). It tapers to a point on the lateral side, giving the margin a triangular outline. The coracoid also shows the coracoid notch lateral to the foramen (Plate XII 2B), which is also seen in *Cetiosaurus oxoniensis* (Upchurch and Martin, 2003), but unlike the latter, the notch in MACN-CH 935 is more shallow, but also more wide, giving the coracoid a heart-shaped appearance on the lateral side.

MACN-CH 935 ilium

This medium-sized ilium is an order of magnitude between the small MACN-CH 933 and MACN-CH 932 and the large PVL 4170 holotype ilium. It has anterior and posterior lobes preserved, and the pubic peduncle and acetabular rim. The dorsal part of the ilium is missing (Plate XII 1). The anterior lobe is offset from the axial plane of the ilium by projecting anteriorly and ventrally, instead of anteriorly as in *Patagosaurus* PVL 4170 (Plate XII 1A). The anterior lobe is also elongated axially, and projects further anteriorly than most ilia of sauropods (e.g. *Patagosaurus*, *Cetiosaurus*, *Mamenchisaurus*, *Omeisaurus*, *Shunosaurus*, *Haplocanthosaurus*, and neosauropods (Hatcher, 1903; Bonaparte, 1979; Bonaparte, 1986a; Tang et al., 2001; Ouyang and Ye, 2002; Upchurch and Martin, 2003;Upchurch et al., 2004). However, the ventral projection is similar to that of *Barapasaurus* (Bandyopadhyay et al., 2010). The pubic peduncle is elongated dorsoventrally, as in PVL 4170 (Plate XII 1A, D). The articular surface of the pubic peduncle is roughly triangular, and rugosely pitted (Plate XII 1C). The acetabulum is wide, as in the holotype PVL 4170 and MACN-CH 932. The posterior lobe has the ischial peduncle preserved, which is blunt and rectangular in shape (Plate XII 1A,D), however, the articular facet of the ischial peduncle is semi-circular and tapers to a point, as in PVL 4170, and is also rugosely pitted (Plate XII 1B). Based on the projection of the dorsal edge of the anterior lobe (Plate XII 1A,D), the dorsal part of the ilium would not

project very high dorsoventrally, which makes it dissimilar to PVL 4170 and MACN-CH 932, 933.

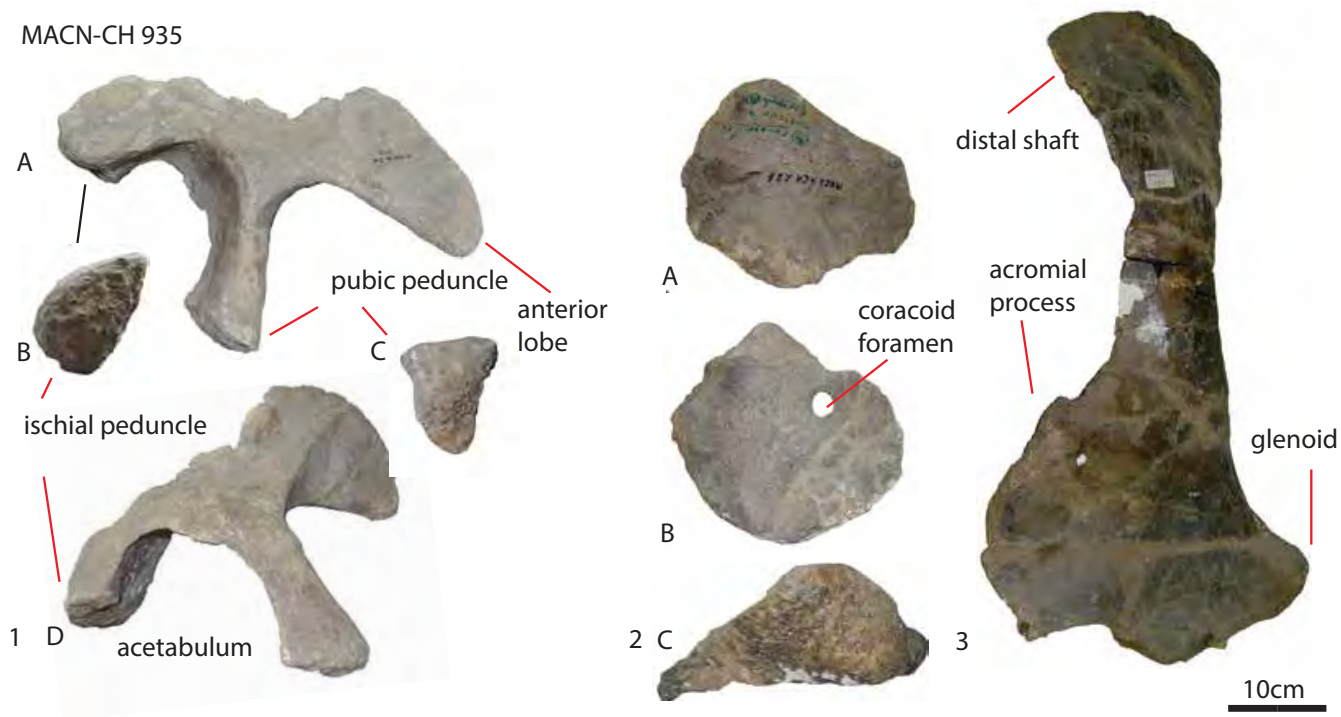

Plate XII: MACN-CH 935 pelvic and appendicular elements. MACN-CH 935 ilium (1) in lateral (A) view, ischial peduncle (B), pubic peduncle (C) and in medial view (D). MACN-CH 935 coracoid (2) in dorsal (A), ventral (B) and lateral (C) view. MACN-CH 935 scapula (3).

Comparison with *Patagosaurus* PVL 4170

Based on similarities with the holotype PVL 4170 in the dorsal neural arches, in particular the lamination and the presence of extensive pneumatization in the neural arch with inclusion of the CDF, as well as the neural spine, zygapophyses, and hyposphene, this specimen is most likely a *Patagosaurus*. Moreover, the caudals are similar to those of the holotype PVL 4170.

Novel material

The scapula and coracoid of the holotype were never recovered for this study, therefore the material for MACN-CH 935 is novel material with the placement of the distal scapular shaft an important morphological character distinct from other sauropods. This element has several rib fragments preserved, which the holotype PVL 4170 does not have. The ribs are badly preserved, however, the heads show a typical sauropod dorsal rib, and the shaft shows that it was transversely slightly flattened.

Comparison with *Volkheimeria*

MACN-CH 935 differs from *Volkheimeria* PVL 4077 in the elongation of the dorsal neural arches and spines, which is a shared characteristic with *Patagosaurus*, and which *Volkheimeria* does not have. Moreover, MACN-CH 935 lacks the accessory oblique lamina on the lateral side of the neural arch that *Volkheimeria* possesses. There is no other material for comparison between the two specimens.

Ontogenetic stage

Based on the presence of complex lamination and fossae, this specimen was at an advanced stage of development. However, the unfused dorsal neural arches show that it was not yet

an adult, therefore it was likely in MOS 3 or 4 and a subadult, slightly smaller than the holotype specimen.

PVL 4617

A large ungual phalanx was recovered from Cerro Condor Norte (Plate XIII A-D). It is a stout element, which tapers towards its distal end, although not as sharply as in MACN-CH 932. It has one single groove running along the lateral margin (Plate XIII A), constricting the midsection of the claw slightly, which bulges laterally, dorsally and ventrally of this groove, as in most sauropods (Upchurch, et al., 2004). A similar large ungual is known from the Middle Jurassic of Morocco (R. Allain, pers. comm.), however, the provenance of that specimen is unknown. A similarly large ungual is known from the Cañadón Asfálto Fm, and is housed in the MPEF-PV collections, however, it is uncertain whether this specimen is *Patagosaurus* (MPEF-PV 1359). Large unguals in sauropods are conservative in morphology, and therefore do not give much information (Upchurchet al., 2004), except in association with ichnofossils (Wilson, 2005). MACN-CH 4617 could be the main large ungual, and the smaller, sharper and more slender MACN-CH 932 element could be the second ungual of *Patagosaurus*.

Plate XIII: PVL 4617 ungual phalanx in medial (A), lateral (B), dorsal (C) and ventral (D) views.

PVL 4076

This specimen (see Plate XIV) provides the only cranial element from Cerro Condor Norte; a premaxilla with dentition preserved. It is a stout, square element, showing in lateral/labial view, a dorsoventrally high, oblique anterior rim of the snout, and a high, near vertical maxillary articular surface on the distal lateral side (Plate XIV A). The lateral surface shows rugose striations, as well as deep pits, which are probably nutrient foramina for blood vessels (Plate XIV A). The dorsal side tapers to a point, giving the premaxilla a pentagonal appearance in lateral view. In medial view, the dorsal rim shows a sharp, hook-shaped protrusion of the nasal process for the attachment to the naris (Plate XIV B,D). The ventral side shows four large, pentagonal alveoli bearing one erupted tooth and three unerupted teeth (Plate XIV B, E). The morphology of the tooth shows denticles (Plate XIV E, F) and the

enamel wrinkling consists of rugose anastomosing ridges intersperced with pits and grooves. The morphotype of this enamel wrinkling has been discussed elsewhere (Holwerda et al., 2015). Dorsal to these alveoli, interdental plates are visible, as well as a prominent nutrient groove, which runs transversely across the medial surface of the premaxilla.

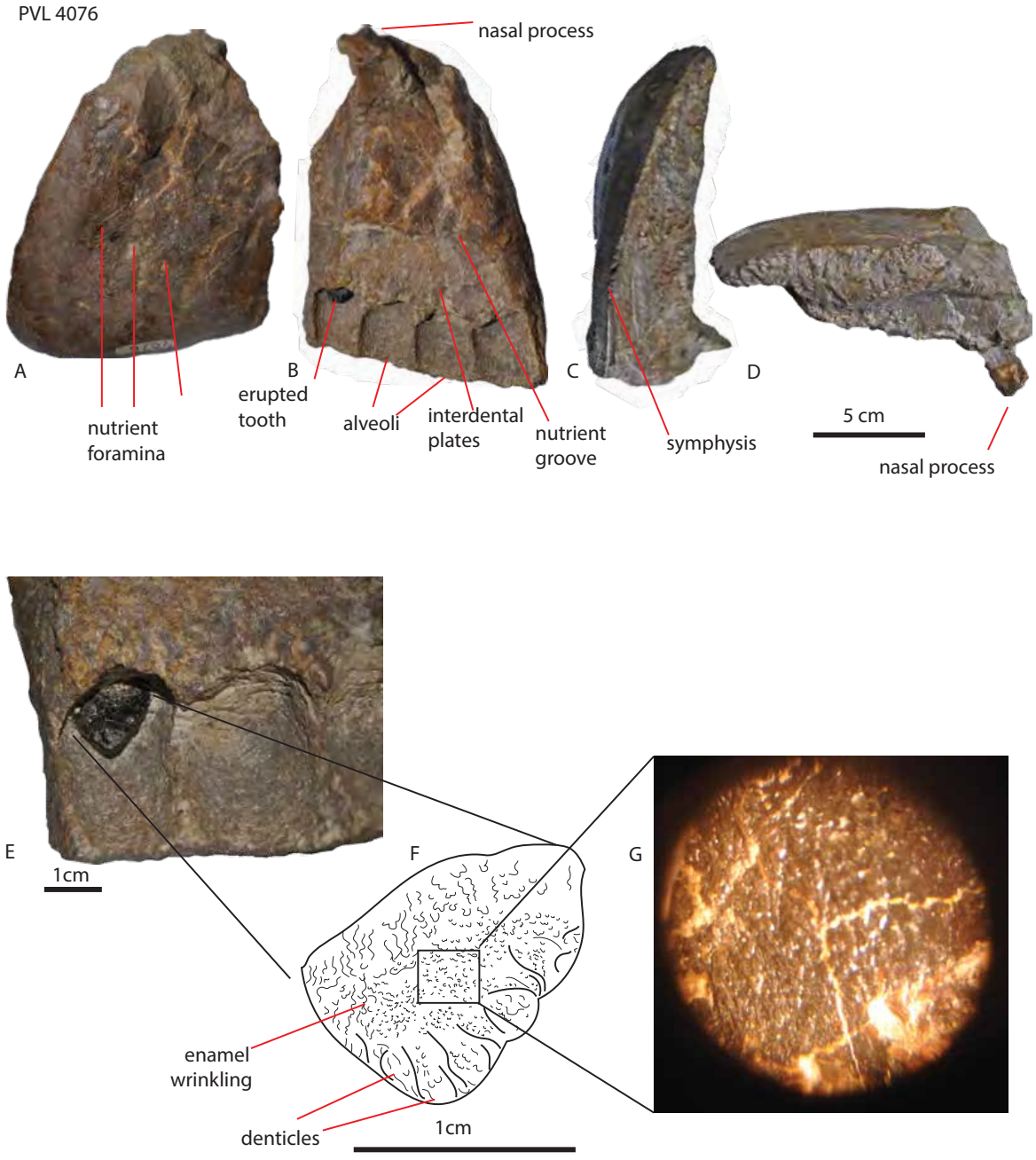

Plate XIV: PVL 4076 premaxilla in labial (A), lingual (B), proximal (C) and dorsal (D) views. Closeup of tooth (E) with schematic (F) with enamel wrinkling details (G).

Specimen MACN-CH 4076 also provides axial material; three cervicals, one anterior dorsal, and one anterior-middle caudal.

The first and anteriormost of these cervicals (Plate XV 1A-E) shows a relatively small and anteriorly tapering condyle, with a nose-like protrusion on the anteriormost point of the condyle (Plate XV 1A, C,D,E). In anterior view, this condyle is dorsoventrally deformed by compression (Plate XV 1A). The cotyle is also deformed, as is seen in posterior view, and the centrum is transversely also more flattened due to taphonomy (Plate XV 1B). In lateral view, the centrum is elongated, and shows a constriction just behind the condyle, giving the first 1/3rd of the centrum a concave lateral profile, and the posterior part a convex profile ventrally (Plate XV 1C,D). The pleurocoel on the lateral side of the centrum however, is well-preserved, and shows an anteriorly excavated side of the condyle. The pleurocoel runs to about 2/3rd of the lateral side of the centrum, and shows well-defined anterior, posterior, dorsal and ventral boundaries (Plate XV 1C,D). Moreover, the pleurocoel displays perforation in the midsection, showing evidence of only a thin septum separating the pleurocoel from its counterpart, as seen in the holotype PVL 4170. The neural arch is damaged, however, the right prezygapophysis is preserved, and projects anteriorly and dorsally, resting on a stout beam, as in the holotype PVL 4170 (Plate XV 1C,D). It is supported from the ventral side by a stout prdl, which connects posterior to the prezygapophyseal stalk to the diapophysis. In anterior view, the prezygapophyseal articular surface is canted medially, and is rugosely pitted. The diapophysis is semicircular in lateral view, and projects ventrally in anterior view (Plate XV 1A,C,D). The postzygapophyses are damaged, however, the tpols are visible, and they meet ventral to the neural arch (Plate XV 1B). The neural spine is dorsoventrally elongated, and shows a rhomboid shape. It is rugosely striated in anterior view.

The second cervical (Plate XV 2A-F) shows a centrum similar to the first, which is also elongated axially, and constricted ventrally, posterior to the condyle. It shows a similar anterior projection of the condyle, which is also seen in anterior cervicals of *Patagosaurus* PVL 4170 (Plate XV 2A). In this specimen however, the right parapophysis is well-preserved, and shows a projection posteriorly, where the parapophysis tapers to a point (Plate XV 2 A, C, D). In ventral view, a stout ventral keel is seen to run over the anterior 2/3rd of the centrum. The pleurocoel on the lateral side of the centrum is equally deep and perforated, as in the first element (Plate XV 2 C,D).

Both prezygapophyseal bases are preserved in this element (Plate XV 2C,D). The articular surfaces are canted medially. The prdl and the tprl meet on the ventral side of the articular surface in an inverted V-shape, showing triangular and deep cprfs in between. The postzygapophyses are better preserved, showing a dorsventrally high projection of the podl, and a dorsoventrally elongated tpol (Plate XV 2B). They also show epipophyses, which are also present in the holotype PVL 4170.

One dorsal neural arch (Plate IX d) is preserved, it is similar to anterior dorsals of PVL 4170 (11,12). It shows a stout hyposphene and hypantrum/stprl complex (Plate XV 3A,B), with transversely wide prezygapophyses (Plate XV 3A,C), which project anteriorly and create an angle of 90 degrees with the neural spine. It is supported by stout cprls from the ventral side. Posteriorly, the postzygapophyses are small triangular protrusions, and are supported by thick tpols from the ventral side, and by thick, laterally flaring spols (Plate XV 3B). Two large stout sprls flare laterally from the neural spine (Plate XV 3A). The diapophyses project laterally and are slightly convex dorsally (Plate XV 3A,B). Ventral to the diapophyses, open CDF's are visible, infilled with sediment (Plate XV 3C,D).

The neural spine is transversely wide, which is only seen in anterior dorsals of PVL 4170. They show deep sprf, spof, and spdfs (Plate XV 3A,B).

One anterior-to-middle caudal is preserved for this specimen (Plate XV 4A-E); it is slightly concave on its anterior articular surface and convex on its posterior articular surface, as in MACN-CH 935 and also as in mamenchisaurids (Ouyang and Ye, 2002).

The neural spine projects dorsally and posteriorly, and displays a slight sinusoidal curve, as in PVL 4170 (Plate XV 4C). Ventrally, no chevron facets are seen, which is unlike the holotype PVL 4170.

This specimen was originally said to possess a femur and tibia (Bonaparte, 1986a), however, no such association has been uncovered in the Instituto Miguel Lillo collections (nor in the quarry map).

PVL 4076

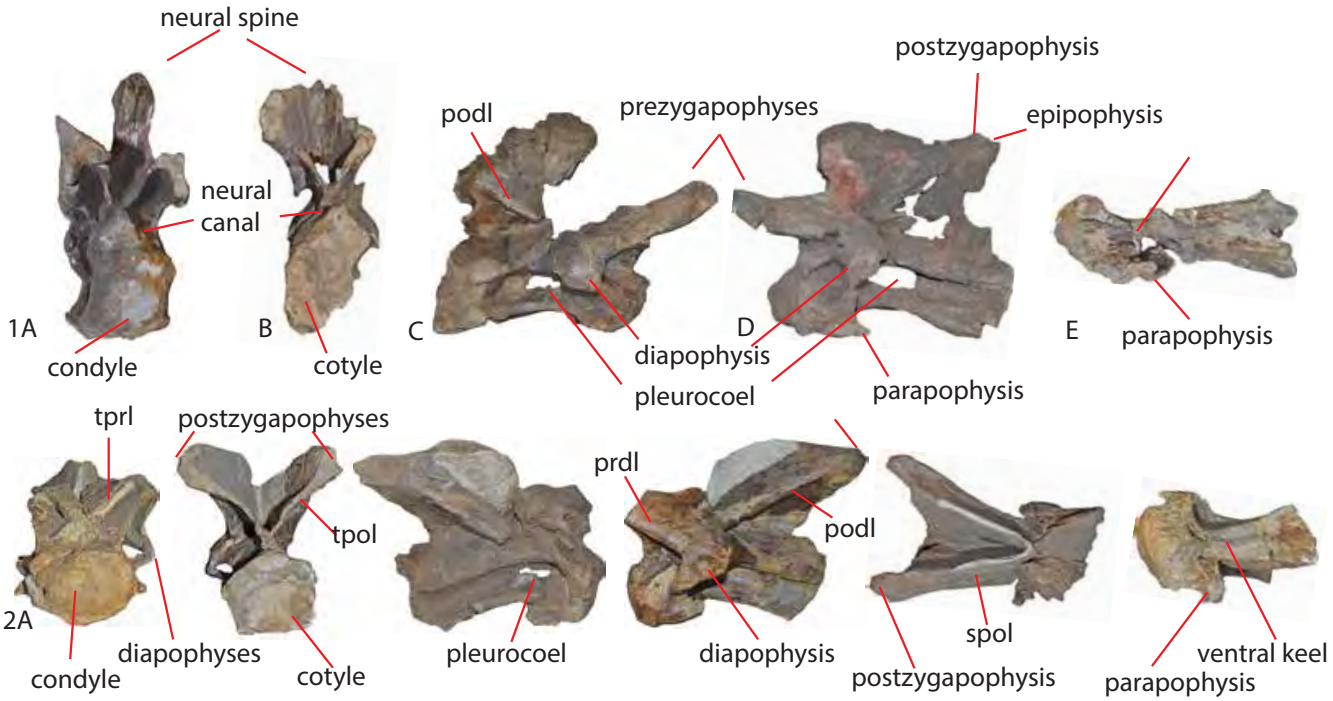
neural spine
neural canal
1A
condyle
B
cotyle
podl
prezygapophyses
C
diapophysis
pleurocoel
postzygapophysis
epipophysis
D
parapophysis
E
parapophysis
tprl
postzygapophyses
tpol
2A
condyle
diapophyses
cotyle
pleurocoel
prdl
podl
diapophysis
spol
postzygapophysis
ventral keel
parapophysis

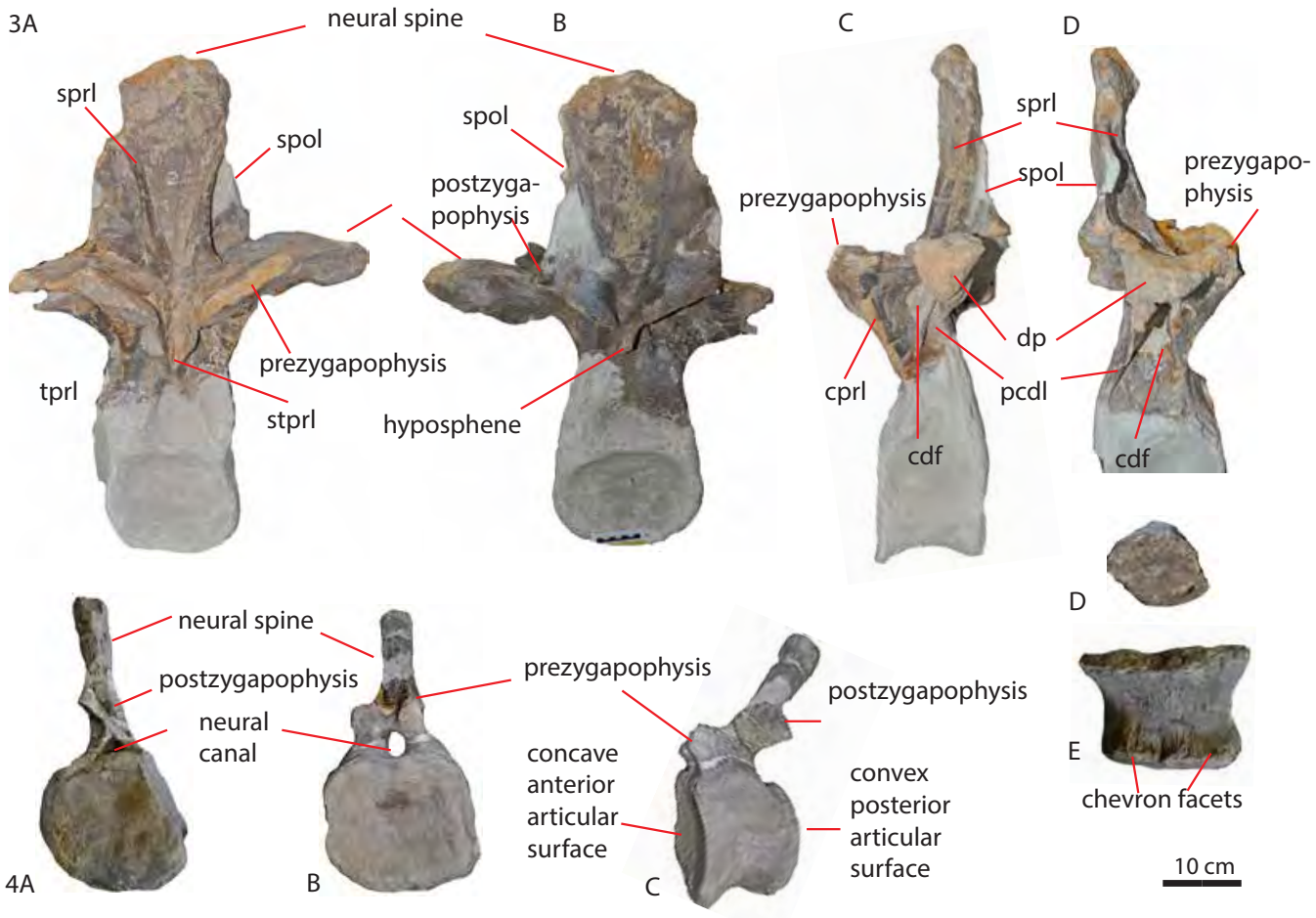
3A
neural spine
B
C
D
sprl
spol
postzyga-
pophysis
prezygapophysis
tprl
stprl
hyposphene
sprl
spol
prezygapophysis
dp
cprl
pcdl
cdf
prezygapo-
physis
cdf
D
neural spine
postzygapophysis
neural canal
4A
B
prezygapophysis
concave anterior articular surface
C
postzygapophysis
convex posterior articular surface
E
chevron facets
10 cm

Plate XV: PVL 4076 axial elements. PVL 4076 cervical 1 in anterior (A)l posterior (B), right lateral (C), left lateral (D) and ventral (E) views. PVL 4076 cervical 2 in anterior (A), posterior (B), right lateral (C), left lateral (D), dorsal (E), and ventral views (F). PVL 4076 dorsal 3 in anterior (A), posterior (B), left lateral (C) and right lateral (D) views. PVL 4076 caudal 4 in posterior (A), anterior (B), anterolateral (C) views, with neural spine summit (D) and ventral view (E). Abbreviations: cdf = centrodiapophyseal fossa, cprl = centroprezygapophyseal lamina, dp = diapophysis, pcdl = posterior centrodiapophyseal lamina, podl = postzygodiapophyseal lamina, sprl = sprinoprezygapophyseal lamina, spol = spinopostzygapophyseal oamina, stprl = single intraprezygapophyseal lamina, tprl = intraprezygapophyseal lamina.

MACN-CH 1986

One large femur (Plate XVI) is preserved in the MACN collections. It is unfortunately encased in a frame, which makes complete views impossible. As it is not mentioned in the original material list from the collections of the MACN, the provenance is unclear. However, the Cerro Condor Norte quarry map shows a large femur which could match this specimen. Both PVL 4075 and PVL 4076 are said to contain femora by Bonaparte in the original 1986 description, though neither was found in the collections. Therefore, the exact association of this specimen remains unclear. The posterior side is, however, exposed, and shows a transversely wide and anteroposteriorly compressed shaft, as in the holotype PVL 4170. The fourth trochanter is visible as a rugose projection on the medial side (Plate XVI). The femoral head projects medially, and is rounded, however, its medialmost side shows a tapering to a point. The greater trochanter is not very well developed and presents only as a rugose dorsal protrusion (Plate XVI). In dorsal view, the shaft is anteroposteriorly compressed medial to the greater trochanter, after which the femoral head widens the shaft to the anterior and posterior sides (Plate XVI). The surface is rugosely pitted, as in PVL 4170.

The distal end of the shaft shows prominent tibial and fibular condyles, with a large triangular depression in between, as in PVL 4170.

A tibia is associated with this specimen according to the MACN-CH *Patagosaurus* materials list, however, it could not be located in the collections. It could be that this is in fact the MACN-CH 1299 tibia (see Cerro Condor Sur specimens, MACN-CH 1299).

Plate XVI MACN-CH 1986 femur in posterolateral, and dorsal view, with close-ups in posterior view.

3.5 Cerro Condor Sur material

The Cerro Condor Sur material consists of several individuals, but also many isolated and/or fragmentary remains. Some material can be ascribed to *Patagosaurus*, and this is where the description starts. Two specimens are described as having no affinities with *Patagosaurus*, and which might be new, unnamed taxa. Finally, some material is not informative enough for any taxonomical assignation, and will remain Sauropoda indet.

3.5.1 *Patagosaurus* referable material

MACN-CH 936

This specimen consists only of a cervical and anterior-mid dorsal series. The anteriormost eight cervicals (Plate XVI), however, are currently part of a traveling exhibition and could not be viewed for study, only lateral images being available for reference. The other five more posterior cervicals (Plate XVII, XVIII) are present in the MACN collections, together with four large dorsals. Because there is no quarry map or specific notes on the excavation of the Cerro Condor Sur specimens, it is not entirely certain whether these vertebrae were found in association or not.

The axis is an elongated, slender element with a sharply protruding odontoid on the anterior side, and large parapophyses ventral to the condyle (PlateXVIIaxis). The ventral side of the centrum is concave, directly posterior to the parapophyses. This is also seen in the Rutland *Cetiosaurus* and in *Mamenchisaurus* (Ouyang and Ye, 2002; Upchurch and Martin, 2002), and differs from that of *Tazoudasaurus* (Allain and Aquesbi, 2008). The centrum also has a deep, elongated pleurocoel that stretches from directly posterior to the condyle, to about

the height of the neural canal on the posterior side of the centrum. It is compartmentalized into two smaller oval depressions, which are embedded in a larger, oval shallow depression, a condition that is less pronounced, but similar to, those of *Jobaria*, and neosauropods (Sereno et al., 1999; Upchurch et al., 2004). The anterior end of the neural spine is broken away, however, the neural spine summit is present. It is an oblique dorsal structure with the highest point at around the height of the neural canal on the posterior side of the centrum. It is dorsoventrally higher than the neural spine on the axis of the Rutland Cetiosaurus and that of *Tazoudasaurus* (Upchurch and Martin, 2002; Allain and Aquesbi, 2008). The axis has postzygapophyses, which are present as small triangular protrusions. It also shows epipophyses on the dorsal side of the postzygapophyses.

The first eight cervicals, besides the axis, are only visible in lateral view (PlateXVIIcervical 1-8). The first six are elongated, and have slender centra. In the first of these cervicals (PlateXVIIcervical 1), the pleurocoel is one deep depression, which has the anterior deepest depression perforating the centrum to the other lateral side, in an oval shape. The centrum is opisthocoelous, with the condyle offset from the axial plane by bending ventrally, and thus lying in a lower ventral plane than the cotyle. This is also seen in anterior cervicals of *Amygdalodon* (Cabrera, 1947; Rauhut, 2003), *Spinophorosaurus*, the Rutland *Cetiosaurus*, and to some extent in *Mamenchisaurus* (Ouyang and Ye, 2002; Upchurch and Martin, 2002; Remes et al., 2009).

The second of the cervicals (PlateXVIIcervical 2) shows a less pronounced offset of the condyle towards the rest of the centrum, which is also the common condition in *Patagosaurus* PVL 4170. This element is strongly opisthocoelous, and the element shows prominent, round parapophyses, which are present directly posterior to the condyle, and are confluent with the condylar rim on the ventral posterior side of the condyle, as in the

holotype PVL 4170. The pleurocoel is present as an elongated oval depression, which runs along almost the entire axial length of the centrum, and has clear anterior, dorsal, ventral and posterior boundaries. The element has no neural spine or diapophyses.

The third element (PlateXVIIcervical 3) shows a shortening of the centrum, as is typical of PVL 4170 cervicals. It shows a similar pleurocoel as in the second element on the lateral side, however, this pleurocoel is only pierced in its anterior 1/3rd, showing an oval fenestra. As in the holotype, the posterior ventral half of the centrum is ventrally lower than the rest of the centrum. The prezygapophyses project prominently anteriorly as two stout beams; these project further anteriorly than the postzygapophyses project posteriorly; the prezygapophyses project almost over 1/3rd of the axial length of the preceding centrum. The elongation of the neural arch, also a feature seen in the holotype PVL 4170, is seen, with an elevation of the postzygapophyses and a high projection of the podl. The neural spine is dorsoventrally also elongated.

The fourth element (PlateXVIIcervical 4) is slightly different from the third, and is likely to not be the fourth but the second real cervical, since the size of the cervical is smaller than the third, and the centrum is less elongated. Moreover, the condyle is much smaller dorsoventrally than the centrum, making it appear offset dorsally from the centrum. This small condyle size is seen in *Amygdalodon* (Rauhut, 2003), however, the offset of the condyle in *Amygdalodon* is towards the ventral side. The centrum does show a pleurocoel consistent with the other cervicals in this series, however, being well-defined on all sides, and being perforated. However, the perforation is in the posterior half of the pleurocoel, and not in the anterior half. Thus, together with the lower projection of the neural spine, and the prominently anteriorly projecting prezygapophyseal stalks, this element probably would be more naturally placed as the second or third cervical; the pneumaticity running

from the posterior half of the pleurocoel being perforated to the anterior side in more posterior cervicals.

The fifth element (PlateXVII cervical 5) has a more elongated centrum as in the third element. The cotyle is large and round, and the parapophyses are prominently visible as bulging, rugose protrusions at the ventral posterior side of the condyle. The cotyle is anteriorly and ventrally offset from the rest of the centrum. The centrum shows a prominent pleurocoel, which is well-defined on all four boundaries, however, it is not completely perforated anywhere. The ventral side of the centrum is constricted posterior to the condyle, as in PVL 4170. The prezygapophyses are prominent, as can be seen in the first cervicals of the holotype PVL 4170. They project anteriorly on stout stems, which are more than half of the centrum length of the centrum length. The neural spine is not projecting as high as in the third element, which is an interesting feature, while *Patagosaurus* cervicals are characterized by the high projection of the podl. This could mean that either the spine is damaged in this element, or that the fifth cervical has a low neural spine to allow for a larger musculature, for instance for the stability of the neck, which is a feature seen in modern archosaurs (see Van Der Leeuw et al., 2001). More research on the biomechanics of the neck of basal sauropods is needed for this, which is outside of the scope of this study.

MACN-CH 936

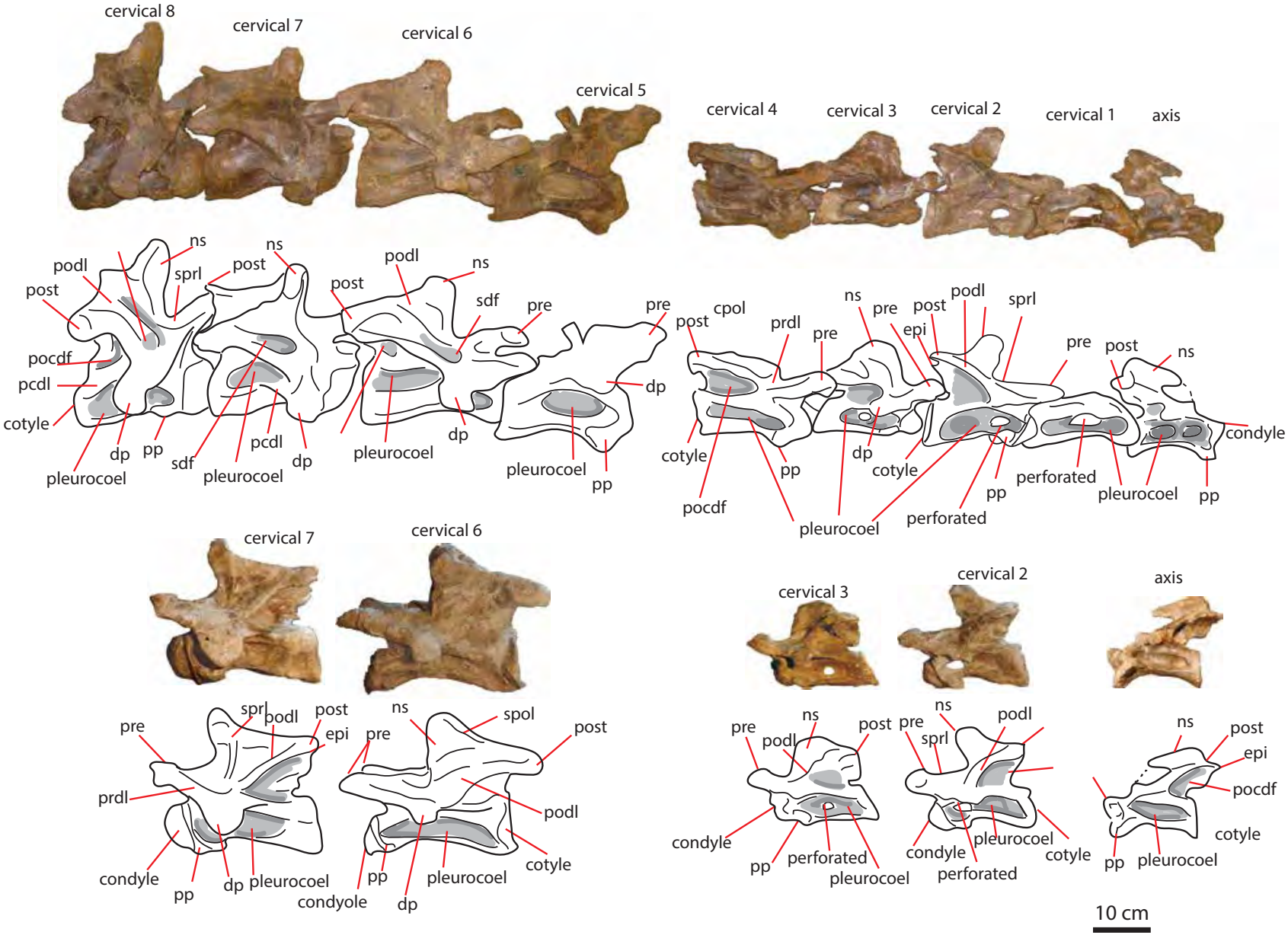
cervical 8
cervical 7
cervical 6
cervical 5
cervical 4
cervical 3
cervical 2
cervical 1
axis
ns
podl
sprl
post
pocdf
pcdl
cotyle
dp
pp
sdf
pleurocoel
sdf
pre
cpol
prdl
epi
condyle
perforated
cervical 7
cervical 6
cervical 3
cervical 2
axis
spol
condyole
10 cm

Plate XVII: MACN-CH 936 cervical series. Upper row: MACN-CH 936 axis and cervicals 1-8 in right lateral view. Bottom row: MACN-CH 936 axis and cervicals 2, 3, 6 and 7 in left lateral view. Abbreviations: cpol = centropostzygapophyseal lamina, dp = diapophysis, epi = epipophysis, nc = neural canal, ns = neural spine, pp = parapophysis, pre = prezygapophysis, po = postzygapophysis, pocdf = postzygapophyseal centrodiapophyseal fossa, podl = postzygadiapophyseal lamina, ppdl= paradiapophyseal lamina, prcdf = prezygapophyseal centrodiapophyseal fossa, sdf = spinodiapophyseal fossa, spof = spinopostzygapophyseal fossa, sprl = spinoprezygapophyseal lamina.

The final four cervicals of this anterior cervical series are more typical of the *Patagosaurus* holotype PVL 4170 series, in that they have short, stout cervical centra, which are strongly constricted directly posterior to the condyle, and have prominent condyles with thick rugose rims, that 'cup' the condyles. These cervicals show, with the high dorsal projection of the neural spine, the elevation of the podl, and stout centrum, an overlap with PVL 4170 (3), (4), (5), and (6).

The condyle of the sixth cervical (Plate XVII cervical 6) shows a ventral extension of the condyle, which has not been seen before in *Patagosaurus*. It could be that this is an extra attachment for the cotyle of the preceding cervical. However, it could also be a deformation of the condyle, caused by taphonomy. The centrum on the lateral side is extensively excavated by pleurocoels which are deepest anteriorly, and which grow more shallow towards the posterior side of the centrum, eventually fading into the centrum at their posterior end. However, whereas in most cervicals the pleurocoel is well-defined by all four borders, the presence of the posterior border fluctuates. The sixth cervical shows a deep anterior oval depression within the pleurocoel, however, this is not entirely perforated, but rather closed by a thin septum. The other three cervicals, the seventh, and eighth do not have this deep depression, but show a pleurocoel similar to those seen in the holotype PVL 4170 (Plate XVII cervical 7,8). The prezygapophyses are prominent, and rest on stout stalks which project anteriorly and dorsally, as in more posterior cervicals of *Patagosaurus* PVL 4170. Moreover, the podl shows a high projection (Plate XVII cervical 7,8), with the postzygapophyses prominently present as triangular posterior protrusions, as well as prominent epipophyses, as seen in PVL 4170. The prezygapophyses are not visible in anterior or dorsal view in order to see pre-epipophyses. The neural spine is elevated dorsoventrally, which increases prominently towards the posterior cervical (the eighth), as in the holotype PVL 4170.

MACN-CH 936

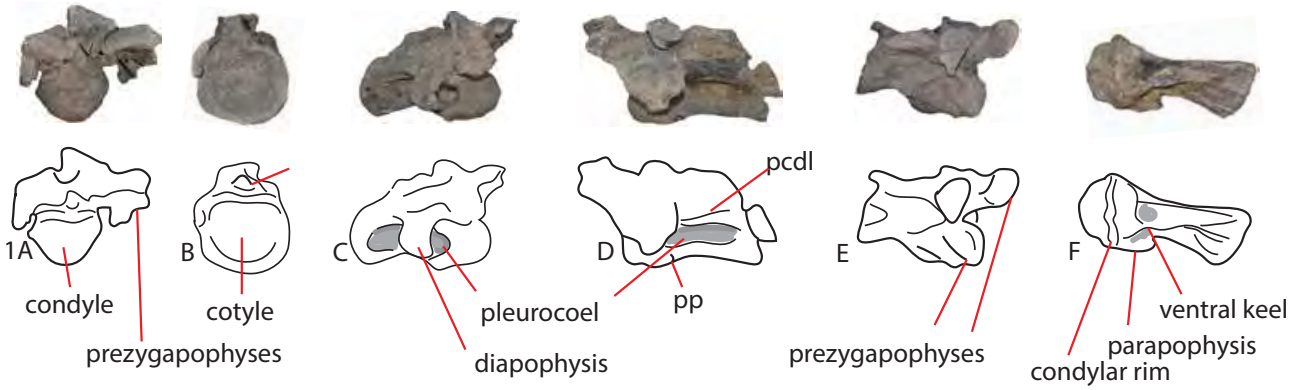
1A
condyle
prezygapophyses
B
cotyle
C
pleurocoel
diapophysis
D
pcdl
pp
E
prezygapophyses
F
ventral keel
parapophysis
condylar rim

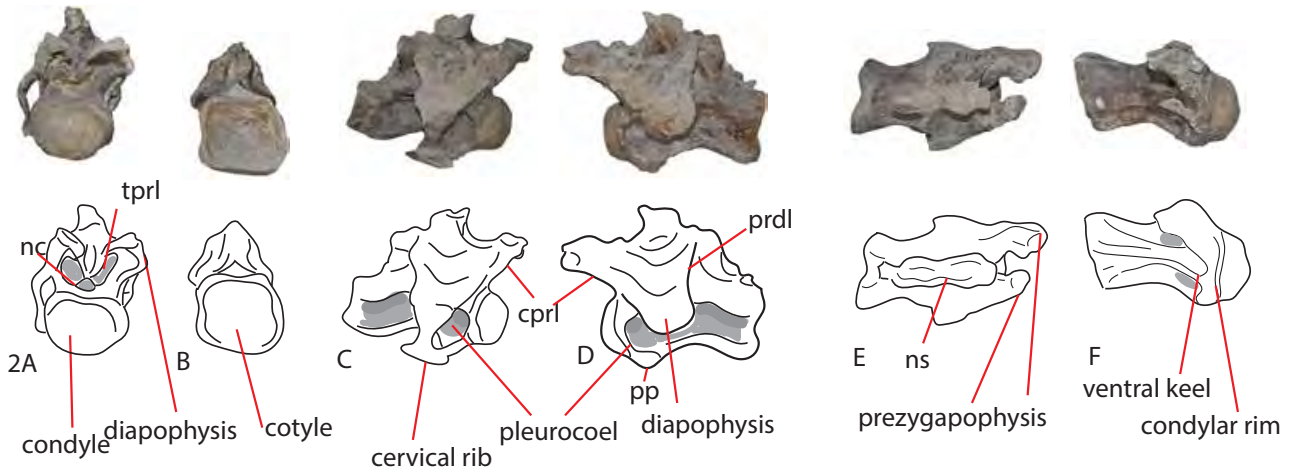
tprl
nc
2A
condyle
diapophysis
B
cotyle
C
cprl
cervical rib
pleurocoel
D
prdl
pp
diapophysis
E
ns
prezygapophysis
F
ventral keel
condylar rim

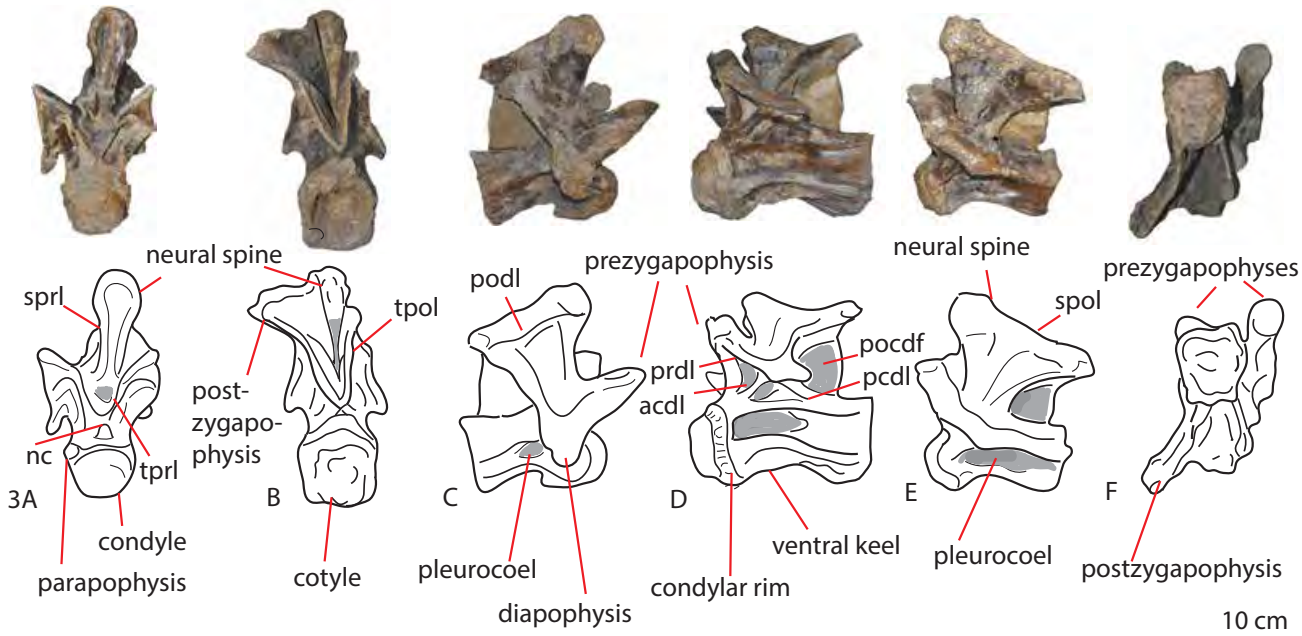
neural spine
sprl
nc
tprl
3A
condyle
parapophysis
post-
zygapo-
physis
tpol
B
cotyle
podl
C
pleurocoel
diapophysis
prezygapophysis
prdl
acdl
D
ventral keel
condylar rim
pocdf
pcdl
neural spine
spol
E
pleurocoel
prezygapophyses
F
postzygapophysis
10 cm

Plate XVIII: MACN-CH 936 posterior cervicals. MACN-CH 936 posterior cervical 1 in anterior (A), posterior (B), right lateral (C), left lateral (D), dorsal (E), and ventral (F) views. MACN-CH 936 posterior cervical 2 in anterior (A), posterior (B), right lateral (C), left lateral (D), dorsal (E), and ventral (F) views. MACN-CH 936 posterior cervical 3 in anterior (A), posterior (B), right lateral (C), ventrolateral (D), left lateral (E), and dorsal (F) views.

Abbreviations: cpol = centropostzygapophyseal lamina, dp = diapophysis, nc = neural canal, ns = neural spine, pp = parapophysis, pre = prezygapophysis, po = postzygapophysis, pocdf = postzygapophyseal centrodiapophyseal fossa, podl = postzygadiapophyseal lamina, ppdl= paradiapophyseal lamina, prcdf = prezygapophyseal centrodiapophyseal fossa, sdf = spinodiapophyseal fossa, spof = spinopostzygapophyseal fossa, sprl = spinoprezygapophyseal lamina, tpol = intrapostzygapophyseal lamina, tprl = intraprezygapophyseal lamina.

There are five more cervical elements in to this series, which are all posterior cervicals (Plate XVIII 1-3, Plate XIX1-2). However, as previously noted, the exact association of these cervicals is unknown, and, moreover, the colour (a dark greyish-brown) of these cervicals is more suggestive of a Cerro Condor Norte provenance. The Cerro Condor Norte quarry map (Figure 1 and Figure 2) does show a few isolated vertebrae, illustrated as dorsals, which could not be identified (Figure 2 grey elements). They will be described here, however, as they are numbered MACN-CH 936. The centra are short and stout, except that of the fourth element of this series, which is more elongated (Plate XVIII 1-3 C-D, Plate XIX1-2 A,B, E,F). They all possess large rounded condyles, deep rounded cotyles, and prominent parapophyses posteroventrally on the condylar rim (Plate XVIII 1-3 A,B, Plate XIX1-2 C,D). The centra show prominent hypapophyses and ventral keels, as in PVL 4170 (Plate XVIII 1-3 F, Plate XIX1-2 A). The centra in lateral view show deep pleurocoels, which are deepest anteriorly and show a faint compartmentalization of the pleurocoel (Plate XVIII 1-3 C,D, Plate XIX1-2 E,F), as in PVL 4170, but not as prominent as in *Klamelisaurus, Mamenchisaurus, Omeisaurus* or neosauropods (Xijing, 1993; Tang et al., 2001; Ouyang & Ye, 2002; Upchurch, Barrett & Dodson, 2004). They are also not perforated as in the anterior cervicals of this series. The neural arches all show prominent prezygapophyseal stalks, and triangular, medially-canted prezygapophyseal articular surfaces, with medial pre-epipophyses present (Plate XVIII 1-3 A,C,D, Plate XIX1-2 E,F). The neural spine of the fourth element in anterior view (Plate XIX1C) is similar to those of middle-posterior cervicals in PVL 4170; it is dorsoventrally elongated, and shows a slight expansion towards the neural spine summit of the sprls towards the lateral side. However, in lateral view, the spine shows a high anterior crest, followed by a steep ventrally-sloping spol, which makes the neural spine triangular in lateral view (Plate XIX1E,F). This is not seen in *Patagosaurus* PVL 4170, although several PVL 4170 cervicals are known to be missing, and one cervical with a high elongation of the

centrum lacks the neural spine. One other structure that differs in this element from the other MACN-CH 936 cervicals is the presence of an extra lamina, on the anterior side of the neural arch, which runs from the anterior half of the prdl to the dorsal rim of the condylar cup (Plate XIX2E). This lamina is not visible on the other lateral side of the cervical, however, as there the diapophysis is preserved, obscuring the lamina. It could therefore be, that this extra lamina is an assymmetrical, unique appearance. The neural spines, where preserved, are elongated, and show thick, dense spine tips, which display an expanding lump-shape dorsally, as well as anteriorly (Plate XIX1-2 E,F). The typical elevation of the podl is also seen (Plate XVII 3C,D,E). One element has a cervical rib preserved (Plate XVII 2C), which might be the only in-situ, attached cervical rib for the entire hypodigm of *Patagosaurus*. It is not as prominent as in neosauropods, but is stout, and curves in a gentle C-shape around the lateral side of the centrum, from the ventrally-directed tip of the diapophysis to the posteroventrally-directed tip of the parapophysis. One tapering posterior protrusion is seen in lateral view.

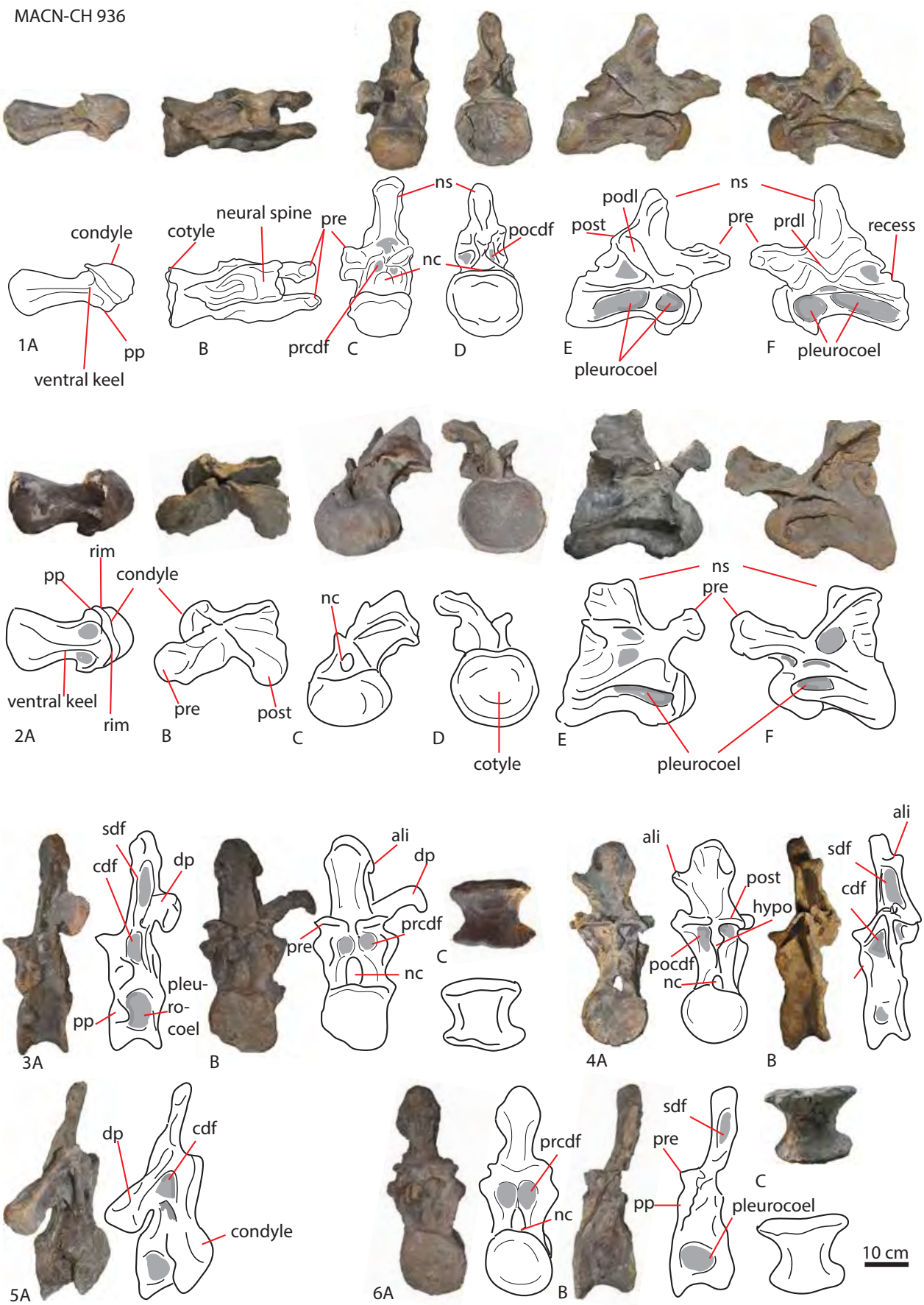
MACN-CH 936
condyle
cotyle
neural spine
pre
ns
pocdf
nc
podl
post
pre
prdl
recess
1A
pp
ventral keel
B
prcdf
C
D
E
pleurocoel
F
pleurocoel
rim
pp
condyle
ventral keel
rim
2A
B
pre
post
C
nc
D
cotyle
ns
pre
E
F
pleurocoel
sdf
cdf
dp
pleu-
ro-
coel
pp
3A
B
ali
dp
prcdf
pre
nc
C
ali
post
hypo
pocdf
nc
4A
B
sdf
cdf
ali
dp
condyle
5A
prcdf
nc
6A
B
sdf
pre
pp
C
pleurocoel
10 cm

Plate XIX (previous page): Posterior cervicals and dorsals of MACN-CH 936. MACN-CH posterior cervical 1 in ventral (A), dorsal (B), anterior (C). posterior (D), right lateral (E) and left lateral (F) views. MACN-CH 936 posterior cervical 2 in ventral (A), dorsal (B), anterior (C). posterior (D), right lateral (E) and left lateral (F) views. MACN-CH 936 dorsal 3 in lateral (A) and anterior (B) and ventral (C) views. MACN-CH 936 dorsal 4 in posterior (A) and lateral (B) views. MACN-CH 936 5 in lateral (A) view. MACN-CH 936 dorsal 6 in anterior (A), lateral (B) and ventral (C) views.

Abbreviations: ali = aliform process, cpol = centropostzygapophyseal lamina, dp = diapophysis, hypo = hypapophysis, nc = neural canal, ns = neural spine, pp = parapophysis, pre = prezygapophysis, po = postzygapophysis, pocdf = postzygapophyseal centrodiapophyseal fossa, podl = postzygadiapophyseal lamina, ppdl= paradiapophyseal lamina, prcdf = prezygapophyseal centrodiapophyseal fossa, sdf = spinodiapophyseal fossa, spof = spinopostzygapophyseal fossa, sprl = spinoprezygapophyseal lamina.

The series also has four anterior-middle dorsals preserved (Plate XIX3-6), the first of which is slightly opisthocoelous, indicating an anterior or anteriormost dorsal (Plate XIX5A). The other three elements have amphicoelous centra (Plate XIX3A,B, 4A,B, 6A,B), and shallow, oval depressions laterally on the centra (Plate XIX3A, 4B, 6B). The lateral sides of the centra show no neurocentral sutures in connection with the neural arch. The anterior dorsal also has one prominent diapophysis, which is directed laterally and ventrally (Plate XIX5A). The dorsal and proximal sides of this diapophysis show rugose rims. The neural spine is not as elevated in this element, as it is in subsequent elements. The other, more middle dorsal elements show prominent elevation of the neural arch and spine, as in PVL 4170 (Plate XIX3B, 4A, 6A). They show, in anterior view, the prominent stpol dividing the anterior face of the neural arch into two parts, both of which show deep cprfs. The neural canal in anterior

view is dorsoventrally elongated. This all morphologically overlaps with PVL 4170 dorsals. The only other preserved diapophysis is directed strongly laterally and slightly dorsally (Plate XIX3B). Anteriorly and posteriorly, prominent hypantrum-hypapophysis complexes are seen (Plate XIX3B, 4A, 6A). The hypantrum is a thickened, rugose ligament, coinciding with the strpl, hinting at the stprl being a precursor to the hypantrum, however, since the hypantrum is not found in the (sub)adult PVL 4170, this is probably an ontogenetic development of the stprl in this taxon. The neural spine is dorsoventrally elongated, but shows a slight fanning out towards the lateral sides of the spine tip. Prominently present are also both medial and lateral sprls and spols, which are only present in the holotype PVL 4170 on the posterior side, hinting at an ontogenetic need for more ligament attachment sites and thus more laminae (Wilson, 2012). Both elements show prominent aliform processes on their neural spines (Plate XIX3B, 4A). These are seen in *Europasaurus* adults (Carballido and Sander, 2014), and are seen only tentatively in the holotype PVL 4170.

Comparison with *Patagosaurus* PVL 4170

MACN-CH 936 shares several features with the holotype of *Patagosaurus fariasi.* The middle cervicals show morphological similarities with the cervicals of the holotype PVL 4170 in that they are stout, have a low EI, show a complex pleurocoel on the lateral side of the centrum, (of which have round prominent condyles which are cupped by thick rugose rims, from which ventral sides the parapophyses expand, and elongated neural arches with neural spines and high projections of the podl.

The dorsals show equally high projection of the neural arch and spine, and the characteristic *Patagosaurus*/basal eusauropod division of the anterior neural arch by the stprl/hypantrum, as well as a posterior rhomboid, prominent hypantrum and stpol, accompanied anteriorly by two oval prcdfs and posteriorly by the triangular pocdfs (Upchurch and Martin, 2002, 2003; Allain and Aquesbi, 2008; Bandyopadhyay et al., 2010).

There are some notable differences, however, as discussed for the fourth cervical, as well as for the dorsals. While that cervical could simply not be represented in the cervical series of the holotype PVL 4170; its dorsal series is more or less complete. The dorsals show a high dorsolateral projection of the diapophysis, which is seen in the Rutland *Cetiosaurus*, *Cetiosaurus oxoniensis* and mamenchisaurids (Zhao, 1993; Tang et al., 2001; Ouyang and Ye, 2002; Upchurch and Martin, 2003, 2003). This high projection is not seen in *Patagosaurus* PVL 4170. Next to this, the dorsals show a prominent aliform process on the lateral side, which is much more pronounced than the faint process on the posterior dorsals of PVL 4170. Finally, these dorsals show a rim that 'cups' the anterior articular surface, which is slightly convex; though this is also convex in the holotype PVL 4170, the rim is not found in these dorsals. The expression of the aliform process could be an ontogenetic one (Carballido et al., 2014); however, as PVL 4170 was a not fully grown individual, and MACN-CH 936 seems to have been fully grown (by lack of visible neurocentral sutures). The projection of the diapophyses and the rim of the articular surfaces are not known to be subject to ontogenetic

changes. Therefore, the associated anterior cervicals MACN-CH 936 axis and 1-8 can safely be referred to *Patagosaurus,* and the posterior cervicals and dorsals are carefully referred to *Patagosaurus*, however, may need to be subjected to further study, possibly with geometric morphometrics in order to compare morphological changes between this specimen and the holotype PVL 4170.

Comparison with *Volkheimeria* PVL 4077

As only the dorsals can be compared, there are only three elements to possibly show morphological overlap with *Volkheimeria* PVL 4077. However, the neural arches do not show the oblique accessory lamina seen in *Volkheimeria*, and the axial elongation of the dorsal neural spines is also not seen.

Ontogenetic stage of MACN-CH 936

As indicated before, the neurocentral sutures of MACN-CH 936 are not visible, indicating a fully-grown animal, or at least an animal of sexual maturity (Brochu, 1996; Birkemeier, 2011; Tschopp and Mateus, 2017). While there are still sutures visible in PVL 4170, this indicates the holotype to be a subadult, or an adult that is still growing. The more developed aliform process could be another indication of ontogenetic maturity, as these are also seen on adult *Europasaurus* dorsals (Carballido and Sander, 2014).

MACN-CH 1299

This is a series of caudals, a femur and a tibia. The femur unfortunately could not be retrieved from the collections, however the tibia could be photographed from the lateral side, as it was present in the collections, but could not be taken from the depository due to health and safety issues.

The caudal series (Plate XX1-7) consists of four anterior and two anterior-middle caudals. Most are well-preserved, however only two have one or two transverse processes preserved (Plate XX1A,B, 2A,B). The anterior caudals show a dorsoventrally elongated, oval centrum in anterior and posterior view (Plate XX2A,B 3A,B 5A, 7A,B), and an axially shortened centrum in lateral view (Plate XX3C, 5B). There is some slight damage to the articular surfaces, however. The anteriormost caudals show an anterior articular surface that is slightly convex (Plate XX2A, 3A), and a posterior articular surface that is slightly concave (Plate XX2B, 3B). The two following caudals, however, show the opposite on the articular surfaces; the anterior surface is slightly concave (Plate XX5B, 6C), and the posterior slightly convex. The middle caudals show this even more prominently (Plate XX1C, 4C). This is also seen in mamenchisaurids (Ouyang and Ye, 2002), however, mamenchisaurids show a far more prominent caudal posterior convexity. The posterior articular convexity persists through the other caudals as well, towards the middle caudals. This is also seen in anterior caudals of *Cetiosauriscus stewarti* (Charig, 1993; Noè et al., 2010), as well as in caudal vertebrae of Late Jurassic Portuguese non-neosauropod eusauropods (Mocho et al., 2017).

The centra of the anterior caudals show small oval depressions on the lateral sides, underneath the base of the transverse processes (Plate XX3C, 5B, 6C). The centra of the anterior vertebrae show neurocentral sutures, however, these are fused. The anterior caudal with the right diapophysis preserved, shows a short, stout, distally-tapering

transverse process (Plate XX2A,B), which projects laterally and slightly ventrally at an oblique angle. The middle caudal that has the transverse processes preserved shows short, stout processes, that are directed laterally and ventrally, and fan out slightly towards the anterior and posterior side at their distal end (Plate XX1A, C). They also curve slightly around the centrum, in a C-shape, in anterior view.

The neural arch of the anterior caudals in anterior view shows an elevation of the prdl and podl (Plate XX2A,B, 3A,B, 5A, 6A,B, 7A,B), showing a triangular sheet of bone surrounding the neural canal; which is defined by Gallina and Otero (2009) as the anterior caudal transverse process complex (ACTP), the morphology of which can be used as a diagnostic feature for sauropod systematics. The ACTP complex of MACH-CH 1299 is also seen in *Cetiosaurus oxoniensis*, *Cetiosauriscus stewarti* (Charig, 1993; Upchurch & Martin, 2003; Noè, Liston & Chapman, 2010) and an unnamed sauropod caudal from the Callovian of Peterborough, UK (Holwerda and Liston, 2017), and to some extent in *Haestasaurus* (Upchurch et al., 2015), as well as *Haplocanthosaurus*, mamenchisaurids, *Camarasaurus* and *Giraffatitan* (Hatcher, 1903; Ouyang and Ye, 2002; Gallina and Otero, 2009; Taylor, 2009; Foster and Wedel, 2014). The middle caudals do not have a prominent ACTP complex, as in PVL 4170 (Gallina and Otero, 2009); the prdl and podls are more closely aligned to the vertebral body. All caudals show prominent, anterodorsally projecting, tapering prezygapophyses, which are triangular in shape in anterior view, and which cant slightly medially, as in *Patagosaurus* PVL 4170. The neural canal is round, both in anterior as well as posterior view.

The neural spine in the anterior vertebrae shows a strong projection posterodorsally (Plate XX, 3C, 5B, 6C), at an angle of about 60 degrees to the vertical, and shows in lateral view an anterior bulging and posterior concavity of the sprls and spls, giving the spine a curved appearance. This is so far not seen in any other sauropod, and could be taken as an additional autapomorphy for *Patagosaurus*. The middle caudals show an oblique projection

of the spine at the same angle. The spine in all caudals is rugosely striated anteriorly and posteriorly. The spinal summit in the anterior caudals is rhomboid in appearance in anterior and posterior view, but shows the characteristic saddle-shape in lateral view (Plate XX3B, 6C), as seen in *Spinophorosaurus,* and *Cetiosauriscus stewarti* (Charig, 1993; Remes et al., 2009; Noè et al., 2010).

A tibia is associated with MACN-CH 1299. The tibia (Plate XX8) is a relatively short element, and is anteroposteriorly compressed and transversely wide, as is also the case for the femur of PVL 4170, as well as the small juvenile tibia of MACN-CH 933. The proximal end flares out further transversely than the distal end, as in most sauropods, and the midshaft is most slender at about 1/3rd dorsally from the distal end. It does not show a prominent cnemial crest, nor does it show a prominent distal expansion of the medial malleolus, which is also similar to the small juvenile tibia of MACN-CH 933. This is perhaps not an ontogenetic change in tibial morphology, but a typical tibial morphology for *Patagosaurus*. There is a slight torsion in the shaft, however, which could be due to taphonomy.

Comparison with *Patagosaurus* PVL 4170

MACN-CH 1299 shares the elongated neural spine with the holotype PVL 4170 anterior caudals (though PVL 4170 does not preserve the anteriormost caudals). It also shares the presence of a saddle-shaped neural spine summit, seen in lateral view. The differences are the complex ACTP of MACN-CH 1299, which is not shared in PVL 4170, as well as the lack of heart-shaped anterior articular surfaces, seen in PVL 4170, however, this could be due to taphonomic damage in the former. The associated middle caudals of MACN-CH 1299 do resemble the holotype PVL 4170 middle caudals, therefore, this specimen may safely be referred to *Patagosaurus*.

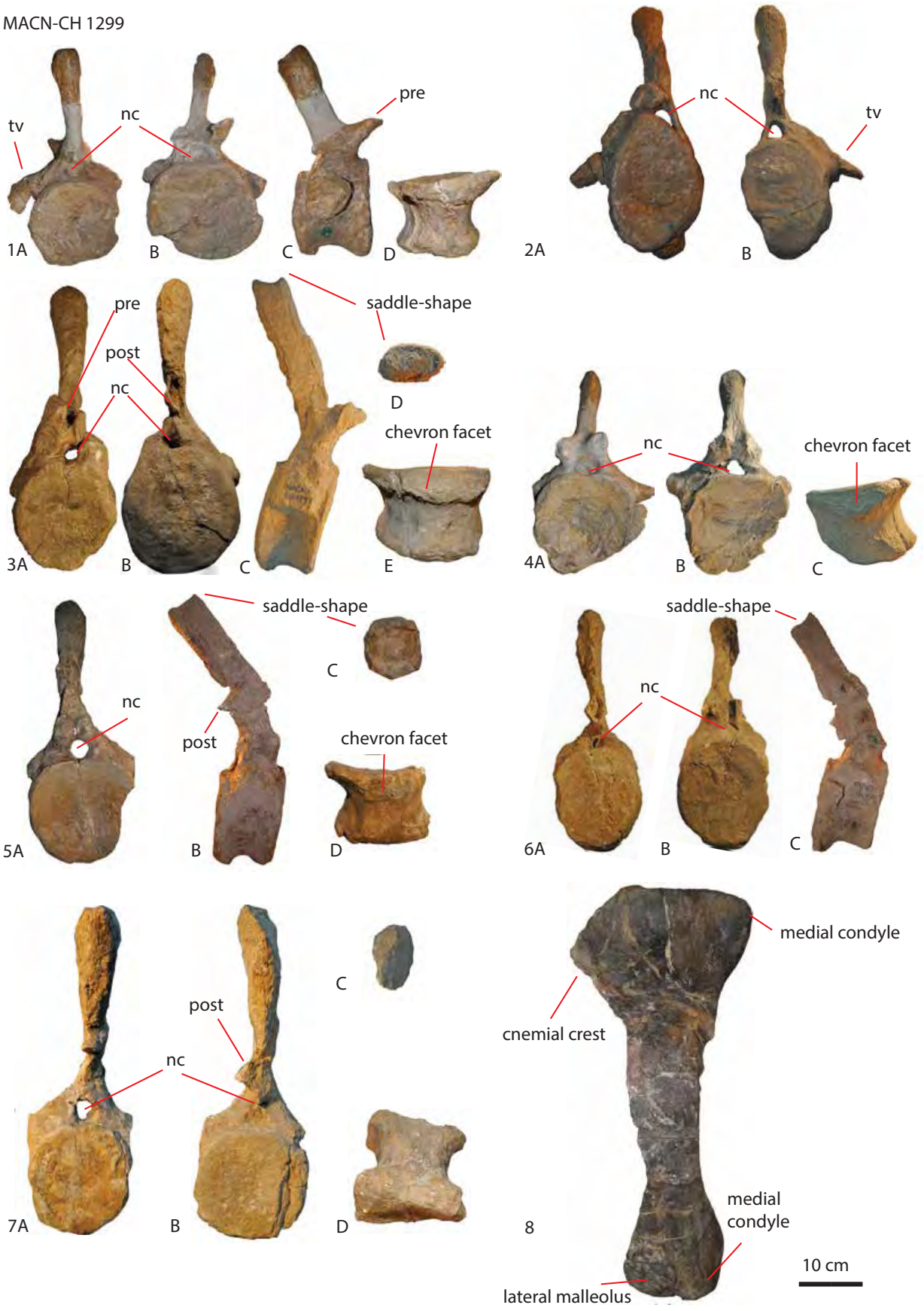
MACN-CH 1299
tv
nc
pre
1A
B
C
D
2A
nc
tv
B
pre
post
nc
saddle-shape
D
chevron facet
3A
B
C
E
4A
nc
chevron facet
B
C
nc
saddle-shape
C
post
chevron facet
5A
B
D
6A
nc
saddle-shape
B
C
post
nc
C
7A
B
D
8
medial condyle
cnemial crest
medial condyle
lateral malleolus
10 cm

Plate XX (previous page): MACN-CH 1299 caudal series and tibia. MACN-CH 1299 caudal 1 in posterior, anterior, lateal and ventral views. MACN-CH 1299 caudal 2 in anterior (A) and posterior views (B). MACN-CH 1299 caudal 3 in anterior (A), posterior (B), lateral (C), dorsal (D) and verntral (E) views. MACN-CH 1299 caudal 4 in anterior (A), posterior (B), and ventral (C) views. MACN-CH 1299 caudal 5 in anterior (A) , lateral (B), dorsal (C), and ventral views (D). MACN-CH 1299 caudal 6 in posterior (A), anterior (B), lateral (C) views. MACN-CH 1299 caudal 7 in posterior (A), anterior (B), dorsal (C) and ventral (D) views. MACN-CH 1299 tibia (8). Abbreviations: nc = neural canal, ns = neural spine, pre = prezygapophysis, post = postzygapophysis, tv = transverse process.

MACN-CH 231

This series consists of two complete anterior-mid caudal vertebrae, and one posterior caudal vertebra. One of the anterior-mid caudals, however, is filed under two numbers; MACN-CH 231 and 223. As it matches the first MACN-CH 230 element in morphology as well as size, it will be described here.

The first element (Plate XXI1) is a well-preserved caudal, with only the distal tip of the left diapophysis missing. The centrum is amphicoelous, dorsoventrally longer than axially or transversely wide, indicating that it is a still more anterior caudal (Plate XXI1C,D). The centrum is mildly constricted transversely in its midsection, showing a concave ventral side and a ventral lip on both anterior and posterior ventral sides, as well as a shallow, rounded depression on each lateral side of the centrum, below the diapophyses.

The anterior articular surface is oval, and has a slight semi-circular indentation below the neural canal, rendering the dorsal half of the articular surface heart-shaped (Plate XXI1A). This dorsal end is also slightly thicker and more rugose than the rest of the articular anterior

rim, giving it a 'lip'-like appearance. The posterior articular surface is also oval, but less transversely flattened than the anterior one (Plate XXI1B). It does not show a lip-like structure on the dorsal rim. As in many sauropods, the anterior surface has a slight bulge, and the posterior one a slight indentation, just below the centre of the articular surface.

The neural canal in anterior view is slightly teardrop-shaped, whereas in posterior view it is more oval (Plate XXI1A,B).

The prezygapophyses are prominent, and project anteriorly and dorsally at an oblique angle (Plate 1A,C,D). In anterior view, they are triangular, and are canted medially, as in the caudals of MACN-CH 935. They are supported ventrally by the prdl, which curves over the neural arch towards the dorsal distal tip of the diapophyses, and by the smaller tprls. The diapophyses, supported from the ventral side by the acdl and pcdl, project laterally and veer slightly dorsally, as slender, distally-tapering stalks. The postzygapophyses are much smaller than the prezygapophyses, and project mainly posteriorly, visible as small triangular processes.

The neural spine is elongated, as in PVL 4170 and MACN-CH 935, and in lateral view is seen to curve in a gentle sinusoidal form from prezygapophyses to the tip of the spine, and similarly from the postzygapophyses to the posterior tip of the spine. This gives the spine a sinusoidal appearance (Plate XXI1C,D). The tip of the spine is a rhomboid bulge, as in PVL 4170.

The second element (Plate XXI2) is similar to the first in the appearance of the centrum, neural arch and spine. However, it shows more rounded, shorter prezygapophyses in lateral view (Plate XXI2A,B), and has a slightly more oblique and less sinusoidal spine. The spine summit is saddle-shaped in lateral view (Plate XXI2 B). This element also shows the spine to be slightly longer (Plate XXI2C); however, the centrum is smaller.

The third element (Plate XXI3) is a small posterior caudal. It is well-preserved, and only a small part of the posterior articular surface is missing. It is an axially elongated, slender element (Plate XXI3A,B), and is transversely compressed in the midsection, showing a symmetrically shaped centrum, with both anterior and posterior articular surfaces fanning out dorsally and ventrally on both articular ends of the centrum. The centrum is amphicoelous, with both the anterior and posterior articular surfaces being slightly concave (Plate XXI3 C,D). There are no diapophyses present, and the postzygapophyses are also either only rudimentarily present or no longer present. The prezygapophyses project anteriorly and slightly dorsally at a low angle, and taper to a point anteriorly (Plate XXI3A,B, D). The neural spine is slightly more elongated than the prezygapophyseal stalks, and is seen to project slightly posteriorly and dorsally at a low angle. It too tapers to a point towards its distal end.

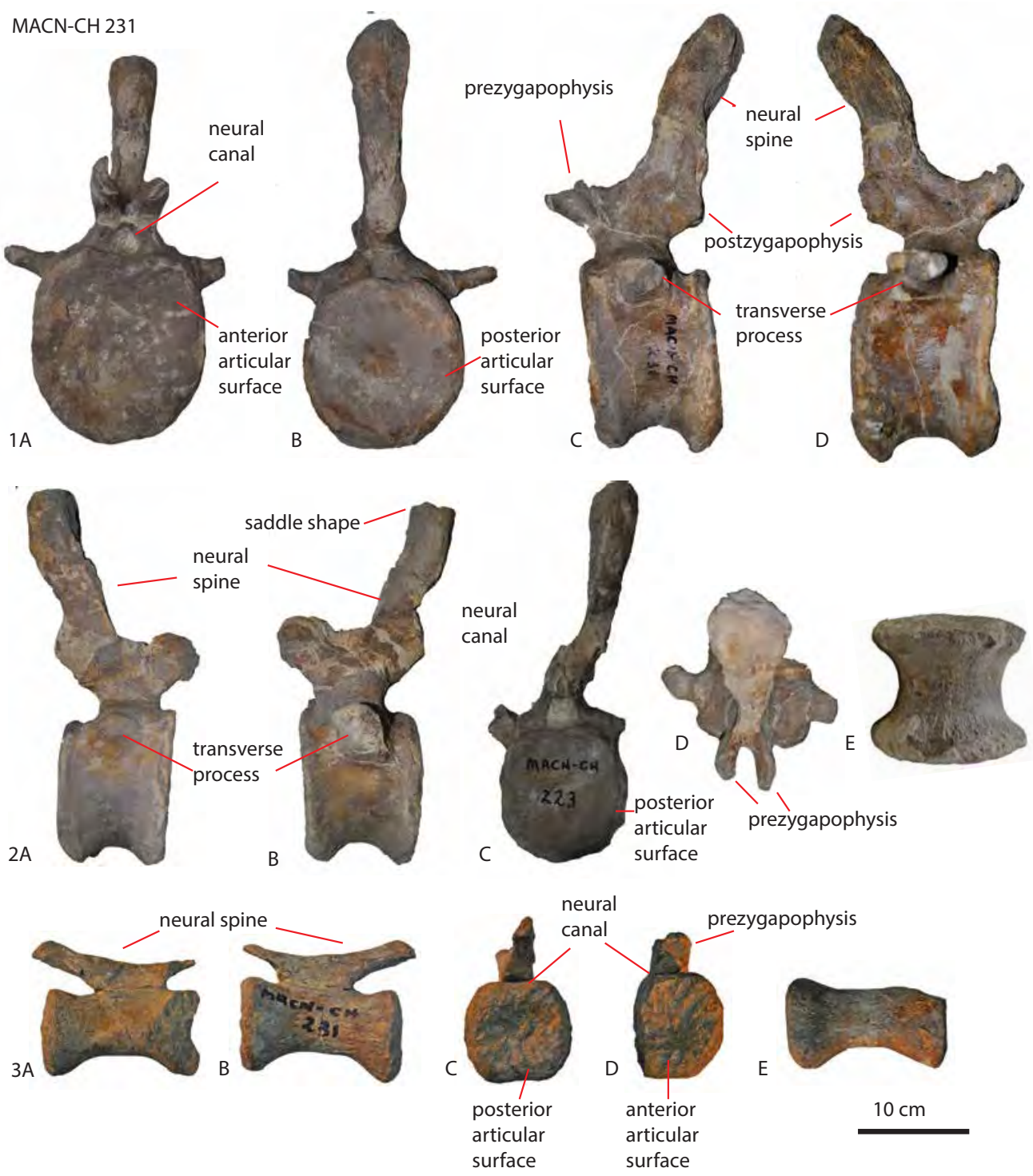

Plate XXI: MACN-CH 231 caudals. MACN-CH 231 caudal 1 in anterior (A), posterior (B), left (C) and right lateral views (D). MACN-CH 231 caudal 2 in right lateral (A) left lateral (B) posterior (C), dorsal (D), and ventral (E) views. MACN-CH 231 caudal 3 in right lateral (A), left lateral (B), posterior (C), anterior (D), and ventral (E) views.

Comparison with PVL 4170

The caudals are similar to *Patagosaurus* PVL 4170 as well as MACN-CH 935 in having an elongated neural spine, which shows a sinusoidal curvature in lateral view, together with a saddle-shaped spine summit in lateral view. The slightly more convex posterior articular surface is also similar to both MACN-CH 935, MACN-CH 1299.

Ontogenetic stage

This caudal series belongs to an adult, or subadult, as there are no neurocentral sutures visible, and the caudals are completely fused. MACN-CH 935, however, does have unfused dorsal neurocentral sutures, and fused caudal neurocentral sutures. Therefore, this individual was in MOS 3 or 4 when it died.

3.5.2 Specimens that are not *Patagosaurus* or cannot be ascribed to any taxon

MACN-CH 934

This specimen from Cerro Condor Sur consists of several dorsal neural arches and spines, one partial sacral neural arch and spine, one middle caudal vertebra, and a left pubis. Originally, a large ilium was ascribed to this specimen (Bonaparte, 1986a), however, this ilium could not be retrieved from the collections, as it is part of a traveling exhibition, and moreover, it is too large to belong to this small juvenile specimen.

Cranial elements

Two maxillae were found associated with this specimen (Plate XXI), one of which bears several teeth (Plate XXIIA). The dentition (see close-up in Plate XXIIF) is extensively described elsewhere (Holwerda et al., 2015), where it was found to be unlike any other sauropod dentition in the Cañadón Asfálto Fm. In medial/lingual view, the left maxilla shows at least 9 alveoli, some of which show teeth (Plate XXIIA). Interdental plates are present, as in all sauropods (Plate XXIIA, I). Replacement teeth are not visible. In lateral view, the labial side of the maxillae is bulging slightly towards the lateral side (Plate XXIIB,H). Here, the bone shows shallow but wide grooves that run dorsoventrally, probably functioning to accommodate blood vessels. The symphysis of the toothbearing maxilla (Plate XXIIC) shows a gently convex curvature, which is similar to that of *Shunosaurus*, *Spinophorosaurus*, *Europasaurus* and *Jobaria* (Chatterjee and Zheng, 2002; Sereno et al., 2007; Remes et al., 2009; Marpmann et al., 2015), as well as an unnamed sauropod from the Bagual Locality of the Cañadón Asfálto Fm. (Pol et al., 2009), and unlike the abrupt tapering as in *Mamenchisaurus* or *Camarasaurus* (Madsen et al., 1995; Ouyang and Ye, 2002; Chatterjee and Zheng, 2005). The anterior side of the maxilla of *Omeisaurus* is not clearly visible (Tang

et al., 2001). Dorsal to the symphysis, a hook-shaped nasal process is seen (Plate XXIIA,B,C). The posterior ventral side of the maxilla shows a rectangular posterior protrusion, that is ventrally mildly rounded, for attachment to the jugal (Plate XXIIB). This side of the maxilla also dorsally accommodates at the distalmost point a small dorsal lacrimal process (Plate XXIIA,B,I). Anterior to this, the lacrimal process is encasing a teardrop-shaped antorbital fenestra. The antorbital fenestra is about twice as high as it is wide, as in *Camarasaurus,* but unlike *Europasaurus* (Marpmann et al., 2015). The distal shape of the maxilla, with jugal and lacrimal process, is similar to that of *Shunosaurus*, *Mamenchisaurus* and *Camarasaurus* (Chatterjee and Zheng, 2002, 2005; Ouyang and Ye, 2002). Furthermore, the jugal process of the maxilla shows a retraction towards the dorsal side, which is more pronounced than in any of the maxillae of *Shunosaurus*, *Mamenchisaurus*, *Spinophorosaurus*, *Jobaria*, *Camarasaurus*, *Omeisaurus* (Madsen et al., 1995; Tang et al., 2001; Chatterjee and Zheng, 2002, 2005; Sereno et al., 2007; Remes et al., 2009), and unlike in the unnamed Cañadón Asfálto Fm. sauropod (Pol et al. , 2009), but which is seen to a lesser extent in *Europasaurus* and diplodocids (Berman and McIntosh, 1978; Whitlock et al., 2010; Barrett et al., 2011; Tschopp and Mateus, 2013b; Marpmann et al., 2015). The ectopterygoid process is only visible in dorsal view (Plate XXIIG), unlike in *Europasaurus* (Marpmann et al., 2015). Finally, the anterior, dorsal, ascending process of the maxilla (Plate XXIIA,B) is an abruptly-tapering, oblique, and elongated structure, that curves sinusoidally towards the dorsal side. This high projection of the ascending process of the maxilla is only seen in *Camarasaurus* and *Europasaurus* (Madsen et al., 1995; Chatterjee and Zheng, 2005; Marpmann et al., 2015). Given the height of the ascending process and the anterior protrusion of the hook-shaped process, the fenestra for the nasal would have been both dorsoventrally elongated, as well as axially wide, which is seen in *Spinophorosaurus*, *Jobaria* and *Europasaurus* (Sereno et al., 2007; Remes et al., 2009; Marpmann et al., 2015).

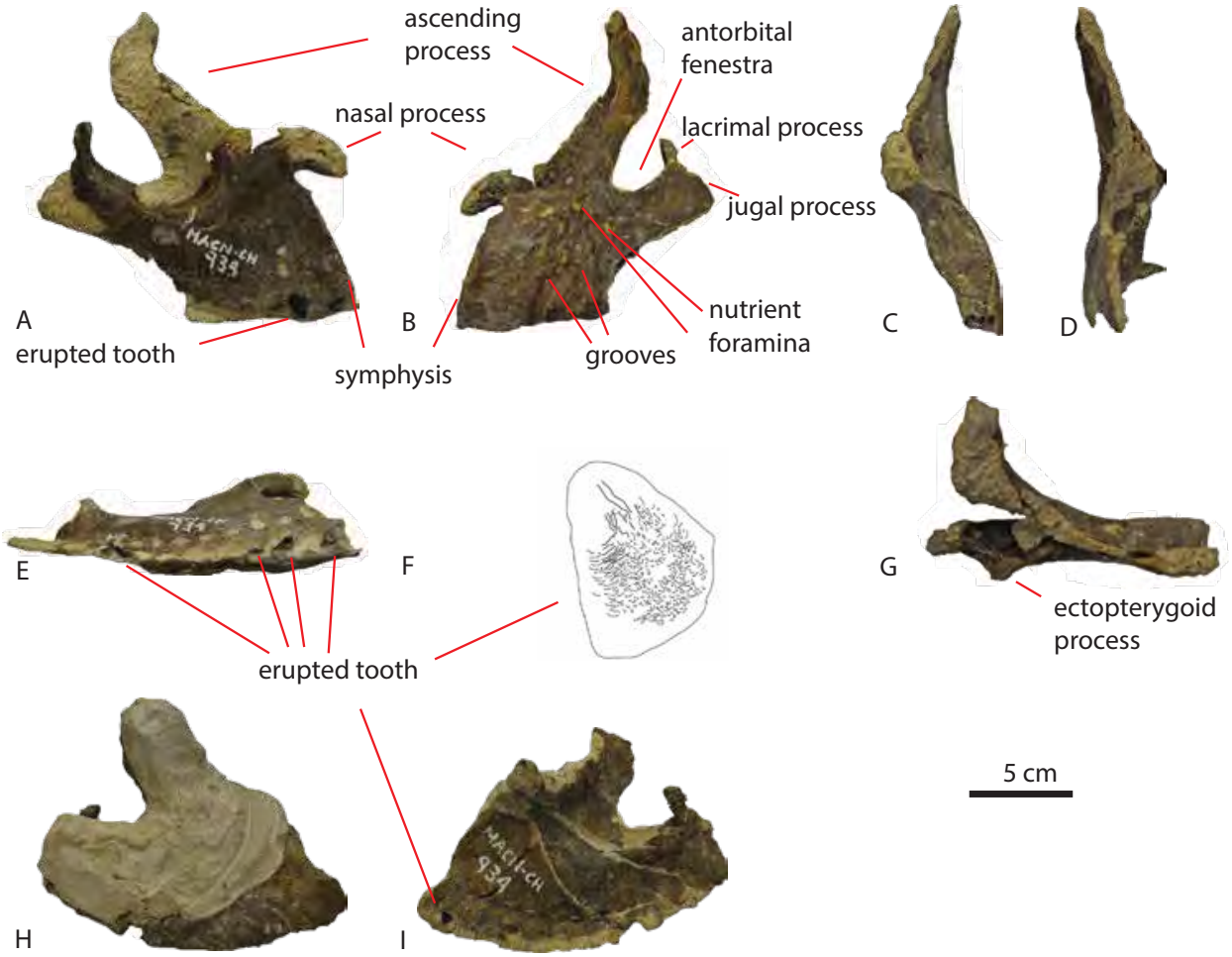

Plate XXII: MACN-CH 934 cranial elements. MACN-CH 934 left maxilla in lingual (A), labial (B), anterior (C), posterior (D) views. MACN-CH 934 right maxilla in ventral view, with close-up of erupted tooth (F), dorsal view (G) labial (H) and lingual (I) views.

Two anterior to mid dorsals are preserved (Plate XXIII1,3). The anteriormost of these two has both zygapophyses, diapophyses and neural spine preserved (Plate XXIII1A-D). In anterior view, the neural arch is wide, and shows two rounded, laterally fanning parapophyses (Plate XXIII1A). An opening for the neural canal is visible, which is semicircular and transversely broad. The posterior neural canal is evenly semicircular with a broad transverse base (Plate XXIII1B). In lateral view, the neural arch is less axially elongated. The CDF is visible as a transversely narrow, dorsoventrally elongated triangle, and is infilled with sediment (Plate XXIII1C,D). One oblique accessory lamina divides the CDF in two, as in *Volkheimeria* and possibly *Lapparentosaurus*. The prezygapophyses are not prominently present; they are small rounded lateral extensions of the tprls, which are prominently present as a curved V-shape. The tprls join ventrally in the stprl, which ends right above the neural canal in a hypanthrum structure (Plate XXIII1A). Though the holotype PVL 4170 shows stprl structures, which may serve as connection to the hyposphene, this structure is not seen so clearly in the other juvenile *Patagosaurus* specimen MACN-CH 932 (already slightly larger than MACN-CH 934). Two small oval cprfs are visible on the lateral sides of the stprl. They are flanked laterally by small vertical cprls, which support the prezygapophyses from below. The postzygapophyses are widely-spaced, with a large oval spof in between. The articular surfaces are triangular and rugose (Plate XXIII1B). Below the tpols, a rhomboid, symmetrical hyposphene is present, which is supported ventrally by the cpols and the stpol. The diapophyses project laterally and slightly dorsally. The dorsal side is convex, while the ventral side is concave, due to a prominent convexly curving prdl, and a convexly curving pcdl (Plate XXIIIA,B) The diapophyses are further supported by convexly curving acdls. Finally, this dorsal has a short, stout, oblique spdl, which is not present in PVL 4170. Large, oval, laterally elongated fossae are visible on the ventral side of each diapophysis (Plate XXIII1B). The diapophyses show circular depressions at both anterior and posterior distal ends. Posterior depressions are seen in PVL 4170, but anterior ones do not appear in PVL

4170. The neural spine at the base shows an anterior constriction of the sprls, which fan out towards the dorsalend of the spine. In posterior view, the spols create a bell-curve shape via a sinusoidal curvature from the dorsal side to the postzygapophyses, where they are constricted right above the postzygapophyses. Both anterior and posterior sides of the spine are rugosely striated.

The other anterior to mid dorsal is slightly more dorsoventrally elongated than the previous element, especially on the neural spine (Plate XXIII3A,B). The base of the neural arch is transversely wide, as in the previous element, and the parapophyses are prominently present as fanning out lateral structures (Plate XXIII3B). The tprls are not as strongly developed in this element, however. The prezygapophyses in this element are prominent, and rest on thick stalks consisting of the cprl and the prdls (Plate XXIII3B). The prezygapophyses are canted medially and project anteriorly and dorsally. The articular surfaces are triangular. The postzygapophyses are small, triangular processes, which cant medially, and show a small oval spof in between (Plate XXIII3A). Below the postzygapophyses, a prominent rhomboid hyposphene is present, which is supported by two cpols. Small rounded to triangular pocdfs are visible on each lateral side of the hyposphene. The diapophyses are directed laterally and dorsally, as in MACN-CH 934 1 (Plate XXIII1A,B).

Several posterior dorsal neural arches and spines are preserved as well (Plate XXIII2,4-9) with the pre- and postzygapophyses intact, as well as the parapophyses, however, without the diapophyses, except for MACN-CH 934 4 and 6. These posterior dorsals are similar, and seem to form a series, thought the exact order is hard to determine due to missing diapophyses and sedimentary infill.

The neural arch of these dorsals is dorsoventrally short and transversely wide (2A,B, 4C,D, 5A,C, 7A, B, 8A,B, 9A,B),, which is different from PVL 4170 posterior dorsals. In anterior view,

the parapophyses are stout and transversely broader than dorsoventrally high, which is also different from *Patagosaurus* PVL 4170. In lateral view, the neural arch is rectangular, as in PVL 4170, MACN-CH 935 and MACN-CH 932. Relatively narrow triangular CDFs are visible, infilled with sediment (see Plate XXIII2B, 4C, 5C, 8B). In anterior view, the prezygapophyses are canted medially, and have a narrow opening between them. There are two fossae present on the neural arch ventral to the prezygapophyses; the prcdfs which are small paired rounded fossae, and a central fossa that runs along where the stprl usually is located in PVL 4170, but which is not present in these posterior dorsals (though present in the anterior dorsal MACN-CH 934 1). In lateral view, the prezygapophyses project mainly anteriorly (Plate XXIII2B, 4C, 5C, 6A,B, 8B, 9A,B). The postzygapophyses are relatively small, triangular processes that cant medially, similar to the prezygapophyses. They meet ventrally just above the rhomboid, small hyposphene, which is supported by two sets of laminae, which seem to be a splitting of the cpols into a lateral and medial cpol. Lateral to the hyposphene, small rounded pocdfs are visible (Plate XXIII 3A, 4B, F).

The diapophyses are broken in nearly all elements, save for two, and they are also present in the attached neural arches of MACN-CH 934 6). The diapophyses project laterally, dorsally and slightly posteriorly (Plate XXIII 3A,B, 4B, 6A,B). They are supported by the prdl, the ppdl and the pcdl, and also medially by the spdl, as in the anterior dorsals, making them distinct from PVL 4170. The neural spine is constricted at the base, both anteriorly and posteriorly, by a constriction of the sprl and the spols (Plate XXIII2A, 4A,B, 5A,B, 7A, 8A). The posterior side of the neural spine has a clear lateral and medial spol division, which is also seen in the adult PVL 4170. The anterior and posterior surfaces are rugosely striated, whilst the lateral surfaces are mostly taken up by the dorsoventrally elongated, narrow spdfs.

One element (Plate XXIII 6) consists of two dorsal neural arches and spines that are fused together; this is most likely a true association. The exact articulations are difficult to trace, however; the neural arches are still partially embedded in sediment (Plate XXIII6A,B).

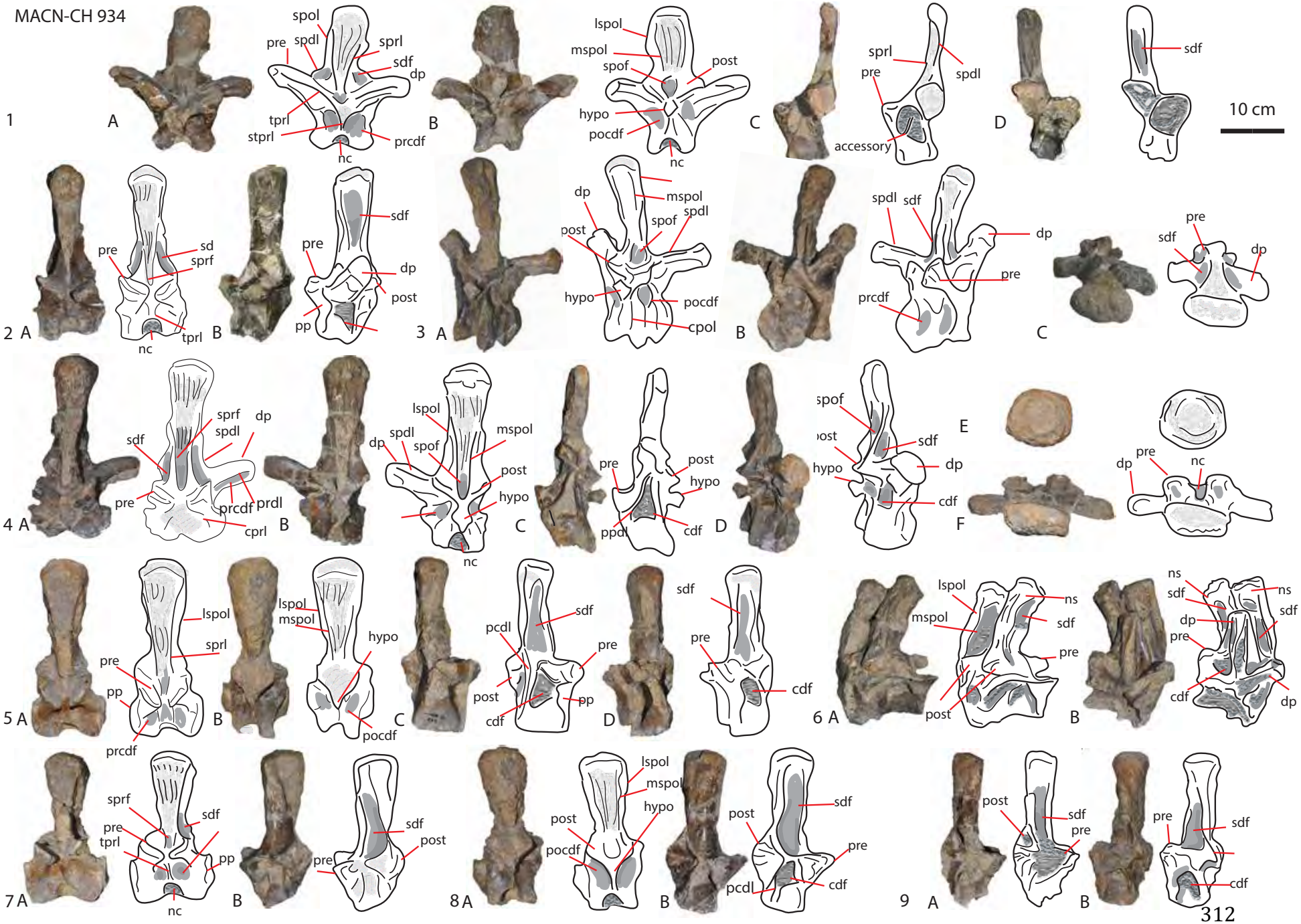
MACN-CH 934
1
A
spol
pre
spdl
sprl
sdf
dp
tprl
stprl
prcdf
nc
B
lspol
mspol
spof
post
hypo
pocdf
nc
C
sprl
pre
spdl
accessory
D
sdf
10 cm
2 A
pre
sd
sprf
tprl
nc
B
sdf
pre
dp
post
pp
3 A
dp
mspol
post
spof
spdl
hypo
pocdf
cpol
B
spdl
sdf
dp
pre
prcdf
C
pre
sdf
dp
4 A
sdf
sprf
spdl
dp
pre
prcdf
prdl
cprl
B
lspol
dp
spdl
spof
mspol
post
hypo
nc
C
pre
post
hypo
ppdl
cdf
D
spof
ost
sdf
hypo
dp
cdf
E
F
dp
pre
nc
5 A
lspol
pre
sprl
pp
prcdf
B
lspol
mspol
hypo
pocdf
C
pcdl
sdf
pre
post
pp
cdf
D
sdf
pre
cdf
6 A
lspol
mspol
ns
sdf
pre
post
B
ns
sdf
sdf
dp
pre
cdf
dp
7 A
sprf
pre
tprl
sdf
pp
nc
B
sdf
pre
post
8 A
lspol
mspol
hypo
post
pocdf
B
post
sdf
pre
pcdl
cdf
9 A
post
sdf
pre
B
pre
sdf
cdf

Plate XXIII (previous page): MACN-CH 934 dorsal neural arches. MACN-CH 934 anterior dorsal 1 in anterior (A), posterior (B), left lateral (C), right lateral (D) view. MACN-CH 934 dorsal 2 in anterior (A) and lateral (B) views. MACN-CH 934 anterior dorsal 3 in posterior (A), anterior (B), and dorsal (C) views. MACN-CH 934 dorsal 4 in anterior (A), posterior (B), left lateral (C), right lateral (D), dorsal (E,F) views. MACN-CH 934 dorsal 5 in anterior (A), posterior (B), right lateral (C) left lateral (D) views. MACN-CH 934 dorsal 6 in right lateral (A) and left lateral (B) views. MACN-CH 934 dorsal 7 in anterior (A), posterior (B) views. MACN-CH 934 dorsal 8 in posterior (A) and lateral (B) views. MACN-CH 934 dorsal 9 in right lateral (A) and left lateral (B) views.

Abbreviations: cdf = centrodiapophyseal fossa, cpol = centropostzygapophyseal lamina, dp = diapophysis, hypo = hyposphene, nc = neural canal, ns = neural spine, pp = parapophysis, pre = prezygapphysis, po = postzygapophysis, pocdf = postzygapophyseal centrodiapophyseal fossa, podl = postzygadiapophyseal lamina, ppdl= paradiapophyseal lamina, prcdf = prezygapophyseal centrodiapophyseal fossa, sdf = spinodiapophyseal fossa, spdl = spinodiapophyseal lamina, spof = spinopostzygapophyseal fossa, l.spol, m. spol = lateral/medial spinopostzygapophyseal lamina, sprf = spinoprezygapophyseal fossa, sprl = spinoprezygapophyseal lamina, tpol = intrapostzygapophyseal lamina, tprl = intraprezygapophyseal lamina, stpol = single intrapostzygapophyseal lamina, stprl = single intraprezygapophyseal lamina.

The only caudal element (Plate XXIV 1A-F) belonging to this specimen is a stout, short, middle caudal, with a partially-preserved neural spine. The centrum is amphicoelous, however, the anterior articular surface is slightly convex, and the posterior one slightly concave (Plate XXIV 1C,D,E). In lateral view, the anterior ventral articular side shows a lip-like structure (Plate XXIV 1C,D). In ventral view, the caudal has a keel-like structure, as well as two chevron facets on the posterior ventral rim. (Plate XXIV 1E) A keel-like structure is seen in a sauropod caudal from the Early Jurassic Whitby Mudstone Formation of the UK (Manning et al., 2015) as well as from the Middle Jurassic Oxford Clay Formation of the UK (Holwerda and Liston, 2017), and finally in neosauropods (e.g. *Barosaurus*). The diapophyses are short and stubby, and taper to a point (Plate XXIV 1F). They are directed laterally and posteriorly. The neural arch is dorsoventrally short and axially stretches no further than the level of the diapophyses. The prezygapophyseal stalks are present, however the prezygapophyses are not preserved. The base of the neural spine is preserved, and seen to project mainly dorsally at an oblique angle, and slightly posteriorly.

Two sacral neural arches (Plate XXIV 2A-D) are associated with this specimen; one neural arch with only the right sacral rib preserved, and one with the partial neural arch preserved. The sacral ribs fan out towards the lateral side, creating a C-shape. The neural spines are elongated and rugose, as in PVL 4170, MACN-CH 932, 933, 934 and 935. The prdl, podl, and sprl and spols are all present, as are the sprf and the spof. The spols divide into a lateral and medial spol, as in the dorsals. This is also seen in sacrals of *Lapparentosaurus* MAA 7. Lastly, a stout spdl is apparent, which is not found in PVL 4170.

Pubis MACN-CH 934

This small left pubis (Plate XXIV 4A-D) is one of two pubes preserved in this specimen, however, only one is available for study in the collections of the MACN. It has a stout shaft, and about ½ of the length comprises the pubic apron (Plate XXIV 4A,B). The shaft is straight both in lateral as well as in anterior and posterior view (Plate XXIV 4A-C). The apron, however, shows a sinusoidal curvature in posterior view, with the ischial peduncle being especially sinusoidal. The articulation surfaces are rugosely pitted. The iliac peduncle is slightly damaged, however, there seems to be a rudimentary hook-shaped ambiens process present on the medial side of the pubis, which is not seen in PVL 4170 (Plate XXIV 4A,B,D). The pubic foramen is large and oval, and not kidney-shaped, as in PVL 4170 or MACN-CH 932.

Ischium MACN-CH 934

A small ischium (Plate XXIV 3A,B) is associated with this specimen. It is a stout, short element, with a wide proximal shaft with a rectangular to triangular peduncle and a more rounded peduncle. The space between the two proximal peduncles is small and shallow, unlike PVL 4170 and MACN-CH 932 and 933. The ischium combined with its mirroring element would have made a more V-shaped distal fusion, instead of a co-planar one, which is similar to the condition found in PVL 4170.

Ilium MACN-CH 934

A small ilium (Plate XXIV 5) is associated with this specimen; it is well-preserved, however, currently on exhibit, therefore only one image of the lateral side is available. The ilium is

axially elongated, as in PVL 4170, and *Cetiosaurus* (Upchurch & Martin, 2003), and has a wide acetabulum, as in PVL 4170. The anterior lobe, however, is rounded in shape, and blunt, and does not taper to a hook-shape as in PVL 4170. The dorsal rim of the ilium is slightly damaged, however, the outline is visible, and suggests a flat dorsal rim, and no convex shape. This is also seen in *Haplocanthosaurus* and *Cetiosauriscus* (Hatcher, 1903; Charig, 1980; Foster and Wedel, 2014; Noè et al., 2010). The ischial peduncle is a rounded, posteroventrally projecting lobe, as in PVL 4170, and it makes a wide angle with the posterior lobe of the ilium, as in PVL 4170. The pubic peduncle is short and stout, and anteriorly convex, which is seen in *Barapasaurus, Tazoudasaurus,* and *Shunosaurus* (Zhang, 1988; Upchurch et al., 2004; Allain and Aquesbi, 2008; Bandyopadhyay et al., 2010).

MACN-CH 934

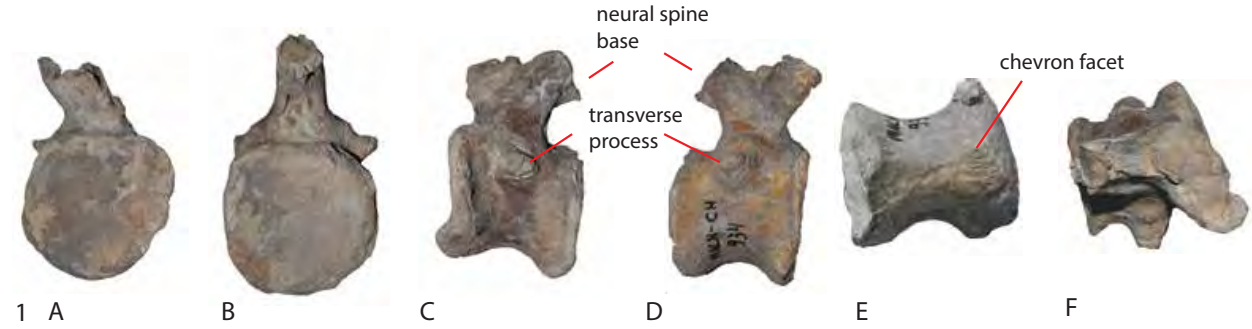

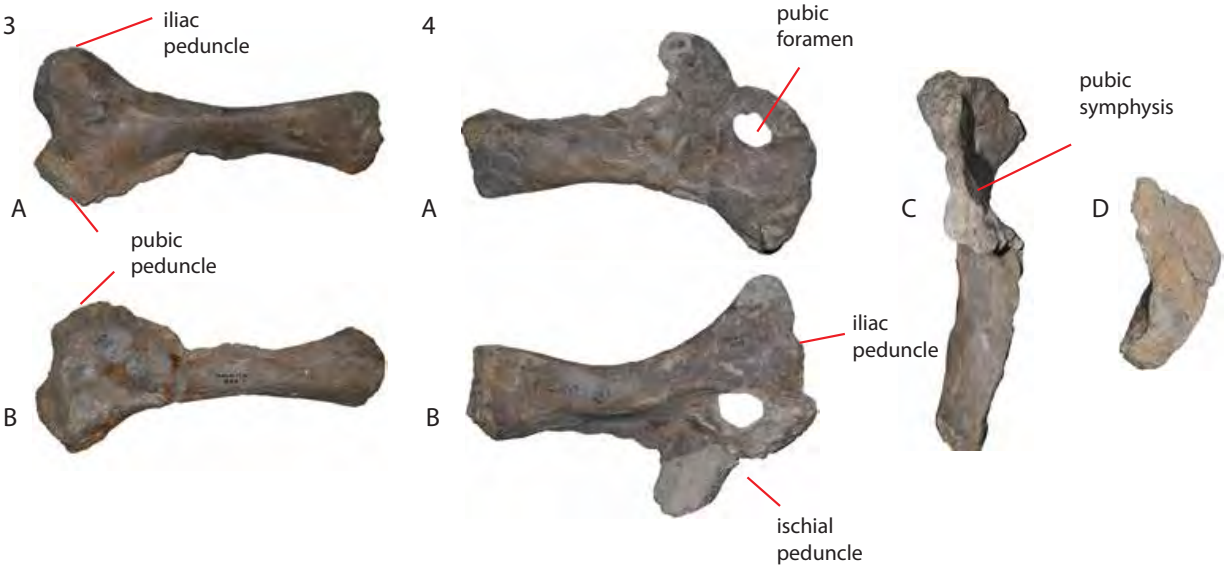

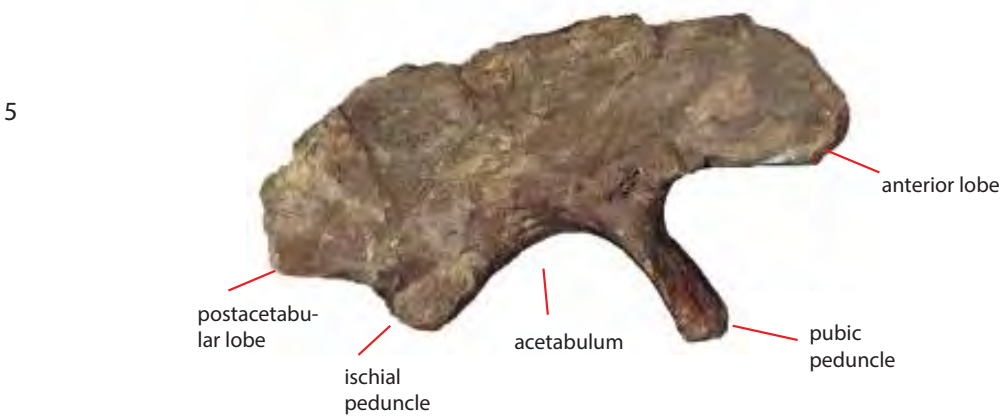

10 cm

Plate XXIV (previous page): MACN-CH 934 ischium, pubis, ilium and caudal and sacral elements. MACN-CH 934 caudal 1 in anterior (A), posterior (B), left lateral (C), right lateral (D), ventral (E) and dorsal (F) views. MACN-CH 934 sacral neural arch and spine in anterior (A), and posterior (B) views, and sacral neural arch in anterior (C) and posterior (D) views. MACN-CH 934 ischium 3 in lateral (A) and medial (B) views. MACN-CH 934 pubis 4 in lateral (A), medial (B), ventral (C) and iliac peduncle (D) views. MACN-CH 934 ilium 5.

Comparison with PVL 4170

The dorsals of MACN-CH 934 show a similar elongation of the neural spine to PVL 4170. The rhomboid hyposphenes match with PVL 4170 and MACN-CH 935 and 932. The lateral spol fanning out towards the ventral side of the neural spine is similar to all *Patagosaurus* dorsals. However, there are some notable differences as well. The presence of a clear hypantrum, for instance, is not seen in the holotype (which is an adult specimen) nor is it seen in any of the juvenile *Patagosaurus* specimens. Furthermore, a clearly developed spdl is seen in MACN-CH 934, which is not present in the juvenile *Patagosaurus*, and also not in the adult *Patagosaurus* (in PVL 4170 only as a subtle incipient lspol+spdl formation, and as an incipient lspol+spdl formation in MACN-CH 936). The occurrence of the spdl in dorsal vertebrae is a widespread feature in sauropods, such as *Tazoudasaurus*, *Mamenchisaurus*, *Omeisaurus*, and basal neosauropods and rebbachisaurids (Wilson, 1999; Allain and Aquesbi, 2008; Mannion, 2009; Carballido et al., 2012), and titanosauriforms (e.g. Carballido et al., 2011; Carballido et al., 2012; Carballido and Sander, 2014; Lacovara et al., 2014). It is, however, neither found as a single clearly present lamina in *Patagosaurus*, nor in the Rutland *Cetiosaurus* or *Cetiosaurus oxoniensis*. This could mean that MACN-CH 934 is not a *Patagosaurus*. Interestingly, the spdl is also present in the sacral neural arch associated with

MACN-CH 934. This lamina has not received much attention in sacrals thus far, but an spdl seems to be present in the sacrals of *Patagosaurus* PVL 4170, as well as *Lapparentosaurus* MAA 7, and also in sacrals of (basal) neosauropods *Haplocanthosaurus* and diplodocids (Hatcher, 1903; Osborn, 1904).

The pubis of MACN-CH 934 also differs in morphology from PVL 4170, as well as MACN-CH 935 and 932. Next to differences pointed out on the apron and pubic foramen, the MACN-CH 934 pubis shows an incipient ambiens process similar to those of *Lapparentosaurus* MAA 117 and diplodocids, which is neither present in *Patagosaurus* nor in *Cetiosaurus* (Upchurch and Martin, 2002, 2003; Upchurchet et al., 2004; Wilhite, 2005). The ilium shows differences with PVL 4170 in the low dorsal rim, non-tapering, blunt anterior lobe and short, anteriorly convex, pubic peduncle, which are more similar to *Haplocanthosaurus, Cetiosauriscus*, and basal sauropods (*Barapasaurus, Tazoudasaurus, Shunosaurus*).

Comparison with *Volkheimeria*

MACN-CH 934 is of a similar size and ontogeny as *Volkheimeria* (see ontogenetic stage below), however, there are similar morphological dissimilarities between the two taxa represented by MACN-CH 934 and PVL 4077. As mentioned before, *Volkheimeria* seems to have less dorsoventrally-elongated neural spines, and rather shows axially-wide neural spines and arches, which MACN-CH 934 clearly does not have. However, the accessory lamina that is shown in the lateral neural arches of *Volkheimeria*, is potentially present in some of the MACN-CH 934 neural arches, though not consistently. These neural arches would need more preparation work done before anything conclusive could be said about this accessory lamina.

Ontogenetic stage of MACN-CH 934

MACN-CH dorsal neural arches show complex lamination, fossae, and neural spine elongation, and therefore will probably be in MOS stage 2. The sacral neural arch, however, shows less prominent features, which could mean that in this taxon, ontogenetic development starts at the anterior side of the axial column and develops posteriorly along the ontogenetic scale. An earlier MOS stage is likely not supported, however, because the spdl is present in this specimen. In early juvenile sauropods, the spdl is not present, which otherwise should be present in adult specimens (Carballido et al., 2012). Moreover, the maxillae show grooves and structures that are not present in sauropods of a very early MOS stage (Marpmann et al., 2015). Due to the unfused state of the neural arches, MOS stage 3 is also probably not likely.

The pubic apron morphology, which matches that of the juvenile *Lapparentosaurus* MAA 117, which is in an early ontogenetic stage, also establishes an early MOS stage, thus MOS 2 is the most likely stage.

MACN-CH 230

This material from Cerro Condor Sur consists of three dorsal vertebrae, two complete and one partially-preserved. The first of these elements (Plate XXV 1) is a posterior dorsal, shown by the high neural arch, neural spine, and axially-short neural arch, as well as the well-developed hyposphene.

The centrum is axially more elongated than the neural arch (Plate XXV 1C,D), and therefore stretches further both anteriorly and posteriorly underneath the neural arch. The centrum in ventral view (Plate XXV 1F) is seen to be symmetrically constricted in the midsection and flaring out mildly towards each articular surface, which are both flat, though the anterior one is very slightly convex, and has a rim as seen on the condylar rims in cervicals and anterior dorsals of PVL 4170. On each lateral side, there is a slight elliptical depression visible (Plate XXV 1C,D). The neural arch is strongly offset towards the posterior side, showing the entire element to cant towards the posterior side. The neural arch in lateral view tapers towards the diapophyses; the anterior tapering is curved by the presence of rugosely undulating parapophyses, and the posterior side shows a small gully for the neural canal. Neurocentral sutures are present on each lateral side of the neural arch. In anterior view, the neural arch shows a wide, open, oval neural canal, and triangularly protruding parapophyses on each lateral side of the neural canal (Plate XXV 1B). The neural canal is followed dorsally by a V-shaped, transversely thick hypantrum, similar to MACN-CH 934, and unlike the lack of hypantrum and presence of the stprl in *Patagosaurus* PVL 4170 and MACN-CH 935. The posterior side of the neural arch shows a teardrop-shaped neural canal, directly followed at its dorsal side by a dorsoventrally-elongated, transversely narrow rectangular hyposphene, which differs from the rhomboidal shape of PVL 4170 (Plate XXV 1A). The prezygapophyses are missing, however, the prdl is seen to curve convexly towards the tip of

the diapophyses. The diapophyses are further supported by the ppdl and the pcdl from the ventral side (Plate XXV 1A,B). The diapophyses are directed strongly dorsally, unlike PVL 4170. A dorsal projection of diapophyses is seen in *Cetiosaurus oxoniensis* as well as the Rutland *Cetiosaurus*, *Mamenchisaurus*, *Klamelisaurus* and *Haplocanthosaurus* (Hatcher, 1903; Xijing, 1993; Ouyang and Ye, 2002; Upchurch and Martin, 2002, 2003). In anterior view, the neural spine shows two sets of ventrally acutely tapering laminae, which seem to be a lateral and medial splitting of the sprls (Plate XXV 1B). This is not seen in *Patagosaurus* PVL 4170. They converge dorsally on the two small aliform processes which are seen on each ventral side of the neural spine summit mass. In posterior view, the triangular postzygapophyses show a shallow, V-shaped spof ventral to the onset of the lateral and medial spols, which are split in an equal fashion, as on the anterior side (Plate XXV A). The lateral spol seems to converge with a short spdl, however, the lamination is damaged here and is not very clearly visible.

The second element (Plate XXV 2) is less well-preserved than the first; the postzygapophyses and part of the posterior neural spine are missing. The centrum is similar to the previous element; it is symmetrical and amphicoelous (Plate XXV 2A). The neural arch is slightly different from the first element; it is axially more elongated, and dorsoventrally more elongated. The neural arch is canted anteriorly, whereas the neural spine is canted posteriorly. Oval depressions and neurocentral sutures are present, as in the previous element (Plate XXV 2A). The parapophyses are rugosely undulating on the lateral side of the neural arch, as in the first element. The diapophyses are directed strongly dorsally, as in the first element (Plate XXV 2A,B). The neural spine shows a similar double pair of lateral and medial sprls and spols.

The third element (Plate XXV 3) from this series only has the centrum and part of the neural arch and a diapophysis preserved. As in the first element, the anterior articular surface of the centrum is slightly convex (Plate XXV B,D). The centrum is not symmetrical, however;

the anterior end is wider than the posterior, and also the anterior side of the centrum is dorsoventrally more elongated, so that the ventral side protrudes further ventrally than the posterior ventral side (which creates a 'lip'-like appearance). The neural canal is more similar in shape for each side, being oval and dorsoventrally elongated (Plate XXV 3A,C). No hyposphene or hypantrum is visible. The neural arch is seen to cant posteriorly, as in the first element, rather than in the second (Plate XXV 3B,D). The right diapophysis is partially preserved, and is shown to project dorsally, as in the previous elements.

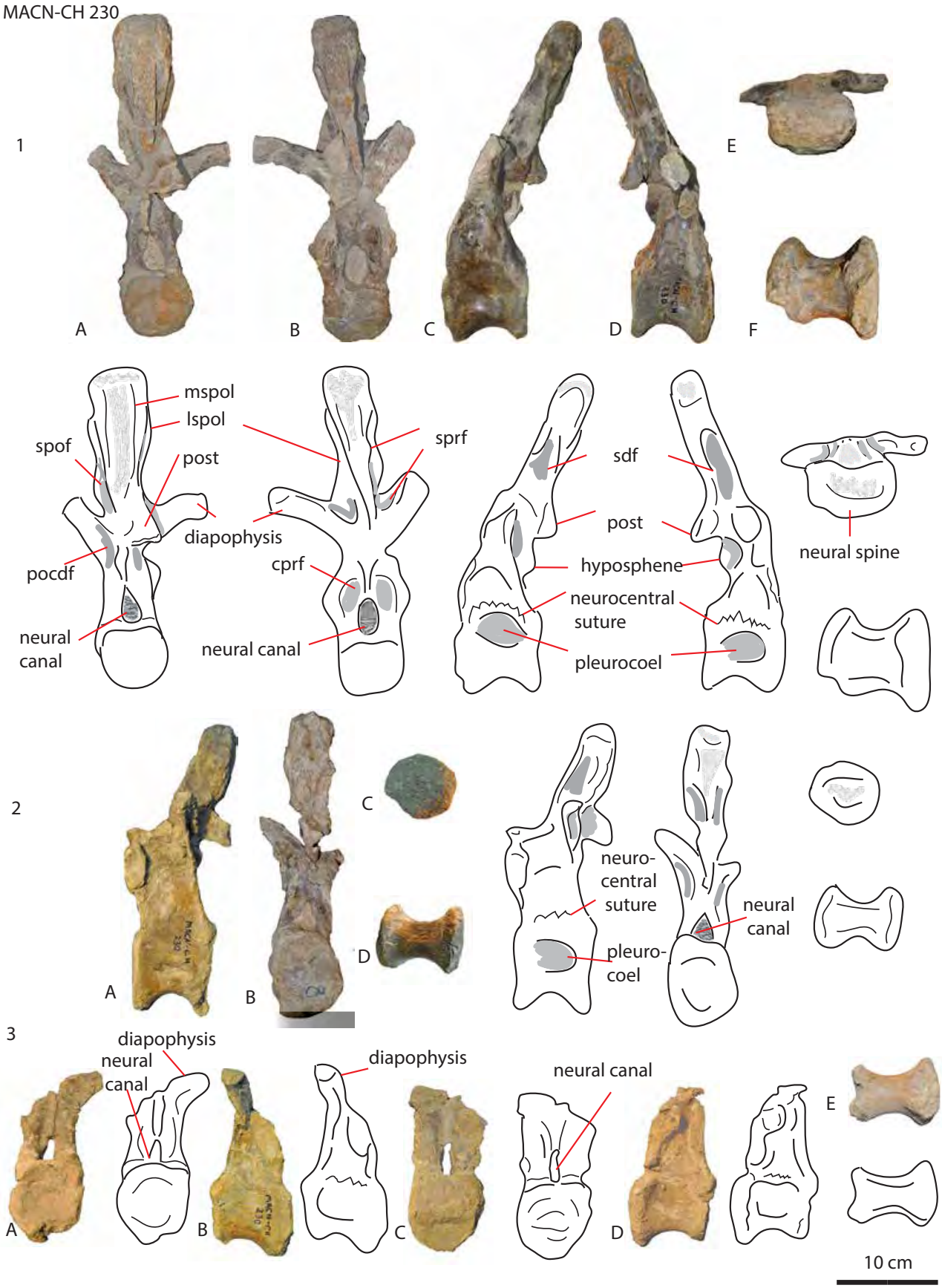
MACN-CH 230
1
A
B
C
D
E
F
mspol
lspol
spof
post
diapophysis
pocdf
neural canal
sprf
cprf
neural canal
sdf
post
hyposphene
neurocentral suture
pleurocoel
neural spine
2
A
B
C
D
neuro-central suture
pleuro-coel
neural canal
3
diapophysis
neural canal
A
B
diapophysis
C
neural canal
D
E
10 cm

Plate XXV (previous page): MACN-CH 230 dorsal series. Dorsal MACN-CH 230 1 in posterior (A), anterior (B), left lateral (C), right lateral (D), dorsal (E) and ventral (F) views. MACN-CH 230 dorsal 2 in lateral (A), posterior (B), dorsal (C) and ventral (D) views. MACN-CH 230 dorsal 3 in anterior (A), right lateral (B), posterior (C), left lateral (D), and ventral (E) views. Abbreviations: dp = diapophysis, nc = neural canal, ns = neural spine, pp = parapophysis, pre = prezygapophysis, po = postzygapophysis, pocdf = postzygapophyseal centrodiapophyseal fossa, podl = postzygadiapophyseal lamina, ppdl= paradiapophyseal lamina, prcdf = prezygapophyseal centrodiapophyseal fossa, sdf = spinodiapophyseal fossa, spof = spinopostzygapophyseal fossa, sprl = spinoprezygapophyseal lamina.

Comparison with PVL 4170

This dorsal series matches *Patagosaurus* PVL 4170 in elongation of the neural arch and neural spine. However, notable differences are the rim over the anterior articular surface, not seen in *Patagosaurus* PVL 4170 (though to some extent seen in MACN-CH 936). Moreover, the lack of pneumaticity in the neural arches, even though this should be evident in at least a sub-adult (see ontogenetic stage), shows that this specimen might be different from *Patagosaurus*. The hypantrum is also not clearly present in PVL 4170, though it is in MACN-CH 934. Finally, the positioning of the diapophyses towards the dorsal side, is clearly different from PVL 4170, as well as any preserved and taphonomically unaltered diapophyses in MACN-CH 932. This could mean this specimen is different from *Patagosaurus fariasi*.

Comparison with *Volkheimeria*

Based on the elongation of the neural arch and spine, this specimen differs greatly from those of *Volkheimeria*. Also, no lateral pneumatic foramina are present, as in *Volkheimeria* PVL 4077 and *Patagosaurus* PVL 4170.

Ontogenetic stage

Based on the complete fusion of the neural arch with the centrum, with neurocentral sutures clearly visible, and the presence of intricate lamination and fossae, as well as the hyposphene and hypantrum complex, this specimen is an adult that was still growing at the time of death, and thus in MOS stage 4 for dorsals (Carballido and Sander, 2014).

MACN-CH 232

This series from Cerro Condor Sur is a mixture of several elements (Plate XXV), which were probably not all found in association, as the size differs per element. Most elements, however, are incomplete and show unfused sutures, indicating a young ontogenetic stage.

The series has a partial cervical centrum, a partial sacral neural arch, three caudal neural arches, several caudal centra, which have unfused neurocentral sutures, a dorsal rib, and an unidentified element, possibly part of an ilium.

The cervical centrum (Plate XXVI 1) is badly preserved, with only the posterior half containing the cotyle, lateral and ventral facets present. However, it shows a prominent pleurocoel (Plate XXVI 1B,C), with clearly defined anterior, posterior, dorsal and ventral margins, as in PVL 4170 cervicals. In ventral view, a ventral keel is visible (Plate XXVI 1A), as in PVL 4170. In posterior view, the cotyle is dorsoventrally flattened, and transversely wide (Plate XXVI 1E). The dorsal rim shows a heart-shaped gully for the neural canal, as in PVL

4170. One small cervical rib shaft is partially preserved (Plate XXVI 2), which is dorsoventrally longer than transversely wide, as in most cervical ribs of sauropods. It is an elongated, slender element, with no cervical head preserved.

The sacral neural arch (Plate XXVI 8) shows a transversely wide and dorsoventrally elongated neural canal (Plate XXVI 8A,B), as in MACN-CH 935, 934 and PVL 4170. The neural arch is transversely wide, and shows lateral flaring out of the sacral ribs, however, this part is not completely preserved. The element shows a partial right prezygapophyseal base (Plate XXVI 8B), which shows that it canted towards the lateral side, with the prezygapophyseal articular surface probably canting towards the medial side. In posterior view, a clear hyposphene is seen as a triangular protrusion (Plate XXVI 8A), with shallow round fossae on each lateral side.

The caudal neural arches and spines show the postzygapophyses to be partially preserved, as well as the neural spine (Plate XXVI 6A,B, 7A-D). The postzygapophyses project posteriorly as triangular protrusions. The spine is rugosely striated on anterior and posterior sides, and in anterior view, the spine widens towards the tip. The tip of caudal neural arch 7 (Plate XXVI 7B,C) itself is saddle-shaped in lateral view (Plate XXVI 7B,C). This is also seen in MACN-CH 1299 and PVL 4170. One small caudal neural arch is preserved (Plate XXVI 9), with only rudimentary prezygapophyses (Plate XXVI 9A), postzygapophyses (Plate XXVI 9B) and a dorsoventrally short, axially wide neural spine preserved. In lateral view, the spine tip shows a faint saddle-shape (Plate XXVI C,D). In anterior and posterior view, the spine is transversely narrow, and shows a slight transverse widening at the tip. All zygapophyses are visible as rounded-to-triangular bulges.

There are two anterior caudal centra (Plate XXVI 3-4), which are dorsoventrally elongated but axially short. These centra are heart-shaped (Plate XXVI 3,4- E,F), with a tapering, pointed ventral side, which in ventral view shows a ventral keel (Plate XXVI 4B). Ventral keels in Jurassic sauropod caudal vertebrae are known from an unnamed caudal from the north of the UK (Manning et al., 2015) and from an unnamed dorsal from the Oxford Clay of Peterborough, UK (Holwerda and Liston, 2017). There are no chevron facets present. Both are amphicoelous (Plate XXVI 3,4C,D). The third small caudal (Plate XXVI 5) is a middle caudal, which a more elongated axial central length (Plate XXVI 5A-D). The anterior articular surface is rounded to rectangular (Plate XXVI 5E), the posterior is rounded (Plate XXVI 5F). It shows neither ventral keel, nor chevron facets, in ventral view (Plate XXVI 5B).

One dorsal rib in two fragments is also preserved at the head (Plate XXVI 11); it is seen to curve convexly dorsally, and has a rugose dorsal/lateral rim for ligament attachment. As in the dorsal ribs of MACN-CH 935, the tuberculum is more elongated and has a larger articular surface than the capitulum (Plate XXVI 11 A-D). Besides a shaft fragment (Plate XXVI B,C) the rest of the shaft is not preserved, but the cross-section is round to rhomboid (Plate XXVI 11 F).

Finally, a D-shaped flat plate-like element is preserved as part of this series (Plate XXVI 1). It is not entirely certain what this element is, however there is a rugose tubercle on the posterior side (Plate XXVI 10 B,D), as well as a thickening at the midsection in dorsal view (Plate XXVI D), therefore it could be a part of the posterior lobe of an ilium, containing the ischial peduncle. However, similar elements have been recovered for *Spinophorosaurus*, and identified as either spinous processes at the end of the tail (Remes et al., 2009) or, alternatively, as clavicles (Tschopp and Mateus, 2013a).


MACN-CH 232
1 A
ventral keel
B
pleurocoel
C
D
unfused neurocentral suture/neural canal
E
2
3A
neural canal
B
chevron facet
C
D
E
F
4 A
unfused neurocentral sutures
B
ventral keel
C
D
E
F
5 A
transverse process
B
C
D
E
F
neural spine
post-zyga-pophysis
prezyga-pophysis
6 A
B
saddle-shape
7 A
B
C
D
hyposphene
preygapophysis
8 A
neural canal
B
9 A
preygapophysis
B
postzygapophysis
neural spine
A
prezygapophysis
B
C
D
10 A
B
C
E
D
11 A
capitulum
tuberculum
B
C
D
E
F
10 cm

Plate XXVI (previous page): MACN-CH 232 elements. MACN-CH 232 1 cervical in ventral (A), left lateral (B), right lateral (C), dorsal (D) and posterior (E) views. MACN-CH 232 cervical rib 2. MACN-CH 232 anterior caudal centrum 3 in dorsal (A), ventral (B), left and right lateral (C,D) anterior (E) and posterior (F) views. MACN-CH 232 anterior caudal centrum 4 in dorsal (A), ventral (B),right and left lateral (C,D), posterior (E) and anterior views (F). MACN-CH 232 middle caudal centrum 5 in dorsal (A), ventral view (B), right lateral (C), left lateral (D), anterior (E), and posterior views (F). MACN-CH 232 caudal neural arch 6 in right lateral (A) and left lateral (B) view. MACN-CH 232 caudal neural arch 7 in anterior (A), left lateral (B), right lateral (C) and dorsal views (D). MACN-CH 232 sacral neural arch 8 in posterior (A) and anterior (B) views. MACN-CH 232 caudal neural arch 9 in anterior (A), posterior (B), right lateral (C), left lateral (B), ventral (C) and dorsal (D) views. MACN-CH 232 plate-like ?iliac element 10 in lateral (A), medial (B), ?ventral (C), ?dorsal (D), and anterior (E) views. MACN-CH 232 dorsal ribfragment 11 in anterior (A), posterior (D) and lateral (E) views, with shaft fragment in anterior (B), posterior (C) and distal (f) views.

Comparison to *Patagosaurus* PVL 4170

Several features of this series show similarities with PVL 4170, as well as to MACN-CH 935. However, the ventral keel of the caudals is a feature not seen in *Patagosaurus*, nor in any of the other anterior caudal centra preserved for any of the PVL or MACN-CH series, save for MACN-CH 934. In the latter caudal, the keel is visible in a more middle caudal centrum, which makes direct comparison with the anterior caudal centra of MACN-CH 232 not possible. The material is not complete enough to make any valid direct comparisons, and therefore must remain sauropod indet.

Comparison to *Volkheimeria*

Even though there is a shared ontogenetic stage (see ontogenetic stage), there is not enough material to compare to *Volkheimeria*.

Ontogenetic stage

Based on unfused neurocentral sutures on all axial elements, including the caudals, as well as only rudimentary forms of zygapophyses and laminae on the small caudal neural arch and spine (Plate XXVI MACN-CH 232 9), these elements was most likely belonged to one or several early juvenile sauropods in MOS stage 1. The caudal neural arches MACN-CH 232 6 and 7 show a slightly more complex morphology; however, they are unfused to any centrum, therefore these belonged to an individual or individuals in MOS stage 2. The ribs, or plate-like structure do not give enough information to confidently assign them to any MOS stage.

MACN-CH 221-223

This material consists of a partially-preserved cervical and three anterior to mid-caudals. Though allegedly from Cerro Condor Sur, the coloration of the bones is more like that of Cerro Condor Norte. Moreover, several axial elements (two ischia, and a sacral centrum and neural arch) that are either MACN-CH 221 or MACN-CH 223 are allegedly in association, however, it is unclear if this is the case.

The cervical (Plate XXVII cervical A-C), misses the neural arch and spine, however, the prezygapophyses are preserved (Plate XXVII cervical B,C). There is no clear sign of any neurocentral sutures, however, there is also no clear sign of damage, therefore, it can be assumed this individual was of an early MOS stage (MOS 2) with unfused neural arches. The centrum is opisthocoelous (Plate XXVII cervical C). It shows a constriction right behind the condyle, after which the centrum widens both dorsoventrally in lateral view, as well as

transversely in ventral view (Plate XXVII cervical A,C). In ventral view, the centrum shows a clearly defined ventral keel, however, the condyle is slightly damaged ventrally. The posterior ventral half of the centrum is also not very well-preserved, however, a shallow, triangular to rectangular depression is seen where the ventral keel merges with the centrum surface (Plate XXVII cervical A). The lateral side of the centrum shows a relatively deep pleurocoel, which is deeper anteriorly than posterior. Finally, the centrum seems slightly flattened dorsoventrally, however, this could be due to taphonomy .

The prezygapophyses are short and stout anterior projections; they project with an angle of about 95-100 degrees to the vertical (PlateXVIIcervical C). The prezygapophyseal stalks are relatively thick in dorsal view, and there is only a narrow, V-shaped space between each stalk, unlike the large U-shaped space of posterior cervicals (PlateXVIIcervical A,B). This, together with the relative elongation of the cervical, shows that it was an anterior to mid-cervical.

MACN-CH 221-223 consists of an isolated partially preserved sacral vertebra, as well as two ischia which are not from the same individual (Plate XXVII). In fact, one ischium has a different collection number, even though it was aggregated with MACN-CH 223. This ischium could be the second ischium belonging to MACN-CH 934 (O.Rauhut, pers.comm.), due to similarities in size. At present it is unclear if this association exists, however, future study on MACN-CH 934 will reveal any further associations.

The sacral (Plate XVII) is probably one of the more anterior ones of the sacrum, as the sacral ribs are anteriorly convex (Plate XVII sacral A), and bend towards the posterior side, which is seen in anterior to middle sacrals (Plate XVII sacral C,D). The anterior articular surface is oval and dorsoventrally longer than transversely wide (Plate XVII sacral A). The posterior articular surface is more teardrop-shaped (Plate XVII B). Both have a flat articular surface. The sacral ribs project from the lateral ventral side as C-shaped, axially flattened plates, which connect dorsally to the neural arch by spdl (Plate XVII sacral C,D). The spdl is dorsally elevated, so

that the neural canal is encased between sheets of bone, as in anterior caudals showing a high projecting ACTP (Gallina and Otero, 2009). This shows the sacral to probably have been more middle-posterior. The neural canal is oval and dorsoventrally longer than transversely wide (Plate XVII sacral A,B). The neural arch is broken, however, two sprl are visible anteriorly, and posteriorly, the ventral base of the postzygapophyses is visible; these are triangular in shape.

The caudals (Plate XXVII) consist of two anterior middle caudals and one middle caudal. None have the complete neural spine preserved, however, all have the centrum, diapophyses, prezygapophyses and part of the neural arch (partially) preserved. The anterior caudals (Plate XXVII caudal 1,2 C,D) show an axially short but dorsoventrally long centrum. The anterior articular surface is oval in shape (Plate XXVII caudal 1,2 A), while the posterior articular surface is slightly more heart-shaped (Plate XXVII caudal 1,2 B). In lateral view, the centrum shows a strong concavity of the ventral surface, with ventral expansions of the articular surfaces on each side (Plate XXVII caudal 1,2 C,D). The neural canal on the anterior side is more triangular in shape, and in posterior view is more oval in shape (Plate XXVII caudal 1,2 A,B). The diapophyses project laterally and posteriorly as small, dorsoventrally flatted protrusions. The articular surface of the diapophyses is rounded to oval in dorsal view (Plate XXVII caudal 1,2 C,D). The prezygapophyses are small and stout, and project anteriorly and strongly dorsally. The neural arch is not clearly developed, however, the base of the neural spine is seen to project dorsally and posteriorly.

The middle caudal (Plate XXVII middle caudal A,B) is more elongated axially than the anterior caudals, and is less elongated dorsoventrally than the anterior ones. The articular surfaces are of a similar shape as in the more anterior caudals. The diapophyses project laterally, and not dorsally, and the base of the neural spine projects strongly posteriorly and slightly dorsally.

The first ischium (Plate XXVII 223 ischium A-C) is stout, and does not possess the slender shaft as in MACN-CH 933. The structure shows a strong curvature which is not seen in any other ischium of the associated material; it curves strongly convexely towards the lateral side. It is unclear whether this is a real-life curvature or if this is caused by taphonomy or a pathology. The proximal end of the ischium shows a rectangular and rugosely pitted ischial peduncle (Plate XXVIII 223 ischium A-C), and a more elongated, triangular pubic peduncle, which is also sharply triangular in lateral view.

The second ischium (numbered MACN-CH 221; Plate XXVIII) is more slender than the first, and smaller, as well as more elongated (Plate XXVII 221 ischium A-G). It does not show the strong curvature of the former ischium MACN-CH 223 (Plate XXVIII 221 ischium A-B). The pubic peduncle is damaged (Plate XXVIII 221 ischium F). The iliac peduncle, however, is also distinguished from the other ischium by being more blunt (Plate XXVIII 221 ischium G). The ischium MACN-CH 221 differs from the first ischium, and was originally thought to belong to MACN-CH 934. The high elongation also offsets it from *Patagosaurus*, therefore it is possible it belonged to the smaller individual that is MACN-CH 934. The slightly damaged proximal end, however, makes it impossible to compare. Future studies (e.g. morphometrics) might find similarities/differences between the elements of MACN-CH 934 and MACN-CH 221.

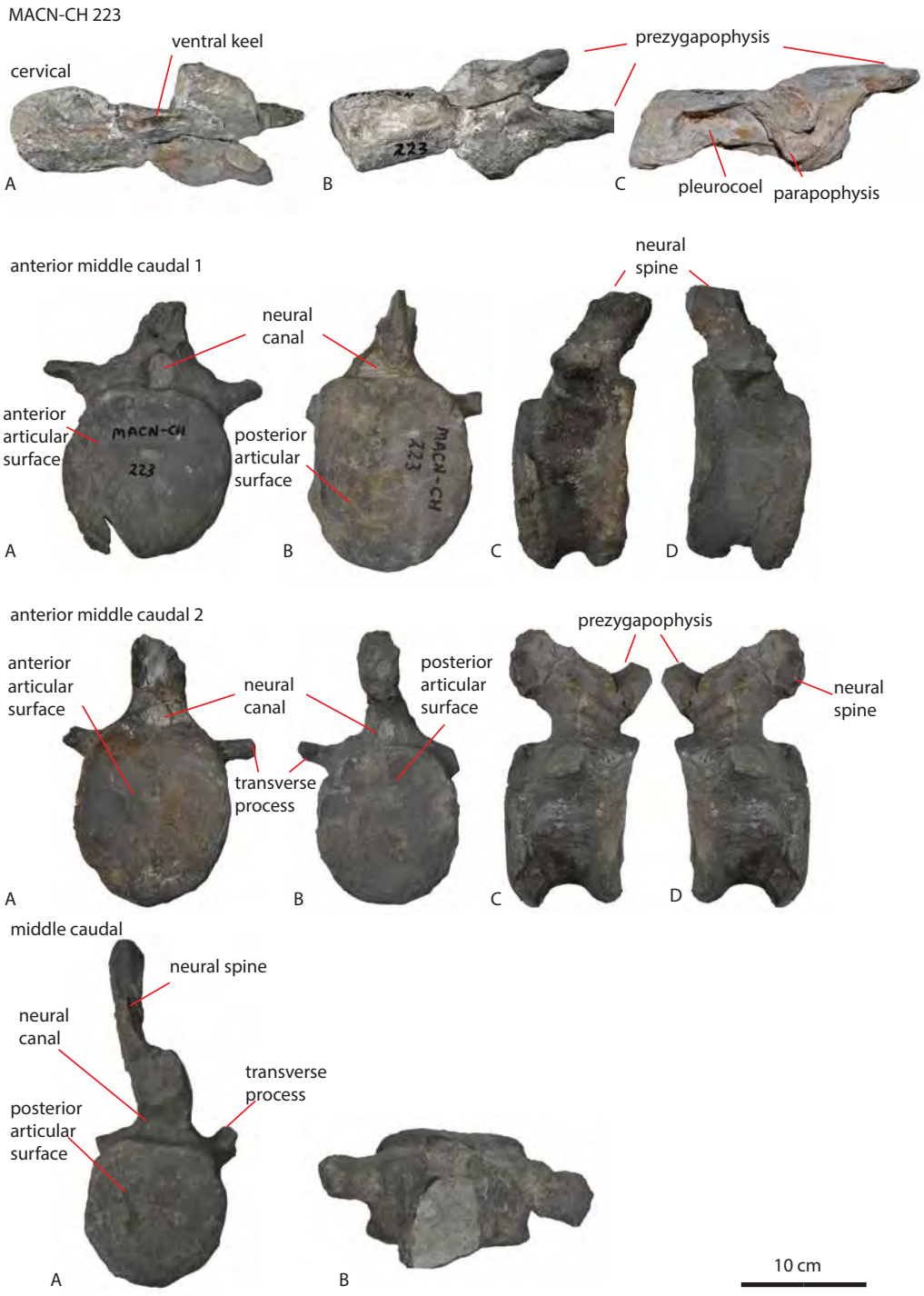

Plate XXVII: MACN-CH 223 elements. MACN-CH 223 cervical in ventral (A), dorsal (B), lateral (C) views. MACN-CH 223 anterior middle caudal in anterior (A), posterior (B), left lateral (C), and right lateral (D) views. MACN-CH 223 middle caudal 2 in anterior (A), posterior (B), right lateral (C), left lateral (D) view. MACN-CH 223 middle caudal in posterior (A) and dorsal (B) views.

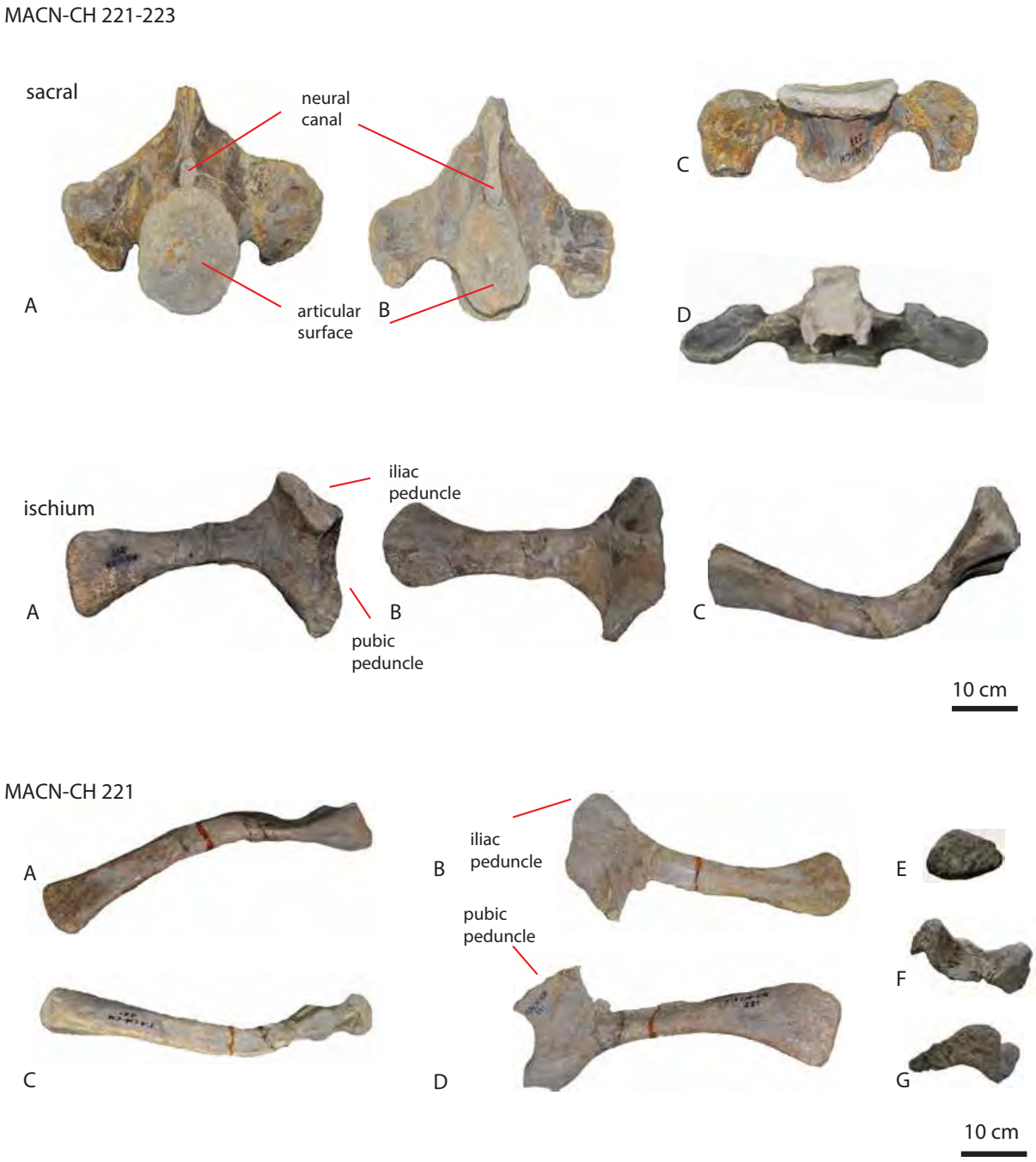

Plate XXVIII: MACN-CH 223-221 elements. MACN-CH 223 sacral centrum and neural arch in anterior (A), posterior (B), ventral (C) and dorsal (D) views. MACN-CH 223 ischium in medial (A), lateral (B) and dorsal (C) views. MACN-CH 221 ischium in dorsal (A), posterior (B), ventral (C), anterior (D) views, with cross-section of the shaft (E), the pubic peduncle (F) and the iliac peduncle (G).

Comparison to *Patagosaurus* PVL 4170

MACN-CH 223 shows similarities with the holotype of Patagosaurus in the elongation of the cervical centrum, the anteriorly projecting and stout prezygapophyses, and the lateral pleurocoel, which is deeper anteriorly.

The sacral vertebra of MACN-CH 223 show similarities with *Patagosaurus i*n that the centrum is dorsoventrally elongated, as well as having C-shaped sacral ribs and a high projection of the spdl running along the lateral sides of the neural arch.

The caudals of MACN-CH 223 show similarities with the holotype caudals, however, these are also more generic basal eusauropod cervical and caudal morphologies (e.g. *Spinophorosaurus, Cetiosaurus, Tazoudasaurus*). Therefore, there is not enough information to definitely assign this material to *Patagosaurus*, though it is likely the material is *Patagosaurus*. There is no novel information on this material, nor can it be compared to *Volkheimeria* PVL 4077.

The ischia, however, are difficult to determine. The first ischium, MACN-CH 223, shows a morphological difference from other confirmed *Patagosaurus* ischia by being strongly convexely curved laterally. None of the elements have any osteological overlap with *Volkheimeria*.

3.6 **Discussion**

3.6.1 Species diversity overview from Cerro Condor Norte and Sur

Based on similarities with the holotype, the following specimens are considered to be *Patagosaurus*; MACN-CH 933, MACN-CH 932, MACN-CH 935 from Cerro Condor Norte, MACN-CH 936, MACN-CH 1299, MACN-CH 232 from Cerro Condor Sur.

MACN-CH 933 shares similarities with cervical centra and dorsal neural arches of the holotype. The femoral morphology is slightly different, as well as the pubis, however, this could be due to ontogeny as MACN-CH 933 is in MOS 1 (see Ontogenetic features further in Discussion). As the tibia ascribed to this specimen is very similar to the adult form in MACN-CH 1299, a case could be made that, due to the morphological dissimilarities between limb bones of these specimens and the holotype, these are an adult and juvenile of a taxon different from *Patagosaurus*. However, as there is not much material to support this assertion, the dorsal vertebral morphology is similar to that of PVL 4170, and as dorsal vertebral morphology is defining for sauropod taxonomy (see Carballido et al., 2012; Wilson, 2012, 2002, 1999; Wilson et al., 2011), the most conservative approach is to see MACN-CH 933 as a juvenile *Patagosaurus*. Moreover, the ilium element is also similar to that of the holotype, in that it shares the prominent hook-shaped anterior lobe that is used to define the holotype. Finally, the dentary and dentition were both already ascribed to *Patagosaurus* in previous studies (Rauhut, 2003; Holwerda et al., 2015).

MACN-CH 932 shares morphological features on the dorsal neural arches with PVL 4170, which are prominent features used to define the holotype; the CDF, the neural spine elongation, the hyposphene. The pubis also shows similarities with the holotype. As there is unfortunately no confirmed humerus or forelimb elements of the holotype, these elements cannot be ascribed to *Patagosaurus* for certain.

MACN-CH 935 shows a clear overlap between the dorsal neural arches of this specimen and the holotype, as well as with MACN-CH 932. It has well-developed pneumatic structures in the CDF, as well as similar dorsal neural arch lamination and hyposphene morphology as PVL 4170. The caudals, moreover, are very similar to anterior caudals of PVL 4170, showing the same dorsoventral elongation of the centrum and the neural spine, together with the saddle-shaped neural spine tip. The ilium of this specimen, however, is different to that of the holotype, and shows more morphological affinities with that of *Barapasaurus* (Bandyopadhyay et al., 2010), and to a lesser extent with that of *Lapparentosaurus*. As the association of this ilium and the rest of MACN-CH 935 is not clear, however, it could be that this ilium represents yet another taxon in the Cerro Condor bonebeds. Unfortunately, the ilium of *Volkheimeria* (Bonaparte, 1979; Bonaparte, 1986a) is incomplete, therefore it cannot be compared with this ilium.

MACN-CH 1299 and MACN-CH 231 both show morphological overlap with *Patagosaurus* PVL 4170 in the caudal vertebral morphology. Even though caudal morphology is conservative in sauropods, anatomical features are becoming more well-known on caudals, making taxonomic comparisons possible (see Mannion et al., 2013; Wedel and Taylor, 2013; Manning et al., 2015; Mocho et al., 2016a, 2016b, 2016c, Holwerda and Liston, 2017). Therefore, through this morphological overlap with the holotype, these specimens can safely be referred to as *Patagosaurus*.

Finally, specimen MACN-CH 936 shows a near-complete anterior cervical series (axis and cervical 1-8), which shows partial overlap with *Patagosaurus* PVL 4170, which lacks a complete cervical series. The anteriormost cervicals shed new light on cervical pneumaticity of *Patagosaurus*, and therefore on early sauropod cervical pneumaticity. The cervicals of prosauropods, as well as mamenchisaurs, *Klamelisaurus*, and neosauropods, are known to be pneumatic (Schwarz et al., 2007; Schwarz and Fritsch, 2006; Wedel, 2007, 2003a, 2003b) and other basal eusauropods show pneumatic structures, however, in these early Jurassic

forms, only *Patagosaurus* so far shows complete perforation of the pleurocoel, which could be a tentative autapomorphy for the taxon. It could also be an ontogenetic signal (see Ontogenetic features in Discussion). With the inclusion of these cervicals, the earlier estimation of Chapter 2 for the holotype that *Patagosaurus* had between around 13-15 cervical vertebrae is demonstrated to be correct.

The specimen MACN-CH 934 from Cerro Condor Sur is shown to be different from *Patagosaurus*, by its dentition in a previous study (Holwerda et al., 2015). The dorsal neural arches were originally ascribed to *Patagosaurus*, however, there are several morphological differences found; most prominently the existence of an spdl, as well as the existence of a hypantrum together with the hyposphene, which is not found in other juvenile *Patagosaurus* or even in the holotype, only in MACN-CH 936, a fully grown adult. Moreover, the presence of an ambiens process on the pubis hints at a more derived taxon than *Patagosaurus*. A phylogenetic analysis, incorporating the characters on dentition, maxillae, and dorsal neural arches as well as on the pubis will clarify the position of this specimen, relative to *Patagosaurus*, *Volkheimeria*, and other Early and Middle Jurassic Gondwanan and Laurasian sauropods.

The specimen MACN-CH 230 from Cerro Condor Sur also shows some differences from the other *Patagosaurus* specimens. First of all, the size and height of this (sub)adult is much smaller than that of the holotype PVL 4170 or of the fully-grown adult MACN-CH 936. Next to this, the positioning of the diapophyses is more similar to those in mamenchisaurs and *Klamelisaurus* than in *Patagosaurus*. This, together with the morphology of the hypantrum, similar to those in the tentatively more derived MACN-CH 934, gives reason to believe that this specimen is also different from *Patagosaurus*, *Volkheimeria*, and, with the positioning of

the diapophyses, also of MACN-CH 934. Therefore, this specimen could possibly be a small sauropod taxon. As the taxon is a (sub)adult and of small size, it could be that it coexisted with the other sauropods in the Cañadón Asfálto Fm by being a 'dwarf-type' sauropod, (Buffetaut et al., 2011)feeding on lower/different vegetation than the dominant, larger taxa. Dinosaurs also tend to reach smaller maximum body sizes during more humid climatic conditions, as is found in the Morrison Fm of the USA (S. Maidment, pers. comm.; Engelmann et al., 2004). By being a dwarf species, resource partitioning by means of vertical stratification would be possible (Engelmann, Chure & Fiorillo, 2004). As Cerro Condor Sur consists of several layers of bonebeds, accumulated over a potentially longer timespan than Cerro Condor Norte, this specimen could come from a different layer than the *Patagosaurus* assemblage, and could indicate some sort of climatic change compared to the conditions of Cerro Condor Norte, and also between the different strata of Cerro Condor Sur. The Cañadón Asfálto Fm does show evidence of climate cycles of more humid and more dry conditions (Volkheimer et al., 2008). Moreover, sauropod dwarfism is known from insular settings from the Late Jurassic of Europe (*Europasaurus*, Carballido and Sander, 2014; Marpmann et al., 2015; Sander et al., 2006) and the Late Cretaceous of Europe (*Magyarosaurus* Stein et al., 2010), and one specimen from the Middle Jurassic of Europe was previously thought to be a dwarf, however, this has been disproved. Finally, one study tentatively concludes that a dwarf-type sauropod existed within a non-insular ecosystem in the Late Jurassic of the Morrison Formation of the USA (Waskow & Sander, 2014; Waskow, 2017). However, there is not much material of specimen MACN-CH 230 to verify dwarfism, and therefore more osteological study and phylogenetic study is necessary for this specimen, as well as more information on vegetation and climate from the Cerro Condor bonebeds.

Other associated material (MACN-CH 219, 223(+221), 231) is too fragmentary to be ascribed to any taxon, and for the time being will remain Sauropoda indet.

To summarize, the dominant taxon in the Cerro Condor bonebeds is by far *Patagosaurus*, followed by *Volkheimeria* and one or two other taxa of sauropods. Interestingly, none of the other specimens have been found to have complete overlap with *Volkheimeria*. This could be due to a sampling and/or preservational bias, where there is more material of *Patagosaurus* to compare material with. However, it could also be that *Volkheimeria* was a more rare taxon during the Early-Middle Jurassic in South-West Gondwana. As *Volkheimeria* is shown to be more basal than *Patagosaurus*, it could be that this type of basal sauropod was diminishing, and that more derived sauropods like *Patagosaurus* and MACN-CH 934 were becoming more dominant. A complete revision of *Volkheimeria* is needed, however, to reappraise phylogenetic relationships with *Patagosaurus* and MACN-CH 934, and possibly MACN-CH 230. Cerro Condor Norte is completely *Patagosaurus* material, which could prove the theory correct that this is a gregarious assemblage (Coria, 1994). However, this cannot be proven for certain, as the dominance of Patagosaurus in the region could show a preservational bias for Cerro Condor Norte.

Cerro Condor Sur is by far the most species-rich assemblage, hinting at a different taphonomical structure and preservation than Cerro Condor Sur. Unfortunately, no complete record of Cerro Condor Sur was ever made, therefore, the precise taphonomy will remain unknown.

3.6.2 New elements to be added to the taxon *Patagosaurus,* with new phylogenetic characters, and implications for the taxon *Patagosaurus*

Characters that are new for *Patagosaurus*, (i.e. not present in the holotype PVL 4170)

New elements from this series of associated specimens, are the cranial elements (MACN-CH 933 dentary, PVL 4076 premaxilla, and dentition), pectoral elements, a humerus, radius and ulna as well as a sternal plate for MACN-CH 932, a tibia for MACN-CH 933 and MACN-CH 1299, as well as a scapula-coracoid complex for MACN-CH 935, and finally, a near-complete cervical series for MACN-CH 936.

The humerus has a low Gracility Index, which can be used as a phylogenetic character, as well as showing a robustness in the forelimbs of *Patagosaurus* compared to other sauropods, even contemporaneous ones. This is in concurrence with the robustness of the hindlimb (the femur), found in Chapter 2. Moreover, the ulna shows traits that are different from *Lapparentosaurus*, as well as from more derived sauropods, in that the triradiate proximal surface is very asymmetrical. The ulna does not contain much phylogenetic information.

The tibiae, both juvenile and adult, show an absence of a pronounced cnemial crest, as well as an absence of the 'step' for the medial malleolus, which can be coded as a phylogenetic character.

The scapular proximal blade is very similar to *Cetiosaurus*, confirming a morphological affinity between the two taxa. The distal shaft, however, is different from other sauropods, and the ventral curvature could be seen as another potential autapomorphy, and therefore as a phylogenetic character. The coracoid shows a wide coracoidal notch, which can be used as a character.

The taxon now has more characters, either as new characters (see next chapter) or as information to code for known characters in existing datamatrices, with which to create a reliable phylogenetic analysis, which will be performed in the next chapter.

Existing morphological details to be coded as phylogenetic characters

The anterior cervical pneumaticity is complicated to use as a character, because other basal sauropods have not received much study in this regard. A revision of pneumatic characters in cervicals of Early – Middle Jurassic sauropods is therefore necessary, which is beyond the scope of this paper. The cervical count can be better established, however, and also the morphology of the pleurocoel is better understood, and these can be used as a phylogenetic character for *Patagosaurus*.

The pneumatic foramen (CDF) which is visible in the holotype PVL 4170 is repeated in several associated specimens (MACN-cH 932, 935, 936) which can be confirmed therefore as phylogenetic character. Also, the small aliform process on posterior dorsals of larger individuals (MACN-CH 935, 936) can be used.

The caudal vertebrae, especially the anterior caudal vertebrae, of the associated specimens confirm the 'saddle-shape' character of the neural spine for *Patagosaurus*. Whether the overall sinusoidal shape of the neural spine of *Patagosaurus* can be used will be investigated in the next chapter.

The slightly convex shape of the femur, shown both in the holotype PVL 4170 and in MACN-CH 933, will be investigated in the last chapter on geometric morphometrics of Jurassic sauropods.

3.6.3 Ontogenetic features on vertebrae of *Patagosaurus*

The ontogenetic stages preserved in *Patagosaurus* associated material are MOS 1; early juvenile (MACN-CH 933), MOS 2; juvenile (MACN-CH 932), and MOS 3-4; mature (MACN-CH 935).

The axial series, both cervicals and dorsals, for the MOS 2 (MACN-CH 932), 3 and 4 (MACN-CH 935 and MACN-CH 936) remain consistent in lamination and distribution of fossae, even the pneumatic CDF structure, when compared with the holotype PVL 4170 (which is in MOS 4). The differences lie in the amount of dorsoventral elongation of the neural arch, and the development of the hyposphene, as well as the aliform process in dorsal vertebrae. This implies that from an early age onwards, most of the characters that are definable at a taxonomic level have appeared, and are a set feature, despite neural arch fusion not yet being present. This is consistent with more derived sauropods in ontogenetic series, and although in *Europasaurus* the laminae complexity is not as high as in *Patagosaurus* MOS 2, it is already complex in a juvenile *Barosaurus* (Hanik et al., 2017; Carballido and Sander, 2014). This might imply a difference in ontogenetic development between more basal and more derived sauropods. A study including other basal sauropod ontogenetic series will clarify this, however, these studies have not been performed yet and are outside the scope of this study (see Allain and Aquesbi, 2008). The difference in the elongation of the neural arch could be attributed to the smaller size of juvenile sauropods. The hyposphene is comparatively larger in juveniles than in adults, which could be a structurally related development; as neurocentral suture support is lacking (Fronimos & Wilson, 2017), the unfused vertebrae would need more structural support, and potentially require larger hyposphenes to interlock into the following vertebrae. The lack of aliform processes in juveniles, and the expression of these in only the latest stage of ontogenetic development,

hints at a similar structural support, moreover, because aliform processes are also absent from juvenile *Europasaurus* (Carballido et al., 2012).

It is interesting to note that there seems to be a discrepancy in the amount and timing of neurocentral suture fusion between dorsal and caudal vertebrae, as seen in MACN-CH 935. However, as said before, neurocentral sutures have been proven to improve axial skeletal stability (Fronimos & Wilson, 2017), possibly implying a more heavy weight and structural load on the tail of *Patagosaurus* during ontogeny, than on dorsal vertebrae. Another explanation is that neurocentral suture fusion is extremely asymmetrical in timing, even between different specimens of the same taxon at similar ontogenetic stages (Danny Vidal pers. comm.). In *Europasaurus*, as well as in an unnamed juvenile titanosaurifom, however, the dorsal and sacral neural arch fusion seems to precede the caudal neural arch fusion (Carballido et al., 2012; Carballido and Sander, 2014; Schwarz et al., 2007b), therefore showing a potential phylogenetic/taxonomic difference. This effect requires further study, which is beyond of the scope of this paper.

For MOS 1, (MACN-CH 933 and possibly MACN-CH 232) however, there are several differences between these juveniles and the adults/later-stage juveniles. First of all, the elongation index (EI) is much lower for these juveniles, implying a stoutness of the cervical series in juveniles, and potentially shorter necks, which in turn imply a difference in feeding ecology. A difference in dentition between young and adult sauropods has already been encountered in several studies (see Díez Díaz et al., 2013, 2012; Holwerda et al., 2015a; Holwerda et al., 2015b). Differences in feeding ecology have also been inferred for juvenile vs. adult diplodocid sauropods (see Holwerda et al., 2015; Whitlock et al., 2010).

Another detail that differentiates MOS 1 cervicals from the later stages, is the absence of the sprf and stprl. This could be due to the lack of elongation of the neural arch in these early juveniles, however, the later-stage juveniles also lack this elongation, but do show an stprl in the dorsals. Cervicals, however, are not preserved for these specimens, therefore it could

still be an early ontogenetic feature. The vertebrae of the early juvenile SMA 0009, however, also lack the single intrazygapophyseal lamina, even though the intrazygapophyseal laminae are present (Carballido et al., 2012).

3.6.4 Ontogenetic features on the axial and appendicular skeleton of *Patagosaurus*

Although there are not many appendicular elements that overlap, there are two femora of different ontogenetic stages, as well as pubes, ischia and ilia.

The femur of MACN-CH 933 shows morphological differences to PVL 4170, which seem to go beyond isometric growth. The femur of MACN-CH 933 is not as transversely wide nor as anteroposteriorly compressed as in the holotype. However, the femoral head and distal condyles are similarly pronounced in both specimens, and the 4th trochanter is placed posteromedially in both. In more derived sauropods, ontogenetic differences in appendicular bones are distributed dissimilarly over the skeleton. Even though substantial differences were found between the scapulae, coracoids, sternal plates and fibulae of adult and juvenile *Camarasaurus*, as well as in the unnamed titanosauriform SMA 0009 and adult titanosauriforms, only small differences were found in the limb bones, and those differences pertain mostly to roughness of articulation surfaces (Foster, 2005; Ikejiri, Tidwell & Trexler, 2005; Tidwell & Wilhite, 2005; Schwarz et al., 2007). Size differences were found to be isometric in the forelimbs of *Venenosaurus* as well (Tidwell & Wilhite, 2005). However, ontogenetic studies on basal sauropods (from the Early or Middle Jurassic) like *Tazoudasaurus* are still in progress (Allain & Aquesbi, 2008). The femur of PVL 4077 is similar in shape to that of MACN-CH 933, which could imply a plasticity in juvenile basal sauropod femora compaired to adults. As the forelimbs in more derived sauropods go through the most ontogenetic changes, the more basal sauropods might have the reverse, and have

more changes happen in the femora instead, hinting at a difference in gait and mobility and thus usage of fore- or hindlimbs.

The tibiae of *Patagosaurus*, however, show very little ontogenetic variation, as they both have the same shape and lack of expansion of the distal shaft, reinforcing the concept of isometrical growth of limb bones in all sauropods.

The ilia of MACN-CH 933, 932, 935 and the holotype are also similar, only differing in size. They show similar tapering of the anterior lobe, as well as a similar shape of the pubic peduncle. However, the size of the acetabulum differs; it is smaller in juveniles than in the more adult specimens. This could be due to the alleged isometric growth of the femoral head, which remains similar in morphology in both MACN-CH 933 and PVL 4170.

The ischia also show an isometric growth, as the length of the shaft increases, but the general morphology remains similar between MACN-CH 933 and PVL 4170. The only pelvic element that changes is the pubis, and this is only between MOS 1 and MOS 2-MOS 3 and 4. The pubis of MOS 1 MACN-CH 933 shows an open pubic foramen, which would probably have been enclosed by cartilage. In several dinosaurs, cartilage is replaced by bone during ontogeny, although this is not yet well-studied in sauropods, and thus far has only been found in early juvenile titanosaurs (Rogers et al., 2016; Hone, Farke & Wedel, 2016). The MACN-CH 932 (MOS 2) pubis is already similar to those of the (sub)adults MACN-CH 935 and PVL 4170.

3.7 Conclusions

Based on comparisons with the holotype, the following specimens can be added to the taxon *Patagosaurus fariasi*:

MACN-CH 933 as the youngest, earliest MOS stage *Patagosaurus*, MACN-CH 932 as a slightly larger, MOS stage 2 *Patagosaurus*, and MACN-CH 935 as a subadult *Patagosaurus* and PVL 4076 and 4176 as adult *Patagosaurus* material, possibly from the holotype, from Cerro Condor Norte.

From Cerro Condor Sur, the specimens MACN-CH 936 and MACN-CH 231 can safely be assigned to *Patagosaurus*.

This leaves the taxon with an ontogenetic series, as well as additional material for phylogenetic analyses.

The specimens MACN-CH 934, as well as MACN-CH 230, are most likely not *Patagosaurus fariasi*, and also probably not *Volkheimeria*. Therefore, they would appear to be different taxa, increasing the species diversity of the Cañadón Asfálto Fm. even more; in addition to *Patagosaurus fariasi*, *Volkheimeria chubutensis*, and an unnamed taxon at the MPEF collection, one taxon based on a juvenile MOS stage 2 sauropod MACN-CH 934 is now confirmed, as well as that of a possible small taxon, the MOS stage 3 or 4 MACN-CH 230.

MACN-CH 232, MACN-CH 219, 223, 244 and 245 do not contain enough information to rule them out as being *Patagosaurus* or another affinity, and this material will remain Sauropoda indet.

3.8 Acknowledgements

Acknowledgements go to Stella Maris Alvarez and Alejandro Kramarz, and the late Jaime Powell, who were invaluable in locating and providing access to most of the specimens in this study, as well as trying to make sense of the many (re)numberings, and incomplete collection references. Many thanks also to the other staff of the MACN for providing good working conditions, electrical heaters, cake for my birthday, and mate.

3.9 References

Alifanov VR., Averianov AO. 2003. *Ferganasaurus verzilini*, gen. et sp. nov., a new neosauropod (Dinosauria, Saurischia, Sauropoda) from the Middle Jurassic of Fergana Valley, Kirghizia. *Journal of Vertebrate Paleontology* 23:358–372.

Allain R., Aquesbi N. 2008. Anatomy and phylogenetic relationships of *Tazoudasaurus naimi* (Dinosauria, Sauropoda) from the late Early Jurassic of Morocco. *Geodiversitas* 30:345–424.

Bandyopadhyay S., Gillette DD., Ray S., Sengupta DP. 2010. Osteology of *Barapasaurus tagorei* (Dinosauria: Sauropoda) from the Early Jurassic of India. *Palaeontology* 53:533–569.

Barrett PM., Benson RB., Upchurch P. 2010. Dinosaurs of Dorset: Part II, the sauropod dinosaurs (Saurischia, Sauropoda) with additional comments on the theropods. In: *Proceedings of the Dorset Natural History and Archaeological Society*. Dorset Natural History and Archaeological Society, 113–126.

Barrett PM., Storrs GW., Young MT., Witmer LM. 2011. A new skull of *Apatosaurus* and its taxonomic and palaeobiological implications. In: *The annual Symposium on Vertebrate Palaeontology and Comparative Anatomy Abstract Volume*. 1606.

Berman DS., McIntosh JS. 1978. Skull and relationships of the Upper Jurassic sauropod *Apatosaurus* (Reptilia, Saurischia). *Bulletin of the Carnegie Museum of Natural History* 8:1–35.

Birkemeier T. 2011. Neurocentral suture closure in *Allosaurus* (Saurischia: Theropoda): sequence and timing. *Journal of Vertebrate Paleontology, Program and Abstracts* 2011:72A.

Bonaparte JF. 1979. Dinosaurs: A Jurassic Assemblage from Patagonia. *Science* 205:1377–1379.

Bonaparte JF. 1986a. The dinosaurs (Carnosaurs, Allosaurids, Sauropods, Cetiosaurids) of the Middle Jurassic of Cerro Cóndor (Chubut, Argentina). In: *Annales de Paléontologie (Vert.-Invert.)*. 325–386.

Bonaparte JF. 1986b. Les dinosaures (Carnosaures, Allosauridés, Sauropodes, Cétosauridés) du Jurassique Moyen de Cerro Cóndor (Chubut, Argentina). *Annales de Paléontologie (Vert.-Invert.)* 72:247–289.

Bonaparte JF. 1996. *Dinosaurios de America del Sur*. Museo Argentino de Ciencias Naturales. 174 pp.

Brochu CA. 1996. Closure of neurocentral sutures during crocodilian ontogeny: Implications for maturity assessment in fossil archosaurs. *Journal of Vertebrate Paleontology* 16:49–62.

Buffetaut E., Gibout B., Launois I., Delacroix C. 2011. The sauropod dinosaur *Cetiosaurus* Owen in the Bathonian (Middle Jurassic) of the Ardennes (NE France): insular, but not dwarf. Carnets de Géologie / Notebooks on Geology, 149-161.

Buffetaut E. 2005. A new sauropod dinosaur with prosauropod-like teeth from the Middle Jurassic of Madagascar. *Bulletin de la Société Géologique de France* 176:467.

Cabaleri N., Volkheimer W., Silva Nieto D., Armella C., Cagnoni M., Hauser N., Matteini M., Pimentel MM. 2010. U-Pb ages in zircons from las Chacritas and Puesto Almada members of the Jurassic Cañadón Asfalto Formation, Chubut province, Argentina. In: *VII South American Symposium on Isotope Geology*. 190–193.

Cabrera A. 1947. Un saurópodo nuevo del Jurásico de Patagonia. *Notas del Museo de la Plata Paleontologia.* 95:1–17.

Carballido JL., Rauhut OW., Pol D., Salgado L. 2011. Osteology and phylogenetic relationships of *Tehuelchesaurus benitezii* (Dinosauria, Sauropoda) from the Upper Jurassic of Patagonia. *Zoological Journal of the Linnean Society* 163:605–662.

Carballido JL., Marpmann JS., Schwarz-Wings D., Pabst B. 2012a. New information on a juvenile sauropod specimen from the Morrison Formation and the reassessment of its systematic position. *Palaeontology* 55:567–582.

Carballido JL., Salgado L., Pol D., Canudo JI., Garrido A. 2012b. A new basal rebbachisaurid (Sauropoda, Diplodocoidea) from the Early Cretaceous of the Neuquén Basin; evolution and biogeography of the group. *Historical Biology* 24:631–654.

Carballido JL., Sander PM. 2014. Postcranial axial skeleton of *Europasaurus holgeri* (Dinosauria, Sauropoda) from the Upper Jurassic of Germany: implications for sauropod ontogeny and phylogenetic relationships of basal Macronaria. *Journal of Systematic Palaeontology* 12:335–387.

Casanovas ML., Santafé JV., Sanz JL. 2001. *Losillasaurus giganteus* , un nuevo saurópodo del tránsito Jurásico-Cretácico de la cuenca de" Los Serranos"(Valencia, España). *Paleontologia i Evolució* 99–122.

Charig AJ. 1980. A diplodocid sauropod from the Lower Cretaceous of England. In: Jacobs LL ed. *Aspects of Vertebrate History. Essays in Honor of Edwin Harris Colbert.* Flagstaff: Museum of Northern Arizona Press, 231–244.

Charig AJ. 1993. *Cetiosauriscus* von Huene, 1927 (Reptilia, Sauropodomorpha). *Bulletin of Zoological Nomenclature* 50:282–283.

Chatterjee S., Zheng Z. 2002. Cranial anatomy of *Shunosaurus*, a basal sauropod dinosaur from the Middle Jurassic of China. *Zoological Journal of the Linnean Society* 136:145–169.

Chatterjee S., Zheng Z. 2005. Neuroanatomy and dentition of *Camarasaurus lentus*. In: Tidwell V, Carpenter K eds. *Thunder-lizards: The sauropodomorph dinosaurs*. Bloomington: Indiana University Press, 199–211.

Chure D., Britt B., Whitlock J., Wilson J. 2010. First complete sauropod dinosaur skull from the Cretaceous of the Americas and the evolution of sauropod dentition. *Naturwissenschaften* 97:379–391.

Cooper MR. 1984. A reassessment of *Vulcanodon karibaensis* Raath (Dinosauria: Saurischia) and the origin of the Sauropoda. *Palaeontologia africana* 25:203–231.

Coria RA. 1994. On a monospecific assemblage of sauropod dinosaurs from Patagonia: implications for gregarious behavior. *Gaia* 10:209–213.

Cúneo R., Ramezani J., Scasso R., Pol D., Escapa I., Zavattieri AM., Bowring SA. 2013. High-precision U-Pb geochronology and a new chronostratigraphy for the Cañadón Asfalto Basin, Chubut, central Patagonia: Implications for terrestrial faunal and floral evolution in Jurassic. *Gondwana Research* 24:1267–1275.

Díez Díaz V., Pereda Suberbiola X., Sanz JL. 2012. Juvenile and adult teeth of the titanosaurian dinosaur *Lirainosaurus* (Sauropoda) from the Late Cretaceous of Iberia. *Geobios* 45:265–274.

Díez Díaz V., Tortosa T., Le Loeuff J. 2013. Sauropod diversity in the Late Cretaceous of southwestern Europe: The lessons of odontology. *Annales de Paléontologie* 99:119–129.

Engelmann GF., Chure DJ., Fiorillo AR. 2004. The implications of a dry climate for the paleoecology of the fauna of the Upper Jurassic Morrison Formation. *Sedimentary Geology* 167:297–308.

Foster JR. 2005. New juvenile sauropod material from Western Colorado, and the record of juvenile sauropods from the Upper Jurassic Morrison Formation. In: Tidwell V, Carpenter K eds. *Thunder-lizards: The sauropodomorph dinosaurs*. Bloomington: Indiana University Press, 141–153.

Foster JR., Wedel MJ. 2014. *Haplocanthosaurus* (Saurischia: Sauropoda) from the lower Morrison Formation (Upper Jurassic) near Snowmass, Colorado. *Volumina Jurassica* 12:197–210.

Fronimos JA., Wilson JA. 2017. Neurocentral Suture Complexity and Stress Distribution in the Vertebral Column of a Sauropod Dinosaur. *Ameghiniana* 54:36–49.

Gallina PA., Otero A. 2009. Anterior caudal transverse processes in sauropod dinosaurs: morphological, phylogenetic and functional aspects. *Ameghiniana* 46:165–176.

Hanik GM., Lamanna MC., Whitlock JA. 2017. A Juvenile Specimen of *Barosaurus* Marsh, 1890 (Sauropoda: Diplodocidae) from the Upper Jurassic Morrison Formation of Dinosaur National Monument, Utah, USA. *Annals of Carnegie Museum* 84:253–263.

Harris JD. 2006. The significance of *Suuwassea emilieae* (Dinosauria: Sauropoda) for flagellicaudatan intrarelationships and evolution. *Journal of Systematic Palaeontology* 4:185–198.

Hatcher JB. 1903. Osteology of *Haplocanthosaurus*, with description of a new species and remarks on the probable habits of the Sauropoda and the age and origin of the *Atlantosaurus* beds: Additional remarks on *Diplodocus*. *Memoirs of the Carnegie Museum* 2:1–72.

Hauser N., Cabaleri NG., Gallego OF., Monferran MD., Nieto DS., Armella C., Matteini M., González PA., Pimentel MM., Volkheimer W., others 2017. U-Pb and Lu-Hf zircon geochronology of the Cañadón Asfalto Basin, Chubut, Argentina: Implications for the magmatic evolution in central Patagonia. *Journal of South American Earth Sciences* 78:190-212.

He X., Li K., Cai K. 1988. *The Middle Jurassic dinosaur fauna from Dashanpu, Zigong, Sichuan. Vol. IV. Sauropod Dinosaurs (2) Omeisaurus tianfuensis*. Chengdu, China: Sichuan Publishing House of Science and Technology. 143 pp.

Holwerda FM., Pol D., Rauhut OWM. 2015. Using dental enamel wrinkling to define sauropod tooth morphotypes from the Cañadón Asfalto Formation, Patagonia, Argentina. *PLOS ONE* 10:e0118100.

Holwerda F., Schmitt A D., Tschopp E. 2015. Ontogenetic differences in tooth replacement rates in adult and juvenile diplodocids. *Journal of Vertebrate Paleontology, Program and Abstracts 36 (Supplement 2),* 145A.

Holwerda FM., Liston JJ. 2017. An anterior sauropod caudal from the Peterborough Oxford Clay: Whose tail is it anyway? PeerJ Preprints 5:e3243v1,.

Hone DWE., Farke AA., Wedel MJ. 2016. Ontogeny and the fossil record: what, if anything, is an adult dinosaur? *Biology Letters* 12:20150947.

Ikejiri T., Tidwell V., Trexler DL. 2005. New adult specimens of *Camarasaurus lentus* highlight ontogenetic variation within the species. In: *Thunder-lizards: the Sauropodomorph dinosaurs*. Bloomington: Indiana University Press, 154–179.

Janensch W. 1935. Die Schädel der Sauropoden *Brachiosaurus*, *Barosaurus* und *Dicraeosaurus* aus den Tendaguruschichten Deutsch-Ostafrikas. *Palaeontographica* Supplement 7:145–298.

Janensch W. 1961. Die Gliedmassen und Gliedmassengürtel der Sauropoden der Tendaguru-Schichten. *Palaeontographica-Supplementbände* 4:177–235.

Lacovara KJ., Lamanna MC., Ibiricu LM., Poole JC., Schroeter ER., Ullmann PV., Voegele KK., Boles ZM., Carter AM., Fowler EK., others 2014. A gigantic, exceptionally complete titanosaurian sauropod dinosaur from southern Patagonia, Argentina. *Scientific Reports* 4:srep06196.

Lallensack JN., Klein H., Milàn J., Wings O., Mateus O., Clemmensen LB. 2017. Sauropodomorph dinosaur trackways from the Fleming Fjord Formation of East Greenland: Evidence for Late Triassic sauropods. *Acta Paleontologica Polonica* 66:(4) 833-843

Liston JJ. 2004a. An overview of the pachycormiform *Leedsichthys*. *Mesozoic Fishes*:379–390.

Liston JJ. 2004b. A re-examination of a Middle Jurassic sauropod limb bone from the Bathonian of the Isle of Skye. *Scottish Journal of Geology* 40:119–122.

Liston JJ., Noè LF. 2004. The tail of the Jurassic fish *Leedsichthys problematicus* (Osteichthyes: Actinopterygii) collected by Alfred Nicholson Leeds-an example of the importance of historical records in palaeontology. *Archives of natural history* 31:236–252.

Liu LKYC-Y., Zheng-Xin JW. 2010. A New Sauropod from the Lower Jurassic of Huili, Sichuan, China. *Vertebrata Palasiatica* 3: 185-202.

Madsen JH., McIntosh JS., Berman DS. 1995. Skull and atlas-axis complex of the Upper Jurassic sauropod *Camarasaurus* Cope (Reptilia: Saurischia). *Bulletin of Carnegie Museum of Natural History* 31:1–115.

Maltese A., Tschopp E., Holwerda FM., Burnham DA. 2018. The real Bigfoot: a pes from Wyoming, USA is the largest sauropod pes ever reported and the northern-most occurrence of brachiosaurids in the Upper Jurassic Morrison Formation. *PeerJ e5250*.

Manning PL., Egerton VM., Romano M. 2015. A New Sauropod Dinosaur from the Middle Jurassic of the United Kingdom. *PLOS ONE* 10:e0128107.

Mannion PD. 2009. A rebbachisaurid sauropod from the Lower Cretaceous of the Isle of Wight, England. *Cretaceous Research* 30:521–526.

Mannion PD., Upchurch P., Barnes RN., Mateus O. 2013. Osteology of the Late Jurassic Portuguese sauropod dinosaur *Lusotitan atalaiensis* (Macronaria) and the evolutionary history of basal titanosauriforms. *Zoological Journal of the Linnean Society* 168:98–206.

Mannion PD., Allain R., Moine O. 2017. The earliest known titanosauriform sauropod dinosaur and the evolution of Brachiosauridae. *PeerJ* 5:e3217.

Marpmann JS., Carballido JL., Sander PM., Knötschke N. 2015. Cranial anatomy of the Late Jurassic dwarf sauropod *Europasaurus holgeri* (Dinosauria, Camarasauromorpha): ontogenetic changes and size dimorphism. *Journal of Systematic Palaeontology* 13:221–263. DOI: 10.1080/14772019.2013.875074.

Marty D., Falkingham PL., Richter A. 2016. Dinosaur Track Terminology: A Glossary of Terms. *Dinosaur Tracks: The Next Steps*. 399pp.

McPhee BW., Bonnan MF., Yates AM., Neveling J., Choiniere JN. 2015. A new basal sauropod from the pre-Toarcian Jurassic of South Africa: evidence of niche-partitioning at the sauropodomorph–sauropod boundary? *Scientific reports* 5:1-12.

Mocho P., Royo-Torres R., Ortega F. 2014. Phylogenetic reassessment of *Lourinhasaurus alenquerensis*, a basal Macronaria (Sauropoda) from the Upper Jurassic of Portugal. *Zoological Journal of the Linnean Society* 170:875–916.

Mocho P., Royo-Torres R., Malafaia E., Escaso F., Narváez I., Ortega F. 2016a. New data on Late Jurassic sauropods of central and northern sectors of the Bombarral Sub-basin (Lusitanian Basin, Portugal). *Historical Biology* 0:1–19.

Mocho P., Royo-Torres R., Malafaia E., Escaso F., Ortega F. 2016b. Systematic review of Late Jurassic sauropods from the Museu Geológico collections (Lisboa, Portugal). *Journal of Iberian Geology* 42:227–250.

Mocho P., Royo-Torres R., Malafaia E., Escaso F., Ortega F. 2017. First occurrences of non-neosauropod eusauropod procoelous caudal vertebrae in the Portuguese Upper Jurassic record. *Geobios* 50:23–36.

Noè LF., Liston JJ., Chapman SD. 2010. 'Old bones, dry subject': the dinosaurs and pterosaur collected by Alfred Nicholson Leeds of Peterborough, England. *Geological Society, London, Special Publications* 343:49–77.

Osborn HF. 1904. Manus, sacrum, and caudals of Sauropoda. *Bulletin of the American Museum of Natural History* 20:181–190.

Ouyang H., Ye Y. 2002. *The first mamenchisaurian skeleton with complete skull, Mamenchisaurus youngi*. Chengdu, China: Sichuan Publishing House of Science and Technology. 138 pp.

P Pol, D., Rauhut, O.W.M., Carballido, J.L., 2009. Skull anatomy of a new basal eusauropod from the Cañadon Asfalto Formation (Middle Jurassic) of Central Patagonia. *Journal of Vertebrate Paleontology, Program and Abstracts 29 (Supplement 3)*, 100A.

Powell JE. 1992. Osteología de Saltasaurus loricatus (Sauropoda-Titanosauridae) del Cretácico Superior del noroeste argentino. *Los Dinosaurios y su entorno biótico. Sanz JL And Buscalioni AD (Eds), Instituto Juan de Valdés, Cuenca, España*, 165–230.

Rauhut OW. 2003a. A dentary of *Patagosaurus* (Sauropoda) from the Middle Jurassic of Patagonia. *Ameghiniana* 40:425–432.

Rauhut OWM. 2003b. Revision of *Amygdalodon patagonicus* Cabrera, 1947 (Dinosauria, Sauropoda). *Fossil Record* 6:173–181.

Remes K., Ortega F., Fierro I., Joger U., Kosma R., Ferrer JMM., Ide OA., Maga A. 2009. A new basal sauropod dinosaur from the Middle Jurassic of Niger and the early evolution of Sauropoda. *PLoS One* 4:e6924.

Rogers RR., Eberth DA., Fiorillo AR. 2010. *Bonebeds: genesis, analysis, and paleobiological significance*. University of Chicago Press. 499 pp.

Rogers KC., Whitney M., D'Emic M., Bagley B. 2016. Precocity in a tiny titanosaur from the Cretaceous of Madagascar. *Science* 352:450–453.

Sander PM. 2000. Longbone histology of the Tendaguru sauropods: implications for growth and biology. *Paleobiology* 26:466–488.

Sander PM., Mateus O., Laven T., Knötschke N. 2006. Bone histology indicates insular dwarfism in a new Late Jurassic sauropod dinosaur. *Nature* 441:739–741.

Schwarz D., Fritsch G. 2006. Pneumatic structures in the cervical vertebrae of the Late Jurassic Tendaguru sauropods *Brachiosaurus brancai* and *Dicraeosaurus*. *Eclogae Geologicae Helvetiae* 99:65–78.

Schwarz D., Frey E., Meyer CA. 2007. Pneumaticity and soft-tissue reconstructions in the neck of diplodocid and dicraeosaurid sauropods. *Acta Palaeontologica Polonica* 52:167–188.

Schwarz D., Ikejiri T., Breithaupt BH., Sander PM., Klein N. 2007. A nearly complete skeleton of an early juvenile diplodocid (Dinosauria: Sauropoda) from the Lower Morrison Formation (Late Jurassic) of north central Wyoming and its implications for early ontogeny and pneumaticity in sauropods. *Historical Biology* 19:225–253.

Sereno PC., Beck AL., Dutheil DB., Larsson HC., Lyon GH., Moussa B., Sadleir RW., Sidor CA., Varricchio DJ., Wilson GP. 1999. Cretaceous sauropods from the Sahara and the uneven rate of skeletal evolution among dinosaurs. *Science* 286:1342–1347.

Sereno PC., Wilson JA., Witmer LM., Whitlock JA., Maga A., Ide O., Rowe TA. 2007. Structural extremes in a Cretaceous dinosaur. *PLoS ONE* 2:e1230.

Stein K., Csiki Z., Rogers KC., Weishampel DB., Redelstorff R., Carballido JL., Sander PM. 2010. Small body size and extreme cortical bone remodeling indicate phyletic dwarfism in *Magyarosaurus dacus* (Sauropoda: Titanosauria). *Proceedings of the National Academy of Sciences* 107:9258–9263.

Tang F., Jing X., Kang X., Zhang G. 2001. *Omeisaurus maoianus: a complete sauropod from Jingyuan, Sichuan*. Beijing, China: China Ocean Press. 112 pp.

Taylor MP. 2009. A re-evaluation of *Brachiosaurus altithorax* Riggs 1903 (Dinosauria, Sauropoda) and its generic separation from *Giraffatitan brancai* (Janensch 1914). *Journal of Vertebrate Paleontology* 29:787–806.

Tidwell V., Wilhite DR. 2005. Ontogenetic variation and isometric growth in the forelimb of the Early Cretaceous sauropod *Venenosaurus*. *Thunder Lizards: the Sauropodomorph Dinosaurs*, 187–198.

Tschopp E., Mateus O. 2013a. Clavicles, interclavicles, gastralia, and sternal ribs in sauropod dinosaurs: new reports from Diplodocidae and their morphological, functional and evolutionary implications. *Journal of Anatomy* 222:321–340.

Tschopp E., Mateus O. 2013b. The skull and neck of a new flagellicaudatan sauropod from the Morrison Formation and its implications for the evolution and ontogeny of diplodocid dinosaurs. *Journal of Systematic Palaeontology* 11:853–888.

Tschopp E., Mateus O. 2017. Osteology of *Galeamopus pabsti* sp. nov. (Sauropoda: Diplodocidae), with implications for neurocentral closure timing, and the cervico-dorsal transition in diplodocids. *PeerJ* 5:e3179.

Upchurch P. 1998. The phylogenetic relationships of sauropod dinosaurs. *Zoological Journal of the Linnean Society* 124:43–103.

Upchurch P., Martin J. 2002. The Rutland *Cetiosaurus*: the anatomy and relationships of a Middle Jurassic British sauropod dinosaur. *Palaeontology* 45:1049–1074.

Upchurch P., Martin J. 2003. The anatomy and taxonomy of *Cetiosaurus* (Saurischia, Sauropoda) from the Middle Jurassic of England. *Journal of Vertebrate Paleontology* 23:208–231.

Upchurch P., Barrett PM., Dodson P. 2004. Sauropoda. In: Weishampel DB, Dodson P, Osmólska H eds. *The Dinosauria. Second edition*. Berkeley, CA: University of California Press, 259–322.

Upchurch P., Mannion PD., Taylor MP. 2015. The Anatomy and Phylogenetic Relationships of "*Pelorosaurus*" *becklesii* (Neosauropoda, Macronaria) from the Early Cretaceous of England. *PLoS One* 10:e0125819.

Van Der Leeuw AH., Bout RG., Zweers GA. 2001. Evolutionary morphology of the neck system in ratites, fowl and waterfowl. *Netherlands Journal of Zoology* 51:243–262.

Volkheimer W., Rauhut OW., Quattrocchio ME., Martinez MA. 2008. Jurassic paleoclimates in Argentina, a review. *Revista de la Asociación Geológica Argentina* 63:549–556.

Volkheimer W., Quattrocchio ME., Cabaleri NG., Narvaez PL., Rosenfeld U. 2015. Environmental and Climatic Proxies for the Cañadón Asfalto and Neuquén Basins (Patagonia, Argentina): Review of Middle to Upper Jurassic Continental and Near Coastal Sequences. *Revista Brasileira De Paleontologia* 18:71–82.

Waskow K., Sander PM. 2014. Growth record and histological variation in the dorsal ribs of *Camarasaurus* sp. (Sauropoda). *Journal of Vertebrate Paleontology* 34:852–869.

Waskow K. 2017. Growth rates of Giants: histological evidence for size related differences in growth models between normal sized diplodocoids and a unique assemblage of dwarfed Late Jurassic diplodocoids from the Mother's Day Quarry (Morrison Formation, Montana, USA). *Journal of Vertebrate Paleontology, Program and Abstracts* 37, 210-211.

Wedel MJ. 2003a. The evolution of vertebral pneumaticity in sauropod dinosaurs. *Journal of Vertebrate Paleontology* 23:344–357.

Wedel MJ. 2003b. Vertebral pneumaticity, air sacs, and the physiology of sauropod dinosaurs. *Paleobiology* 29:243.

Wedel M. 2007. What pneumaticity tells us about 'prosauropods', and vice versa. *Special Papers in Palaeontology* 77:207.

Whitlock JA., Wilson JA., Lamanna MC. 2010. Description of a nearly complete juvenile skull of *Diplodocus* (Sauropoda: Diplodocoidea) from the Late Jurassic of North America. *Journal of Vertebrate Paleontology* 30:442–457.

Wilhite DR. 2005. Variation in the appendicular skeleton of North American sauropod dinosaurs: taxonomic implications. In: Tidwell V, Carpenter K eds. *Thunder-lizards: the Sauropodomorph dinosaurs*. Bloomington: Indiana University Press, 268–301.

Wilson JA. 1999. A nomenclature for vertebral laminae in sauropods and other saurischian dinosaurs. *Journal of Vertebrate Paleontology* 19:639–653.

Wilson JA. 2002. Sauropod dinosaur phylogeny: critique and cladistic analysis. *Zoological Journal of the Linnean Society* 136:215–275.

Wilson JA. 2005. Integrating ichnofossil and body fossil records to estimate locomotor posture and spatiotemporal distribution of early sauropod dinosaurs: a stratocladistic approach. *Paleobiology* 31:400–423.

Wilson JA., Upchurch P. 2009. Redescription and reassessment of the phylogenetic affinities of *Euhelopus zdanskyi* (Dinosauria: Sauropoda) from the Early Cretaceous of China. *Journal of Systematic Palaeontology* 7:199–239.

Wilson JA., D'Emic MD., Ikejiri T., Moacdieh EM., Whitlock JA. 2011. A nomenclature for vertebral fossae in sauropods and other saurischian dinosaurs. *PLoS ONE* 6:e17114.

Wilson JA. 2012. New vertebral laminae and patterns of serial variation in vertebral laminae of sauropod dinosaurs. *Contributions from the Museum of Paleontology, University of Michigan* 32:91–110.

Yates AM. 2003. The species taxonomy of the sauropodomorph dinosaurs from the Löwenstein Formation (Norian, Late Triassic) of Germany. Palaeontology 46:317–337.

Zavattieri AM., Escapa IH., Scasso RA., Olivera D. 2010. Contribución al conocimiento palinoestratigráfico de la Formación Cañadón Calcáreo en su localidad tipo, provincia del Chubut, Argentina. In: *X Congreso Argentino de Paleontología y Bioestratigrafía-VII Congreso Latinoamericano de Paleontología*. 51 pp.

Zhang Y. 1988. *The Middle Jurassic dinosaur fauna from Dashanpu, Zigong, Sichuan, vol. 1: sauropod dinosaur (I): Shunosaurus*. Chengdu, China: Sichuan Publishing House of Science and Technology. 114pp.

Zhao, Z. 1993. A New Mid-Jurassic Sauropod (*Klamelisaurus gobiensis* Gen. Et Sp. Nov.) From Xinjiang, China. *Vertebrata Palasiatica* 2: 243-265.

4 The Phylogeny of *Patagosaurus fariasi* and implications for evolutionary relationships of Early – Middle Jurassic sauropods and their biogeography

Femke M Holwerda[123], Oliver W M Rauhut[13], Diego Pol[45]

1 Staatliche Naturwissenschaftliche Sammlungen Bayerns (SNSB), Bayerische Staatssamlung für Paläontologie und Geologie, Richard-Wagner-Strasse 10, 80333 München, Germany

2 GeoBioTec, Departamento de Ciências da Terra, Faculdade de Ciências e Tecnologia (FCT), Universidade Nova de Lisboa, 2829-526 Caparica, Portugal

3 Department of Earth and Environmental Sciences and GeoBioCenter, Ludwig Maximilians Universität, 80333 München, Germany

4 Consejo Nacional de Investigaciones Científicas y Técnicas (CONICET), Argentina

5 Museo Paleontológico Egidio Feruglio, Avenida Fontana 140, Trelew, Argentina

Author contributions: Conceived the study: FH, DP, OR. Character coding, phylogenetic analysis, interpreting results: FH. Writing the chapter/manuscript in prep: FH.

4.1 Abstract

The phylogenetic position of the early Middle Jurassic sauropod *Patagosaurus fariasi* is investigated. This material comes from two Cerro Condor bonebeds within the Cañadón Asfalto Formation, close to Cerro Cóndor, Patagonia (Argentina).

Newly-described material, together with the original holotype and previously-published associated material has been scored, and its phylogenetic position has been assessed using Gondwanan sauropod taxa from the Early and Middle Jurassic, such as *Vulcanodon, Amygdalodon, Tazoudasaurus, Barapasaurus, Lapparentosaurus, Volkheimeria*, *Spinophorosaurus*, *Jobaria*, and Laurasian Early and Middle Jurassic taxa such as *Gongxianosaurus, Isanosaurus, Shunosaurus, Cetiosaurus, Mamenchisaurus* and *Omeisaurus*, and neosauropods. New phylogenetic characters, based on the redescription of the holotype and associated material, are included in an existing sauropod datamatrix, to which several characters from more recent analyses on basal non-sauropodan sauropodomorphs and basal

sauropods are added. The results show a close phylogenetic relationship between *Cetiosaurus* and *Patagosaurus*, with *Patagosaurus* nested within the Cetiosauridae, and moreover, being retrieved as a derived non-neosauropodan eusauropod. *Barapasaurus,* however, being traditionally retrieved as closely related to both, is excluded from this group, and comes out several nodes more basal from *Patagosaurus+Cetiosaurus*. Furthermore, *Patagosaurus* and the Cetiosauridae are retrieved as more derived than all other Gondwanan and Laurasian Early and Middle Jurassic taxa, save for *Lapparentosaurus, Mamenchisaurus, Omeisaurus*, and the Middle-Late Jurassic turiasaurs and *Jobaria*, making *Patagosaurus* the most derived Gondwanan well-known sauropod from the early Middle Jurassic. However, after adding one specimen originally referred to *Patagosaurus*, MACN-CH 934, which appears to represent a different taxon, as separate OTU (operational taxonomic unit), this specimen comes out more derived than *Patagosaurus, Cetiosaurus, Mamenchisaurus, Omeisaurus*, and *Jobaria*. It comes out as sister-taxon to *Lapparentosaurus*, and close to the base of neosauropods, or as a basal neosauropod. With *Volkheimeria*, also from the Cerro Condor bonebeds, retrieved as a much more basal sauropod than *Patagosaurus* and MACN-CH 934, the Cañadón Asfalto Fm. Cerro Condor bonebeds show a high taxonomic as well as evolutionary diversity in sauropods. Moreover, another specimen ascribed previously to *Patagosaurus*, MACN-CH 230, also comes out different from *Patagosaurus* when used as OUT in this analysis. This could imply an earlier sauropod diversification than previously assumed, and pushes back the evolutionary radiation of sauropods to the Early Jurassic at least, or perhaps even the Late Triassic, with a potential rapid diversification of eusauropods at the latest Early to earliest Middle Jurassic. The high diversity and evolutionary interrelationships between both South and North Gondwanan and West Laurasian sauropods shows a high mobility and few significant physical barriers for sauropod dispersal in the Early and Middle Jurassic.

4.2 Introduction

4.2.1 Sauropod diversification in the Late Triassic-Early Jurassic

Phylogenetic analysis of Late Triassic sauropodomorphs and Early Jurassic sauropods shows that the transition from basal sauropodomorphs to sauropods happened somewhere around the Early Jurassic (see for example Upchurch, 1998; Wilson and Sereno, 1998; Wilson, 2002; Upchurch et al., 2004; Harris, 2006), and that especially (Southern) Gondwana is important for this early transition (Yates and Kitching, 2003; Bonnan and Yates, 2007; Yates et al., 2010; McPhee et al., 2014, 2015; McPhee and Choiniere, 2016). It does depend, however, on which definition of Sauropoda is used; the definition of Salgado et al., (1997) used *Vulcanodon karibaensis* as the first specifier, and *Saltasaurus loricatus* as the second specifying taxon, and the Sauropoda was therefore defined as *Vulcanodon, Saltasaurus*, their most recent common ancestor, and all descendants (Salgado et al., 1997). A more recent, less accepted definition of the Sauropoda is that by Yates, (2005); where the definition includes all sauropods more closely related to *Saltasaurus loricatus* than to *Melanorosaurus readi* (Yates, 2005) making the group more inclusive of Late Triassic taxa. Here, we will adhere to the definition of Salgado et al. (1997), which is inclusive enough for this study and more widely accepted and used. Moreover, *Vulcanodon* and the beds where the material of *Vulcanodon* is from are currently under revision, and the material seems to be older than previously thought (P.Barrett pers.comm.), which makes it a useful taxon for phylogenetic analysis of Early and Middle Jurassic sauropods.

Recent analysis of basal sauropods and basal eusauropods from the Middle, but also from the Early Jurassic, especially from Gondwana, shows a greater diversity than previously assumed (e.g. Allain and Aquesbi, 2008; Läng, 2008; Pol et al., 2009; Remes et al., 2009; Läng and

Mahammed, 2010). According to recent analyses, the diversification of sauropods and their dispersal is influenced by two plausible factors; the first being the Toarcian Anoxic Event and subsequent mass extinction and radiation of new taxa (Bailey et al., 2003; Hesselbo et al., 2007; Hesselbo and Pieńkowski, 2011).

This is thought to be linked to the latest Early-Middle Jurassic radiation of sauropods and other dinosaurs (Allain and Aquesbi, 2008; Läng, 2008; Allain and Läng, 2009; Läng and Mahammed, 2010; Pol and Rauhut, 2012; Rauhut et al., 2016). Another possible determining factor is a physical barrier, likely causing sauropod endemic radiation in South and North Gondwana, in the form of the Central Gondwanan Desert, (the theory of which is reinforced by studies on Jurassic climate; see Hallam, 1985; Parrish, 1993; Scotese et al., 1999; Sellwood and Valdes, 2006; Läng, 2008; Remes et al., 2008; 2009; Volkheimer et al., 2008; Rauhut and López-Arbarello, 2009). Indeed, the Cañadón Asfalto Formation in Patagonia, Argentina, shows evidence of endemism in South Gondwana, (Apesteguía et al., 2011, 2012; Pol and Rauhut, 2012; Pol et al., 2013), as well as a high diversity in sauropods (Becerra et al., 2017; Carballido et al., 2017), and earlier studies (Bonaparte, 1979; Bonaparte, 1986a; Rauhut, 2003a; Pol et al., 2009; Holwerda et al., 2015). A revised phylogeny of one of the Patagonian sauropods, *Patagosaurus fariasi*, with the inclusion of Early and Middle Jurassic Gondwanan (and Laurasian) sauropods, will help to elucidate these evolutionary patterns.

4.2.2 Historical perspective and previous analyses on the phylogenetic position of *Patagosaurus*

The Dinosauria received their first classification as a group in 1842 (Owen, 1842b). The first sauropod, however, was unknowingly also described by Owen one year prior, who gave some fossil remains from localities across England the names *Cetiosaurus* and *Cardiodon,* respectively (Owen, 1841). *Cetiosaurus* was recognized as a large reptile, however, it was

named so because of superficial morphological affinities with cetaceans (Owen 1842a; Taylor, 2010). *Cetiosaurus oxoniensis* was only described more fully by Phillips as a dinosaur some years later (Phillips, 1871), however, it was still also several years before Sauropoda were officially coined, as a group of large dinosaurs, by Marsh (Marsh, 1878). Marsh actually first used the term 'Atlantosauridae' to include *Atlantosaurus* (possibly *Apatosaurus ajax*) and *Apatosaurus* (Marsh, 1877; Taylor 2010), however, one year later recognized the group needed a more inclusive name (Taylor 2010). Marsh went on to subdivide Sauropoda into Atlantosauridae, Morosauridae, Diplodocidae, Pleurocoelidae, and Titanosauridae (Marsh 1895; the last group being incorporated from Lydekker, (1885)). Later on, Janensch divided Sauropoda into two groups, the broad-nosed, spatulate-toothed Bothrosauropodidae, and the high-nosed, narrow-toothed Homalosauridae (Janensch, 1929).

Of all of these groups, however, only Diplodocidae (Marsh, 1884) remains as the original name (although with a different definition, see Calvo and Salgado, (1995); Tschopp, (2013)). The Atlantosauridae were synonymized by Steel (1970) with Camarasauridae (Camarasauridae *sensu* Cope 1877 and Romer 1956). The Titanosauridae as a group currently exists in different definitions as well, however, it has been abandoned by most authors due to *Titanosaurus* being regarded as a nomen dubium (Powell, 1992; Salgado et al., 1997; Wilson and Upchurch, 2003).

The Cetiosauridae, meanwhile, were established by Lydekker in 1888, allegedly as a result of a disagreement between him and colleague and palaeontologist Seeley over *Cetiosaurus* and *Ornithopsis* (Seeley, 1889; Noè et al., 2010), which incentivised Lydekker to create a more inclusive group for these two sauropods. The Cetiosauridae subsequently went on to form a waste-basket group for a long time, with the definition changing from very inclusive to being only a group of Early-Middle Jurassic (basal) sauropods (see e.g. Upchurch and Martin, 2002, 2003; Läng and Mahammed, 2010). The Cetiosauridae were firstly more firmly established when more discoveries were attributed to this group (Seeley 1889, Taylor 2010). While during

Cope's and Marsh's time it was mainly the Morrison Formation of the USA that was the main focus of sauropod research, (with sauropods from the UK serving as base for the Cetiosauridae group), meanwhile, Gondwanan taxa were already being added to the bunch, with Indian and Malagasi taxa being described (Lydekker, 1887, 1893, 1895; Depéret, 1896; Thevenin, 1907), as well as African taxa (Janensch, 1929), and later on in the 20th century, even more Gondwanan taxa (de Lapparent, 1955; Jain et al., 1972, 1975; Raath, 1972; Cooper, 1984). After the 'Bone Wars' of Cope and Marsh, more Laurasian taxa were found and described from China during the 20th century (Wiman, 1929; Young, 1935, 1939, 1958; Dong and Tang, 1984; Zhang, 1988).

When *Patagosaurus* was discovered and described in 1979 and 1986, it was also ascribed to the family of Cetiosauridae (Bonaparte, 1979; Bonaparte, 1986a; Bonaparte, 1986b), to which by now only the taxa *Bothriospondylus, Cetiosaurus, Barapasaurus, Amygdalodon, Volkheimeria, Lapparentosaurus, Patagosaurus* and *Rhoetosaurus* were ascribed (McIntosh, 1981; Bonaparte, 1986b). Bonaparte (1986a,b) created a triad of the cetiosaurs *Patagosaurus, Cetiosaurus* and *Barapasaurus*, based on morphological commonalities he perceived (mostly in the dorsal vertebral morphology). In the same year, another first cladogram (though not used the way it is in current analyses) was made by Gaulthier (Gaulthier, 1986).

However, it was not until 1990 that the first sauropod phylogeny was attempted (though not using any phylogenetic analysis, but rather a study on most likely sauropod relationships found by McIntosh), with a tentative cladogram as a result (McIntosh, 1990a), where *Patagosaurus* was classified under Cetiosauridae (Lydekker, 1888) together with *Cetiosaurus oxoniensis, Haplocanthosaurus*, and *Amygdalodon* (McIntosh, 1990a), together with the Middle Jurassic Moroccan 'cetiosaurid' *Cetiosaurus mogrebiensis,* (currently an enigmatic taxon in need of revision, P.Mannion pers. comm.). This cladogram showed it to be a potential sister-taxon to *Cetiosaurus mogrebiensis*, and more basal to *Cetiosaurus, Shunosaurus, Omeisaurus,*

Mamenchisaurus, Lapparentosaurus and *Bothriospondylus*, and diplodocids, but more derived than *Barapasaurus* and *Vulcanodon* (McIntosh, 1990a).

The next phylogeny, and first 'true' (i.e. with 'modern' phylogenetic analytical methods) phylogenetic analysis, was by Upchurch (1995), who ascribed *Patagosaurus, Cetiosaurus* and *Amygdalodon* to Cetiosauridae, and later *Patagosaurus*, *Cetiosaurus* and *Haplocanthosaurus* (Upchurch, 1998), and where *Shunosaurus, Vulcanodon, Omeisaurus, Mamenchisaurus* and *Euhelopus* were more basal to *Patagosaurus*. The Cetiosauridae *sensu* Upchurch (1995, 1998) are not found in many more recent analyses. Wilson (2002), with the most comprehensive datamatrix at that time, scored *Patagosaurus* as more derived than *Vulcanodon, Barapasaurus* and *Shunosaurus*, but more basal than *Mamenchisaurus* and *Omeisaurus* (Wilson, 2002). The subsequent matrix of Harris (2006), with a focus on diplodocids, recovered *Patagosaurus* as basal to *Mamenchisaurus* and *Haplocanthosaurus*, but more derived than *Omeisaurus*, *Barapasaurus*, *Shunosaurus* and *Vulcanodon*. However, it was not until Allain and Aquesbi, (2008) that Middle Jurassic sauropod phylogenetic relationships got more attention. With the phylogeny of *Tazoudasaurus*, where the term Gravisauria was introduced for the node leading to *Vulcanodon*, *Tazoudasaurus*, and basal sauropods, and where *Patagosaurus* was found to be sister-taxon to *Barapasaurus,* and more derived than *Shunosaurus*, *Tazoudasaurus* and *Vulcanodon*, but more basal to *Omeisaurus* and *Mamenchisaurus* and neosauropods (Allain and Aquesbi, 2008). The subsequent analysis by Läng (2008) and Läng and Mahammed, (2010), which included *Lapparentosaurus*, *Bothriospondylus* and *Cetiosaurus mogrebiensis*, as well as the splitting of *Cetiosaurus oxoniensis* from the Rutland *Cetiosaurus*, showed *Patagosaurus* to be more basal to the Rutland *Cetiosaurus*, and *Mamenchisaurus+Omeisaurus*, but more derived than *Chebsaurus, Cetiosaurus mogrebiensis, Cetiosaurus oxoniensis*, and *Lapparentosaurus* (these forming a polytomy), and more derived than *Shunosaurus, Barapasaurus, Amygdalodon, Tazoudasaurus* and *Vulcanodon*. This was then redefined by Läng as a potential cetiosaurid node, which remains, however, unresolved

(and which to date is the last time Cetiosauridae were included as a group in a sauropod phylogeny). Läng's definition is as follows; 'Cetiosauridae *sensu* Bonaparte (1986b) are paraphyletic and *Barapasaurus* and *Patagosaurus* bound, with the inclusion of a polytomy of *Chebsaurus, Lapparentosaurus, Ferganasaurus, Cetiosaurus mogrebiensis* and *Cetiosaurus oxoniensis*' (Läng, 2008; Läng and Mahammed, 2010).

The polytomy of Läng (2008) and Läng and Mahammed, (2010) shows the great uncertainty of the phylogenetic interrelationships of basal non-neosauropod (eu)sauropods, due to a plethora of missing information and taxonomic uncertainties. The degree to which phylogenetic interrelationships can change by the addition of a new single taxon with new phylogenetic information, as well as new phylogenetic characters, was shown by Remes et al. (2009), where *Patagosaurus* was sister-taxon to *Barapasaurus*, but not to *Cetiosaurus,* and where many shared characteristics were found for *Patagosaurus*+*Barapasaurus*.

The most recent analyses including *Patagosaurus* were by Carballido et al., (2011, 2012), and Carballido and Sander, (2014), where *Patagosaurus* came out more derived than *Cetiosaurus, Barapasaurus, Shunosaurus* and *Tazoudasaurus*, and more basal to *Mamenchisaurus+Omeisaurus*, and neosauropods.

4.2.3 Phylogenetic importance of *Patagosaurus* in relation to its redescription

Although coined in 1979 and described in 1986 (Bonaparte, 1979; Bonaparte, 1986a) *Patagosaurus fariasi*, one of the most abundant and best preserved Gondwanan Middle Jurassic sauropods, did not receive any close attention until recently. Now that the holotype and associated material have been redescribed, and new elements recognized, this new information can be used as additional data for a new phylogenetic study. Most *Patagosaurus* material used for previous phylogenetic analysis has been on the basis of the first monograph by Bonaparte (1986a), which included several associated *Patagosaurus* specimens that are

now no longer considered to be *Patagosaurus* (MACN-CH 934, MACN-CH 230, see Chapter 3). *Patagosaurus*, and most importantly, the associated material including these potential new taxa, are found in even the most fundamental sauropod phylogenetic datamatrices (Upchurch, 1998; Wilson, 2002), therefore leading to a potential long-standing wrong phylogenetic position of the taxon (though clearly unbeknownst to the authors at the time).

Moreover, recent re-dating of the Cañadón Asfalto Formation, where *Patagosaurus* was found, has proven these beds to be much older than previously assumed, being re-dated from the Callovian to the Aalenian-Bajocian (Cúneo et al., 2013; Hauser et al., 2017), giving any evolutionary interrelationships of *Patagosaurus* with other sauropods more significance in light of the early sauropod radiation. Finally, as previous phylogenetic analyses on early sauropods have highlighted, there is much uncertainty on their interrelationships. A new phylogeny including new information on *Patagosaurus* may help shed light on these interrelationships.

4.3 Methods

4.3.1 Coding

Coding was done based on first-hand observation of all *Patagosaurus* material, *Cetiosaurus oxoniensis* and Rutland *Cetiosaurus* material, *Lapparentosaurus* material, *Amygdalodon* material, *Bothriospondylus* material (pruned), *Cetiosauriscus* material (pruned), *Tazoudasaurus, Spinophorosaurus* and *Jobaria* material. All other sauropods in this matrix were coded using photographs, publications and information from previous matrices.

The matrix used is based on Carballido et al., (2012), to which characters were added by McPhee et al., (2014) as well as an unpublished matrix by Rauhut et al. (Holwerda et al., 2016;

Rauhut et al, unpublished data). Next to recoding characters, some new characters were added as well.

4.3.2 Software

The data matrix was coded using Mesquite version 2.75 (Maddison and Maddison, 2010).

The resulting data matrix was analysed in TNT (Goloboff et al., 2008) in TNT version 1.5 (Goloboff and Catalano, 2016).

4.3.3 New characters

Cranial characters:

(104) Enamel surface texture: absent (0); present (1). In previous matrices, this was only one character, since wrinkled enamel is a synapomorphy for Eusauropoda (Upchurch, 1998; Wilson and Sereno, 1998; Wilson, 2002, 2005). However, as enamel wrinkling is used as a way to assess taxonomic diversity in sauropods (see Buffetaut, 2005; Carballido and Pol, 2010; Díez Díaz et al., 2012, 2013, 2014; Holwerda et al., 2015; Barrett et al., 2016; Carballido et al., 2017; Holwerda et al., 2018), this character is extended with the following:

(105) Enamel surface texture (wrinkling) coverage: (0) only partial coverage on tooth surface; (1) wrinkling all over tooth surface. Enamel wrinkling surface coverage differs between clades of sauropods: in many basal sauropods the wrinkling does not cover the entire surface of the tooth, whereas in many eusauropods and camarasaurids the surface is heavily wrinkled, and in Titanosauria, the teeth are smooth again (Upchurch et al., 2004; Buffetaut, 2005; Barrett, 2006; Carballido and Pol, 2010; García and Cerda, 2010; García et al., 2015; Holwerda et al., 2015).

(106) Enamel surface texture: (1) finely wrinkled; (2) coarsely wrinkled; (3) pebbly wrinkled. This character is used to define wrinkling type; as stated before, wrinkling can be fine, coarse,

and in the case of '*Patagosaurus*' MACN-CH 934, 'pebbly' (Bonaparte, 1986a; Holwerda et al., 2015, see Figure 1 therein) This character is unapplicable for all taxa that do not have enamel wrinkling on their dentition.

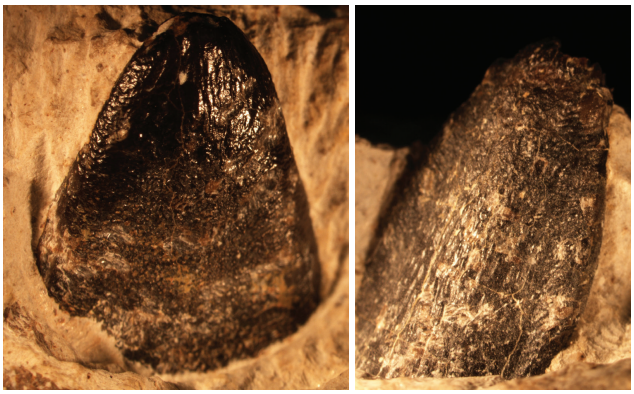

Figure 1: dental enamel wrinkling characters: pebbly (left) and coarse wrinkling (right)

Axial characters:

Cervicals:

(122) pre-epipophyses, absent (0) present (1). This character was added after *Patagosaurus* showed clear pre-epipophyses, or the lateral expansion of a triangular protrusion (separate from the prezygapophyseal facet) of the spinoprezygapophyseal and prezygadiapophyseal lamina (see Figure 2). This feature is seen in more and more sauropods (Russell and Zheng, 1993; Taylor and Wedel, 2013), however, it is not well-studied in most sauropods, (only recently this feature starts to appear as a character, see e.g. Tschopp et al., (2015), and then only in neosauropod-based phylogenies, not in non-neosauropod (eu)sauropod-based phylogenies) and basal eusauropods prove no exception to this.

(123) epipophyses, absent (0) present (1). This character was added after epipophyses were clearly present on *Patagosaurus* (see Figure 2). Epipophyses are small triangular protrusions dorsal to the postzygapophyses, and exist as an expansion of the postzygadiapophyseal laminae together with the intrapostzygapophyseal laminae. Similarly to pre-epipophyses,

epipophyses are not well-studied in sauropods (Russell and Zheng, 1993; Carballido et al., 2011; Taylor and Wedel, 2013; Carballido and Sander, 2014).

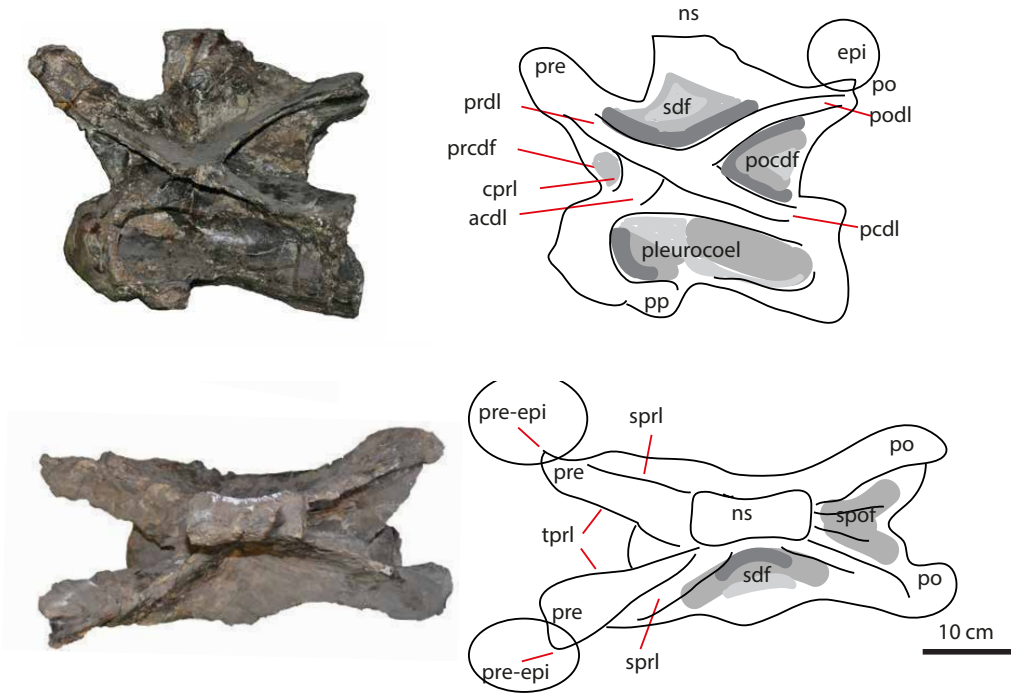

Figure 2: Pre-epipophyses and epipophyses on *Patagosaurus fariasi* cervical PVL 4170 (3) in lateral (above) and dorsal (below) view. (acdl = anterior centrodiapophyseal lamina; cprl = centroprezygapophyseal lamina; epi = epipophyses, pcdl = posterior centrodiapophyseal lamina, prdl = prezygadiapophyseal lamina; pre = prezygapophysis; pre-epi = pre-epipophysis; podl = postzygadiapophyseal lamina; pocdf = postzygacentrodiapophyseal fossa; prcdf=prezygacentrodiapophyseal fossa; sprl = sprinoprezygapophyseal lamina, spof = spinopostzygapophyseal fossa; sdf = spinodiapophyseal fossa; pp=parapophysis, ns=neural spine).

Dorsals:

(172) Anterior dorsals, single intraprezygapophyseal lamina (stprl): (0) absent; (1) present. This character was added as it is a prominent feature in dorsals of *Patagosaurus*. As the neural arch elongates over the axial column, a single lamina appears between the prezygapophyseal bases, which divides the neural arch in half (see 'stprl' in Figure 3). This feature is seen in basal eusauropods like *Tazoudasaurus*, *Barapasaurus*, and *Cetiosaurus oxoniensis* and the Rutland *Cetiosaurus* (Upchurch and Martin, 2002, 2003; Allain and Aquesbi, 2008; Bandyopadhyay et al., 2010) but was not named 'stprl' until 2014 (Carballido and Sander, 2014) though it was already mentioned as a structure, by Upchurch et al., (2004); and by Wilson, (1999, 2012).

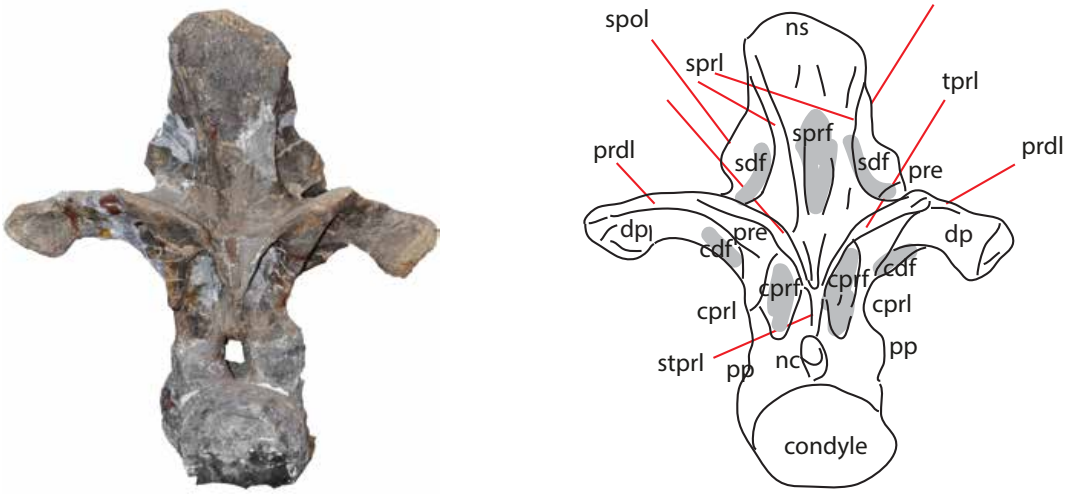

Figure 3: anterior dorsal of *Patagosaurus fariasi* PVL 4170 (11), in anterior view, with the single intraprezygapophyseal lamina (stprl). (prdl = prezygadiapophyseal lamina, cprl = centroprezygapophyseeal lamina, tprl = intraprezygapophyseal lamina, sprl = spinoprezygapophyseal lamina, spol = spinopostzygapophyseal lamina, cdf = centrodiapophyseal fossa, cprf = centroprezygapophyseal lamina, sprf = spinoprezygapophyseal fossa, sdf = spinodiapophyseal fossa, nc = neural canal, dp = diapophyses, pre = prezygapophyses, pp = parapophyses, ns = neural spine.)

(178) Posterior Dorsal vertebra, centrodiapophyseal fossa (CDF): (0) absent; (1) present

(179) Posterior vertebra, internal pneumatic chamber connected to CDF: (0) absent; (1) present. These form one of the characters that (for the time being) define the taxon

Patagosaurus, however, they are also a rudimentary pneumatic feature present in many sauropods in general, and even for saurischians (Wedel, 2003a, 2003b, 2007; Wedel et al., 2005). In *Patagosaurus*, however, the lateral openings connect to an internal pneumatic structure, which is separated from the neural canal. The diapophyses show a ventral triangular fenestra, which connects to an internal pneumatic chamber, which is seen in *Patagosaurus* through a CT scan of a posterior dorsal (see Figure 4, in blue). The fenestrae, however, are seen to some extent in *Tazoudasaurus, Barapasaurus*, and possibly *Cetiosaurus* (Upchurch and Martin 2002, 2003; Allain and Aquesbi, 2008; Bandyopadhyay et al., 2010; Peyer and Allain, 2010). These are not as thoroughly documented as *Patagosaurus*, and possibly not as extensively developed, therefore the exact morphology of this feature, remains a diagnostic character for *Patagosaurus* for the time being. If indeed other sauropods share this character, using this feature as a phylogenetic character may in the future help determine whether or not a clade arises with these morphotypes of internal pneumatic chambers in posterior dorsals. Evidently, more non-neosauropod eusauropod dorsal pneumatic features will need to be studied more thoroughly to finalize this phylogenetic character, and it may well need to be re(de)fined in the future.

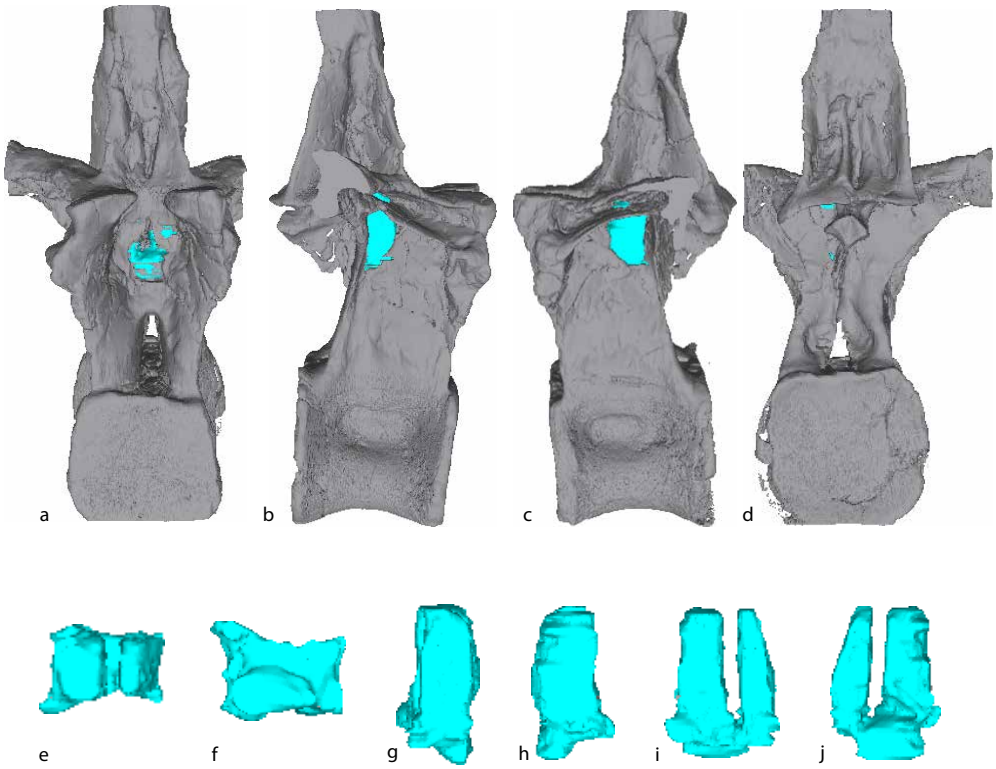

Figure 4: *Patagosaurus* dorsal PVL 4170 (13) CT rendering, with CDF and pneumatic chamber in blue. Dorsal PVL 4170 (13) in anterior (a), lateral (b,c) and posterior (d) view, with the CDF and pneumatic chamber in dorsal (e), ventral (f), lateral (g,h), anterior (i) and posterior (j) views.

Caudals:

(200) Anterior caudal vertebrae, neural spine: (0) flat spine summit; (1) saddle-shaped spine summit. This character was added after seeing the saddle-shaped spine tip of anterior caudals of *Patagosaurus* in lateral view as a potential autapomorphy for the taxon. This feature is also tentatively seen in *Cetiosauriscus*, and also in *Spinophorosaurus,* however, which could lead to more information on interrelationships between these taxa (Heathcote and Upchurch, 2003; Remes et al., 2009).

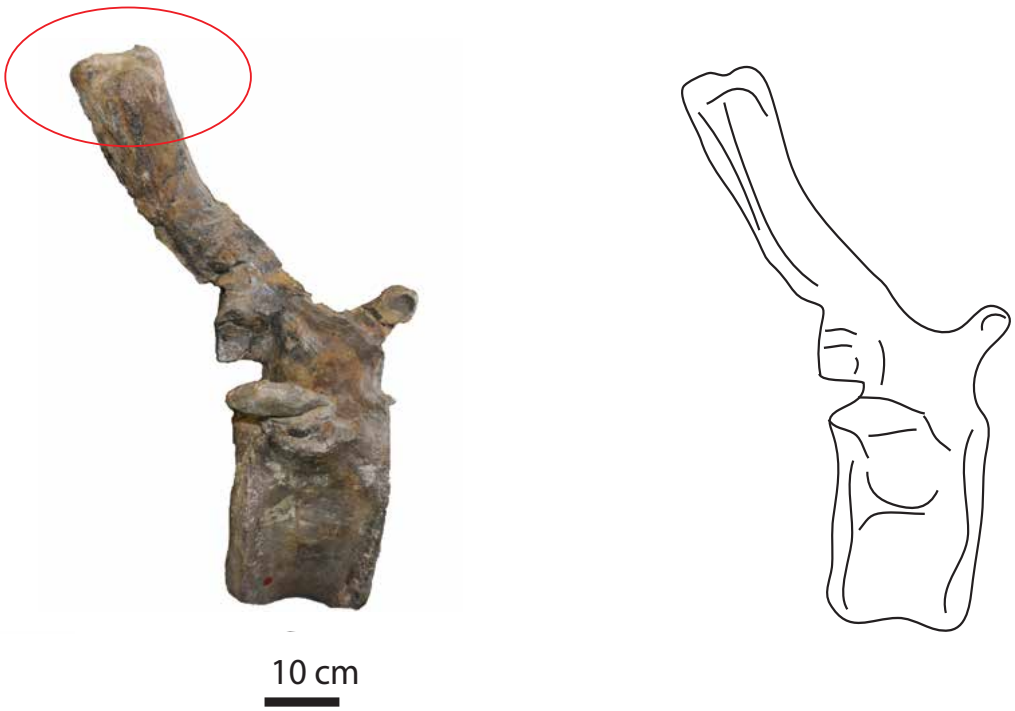

Figure 5: Saddle-shaped dorsal end of neural spine in lateral view (figure and line drawing) on *Patagosaurus* anterior caudal PVL 4170 (20).

4.4 Results

Using just the holotype codings, and no other associated *Patagosaurus* material, the matrix consisted of 350 characters and 78 taxa. Using the following parameters: {1000 replicates, TBR, hold 100000} the analysis gave a best hit of 34 times out of 1000, and 280 most parsimonious trees (mpt's) were found, without overflow.

The tree showed a polytomy, therefore an analysis was performed to trace which taxa were unstable, and therefore jumping positions in the tree, creating an unstable topology.

The command 'pcr . > 0 ; nelsen // {0} ; ' was used to identify unstable taxa. This command is a variant on the IterPCR command of Pol and Escapa, (2009), which reiterates tree calculations so that unstable taxa are found, and created subsequently by Goloboff and Szumik , (2015). The PCR Nelsen command creates a Nelsen Consensus tree after identifying the unstable taxa.

These taxa were subsequently pruned a-posteriori. The taxa were *Cetiosauriscus stewarti* and *Klamelisaurus gobiensis*.

Cetiosauriscus stewarti (not to be confused with *Cetiosauriscus greppini*, a basal titanosauriform from the Late Jurassic of Switzerland, Charig, 1993; Schwarz et al., 2007), is a non-neosauropodan eusauropod from the Oxford Clay Formation of the UK, which is dated to be Callovian-Oxfordian in age (Charig, 1980; Cox et al., 1992; Heathcote and Upchurch, 2003). It is one of the best-preserved sauropods from the Oxford Clay, and has been found to be different from *Cetiosaurus*, being tentatively retrieved as a more derived taxon than *Cetiosaurus*, or even as a basal neosauropod (Charig, 1980, 1993; Heathcote and Upchurch, 2003). It shares morphological features with *Patagosaurus* on the caudal neural spines; however, the taxon has not received any revision or osteological description since 1993, since a renewed attempt at redescription and phylogenetic analysis was discontinued (Charig, 1980, 1993; Heathcote and Upchurch, 2003), and the current information available did not yield enough information to keep this taxon as a viable OTU in this anaylsis (but see third and final analysis). A revision is therefore necessary, which will provide more phylogenetic information, which can subsequently be used in an analysis. This is currently beyond the scope of this study (but promised to be carried out in the near future by Upchurch et al., in prep, P.Upchurch and P.Mannion pers. comm.).

Klamelisaurus gobiensis (Zhao, 1993) is a basal mamenchisaurid from the Middle Jurassic of China. The Mamenchisauridae are currently under revision (e.g. Russell and Zheng, 1993; Barrett, 1999; Ouyang and Ye, 2002; Xing et al., 2015; McPhee et al., 2016a), and, moreover, *Klamelisaurus* itself is also under revision (Moore et al., 2017). It is thought to be more basal to *Mamenchisaurus* and *Omeisaurus*, and thus could give information on Middle Jurassic sauropod diversity from the East of Laurasia, and would be valuable to compare with

Patagosaurus, besides *Shunosaurus*, which is currently the only well-known taxon from this time from the East of Laurasia. Other Chinese taxa are either too fragmentary, difficult to access, or possess very unclear systematic information, therefore these are not used in this analysis (e.g. *Datousaurus*, mamenchisaurs other than *Mamenchisaurus youngi* and *Mamenchisaurus hochuanensis*, Dong and Tang, (1984); Zhang, (1988); Xing et al., (2015)). The thorough revision of *Klamelisaurus* is currently ongoing (Moore et al., 2017); however, therefore there is not enough information on *Klamelisaurus* to keep it as a valid OTU in this analysis.

The TNT file ‚bremsupred' was used to prune the unstable taxa out, by giving the taxa numbers in the bremsupred file. This program calculates Bremer support while excluding the unstable taxa, after which it renders the consensus tree. Bremer support shows the number of steps it takes to break a phylogenetic relation apart (see Bremer, 1994; Goloboff et al., 2008). The results are shown in a simplified consensus tree in Figure 6 and a list of synapomorphic characters is shown in Table 1 (but see Appendix for the complete consensus tree).

The holotype of *Patagosaurus fariasi* is retrieved as not only sister-taxon to *Cetiosaurus*, but as nested within *Cetiosaurus*, and is sister-taxon to the Rutland *Cetiosaurus*. All characters uniting the cetiosaurs are characters of the dorsal vertebrae (see Table 1). The cetiosaur node has a Bremer support of 2 (whereas the Bremer support was 1 for other basal eusauropod nodes). Furthermore, *Barapasaurus*, the other 'cetiosaur', is retrieved as less derived, being sister-taxon to the node of *Spinophorosaurus+Volkheimeria*, which all together are more basal to *Shunosaurus* (and thus are non-eusauropod sauropods) and *Patagosaurus+Cetiosaurus*. *Spinophorosaurus+Volkheimeria* is supported by a weakly developed hyposphene-hypantrum complex, and these are united with *Barapasaurus* in having longitudinal grooves on teeth, and the height of the postzygapophyseal pedicels in middle and posterior dorsals. Moreover,

forcing taxa together in the free edit mode in TNT, takes more than 20 steps to force *Barapasaurus* into a sister-group with *Patagosaurus* and *Cetiosaurus*. In a previous analysis by Remes et al., (2009), *Patagosaurus+Barapasaurus* were only one step removed. Other than this, the tree does not change much from previous analyses, in that *Tazoudasaurus* and *Vulcanodon* come out as sister-taxa, and more basal to *Barapasaurus*, as was previously also found (Allain and Aquesbi, 2008; Läng, 2008). *Patagosaurus* is also still found to be more basal to mamenchisaurs, turiasaurs, *Jobaria*, and neosauropods, which was also found in previous analyses (e.g. Wilson, 2002; Harris, 2006; Carballido et al., 2012, 2015; Carballido and Sander, 2014). However, the re-coding of *Volkheimeria* retrieves this taxon as an overal more basal taxon than previously assumed (it was assumed to be a brachiosaurid, and sister taxon to *Lapparentosaurus* (Bonaparte, 1986b)), and it also is recovered as more basal than *Patagosaurus,* and it forms a sister-group with the North African Middle Jurassic taxon *Spinophorosaurus.*

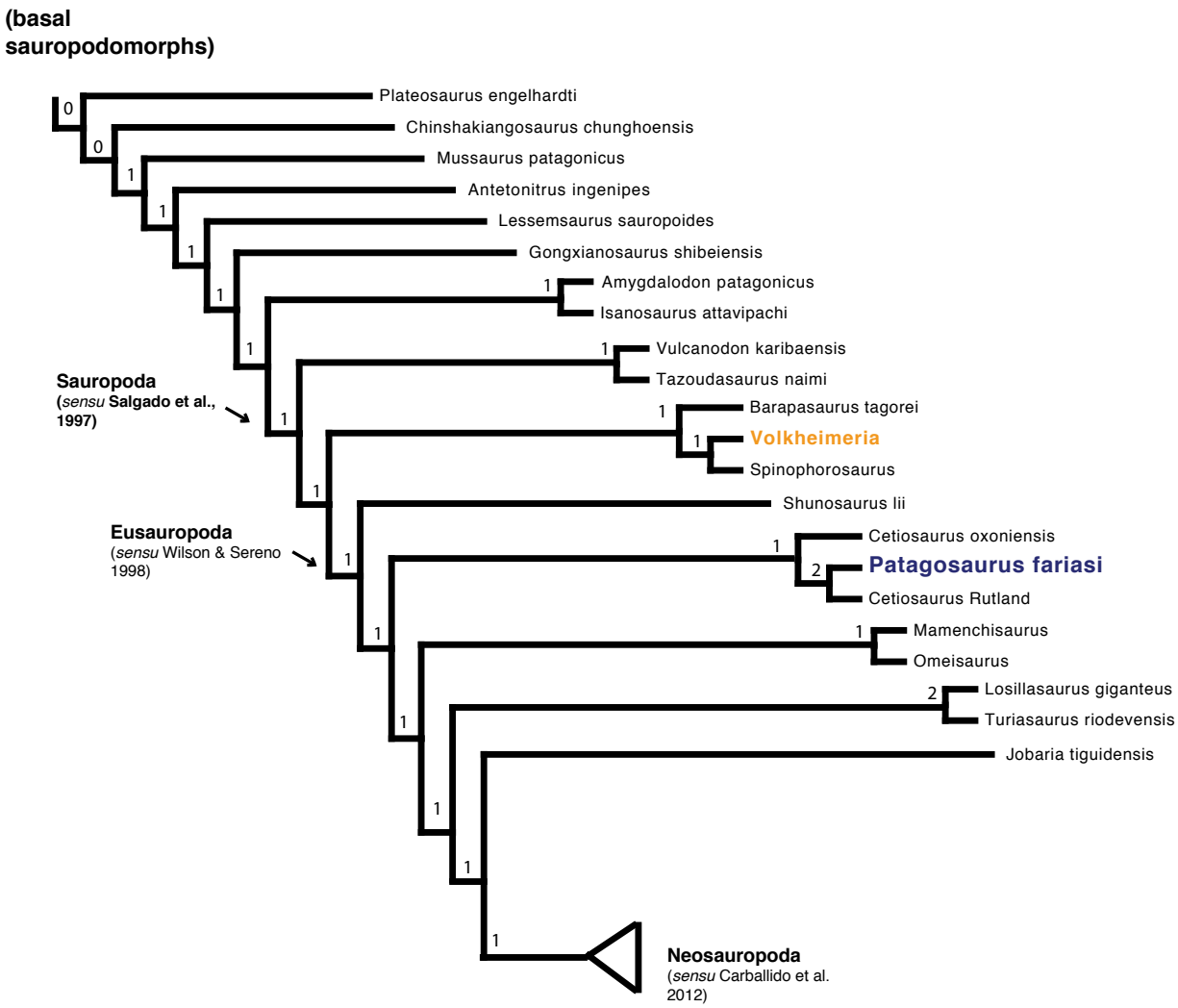

Figure 6: *Patagosaurus fariasi* PVL 4170 Strict consensus tree (simplified) of 280 trees with Bremer support. *Patagosaurus* in blue, *Volkheimeria* in orange.

Table 1: List of synapomorphic characters for the first phylogenetic analysis

Node	Synapomorphies
Spinophorosaurus + Volkheimeria	155: weakly developed hyposphene-hypanthrum complex on posterior dorsals
Barapasaurus + eusauropods	108: presence of longitudinal grooves on teeth
	175: height of pedicels of middle and posterior dorsal postzygapophyses subequal or higher than centrum
Patagosaurus + Rutland Cetiosaurus	123: Complex pleurocoel on cervical centra
	134: laterally expanded neural spine on posterior cervicals
	157: single tpol supporting hyposphene from below
	179: medial spol on posterior dorsals
Cetiosaurus + Patagosaurus + Rutland *Cetiosaurus*	164: pcpl absent on middle and posterior dorsals
	165: slightly dorsoventrally compressed dorsal centrum
	175: height of pedicels of middle and posterior dorsal postzygapophyses subequal or higher than centrum
	217: presence of ventral longitudinal hollow on anterior and middle caudals
Mamenchisaurus + eusauropods	115: presence of pleurocoels within cervical centra
	137: 12 or more dorsal vertebrae
	138: pleurocoels in dorsal centra
	148: single neural spines on dorsal vertebrae
	174: dorsal contact of spdl + lspol
	192: dorsoventral length sacral ribs
	238: size scapular acromion process

The second phylogenetic analysis was performed using the same matrix, but adding the associated material for *Patagosaurus*. All material that could safely be referred to *Patagosaurus* was selected, and material that did not have any overlap with the holotype, and thus provided new information, was coded for.

This material mainly represented pectoral and appendicular elements, and gave new (or simply not coded for) information on the scapula and coracoid, sternal plate, humerus, radius, ulna, tibia, and pes of *Patagosaurus fariasi*.

Additionally, cranial elements, a dentary and a premaxilla, could be added to this new information. However, there were not many cranial characters that could be coded for, as most cranial characters for tooth-bearing bones are for the association with articulated cranial elements, and these *Patagosaurus* cranial elements are isolated. The dentition, however, gives many characters, and new characters were added for the dentition, based on previous analysis (Holwerda et al., 2015).

Moreover, MACN-CH 934, a juvenile specimen from Cerro Condor Sur, thought to not be *Patagosaurus,* characterized by the presence of a clear spdl on dorsal and sacral neural arches, well-developed hyposphene-hypantrum complexes, and an ambiens process on the pubis, among others, was coded as a separate OTU to determine its phylogenetic position in the tree.

More Gondwanan taxa were added for this analysis; *Lapparentosaurus madagascariensis* (Bonaparte, 1986b), *Bothriospondylus* (Lydekker, 1895; Läng, 2008; Mannion, 2010), and *Klamelisaurus* as well as *Cetiosauriscus* were recoded in an attempt to counteract the unstable taxon effect for these two taxa. *Lapparentosaurus* and *Bothriospondylu*s are two Middle Jurassic sauropods from Madagascar, for which the associations are not entirely clear, but which both have information on East-Gondwanan sauropod morphology. *Lapparentosaurus* is a juvenile sauropod, first described by Bonaparte (1986b); and more recently by Läng (2008). The latter retrieved it as a basal non-neosauropod eusauropod, the former retrieved it as a brachiosaurid, closely related to *Volkheimeria*. *Bothriospondylus* is known from several

localities, and the skeletal association is not well-defined for this taxon. The type material from the NHM was recently redescribed, however, showing that the taxon is most likely invalid (Mannion, 2010). The large specimen from Madagascar might even be an adult *Lapparentosaurus* (P. Mannion, pers. comm.) Nevertheless, the associated material has morphological information which could be coded for phylogenetic analysis (Läng, 2008).

Rhoetosaurus brownei (Longman, 1927) was originally scheduled for inclusion in this analysis, however the material is poorly preserved, and the specimen is currently under preparation (see Nair and Salisbury, 2012; J.Nair pers. comm.). This is the eastern-most Gondwanan sauropod known from the Middle Jurassic. Therefore, in future analyses, the inclusion of this taxon as an OTU would be helpful for sauropod evolutionary study.

The same procedure as for the first analysis was repeated. However, the addition of these extra taxa made the tree more unstable; after a TBR with 1000 replicates, 26451 trees were found. However, not all trees were found yet, and when trees were taken from RAM, 27002 trees were found with a best TBR score of 1090 (in contrast to 280 trees in the first analysis).

The same unstable taxa search with PCR and Nelsen was performed, which again gave *Cetiosauriscus*, *Klamelisaurus*, and now also *Bothriospondylus* as unstable taxa, which were then pruned a-posteriori. *Lapparentosaurus* was found to be stable.

Despite having to prune taxa, the resulting tree was well-resolved, see Figure 7:

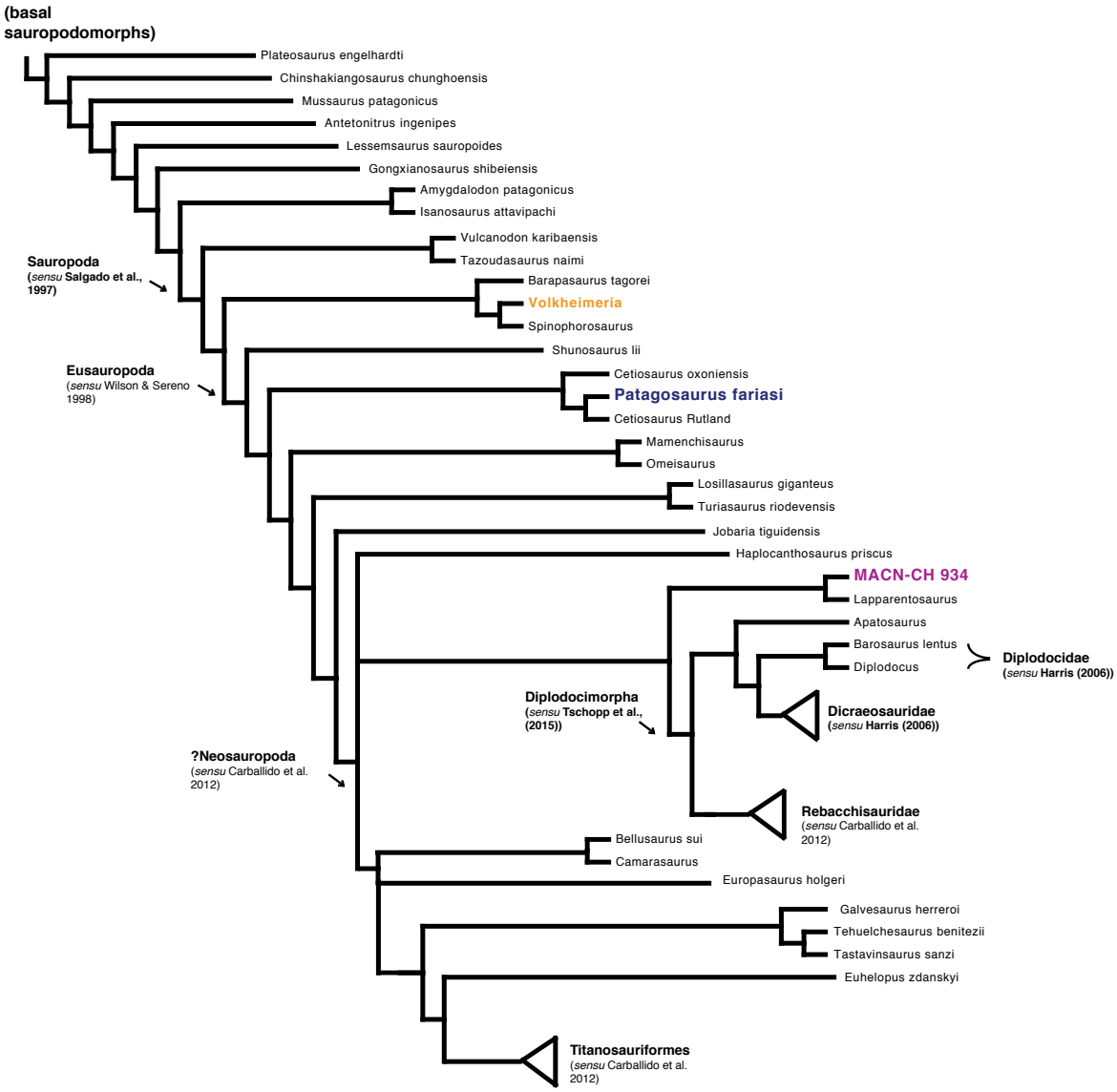

Figure 7: Strict Consensus tree of 27002 trees of all *Patagosaurus* material, (in blue), MACN-CH 934 (in purple), and *Volkheimeria* (in orange).

The position of *Patagosaurus*, as well as *Cetiosaurus*, does not change in this analysis; when a Bremer support analysis was run in between analyses, the Bremer support for the 'cetiosaurs' also does not change. *Patagosaurus* is still nested within the Cetiosauridae, and it is still more derived than the other Middle Jurassic Gondwanan and Laurasian sauropods, except for *Mamenchisaurus, Omeisaurus, Jobaria,* and the Late Jurassic turiasaurs. However, in this analysis, MACN-CH 934 comes out more derived than any of these Middle Jurassic sauropods,

and ends up as sister-taxon to *Lapparentosaurus*, and also as the most basal clade of Diplodocimorpha, and MACN-CH 934 + *Lapparentosaurus* being sister-group to the clade uniting rebbachisaurids and flagellicaudatans. It takes 6 additional steps to move these two taxa to the 'cetiosaur' node. See Table 2 for synapomorphies. MACN-CH 934 and *Lapparentosaurus* are united by dorsal vertebral characters, namely the position of the transverse processes, the existence of a spinodiapophyseal lamina (note that *Patagosaurus* and both cetiosaurs explicitly do not have an spdl) and a transversely narrower spine than anteroposteriorly (which is reversed in *Patagosaurus* and the cetiosaurs). MACN-CH 934+*Lapparentosaurus* and all 'neosauropods' (see below) are united by dental characters, the absence of an aliform process on dorsals, and the presence of a medial spinopostzygapophyseal lamina (mspol), see Table 2. *Haplocanthosaurus*, a basal neosauropod, (Hatcher, 1903; McIntosh and Williams, 1988; Foster and Wedel, 2014) comes out in a trichotomy with the two major lineages of neosauropods.

Note the '?Neosauropoda', this is because the base of Neosauropoda is unclear in this tree, as a trichotomy makes the usage of the definition of Neosauropoda (*Saltasaurus*, *Diplodocus*, and all their descendants) not possible. The same issue goes for Diplodocoidea, which is *Diplodocus*, but not *Saltasaurus* (Tschopp et al., 2015). Therefore, Diplodocimorpha (*Rebbachisaurus* + *Diplodocus* (Tschopp et al., 2015) is used here.

Table 2: List of synapomorphies for results of the second phylogenetic analysis

Node	Synapomorphies
MACN-CH 934 *+ Lapparentosaurus*	140: transverse processes of dorsals directed slightly dorsally
	169: spinodiapophyseal (spdl) present in posterior dorsals
	183: neural spine narrower transversely than anteroposteriorly
MACN-CH 934 *+ Lapparentosaurus* + ?neosauropods	97: more than four replacement teeth
	103: cylindrical tooth shape
	106: fine or pebbly wrinkling of tooth enamel
	110: SI (Slenderness Index, *sensu* (Upchurch, 1998)) of 3-4 for teeth
	167: absence of aliform process on dorsal vertebrae
	180: medial spinopostzygapophyseal lamina (mspol) present on dorsal vertebrae

The third analysis used this same matrix; however, MACN-CH 230, which might also be different from *Patagosaurus,* (see Chapter 3) was added as an OTU. As mentioned in the revision of the associated material, specimen MACN-CH 230, consisting of several dorsal vertebrae, shows some dissimilarities with both the *Patagosaurus* holotype, the *Patagosaurus* associated material, and with MACN-CH 934, as well as with *Volkheimeria*. Therefore, as a test to see whether this dorsal vertebral morphology validates a different taxonomic origin, or to see if the differences are more to do with serial and/or ontogenetic variation, the specimen was scored in the matrix, together with all *Patagosaurus* material, as well as MACN-CH 934.

The matrix, however, showed many overflows when run with a traditional TBR with 100 and 1000 multiplications, and showed a hit score of only 6 out of 100, and 10 out of 1000, with a best hit of 1103. A subsequent multiplication with trees from RAM showed a best hit of 1155 and still overflow of trees, with 3144 trees found.

The resulting Strict Consensus tree is shown in Figure 8. Interestingly, in this analysis, *Bothriospondylus* was not found to be an unstable taxon, and did not consequently needed pruning. Moreover, *Cetiosauriscus* and even *Klamelisaurus* did not need pruning. *Klamelisaurus*, however, does come out in a far more basal position than expected for an alleged mamenchisaur, showing the need for more work on this specimen.

The results show no change for the *Patagosaurus*+*Cetiosaurus* relationships, and also MACN-CH 934 remains at the same tree node; at the base of Diplodocimorpha. However, *Lapparentosaurus* jumped back in the tree, towards a more basal position than as sister taxon to MACN-CH 934. *Lapparentosaurus* is here nested with MACN-CH 230, together with *Cetiosauriscus*, and is sister taxon to *Bothriospondylu*s. Moreover, specimen MACN-CH 230 (together with the formerly mentioned taxa) comes out as sister group to *Cetiosaurus*+*Patagosaurus*+Rutland *Cetiosaurus*. However, it only takes 3 additional steps to move MACN-CH 230 to *Cetiosaurus*+*Patagosaurus*. It takes 20 additional steps to move *Lapparentosaurus* to this group. MACN-CH 230, *Cetiosauriscus*, *Lapparentosaurus* and *Bothriospondylus* are united by the presence of a medial spinopostzygapophyseal lamina, the absence of the centrodiapophyseal fossa, and the presence of a centropostzygapophyseal lamina (see Table 3). *Spinophorosaurus, Barapasaurus and Volkheimeria* are basal to *Cetiosaurus+Patagosaurus*, as in the previous analysis. However, it only takes an additional 2 steps to move *Spinophorosaurus* to be a sister taxon to *Patagosaurus.* Moving MACN-CH 934 to *Patagosaurus* takes an additional 7 steps. The vulcanodontids *Vulcanodon+Tazoudasaurus*

remain in a similar place on the tree topology. Bootstrap GC values were not high for this tree, not going over 32% for any of the basal eusauropod nodes.

The jumping of *Lapparentosaurus* and the low amount of steps necessary to move *Spinophorosaurus* shows that these taxa need more morphological information before their phylogenetic position can by analysed with more confidence. The position of MACN-CH 934 as a basal neosauropod seems to be stable, as well as the *Patagosaurus+Cetiosaurus* group.

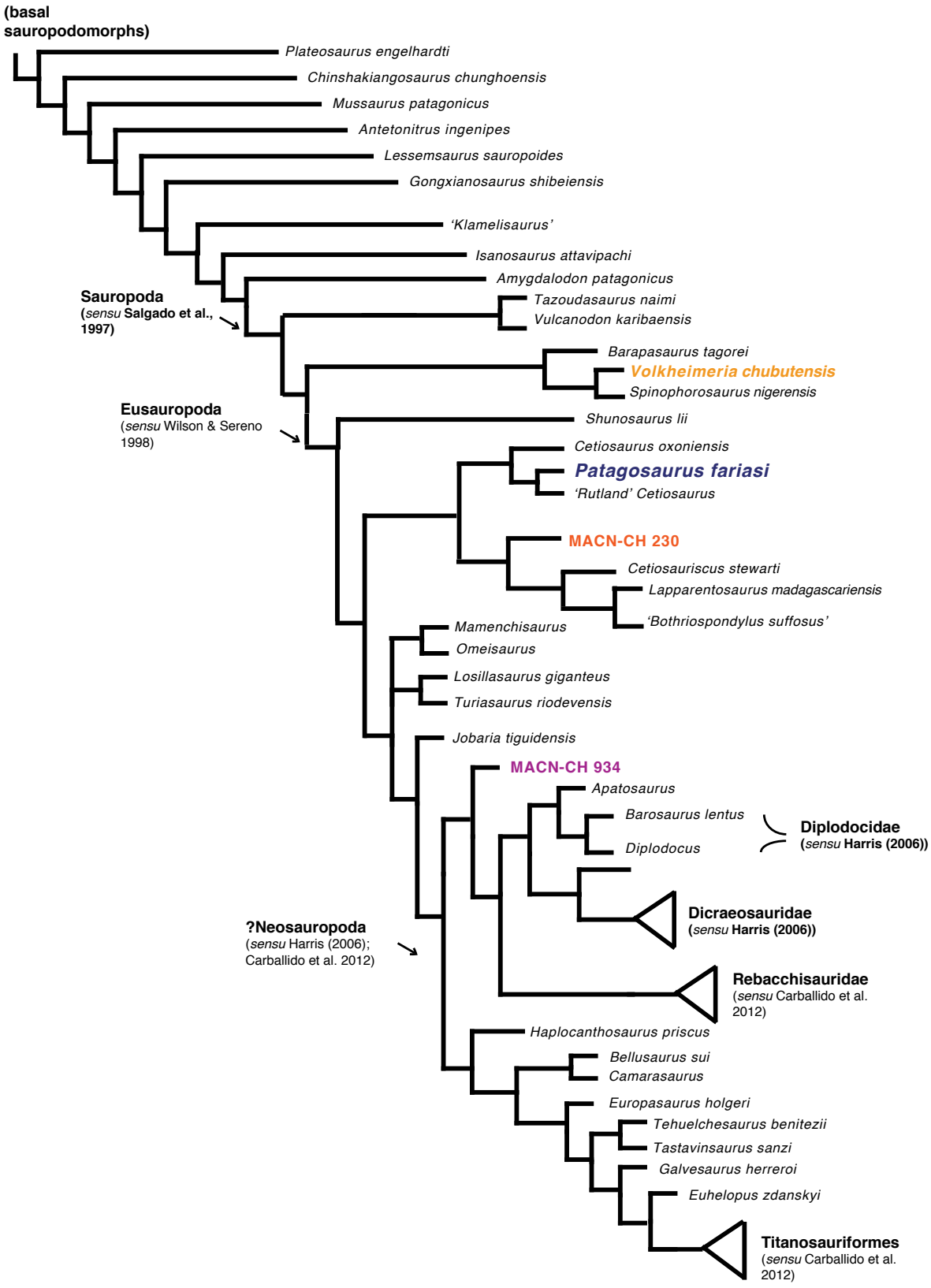

Figure 8: Strict Consensus tree of all *Patagosaurus* material (in blue), including MACN-CH 934 (purple), *Volkheimeria* (in light orange) and MACN-CH 230 (in dark orange) as separate OTU's.

Table 3: synapomorphies of third phylogenetic analysis

Node	Synapomorphies
MACN-CH 230 + ‘cetiosaurs‘	165: absence of posterior centroparapophyseal lamina (pcpl)
	176: height of neural arch subequal or greater than height of centrum
	205: presence of (rudimentary) ventrolateral ridges on caudal vertebrae
	218: absence of ventral longitudinal hollow on caudal vertebrae
	261: relatively low (0.6) humerus to femur ratio
MACN-CH 230 + *Lapparentosaurus* + *Bothriospondylus*	169: presence of accessory spinodiapophyseal lamina
	177: presence of centropostzygapophyseal lamina
	179: absence of centdodiapophyseal fossa (CDF)

The characters that unite *Cetiosaurus*, *Patagosaurus*, the Rutland *Cetiosaurus*, with MACN-CH 230, *Cetiosauriscus, Lapparentosaurus*, and *Bothriospondylus*, are mainly characters that distinguish them from neosauropods (i.e. characters found in neosauropods, but not in non-neosauropod eusauropods), such as the absence of a longitudinal ventral hollow on caudals, the presence of only a rudimentary ventrolateral crest (as opposed to a prominent one, see Tschopp et al., 2015), the height of the neural arch, and the absence of the pcpl (see Table 3).

4.5 Discussion and conclusions

4.5.1 Phylogenetic signal

The position of *Patagosaurus* as a derived non-neosauropodan eusauropod, sister taxon to the Rutland *Cetiosaurus*, and being nested within *Cetiosaurus*, has a slightly higher Bremer support, and remains stable even though other taxa are unstable and jump positions frequently in different analyses. *Barapasaurus*, attributed as sister-taxon to *Patagosaurus*, is no longer closely-related to *Patagosaurus* in this analysis; in fact it is considerably more basal *to Patagosaurus*. This is contra Allain and Aquesbi, (2008) and Remes et al., (2009), where these latter taxa are found to be closely related. At first sight, the morphology does not differ that much between the original Cetiosaur triad proposed by Bonaparte (1986a,b). The lamination on the neural arches of *Barapasaurus,* however, especially on dorsal vertebrae, is considerably less elaborate than in *Patagosaurus*, or in the Rutland *Cetiosaurus*. Moreover, on closer inspection, there are many morphological similarities between *Cetiosaurus* and *Patagosaurus* that are missing in *Barapasaurus*, such as the expansion of the transverse processes to the lateral side, the lateral and medial spols, the small aliform process, cpols and stpol, and also in the appendicular elements, such as the tapering anterior lobe of the ilium, the axial elongation of the ilium, the morphology of the scapular blade and the transverse width and anteroposterior compression of the femur.

However, *Barapasaurus* is in need of revision, as some parts of the taxon are, just as *Patagosaurus*, uncovered from different localities, and may not belong to *Barapasaurus*, and therefore the holotype and associated specimens might be composite specimens (Bandyopadhyay et al., 2010; O.Rauhut, D.Pol pers. comm.). Therefore, the phylogeny of *Barapasaurus* is likely to remain uncertain until a thorough revision of all material has been performed.

The close affinities of *Patagosaurus* and *Cetiosaurus* could still be a result of biased coding, as the *Cetiosaurus* material (both *C. oxoniensis* and the Rutland material) is easily accessed, and generally well-preserved, and therefore will provide more phylogenetic information than many other basal sauropods. The Rutland *Cetiosaurus* has, in the last decade or so, been considered to be a separate genus from *Cetiosaurus* (e.g. Läng, 2008, J.Martin pers. comm., P.Mocho pers. comm.). A new phylogenetic analysis including the Rutland *Cetiosaurus* as separate OTU from *C. oxoniensis* is proposed, however, and if more information on *Cetiosaurus* should arise from this, this could potentially break the *Patagosaurus+Cetiosaurus* clade apart. Finally, as *Cetiosaurus mogrebiensis* has not been coded for this analysis, a potential polytomy could not form with any unstable cetiosaurids, and perhaps in future analyses the *Cetiosaurus+Patagosaurus* relationship will fall apart, as is demonstrated by Läng in 2008. *Cetiosaurus mogrebiensis* is unfortunately not accesseable for study for the coming years, as the specimen will need significant preparation (R. Allain pers. comm.).

However, this analysis does confirm the original assessment of Bonaparte in 1986a, in that *Patagosaurus* and *Cetiosaurus* share a close phylogenetic affinity. Both are from roughly the same age; *Patagosaurus* being Aalenian-Bajocian, *Cetiosaurus oxoniensis* ranging from Bajocian to Callovian, and the Rutland *Cetiosaurus* being Bajocian in age (Cox et al., 1992; Upchurch and Martin, 2002, 2003; Barrett, 2006; Liston, 2004a,b; Noè et al., 2010; Cúneo et al., 2013; Hauser et al., 2017). The close affinity shows a global radiation of sauropods well into the late Early and early Middle Jurassic, which suggests much earlier global radiation of sauropods, and indeed, several early sauropods are known from both Gondwana, but also from Laurasia from recent studies (McPhee et al., 2016b; Lallensack et al., 2017; Rauhut et al., in prep). However, biogeographical analyses need to validate this assumption, which is a topic for future research and analyses.

The positions of *Lapparentosaurus* and *Bothriospondylus* show a need for more information on both taxa. *Bothriospondylus* was too unstable to remain in the analysis for the first two runs, both when the *Patagosaurus* holotype was included, as well as with all of the associated material subsequently included. The third analysis, with the inclusion of MACN-CH 230, gave a tree that showed low support for the nodes. *Bothriospondylus* does not feature often in phylogenetic analysis, and the taxon is not considered valid by some authors (Mannion, 2010); however, others point out the need for more inclusion of the Madagascar material from the collections in the MNHN Paris (Läng, 2008; Läng and Mahammed, 2010), and, if the *Bothriospondylus* material is indeed an adult *Lapparentosaurus*, the close affiliation in the phylogenetic analysis of both would support this. *Lapparentosaurus,* however, has long been included in phylogenetic analyses, although it comes out in different positions, and this analysis proves no exception. However, in the more stable tree outcomes, *Lapparentosaurus* is a basal neosauropod, as is MACN-CH 934 consistently. This is unusual, but not impossible for the Middle Jurassic. Isolated possible neosauropod teeth are found in the early Middle Jurassic of Argentina, see for example (Carballido et al., 2017). Moreover, a neosauropod is known from the Cañadón Calcáreo Formation, which is only slightly younger than the Cañadón Asfalto Formation (Rauhut et al., 2015). The characters that unite these sauropods with neosauropods are based on dentition, with some conflicting characters (e.g. enamel wrinkling pattern), which shows that the characters need more study. Moreover, the interrelationships between the more derived non-neosauropod eusauropods are still not well understood (e.g. *Jobaria*, as the original description by Sereno et al., (1999) is based on a composite specimen (O.Rauhut and E.Tschopp pers. comm.)) and the turiasaurs (Mocho et al., 2014, 2016)), and even some probably basal neosauropods still change positions between analyses (e.g. *Haplocanthosaurus*, Foster and Wedel, 2014). *Lapparentosaurus*, however, comes out as a non-neosauropodan eusauropod in Läng's analysis (Läng, 2008), and in Mannion's 2013 analysis of Late Jurassic sauropods, it is retrieved at one step before the node of neosauropods

(Mannion et al., 2013), which shows a consistently more derived position in recent phylogenetic analyses (Mannion et al., 2013).

The position of S*pinophorosaurus* is also still unclear, as this taxon shows derived features that indicate a close morphological affinity with *Patagosaurus*, yet it is retrieved as more basal (however, moving it closer to *Patagosaurus* only takes a few extra steps). A complete osteology of *Spinophorosaurus* is in the making, however (D. Vidal & F. Knoll, pers. comm.), and will provide more information on this taxon, as several authors noted derived characters on the material, which might alter the phylogenetic placing (J. Carballido, pers. comm.).

Finally, the sister group relationships of *Cetiosaurus*, *Patagosaurus*, Rutland *Cetiosaurus*, and MACN-CH 230, *Cetiosauriscus*, *Lapparentosaurus* and *Bothriospondylus,* being retrieved as derived non-neosauropod eusauropods in the third phylogenetic analysis, could potentially hail a new grouping of the Cetiosauridae, as early Middle Jurassic, Gondwanan and west Laurasian-dwelling, derived non-neosauropodan eusauropods, with a distinct set of characteristics which separates them from more basal non-neosauropodan eusauropods (such as *Volkheimeria*), and which also separates them from the mamenchisaurids. This is further supported by the characters uniting this group of non-neosauropod eusauropods, which is the absence of characters shared by neosauropods. Again, however, as the relationships of the Malagasi sauropods are not well understood, and *Cetiosauriscus* is retrieved as either a derived non-neosauropodan eusauropod, or a basal neosauropod (Charig, 1980; Upchurch and Heathcote, 2003), this claim cannot be made certain until more studies have been performed (and until the interrelationships of basal neosauropods are better understood as well). Furthermore, the low number of additional steps necessary to force MACN-CH 230 to be the sister taxon to *Patagosaurus* also make it unclear whether this is a small specimen of *Patagosaurus* with larger intraspecific changes than the other *Patagosaurs* (e.g. MACN-CH 935, 933, etc.), or really a taxon on its own.

4.5.2 Biogeographic implications

Previous studies have suggested an Early-Middle Jurassic Southern Gondwanan endemism of sauropods, (see Allain and Aquesbi, 2008; Rauhut and López-Arbarello, 2009; Pol et al., 2011; Apesteguia et al., 2012; Pol and Rauhut, 2012;). This endemism was theorized to be possibly related to the presence of the Central Gondwanan Desert (see e.g. Remes et al., 2009) as a physical barrier between South and North Gondwana (as well as Laurasia).

However, with the breaking-up of the close affinity between *Patagosaurus* and *Barapasaurus*, and furthermore, with the close affinity of *Patagosaurus*, a South-West Gondwanan sauropod, and *Cetiosaurus*, a Mid-Laurasian sauropod, other patterns are indicated by this sauropod phylogeny (see Figure 9). First of all, *Volkheimeria*, discovered together with *Patagosaurus* from the Cerro Condor bonebeds in the Cañadón Asfalto Formation, shows affinities with *Spinophorosaurus,* a sauropod from the Middle Jurassic of Niger, which was more or less North-East Gondwana. Moreover, both the associated specimens of *Patagosaurus*, MACN-CH 934 and MACN-CH 230, come out in subsequent analyses as closely-related to *Lapparentosaurus*, and *Bothriospondylus*, respectively, which are taxa from Madagascar, in South-East Gondwana. A potential explanation for these affinities is the periodical absence/intermittent presence of the Gondwanan desert as a barrier, be it seasonal with a wet season and a dry season, or with climatic cyclicity. The Cañadón Asfalto Formation has been proven to show climatic cyclicity, with alternating dry and more humid conditions (Escapa et al., 2008; Volkheimer et al., 2008; Cúneo et al., 2013). Another option is that the desert was not a barrier at all, and that the sauropods dispersed freely over the continent of Gondwana, and even went north to Laurasia. The edges of the desert were thought to be more temperate and could allow for migration (Rauhut and López-Arbarello, 2009). Migration has

been proven for Late Jurassic sauropods, and Middle Jurassic ichnofossils show that sauropods traveled for long distances (Manley, 1991; Meyer, 1993; Foster et al., 2000; Fricke et al., 2011). Unfortunately, there is as yet very little recorded on Early-Middle Jurassic terrestrial sediments from the west of Laurasia (i.e. current North America), safe for tridactyl footprints and theropod remains (Kvale et al., 2001). However, as the United Kingdom is proven to be an island archipelago with shallow seas, lagoons, and sand banks, (long-term) migration of sauropods between South Gondwana and Midwest Laurasia is hypothetically possible (Day et al., 2004; M.Barron pers. comm.). As said in the previous part of this Chapter, the phylogenetically close relationships of the 'cetiosaurs' (*Cetiosaurus*, *Patagosaurus*, Rutland *Cetiosaurus*, and MACN-CH 230, *Cetiosauriscus*, *Lapparentosaurus* and *Bothriospondylus*), if correct, prove that a group of sauropods were 'cosmopolitan' i.e. widespread, and migrating. Their separation from the Chinese sauropods is supported by previous works (e.g. Russell, 1993; Wilson and Upchurch, 2009) which states that, by the existence of a sea barrier in the Jurassic, the Chinese sauropods were the only real endemic group of sauropods.

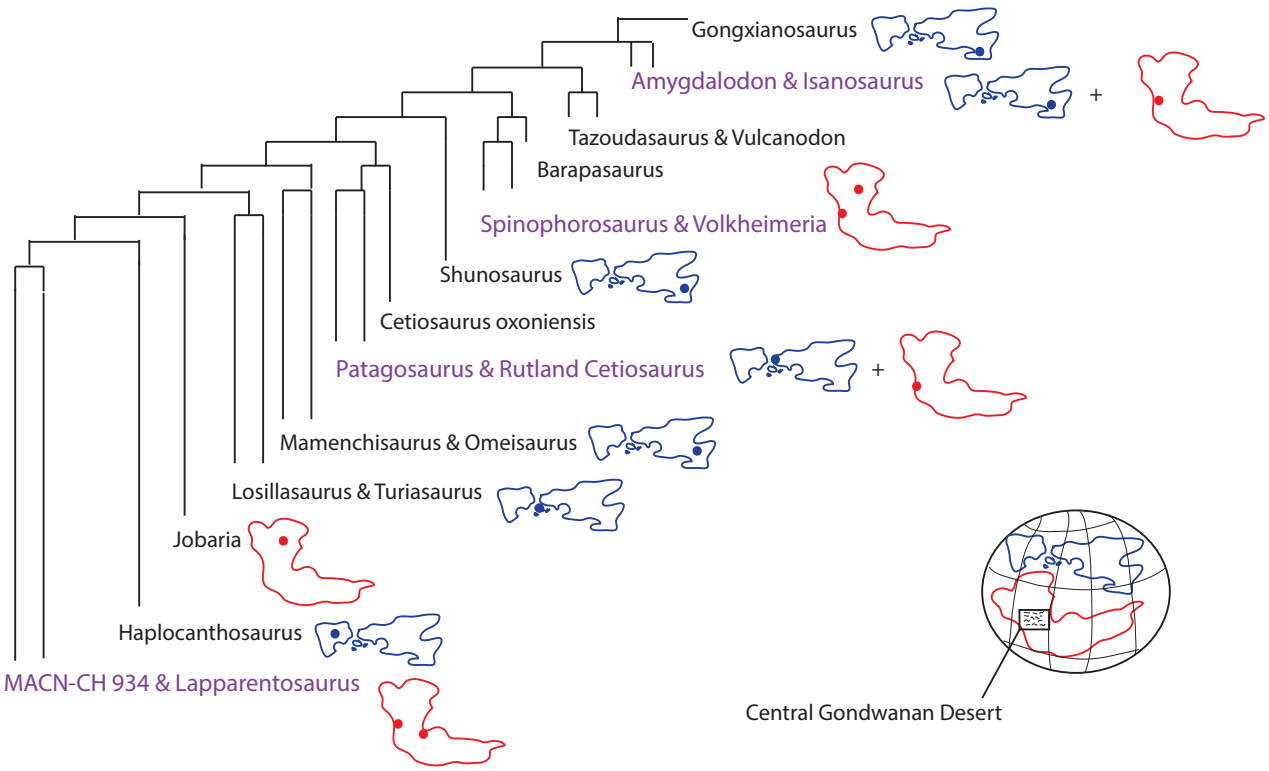

Figure 9: Simplified phylogenetic analysis of most relevant taxa (in purple). Gondwanan (red) and Laurasian (blue) provenances. Note that this is not a formal biogeographic analysis.

A preliminary biogeographical analysis using the programme RASP (Reconstruct Ancestral State in Phylogenies) using the Bayesian Binary Method is shown in Figure 10. Any further biogeographical analysis (with an application of S-DIVA and Lagrange methods) is not yet possible as the tree is not fully resolved (A. Cau Pers. Comm.). However, this data will be used in the future for a biogeographical analysis with another research group. Figure 9 repeats the aforementioned conclusions, with a mix of both Early/Middle Jurassic Laurasian and Gondwanan taxa showing close phylogenetic affinities.

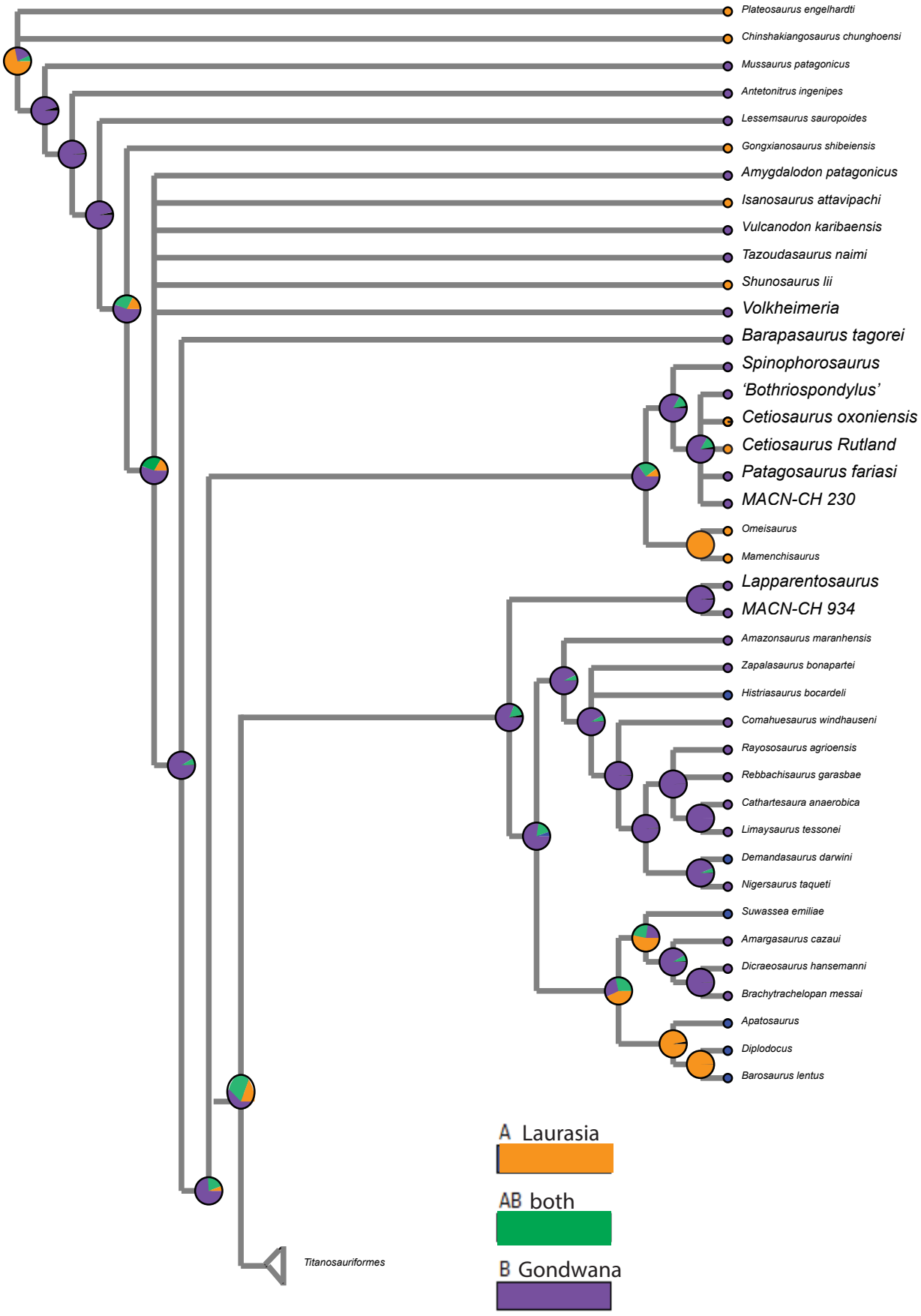

Figure 10: Preliminary Bayesian biogeographical analysis using RASP. Relevant taxa highlighted.

To summarize, this phylogenetic analysis gives new information and sheds new light on several relationships of *Patagosaurus* with contemporaneous sauropods. It also shows that several taxa need a similar redescription, to generate more morphological data in order to render a more accurate phylogeny. Therefore, this current analysis is definitely not enough to make any clear assumptions, and in future analysis a larger dataset should be provided. Moreover, in the future, more research on climatic and vegetation conditions for the South of Gondwana in the Middle Jurassic might aid this sauropod biogeographical interpretation.

4.5.3 Phylogenetic implications for the Cañadón Asfalto Formation sauropods

Within the Cañadón Asfalto Formation sauropod community, a high phylogenetic diversity is seen, with a relatively-derived non-neosauropod eusauropod position for *Patagosaurus*, potential neosauropod affinities for MACN-CH 934, and a more basal non-eusauropod sauropod position for *Volkheimeria*, MACN-CH 230, which comes out as a derived non-neosauropod eusauropod like *Patagosaurus*, and possibly yet another taxon, MACN-CH 232 (see Table 4).

The MACN-CH 934 material is moderately preserved, and it has both cranial, as well as axial material preserved, and pelvic elements, which give it enough information to be considered a new taxon, and it consequently will be analysed more thoroughly in the future. Moreover, its phylogenetic position is far enough removed from *Patagosaurus* and *Volkheimeria* to show a real phylogenetic signal. The position of MACN-CH 230, however, is more complicated. It could be a product of serial variation, or ontogeny, and, as it only has dorsal elements so far, it might not show a true signal, even though dorsal morphology is important for sauropod systematics.

Table 4 (next page): Sauropod diversity in major Middle Jurassic ecosystems known thus far. ([1] Remes, 2009, [2,3,4] Foster, 2003; Tschopp and Mateus, 2013, 2017, [5,6,7,8,9] Mannion et al., 2013, 2012; Mateus et al., 2014; Mocho et al., 2017, 2016, [10,11,12] Noè et al., 2010; Royo-Torres and Upchurch, 2012; Holwerda and Liston, 2017; , [13,14,15,16] He et al., 1988; Zhang, 1988; Zhao, 1993; Xing et al., 2015 17,18 Upchurch and Martin, 2002, 2003).

Formation/Locality/Age	Clade	Genera/Taxa
Tendaguru, Africa, Kimmeridgian-Tithonian[1]	Diplodocidae	*Tornieria* *Australodocus*
	Dicroaeosauridae	*Dicraeosaurus*
	Titanosauriformes	*Giraffatitan* *Janenschia* *Tendaguria*
Morrison Fm, USA, Kimmeridgian-Tithonian[2,3,4]	Diplodocoidea	*Amphicoelias* *Barosaurus*
	Diplodocidae	*Diplodocus* *Apatosaurus* *Suuwassea* *Kaatedocus* *Galeamopus*
	Macronaria	*Camarasaurus* *Cathetosaurus*
	Titanosauriformes	*Brachiosaurus*
	Neosauropoda	*Haplocanthosaurus*
Lourinhã Fm, Portugal, Kimmeridgian-Tithonian[5,6,7,8,9]	Eusauropoda	indet
	Diplodocidae	*Dinheirosaurus*
	Titanosauriformes	*Lusotitan*
	Macronaria	*Lourinhasaurus*
	Turiasauria	*Zby*
Peterborough Oxford Clay Fm, UK, Callovian-Oxfordian[10,11,12]	Eusauropoda/?Neosauropoda	*Cetiosauriscus*
	Turiasauria	BMNH R3777
	Diplodocoidea	PETMG R272
	Diplodocidae	LEICT G. 418.1956.21.0
	Brachiosauridae	BMNH R1984
	Neosauropoda	PETMG R85
Cañadón Asfálto Fm, Argentina, Aalenian-Bajocian	Sauropoda	*Volkheimeria*
	Eusauropoda (Cetiosauridae?)	*Patagosaurus* MACN-CH 230
	Eusauropoda	'Bagual sauropod'
	Neosauropoda	?MACN-CH 232 MACN-CH 934
Zigong Province & Sichuan Province, China, ~Bathonian-Callovian[13,14,15,16]	Eusauropoda	*Shunosaurus*
	Mamenchisauridae	*Omeisaurus* *Mamenchisaurus sp* *Klamelisaurus*
Forest Marble/Great Oolite, UK , Bajocian-Bathonian[17,18]	Eusauropoda (Cetiosauridae?)	*Cetiosaurus oxoniensis* Rutland *Cetiosaurus* Gloucestershire *Cetiosaurus*
	Eusauropoda (Cetiosauridae?)	
	Eusauropoda (Cetiosauridae?)	

	?Neosauropoda	*Cetiosaurus glymptoniensis*

The high diversity, however, in having three or four sauropod taxa from these bonebeds, as well as having yet another sauropod (potentially derived non-neosauropod eusauropod) taxon in the Cañadón Asfalto Formation (Pol et al., 2009), could still point to a Patagonian Gondwanan form of endemic radiation, as this is not seen in other Middle Jurassic sites yet (Pol et al., 2011; Apesteguia et al., 2012; Pol and Rauhut, 2012; Becerra et al., 2013; Holwerda et al., 2015). However, as the previous part of this Chapter made clear that migration was not impossible, this local diversity could also be a sampling artefact, as many sites in Gondwana have not been as extensively studied and excavated as the Cañadón Asfalto Formation. Table 4 shows a comparison between the diversity in sauropod genera of the Cañadón Asfalto Formation, and other Jurassic diversity 'hotspots', i.e. localities with a high generic number of sauropods. Although not as species rich as many of the other, more 'classic', localities, the Cañadón Asfalto Formation is also definitely not species-poor.

Only further study on Gondwanan taxa and localities (which is currently ongoing for some; P. Barrett pers. comm.) can further elucidate the true biogeographic patterns. Future studies of the Cetiosaurs (e.g. the Rutland *Cetiosaurus*, and other '*Cetiosaurus*' material from collections in the UK) might also show a high taxic diversity in the UK, similar as seen in Argentina.

This, together with high diversity patterns and interrelationships between Early Jurassic and Middle Jurassic sauropods in this analysis, along with the high diversity of the Cañadón Asfalto Fm. sauropods in the early Middle Jurassic, demonstrates the early sauropod diversification and radiation event in the Early Jurassic, and definitely pushes the boundaries of sauropod diversification and radiation further back to the Early Jurassic.

4.6 Acknowledgements go to José Luis Carballido for his great help in resolving many phylogenetic characters. Many thanks also to Emanuel Tschopp, Veronica Díez Díaz, Andrew Moore, and David Button. Andrea Cau and Neil Brocklehurst are thanked for help in a preliminary biogeographical analysis. The authors are also grateful to William Orsi for his help an early biogeographical analysis. Logistical acknowledgements go to the entire team of the MEF in Trelew, but especially to Ana and Andres.

4.7 References

Allain R., Aquesbi N. 2008. Anatomy and phylogenetic relationships of *Tazoudasaurus naimi* (Dinosauria, Sauropoda) from the late Early Jurassic of Morocco. *Geodiversitas* 30:345–424.

Allain, R., Läng, É., 2009. Origine et évolution des saurischiens. *Comptes Rendus Palevol* 8:243–256.

Apesteguia, S., Gomez, R.O., Rougier, G.W., 2012. A basal sphenodontian (Lepidosauria) from the Jurassic of Patagonia: new insights on the phylogeny and biogeography of Gondwanan rhynchocephalians. *Zoological Journal of the Linnean Society* 166:342–360.

Bailey, T.R., Rosenthal, Y., McArthur, J.M., Van De Schootbrugge, B., Thirlwall, M.F., 2003. Paleoceanographic changes of the Late Pliensbachian–Early Toarcian interval: a possible link to the genesis of an Oceanic Anoxic Event. *Earth and Planetary Science Letters* 212:307–320.

Bandyopadhyay, S., Gillette, D.D., Ray, S., Sengupta, D.P., 2010. Osteology of *Barapasaurus tagorei* (Dinosauria: Sauropoda) from the Early Jurassic of India. *Palaeontology* 53:533–569.

Barrett, P.M., 1999. A sauropod dinosaur from the lower Lufeng Formation (Lower Jurassic) of Yunnan province, People's Republic of China *Journal of Vertebrate Paleontology* 19:785–787.

Barrett, P.M., 2006. A sauropod dinosaur tooth from the Middle Jurassic of Skye, Scotland. *Transactions of the Royal Society of Edinburgh, Earth and Environmental Sciences* 97:25–29.

Barrett, P.M., Pouech, J., Mazin, J.-M., Jones, F.M., 2016. Teeth of embryonic or hatchling sauropods from the Berriasian (Early Cretaceous) of Cherves-de-Cognac, France. *Acta Palaeontolica Polonica* 61:591–596.

Becerra, M.G., Pol, D., Marsicano, C.A., Rauhut, O.W.M., 2013. The dentition of *Manidens condorensis* (Ornithischia; Heterodontosauridae) from the Jurassic Cañadón Asfalto Formation of Patagonia: morphology, heterodonty and the use of statistical methods for identifying isolated teeth. *Historical Biology* 26:480-492.

Becerra, M.G., Gomez, K.L., Pol, D., 2017. A sauropodomorph tooth increases the diversity of dental morphotypes in the Cañadón Asfalto Formation (Early–Middle Jurassic) of Patagonia. *Comptes Rendus Palevol*. 1030:1-9.

Bonaparte, J.F., 1979. Dinosaurs: A Jurassic Assemblage from Patagonia. *Science* 205:1377–1379.

Bonaparte JF. 1986a. The dinosaurs (Carnosaurs, Allosaurids, Sauropods, Cetiosaurids) of the Middle Jurassic of Cerro Cóndor (Chubut, Argentina). *Annales de Paléontologie (Vert.-Invert.)*. 72:325–386.

Bonaparte, J.F., 1986b. The early radiation and phylogenetic relationships of the Jurassic sauropod dinosaurs, based on vertebral anatomy, in: Padian, K. (Ed.), The Beginning of the Age of Dinosaurs. Cambridge University Press, Cambridge, 247–258.

Bonnan, M.F., Yates, A.M., 2007. A new description of the forelimb of the basal sauropodomorph *Melanorosaurus*: implications for the evolution of pronation,

manus shape and quadrupedalism in sauropod dinosaurs. *Special Papers in Palaeontology* 77:157–168.

Bremer, K., 1994. Branch support and tree stability. *Cladistics* 10:295–304.

Buffetaut E. 2005. A new sauropod dinosaur with prosauropod-like teeth from the Middle Jurassic of Madagascar. *Bulletin de la Société Géologique de France* 176:467-473.

Calvo, J.O., Salgado, L., 1995. *Rebbachisaurus tessonei* sp. nov. A new sauropod from the Albian-Cenomanian of Argentina; new evidence on the origin of the Diplodocidae. *Gaia* 11:13–33.

Carballido, J.L., Pol, D., 2010. The dentition of *Amygdalodon patagonicus* (Dinosauria: Sauropoda) and the dental evolution in basal sauropods. *Comptes Rendus Palevol* 9:83–93.

Carballido, J.L., Rauhut, O.W.M., Pol, D., Salgado, L., 2011. Osteology and phylogenetic relationships of *Tehuelchesaurus benitezii* (Dinosauria, Sauropoda) from the Upper Jurassic of Patagonia. *Zoological Journal of the Linnean Society* 163:605–662.

Carballido, J.L., Salgado, L., Pol, D., Canudo, J.I., Garrido, A., 2012. A new basal rebbachisaurid (Sauropoda, Diplodocoidea) from the Early Cretaceous of the Neuquén Basin; evolution and biogeography of the group. *Historical Biology* 24:631–654.

Carballido, J.L., Sander, P.M., 2014. Postcranial axial skeleton of *Europasaurus holgeri* (Dinosauria, Sauropoda) from the Upper Jurassic of Germany: implications for sauropod ontogeny and phylogenetic relationships of basal Macronaria. *Journal of Systematic Palaeontology* 12:335–387.

Carballido, J.L., Pol, D., Ruge, M.L.P., Bernal, S.P., Páramo-Fonseca, M.E., Etayo-Serna, F., 2015. A new Early Cretaceous brachiosaurid (Dinosauria, Neosauropoda) from northwestern Gondwana (Villa de Leiva, Colombia). *Journal of Vertebrate Paleontology* 35:e980505.

Carballido, J.L., Holwerda, F.M., Pol, D., Rauhut, O.W., 2017. An early jurassic sauropod tooth from patagonia (cañadón asfalto formation): implications for sauropod diversity. *Publicacion Electronica de Paleontológica Argentina* 17:50-57.

Charig, A.J., 1993. Case 1876. *Cetiosauriscus* von Huene, 1927 (Reptilia, Sauropodomorpha): proposed designation of *C. stewarti* Charig, 1980 as the type species. *Bulletin of Zoological Nomenclature* 50:282–283.

Charig, A.J., 1980. A diplodocid sauropod from the Lower Cretaceous of England, in: Jacobs, L.L. (Ed.), Aspects of Vertebrate History. Essays in Honor of Edwin Harris Colbert. Museum of Northern Arizona Press, Flagstaff, 231–244.

Cope, E.D., 1877. On *Amphicoelias*, a genus of saurians from the Dakota Epoch of Colorado. *Paleontological Bulletin* 27:1–5.

Cox, B.M., Hudson, J.D., Martill, D.M., 1992. Lithostratigraphic nomenclature of the Oxford Clay (Jurassic). *Proceedings of the Geological Association* 103:343–345.

Cúneo, R., Ramezani, J., Scasso, R., Pol, D., Escapa, I., Zavattieri, A.M., Bowring, S.A., 2013. High-precision U–Pb geochronology and a new chronostratigraphy for the Cañadón Asfalto Basin, Chubut, central Patagonia: Implications for terrestrial faunal and floral evolution in Jurassic. *Gondwana Research* 24:1267–1275.

Day, J.J., Norman, D.B., Gale, A.S., Upchurch, P., Powell, H.P., 2004. A Middle Jurassic dinosaur trackway site from Oxfordshire, UK. *Palaeontology* 47: 319–348.

Depéret, C., 1896. Note sur les dinosauriens sauropodes et théropodes du Crétacé supérieur de Madagascar. *Société Géologique Francais Bulletin* 24:176–194.

Díaz, Díaz, V., Suberbiola, X.P., Sanz, J.L., 2012. Juvenile and adult teeth of the titanosaurian dinosaur Lirainosaurus (Sauropoda) from the Late Cretaceous of Iberia. *Geobios* 45, 265–274.

Díez Díaz, V., Tortosa, T., Le Loeuff, J., 2013. Sauropod diversity in the Late Cretaceous of southwestern Europe: The lessons of odontology. *Annales Paleontologie* 99:119–129.

Díez Díaz, V., Ortega, F., Sanz, J.L., 2014. Titanosaurian teeth from the Upper Cretaceous of "Lo Hueco" (Cuenca, Spain). *Cretaceous Research* 51: 285–291.

Dong, Z., Tang, Z., 1984. Note on a new mid-Jurassic sauropod (*Datousaurus bashanensis* gen. et sp. nov.) from Sichuan Basin, China. *Vertebrata Palasiata* 22:69–75.

Escapa, I.H., Sterli, J., Pol, D., Nicoli, L., 2008. Jurassic tetrapods and flora of Cañadón Asfalto Formation in Cerro Cóndor area, Chubut province. *Revision de Asociascion Geológica Argentina* 63:613–624.

Foster, J.R., Hamblin, A.H., Lockley, M.G., 2000. The oldest evidence of a sauropod dinosaur in the western United States and other important vertebrate trackways from Grand Staircase-Escalante National Monument, Utah. *Ichnos* 7:169–181.

Foster, J.R., 2003. Paleoecological analysis of the vertebrate fauna of the Morrison Formation (Upper Jurassic), Rocky Mountain Region, U.S.A. *New Mexico Museum of Natural History and Science Bulletin* 23:2–100.

Foster, J.R., Wedel, M.J., 2014. Haplocanthosaurus (Saurischia: Sauropoda) from the lower Morrison Formation (Upper Jurassic) near Snowmass, Colorado. *Volumina Jurassica* 12:197–210.

Fricke, H.C., Hencecroth, J., Hoerner, M.E., 2011. Lowland-upland migration of sauropod dinosaurs during the Late Jurassic epoch. *Nature* 480:513-515.

García, R.A., Cerda, I.A., 2010. Dentition and histology in titanosaurian dinosaur embryos from Upper Cretaceous of Patagonia, Argentina. *Palaeontology* 53:335–346.

García, R.A., Salgado, L., Fernández, M.S., Cerda, I.A., Paulina Carabajal, A., Otero, A., Coria, R.A., Fiorelli, L.E., 2015. Paleobiology of titanosaurs: reproduction, development,

histology, pneumaticity, locomotion and neuroanatomy from the South American fossil record. *Ameghiniana* 52:29–68.

Gaulthier, J. 1986. Saurischian monophyly and the origin of birds. *Memoirs of the California Academy of Sciences* 8, 1-55.

Goloboff, P.A., Farris, J.S., Nixon, K.C., 2008. TNT, a free program for phylogenetic analysis. *Cladistics* 24:774–786.

Goloboff, P.A., Szumik, C.A., 2015. Identifying unstable taxa: Efficient implementation of triplet-based measures of stability, and comparison with Phyutility and RogueNaRok. *Molecular Phylogenetic Evolution* 88:93–104.

Goloboff, P.A., Catalano, S.A., 2016. TNT version 1.5, including a full implementation of phylogenetic morphometrics. *Cladistics* 32:221–238.

Hallam, A., 1985. A review of Mesozoic climates. *Journal of the Geological Association* 142:433–445.

Harris, J.D., 2006. The significance of *Suuwassea emilieae* (Dinosauria: Sauropoda) for flagellicaudatan intrarelationships and evolution. *Journal of Systematic Paleontology* 4:185–198.

Hatcher, J.B., 1903. Osteology of *Haplocanthosaurus*, with description of a new species and remarks on the probable habits of the Sauropoda and the age and origin of the *Atlantosaurus* beds: Additional remarks on *Diplodocus*. *Memoirs of the Carnegie Museum* 2:1–72.

Hauser, N., Cabaleri, N.G., Gallego, O.F., Monferran, M.D., Nieto, D.S., Armella, C., Matteini, M., González, P.A., Pimentel, M.M., Volkheimer, W., Reimold, W. M. 2017. U-Pb and Lu-Hf zircon geochronology of the Cañadón Asfalto Basin, Chubut, Argentina: Implications for the magmatic evolution in central Patagonia. *Journal of South American Earth Sciences* 78:109-212.

He, X., Li, K., Cai, K., 1988. The Middle Jurassic dinosaur fauna from Dashanpu, Zigong, Sichuan. Vol. IV. Sauropod Dinosaurs (2) *Omeisaurus tianfuensis*. Sichuan Publishing House of Science and Technology, Chengdu, China, 143 pp.

Heathcote, J., Upchurch, P., 2003. The relationships of *Cetiosauriscus stewarti* (Dinosauria; Sauropoda): implications for sauropod phylogeny. *Journal of Vertebrate Paleontology, Program and Abstracts 23 (Supplement)*, 60A.

Hesselbo, S.P., Jenkyns, H.C., Duarte, L.V., Oliveira, L.C., 2007. Carbon-isotope record of the Early Jurassic (Toarcian) Oceanic Anoxic Event from fossil wood and marine carbonate (Lusitanian Basin, Portugal). *Earth and Planetary Science Letters* 253:455–470.

Hesselbo, S.P., Pieńkowski, G., 2011. Stepwise atmospheric carbon-isotope excursion during the Toarcian oceanic anoxic event (Early Jurassic, Polish Basin). *Earth and Planetary Science Letters* 301:365–372.

Holwerda, F.M., Pol, D., Rauhut, O.W.M., 2015. Using dental enamel wrinkling to define sauropod tooth morphotypes from the Cañadón Asfalto Formation, Patagonia, Argentina. PLOS ONE 10:e0118100.

Holwerda, F.M., Rauhut, O.W.M., Furrer, H. 2016. Sauropodomorph diversity in the European Triassic: a new sauropodiform from the Norian–Rhaetian of Switzerland. *Journal of Vertebrate Paleontology Program and Abstracts 37 (Supplement),* 148A.

Holwerda, F.M., Liston, J.J., 2017. An anterior sauropod caudal from the Peterborough Oxford Clay: Whose tail is it anyway? PeerJ Preprints 5:e3243v1.

Holwerda, F.M., Díez Díaz, V., Blanco, A., Montie, R., Reumer, J.W.F. (2018). Late Cretaceous sauropod tooth morphotypes may provide supporting evidence for faunal connections between North Africa and Southern Europe. *PeerJ* 6:e5925.

Janensch, W., 1929. Material und Formengehalt der Sauropoden in der Ausbeute der Tendaguru-Expedition. *Palaeontographica-Supplement* 1–34.

Kvale, E.P., Johnson, A.D., Mickelson, D.L., Keller, K., Furer, L.C., Archer, A.W., 2001. Middle Jurassic (Bajocian and Bathonian) dinosaur megatracksites, Bighorn Basin, Wyoming, USA. *Palaios* 16:233–254.

Lallensack JN., Klein H., Milàn J., Wings O., Mateus O., Clemmensen LB. 2017. Sauropodomorph dinosaur trackways from the Fleming Fjord Formation of East Greenland: Evidence for Late Triassic sauropods. *Acta Paleontologica Polonica* 66:(4) 833-843.

Läng, É., 2008. Les cétiosaures (Dinosauria, Sauropoda) et les sauropodes du Jurassique moyen: révision systématique, nouvelles découvertes et implications phylogénétiques (Ph. D. dissertation). Centre de recherche sur la paléobiodiversité et les paléoenvironnements, Paris, France. 639 pp.

Läng, E., Mahammed, F., 2010. New anatomical data and phylogenetic relationships of Chebsaurus algeriensis (Dinosauria, Sauropoda) from the Middle Jurassic of Algeria. *Historical Biology* 22, 142–164.

Liston, J.J., 2004a. “Clear as the difference between an arm and a leg?”: A reexamination of the Skye sauropod discoveries. *Quarterly Journal of the Dinosaur Society* 4:18–21.

Liston, J.J., 2004b. A re-examination of a Middle Jurassic sauropod limb bone from the Bathonian of the Isle of Skye *Scottish Journal of Geology* 40:119–122.

Longman, H.A., 1927. The giant dinosaur: *Rhoetosaurus brownei*. Queensland Museum. *Memoirs of the Queensland Museum* 9:1-18.

Lydekker, R., 1893. On the extinct giant birds of Argentina. *Ibis* 35:40–47.

Lydekker, R., 1895. On bones of a sauropodous dinosaur from Madagascar. *Quarterly Journal of the Geological Society* 51:329–336.

Lydekker, R., 1888. Catalogue of the Fossil Reptilia and Amphibia in the British Museum (Natural History). Part I. Containing the Orders Ornithosauria, Crocodilia, Dinosauria, Squamata, Rhynchocephalia, and Proterosauria. *British Museum of History London,* 309 pp.

Lydekker, R., 1887. On certain dinosaurian vertebrae from the Cretaceous of India and the Isle of Wight. *Quarterly Journal of the Geological Society* 43:156–160.

Lydekker, R., 1885. Indian Pretertiary Vertebrata. Vol I. Part 5. The Reptilia & Amphibia of the Maleri and Denwa Groups. *Memoirs of the Geological Survey India Palaeontolica Indica* 5:1–38.

Maddison, W.P., Maddison, D.R., 2010. Mesquite: a modular system for evolutionary analysis. 2011; Version 2.75. (See Mesquiteproject Orgmesquitedownloaddownload.html).

Manley, K., 1991. Gastrolith identification and sauropod dinosaur migration. *Geological Society of America Abstracts with Programs*, 23:4-45.

Mannion, P.D., 2010. A revision of the sauropod dinosaur genus '*Bothriospondylus*' with a redescription of the type material of the Middle Jurassic form '*B. madagascariensis*.' *Palaeontology* 53:277–296.

Mannion, P.D., Upchurch, P., Mateus, O., Barnes, R.N., Jones, M.E.H., 2012. New information on the anatomy and systematic position of *Dinheirosaurus lourinhanensis* (Sauropoda: Diplodocoidea) from the Late Jurassic of Portugal, with a review of European diplodocoids. *Journal of Systematic Palaeontology* 10:521–551.

Mannion, P.D., Upchurch, P., Barnes, R.N., Mateus, O., 2013. Osteology of the Late Jurassic Portuguese sauropod dinosaur *Lusotitan atalaiensis* (Macronaria) and the evolutionary history of basal titanosauriforms *Zoological Journal of the Linnean Society* 168:98–206.

Marsh, O.C., 1877. Notice of some new dinosaurian reptiles from the Jurassic Formation. *American Journal of Science* 14:514–516.

Marsh, O.C., 1878. Notice of new dinosaurian reptiles. *American Journal of Science* 15:241–244.

Marsh, O.C., 1884. Principal characters of American Jurassic dinosaurs. Part VII. On the Diplodocidae, a new family of the Sauropoda. *American Journal of Science* 27:160–168.

Marsh, O.C., 1895. On the affinities and classification of the dinosaurian reptiles. *American Journal of Science* 38:483–498.

Mateus, O., Mannion, P.D., Upchurch, P., 2014. *Zby atlanticus*, a new turiasaurian sauropod (Dinosauria, Eusauropoda) from the Late Jurassic of Portugal. *Journal of Vertebrate Paleontology* 34:618–634.

McIntosh, J.S., 1981. Annotated catalogue of the dinosaurs (Reptilia, Archosauria) in the collections of Carnegie Museum of Natural History. *Bulletin of the Carnegie Museum of Natural History* 18:1–67.

McIntosh, J., Williams, M., 1988. A new species of sauropod dinosaur, *Haplocanthosaurus delfsi* sp. nov., from the Upper Jurassic Morrison Fm. of Colorado. *Kirtlandia* 43:3–26.

McIntosh, J.S., 1990a. Species determination in sauropod dinosaurs with tentative suggestions for their classification, in: Carpenter, K., Currie, P.J. (Eds.), Dinosaur Systematics: Perspectives and Approaches. Cambridge University Press, New York, 53–69.

McIntosh, J.S., 1990b. Sauropoda, in: Weishampel, D.B., Dodson, P., Osmólska, H. (Eds.), The Dinosauria. University of California Press, Berkeley, CA, 345–401.

McPhee, B.W., Yates, A.M., Choiniere, J.N., Abdala, F., 2014. The complete anatomy and phylogenetic relationships of *Antetonitrus ingenipes* (Sauropodiformes, Dinosauria): implications for the origins of Sauropoda. *Zoological Journal of the Linnean Society* 171:151–205.

McPhee, B.W., Choiniere, J.N., Yates, A.M., Viglietti, P.A., 2015. A second species of *Eucnemesaurus* Van Hoepen, 1920 (Dinosauria, Sauropodomorpha): new information on the diversity and evolution of the sauropodomorph fauna of South Africa's lower Elliot Formation (latest Triassic). *Journal of Vertebrate Paleontology* 35:e980504.

McPhee, B.W., Upchurch, P., Mannion, P.D., Sullivan, C., Butler, R.J., Barrett, P.M., 2016a. A revision of *Sanpasaurus yaoi* Young, 1944 from the Early Jurassic of China, and its relevance to the early evolution of Sauropoda (Dinosauria). *PeerJ* 4, e2578.

McPhee, B.W., Choiniere, J.N., 2016b. A hyper-robust sauropodomorph dinosaur ilium from the Upper Triassic–Lower Jurassic Elliot Formation of South Africa: Implications for the functional diversity of basal Sauropodomorpha. *Journal of African Earth Sciences* 123:177–184.

Meyer, C.A., 1993. A sauropod dinosaur megatracksite from the Late Jurassic of northern Switzerland. *Ichnos* 3:29–38.

Mocho, P., Royo-Torres, R., Ortega, F., 2014. Phylogenetic reassessment of *Lourinhasaurus alenquerensis*, a basal Macronaria (Sauropoda) from the Upper Jurassic of Portugal. *Zoological Journal of the Linnean Society* 170:875–916.

Mocho, P., Royo-Torres, R., Malafaia, E., Escaso, F., Ortega, F., 2016. Systematic review of Late Jurassic sauropods from the Museu Geológico collections (Lisboa, Portugal). *Journal of Iberian Geology* 42:227–250.

Moore A., Xu X., Clark J. 2017. Anatomy and systematics of *Klamelisaurus gobiensis*, a mamenchisaurid sauropod from the Middle-Late Jurassic Shishugou Formation of China. *Journal of Vertebrate Paleontology, Program and Abstracts*, *37 (Supplement 2),* 165A.

Nair, J.P., Salisbury, S.W., 2012. New anatomical information on *Rhoetosaurus brownei* Longman, 1926, a gravisaurian sauropodomorph dinosaur from the Middle Jurassic of Queensland, Australia. *Journal of Vertebrate Paleontology* 32:369–394.

Noè, L.F., Liston, J.J., Chapman, S.D., 2010. 'Old bones, dry subject': the dinosaurs and pterosaur collected by Alfred Nicholson Leeds of Peterborough, England. *Geological Society Special Publications* 343:49–77.

Ouyang, H., Ye, Y., 2002. *The first mamenchisaurian skeleton with complete skull, Mamenchisaurus youngi*. Sichuan Publishing House of Science and Technology, Chengdu, China, 138 pp.

Owen R. 1841. Report on British fossil reptiles. *Reports of the British Association for the Advancement of Science* 11:60-204.

Owen, R., 1842a. A description of a portion of the skeleton of *Cetiosaurus*, a gigantic extinct saurian occurring in the Oolitic Formation of different parts of England. *Proceedings of the Geological Society of London* 457–462.

Owen, R., 1842b. Report on British Fossil Reptiles Pt. II. *Reports of the British Association of Advanced Science* 1841:60–204.

Parrish, J.T., 1993. Climate of the supercontinent Pangea. *Journal of Geology* 101:215–233.

Peyer, K., Allain, R., 2010. A reconstruction of *Tazoudasaurus naimi* (Dinosauria, Sauropoda) from the late Early Jurassic of Morocco. *Historical Biology* 22:134–141.

Phillips, J., 1871. Geology of Oxford and the Valley of the Thames. Clarendon Press, Oxford, 390pp.

Pol, D., Escapa, I.H., 2009. Unstable taxa in cladistic analysis: identification and the assessment of relevant characters. *Cladistics* 25: 515–527.

Pol, D., Rauhut, O.W.M., Carballido, J.L., 2009. Skull anatomy of a new basal eusauropod from the Cañadon Asfalto Formation (Middle Jurassic) of Central Patagonia. *Journal of Vertebrate Paleontology Program and Abstracts 29 (suppl. 3),* 100A.

Pol, D., Rauhut, O.W.M., Becerra, M., 2011. A Middle Jurassic heterodontosaurid dinosaur from Patagonia and the evolution of heterodontosaurids. *Naturwissenschaften* 98:369–379.

Pol, D., Rauhut, O.W.M., 2012. A Middle Jurassic abelisaurid from Patagonia and the early diversification of theropod dinosaurs. *Proceedings of the Royal Society Biology Letters* 279:3170–3175.

Pol, D., Carballido, J.L., Rauhut, O.W.M., Rougier, G.W., Sterli, J., 2013. Biogeographic distribution patterns of tetrapods during the Jurassic: new information from the Cañadón Asfalto Basin, Patagonia, Argentina. Journal of Vertebrate Paleontology Program and Abstracts 33 (supplement) 192A.

Powell, J.E., 1992. Osteología de *Saltasaurus loricatus* (Sauropoda-Titanosauridae) del Cretácico Superior del noroeste argentino. In: Sanz Jl Buscalioni Ad (Eds) Los Dinosaur. Su Entorno Biótico, Inst. Juan Valdés Cuenca Espana, 165–230.

Rauhut, O.W.M., 2003. A dentary of *Patagosaurus* (Sauropoda) from the Middle Jurassic of Patagonia. *Ameghiniana* 40: 425–432.

Rauhut, O.W.M., Lopez-Arbarello, A., 2008. Archosaur evolution during the Jurassic: a southern perspective. *Revision Asociacion Geológica Argententina* 63: 557–585.

Rauhut, O.W., López-Arbarello, A., 2009. Considerations on the age of the Tiouaren Formation (Iullemmeden Basin, Niger, Africa): implications for Gondwanan Mesozoic terrestrial vertebrate faunas. *Palaeogeography Palaeoclimatology Palaeoecology* 271:259–267.

Rauhut, O.W.M., Carballido, J.L., Pol, D. (2015). A diplodocid sauropod dinosaur from the Late Jurassic Cañadón Calcáreo Formation of Chubut, Argentina. *Journal of Vertebrate Paleontology* 35:1-8.

Rauhut, O.W.M., Hübner, T., Lanser, K.-P., 2016. A new megalosaurid theropod dinosaur from the late Middle Jurassic (Callovian) of north-western Germany: Implications for theropod evolution and faunal turnover in the Jurassic. *Palaeontologia Electronica* 19:1–65.

Rauhut, O.W.M., Holwerda, F.M., Furrer, H. (in prep). Sauropodomorph diversity in the European Triassic: a new sauropodiform from the Norian–Rhaetian of Switzerland.

Remes, K., 2009a. Taxonomy of Late Jurassic diplodocid sauropods from Tendaguru (Tanzania). *Fossil Record* 12:23–46.

Remes, K., Ortega, F., Fierro, I., Joger, U., Kosma, R., Ferrer, J.M.M., Ide, O.A., Maga, A., 2009b. A new basal sauropod dinosaur from the Middle Jurassic of Niger and the early evolution of Sauropoda. *PLoS One* 4:e6924.

Romer, A., 1956. Osteology of the Reptiles. University of Chicago Press, Chicago.

Royo-Torres, R., Upchurch, P., 2012. The cranial anatomy of the sauropod *Turiasaurus riodevensis* and implications for its phylogenetic relationships. *Journal of Systematic Palaeontology* 10:553–583.

Russell, D.A., 1993. The role of Central Asia in dinosaurian biogeography. *Canadian Journal of Earth Sciences* 30:2002–2022.

Russell, D.A., Zheng, Z., 1993. A large mamenchisaurid from the Junggar Basin, Xinjiang, People's Republic of China. *Canadian Journal of Earth Sciences* 30:2082–2095.

Salgado, L., Coria, R.A., Calvo, J.O., 1997. Evolution of titanosaurid sauropods: Phylogenetic analysis based on the postcranial evidence. *Ameghiniana* 34:3–32.

Schwarz, D., Wings, O., Meyer, C., 2007. Revision of *Cetiosauriscus greppin*i: the revival of a Late Jurassic sauropod from Switzerland. *Journal of Vertebrate Paleontology Program and Abstracts 27, 3 (supp)* 143A.

Scotese, C.R., Boucot, A.J., McKerrow, W.S., 1999. Gondwanan palaeogeography and pal1 oclimatology . *Journal of African Geosciences* 28:99–114.

Seeley, H.G., 1889. Note on the pelvis of Ornithopsis. *Quarterly Journal of the Geology Association* 45:391–397.

Sellwood, B.W., Valdes, P.J., 2006. Mesozoic climates: General circulation models and the rock record. *Sedimentary Geology* 190, 269–287

Sellwood, B.W., Valdes, P.J., 2008. Jurassic climates. *Proceedings of the Geological Association*. 119:5–17.

Sereno, P.C., Beck, A.L., Dutheil, D.B., Larsson, H.C.., Lyon, G.H., Moussa, B., Sadleir, R.W., Sidor, C.A., Varricchio, D.J., Wilson, G.P., 1999. Cretaceous sauropods from the Sahara and the uneven rate of skeletal evolution among dinosaurs. *Science* 286:1342–1347.

Steel, R., 1970. Saurischia. *Handbuch die Paläoherpetologie* 14, 1-87.

Taylor, M.P., 2010. Sauropod dinosaur research: a historical review. *Geologial Society. Lonen Special Publication* 343-361.

Taylor, M.P., Wedel, M.J., 2013. Why sauropods had long necks; and why giraffes have short necks. *PeerJ* 1:e36.

Thevenin, A., 1907. Paléontologie de Madagascar IV - Dinosauriens. *Annales Paléontoogie*. 2: 121–136.

Tschopp, E., 2013a. A specimen-based phylogenetic analysis of Diplodocidae (Dinosauria: Sauropoda). *Journal of Vertebrate Paleontology Program and Abstracts 34, (Supplement)* 241A.

Tschopp, E., Mateus, O., 2013b. The skull and neck of a new flagellicaudatan sauropod from the Morrison Formation and its implication for the evolution and ontogeny of diplodocid dinosaurs. *Journal of Systematic Palaeontology* 11, 853–888.

Tschopp, E., Mateus, O., Benson, R.B.J., 2015. A specimen-level phylogenetic analysis and taxonomic revision of Diplodocidae (Dinosauria, Sauropoda*). PeerJ* 3:e857.

Tschopp, E., Mateus, O., 2017. Osteology of *Galeamopus pabsti* sp. nov. (Sauropoda: Diplodocidae), with implications for neurocentral closure timing, and the cervico-dorsal transition in diplodocids. *PeerJ* 5:e3179.

Upchurch, P., 1998. The phylogenetic relationships of sauropod dinosaurs. *Zoological Society of the Linnean Society* 124:43–103.

Upchurch, P., Martin, J., 2002. The Rutland *Cetiosaurus*: the anatomy and relationships of a Middle Jurassic British sauropod dinosaur. *Palaeontolog*y 45:1049–1074.

Upchurch, P., Martin, J., 2003. The anatomy and taxonomy of *Cetiosaurus* (Saurischia, Sauropoda) from the Middle Jurassic of England. *Journal of Vertebrate Paleontology*. 23:208–231.

Upchurch, P., Barrett, P.M., Dodson, P., 2004. Sauropoda, in: Weishampel, D.B., Dodson, P., Osmólska, H. (Eds.), The Dinosauria. Second Edition. University of California Press, Berkeley, CA, 259–322.

Volkheimer, W., Rauhut, O.W., Quattrocchio, M.E., Martinez, M.A., 2008. Jurassic paleoclimates in Argentina, a review. *Revision de Associacion Geológica Argentina* 63:549–556.

Wedel, M.J., 2003a. The evolution of vertebral pneumaticity in sauropod dinosaurs. *Journal of Vertebrate Paleontology* 23:344–357.

Wedel, M.J., 2003b. Vertebral pneumaticity, air sacs, and the physiology of sauropod dinosaurs. *Paleobiology* 29, 243-255.

Wedel, M.J., Wilson, J.A., Rogers, K.C., 2005. Postcranial skeletal pneumaticity in sauropods and its implications for mass estimates. in: Curry Rogers, K.A., Wilson, J.A. (Eds.), The Sauropods: Evolution and Paleobiology. University of California Press, Berkeley, CA, 201–228.

Wedel, M., 2007. What pneumaticity tells us about prosauropods', and vice versa. *Special* papers in *Palaeontology* 77:207-222.

Wilson, J.A., Sereno, P.C., 1998. Early evolution and higher-level phylogeny of sauropod dinosaurs. *Journal of Vertebrate Paleontology* 18:1–79.

Wilson, J.A., 1999. A nomenclature for vertebral laminae in sauropods and other saurischian dinosaurs. *Journal of Vertebrate Paleontology* 19:639–653.

Wilson, J.A., 2002. Sauropod dinosaur phylogeny: critique and cladistic analysis. *Zoological journal of the Linnean Society* 136,:215–275.

Wilson, J.A., Upchurch, P., 2003. A revision of *Titanosaurus* Lydekker (Dinosauria-Sauropoda), the first dinosaur genus with a 'Gondwanan'distribution. *Journal of Systematic Palaeontology* 1:125–160.

Wilson, J.A., 2005. Overview of sauropod phylogeny and evolution, in: Curry Rogers, K.A., Wilson, J.A. (Eds.), The Sauropods: Evolution and Paleobiology. University of California Press, Berkeley, CA, 15–49.

Wilson, J.A., Upchurch, P., 2009. Redescription and reassessment of the phylogenetic affinities of *Euhelopus zdanskyi* (Dinosauria: Sauropoda) from the Early Cretaceous of China. *Journal of Systematic Palaeontology* 7:199–239.

Wilson, J.A., 2012. New vertebral laminae and patterns of serial variation in vertebral laminae of sauropod dinosaurs. *Contributions of the Museum of Paleontology University of Michichian* 32:91–110.

Wiman, C., 1929. Die Kreide-Dinosaurier aus Shantung. *Palaeontoliga Sinica* ,:1–67.

Xing, L., Miyashita, T., Zhang, J., Li, D., Ye, Y., Sekiya, T., Wang, F., Currie, P.J., 2015. A new sauropod dinosaur from the Late Jurassic of China and the diversity, distribution, and relationships of mamenchisaurids. *Journal of Vertebrate Paleontology* 35:e889701.

Xing, L., Miyashita, T., Zhang, J., Li, D., Ye, Y., Sekiya, T., Wang, F., Currie, P.J., 2015. A new sauropod dinosaur from the Late Jurassic of China and the diversity, distribution, and relationships of mamenchisaurids. *Journal of Vertebrate Paleontology*. 35:e889701.

Yates, A.M., Kitching, J.W., 2003. The earliest known sauropod dinosaur and the first steps

towards sauropod locomotion. *Proceedings of the Royal Society London B: Biological Sciences* 270:1753–1758.

Yates, A., 2005. The skull of the Triassic sauropodomorph, *Melanorosaurus readi*, from South Africa and the definition of Sauropoda*, Journal of Vertebrate Paleontology Program and Abstracts (supp)* 132A.

Yates, A.M., Bonnan, M.F., Neveling, J., Chinsamy, A., Blackbeard, M.G., 2010. A new transitional sauropodomorph dinosaur from the Early Jurassic of South Africa and the evolution of sauropod feeding and quadrupedalism *Proceedings of the Royal Society of London B: Biological Sciences* 277:787–794.

Young, C.-C., 1939. On a new sauropoda, with notes on other fragmentary reptiles from Szechuan. *Bulletin of the Geological Society China* 19:279–315.

Young, C.-C., 1958. New sauropods from China. *Vertebrata Palasiatica*. 2:1–28.

Zhang Y. 1988. *The Middle Jurassic dinosaur fauna from Dashanpu, Zigong, Sichuan, vol. 1: sauropod dinosaur (I): Shunosaurus*. Chengdu, China: Sichuan Publishing House of Science and Technology, 114 pp.

Zhao, X., 1993. A new mid-jurassic sauropod (*Klamelisaurus gobiensis* gen. et sp. nov.) from Xinjiang, China. *Vertebrata Palasiatica* 31: 132-138.

5 Evolutionary trends in Jurassic sauropod hindlimb morphology using geometric morphometrics

Femke M. Holwerda[1,2], Oliver W.M. Rauhut and Anneke H. van Heteren[3]

1 Staatliche Naturwissenschaftliche Sammlungen Bayerns (SNSB), Bayerische Staatssamlung für Paläontologie und Geologie, Richard-Wagner-Strasse 10, 80333 München, Germany, f.m.holwerda@gmail.com

2 Department of Earth and Environmental Sciences and GeoBioCenter, Ludwig Maximilians Universität, 80333 München, Germany

3 Staatliche Naturwissenschaftliche Sammlungen Bayerns (SNSB), Zoologische Staatssammlung München, Münchhausenstrasse 21, 81247 München, Germany

Author contributions: research idea: FH, OR. Ran analyses: FH,AvH. Wrote the paper: FH

5.1 Abstract

Geometric morphometrics has been used as a tool for measuring and quantifying morphological differences between skeletal elements of extinct organisms in previous studies, but has not been used much in studying sauropod dinosaurs. Here, several sauropod femora and tibiae from both the Late Triassic as well as the Early, Middle and Late Jurassic are analysed in order to explore differences in shape of hindlimbs from these giant dinosaurs. Moreover, ontogenetic differences were studied in several taxa. Morphological changes from Late Triassic/Early Jurassic femora are mainly centred around the fourth trochanter, the lateral bulge and the greater trochanter, whilst the tibiae show the largest variability in the cnemial crest, and the distal end of the shaft. An evolutionary allometric trend is observed in especially femora from Triassic to Early-Middle Jurassic sauropods, whilst after the Middle Jurassic femora only seem to increase in size, without associated allometric size changes. A tentative ontogenetic allometric trend is observed in both femora and tibiae, however, larger sample sizes would be necessary to obtain a clear trend, which is not always possible in studying sauropod dinosaurs. This study shows that geometric morphometrics is a useful tool for future expansion of evolutionary studies of sauropods.

Keywords: Sauropoda, Eusauropoda, femur, tibia, functional morphology

5.2 Introduction

The Early and Middle Jurassic are widely regarded as the critical time for sauropod species radiation and worldwide dispersal (Upchurch et al., 2004; Barrett and Upchurch, 2005; McPhee et al., 2015; McPhee and Choiniere, 2016). The accepted theory is that the common ancestor of Early Jurassic non-sauropodomorph sauropods had its provenance in South Africa, South Gondwana at the time (Yates and Kitching, 2003; Bonnan and Yates, 2007; Yates et al., 2010; McPhee et al., 2014, 2015; McPhee and Choiniere, 2016).

One of the major anatomical alterations arising from the sauropodomorph-sauropod transition in the Late Triassic is the shape of the limb bones, which became straight and columnar-like to bear more weight and create an obligatory quadrupedal lifestyle (Upchurch et al., 2004; Yates et al., 2010; McPhee et al., 2015). The sauropod femur, therefore, is an important component of sauropod evolution, since femoral morphology determined quadrupedality and locomotion, and thus major changes in sauropod palaeobiology (see Carrano, 2005; Yates et al., 2010). An alteration in femoral morphology is further seen in the rise of the neosauropods in the Late Jurassic (Upchurch et al., 2004; Bonnan, 2007). The Early and Middle Jurassic, however, have a generally poor sauropod body fossil record, and limb bones are scarce, with the exceptions coming from a few taxa from mainly Gondwana (e.g. *Patagosaurus, Tazoudasaurus, Volkheimeria, Spinophorosaurus, Jobaria,* (Bonaparte, 1979, 1986; Sereno et al., 1999; Allain and Aquesbi, 2008; Remes et al., 2009)), and even fewer from Laurasia (e.g. *Cetiosaurus, Shunosaurus* (Zhang, 1988; Upchurch and Martin, 2003)).

To compare general morphological differences between Early-Middle Jurassic and Late Jurassic sauropod femora, a dataset of photographs was created, including several Early and Middle Jurassic sauropods, and Late Jurassic sauropod taxa, mainly from Gondwana, and an additional few taxa from Laurasia, which was then subjected to geometric morphometric

analysis. One final Triassic sauropod femur specimen (*Isanosaurus,* Buffetaut et al., (2000)) was added as evolutionary base line. A second dataset using images of tibiae of several Early, Middle and Late Jurassic sauropod taxa was also generated, however, tibiae (or images thereof) appropriate for study were found to be sparser. Geometric morphometric analyses have been relatively sparsely used on sauropods thus far, though results seem promising for the elucidation of sauropodiform palaeobiology (Curry Rogers and Forster, 2001; Bonnan, 2004, 2007; Canudo and Cuenca-Bescós, 2004; Yates et al., 2010). Moreover, geometric morphometrics has proven to be useful for phylogenetic and evolutionary developmental research on mammals (Cardini et al., 2009; van Heteren et al., 2014, 2016), but also reptiles besides sauropods; crocodiles (Reed et al., 2010), theropods (Foth and Rauhut, 2013a,b; Hendrickx and Mateus, 2016), and ornithischians (Boehmer and Rauhut, 2010; Brusatte et al., 2012; Hedrick and Dodson, 2013; Hendrickx et al., 2014). Sauropodomorph limb bones from the Late Triassic, as well as titanosauriform femora from the Early Cretaceous, have been subjected to geometric morphometric analysis in previous studies (Canudo and Cuenca-Bescós, 2004; Yates et al., 2010). Therefore, additional geometric morphometric analysis on Early and Middle Jurassic sauropods may help to understand early sauropod evolution in the Jurassic, when sauropod diversification took place. This in turn may shed light on early sauropod evolutionary adaptations, especially concerning stance, gait and locomotion.

5.3 Materials and Methods

To assess the morphological data, pictures of femora and tibiae of Triassic and Early, Middle and Late Jurassic sauropods were collected during collection visits, as well as from publications and literature. The emphasis was laid on Early and Middle Jurassic sauropods, as a) these are the taxa that are from the time of major sauropod radiation, and b) these taxa have not yet been subjected to geometric morphometric analysis, which thus would add knowledge to non-sauropod sauropodomorph and Jurassic neosauropod morphometric data

interpretations of previous datasets (Curry Rogers and Forster, 2001; Bonnan, 2004, 2007; Canudo and Cuenca-Bescós, 2004; Boehmer and Rauhut, 2010; Yates et al., 2010). The taxa used are (see Table 1): *Patagosaurus fariasi, Volkheimeria chubutensis, Tazoudasaurus naimi, Cetiosaurus oxoniensis, Shunosaurus lii, Isanosaurus attavipachi, Jobaria tiguidensis, Lapparentosaurus madagascariensis, Bothriospondylus suffosus, Tornieria africana, Lourinhasaurus alenquerensis, Apatosaurus louisae* (Gilmore, 1936; Bonaparte, 1979, 1986; Dantas et al., 1998; Sereno et al., 1999; Buffetaut et al., 2000; Upchurch and Martin, 2003; Remes, 2006; Allain and Aquesbi, 2008; Läng, 2008; Remes et al., 2009; Mocho,et al., 2013).

Table 1: Provenance, age and ontogeny of taxa used for geometric morphometrics.

Taxon	Provenance	Age	Ontogenetic stage	Element(s) used
Isanosaurus	Thailand, East Laurasia	Late Triassic	Adult	Femur
Tazoudasaurus	Morocco, North Gondwana	Early Jurassic	Juvenile and subadult	Femora and tibiae
Volkheimeria	Argentina, South Gondwana	Middle Jurassic	Juvenile	Femur and tibia
Patagosaurus	Argentina, South Gondwana	Middle Jurassic	Adult and juvenile	Femora and tibiae
Cetiosaurus	United Kingdom, Laurasia	Middle Jurassic	Adult	Femur and tibia
Shunosaurus	China, East Laurasia	Middle Jurassic	Adult	Femur
Jobaria	Niger, North Gondwana	Middle-Late Jurassic	Adult	Femur
Lapparentosaurus	Madagascar, East Gondwana	Middle Jurassic	Juvenile	Femur
Bothriospondylus	Madagascar, East Gondwana	Middle Jurassic	Adult	Femur
Tornieria	Tanzania, South Gondwana	Late Jurassic	Adult	Femur and tibia
Lourinhasaurus	Portugal, Laurasia	Late Jurassic	Adult	Femur
Apatosaurus	United States, Laurasia	Late Jurassic	Adult	Femur

Images of the posterior side of femora, including a scale, were imported into tpsUtil to create a tps file, then tpsDig was used to place the landmarks and add the scale (Rohlf &

Slice, 1990; Rohlf, 2005, 2010). For the image of the femur of *Shunosaurus* from (Zhang, 1988), no scale could be determined. The landmarks were adapted from those of Canudo and Cuenca-Bescós (2005). Twenty landmarks were selected on the images (see Figure 1A).

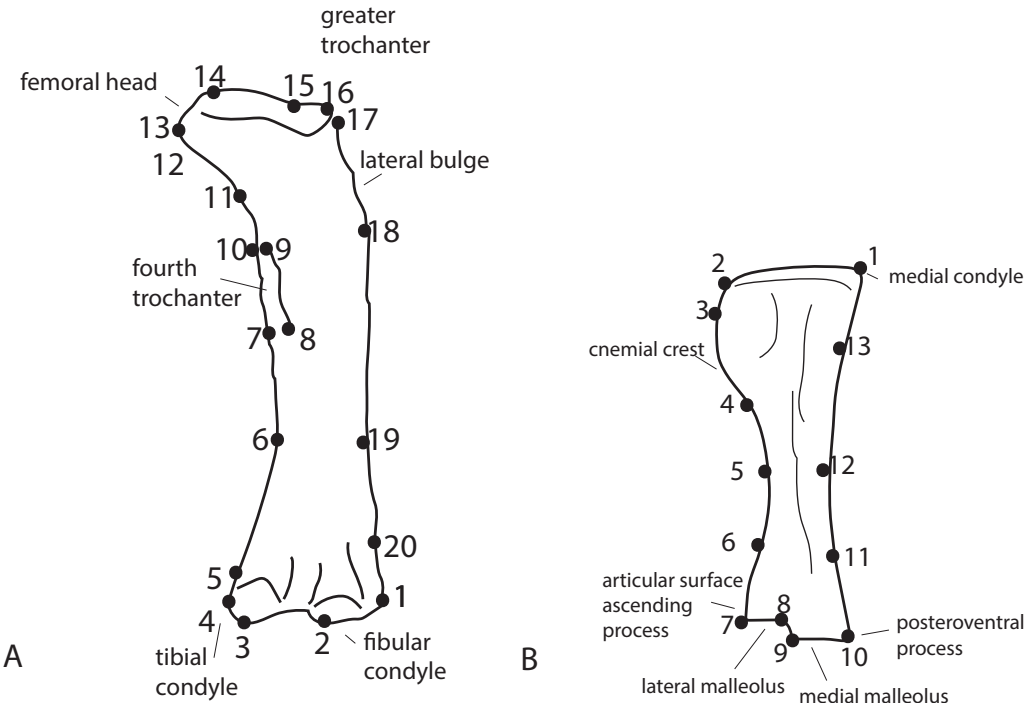

Figure 1: landmarks and key morphological features on femur (A), based on Canudo and Cuenca-Bescós (2005) and on tibia (B), based on Remes et al., (2009).

These landmarks are:

1. Lateral end of the fibular condyle.

2. Distal end of the fibular condyle.

3. Distal end of the tibial condyle. This is the medial end of the baseline.

4. Medial end of the tibial condyle.

5. Proximal end of the tibial condyle.

6. Medial point where the diaphysis has its minimum medial lateral diameter.

7. Medial projection on the outline, parallel to the distal end of the fourth trochanter.

8. Distal end of the fourth trochanter (may coincide with landmark 7). In several basal sauropods, the fourth trochanter projects medially, therefore landmarks 7 and 8 may coincide.

9. Proximal end of the fourth trochanter.

10. Medial projection on the outline of the proximal end of the fourth trochanter (may coincide with landmark 9).

11. Mediodistal end of the articular head.

12. Point of small medial protrusion, ventral to landmark 13. Changed from: point of inflexion between the concave and convex profile of the articular head. This landmark's definition was altered as no sauropod femoral condyle in this dataset was completely rounded; femoral heads had more triangular or even rectangular projections.

13. Point of greatest medial distal convexity of the articulated head.

14. The most proximal point of the articular head.

15. Most depressed point between the greater trochanter and the articular head. Coincides with the depression of the intertrochanteric fossa.

16. Greater trochanter, which coincides with landmark 17 in some more basal taxa.

17. Latero-proximal corner of the greater trochanter.

18. Greatest lateral expansion of the proximal third. This expansion is the most lateral end of the femur or "Lateral Bulge" of Salgado et al. (1997).

19. Lateral part where the diaphysis acquires its minimum diameter (opposite to landmark 6).

20. Lateral projection at the proximal beginning of the fibular condyle.

Landmarks were taken as accurately as possible. Some femora, however, are on exhibition, with metal struts around them, which might obscure the 'true' landmarks. For *Patagosaurus* PVL 4170 (the holotype) the femoral head is obscured by the ilium, since the specimen is mounted at the Instituto Miguel Lillo, Tucuman, Argentina. This was corrected for by

creating a drawing of the femur on the basis of pictures from other angles of the femoral head, as well as direct measurements form the specimen.

For the tibiae, no geometric morphometric data on sauropod tibiae exists thus far, to our knowledge. As such, we selected thirteen landmarks on the tibiae to reflect functional morphology. Tibiae were viewed in posterior/posterolateral view, as this shows the cnemial crest as well as the articular surface for the ascending process, where the attachment surface for the lateral malleolus is, and the posteroventral process where the medial malleolus attaches. These landmarks are shown in Figure 1B, which is based on a tibia of *Spinophorosaurus* (Remes et al., 2009).

1. Medial-most protrusion of the medial condyle at the proximal end of the tibia
2. Dorsalmost protrusion of the dorsal side of the cnemial crest on the proximal articular surface of the tibia
3. Lateral-most expansion of the cnemial crest
4. Ventral-most point of the cnemial crest on the lateral side of the tibia
5. Transversely narrow-most part of the shaft of the tibia on the lateral side (corresponds to landmark 12)
6. Point from which the lateral side of the shaft of the tibia flares out laterally and distally (corresponds with landmark 11, however is not always on the same transverse plane)
7. Lateral-most distal point of the tibia, the lateral end of the articular surface of the ascending process
8. Notch between lateral and medial malleolus
9. lateral distal end of the posteroventral process, where the medial malleolus attaches
10. Medial distal end of the posteroventral process
11. Medial point from which the medial side of the shaft of the tibia flares out distally
12. Medial side of transversely most narrow part of the tibial shaft (corresponds with 5)

13. Medial proximal point from where proximal end of the tibia flares out medially and dorsally.

After this, the datasets were loaded in MorphoJ (version 1.06d), an integrated program package for geometric morphometrics (Klingenberg, 2011). This program performs (amongst others), Procrustes superimposition, regression and principal component analysis (PCA). Using MorphoJ, raw 2D coordinates were scaled, rotated and translated by Procrustes superimposition. MorphoJ uses a full Procrustes fit and projects the data on to a Euclidean space tangent to shape space by orthogonal projection. Reflection was used to make left and right femoral specimens comparable. Specimens were aligned by principal axes, although the choice of alignment does not influence the statistical results, only the visualisations. It should be noted that the sample sizes used in this study are very small, potentially resulting in overfitting the data. Nevertheless, the analyses help to visualise morphological variability between the specimens, although future analyses with more specimens would be recommendable. Differences between species were assessed in morphospace by performing PCA. The landmark configurations of the sauropod specimens were subjected to PCA. The number of PCs to be interpreted was based on the amount of variance they explained. We aimed to explain approximately 75% of variance. The shape changes associated with the PCs are displayed next to the axes and represent a the shapes corresponding to +0,1 and -0,1 on the axes. The Procrustes coordinates served as the dependent variables. To assess any potential allometric effect in the data, a regression analysis of the Procrustes coordinates on to log centroid size was performed. The sample size is so small that no statistical significance tests can be performed. Nevertheless, a multivariate regression of the Procrustes coordinates on to log centroid size can elucidate morphological diversity among sauropods (Yates et al., 2010).

5.4 Results

The principal component analysis on the femoral dataset shows that PC1 accounts for 42,3% of the variance, and PC2 16,2%. PC1 corresponds to a shift of the fourth trochanter, and a more dorsal and lateral shift of the lateral bulge, a variability in size and position of the smallest circumference of the femoral shaft, and finally a distal lateral variability of the greater trochanter (see Fig. 2). PC2 corresponds to a medial shift of the fourth trochanter. PC3 and PC4 account for 10,5% and 7,9% of the variance and correspond to decrease in the lateral bulge and an enlargement of the fourth trochanter, respectively (not shown).The scatterplot of PC1 vs PC2 shows that the Triassic *Isanosaurus* is isolated from the Jurassic cluster of taxa (Fig 2). *Isanosaurus* has a relatively ventrally projected lateral bulge, a rather dorsally projected fourth trochanter and a rather small greater trochanter. *Cetiosaurus* occupies an intermediate position between Isanosaurus and other Jurassic sauropods (Fig. 2). *Vulcanodon* and *Patagosaurus* are slightly separated from the rest of the Jurassic cluster by having higher PC2 scores and relatively low PC1 scores (Fig. 2); both taxa having an obliquely positioned fourth trochanter, even though both taxa are morphologically far apart (see Fig. 3).

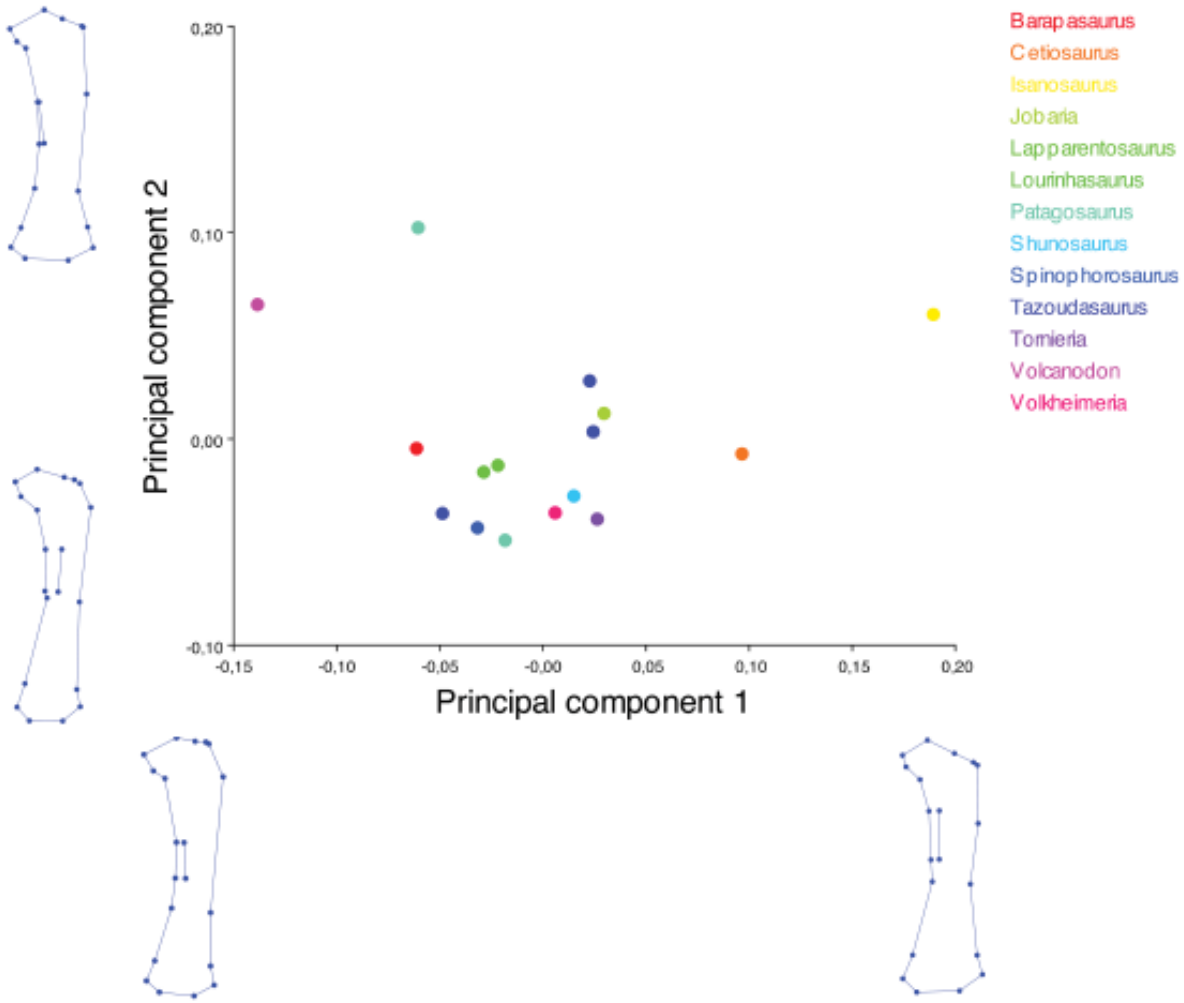

Figure 2: PC1 vs PC2 plot of the principal component analysis on the the femora (see legend for colour coding of taxa).

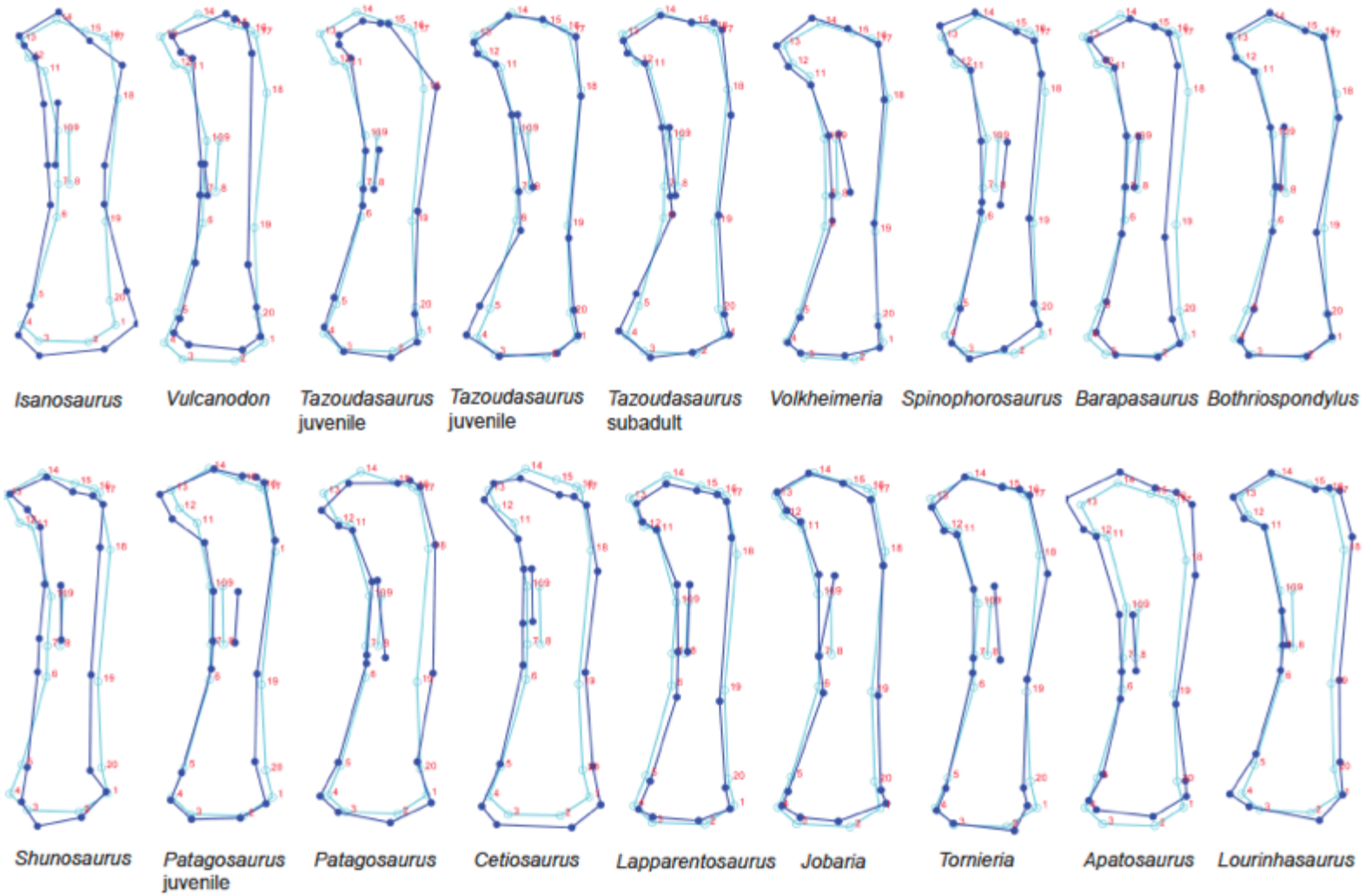

Figure 3: Outlines of sauropod femora. Dark blue lines indicate individual variation from the light blue mean outlines.

The regression analysis of femora of all adult specimens (with the exclusion of *Shunosaurus*, because no reliable scale was available from literature) is not statistically significant (p=0,39). The regression scores (Figure 4) tentatively show that from the Triassic to the Early-Middle Jurassic, femoral morphology changes drastically, although there is only one Triassic specimen in the dataset. In the Middle to Late Jurassic only femoral size increases (see Fig. 4) without an associated directional shape change. Middle Jurassic sauropods cluster around a log centroid size of 7,5, whereas there is much more spread in the centroid sizes of early and late Jurassic sauropods.

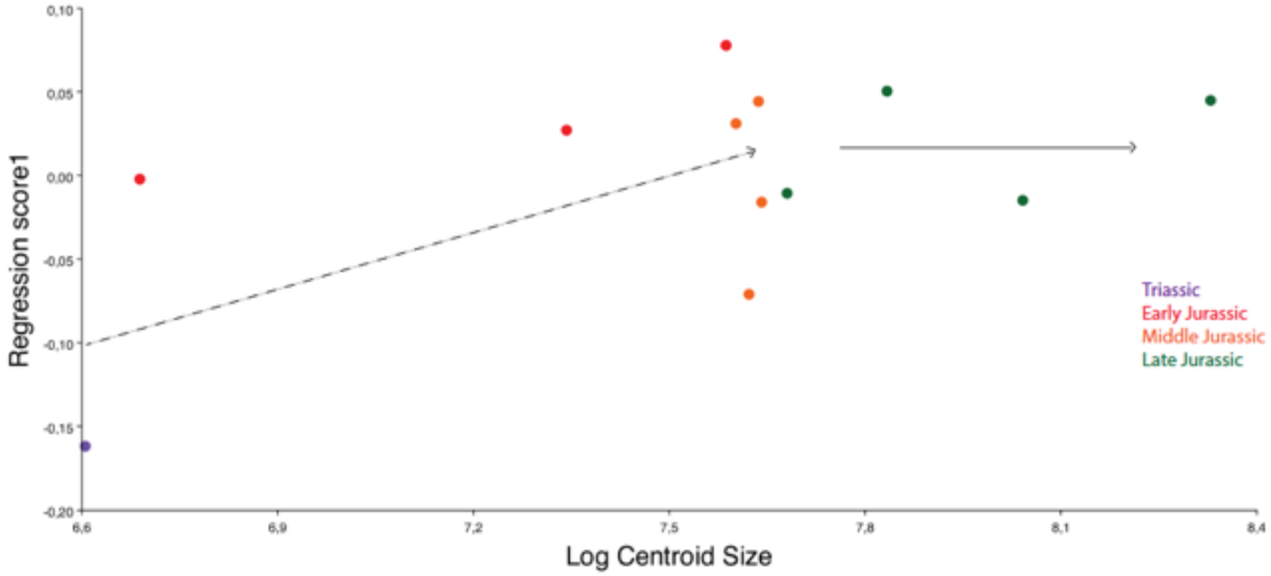

Figure 4: Regression analysis of the Procrustes coordinates on log centroid size, representing evolutionary allometry in adult sauropod femora (Triassic in purple, Early Jurassic in red, Middle Jurassic in orange, Late Jurassic in green).

A second regression was performed with only those species that are represented by at least one juvenile specimen. The *Tazoudasaurus* specimens (both juvenile and subadult specimens) seem to form an allometric trend, as well as the juvenile and adult *Patagosaurus* (Fig. 5). *Lapparentosaurus* seems to follow a similar trend, but *Volkheimeria* seems to have

lower regression scores than expected for its size. The regression analysis again is not statistically significant here (p=0,84).

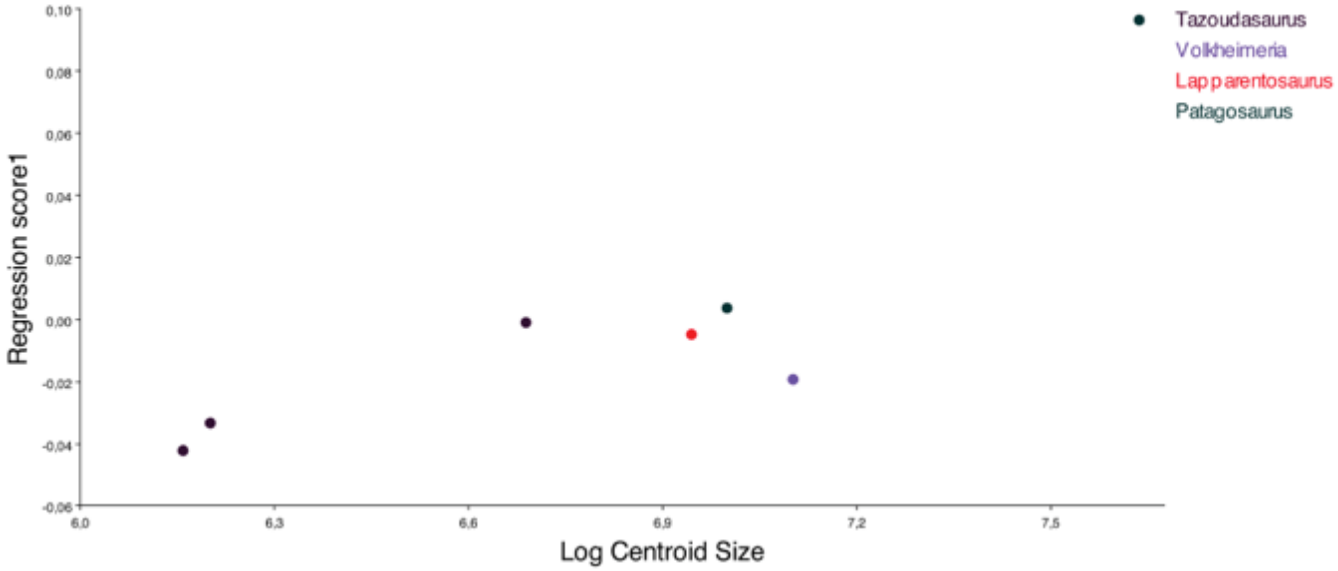

Figure 5: Regression analysis of the Procrustes coordinates on log centroid size, representing ontogenetic allometry in adult and juvenile sauropod femora (*Tazoudasaurus* in dark purple, *Volkheimeria* in blue, *Lapparentosaurus* in red, *Patagosaurus* in green).

The principal component analysis on the adult sauropod tibiae shows that PC1 accounts for 43,8% of the variance, whilst PC2 accounts for 23,2% of the variance and PC3 accounts for 18.3%. PC1 corresponds to variability of the placement of the narrowest part of the diaphysis, the medial malleolus at the distal end of the shaft, as well the shape of the cnemial crest of the tibia. PC2 corresponds with the variability of the distal placement of the ascending process, as well as the width of the medial malleolus (see Fig. 6). PC3 is not figured, but corresponds to a more proximal onset of the posteroventral process and medial malleolus and a broader distal articular surface.

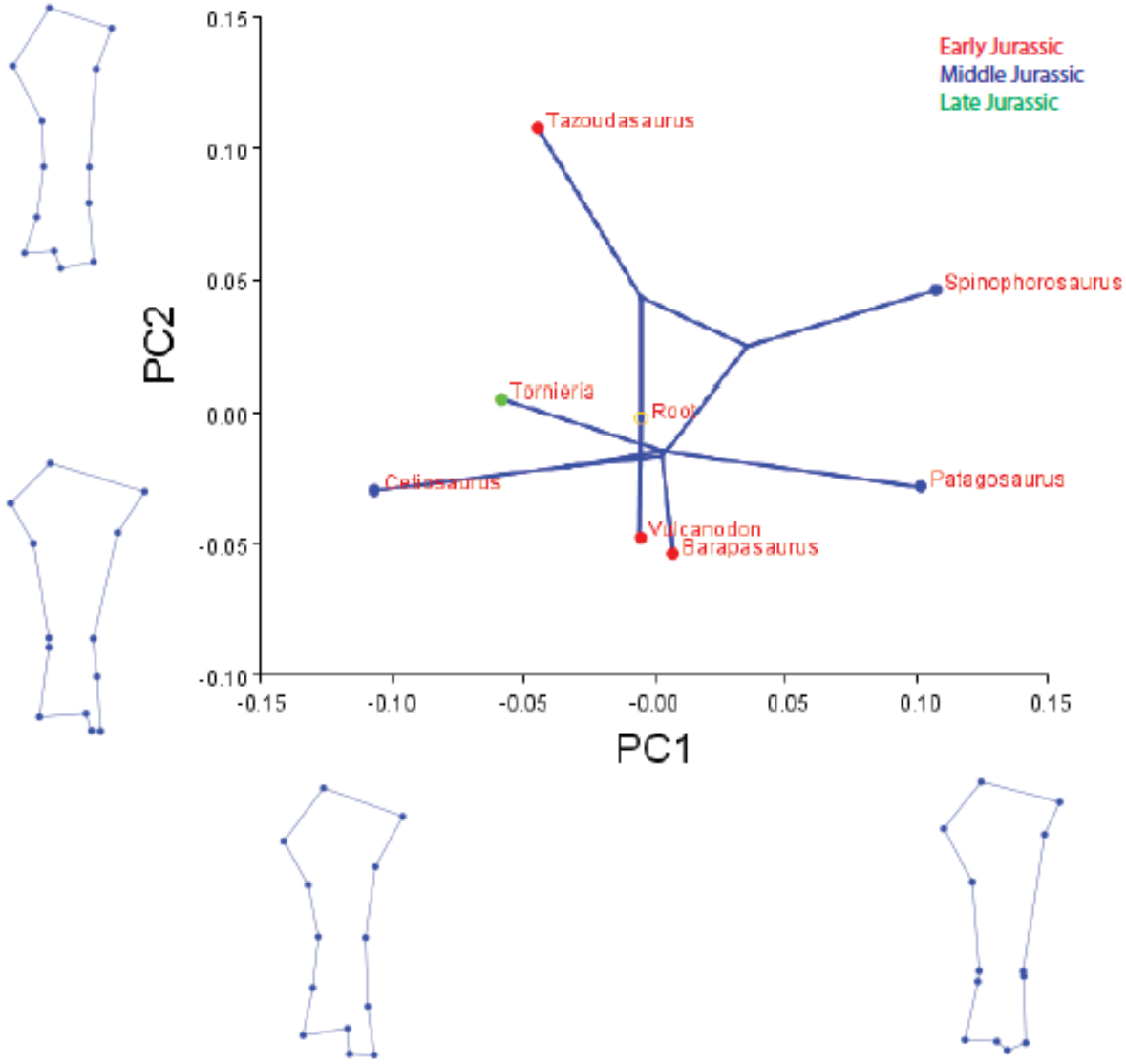

Fig. 6: PC1 vs PC2 of the principal component analysis on the adult tibiae with the phylogeny overlain. The colours represent whether the specimens are Early (red), Middle (blue) or Late Jurassic (green).

The Early Jurassic sauropods vary primarily along PC2 (Fig. 7). The posteroventral process of *Tazoudasaurus* starts to flare relatively far distally along the shaft, whereas *Vulcanodon* and *Barapasaurus* show a more proximal and less abrupt flaring towards the posteroventral process and medial malleolus (Fig. 7). Additionally, *Tazoudasaurus* is more robust (i.e., broader diaphysis and epiphyses) than the other two (Fig. 7). Middle Jurassic sauropods primarily display morphological variation along PC1 (Fig. 6). *Cetiosaurus* has a relatively

broader distal articular surface with a relatively wider medial malleolus compared to the other taxa, whereas *Spinophorosaurus* and *Patagosaurus* show a relatively smaller posteroventral process and medial malleolus (narrow and flat, respectively, Fig. 7).

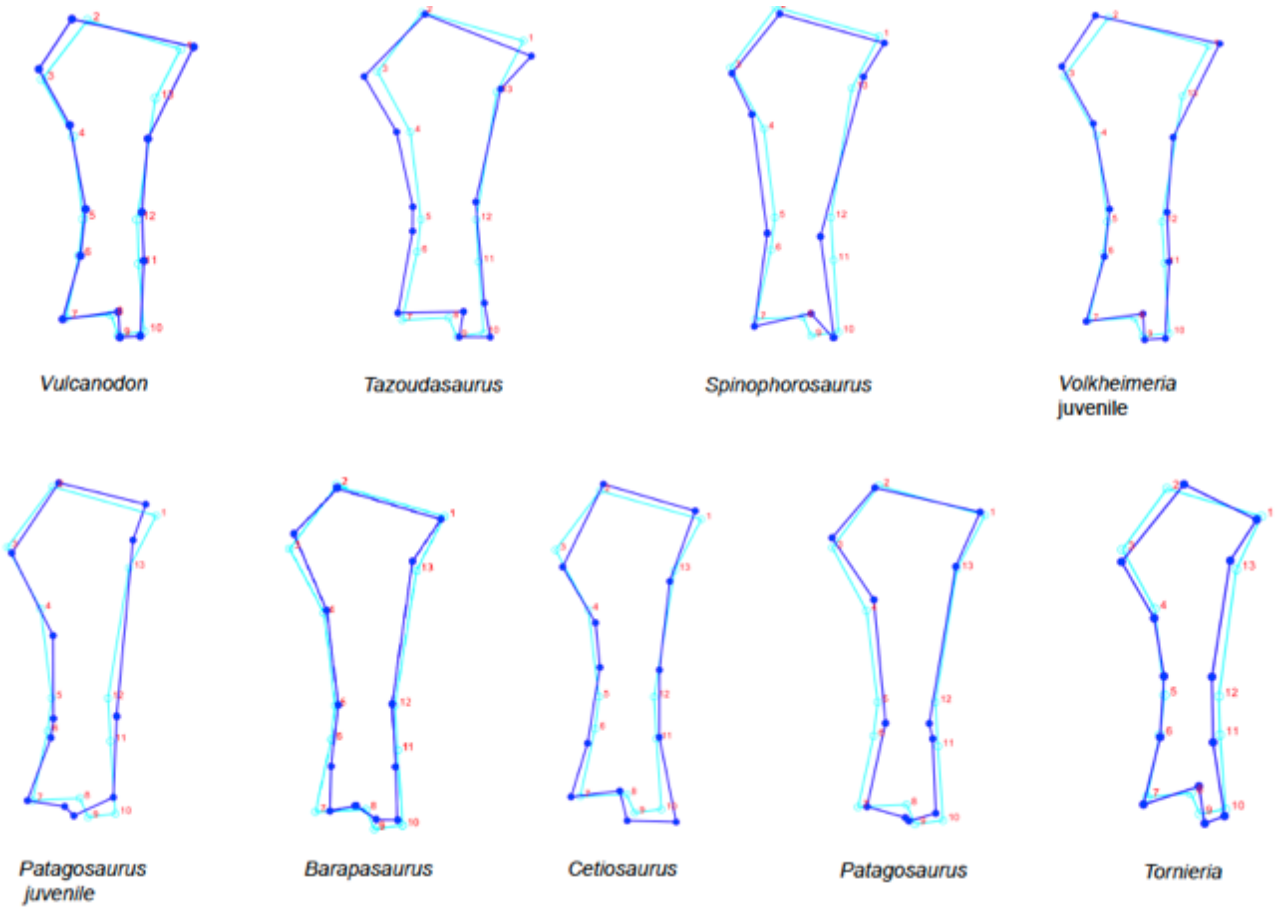

Figure 7: Morphological outlines of sauropod tibiae. Dark blue lines indicate individual variation from the light blue mean outlines

Regression analysis on the dataset of the adult tibiae was not statistically significant (p= 0,74) and does not show any obvious evolutionary allometric trends; even though the Late Jurassic specimen shows larger size, many of the Early and Middle Jurassic specimens also display larger sizes, with the exception of the juvenile specimens (Fig. 8).

Regression analysis without juvenile specimens (*Tazoudasaurus* and *Patagosaurus*) does not show any clear trend either.

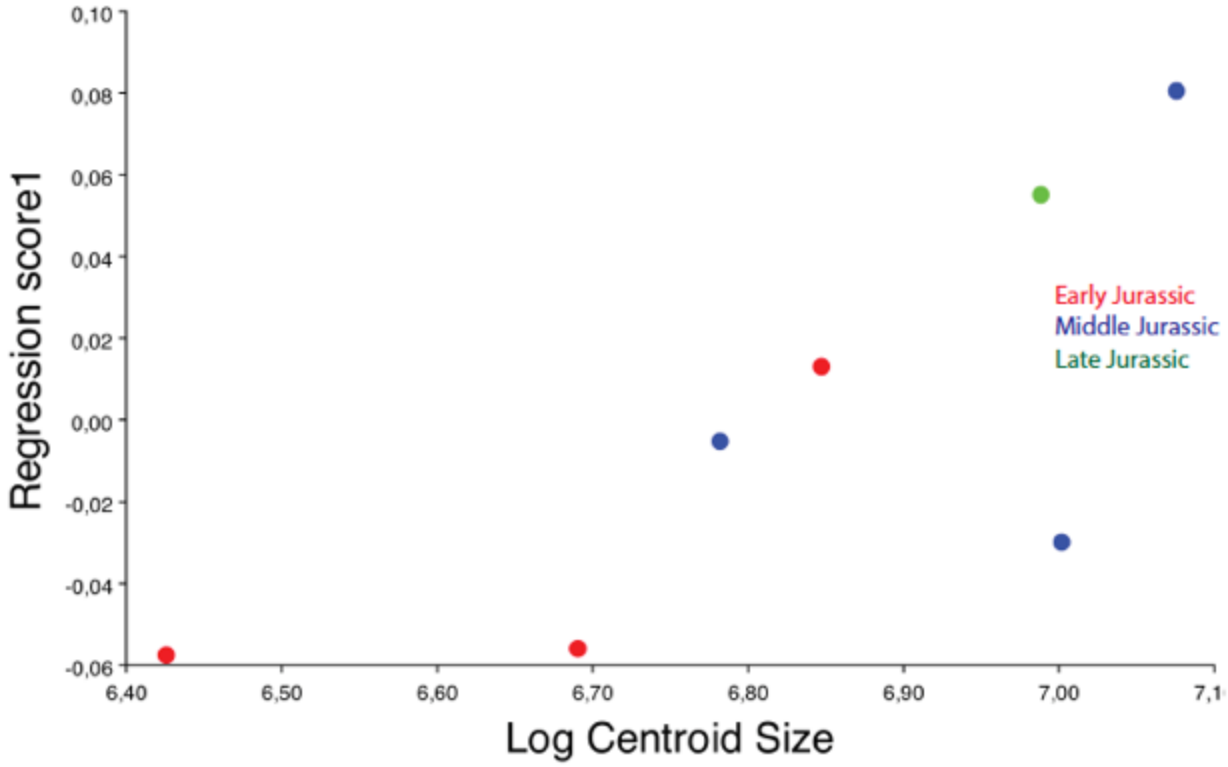

Fig. 8: Regression analysis of the Procrustes coordinates on log centroid size, representing evolutionary allometry in adult sauropod tibiae (Early Jurassic in red, Middle Jurassic in blue, Late Jurassic in green).

5.5 Discussion

Shape variability

The principal component analyses for the femora and the tibiae (Figs. 2 and 6) show no clear separation between Early, Middle and Late Jurassic sauropods, and hindlimb morphology seems to be highly variable. There is, however, a difference between the femora and the tibiae. Whereas the femora seem to display no pattern at all (regarding shape variability), the tibiae display different patterns of variability between the Early and Middle Jurassic sauropods. Naturally, sample sizes are rather small and the principal component analyses might be overfitted, but this might also represent an actual signal. If the latter is the case, a possible explanation might be that Early and Middle Jurassic sauropods partitioned the available niches in different ways. Early Jurassic sauropods differ mostly in terms of diaphysis shape, which may be related to graviportal capabilities of the limbs. Indeed, *Tazoudasaurus*, has the most robust tibia of all three Early Jurassic sauropods, and displays a broad distal flaring of the tibial shaft, whereas *Vulcanodon* and *Barapasaurus* display more slender and straight distal tibial shafts. These differences could be ontogenetic, however, it could also mean that in the Early Jurassic, not just the femora, but the tibiae were subjected to major morphological changes during early sauropod evolution as well.

Middle Jurassic sauropods, on the other hand, primarily display differences in the morphology of the posteroventral process and the medial malleolus. *Spinophorosaurus* and *Patagosaurus* show the posteroventral process and medial malleolus to be relatively narrow and flat compared to the other sauropods, and *Cetiosaurus* shows a relatively countermorphology of these latter features. These show a difference in distal articulation surface space of the tibia, related to the accommodation space for the astragalus and calcaneum, as well as the fibula, which are in turn related to the orientation of the sauropod pes (Nair and Salisbury, 2012), and thus stance. Large ossified calcanea provide stability

(Bonnan, 2000), but less flexibility, the latter which is one of the traits that was probably traded in for larger body size in the evolution of sauropod gigantism (Sander, 2013). Basal sauropods are known to have a different gait from neosauropods (Bonnan, 2000; Nair and Salisbury, 2012), and this study might fill in the 'gap' in the morphological changes of Middle Jurassic non-neosauropod eusauropods, as well as basal neosauropods, showing the variability of tibial morphology to be continuous throughout the Jurassic.

Evolutionary allometric trends

The regression analysis for the femora shows an allometric evolutionary trend for sauropod femoral morphology from the Late Triassic to the Early/Middle Jurassic, whereas from the Middle/Late Jurassic size rather than morphological increase is seen. In an earlier study on Triassic sauropodiform femoral morphology, a similar evolutionary allometric trend was observed through Triassic and Early Jurassic specimens (Yates et al., 2010). This corresponds with phylogenetic studies indicating the start of sauropod diversity to be around the Late Triassic and Early Jurassic. The significance of the morphological changes could therefore correspond to the before-mentioned change from facultative bipedality/quadrupedality to obligatory quadrupedality, which is seen in the sauropodiform-sauropod transition phase in the Late Triassic and Early Jurassic (Yates et al., 2010; McPhee et al., 2015; McPhee and Choiniere, 2016). Why then this evolutionary allometry would end in the Middle Jurassic, is less clear. From the Middle to Late Jurassic, only changes in size are seen in this analysis, whilst from an evolutionary point of view, the major radiation of neosauropds took place between the Middle and Late Jurassic (Alifanov and Averianov, 2003; Barrett and Upchurch, 2005; Upchurch and Mannion, 2009; Mannion and Upchurch, 2010; Rauhut et al., 2015). A positive evolutionary allometric trend would have therefore been expected to continue in sauropod femoral morphology from this time. One explanation could be that the sauropod femur was a less complex bone in neosauropod development as it was in sauropodiform-

sauropod development, and was only necessary in neosauropods as a vertical strut to support graviportal locomotion. Moreover, in a study on geometric morphometrics in neosauropod limb bones, a higher variance was found in humeri (forelimbs) than in femora (hindlimbs) (Bonnan, 2007), which together with this study, hints at a conservative morphology of the femur during Middle and Late Jurassic sauropod evolution. The main myological changes from sauropodiform to sauropod in hindlimbs are found to be the reduction and elongation of the major muscle groups from the ilium to the femur and from the femur to the tibia (Fechner, 2009), which again corresponds with the drastic shape changes observed in the Early Jurassic femur specimens. The further changes in size can relate to an increase in eccentricity of the femur, which was necessary for support (Wilson and Carrano, 1999).

When the regression analysis of the femora (Fig. 4) is compared to that of the tibiae (Fig. 8) there is a distinct difference, especially in Middle Jurassic specimens. The tibiae show a diversity of sizes, whereas Middle Jurassic sauropod femora show a clustering around a log centroid size of 7,5, whereas there is much more spread in the centroid sizes of early and late Jurassic sauropods. It might be possible that sauropod femoral development plateaus around the Middle Jurassic, which could relate to the rise of neosauropods in the Middle Jurassic, which then replaced non-neosauropod eusauropods. The intermediate positon of *Cetiosaurus* between basal sauropods and neosauropods in this study would then be in line with its phylogenetic position of derived non-neosauropod eusauropod (Läng and Mahammed, 2010; Carballido and Sander, 2014). To confirm the trend of Middle Jurassic femoral developmental stagnation, the largest of the eusauropods, turiasaurs and mamenchisaurs, need to be subjected to a similar study, which is beyond the scope of this current study, but which would be an aim for future study.

Ontogenetic allometric trends

Both isometric as well as allometric ontogenetic growth trends have been found in saurischia (Smith, 1997, 1998; Tidwell and Wilhite, 2005). With ontogeny, diagnostic features develop, as well as the eventual adult shape (Curry, 1999; Ikejiri, 2004; Schwarz et al., 2007; Tschopp and Mateus, 2013; Carballido and Sander, 2014). In this analysis, however, only tentative allometric ontogenetic trends were identified, as the sample size is too small to be conclusive. Unfortunately Middle Jurassic sauropod body fossils are still rare, and femora seem to preserve more easily than tibiae.

As juvenile sauropod material from more basal sauropods such as *Patagosaurus* is rare (Schwarz et al., 2007; García and Cerda, 2010; Carballido et al., 2012; Carballido and Sander, 2014), these analyses could help in the understanding of the ontogeny of basal sauropods. The tentative ontogenetic allometry found in *Patagosaurus* and *Tazoudasaurus* does hint at Early and Middle Jurassic sauropod ontogenetic trends to follow that of the more derived neosauropods. Future directions for these comparisons would include more data, however, such as more Laurasian taxa, particularly from China, such as *Shunosaurus*, *Klamelisaurus*, and *Mamenchisaurus*, for which current redescriptions and new analyses are being performed (Zhao and Downs, 1993; Zhang, 1988; Ouyang and Ye, 2002; Xing et al., 2015; Moore, Xu and Clark, 2017).

5.6 Conclusions

To summarize, an evolutionary allometric trend is seen in sauropod femora from the Late Triassic through to the Early/Middle Jurassic, whilst femora from sauropods from the Middle and Late Jurassic do not follow any allometric trend anymore, and only increase in size, which reflects the trends observed in the onset of sauropod gigantism where femora become larger and more robust to provide stability for graviportal posture. Tibiae show a high morphological variability throughout the Jurassic, which could be related to high variability in

sauropod stance and gait. Tentative ontogenetic allometry is found both in femora as well as in tibiae of this dataset, however, the sample size is too small to be conclusive.

5.7 **References**

Alifanov VR., Averianov AO. 2003. F*erganasaurus verzilini*, gen. et sp. nov., a new neosauropod (Dinosauria, Saurischia, Sauropoda) from the Middle Jurassic of Fergana Valley, Kirghizia. *Journal of Vertebrate Paleontology* 23:358–372.

Allain R., Aquesbi N. 2008. Anatomy and phylogenetic relationships of *Tazoudasaurus naimi* (Dinosauria, Sauropoda) from the late Early Jurassic of Morocco. *Geodiversitas* 30:345–424.

Barrett PM., Upchurch P. 2005. Sauropodomorph diversity through time. In: *The Sauropods: evolution and paleobiology*. 125–156.

Boehmer C., Rauhut OWM. 2010. 3D morphometric analysis of the presacral vertebrae of *Plateosaurus*: implications for vertebral evolution in sauropodomorph dinosaurs. *Journal of Vertebrate Paleontology, Program and Abstracts*:61A.

Bonaparte JF. 1979. Dinosaurs: A Jurassic Assemblage from Patagonia. *Science* 205:1377–1379.

Bonaparte JF. 1986. Les dinosaures (Carnosaures, Allosauridés, Sauropodes, Cétosauridés) du Jurassique Moyen de Cerro Cóndor (Chubut, Argentina). *Annales de Paléontologie (Vert.-Invert.)* 72:247–289.

Bonnan MF. 2000. The presence of a calcaneum in a diplodocid sauropod. *Journal of Vertebrate Paleontology* 20:317–323.

Bonnan MF. 2004. Morphometric analysis of humerus and femur shape in Morrison sauropods: implications for functional morphology and paleobiology. *Paleobiology* 30:444–470.

Bonnan MF. 2007. Linear and geometric morphometric analysis of long bone scaling patterns in Jurassic neosauropod dinosaurs: their functional and paleobiological implications. *The Anatomical Record: Advances in Integrative Anatomy and Evolutionary Biology* 290:1089–1111.

Bonnan MF., Yates AM. 2007. A new description of the forelimb of the basal sauropodomorph *Melanorosaurus*: implications for the evolution of pronation, manus shape and quadrupedalism in sauropod dinosaurs. *Special Papers in Palaeontology*:157–168.

Brusatte SL., Sakamoto M., Montanari S., Harcourt Smith WEH. 2012. The evolution of cranial form and function in theropod dinosaurs: insights from geometric morphometrics. *Journal of Evolutionary Biology* 25:365–377.

Buffetaut E., Suteethorn V., Cuny G., Tong H. 2000. The earliest known sauropod dinosaur. *Nature* 407:72.

Canudo JI., Cuenca-Bescós G. 2004. Morphometric approach to Titanosauriformes (Sauropoda, Dinosauria) femora: Implications to the paleobiogeographic analysis. In: *Morphometrics*. Springer, 143–156.

Carballido JL., Marpmann JS., Schwarz-Wings D., Pabst B. 2012. New information on a juvenile sauropod specimen from the Morrison Formation and the reassessment of its systematic position. *Palaeontology* 55:567–582.

Carballido JL., Sander PM. 2014. Postcranial axial skeleton of *Europasaurus holgeri* (Dinosauria, Sauropoda) from the Upper Jurassic of Germany: implications for sauropod ontogeny and phylogenetic relationships of basal Macronaria. *Journal of Systematic Palaeontology* 12:335–387.

Cardini A., Nagorsen D., O'Higgins P., Polly PD., Thorington Jr RW., Tongiorgi P. 2009. Detecting biological distinctiveness using geometric morphometrics: an example case from the Vancouver Island marmot. *Ethology Ecology & Evolution* 21:209–223.

Carrano MT. 2005. The evolution of sauropod locomotion: morphological diversity of a secondarily quadrupedal radiation. In: *The Sauropods: Evolution and Paleobiology*. Berkeley, CA: University of California Press, 229–251.

Curry KA. 1999. Ontogenetic histology of *Apatosaurus* (Dinosauria: Sauropoda): new insights on growth rates and longevity. *Journal of Vertebrate Paleontology* 19:654–665.

Curry Rogers K., Forster CA. 2001. The last of the dinosaur titans: a new sauropod from Madagascar. *Nature* 412:530–534.

Dantas, P., J. Sanz, C. Marques da Silva, F. Ortega, V. Santos, and M. Cachão. 1998. *Lourinhasaurus* n. gen. novo dinossáurio saurópode do Jurássico superior (Kimeridgiano superior-Titoniano inferior) de Portugal. Actas Do V Congresso Nacional de Geologia.-Comunicações Do Instituto Geológico e Mineiro 84:91–94.

Fechner R. 2009. Morphofunctional evolution of the pelvic girdle and hindlimb of Dinosauromorpha on the lineage to Sauropoda. PhD Thesis Thesis. LMU.

Foth C., Rauhut OWM. 2013a. Macroevolutionary and Morphofunctional Patterns in Theropod Skulls: A Morphometric Approach. *Acta Palaeontologica Polonica* 58:1–16.

Foth C., Rauhut OWM. 2013b. The good, the bad, and the ugly: the influence of skull reconstructions and intraspecific variability in studies of cranial morphometrics in theropods and basal saurischians. *PLoS ONE* 8:e72007.

GARCÍA RA., CERDA IA. 2010. Dentition and histology in titanosaurian dinosaur embryos from Upper Cretaceous of Patagonia, Argentina. *Palaeontology* 53:335–346.

Gilmore CW. 1936. *Osteology of Apatosaurus: With Special Reference to Specimens in the Carnegie Museum*. Board of trustees of the Carnegie institute.

Hedrick BP., Dodson P. 2013. Lujiatun psittacosaurids: understanding individual and taphonomic variation using 3D geometric morphometrics. *PLoS One* 8:e69265.

Hendrickx, C., R. Araújo, and O. Mateus. 2014. The Nonavian Theropod Quadrate II: Systematic Usefulness, Major Trends and Cladistic and Phylogenetic Morphometrics Analyses. PeerJ Preprints/380v2.

Hendrickx, C., O. Mateus, and E. Buffetaut. 2016. Morphofunctional Analysis of the Quadrate of Spinosauridae (Dinosauria: Theropoda) and the Presence of *Spinosaurus* and a Second Spinosaurine Taxon in the Cenomanian of North Africa. PloS One 11:e0144695.

van Heteren AH., MacLarnon A., Soligo C., Rae TC. 2014. Functional morphology of the cave bear (Ursus spelaeus) cranium: a three-dimensional geometric morphometric analysis. *Quaternary International* 339:209–216.

van Heteren AH., MacLarnon A., Soligo C., Rae TC. 2016. Functional morphology of the cave bear (Ursus spelaeus) mandible: a 3D geometric morphometric analysis. *Organisms Diversity & Evolution* 16:299–314.

Ikejiri T. 2004. Anatomy of *Camarasaurus lentus* (Dinosauria: Sauropoda) from the Morrison Formation (Late Jurassic), Thermopolis, central Wyoming, with determination and interpretation of ontogenetic, sexual dimorphic, and individual variation in the genus. Master Thesis Thesis. Fort Hays State University, Kansas, UMI.

Klingenberg CP. 2011. MorphoJ: an integrated software package for geometric morphometrics. *Molecular Ecology Resources* 11:353–357.

Läng É. 2008. Les cétiosaures (Dinosauria, Sauropoda) et les sauropodes du Jurassique moyen: révision systématique, nouvelles découvertes et implications phylogénétiques. Ph. D. dissertation Thesis. Paris, France: Centre de recherche sur la paléobiodiversité et les paléoenvironnements.

Läng E., Mahammed F. 2010. New anatomical data and phylogenetic relationships of Chebsaurus algeriensis (Dinosauria, Sauropoda) from the Middle Jurassic of Algeria. *Historical Biology* 22:142–164.

Mannion PD., Upchurch P. 2010. Completeness metrics and the quality of the sauropodomorph fossil record through geological and historical time. *Paleobiology* 36:283–302.

McPhee BW., Yates AM., Choiniere JN., Abdala F. 2014. The complete anatomy and phylogenetic relationships of *Antetonitrus ingenipes* (Sauropodiformes, Dinosauria): implications for the origins of Sauropoda. *Zoological Journal of the Linnean Society* 171:151–205.

McPhee BW., Bonnan MF., Yates AM., Neveling J., Choiniere JN. 2015. A new basal sauropod from the pre-Toarcian Jurassic of South Africa: evidence of niche-partitioning at the sauropodomorph–sauropod boundary? *Scientific reports* 5.

McPhee BW., Choiniere JN. 2016. A hyper-robust sauropodomorph dinosaur ilium from the Upper Triassic–Lower Jurassic Elliot Formation of South Africa: Implications for the functional diversity of basal Sauropodomorpha. *Journal of African Earth Sciences* 123:177–184.

Mocho P., Royo-Torres R., Ortega F. 2013. New approach to *Lourinhasaurus alenquerensis* (Macronaria, Camarasauromorpha) from the Portuguese Upper Jurassic. In: Torcida Fernández-Baldor F, Huerta P eds. *Abstract Book*. Salas de los Infantes (Burgos), Spain: Colectivo Arqueológico y Paleontológico de Salas, C.A.S., 91.

Moore A., Xu X., Clark J. 2017. Anatomy and systematics of *Klamelisaurus gobiensis*, a mamenchisaurid sauropod from the Middle-Late Jurassic Shishugou Formation of China. In: Calgary, Canada: Taylor & Francis, 165A.

Nair JP., Salisbury SW. 2012. New anatomical information on *Rhoetosaurus brownei* Longman, 1926, a gravisaurian sauropodomorph dinosaur from the Middle Jurassic of Queensland, Australia. *Journal of Vertebrate Paleontology* 32:369–394.

Ouyang H., Ye Y. 2002. *The first mamenchisaurian skeleton with complete skull,* Mamenchisaurus youngi. Chengdu, China: Sichuan Publishing House of Science and Technology, 138pp.

Rauhut OWM., Carballido JL., Pol D. 2015. A diplodocid sauropod dinosaur from the Late Jurassic Cañadón Calcáreo Formation of Chubut, Argentina. *Journal of Vertebrate Paleontology* 35:e982798.

Reed DA., Porro LB., Holliday CM., Lemberg JB., Metzger KA., Ross CF. 2010. Multidimensional analysis of mandibular function in Alligator mississippiensis using geometric morphometrics and finite element modeling. In: *Integrative And Comparative Biology*. Oxford University Press, Oxford, UK, E144–E144.

Remes K. 2006. Revision of the Tendaguru sauropod dinosaur *Tornieria africana* (Fraas) and its relevance for sauropod paleobiogeography. *Journal of Vertebrate Paleontology* 26:651–669.

Remes K., Ortega F., Fierro I., Joger U., Kosma R., Ferrer JMM., Ide OA., Maga A. 2009. A new basal sauropod dinosaur from the Middle Jurassic of Niger and the early evolution of Sauropoda. *PLoS One* 4:e6924.

Rohlf FJ. 2005. tpsDig program, version 2.04, ecology and evolution, SUNY at Stony Brook. *See http://life. bio. sunysb. edu/morph*.

Rohlf FJ. 2010. TpsDig, ver. 2. 16. *Department of Ecology and Evolution, State University New York at Stony Brook, New York*.

Rohlf FJ., Slice D. 1990. Extensions of the procrustes method for the optimal superimposition of landmarks. *Systematic Biology* 39:40–59.

Sander PM. 2013. An evolutionary cascade model for sauropod dinosaur gigantism - overview, update and tests. *PLoS ONE* 8:e78573.

Schwarz D., Ikejiri T., Breithaupt BH., Sander PM., Klein N. 2007. A nearly complete skeleton of an early juvenile diplodocid (Dinosauria: Sauropoda) from the Lower Morrison Formation (Late Jurassic) of north central Wyoming and its implications for early ontogeny and pneumaticity in sauropods. *Historical Biology* 19:225–253.

Sereno PC., Beck AL., Dutheil DB., Larsson HC., Lyon GH., Moussa B., Sadleir RW., Sidor CA., Varricchio DJ., Wilson GP. 1999. Cretaceous sauropods from the Sahara and the uneven rate of skeletal evolution among dinosaurs. *Science* 286:1342–1347.

Smith D. 1997. Cranial allometry in Coelophysis: preliminary results. In: *Southwest Paleontological Symposium Proceedings*. 41–48.

Smith DK. 1998. A morphometric analysis of *Allosaurus*. *Journal of Vertebrate Paleontology* 18:126–142.

Tidwell V., Wilhite DR. 2005. Ontogenetic variation and isometric growth in the forelimb of the Early Cretaceous sauropod Venenosaurus. *Thunder Lizards: the Sauropodomorph Dinosaurs*, 187–198.

Tschopp E., Mateus O. 2013. The skull and neck of a new flagellicaudatan sauropod from the Morrison Formation and its implication for the evolution and ontogeny of diplodocid dinosaurs. *Journal of Systematic Palaeontology* 11:853–888.

Upchurch P., Martin J. 2003. The anatomy and taxonomy of *Cetiosaurus* (Saurischia, Sauropoda) from the Middle Jurassic of England. *Journal of Vertebrate Paleontology* 23:208–231.

Upchurch P., Barrett PM., Dodson P. 2004. Sauropoda. In: Weishampel DB, Dodson P, Osmólska H eds. *The Dinosauria. Second edition*. Berkeley, CA: University of California Press, 259–322.

Upchurch P., Mannion PD. 2009. The first diplodocid from Asia and its implications for the evolutionary history of sauropod dinosaurs. *Palaeontology* 52:1195–1207.

Wilson JA., Carrano MT. 1999. Titanosaurs and the origin of ”wide-gauge” trackways: a biomechanical and systematic perspective on sauropod locomotion. *Paleobiology* 25:252–267.

Xing L., Miyashita T., Zhang J., Li D., Ye Y., Sekiya T., Wang F., Currie PJ. 2015. A new sauropod dinosaur from the Late Jurassic of China and the diversity, distribution, and relationships of mamenchisaurids. *Journal of Vertebrate Paleontology* 35:e889701.

Yates AM., Bonnan MF., Neveling J., Chinsamy A., Blackbeard MG. 2010. A new transitional sauropodomorph dinosaur from the Early Jurassic of South Africa and the evolution of sauropod feeding and quadrupedalism. *Proceedings of the Royal Society B: Biological Sciences* 277:787–794.

Yates AM., Kitching JW. 2003. The earliest known sauropod dinosaur and the first steps towards sauropod locomotion. *Proceedings of the Royal Society of London. Series B: Biological Sciences* 270:1753–1758.

Zhang Y. 1988. *The Middle Jurassic dinosaur fauna from Dashanpu, Zigong, Sichuan, vol. 1: sauropod dinosaur (I): Shunosaurus*. Chengdu, China: Sichuan Publishing House of Science and Technology, 114 pp.

Zhao XJ., Downs TBW. 1993. A new Middle Jurassic sauropod subfamily (Klamelisaurinae subfam. nov.) from Xinjiang Autonomous Region, China. *Vertebra PalAsiatic* 31:132–138.

6 Conclusions

6.1 General Conclusions of Chapter 2-5

The Argentine early Middle Jurassic sauropod taxon *Patagosaurus fariasi* BONAPARTE 1979 is an important taxon for early sauropod evolutionary research. It is from a time where sauropod diversification started, and has numerous skeletal elements preserved, adding information for taxonomic and phylogenetic research. Therefore, the holotype of *Patagosaurus fariasi* has been revised, and new diagnostic features are found and compared to other Jurassic sauropods. The principle diagnostic characters based on the holotype of *Patagosaurus*, PVL 4170, (Chapter 2) are the following: the cervicals are opisthocoelous, both cervicals and anterior dorsals show marked pleurocoels, which are deep in the cervicals. *Patagosaurus* does not show the internal pneumatic structure in the pleurocoels that neosauropods display. The pleurocoel is more shallow in the dorsals, as was also noted by Bonaparte in the original 1986 osteological description.

The presence of a single intraprezygapophyseal and single intrapostzygapophyseal lamina in the dorsal vertebrae is another diagnostic feature for *Patagosaurus*, Previously, these laminae were noted only for *Camarasaurus* and the titanosauriform *Tehuelchesaurus.* The presence of a small stprl accompanied by a large oval centroprezygapophyseal fossa on either lateral side, is however shared with many other eusauropods, therefore this combination may not be a definitive diagnostic character.

The centrodiapophyseal fossa (CDF) pneumatic structure on the dorsal neural arches, appearing first in the middle dorsal neural arches and expanding in the posterior dorsal neural arches, is the key feature that Bonaparte mentioned in the

original osteological descriptions for *Patagosaurus*, also using it to distinguish this sauropod from the other sauropod from the Cañadón Asfalto Formation, *Volkheimeria*. This feature is still one of the main autapomorphies for *Patagosaurus,* and marks new pneumatic features for basal eusauropods that were previously unknown. However, more basal non-neosauropod eusauropods may have this structure (e.g. *Cetiosaurus, Barapasaurus, Tazoudasaurus, Spinophorosaurus*), therefore future research will show if the presence/absence of a pneumatic structure is a diagnostic feature alone, or if it is the combination of this feature with the ventral pneumatic air chamber that is well-separated from the neural canal. A detailed pneumatic study is beyond the scope of this thesis. However, as pneumaticity in sauropods is well-known in neosauropods, but not well understood for basal non-neosauropodan eusauropods, *Patagosaurus* is the first taxon to give conclusive evidence for this structure. The elongated neural spines, which are not straight but curve convexly posteriorly at 2/3rd of the height of the spine, that are seen in the anterior caudals of *Patagosaurus,* are another diagnostic feature that is not seen in other sauropods, even though anterior neural spine elongation is seen in *Cetiosauriscus*, as well as in diplodocids. The wide acetabulum of the ilium, as well as the anteriorly projecting and elongated pubic peduncle, are diagnostic features for the ilium of *Patagosaurus.* The femur that is slightly convex towards the lateral side shows a possible gait modification that is diagnostic for *Patagosaurus* and that has not been found in other Jurassic sauropods.

To summarize Chapter 2, *Patagosaurus fariasi* shows a set of morphological features that are typically eusauropod and are shared with other eusauropods. However,

some elements seem to be slightly more derived, and are found in derived non-neosauropodan eusauropods and/or neosauropods.

The alpha taxonomy of Patagosaurus thus re-established; the associated material has been analysed in a similar way. Based on comparisons of the associated *Patagosaurus* material with the holotype (Chapter 3), the following specimens can be confirmed to belong the taxon *Patagosaurus fariasi*:

MACN-CH 933 as the youngest, earliest MOS stage 1 *Patagosaurus*, MACN-CH 932 as a slightly larger, MOS stage 2 *Patagosaurus*, and MACN-CH 935 as a subadult *Patagosaurus* and PVL 4076 and 4176 as adult *Patagosaurus* material, possibly belonging to the holotype, from Cerro Condor Norte.

From Cerro Condor Sur, the specimens MACN-CH 936 and MACN-CH 231 can safely be assigned to *Patagosaurus*.

This leaves the taxon with an ontogenetic series from MOS 1 to MOS 3/4, covering all ontogenetic stages known for sauropods, as well as providing additional skeletal material and characters for phylogenetic analyses.

The specimen MACN-CH 934, as well as MACN-CH 230, are most likely not *Patagosaurus fariasi*, and also probably not *Volkheimeria*. Therefore, they would appear to be different taxa, increasing the species diversity of the Cañadón Asfálto Fm. even more; in addition to *Patagosaurus fariasi*, *Volkheimeria chubutensis*, and an unnamed taxon at the Museo Paleontológico Egidio Feruglio collection in Trelew, Argentina, one taxon based on juvenile (MOS stage 2) sauropod material MACN-CH 934 is now confirmed, as well as that of a possible small taxon, the MOS stage 3 or 4 MACN-CH 230.

The specimens MACN-CH 232, MACN-CH 219, and MACN-CH 223 do not contain enough information to rule them out as being *Patagosaurus* or another affinity, and this material will remain indeterminate sauropods.

The phylogenetic analysis of Chapter 4, using the combined results from Chapter 2 and 3, shows that within the Cañadón Asfálto Formation sauropod community a high phylogenetic diversity is seen, with a relatively-derived position for *Patagosaurus*, potential neosauropod affinities for MACN-CH 934, and a more basal position for *Volkheimeria*, and possibly yet another taxon, MACN-CH 230, which comes out between *Volkheimeria* and *Patagosaurus*.

The MACN-CH 934 material is moderately preserved, and it has both cranial, as well as postcranial material preserved, which provide enough information for it to be considered a new taxon, and it consequently will be analysed more thoroughly in the future. Moreover, its phylogenetic position is far enough removed from *Patagosaurus* and *Volkheimeria* to show a real phylogenetic signal. The phylogenetic position of MACN-CH 230, however, is more complicated. The result could be a product of serial variation, ontogeny, or even hybridization, and as this specimen only has dorsal elements known thus far, the results may not show a true phylogenetic signal. However, the high diversity resulting from the phylogeny, in having three or four sauropod taxa from these bonebeds, as well as having yet another undescribed sauropod taxon from the Cañadón Asfálto Formation, could point to a Patagonian Gondwanan form of endemic radiation, as this has yet to be seen in other Middle Jurassic sites. This, together with the high diversity patterns and interrelationships between Early Jurassic and Middle Jurassic sauropods in this

analysis, demonstrates early sauropod diversification and radiation in the Early Jurassic, and moreover, pushes the boundaries of sauropod diversification and radiation further back to the Early Jurassic, or even the Late Triassic.

Moreover, the phylogenetic relationships of *Patagosaurus* with other sauropods in Gondwana and Laurasia show high dispersal rates of sauropods from different regions in Gondwana and Laurasia in the Early and Middle Jurassic, which were not hindered by physical barriers such as deserts. Principal component analysis shows that there is less diversity within Gondwana than there is within Laurasia, showing potentially less mobility in Laurasian sauropods, and therefore higher endemism in general, than in Gondwana. A better understanding of Laurasian sauropods may help to elucidate these patterns.

Finally, a brief overview of morphological diversity, using geometric morphometrics (Chapter 5) between different ontogenetic stages of limb bones (femora and tibiae) of *Patagosaurus* and also between different Jurassic sauropods, has been performed as preliminary assessment into evolutionary and ontogenetic trends in Jurassic sauropod limb bones. After analyzing femora and tibiae from juvenile and adult Jurassic sauropods, a tentative allometric trend is seen between tibiae of *Patagosaurus*, *Tazoudasaurus* and *Lapparentosaurus*, but not with *Volkheimeria*. However, there might not be enough information to provide conclusive evidence of any ontogenetic trend, as juvenile sauropod material is extremely rare.

The adult *Patagosaurus* femur shows an offset from the datamatrix in general, but also from the juvenile *Patagosaurus*.

Furthermore, tibial morphological variability amongst Jurassic sauropods is highest amongst early Jurassic sauropods, especially concerning the cnemial crest and distal end of the tibia, probably reflecting on muscle attachments. This variability is not seen in Middle to Late Jurassic sauropods, thus indicating that the tibiae were subject to morphological changes in early sauropod evolution, as a result of obligatory graviportal motion. Future analyses will determine whether the morphological trends found in this study reflect on Early and Middle Jurassic sauropod gait, compared to that of Late Jurassic and Cretaceous sauropods.

The morphological trends amongst femora mainly reflect on an increase in size between Triassic, Early and Middle Jurassic sauropods, and is seen less between Middle and Late Jurassic sauropods. This could correspond to an overal increase in sauropod body size and consequent femoral adaptation. This trend does reflect well on the phylogenetic analysis of Chapter 4, as well as earlier studies, where major sauropod diversification is shown to have taken place in the Early-Middle Jurassic. Future studies, having a larger sample size and including more Jurassic and Triassic sauropods, may help to elucidate these patterns.

6.2 Future research

Future directions for Early and Middle sauropod research would include the incorporation of more data on lesser-known Jurassic sauropods, such as Laurasian taxa, like *Cetiosauriscus*, but particularly those from China, such as *Shunosaurus*, *Klamelisaurus* and *Mamenchisaurus*, for which current redescriptions and new analyses are either currently performed or scheduled. *Lapparentosaurus*, a key taxon to understanding the phylogenetic relationships with the new taxon from the *Patagosaurus* sample, MACN-CH 934, also is in need of a reassessment.

In order to see pneumatic trends in non-neosauropodan eusauropods, and for comparative purposes with *Patagosaurus*, the closely-related *Cetiosaurus* (both *C. oxoniensis* and the Rutland *Cetiosaurus*) requires an assessment of its pneumatic vertebral features. CT-scanning of middle and posterior dorsal vertebrae of other sauropods such as *Tazoudasaurus* and *Barapasaurus* would also significantly expand on the current state of understanding of early sauropod vertebral pneumaticity.

In order to elucidate evolutionary morphological trends in the limb bones of sauropods, and to build on the preliminary study in this thesis, more appendicular elements of Triassic and Middle Jurassic non-neosauropodan eusauropods should be analysed. Moreover, geometric morphometric comparisons between fore- and hindlimbs would be useful, as this was outside of the scope of the present study.

Finally, a future, more extensive phylogenetic analysis utilising all new data listed above, which needs to be rendered over the coming years, would further clarify the

position of *Patagosaurus* with respect to other sauropods, and consequently would aid greatly in further resolving the early evolution of basal eusauropods.

Appendix Chapter 3

Appendix A: material list of *Patagosaurus* material in PVL and MACN-CH, amended from original list

Locality	Collection reference	holotype/collected	adult/juvenile	material
Cerro Condor Norte	PVL 4170	holotype	3 adults 1 juvenile	anterior cervical vertebrae
Cerro Condor Norte	PVL 4170	holotype		posterior cervical vertebrae
Cerro Condor Norte	PVL 4170	holotype		anterior dorsals articulated to the last cervical
Cerro Condor Norte	PVL 4170	holotype		mid- and posterior dorsals
Cerro Condor Norte	PVL 4170	holotype		dorsal centra
Cerro Condor Norte	PVL 4170	holotype		the complete sacrum of vertebrae
Cerro Condor Norte	PVL 4170	holotype		proximal caudal vertebrae
Cerro Condor Norte	PVL 4170	holotype		a collection of mid- and distal caudal vertebrae
Cerro Condor Norte	PVL 4170	holotype		incomplete ribs
Cerro Condor Norte	PVL 4170	holotype		haemal arches
Cerro Condor Norte	PVL 4170	holotype		right ilium
Cerro Condor Norte	PVL 4170	holotype		ischia partly fused but broken in their proximal regions
Cerro Condor Norte	PVL 4170	holotype		right pubis
Cerro Condor Norte	PVL 4170	holotype		proximal part of the right scapula associated with the broken coracoid
Cerro Condor Norte	PVL 4170	holotype		proximal part of the right humerus
Cerro Condor Norte	PVL 4170	holotype		right femur
Cerro Condor Norte	MACN-CH 932	hypodigm	small/medium	cervical centra
Cerro Condor Norte	MACN-CH 932	hypodigm		anterior dorsal centrum
Cerro Condor Norte	MACN-CH 932	hypodigm		neural dorsal arches
Cerro Condor Norte	MACN-CH 932	hypodigm		dorsal vertebral centra
Cerro Condor Norte	MACN-CH 932	hypodigm		sacral neural arch
Cerro Condor Norte	MACN-CH 932	hypodigm		sacral vertebral centra
Cerro Condor Norte	MACN-CH 932	hypodigm		sacral ribs
Cerro Condor Norte	MACN-CH 932	hypodigm		right scapula
Cerro Condor Norte	MACN-CH 932	hypodigm		Right coracoid
Cerro Condor Norte	MACN-CH 932	hypodigm		Right humerus
Cerro Condor Norte	MACN-CH 932	hypodigm		Right radius
Cerro Condor Norte	MACN-CH 932	hypodigm		Right ulna
Cerro Condor Norte	MACN-CH 932	hypodigm		(right?) pubis
Cerro Condor Norte	MACN-CH 932	hypodigm		(right?) metatarsals
Cerro Condor Norte	MACN-CH 932	hypodigm		(right?) phalanges
Cerro Condor Norte	MACN-CH 932	hypodigm		(right?) ungual phalanx
Cerro Condor Norte	MACN-CH 933	hypodigm	juvenile	incomplete left dentary
Cerro Condor Norte	MACN-CH 933	hypodigm		cervical centra
Cerro Condor Norte	MACN-CH 933	hypodigm		anterior dorsal centra
Cerro Condor Norte	MACN-CH 933	hypodigm		neural dorsal arches
Cerro Condor Norte	MACN-CH 933	hypodigm		dorsal centra
Cerro Condor Norte	MACN-CH 933	hypodigm		sacral neural arch
Cerro Condor Norte	MACN-CH 933	hypodigm		pubis
Cerro Condor Norte	MACN-CH 933	hypodigm		ilium fragment
Cerro Condor Norte	MACN-CH 933	hypodigm		right femur
Cerro Condor Norte	MACN-CH 933	hypodigm		(right?) tibia
Cerro Condor Norte	MACN-CH 935	hypodigm	large adult	Mid-dorsal vertebral neural arches
Cerro Condor Norte	MACN-CH 935	hypodigm		dorsal centra
Cerro Condor Norte	MACN-CH 935	hypodigm		sacral vertebrae with ribs
Cerro Condor Norte	MACN-CH 935	hypodigm		sacral centrum
Cerro Condor Norte	MACN-CH 935	hypodigm		fused sacral neural arches
Cerro Condor Norte	MACN-CH 935	hypodigm		sacral neural arch with neural spine
Cerro Condor Norte	MACN-CH 935	hypodigm		proximal caudal centrum
Cerro Condor Norte	MACN-CH 935	hypodigm		mid and distal caudal vertebrae
Cerro Condor Norte	MACN-CH 935	hypodigm		incomplete neural spines (from where?)
Cerro Condor Norte	MACN-CH 935	hypodigm		chevrons
Cerro Condor Norte	MACN-CH 935	hypodigm		proximal sections of dorsal ribs
Cerro Condor Norte	MACN-CH 935	hypodigm		ilium fragment with acetabular cavity
Cerro Condor Norte	MACN-CH 935	hypodigm		right pubis
Cerro Condor Norte	MACN-CH 935	hypodigm		ischia?
Cerro Condor Sur	PVL 4076	collected material	large adult	Mid-cervical vertebrae
Cerro Condor Sur	PVL 4076	collected material		left premaxilla
Cerro Condor Sur	PVL 4076	collected material		incomplete posterior cervical vertebrae
Cerro Condor Sur	PVL 4076	collected material		dorsal centra
Cerro Condor Sur	PVL 4076	collected material		anterior dorsal neural arch
Cerro Condor Sur	PVL 4076	collected material		dorsal centrum with part of neural arch
Cerro Condor Sur	PVL 4076	collected material		dorsal rib fragments
Cerro Condor Sur	PVL 4076	collected material		mid and mid proximal caudal vertebrae
Cerro Condor Sur	PVL 4076	collected material		incomplete right pubis
Cerro Condor Sur	PVL 4076	collected material		right femur
Cerro Condor Sur	PVL 4076	collected material		right tibia
Cerro Condor Sur	PVL 4075	collected material	large adult	dorsal centra
Cerro Condor Sur	PVL 4075	collected material		scapula
Cerro Condor Sur	PVL 4075	collected material		left humerus
Cerro Condor Sur	PVL 4075	collected material		proximal fragment of ischium
Cerro Condor Sur	PVL 4075	collected material		left femur
Cerro Condor Sur	PVL 4617	collected material		incomplete caudal vertebrae
Cerro Condor Sur	PVL 4617	collected material		cervical rib
Cerro Condor Sur	PVL 4617	collected material		scapula
Cerro Condor Sur	PVL 4617	collected material		coracoid
Cerro Condor Sur	PVL 4617	collected material		ungual phalanx
Cerro Condor Sur	MACN-CH 934	collected material	juvenile	dorsal neural arches
Cerro Condor Sur	MACN-CH 934	collected material		ilium
Cerro Condor Sur	MACN-CH 934	collected material		pubis
Cerro Condor Sur	MACN-CH 934	collected material		ischium
Cerro Condor Sur	MACN-CH 934	collected material		several appendicular elements
Cerro Condor Sur	MACN-CH 934	collected material		left and right maxilla
Cerro Condor Sur	MACN-CH 219			
Cerro Condor Sur	MACN-CH221,223			
Cerro Condor Sur	MACN-CH 230,231,232	collected material	?	dentary
Cerro Condor Sur	MACN-CH 936			vertebras cervicales mid- posterior and dorsals
Cerro Condor Norte?	MACN-CH 1986			

Appendix Chapter 4

Appendix A: character matrix

nr	Character	State (0)	State (1)	State (2)	State (3)	State (4)
1	Posterolateral processes of premaxilla and lateral processes of maxilla, shape	without midline contact	with midline contact forming marked narial depression, subnarial foramen not visible laterally			
2	Premaxillary anterior margin shape	without step	with marked step but short step	with marked and long step		
3	Premaxila, ascending process shape in lateral view	convex	concave, with a large dorsal projection	sub-rectilinear and directed posterodorsally		
4	Premaxilla, external surface	without anteroventrally orientated vascular grooves originating from an opening in the maxillary contact	vascular grooves present			
5	Maxillary border of external naris, length	short, making up much less than one-fourth narial perimeter	long, making up more than one third narial perimeter			
6	Maxilla, foramen anterior to the preantorbital fenestra	absent	present			
7	Preanteorbital fenestra	absent	present, being wide and laterally opened			
8	Subnarial foramen and exterior maxillary foramen, position	well distanced from one another	separated by narrow bony isthmus			
9	Antorobital fenestra	much shorter than orbital maximum diameter, less than 85% of orbit	subequal to orbital maximum diameter, greater than 85% orbit			
10	Antorbital	straight or	concave			

	fenestra, shape of dorsal margin	convex				
11	Antorbital fossa	present	absent			
12	External nares position	terminal	retracted to level of orbit	retracted to a position between orbits		
13	External nares, maximum diameter	shorter	or longer than orbital maximum diameter			
14	Orbital ventral margin, anteroposterior length	broad, with subcircular orbital margin	reduced, with acute orbital margin			
15	Lacrimal, anterior process	present	absent			
16	Jugal contribution to the ventral border of the skull	present	absent			
17	Quadratojugal-Maxila contact	absent or small	broad			
18	Jugal-ectopterygoid contact	present	absent			
19	Jugal, contribution to antorbital fenestra	very reduced or absent	large, bordering approximately one-third its perimeter			
20	Quadratojugal, position of anterior terminus	posterior to middle of orbit	anterior margin of orbit or beyond			
21	Quadratojugal, anterior process length	short, anterior process shorter than dorsal process	long, anterior process more than twice as long as dorsal process			
22	Quadratojugal, angle between anterior and dorsal processes	less than or equal to 90°, so that the quadrate shaft is directed dorsally	greater than 90°, approaching 130°, so that the quadrate shaft slants posterodorsally			
23	Ventral edge of anterior surface of the quadratojugal	straigth, not expanded ventrally	concave due to a ventral expansion of the anterior region			
24	Squamosal contribution to the supratemporal fenestra	present, the squamosal is well visible in dorsal view	reduced or absent			
25	Squamosal-quadratojugal contact	present	absent			

26	Squamosal, posteroventral margin	smooth	"with prominent, ventrally directed "prong"			
27	Prefrontal posterior process size	small, not projecting far posterior of frontal-nasal suture	elongate, approaching parietal			
28	Prefrontal, posterior process shape	flat	hooked			
29	Prefrontal, anterior process	absent	present			
30	Prefrontal-Frontal contact width	large, equal or longer that the anteroposterior length of the prefrontal	narrow, less than half the anteroposterior length of the prefrontal			
31	Postorbital, ventral process shape	transversely narrow	broader transversely than anteroposteriorly			
32	Postorbital, posterior process	present	absent			
33	Postorbital, posterior margin articulating with the squamosal	with tapering posterior process	with a deep posterior process			
34	Frontal contribution to supratemporal fossa	present	absent			
35	Frontals, midline contact (symphysis)	sutured	or fused in adult individuals			
36	Frontal, anteroposterior length	approximately twice	or less than minimum transverse breadth			
37	Frontal-nasal suture, shape	flat or slightly bowed anteriorly	V-shaped, pointing posteriorly			
38	Frontals, dorsal surface	without paired grooves facing anterodorsally	grooves present, extend on to nasal			
39	Frontal, contribution to dorsal margin of orbit	less than 1.5 times the contribution of prefrontal	at least 1.5 times the contribution of prefrontal			
40	Parietal occipital process, dorsoventral	short, less than the diameter of	deep, nearly twice the diameter of the foramen			

	height	the foramen magnum	magnum			
41	Parietal, contribution to post-temporal fenestra	present	absent			
42	Parietal, distance separating supratemporal fenestrae	less than	or twice the long axis of supratemporal fenestra			
43	Postparietal foramen	absent	present			
44	Paroccipital process distal terminus	straight, slightly expanded surface	rounded, tongue-like process			
45	Supratemporal fenestra	present	absent			
46	Supratemporal fenestra, long axis orientation	anteroposterior	transverse			
47	Supratemporal fenestra, maximum diameter	much longer than	or subequal to that of foramen magnum			
48	Supratemporal region, anteroposterior length	temporal bar longer	or shorter anteroposteriorly than transversely			
49	Supratemporal fossa, lateral exposure	not visible laterally, obscured by temporal bar	visible laterally, temporal bar shifted ventrally			
50	Supraoccipital sagital nucheal crest	broad, weakly developed	narrow, sharp and distinct			
51	Laterotemporal fenestra, anterior extension	posterior to orbit	ventral to orbit			
52	Quadrate fossa	absent	present			
53	Quadrate fossa, depth	shallow	deeply invaginated			
54	Quadrate fossa, orientation	posterior	posterolateral			
55	Quadrate, articular surface shape	quadrangular in ventral view, oriented transversely	roughly triangular in shape or thin, crescent-shaped surface with anteriorly directed medial process			
56	Quadrate, articular surface shape	quadrangular in ventral view, oriented transversely	thin, crescent-shaped surface with anteriorly directed medial process			

		or roughly triangular in shape				
57	Palatobasal contact, shape	pterygoid with small facet	dorsomedially orientated hook	or rocker-like surface for basipterygoid articulation		
58	Pterygoid, transverse flange (i.e. ectopterygoid process) position	posterior of orbit	between orbit and antorbital fenestra	anterior to antorbital fenestra		
59	Pterygoid, quadrate flange size	large, palatobasal and quadrate articulations well separated	small, palatobasal and quadrate articulations approach			
60	Pterygoid, palatine ramus shape	straight, at level of dorsal margin of quadrate ramus	stepped, raised above level of quadrate ramus			
61	Pterygoid, sutural contact with ectopterygoid	broad, along the medial or lateral surface	narrow, restricted to the anterior tip of the ectopterygoid			
62	Palatine, lateral ramus shape	plate-shaped (long maxillary contact)	rod-shaped (narrow maxillary contact)			
63	Epipterygoid	present	absent			
64	Vomer, anterior articulation	maxilla	premaxilla			
65	Supraoccipital, height	twice subequal to	or less than height of foramen magnum			
66	Paroccipital process, ventral non-articular process	absent	present			
67	Crista prootica, size	rudimentary	expanded laterally into dorsolateral process			
68	Basipterygoid processes, length	short, approximately twice	or elongate, at least four times basal diameter			
69	Basipterygoid processes, angle of divergence	approximately 45°	less than 30°			
70	Basal tubera, anteroposterior depth	approximately half dorsoventral height	sheet-like, 20% dorsoventral height			

71	Basal tubera, breadth	much broader than	or narrower than occipital condyle			
72	Basal tubera	distinct from basipterygoid	reduced to slight swelling on ventral surface of basipterygoid			
73	Basal tubera, shape of posterior face	convex	sligthly concave			
74	Basioccipital depression between foramen magnum and basal tubera	absent	present			
75	Basisphenoid/basipterygoid recess	present	absent			
76	Basisphenoid/quadrate contact	absent	present			
77	Basisphenoid, sagital ridge between basipterygoid processes	absent	present			
78	Basipterygoid processes, orientation	perpendicular to	or angled approximately 45° to skull roof			
79	Basipterygoid, area between the basipterygoid processes and parasphenoid rostrum	is a mildly concave subtriangular region	forms a deep slot-like cavity that passes posteriorly between the bases of the basipterygoid processes			
80	Occipital region of skull, shape	anteroposteriorly deep, paroccipital processes oriented posterolaterally	flat, paroccipital processes oriented transversely			
81	Dentary, depth of anterior end of ramus	slightly less than that of dentary at midlength	150% minimum depth			
82	Dentary, anteroventral margin shape	gently rounded	sharply projecting triangular process			
83	Dentary symphysis, orientation	angled 15° or more anteriorly to	or perpendicular to axis of jaw ramus			
84	Dentary, cross-sectional shape of symphysis	oblong or rectangular	subtriangular, tapering sharply towards ventral extreme	subcircular		
85	Dentary,	absent	present			

	tuberocity on labial surface near symphysis					
86	Mandible, coronoid eminence	strongly expressed, clearly rising above plane of dentigerous portion	absent			
87	External mandibular fenestra	present	absent			
88	Surangular depth	less than twice	or more than two and one-half times maximum depth of the angular			
89	Surangular ridge separating adductor and articular fossae	absent	present			
90	Adductor fossa, medial wall depth	shallow	deep, prearticular expanded dorsoventrally			
91	Splenial posterior process, position	overlapping angular	separating anterior portions of prearticular and angular			
92	Splenial posterodorsal process	present, approaching margin of adductor chamber	absent			
93	Coronoid, size	extending to dorsal margin of jaw	reduced, not extending dorsal to splenial	absent		
94	Tooth rows, shape of anterior portions	narrowly arched, anterior portion of tooth rows V-shaped	broadly arched, anterior portion of tooth rows U-shaped	rectangular, tooth-bearing portion of jaw perpendicular to jaw rami		
95	Tooth rows, length	extending to orbit	restricted anterior to orbit	restricted anterior to antorbital fenestra	restricted anterior to subnarial foramen	
96	Dentary teeth, number	greater than 20	10-17	9 or fewer		
97	Replacement teeth per alveolus, number	two or fewer	more than four			
98	Lateral plate	absent	present			
99	Teeth, orientation	perpendicular	or oriented anteriorly relative to jaw margin			

100	Tooth crowns, orientation	aligned along jaw axis, crowns do not overlap	aligned slightly anterolingually, tooth crowns overlap			
101	Crown-to-crown occlusion	absent	present			
102	Occlusal pattern	interlocking, V-shaped facets	high-angled planar facets	low-angled planar facets		
103	Tooth crowns, cross-sectional shape at mid-crown	elliptical	D-shaped	cylindrical		
104	Enamel surface texture (wrinkling)	absent	present			
105	Enamel surface texture (wrinkling) coverage	only partial coverage on tooth surface	wrinkling all over tooth surface			
106	Enamel surface texture	smooth	finely wrinkled	coarsely wrinkled	pebbly wrinkled	
107	Thickness of enamel asymmetric labiolingually	absent	present			
108	Marginal tooth denticles	present	absent on posterior edge	absent on both anterior and posterior edges		
109	Teeth, longitudinal grooves on lingual aspect	absent	present			
110	SI values for tooth crowns	less than 3.0	3.0-4.0	4.0-5.0	more than 5.0	
111	Cervical vertebrae, number	10 or fewer	12	13-14	15	16 or more
112	Atlas, intercentrum occipital facet shape	rectangular in lateral view, length of dorsal aspect subequal to that of ventral aspect	expanded anteroventrally in lateral view, anteroposterior length of dorsal aspect shorter tan that of ventral aspect			
113	Cervical centra, articulations	amphicoelous	opisthocoelous			
114	Cervical centra, ventral surface	is flat or slightly convex transversely	transversely concave			
115	Cervical centra, midline keels on	prominent and plate-like	reduced to low ridges or absent			

	ventral surface					
116	Cervical centra, pleurocoels	absent	present with well defined anterior, dorsal, and ventral edges, but not the posterior one	present, with well defined edges	present but very reduced in size	
117	Cervical centra, pleurocoels	singles without division	divided by a bone septum, resulting in an anterior and a posterior lateral excavation	divided in three or more lateral excavations, resulting in a complex morphology	with a well defined anterior excavation and a posterior smooth fossa	
118	Cervical vertebrae, height divided width (measured in its posterior articular surface)	higher than 1.1	around 1	between 0.9 and 0.7	smaller than 0.7	
119	Cervical centra, small notch in the dorsal margin of the posterior articular surface	absent	present			
120	Cervical vertebrae, neural arch lamination	well developed, with well marked laminae and fossae	rudimentary, with diapophyseal laminae absents or very slightly marked			
121	Cervical vertebrae with an accessory lamina, which runs from the postzygodiapophyseal lamina (PODL) up to the spinoprezygapophyseal lamina (SPRL)	absent	present			
122	Cervical vertebra, pre-epipophyses	absent	present			
123	Cervical vertebra, epipophyses	absent	present			
124	Cervical centra, internal pneumaticity	absent	present with singles and wide cavities	present, with several small and complex internal cavities		
125	Anterior cervical vertebrae, prespinal lamina	absent	present			
126	Anterior cervical vertebrae, neural	single	bifid			

	spine shape					
127	Middle and posterior cervical vertebrae, prespinal lamina	absent	present			
128	Middle cervical vertebrae, lateral fossae on the prezygapophysis process	absent	present			
129	Middle, cervical vertebrae, height of the neural arch	less than the height of the posterior articular surface	higher than the height of the posterior articular surface			
130	Middle cervical centrum, anteroposterior length divided the height of the posterior articular surface	less than 4	more than 4			
131	Middle and posterior cervical vertebrae, morphology of the centroprezygapophyseal lamina	single	dorsally divided, resulting in a lateral and medial lamina, being the medial lamina linked with the intraprezygapophyseal lamina and not with the prezygapophysis	divided, resulting in the presence of a ?true? divided centroprezygapophyseal lamina, which is dorsally connected to the prezygapophisis		
132	Middle and posterior cervical vertebrae, morphology of the centropostzygapophyseal lamina (CPOL)	single	divided, with the medial part contacting the intrapostzygapophyseal lamina			
133	Middle and posterior cervical vertebrae, articular surface of zygapophyses	flat	transversally convex			
134	Posterior cervical vertebrae, lateral profile of the neural spine	displays steeply sloping cranial and caudal faces	displays steeply sloping cranial face and noticeably less steep caudal margin			
135	Posterior cervical vertebrae, neural	without a great lateral	laterally expanded, being			

	spine shape	expansion	equal or wider than the vertebral centrum			
136	Posterior cervical and anterior dorsal vertebrae, neural spine shape	single	bifid			
137	Posterior cervical and anterior dorsal bifid neural spines, median tubercle	absent	present			
138	Number of dorsal vertebrae	14 or more	13	12	10	
139	Dorsal centra, pleurocoels	absent	present			
140	Dorsal vertebrae, transverse processes	are directed laterally or slightly upwards	are directed strongly dorsolaterally			
141	Dorsal vertebrae, distal end of the transverse process	curves smoothly into the dorsal surface of the process	is set off from the dorsal surface, the latter having a distinct dorsally facing flattened area			
142	Dorsal vertebrae, non bifid neural spine in anterior or posterior view	posses subparallel lateral margins	posses lateral margins which slightly diverge dorsally	posses lateral margins which strongly diverge dorsally		
143	Dorsal centra, pneumatic structures	absent, dorsal centra with solid interna structure	present, dorsal centra with simple and bigs air spaces	present, dorsal centra with small and complex air spaces		
144	Anterior and middle dorsal neural spines, spinoprezygapophyseal lamina (SPRL)	absent	present			
145	Posterior dorsal neural spines, spinoprezygapophyseal lamina (SPRL)	absent	present			
146	Dorsal vertebrae, single not bifid neural spines, single prespinal lamina (PRSL)	absent	present			
147	Dorsal vertebrae, single not bifid neural spines,	rough and wide, present in	rough and wide, extended trough almost all the	smooth and narrow		

	single prespinal lamina (PRSL)	the dorsalmost part of the neural spine	neural spine			
148	Dorsal vertebrae with single neural spines, middle single fossa projected trought the middline of the neural spine	present	absent			
149	Dorsal vertebrae with single neural spines, middle single fossa, projected through the midline of the neural spine	relatively wide median simple fossa	a thin median simple fossa	extremely reduced median simple fossa		
150	Anterior dorsal centra, articular face shape	amphicoelous	opisthocoelous			
151	Anterior and middle dorsal centra, pleurocoels	have rounded caudal margins	have tapering, acute caudal margins			
152	Middle dorsal neural arches in lateral view, anterior edge of the neural spine	project anteriorly to the diapophysis	converge with the diapophysis	project posteriorly to the diapophysis		
153	Anterior and middle dorsal vertebrae, zygapophyseal articulation angle	horizontal or slightly posteroventrally oriented	posteroventraly oriented (around 30º)	strongly posteroventraly oriented (more than 40º)		
154	Middle to posterior dorsal centra, ventral surface	convex transversely	flattened	is slightly concave, sometimes with one or two crests		
155	Middle dorsal vertebrae, hyposphene-hypantrum system	present	absent			
156	Posterior dorsal vertebrae, hyposphene-hypantrum system	present and well developed, usually with a rhomboid shape	present and weakly developed, mainly as a laminar articulation	absent or only present in posteriormost dorsal vertebrae		
157	Middle and posterior dorsal vertebrae, transverse processes length	short	long (projecting along 1.5 the articular surface width)			

158	Mid and posterior dorsal vertebrae with a single lamina (the single TPOL) supporting the hyposphene or postzygapophysis from below	absent	present			
159	Middle and posterior dorsal vertebrae, neural canal in anterior view	entirely surrounded by the neural arch	enclosed in a deep fossa, enclosed laterally by pedicels			
160	Middle and posterior dorsal vertebrae, neural spine height	approximately twice the centrum length	for times the centrum length			
161	Middle and posterior dorsal neural spines orientation	vertical	slightly inclined, with an angle of around 70 degrees	strongly inclined, with an angle not bigger than 40 degrees		
162	Middle and posterior dorsal neural arches, centropostzygapophyseal lamina (CPOL), shape	simple	divided			
163	Middle and posterior dorsal neural arches, anterior centroparapophyseal lamina (ACPL)	absent	present			
164	Middle and posterior dorsal neural arches, prezygoparapophyseal lamina (PRPL)	absent	present			
165	Middle and posterior dorsal neural arches, posterior centroparapophyseal lamina (PCPL)	absent	present			
166	Middle and posterior dorsal centrum in transverse section (height: width ratio)	subcircular (ratio, similar to 1 or a bit higher)	slightly dorsoventrally compressed (ratios between 0.8 and 1)	strongly compressed (ratios below 0.8)		
167	Middle and posterior dorsal	absent	present but do not project far	present and project far		

	vertebrae neural spine, triangular aliform processes		laterally (not as far as caudal zygapophyses)	laterally (as far as caudal zygapophyses)		
168	Middle and posterior dorsal vertebrae, spinodiapophyseal lamina (SPDL)	absent	present			
169	Middle and posterior dorsal vertebrae, accessory spinodiapophyseal lamina	absent	present			
170	Dorsal vertebrae, spinodiapophyseal webbing	lamina follows curvature of neural spine in anterior view	lamina "festooned" from spine, dorsal margin does not closely follow shape of neural spine and diapophysis			
171	Anterior dorsal vertebrae, spinopostzygapophyseal lamina (SPOL)	absent	present			
172	Anterior dorsals, single intraprezygapophyseal lamina (stprl)	absent	present			
173	Middle and posterior dorsal neural spines, lateral spinopostzygapophyseal lamina (lSPOL)	absent	present			
174	Middle and posterior dorsal neural arches, spinodiapophyseal lamina (SPDL) and spinopostzygapophyseal lamina (lSPOL) CONTACT	absent	present			
175	Middle and posterior dorsal vertebrae, spinodiapophyseal (SPDL) and spinopostzygapophyseal lamina	ventral, well separated from the triangular aliform process	dorsal, forms part of the triangular aliform process			

	(lSPOL) contact					
176	Middle and posterior dorsal vertebrae, height of neural arch below the postzygapophyses (pedicel)	less than height of centrum	subequal to or greater than height of centrum			
177	Middle and Posterior dorsals, absence of the centropostzygapophyseal laminae (cpol)	absent	present			
178	Posterior Dorsal vertebra, centrodiapophyseal fossa (CDF)	absent	present			
179	Posterior vertebra, internal pneumatic chamber connected to CDF	absent	present			
180	Posterior Dorsal vertebrae, medial spinopostzygapophyseal lamina (mSPOL)	absent	present and forms part of the median posterior lamina			
181	Posterior dorsal vertebrae, transverse processes	lie posterior, or posterodorsal, to the parapophysis	lie vertically above the parapophysis			
182	Posterior dorsal centra, articular face shape	amphicoelous	slightly opisthocoelous	opisthocoelous		
183	Posterior dorsal vertebrae, neural spine	narrower transversely than anteroposteriorly	broader transversely than anteroposteriorly			
184	Posterior dorsal vertebra, posterior centrodiapophyseal lamina (PCDL)	has an unexpanded ventral tip	expands and may bifurcate toward its ventral tip			
185	Cervical ribs, distal shafts of longest cervical ribs	are elongate and form overlapping bundles	are short and do not project beyond the caudal end of the centrum to which they are attached			
186	Cervical ribs, angle between the capitulum and tuberculum	greater than 90°, so that the rib shaft lies close to	less than 90°, so that the rib shaft lies below the ventral margin of			

		the ventral edge of the centrum	the centrum			
187	Dorsal ribs, proximal pneumatopores	absent	present			
188	Anterior dorsal ribs, cross-sectional shape	subcircular	plank-like, anteroposterior breadth more than three times mediolateral breadth			
189	Sacral vertebrae, number	3 or fewer	4	5	6	
190	Sacrum, sacricostal yoke	absent	present			
191	Sacral vertebrae contributing to acetabulum	numbers 1-3	numbers 2-4			
192	Sacral neural spines length	approximately twice length of centrum	approximately four times length of centrum			
193	Sacral ribs, dorsoventral length	low, not projecting beyond dorsal margin of ilium	high extending beyond dorsal margin of ilium			
194	Pleurocoels in the lateral surfaces of sacral centra	absent	present			
195	Caudal vertebrae, number	35 or fewer	40 to 55	increased to 70-80		
196	Caudal bone texture	solid	spongy, with large internal cells			
197	Caudal transverse processes	persist through caudal 20 or more posteriorly	disappear by caudal 15	disappear by caudal 10		
198	First caudal centrum or last sacral vertebra, articular face shape	flat	procoelous	opisthocoelous	biconvex	
199	First caudal neural arch, coel on lateral aspect of neural spine	absent	present			
200	Anterior caudal vertebrae, neural spine	flat spine summit	saddle shaped spine summit			
201	Anterior caudal vertebrae,	ventral surface	directed dorsally			

	transverse processes	directed laterally or slightly ventrally				
202	Anterior caudal centra (excluding the first), articular face shape	amphiplatyan or amphicoelous	procoelous/distoplatyan	Slightly Procoelous	Procoelous	posterior surface markedly more concave than the anterior one
203	Anterior caudal centra, pleurocoels	absent	present			
204	Anterior caudal vertebrae, ventral surfaces	convex transversely	concace transversely			
205	Anterior and middle caudal vertebrae, ventrolateral ridges	absent	present			
206	Anterior and middle caudal vertebrae, triangular lateral process on the neural spine	absent	present			
207	Anterior caudal transverse processes shape	triangular, tapering distally	"wing-like", not tapering distally			
208	Anterior caudal neural spines, transverse breadth	approximately 50% of	or greater than anteroposterior length			
209	Anterior caudal transverse processes, proximal depth	shallow, on centrum only	deep, extending from centrum to neural arch			
210	Anterior caudal transverse processes, diapophyseal laminae (ACDl, PCDL, PRDL, PODL)	absent	present			
211	Anterior caudal transverse processes, anterior centrodiapophyseal lamina (ACDL), shape	single	divided			
212	Anterior caudal	absent	present			

	vertebrae, hyposphene ridge					
213	Anterior caudal centra, length	approximately the same	or doubling over the first 20 vertebrae			
214	Anterior caudal neural arches, spinoprezygapophyseal lamina (SPRL)	absent, or present as small short ridges that rapidly fade out into the anterolateral margin of the spine	present, extending onto lateral aspect of neural spine			
215	Anterior caudal neural arches, spinoprezygapophyseal lamina (SPRL)-spinopostzygapophyseal lamina (SPOL) contact	absent	present, forming a prominent lamina on lateral aspect of neural spine			
216	Anterior caudal neural arches, prespinal lamina (PRSL)	absent	present			
217	Middle caudal centra, shape	cylindrical	with flat ventral margin	quadrangular, flat ventrally and laterally		
218	Anterior and middle caudal centra, ventral longitudinal hollow	absent	present			
219	Middle caudal centra, articular face shape	amphiplatyan or amphicoelous	procoelous/distoplatyan	slightly Procoelous	procoelous	
220	Middle caudal vertebrae, location of the neural arches	over the midpoint of the centrum with approximately subequal amounts of the centrum exposed at either end	on the anterior half of the centrum			
221	Middle caudal vertebrae, height of the pedicels below the prezygapophysis	low with curved anterior edge of the pedicel	high with vertical anterior edge of the pedicel			
222	Middle caudal	anteriorly	vertical	slightly	strongly	

	vertebrae, orientation of the neural spines			directed posteriorly	directed posteriorly	
223	Posterior caudal vertebrae, neural spine strongly displacced posteriorly	absent	present			
224	Middle caudal vertebrae, ratio of centrum length to centrum height	less than 2, usually 1.5 or less	2 or higher			
225	Anterior-posterior caudal vertebrae (those with still well developed neural spine) , neural spine orientation	vertical	slightly directed posteriorly	strongly directed posteriorly		
226	Posterior Caudals centra, articular face shape	anphyplatic	procoelous	opisthocoelous		
227	Posterior caudal centra, shape	cylindrical	dorsoventrally flattened, breadth at least twice height			
228	Posterior caudal vertebrae, ratio of length to height	less than 5, usually 3 or less	5 or higher			
229	Distalmost caudal centra, articular face shape	platycoelous	biconvex			
230	Distalmost biconvex caudal centra, number	10 or fewer	more than 30			
231	Distalmost biconvex caudal centra, length-to height ratio	less than 4	greater than 5			
232	Forked chevrons with anterior and posterior projections	absent	present			
233	Forked chevrons, distribution	distal tail only	throughout middle and posterior caudal vertebrae			
234	Chevrons, crus bridging dorsal margin of haemal canal	present	absent			
235	Chevron haemal canal, depth	short, approximately 25%	or long, approximately 50% chevron length			
236	Chevrons	persisting	disappearing by			

		throughout at least 80% of tail	caudal 30			
237	Posterior chevrons, distal contact	fused	unfused (open)			
238	Posture	bipedal	columnar, obligatory quadrupedal posture			
239	Scapular acromion process, size	Narrow	broad, width more than 150% minimum width of blade			
240	Scapular blade, orientation respect to coracoid articulation	perpendicular	forming a 45º angle			
241	Scapular blade, shape	acromial edge not expanded	rounded expansion on acromial side	racquet-shaped		
242	Scapula, acromion process dorsal margin	concave or straight	with V-shaped concavity	with U-shaped concavity		
243	Scapula, highest point of the dorsal margin of the blade	lower than the dorsal margin of the proximal end	at the same height than the dorsal margin of the proximal end	higher than the dorsal margin of the proximal end		
244	Scapula, development of the acromion process	undeveloped	well developed			
245	Scapular length/minimum blade breadth	5.5 or leas	5.5 or more			
246	Scapula, ventral margin with a well developed ventro medial process	absent	present			
247	Scapular, acromial process position	lies nearly glenoid level	lies nearly midpoint scapular body			
248	Scapular acromion length	less than 1/2 scapular length	at least 1/2 scapular length			
249	Glenoid scapular orientation	relatively flat or laterally facing	strongly beveled medially			
250	Scapular blade, cross-sectional shape at base	flat or rectangular	D-shaped			
251	Coracoid, proximodistal length	less than the length of scapular	approximately twice the length of scapular			

		articulation	articulation			
252	Coracoid, anteroventral margin shape	rounded	rectangular			
253	Dorsal margin of the coracoid in lateral view	reaches or surpasses the the level of the dorsal margin of the scapular expansion	lies below the level of the scapular proximal expansion and separated from the latter by a V-shaped notch			
254	Coracoid, Infraglenoid deep groove	absent	present			
255	Coracoid, infraglenoid lip	absent	present			
256	Sternal plate, shape	oval	crescentic			
257	Prominent posterolateral expansion of the sternal plate producing a kidney-shaped profile in dorsal view	absent	present			
258	Prominent parasagital oriented ridge on the dorsal surface of the sternal plate	absent	present			
259	Ridge on the ventral surface of the sternal plate	absent	present			
260	Ratio of maximum length of sternal plate to the humerus length	less than 0,75, usually less than 0,65	greater than 0,75			
261	Humerus-to-femur ratio	less than 0.60	0.60 to 0.90	greater than 0.90		
262	Humeral deltopectoral attachment, development	prominent	reduced to a low crest or ridge			
263	Humeral deltopectoral crest, shape	relatively narrow throughout length	markedly expanded distally			
264	Humeral midshaft cross-section, shape	circular	elliptical			
265	Humerus, RI (sensu Wilson and Upchurch, 2003)	Gracile (less than 0,27)	medium (0,28-0,32)	Robust (more than 0,33)		
266	Humeral distal	restricted to	exposed on			

	condyles, articular surface shape	distal portion of humerus	anterior portion of humeral shaft			
267	Humeral distal condyle, shape	divided	flat			
268	Humeral, lateral margin	medially deflected	almost straight until the half length or even more			
269	Humeral proximolateral corner, shape	rounded, the dorsal surface is well convex	pronounced / square, the dorsal surface low, almost flat			
270	Ulnar proximal condyle, shape	subtriangular	triradiate, with deep radial fossa			
271	Ulnar proximal condylar processes, relative lengths	subequal	unequal, anterior arm longer			
272	Ulnar olecranon process, development	prominent, projecting above proximal articulation	rudimentary, level with proximal articulation			
273	Ulna, length-to-proximal breadth ratio	gracile	stout			
274	Radial distal condyle, shape	round	subrectangular, flattened posteriorly and articulating in front of ulna			
275	Radius, distal breadth	slightly larger than midshaft breadth	approximately twice midshaft breadth			
276	Radius, distal condyle orientation	perpendicular to long axis of shaft	beveled approximately 20º proximolaterally relative to long axis of shaft			
277	Carpal bones, number	3 or more	2 or fewer			
278	Carpal bones, shape	round	block-shaped, with flattened proximal and distal surfaces			
279	Metacarpus, shape	spreading	bound, with subparallel shafts and articular surfaces that extend half their length			
280	Metacarpals, shape of proximal surface in articulation	gently curving, forming a 90arc	U-shaped, subtending a 270arc			

281	Longest metacarpal-to-radius ratio	close to 0.3	0.45 or more			
282	Metacarpal I, length	shorter than metacarpal IV	longer than metacarpal IV			
283	Metacarpal I, distal condyle shape	divided	undivided			
284	Metacarpal I distal condyle, transverse axis orientation	beveled approximately 20º respect to axis of shaft	proximodistally or perpendicular with respect to axis of shaft			
285	Manual digits II and III, phalangeal number	2- 3-4-3-2 or more	reduced, 2-2-2-2-2 or less	absent or unossified .		
286	Manual phalanx I.1, shape	rectangular	wedge-shaped			
287	Manual nonungual phalanges, shape	longer proximodistally than broad transversely	broader transversely than long proximodistally			
288	Pelvis, anterior breadth	narrow, ilia longer anteroposteriorly than distance separating preacetabular processes	broad, distance between preacetabular processes exceeds anteroposterior length of ilia			
289	Ilium, ischial peduncle size	large, prominent	low, rounded			
290	Ilium, dorsal margin shape	flat	semicircular			
291	Ilium, preacetabular process shape	pointed, arching ventrally	semicircular, with posteroventral excursion of cartilage cap			
292	Ilium, preacetabular process orientation	anterolateral to body axis	perpendicular to body axis			
293	Highest point on the dorsal margin of the ilium	lies caudal to the base of the pubic process	lies cranial to the base of the pubic process			
294	Pubis length respect to ischium	pubis slightly smaller or subequal to ischium	pubis larger (120% +) than ischium			
295	Pubis, ambiens process development	small, confluent with anterior margin of	projects anteriorly from anterior margin of pubis			

		pubis prominent,				
296	Pubic apron, shape	flat (straight symphysis)	canted anteromedially (gentle S-shaped symphysis)			
297	Puboischial contact, length	approximately one third total length of pubis	one-half total length of pubis			
298	Ischium, acetabular articular surface	maintains approximately the same transverse width throughout its length	is transversely narrower in its central portion and strongly expanded as it approaches the iliac and pubic articulations			
299	Ischium, iliac peduncle with constriction or "neck"	absent	present			
300	Ischium, elongate muscle scar on proximal end	absent	present			
301	Ischial blade, shape	emarginate distal to pubic peduncle	no emargination distal to pubic peduncle			
302	Ischia pubic articulation	less or equal to the anteroposterior length of pubic pedicel	greater than the anteroposterior length of pubic pedicel			
303	Ischia, anteroposterior pubic pedicel width divided the total length of the ischium	less than 0,5	0,5 or grate	Large		
304	Ischial distal shaft, shape	triangular, depth of ischial shaft increases medially	bladelike, medial and lateral depths subequal			
305	Ischial distal shafts, cross-sectional shape	V-shaped, forming an angle of nearly 50º with each other	flat, nearly coplanar			
306	Ischia, distal end	is only slightly expanded	is strongly expanded dorsoventrally			
307	Ichium, angle	forming an	a close angle (less	close angle		

	formed between the shaft and the acetabular line	almost right angle (80-110°) or	than 70°)	(less than 70°)		
308	Femur, fourth trochanter development	prominent	reduced to crest or ridge			
309	Femur, lesser trochanter	present	absent			
310	Femur midshaft, transverse diameter	subequal to anteroposterior diameter	125-150% anteroposterior diameter	at least 185% anteroposterior diameter		
311	Femur, lateral bulge (marked by the lateral expansion and a dorsomedial orientation of the laterodorsal margin of the femur, which starts below the femur head ventral margin)	absent	present			
312	Femur, pronounced ridge on posterior surface between greater trochanter and head	absent	present			
313	Femur head position	perpendicular to the shaft, rises at the same level than the greater trochanter	dorsally directed, rises well above the level of the greater trochanter			
314	Femur, distal condyles relative transverse breadth	subequal	tibial much broader than fibular			
315	Femur, distal condyles orientation	perpendicular or slightly beveled dorsolaterally	or beveled dorsomedially approximately 10 relative to femoral shaft			
316	Femur, distal condyles articular surface shape	restricted to distal portion of femur	expanded onto anterior portion of femoral shaft			
317	Situation of the femoral fourth trochanter	on the caudal surface of the shaft, near the	on the caudomedial margin of the shaft			

		midline				
318	Tibial proximal condyle, shape	narrow, long axis anteroposterior	expanded transversely, condyle subcircular			
319	Tibial cnemial crest, orientation	projecting anteriorly	or laterally			
320	Tibia, distal breadth	approximately 125%	more than twice midshaft breadth			
321	Tibial distal posteroventral process, size	broad transversely, covering posterior fossa of astragalus	shortened transversely, posterior fossa of astragalus visible posteriorly			
322	Fibula, proximal tibial scar, development	not well-marked	well-marked and deepening anteriorly			
323	Fibula, lateral trochanter	absent	present			
324	Fibular distal condyle, size	subequal to shaft	expanded transversely, more than twice midshaft breadth			
325	Astragalus, shape	rectangular	wedge shaped, with reduced anteromedial corner			
326	Astragalus, fibular facet	faces laterally	faces posterolaterally, anterior margin visible in posterior view			
327	Astragalus, foramina at base of ascending process	present	absent			
328	Astragalus, ascending process length	limited to anterior two-thirds of astragalus	extending to posterior margin of astragalus			
329	Astragalus, posterior fossa shape	undivided	divided by vertical crest			
330	Astragalus, transverse length	50% more than	or subequal to proximodistal height			
331	Calcaneum	present	absent or unossified			
332	Distal tarsals 3 and 4	present	absent or unossified			
333	Metatarsus, posture	bound	spreading			
334	Metatarsal I proximal condyle,	perpendicula	angled ventromedially			

	transverse axis orientation	r to	approximately 15º to axis of shaft			
335	Metatarsal I distal condyle, transverse axis orientation	perpendicular to	angled dorsomedially to axis of shaft			
336	Metatarsal I distal condyle, posterolateral projection	absent	present			
337	Metatarsal I, minimum shaft width	less than that of metatarsals IIIV	or greater than that of metatarsals IIIV			
338	Metatarsal I and V proximal condyle, size	smaller than	or subequal to those of metatarsals II and IV			
339	Metatarsal III length	more than 30%	or less than 25% that of tibia			
340	Metatarsals III and IV, minimum transverse shaft diameters	subequal to	or less than 65% that of metatarsals I or II			
341	Metatarsal V, length	shorter than	or at least 70% length of metatarsal IV			
342	Pedal nonungual phalanges, shape	longer proximodistally than broad transversely	broader transversely than long proximodistally			
343	Pedal digits II-IV, penultimate phalanges, development	subequal in size to more proximal phalanges	rudimentary or absent			
344	Pedal unguals, orientation	aligned with	or deflected lateral to digit axis			
345	Pedal digit I ungual, length relative to pedaldigit II ungual	subequal	25% larger than that of digit II			
346	Pedal digit I ungual, length	shorter	or longer than metatarsal I			
347	Pedal ungual I, shape	broader transversely than dorsoventrally	sickle-shaped, much deeper dorsoventrally than broad transversely			
348	Pedal ungual IIIII, shape	broader transversely than dorsoventrally	sickle-shaped, much deeper dorsoventrally than broad transversely			
349	Pedal digit IV	subequal in	rudimentary or			

	ungual, development	size to unguals of pedal digits II and III	absent			
350	Unguals of pedal digit II and III, proximal dimensions	as broad as deep	significantly broader than deep			

Note: the matrix remains the same, only the *Patagosaurus* input changes. For the holotype (PVL 4170) scoring, the following characters were coded:

??
???????????????????????0110111200102?10011210011100000110110?3000010
10?0010000001100?11011000111[0 1]01011100[0
1]0????21?0??0010010000100?00?000000?0002002?01??????0??1??????????????
?????1001011011010101001101000???01100000100000?11001110111001110?
????????????????????????????

For MACN-CH 230 the following characters were coded:

MACN_230
??
??31110
1000?1?1002001100010110010?111??100010110???????????????????????????
??
??

The following taxa and their coding are used (in phylogenetic order):

Basal sauropodomorphs

'Plateosaurus_engelhardti'
0000000000000000000000000001000000000010000?00000?0000??000000
000000000??00000?0000???0000000000000?0?00?0?000000?00?1010??00?000?0
00000?000000000?1?0?00000000000000000??0?0??0???000000????0?000?0????0
00??0?000???0?000000 2?010000????0???00000000?000000?0?0???000000000000
0?00000000100000000000?0000000?0000000000000?00000000000000000000
00000000000

'Chinshakiangosaurus_chunghoensis'
??
????????????0?0???00?????0?1?10???0101?010??0??0??0????????????????????
??0??????0????????????????????????
??
??????????????????0??

'Mussaurus_patagonicus'

0000000000000000000100?00?010?0000000?00????000??0?0??????????
??????????????1?1???00000??0?0??010?0[0 1]0[0 1]?[0
1]0??00??0?1010??0000000???0?0??00000000?1?0?000??000000000000??0?0??0
???000000???10?000?0????000??0?0?0???0?00?0002?01000?????0???00000000?
000000?0?????00000000000?0?000??000000?0[0
1]0000000?00?000??00000?0000000?0?0???00??000??000?0000000???00?0

'Antetonitrus_ingenipes'

??
??0??0?10??????????0?????0??000
0001121?0?000000000000000000??0?1??0???00000???????0???0????000??0?0?0?
??0??000002?0?000?????0????0?1010??0000??????????0000?0??0110?000??000?
00?0?????????????????????00100000010001?01????????001?1?000?????????

'Lessemsaurus_sauropoides'

??
??????????????????????????????????????0?????????0010???10??00000?0???000??00
000010?1?0?0000000000?000000??1?1??0???00000???????????0?????????????????
??????????????????????????0010100?000000?0??????110010[0
1]001110000??000?00?0??00000?00???????000000000000001000????0?0000??00?
?1??000??00????

'Gongxianosaurus_shibeiensis'

????????????1???
??????????????????????????????????1101?2????0??0?10??????????0?????????0??
????????0???0??0?0????000??????????
????00???01000?????0????001000??000?00?0??????1000?0?00?01?00000?0?????
??????????????????????111???0?????01??0???????0000?1?000000100000

Basal (non-neosauropod) sauropods

'Amygdalodon_patagonicus'

??1?
??1????????????????????????????1101112021???1????1??????????00????????0??
?0????1?????1????0??????0?????????????????00???0????????0?????00???????????
??0000???0???0??
??

'Isanosaurus_attavipachi'

??
??1??0?10??????????0????????0???
???0?1???0????????0??????10?1?1??0???0?0????????????????????????????????
??????????????????????000000??000???
??????????????????1110010001????????????????????????????????

'Vulcanodon_karibaensis'
????????????????????????????????0????????????????????????????????
??
??1????0?0?0???00???0?100????
?01??????????????00??10?????0??????????????1101?0???1110100????0??????
?1?????0000000?010??101??????1000?0000?1000010?100100100?011001

'Tazoudasaurus_naimi'
????????????????????????????????00?10?????????01?????0?????????????????
????????????100???0011???0?00?00101112?000??1000?0010??0000010000?000
?00000110?000?0000001100011?001001111?001?00010??00???????0?00?000000
001001?0?0000002002000??1100??1000000???????0?00?????1101101101?1010
0?100?001?0101?????00000000?10?0101010000?000?0?00010100?00?011?0?000
1010?1

Basal (non-neosauropod) eusauropods

'Shunosaurus_lii'
0100100000110110000010000000??000001001??000000110110000010001
1000000000??000001100?0000?101?110??01101112?20120100100010??00000100
00100?101000110?1?1?0000000000011101[0 1]??1?1[0
1]?0???00010000010?00010100?000000000100100?00?0002001?00???1110101000
00010??000010000100110110100101010001000001101011000001000000???0?011
100110001101?100?10?001111011101l1?111110

Volkheimeria
??
??10?200010??0?0????????????000
0011120?0000001000000111000?1?1??0??????????????0?????????????????????
???????002?????????????????1???
?01??0?001?00?0001?001010101001?????????????????????????????????

'Barapasaurus_tagorei'
??
????????????????????????????????101112?010??1000?0?0???0???0100????0??00
00011??0?1???1010010?01110010011111?1?1100010???01100?0?0?0??000000001
00??0??000?010???0?0??1?00?011000000000000?00??????101101001110100???
????????011000?01000000010?0111000100?0101111??1?10???010???????1??11?
0

Spinophorosaurus
??
????????????????????????????????011?????????????????????0000000???100??00?
?0110?0?1000?010?100?????00??110??0???000[0
1]0?????????????????1???
?????0??
?????????????????????

Lapparentosaurus

??
????????????????????????2211101?021110011??100101?????1?????0????????10
?00100?00??10?01?0100011??001?111??011010?01???????01?????????????????
?????????????????????????1000000110001l0?1?????011011011011005????????
?????01100?000000?000110001101010017???????110000?????????????????????

Bothriospondylus

??
????????????????????????????????1011110?10??10?2011?????????????????10?
?1??????10???????0?????????????????????0???????1???1?0?00??0?01?0???????
??010?????1???1110?????????????
??????001??????????011000100????????????????????????????????

'Cetiosaurus_oxoniensis'

??
??101102?00??000001011010071?01
000110?00????20010100?1101000?111[0 1]?1011000[0
1]0?10??????0?02?00000010?0?0?100?000000200?000??????????00000001??0???
1???01000?0110??01100100???????????011000001000000l?0?011100110011007?
??????????????????????????

Cetiosaurus_Rutland

??
??101111?0??110000?01?0010?111
??011????100????01100?11?1?00?111[0 1]01011100[0
1]0?????????????????0???
????????????????????????10000???0110????1?????????????????????????????
??????????????????????

'Patagosaurus_fariasi'

??
????????????????????????????????0110111200102?100112100111000000110110?3
00001010?00100000001100?11011000111[0 1]01011100[0
1]0????21?0??001001000010071007?000000?0002002?01??????0??1?????????????
??????100101101101010100110100007??0110000010000007110011101110011107?
??????????????????????????????

Patagosaurus_934

??
????????????????????????????????011021130211?????????????????????????????00
12110?1???11?0001000?111001111?1110???10000?????????????????????????????
??
??

Cetiosauriscus_stewarti

??
??
??1?????????????
??
??

Mamenchisaurs

Omeisaurus

11001?0000110?1????010???000???00101001100000101101l?000?1???11
100?0?0??00?0?00110000000?1???111??0110111201004011123000??[1
2]000101100100?21000[1
2]11100110000010010O?111101001?11?0???00210010?2110100?10000000000010
0100?00?0002001?00???1100001100000??000?0000000100110110100101010001O
0000011101100000100000001O?1111000000001011??00101001111111111111111
110

Mamenchisaurus

11101?0?001110110001l0??0?00???00?010010000?010?1?111000?0???10
1?00??????0?0???1100???00110111100?01101112?1004011123[1
2]000??2000101100101021001211100110110010010001100210011?110???102100
1002??0?00?1100030000001001O0?00?0002002?0????1100?0110?0?0?1????00?0?
0????1101101001110100110l?0001???1100000??00000010?0111000100011O1?11
001110?11?101?1?1111??1???

Klamelisaurus

??
??1???????????000??0?????0??????
??
??
??

Turiasaurs

'Turiasaurus_riodevensis'

??
??????????????????????????????1011120001??111201000??00100101?0101??1
1[0
1]1011100010??000001000111011001?1110???0?1100100???????0???002000?0?1
??????????????????200?????????1??????????????????00??0?10110100????10011110
000111??????????????????????????????00??11?101010?11???11???1?10?111?

'Losillasaurus_giganteus'

??1
0?????0????1??????????????1??1?110101000?0??101201000??0000010110100??1
111011100110100010O?000111011001?1111???00110???????????0???00200?10[0

1]100??00000??????1?????????????????????????????????????1011010?????1?????
?????????01?0??010?0?00?11?0??

'Jobaria_tiguidensis'
11001?000011111?010010??0000??10010100?1000001011011 10???10??11
?000??00?00?0?0?1100000???????1100?01101???00001?1??221?00??0000010010
100?201010110?0[0
1]1?11000001000111011001?1110???000000100211 01?10100?000??000100?00?1
00000200100????1?00101101010????01000000????1101101001110100011100001
11111000?0100000011?0111000100?1101110111110011110111 1?????????

Neosauropods

'Haplocanthosaurus_priscus'
??
??[1 2 3
4]?101221?00?1100001001010 0?0111101110011011000101000110011001011011
1100110110021101 1?0100100000000100100?10000120010???????10??11000211?
000100?00?000?????????????????????????????111000?0100000001100111000100
1????????1?????????????????????????

Macronaria

Camarasaurus
11101000001111110100000000000010010100010100010110111000 1101?1
1100000000001000011000001111111110?01101?12021010101232?0[0
1]1?10100101101011210011110?00101100000100011012100 1?1110???00210010?
21101110100?0000000110010 0?10000020010000??[0 1]0[0
1]0101101000101001001000000011011010011101001111110011111100000110000
0101100111000100111011101011100111101111111111111110

'Bellusaurus_sui'
1?????0???11?????????????????????????10???0???0??????110?????????????
000?????????????????????????1101011 01?12?210??101222000??10000101101 00?
?10011111101101100000100011011100 1?1110???002101?0?2??0?1?0?10?030000
0110?100010000???0?000?????????11[0
1]000010100100?00??????10110100111010????1????????11000?01100001011001
1101010001101?????????????????????????????

'Europasaurus_holgeri'
11101?0?001111?0010010000?????10?1?00?01001?01011?1110000101???
?100000001110?0?1100???1111?111110101101?12?210?0101202100??110111011
0100??10011111101102100000100011001 1001?1101???00210010021?001?0?00?0
0000000010000001000002001000 0??0?10??1100000101001001000 0????101101001
110100??11?????1111101?0110000?0110?111000100?1101110101110?11?1???1
??1?1??11??

'Galvesaurus_herreroi'
??
??111220001??2??0??12001????1?
011111101111100??0?0001101[1
2]1001?1110???0020001012110???0????01000?0?100?0???0011???0?000?????1??
?1???????????1?????00000?101[0
1]0100????????????????????????????????0101100????????????????????????????
?????????????

'Tehuelchesaurus_benitezii'
??
??[0 1
2]10001110?0010210010110001001?01001?11?0???00201??01[1 2
3]1???1???1100000101001001115????
11001010[0
1]1110100????????????1????0011000?10110011110000011?????????????????????
????????????

'Tastavinsaurus_sanzi'
??
??1001
1?10?00????0?000100011011100??10?0???01210??0?21101100100?01000001100
10001001111000000???0?1011???
????111101101100001011001111011?011101110???????111111101117100111?

'Euhelopus_zdanskyi'
01?010000111??110??????0???????00???????????0??????11?????01?1????
??????????????100???1??????111??11101112?2004?111220101??2000010?1?001
1111112101101111110??0?100?111011101?1110???0021101113??01?????????????
????????????????????????????????1100000?110?000?00??????10110101?????????
?????????1110?10011000010110011110010001101110l?11?00?11101?11?1???11
??0

Basal titanosauriforms

'Brachiosaurus_altithorax'
12101?00??11??1???????????000?10?1110?01000?01011??110??????????0
?000000111??0?1?????????????1210?0?101112?201??11?232?00112000111???1?
???10?1111100110000001010?111121001?1100???10211?????????????????0????
??10100001?????????
????????????????????????????????1120001000????????0????????????????????????

'Giraffatitan_brancai'
12101000001111110100100010000010010100010000010110111000010l?1
1100000000l110?0011000001111112121O?00101112020l?0111232[0
1]00?12000111110100?2100111110011010200101010l1[0
1]121001?1100???1021?0111211011?0100?0100000100100?1000102001000????

?10??1101000?000010011000000210100101111010011111111101111101101100001011001121001001110111111?1110011110111?11?1??11?0

'Paluxysaurus_jonesi'
????1?????12??
??????????????????????????????[0 1
2]?0?00?01112?201??111232000??2000011110100??1[0 1]002111[1
2]??1111?000010101111?1[0
1]01?11?0???00210?11121?????0????010??001100000010001020010000??0?10??
110?000?0??01[0
1]0?100????2101001011110 1?0??1?1?11???11??0?1011?000101100112101 1?0101
0111??????????????????????????

'Venenosaurus_dicrocei'
??
??
??11???????0????0?10??00?001000
100010000?000?????????11?00001?10?1?????????????????1?10100????1?????
???????101?0000101?00??

Cedarosaurus
??
??100?
2?????????????0?????1?????????????????2?1???????????0????010??000?0?0?00
10?1100000100???????????0?00010???1011???????2100001111 1??00??????????
??????????????????????11210110????0?????????????????????????????

'Erketu_ellisoni'
??
??????????????????????????????????????0111221?00??201001101010?????
??01?????????????????????????
??????????????????????????????????????1?????????????????????????????
??????????????????????????????111?1101?111?0?????????????????

'Chubutisaurus_insignis'
??
??1???
2?10?0011?110??01?10???1?10???10?0???0?210??11???????010??01000?0?10??0
???0001???0?000?????10??1110000111001?????????1101001111??0110??11111
1?????????????000101101112101100111 1?????????????????1???????????

'Tendaguria_tanzaniensis'
??
??111232000?????0????00100??10
0??1?121?1011???0???????????001?????????????????????????????????????
??
??

'Wintonotitan_wattsi'
??
??1???
21?121??1?20?????????????1??1??????????21???????????001???01011???????0?
010001???0?000?????10??11100001110?1????????????01000??1??0?10??111????
???11????????00010?10??

'Ligabuesaururs_lenzai'
??
??????????????????????????[0 1
2]?0?00101112?201??1?12?3?00??2??0???000010??1001210111?111110000101?1
1?111001?1110???00211??
??110000111011??????????210100011?????????????????????????????????????1
1210?100111011101?????????????????????????

'Phuwiangosaurus_sirindhornae'
??????????????????????10?????100101????????0??????111??????????10
00110?1100?0?1?????????????????????121112?201[2 3
4]?101223?0???201001110010 1?21[0 1]012111100111110100101011112 1[0
1]01?1110???002101???2????1??????0100?00010?1?00110011100100000??0?10??
110000010001??????11????10?0000?1101110????????????1100110110001?01100
1121?010011111110?????????????????????????

'Andesaurus_delgadoi'
??
??10?1
2?10?1??111??0?0101?111?11001?1110???00211?????????001?1?02011000?0?0
0???0?01020010?0??????????????????0????????????????????????????????????
????????1011000110??00??2??????1????????????????????????????

'Mendozasaurus_neguyelap'
??
??1?1????00??2??0???000110??100
021?121?112????0??01???????0?1????????????????????????0????02000000100000
0010?210200110?????????1110000100011?????1?????10?100011??0?????11????
??????????????????????112101?????10??1?????????????1?1???????????

'Malarguesaurus_florenciae'
??
??
??0?1??0100000010?00?0
00?2111000110?????????1??
??????????????????????2100????????????????????????????????????

'Argentinosaurus_hunculensis'
??

??1001
20?121?112110000001?111121101?1110???00211????[2
3]??
??????????????????????????1?????????????????????????????0????????????????
????????????????

'Epachthosaurus_sciuttoi'
??
??0???1001
2110?1?1111?0000002?111211101?1110???00211??103???????110?030??001???1
0??10?3?010?010?????????????????????0?????????????111100011?00?10????????
???11?11?1?1??001?1????1121001101?101?101??????111011111111?01111?

'Malawisaurus_dixeyi'
1120????????1??1???0??????
?????????0???100??????????1?10???1?1112?20???101303?10??21010110?0100??
1101211121?1122?1200?0201?01110?1?1110????02110?1?????????1???0300?000
100??0?101010100000????0?11??1???????????00?00110???10110111110001?0??
1??111????1?????????001111100?1210???????11110????????1?????????????1???

'Nemegtosaurus_mongoliensis'
0020?11?0?12?10?010111?10?0010101101?0?0110?01010?1111??2111011
?1100010??00100?1101??011??01?1210?00122112?202????????????????????????
????????????????????????0??
?????0??
??

'Rapetosaurus_krausei'
00201?1?1012?1010?01?1110?0011?00001?0?0110?01010?1111??21111??
?11?0100???1110?1101??011?????1210?00122112?20?40101303?10??210101101
0110??10002[0
1]0121?1122112000020111201101?11?0???11211????3???????????03???????00??
0????3?020?21???????????1110000??????00?001?????10121001 1?00110????1?1?
???111101101100 01??11?011?111111?????????????????????????????????????

'Isisaurus_colberti'
??
??10?301?10??2101010000100??10
00200121?1112?120010001110010 01?11?0????1210?1?13110?0??????030?10011
00000?10131020011 0????0?11?010100000?001000?00??????101111?11101??????
????????110111?01100011111 01???

'Tapuiasaurus_macedoi'
002?111?0012?1010?0111100??0111011?1000?0???01011?1?1????11111?
??1?0000???1110??101????0??1??1210?00122112020[2
3]??1??????0???2?0??11????????100021?121?1112?120?0000110??1101?11?????
??11???11???10?

101???????1?????110011?????1?????????????????????????1?2???????????1????
??????????????1110?111?

'Trigonosaurus_pricei'
??
??101103?10??20?0011000100?31[
0 1]11210121?1122[0
2]1200002?111211101?11?0????1211??
??
??

'Alamosaurus_sanjuanensis'
??????????????1??
??????????????????????????????122112?201??1?1303?10??2000?00000100??1
0?1[1 2]10121?1?12212000020110211?01?1110???00210?1?1[2
3]1?0??00231?03001001100000?1013101110100???0?11111110000000011111101
10?1?1110100111001111??1111112???????1????00?1111100112???111??111111??
?????1?????????????????

'Opisthocoelicaudia_skarzynskii'
??
??1001
200121?11[1
2]22120010201112111101?1110???01210??1131?0?00?221?0?011001100100?101?
1020002001000?111110000000?00111101111011111121011110111??1111112??
11111110110001?11101112101110111111101011011111101111111011110

'Neuquensaurus_australis'
??
??101[2
3]03000??2??00??000100??1111200121?112211200002?111211101?1110???0121
1????31?0???1?30?030??001100??0?1013?021?011?1?0??????11100?0000010110
111?????11121001110111?????????????1111?101?000111110011210111?1111?1
0101101??1110?????1????????

'Saltasaurus_loricatus'
????????????????????????????00?????1010???010?01?????????????????01
00010??1?????1?????????????????????????????101303000??2001010000100?
?1111200121?1122112000020111111101?1110???01211????311010?1?1??030110
01100??0?10131021101101?0??11?011100000000101101111O???11121001110111
1???????????1111111011000111110011210111111111110?????????????????????
????

'Amazonsaurus_maranhensis'
??
??1???
111????10??0???????????0?1?01?11?????1?????????????0????000[0

1]?0?1???0?1[0
1]1100002?1?00??????10??
????0??

'Zapalasaurus_bonapartei'
??
??11?221001???00?????????????
??1001000110?011
00100002011 00???
?????????000?0?11?0????????????????????????????????????

'Histriasaurus_bocardeli'
??
??1101
?????????10?010??00???001011?11?0???1?010????????????????????????
??
??

'Comahuesaurus_windhauseni'
??
????????????????????????????122111?203????????????????????????110
11110?0210220?1??1??0???001111?11?????1?01??????????0?0?20?1400000?10?
0????10002011?0??????10??1???????????00?001?????10110111?????????????
???????????010100000 11?0211000100????????????????????????????

'Rayososaurus_agrioensis'
??
??
??
??????????????????????102111001001????????????????????????????????
??????????????????2?1????????????????????????????????????

Rebbachisaurids

'Rebbachisaurus_garasbae'
??
????????????????????????????21110????????????????????????????1101
1?110?02?0??0121011001110 01011?11?1???11010???????1?????????????????
??????????????????????11021?1001001????????????????????????????????
??

'Cathartesaura_anaerobica'
??
????????????????????????????????????110221001??1??0???000100?????
??1????0111000?1
1?100012?1??0???????????1?21110011?1?????????????????????????????????
??????????????????2110001????????????????????????????????

'Limaysaurus_tessonei'

??????????1?01????1?1??0000??11??0011111?001?0?10111011?20?????1
00101010110?101?????????????????????1221111203??110221001??100001000010
0??11011110?021011012101100110001011?11?1???110101?0???????[1 2]01[0
2]0?14000001100001111000020110011?1??10??110211100110100100111???11010
01011110100????????????11???00101100001101211000?001?10??1?11???0??100
01111??????????

'Demandasaurus_darwini'

?0?0??
?????????????10120?????????2?2?1?01221111203??110231001??1000010200100?
?11??1?10?02????0?1?01101111100101??11?????1?01011???????????20?1400010
11001?1010100??0??00??????10??
??????????????????111????1?1211010100????????????????????????????????

'Nigersaurus_taqueti'

00201?10101100?1??1111??0000??11??0011110??11????0111011?2??????
100100010??0?1?1101200100????2301?0012211112032?110221001??1000010200
100?211?11110?021012011111101111001011?11?1???100101?00???1????????14
0??1?1?0?0?1011?00120110011?11010??1102121000001100?00??????10100101??
??????????????????110??0???111??????1211010100?????????1?????????????????
???????

'Suwassea_emiliae'

0121???1???2?????????1??01???????00?00??11100?0??1??0?10????????0
????0?0?????????1?11?????????2?2????1??21110????0111221000??100101010???1
??110?11?????1021?????????????????1?????????????1100???????0?????1???????
????????????????????????????????0000?000????????????????2?????????????????
??

'Amargasaurus_cazaui'

???????????2?011?????????100??10?0110001111001111?????????????0
011101001?0?111?????????????????????????????????1111021100????1?1101001?1
0?01020110?1?1?1100210110?10?001001?11?0???000101??02??1?????0??0?0??0
??????010???0?020?????????????????1??0??????0?1??????????1101101001010?00??
???????????11001?????????????????1110?0?001????????1?????????????????????

'Dicraeosaurus_hansemanni'

0021???1???2??01?????????100???0?0110001111001111111?????1?0???10
001110100010?11111011????????2311?0011211102031111021100??0?1?110110
1?11201020110?1?1?1100010110110000010 01?11?1???00010110021?1?0?0110?02
000011100101010000020 12?0?1?11?00??1100000???00100??0?????11011010011
10?????????????1110000110000??0010111000100111011101111 10??111111?1
1????11???

'Brachytrachelopan_messai'
??
??1?0?11?????0????????????2010
20110?1?1?1?000101101100001001?11?1???000101????????????????????????
??
??

Apatosaurus
00201?11111201111?111100101100?00101000111010101101100100 20?01
?000010000000000101?1?001???????2311?000121110 2?331111231?0011201?1102
101?1131000?110?021011000011001111001001111?0???10010110021?11120110?
020000111111011100000 2012?011111100101100000 1?0011001?00000?11012010
010101001111000011111100001100000 1?00101111001001110111011101111111
1111?1111?1110

Diplodocus
00201011111201111111110010110010010100011101010110110010020101
100001000010100101110001101101?2311?100121110203311112 31?0011201?011
2111?1131000111??021011000011001111001001111?0???101101100211111201 1
0?021110111111111121000 3012?011111100101100000 0?1001001?000000110110
1001110100???????????1110000011000000?00101110001011110 1?1011111001111
111111111?11110

'Barosaurus_lentus'
??
??3?111231?0011?00?1112011?11310
001110?021011000011001111001001?11?0???1001011002????0?0110?021110111
1111111210003012?011?11?00?01???000????????1??0??????0?00?0????????????
????????11??0?11?0???????10111000???11????????1??????????????????????

ccode + 11 57 94 95 107 109 116 117 123 148 155 166 221 224 240.242 260 264
307 309 *;

Appendix Chapter 5

Appendix A: PCA Analysis

Dataset 'Combined dataset '

20 landmarks in 2 dimensions.
The dataset contains 9 observations, of which 9 are included for analyses.

Average shape:

Lmk.	Axis 1 (x)	Axis 2 (y)
1	0,29552418	-0,08517905
2	0,32315778	-0,03170936
3	0,31588216	0,06138697
4	0,28940144	0,09458593
5	0,23611067	0,06745492
6	0,08248801	0,01641398
7	0,02224716	0,01568538
8	0,02118772	-0,00222671
9	-0,07908498	0,00320403
10	-0,07886183	0,01737442
11	-0,17539355	0,04289093
12	-0,20427257	0,07997957
13	-0,23558700	0,09303073
14	-0,27346083	0,03665514
15	-0,25666005	-0,02992671
16	-0,24684284	-0,06276257
17	-0,24003756	-0,07574513
18	-0,13487642	-0,09294148
19	0,09515001	-0,07225241
20	0,24392852	-0,07591858

Procrustes sums of squares: 0.07086170829490836
Tangent sums of squares: 0.07008774309057351

Data matrices in this dataset:
- Combined dataset , raw data
- Combined dataset , centroid size
- Combined dataset , Procrustes coordinates

Dataset 'PC scores, CovMatrix, Combined dataset , Procrustes coordinates'

20 landmarks in 1 dimensions.
The dataset contains 9 observations, of which 9 are included for analyses.

Data matrices in this dataset:
- PC scores, CovMatrix, Combined dataset , Procrustes coordinates

Dataset 'PC scores, CovMatrix, Combined dataset , Procrustes coordinates'

20 landmarks in 1 dimensions.
The dataset contains 9 observations, of which 9 are included for analyses.

Data matrices in this dataset:
- PC scores, CovMatrix, Combined dataset , Procrustes coordinates

Principal Component Analysis:

	Eigenvalues	% Variance	Cumulative %
1.	0,00395489	45,142	45,142
2.	0,00147751	16,865	62,007
3.	0,00136406	15,570	77,577
4.	0,00073516	8,391	85,968
5.	0,00044802	5,114	91,082
6.	0,00041675	4,757	95,839
7.	0,00020315	2,319	98,158
8.	0,00016141	1,842	100,000

Total variance: 0,00876097

Variance of the eigenvalues: 0,0000005148611
Eigenvalue variance scaled by total variance: 0,00671
Eigenvalue variance scaled by total variance and number of variables: 0,24838

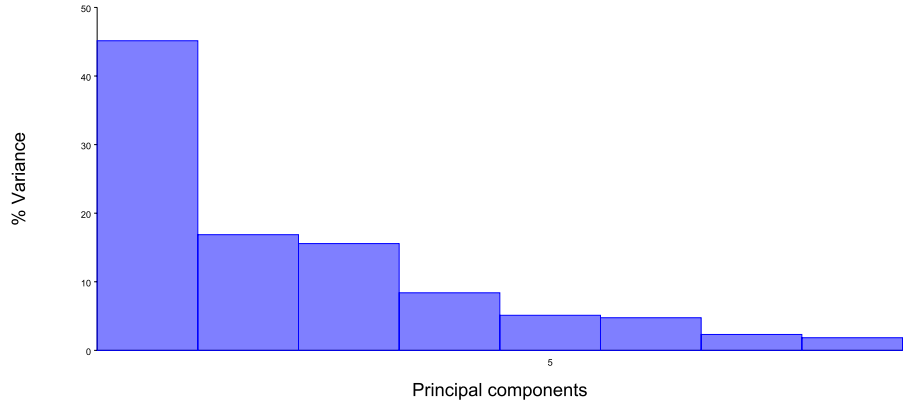

Principal Component Coefficients

	PC1	PC2	PC3	PC4	PC5	PC6	PC7	PC8
x1	-0,165793	-0,150024	0,142942	-0,209368	-0,009302	0,018263	0,167025	0,076770
y1	-0,000355	-0,025868	0,260206	0,020508	-0,037275	-0,075292	0,247207	-0,225965
x2	-0,089053	-0,218770	-0,101358	-0,168855	-0,011879	-0,013419	-0,146723	-0,002250
y2	0,013724	0,180717	0,303340	-0,053335	0,290167	0,099971	-0,160696	0,340782
x3	-0,141935	-0,151086	-0,055242	0,034470	-0,214469	0,136021	0,018950	-0,124706
y3	-0,006653	-0,167079	-0,116860	-0,134760	0,092475	-0,107214	-0,074147	0,377705
x4	-0,117174	-0,128924	-0,014168	0,093157	0,084536	0,035604	0,096581	-0,089425
y4	0,029229	-0,096779	-0,164481	-0,115472	-0,274458	-0,192207	-0,102468	0,039845
x5	-0,147805	0,133789	0,197774	0,245249	0,109551	0,053219	-0,306385	-0,024021
y5	-0,004004	0,061692	-0,063455	0,154326	-0,244739	-0,033525	-0,142348	-0,064867
x6	0,195996	0,357950	-0,074445	-0,134573	-0,170857	0,153178	-0,037758	0,067114
y6	0,068604	-0,086436	-0,157748	0,088514	0,056266	0,210155	0,014764	-0,095647
x7	0,238731	0,222255	0,078358	0,153468	-0,026694	-0,121816	-0,031764	-0,026445
y7	0,000795	-0,030831	-0,144929	0,129029	0,051922	0,126920	-0,090614	-0,126452
x8	0,250691	0,199212	0,109433	0,118616	0,055715	-0,038510	-0,078506	-0,152948
y8	-0,047764	0,076425	-0,247292	-0,167352	0,296601	-0,023492	-0,459408	-0,249176
x9	0,430762	-0,304031	0,011912	0,021853	0,214073	-0,067480	0,002771	-0,052385
y9	0,006685	0,018188	-0,277041	-0,244555	-0,081401	-0,302306	0,262038	0,039526
x10	0,429550	-0,311332	0,019297	0,027286	0,213110	-0,086274	0,076661	-0,004005
y10	-0,050157	0,000732	-0,110209	0,121316	-0,111706	-0,054725	-0,043975	-0,109116
x11	-0,078321	-0,271360	0,058493	0,136279	-0,166776	0,325826	-0,009434	0,412926

y11 0,006299 0,100838 -0,049625 0,094879 -0,005468 -0,270248 0,063657 -0,169198
x12 -0,053144 -0,096865 0,271649 -0,142520 -0,188985 -0,215884 -0,163433 -0,075725
y12 0,029591 -0,113994 -0,148968 0,306012 -0,130243 0,043274 0,052365 0,148088
x13 -0,042757 0,019590 0,160664 -0,235860 -0,316554 -0,168615 -0,052841 -0,044515
y13 0,120765 -0,086343 0,112621 0,258613 -0,062875 -0,098397 -0,065436 0,078331
x14 -0,138683 -0,021110 -0,063282 -0,175565 -0,112123 0,058155 -0,085758 -0,096757
y14 0,068444 0,108888 -0,060589 -0,136750 0,208751 -0,037425 0,349137 0,205714
x15 -0,108403 -0,127619 -0,189817 -0,025954 0,179932 -0,000387 -0,007245 -0,105505
y15 -0,076127 0,124307 0,093577 -0,051827 -0,069786 -0,029665 -0,092658 0,285556
x16 -0,145317 0,121781 -0,169396 0,252374 0,023374 -0,223740 -0,067764 0,191541
y16 -0,071789 -0,109191 0,101305 -0,365601 0,154208 0,262037 -0,080588 -0,129418
x17 -0,175110 0,042019 -0,189720 0,162585 0,072595 -0,063427 0,035502 0,082370
y17 -0,038424 0,047394 0,123506 -0,067136 0,088231 0,138996 -0,118698 0,006546
x18 -0,281562 0,167799 -0,186557 0,105123 0,191971 0,230961 0,314934 -0,132012
y18 -0,073643 0,076285 0,161459 0,025432 -0,008870 0,027571 0,109035 -0,023275
x19 0,341231 0,350252 -0,204725 -0,212856 -0,176369 0,299012 0,090109 0,072944
y19 -0,015124 -0,025457 0,153365 0,094656 -0,112039 0,132100 0,218518 -0,116512
x20 -0,201903 0,166473 0,198187 -0,044908 0,249150 -0,310689 0,185077 0,027034
y20 0,039904 -0,053488 0,231816 0,043502 -0,099761 0,183471 0,114316 -0,212468

Appendix B

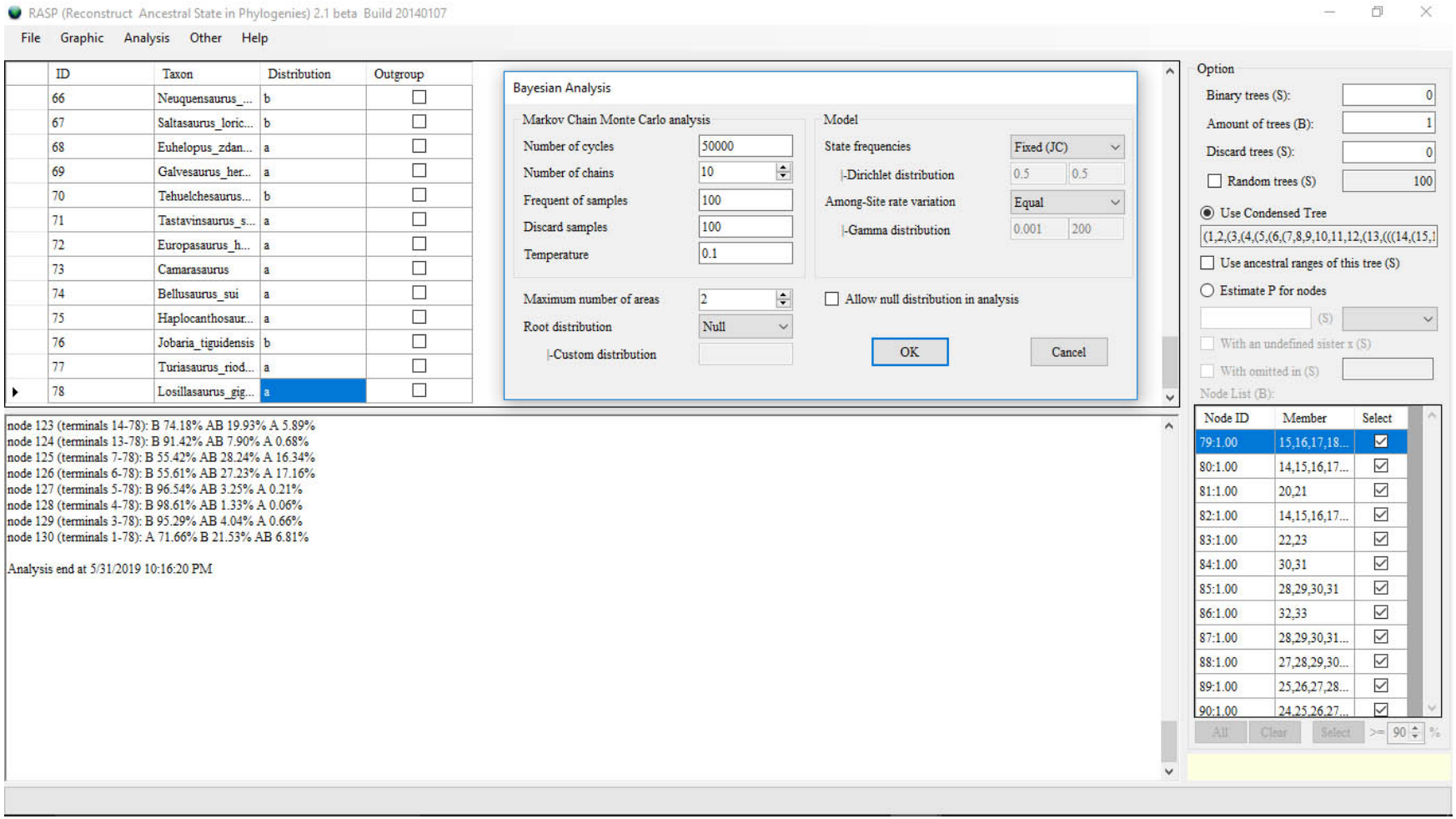
RASP (Reconstruct Ancestral State in Phylogenies) 2.1 beta Build 20140107
File
Graphic
Analysis
Other
Help
ID
Taxon
Distribution
Outgroup
66 Neuquensaurus_... b
67 Saltasaurus_loric... b
68 Euhelopus_zdan... a
69 Galvesaurus_her... a
70 Tehuelchesaurus... b
71 Tastavinsaurus_s... a
72 Europasaurus_h... a
73 Camarasaurus a
74 Bellusaurus_sui a
75 Haplocanthosaur... a
76 Jobaria_tiguidensis b
77 Turiasaurus_riod... a
78 Losillasaurus_gig... a
Bayesian Analysis
Markov Chain Monte Carlo analysis
Number of cycles 50000
Number of chains 10
Frequent of samples 100
Discard samples 100
Temperature 0.1
Model
State frequencies Fixed (JC)
|-Dirichlet distribution 0.5 0.5
Among-Site rate variation Equal
|-Gamma distribution 0.001 200
Maximum number of areas 2
Root distribution Null
|-Custom distribution
Allow null distribution in analysis
OK
Cancel
node 123 (terminals 14-78): B 74.18% AB 19.93% A 5.89%
node 124 (terminals 13-78): B 91.42% AB 7.90% A 0.68%
node 125 (terminals 7-78): B 55.42% AB 28.24% A 16.34%
node 126 (terminals 6-78): B 55.61% AB 27.23% A 17.16%
node 127 (terminals 5-78): B 96.54% AB 3.25% A 0.21%
node 128 (terminals 4-78): B 98.61% AB 1.33% A 0.06%
node 129 (terminals 3-78): B 95.29% AB 4.04% A 0.66%
node 130 (terminals 1-78): A 71.66% B 21.53% AB 6.81%
Analysis end at 5/31/2019 10:16:20 PM
Option
Binary trees (S): 0
Amount of trees (B): 1
Discard trees (S): 0
Random trees (S) 100
Use Condensed Tree
(1,2,(3,(4,(5,(6,(7,8,9,10,11,12,(13,(((14,(15,1
Use ancestral ranges of this tree (S)
Estimate P for nodes
(S)
With an undefined sister x (S)
With omitted in (S)
Node List (B):
Node ID
Member
Select
79:1.00 15,16,17,18...
80:1.00 14,15,16,17...
81:1.00 20,21
82:1.00 14,15,16,17...
83:1.00 22,23
84:1.00 30,31
85:1.00 28,29,30,31
86:1.00 32,33
87:1.00 28,29,30,31...
88:1.00 27,28,29,30...
89:1.00 25,26,27,28...
90:1.00 24,25,26,27...
All
Clear
Select
>= 90 %